The Dissertation Committee for Alan Ronald Meis Certifies that this is the approved version of the following dissertation:

Synthesis of Homoaporphine-Type Alkaloids via Intramolecular Phenol Alkylation, Design and Synthesis of a New Class of *Trypanosoma brucei* Growth Inhibitors, and Neurons That Matter: Using Light To Tag Neuronal Ensembles Based On Function

Committee:

Stephen F. Martin, Supervisor

Jonathan L. Sessler

Eric V. Anslyn

Adrian T. Keatinge-Clay

Boris V. Zemelman

Synthesis of Homoaporphine-Type Alkaloids via Intramolecular Phenol Alkylation, Design and Synthesis of a New Class of *Trypanosoma brucei* Growth Inhibitors, and Neurons That Matter: Using Light To Tag Neuronal Ensembles Based On Function

by

Alan Ronald Meis, B.S.

Dissertation

Presented to the Faculty of the Graduate School of

The University of Texas at Austin

in Partial Fulfillment

of the Requirements

for the Degree of

Doctor of Philosophy

The University of Texas at Austin

May 2017

Dedication

To my first teacher, mentor, and inspiration, for whom I would not be here without,

Dr. Ronald J. Meis

Acknowledgements

The personal successes that I have achieved throughout my graduate studies would not have been possible without the support of numerous individuals. First and foremost, I must thank my loving parents, whose unconditional love and support has allowed me to become the person that I am today. To my mother Darlene Meis, thank you for teaching me how to be a responsible individual and setting an example as to what it means to be a compassionate and caring person. To my father Ronald Meis, thank you for questioning, yet supporting, every decision I have ever made. You instilled an inquisitive and knowledge seeking mindset that ultimately led me to become a scientist. To my brother Andy Meis, your tenacity in the face of hardships has deeply inspired me. As brothers, we will always be there for each other.

Most notably, thank you Professor Stephen F. Martin for allowing me to join your group when I was left without one. I can honestly say that joining the Martin group was the best possible decision for my graduate career. Your never ending technical expertise and motivational words have influenced me in more ways than I can describe. More importantly, your thought provoking questions have shaped me into the independent scientist that I am today.

I would like to thank Danny Klosowski for being a friend both inside and outside of the lab. From our adventures through candidacy to learning about neurobiology, my time in graduate school would not have been nearly as productive or fun without you.

I am deeply grateful for the technical advice and personal friendship of Dr. James Sahn. You helped me through synthetic challenges on every one of my projects, but more importantly you became a dear friend.

I must thank Lance Lepovitz for working with me on our African sleeping sickness project. I am quite impressed how you matured as a scientist throughout the course of this project to make it your own. I truly believe that our project would not have been nearly as successful or interesting without your work.

The entirety of my graduate experience would not have been the same without my closest friends: Igor Kolesnichenko and Tom Luong. We have been through this journey together since the beginning. It is almost unbelievable to think that we are all on our way to the next chapters of our own lives. But needless to say, we would not have made it this far without each other. Bobateers 4 life!

I would also not have made it through graduate school without the friendships of Dr. Charles Seipp, Dr. William Montgomery, and Dr. Timothy Hodges. We all started in the Magnus lab together, and remained dear friends throughout the course of our own graduate studies.

I would to thank Professor Phil Magnus for taking me on as a first-year graduate student. Though our time was cut short, the lessons I learned from you have been both innumerable and invaluable to my chemical career.

Finally, I would like to thank the entire Martin lab, both past and present members, who have helped me along the way. From ridiculous antics to thought provoking conversations, I would not have survived the past five years without the help of Katie Linkens, Zach White, Sean Blumberg, Caleb Heathcox, Alex Goodnough, Rachel Wypych, Mike Wood, Chris Farley, and Zhipeng Wang.

Synthesis of Homoaporphine-Type Alkaloids via Intramolecular Phenol Alkylation, Design and Synthesis of a New Class of *Trypanosoma brucei* Growth Inhibitors, and Neurons That Matter: Using Light To Tag Neuronal Ensembles Based On Function

Alan Ronald Meis, Ph.D.

The University of Texas at Austin, 2017

Supervisor: Stephen F. Martin

The synthesis of a homoaporphine-type alkaloid was accomplished in 10-steps. The synthesis featured a synthetic strategy to establish the key quaternary center through an early Suzuki cross coupling and a late-stage *p*-phenolic *C*-alkylation reaction, which proceeded in high yields.

A medicinal chemistry and rational drug design approach was undertaken to design and synthesize a new class of *Trypanosoma brucei* growth inhibitors. This hit-to-lead strategy resulted in compounds with up to a 25-fold increase in efficacy towards *T. brucei* growth inhibition, with respect to the initial hit compound, and a single compound with activity in sub-micromolar concentrations.

A collaborative effort has begun to develop a function based method to label or tag neurons. We have developed a photocaged derivative of erythromycin A in order to control gene expression within neurons using light. The photochemical properties of the photocaged-erythromycin derivative were studied and *in vitro* proof of principle assays are currently underway.

Table of Contents

List of Tables

List of Figures

List of Schemes

P-PHENOLIC *C*-ALKYLATION AS A STRATEGY TO ACCESS HOMOPROAPORPHINE AND HOMOAPORPHINE ALKALOIDS

Chapter 1: Previous Synthetic Studies Towards Natural and Unnatural Homoaporphine Alkaloids

1.1. NATURAL PRODUCTS AND ISOLATION

Homoaporphine alkaloids are a class of naturally occurring 1-phenethylisoquinoline alkaloids containing a tetracyclic core with a 7-membered ring (**1.1**) (Figure 1.1). The naturally occurring homoaporphines are generally *N*-methylated on the isoquinoline ring and penta-oxygenated on the biaryl moiety.[1,2] Variations of the *O*-methyl or hydroxyl substitution patterns give rise to the various members in the alkaloid family.

Figure 1.1. Generalized homoaporphine skeleton (**1.1**) and numbering convention, examples of homoaporphine natural products

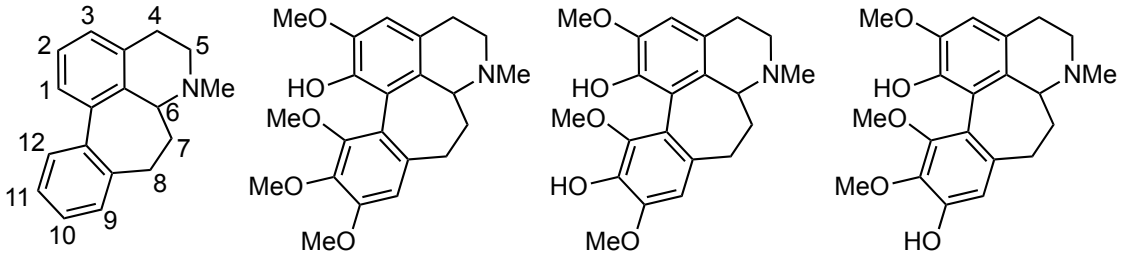

1.1 (±)-kreysigine (**1.2**) (±)-multifloramine (**1.3**) (±)-floramultine (**1.4**)

The first reported isolation of these compounds came from Bradbury and Badger in 1960. Upon extraction from dried *Kreysigia multiflora*, they isolated three previously unknown alkaloids.[3] Further isolation and synthetic studies by Battersby characterized

the structures of (±)-kreysigine (**1.2**), (-)-multifloramine (**1.3**), and (+)-floramultine (**1.4**).[4,5] Since these initial studies, 17-naturally occurring homoaporphine alkaloids have been isolated from the Lilaceae family of plants, specifically from the genera: *Androcymbium, Colchicum, Kreysigia, Bulbocodium, Iphigenia, Merendera, and Gloriosa*. Interestingly, it was found that the stereochemistry of these compounds at C6 depends on the genus of plant from which they were isolated. For instance, all compounds isolated from the genus *Androcymbium* were found to be dextrorotatory, while compounds from the *Colchicum* genus were isolated as either the dextrorotatory or levorotatory configurations. Furthermore, of the three homoaporphine alkaloids isolated from *Kreysigia multiflora*, both floramultine (**1.4**) and multifloramine (**1.3**) were isolated as the levorotatory isomer, yet both stereoisomers of kreysigine (**1.2**) were isolated from the same source.[1]

1.2. BIOSYNTHESIS OF HOMOAPORPHINE ALKALOIDS

In discussing the biosynthetic pathway towards homoaporphine alkaloids, it is interesting to note that these compounds are biosynthetically related to the alkaloid colchicine (**1.7**). The biosynthesis of colchicine has been shown to proceed through a *para*-*para*-oxidative phenolic coupling from automnaline (**1.5**) (Scheme 1.1) to give the hexadienone androcymbine (**1.6**), the biosynthetic precursor of colchicine (**1.7**). Conversely, the homoaporphine alkaloids are thought to arise through an *ortho*-*para*-oxidative phenolic coupling

Scheme 1.1. Biosynthesis of floramultine (**1.4**) and colchicine (**1.7**) from automnaline (**1.5**)

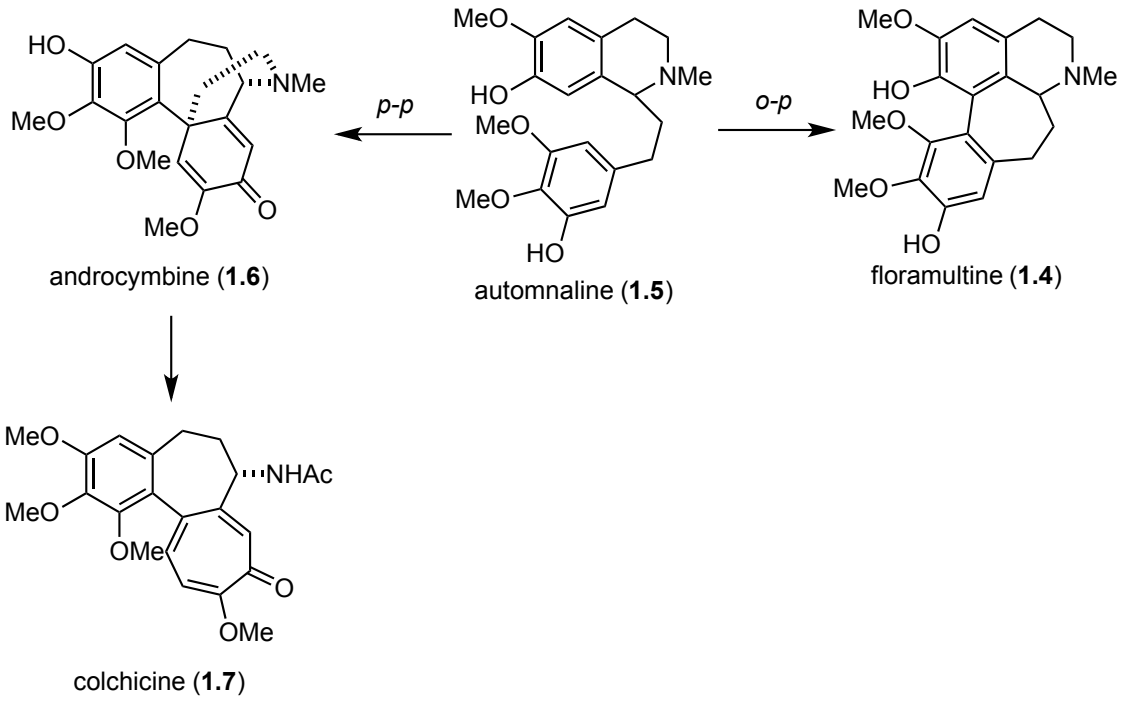

Given the co-occurrence of homoaporphine alkaloids with tropolone alkaloids from natural sources, Battersby et. al. undertook studies to show that homoaporphines, specifically floramultine (**1.4**), could arise from automnaline (**1.5**).[6] In this study, synthetic radiolabeled samples of automnaline (**1.5**) were fed to *Kreysigia multiflora*. Upon isolation and treatment with diazomethane, they isolated pure radiolabeled *O*-methylkreysigine, suggesting that the homoaporphine alkaloids can arise from a direct *ortho-para*-oxidative phenolic coupling of automnaline (**1.5**).

While the previous study was a good indication that some homoaporphine alkaloids could arise from automnaline (**1.5**), this study did not explain the occurrence of

homoproaporphine alkaloids with the differing substitution patterns found in nature. The homoproaporphine kreysiginone (**1.9**) (Scheme 1.2) was isolated in small quantities from *Kreysigia multiflora*.[7] The presence of **1.9** indicates that some of these compounds may arise from the *ortho-para*-oxidative phenolic coupling of phenethylisoquinoline precursors, like **1.8**. The *ortho-para*-oxidative phenolic coupling of **1.8** would yield kreysiginone (**1.9**), of which, dienone-phenol rearrangement would yield the corresponding homoaporphine **1.10**. While this second potential biosynthetic pathway has yet to be proven via tracer studies, it's analogous to the biosynthetic formation of the homologous aporphine alkaloids.[8]

Scheme 1.2. Homoaporphine biosynthesis from isolated intermediate kreysiginone (**1.9**)

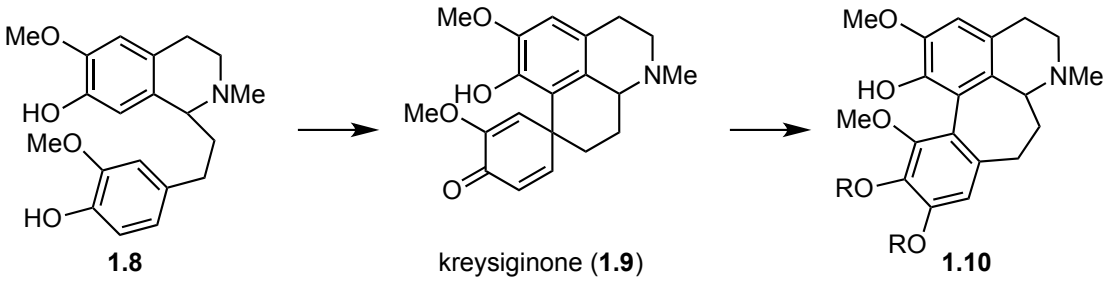

1.3. PREVIOUS SYNTHETIC STUDIES

A number of synthetic efforts towards the synthesis of homoaporphine alkaloids have been reported since their discovery in 1960. Strategically, all of these approaches (with one exception) focus on constructing the phenethylisoquinoline scaffold and subsequent formation the key biaryl bond. Many synthetic efforts have been made to

effect a biomimetic *o*-*p*-oxidative phenolic coupling strategy to form this bond, but this method has been met with limited success throughout the history of these (and related) alkaloids. The following sections summarize the synthetic efforts towards both natural and unnatural homoaporphines and is organized by key bond transformation.

1.3.1. Oxidative Phenolic Coupling Strategies

1.3.1.1. Battersby's Approach

The first reported synthesis of a homoaporphine alkaloid was Battersby's synthesis of (±)-multifloramine (**1.3**) (Scheme 1.3).[5] This synthesis was performed to confirm the structural assignment of (±)-kreysigine (**1.2**), (±)-multifloramine (**1.3**), and (±)-floramultine (**1.4**). In this route, diphenol **1.11** was prepared according to "standard methods". Treatment of **1.11** with potassium ferricyanide in a biphasic mixture led to homoproaporphine **1.12** in 49% yield. Subsequent dienone-phenol rearrangement in concentrated sulfuric acid led to (±)-multifloramine (**1.3**) in 45% yield.

The key step in this synthesis was the *o*-*p*-oxidative phenolic coupling. In this sequence, (±)-multifloramine (**1.3**) was synthesized from **1.11** in two steps with an overall yield of 22%. Throughout his studies of homoaporphines, Battersby performed this reaction on a number of different phenolic phenethylisoquinoline substrates and in each case the yields were quite poor (~30-50%).[4,7]

Scheme 1.3. Battersby's approach to (±)-multifloramine (**1.3**)

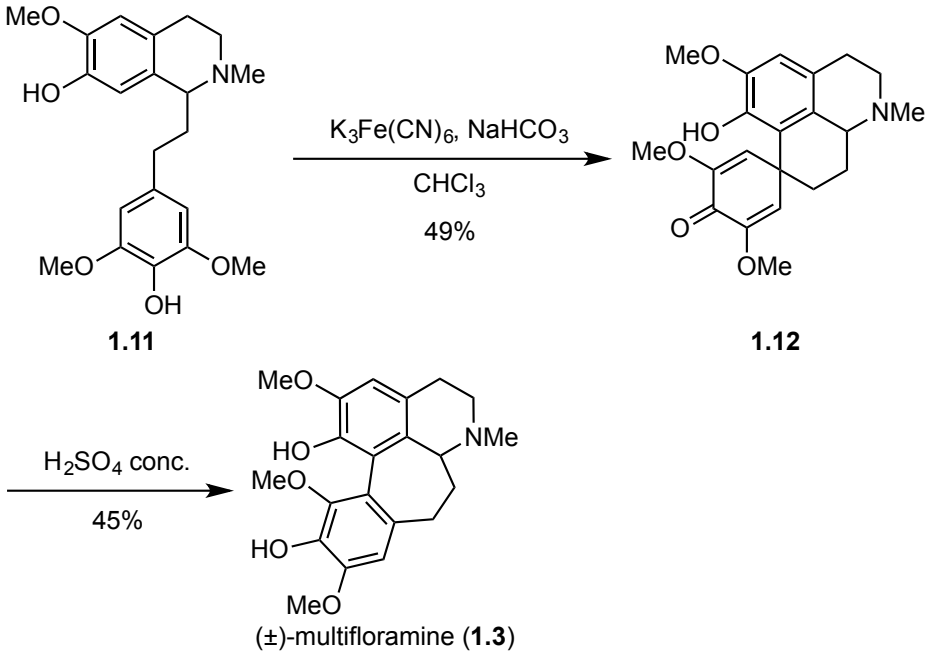

1.3.1.2. Kupchan's Synthesis of (±)-Kreysigine and (±)-Multifloramine

In a series of studies, Kupchan used the same late stage oxidative phenolic coupling strategy to synthesize (±)-kreysigine (**1.2**) and (±)-multifloramine (**1.3**). The major difference in this method was the use of vanadium (V) oxytrifluoride as the oxidant.[9,10] The use of this reagent allowed for the oxidative phenolic coupling to occur on monophenolic substrates. When phenol **1.13** was oxidized using vanadium (V) oxytrifluoride, the *N*-trifluoroacetamide of kreysigine **1.14** was isolated in 46% yield, as well as the homoproaporphine **1.15** in 4% yield (Equation 1.1). However, when the *N*-methyl derivative **1.16** was subjected to the same conditions, the major product was the corresponding homoproaporphine **1.12** in 54% yield, and (±)-kreysigine (**1.2**) was only

isolated in 16% yield (Equation 1.2). The homoproaporphine **1.12** was transformed into (±)-multifloramine (**1.3**) in 72% yield via treatment with boron trifluoride etherate (Equation 1.3).

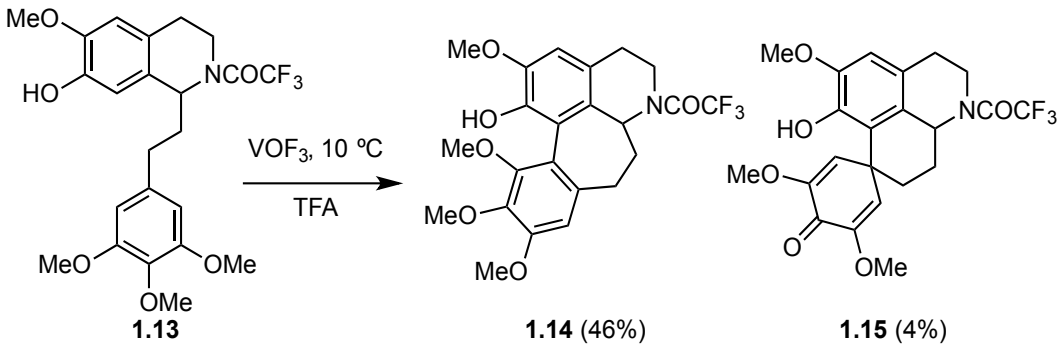

1.13 **1.14** (46%) **1.15** (4%) **(1.1)**

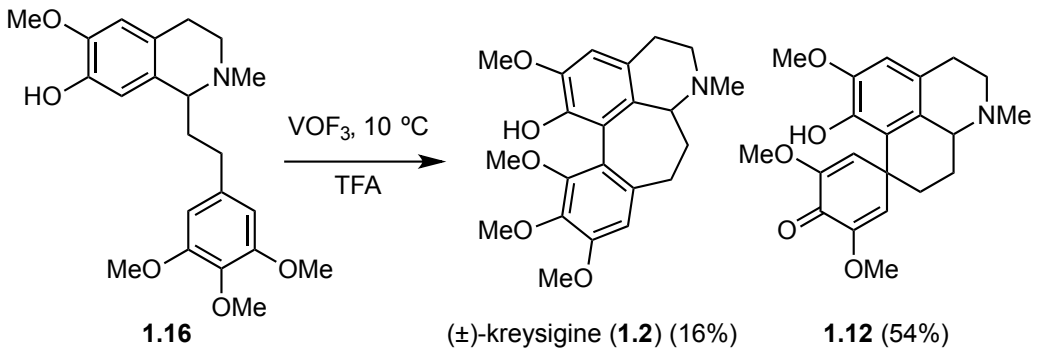

1.16 (±)-kreysigine (**1.2**) (16%) **1.12** (54%) **(1.2)**

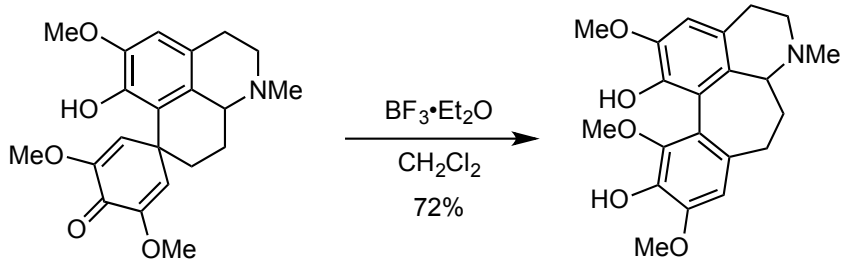

1.12 (±)-multifloramine (**1.3**) **(1.3)**

The fact that the corresponding homoproaporphines **1.15** and **1.12** were isolated in each example has rather interesting mechanistic implications. Given the acidic reaction

conditions, it is reasonable that the formation of (±)-kreysigine (**1.2**) and **1.14** could arise through a homoproaporphine-type intermediate **1.17** (Scheme 1.4). However, dienone-phenol rearrangement of the isolated homoproaporphines **1.15** and **1.12** would lead to the corresponding (±)-multifloramine analogues, instead of the isolated (±)-kreysigine derivatives **1.14** and **1.2**. For this reason, Kupchan proposed that oxidation of the starting material yields homoproaporphine-type intermediate **1.17**. This homoproaporphine-type intermediate could then undergo a dienone-phenol rearrangement to give the (±)-kreysigine compounds **1.14** and **1.2** (Path A, Scheme 1.4) or hydrolyze to the corresponding homoproaporphines **1.15** and **1.12** upon aqueous work-up (Path B, Scheme 1.4).

Scheme 1.4. Proposed mechanistic rationale for observed homoproaporphine and homoaporphine products

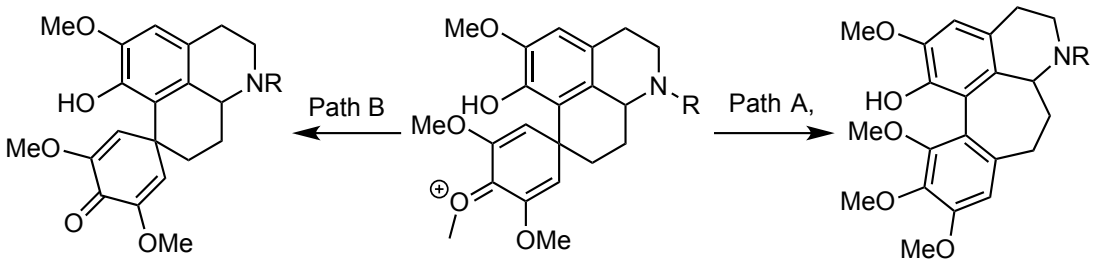

1.15: R = $COCF_3$
1.12: R = Me

1.17

1.14: R = $COCF_3$
1.2: R = Me

In these reports, the syntheses of **1.13** and **1.16** were merely commented upon. The authors state that **1.13** and **1.16** were synthesized according to "standard methods".[11] These methods include the condensation of substituted phenethylamine **1.18** and

phenylpropionic acid **1.19**, followed by Bischler-Napieralski cyclization and sodium borohydride reduction to give the corresponding phenethylisoquinoline **1.21** (Scheme 1.5). Compound **1.21** was either treated with trifluoroacetic anhydride or formaldehyde and sodium cyanoborohydride, followed by hydrogenolysis to give substrates **1.13** or **1.16**, respectively.

Scheme 1.5. General methods used to synthesize phenethylisoquinolines **1.13** and **1.16**

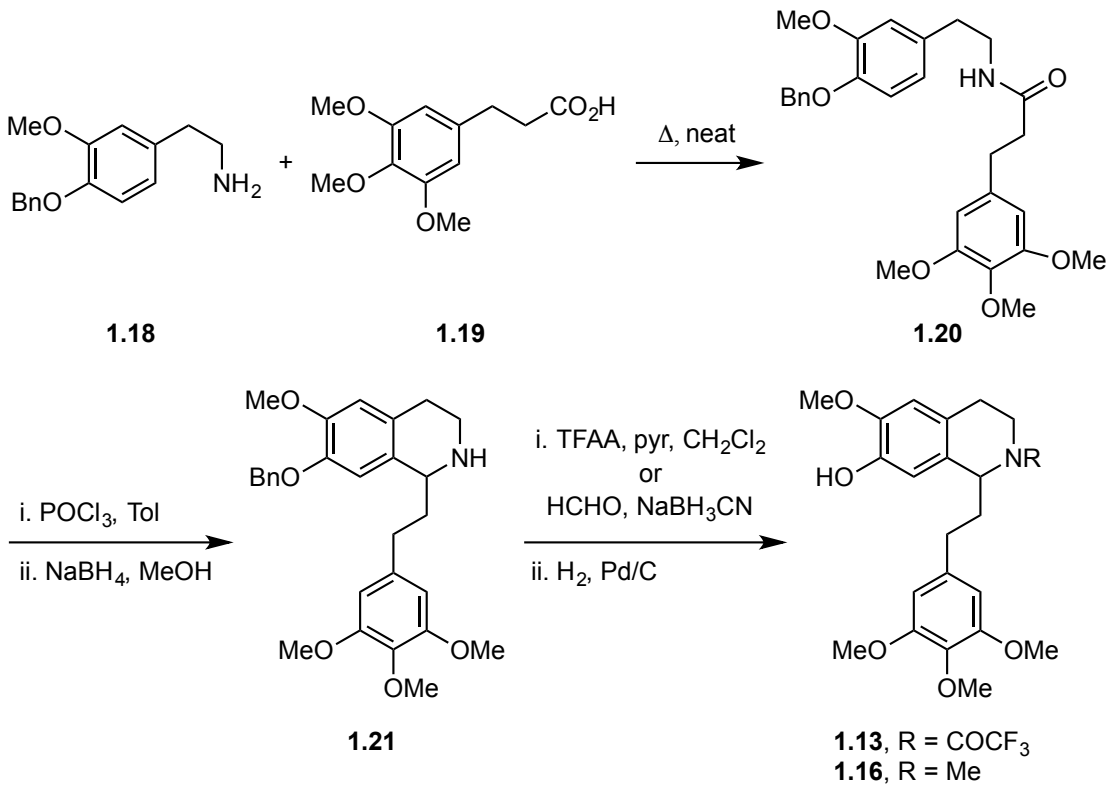

To summarize, Kupchan synthesized (±)-kreysigine (**1.2**) and (±)-multifloramine (**1.3**) in 16% and 39% yield, respectively, from **1.16**. While the overall yield cannot be

determined, (±)-kreysigine (**1.2**) and (±)-multifloramine (**1.3**) were synthesized in a total of six- and seven-steps, respectively.

1.3.1.3. Thallium(III) Trifluoroacetate (TTFA) Oxidative Nonphenolic Coupling

In the early 1980s, it was found that thallium (III) trifluoroacetate (TTFA) could effect an oxidative nonphenolic coupling. As shown in Equation 1.4, this reagent, in conjunction with catalytic boron trifluoride, was used rather elegantly to effect the oxidative coupling of benzyloxy-phenethylisoquinoline **1.22** to yield (±)-kreysigine (**1.2**) directly in 40% yield.[12]

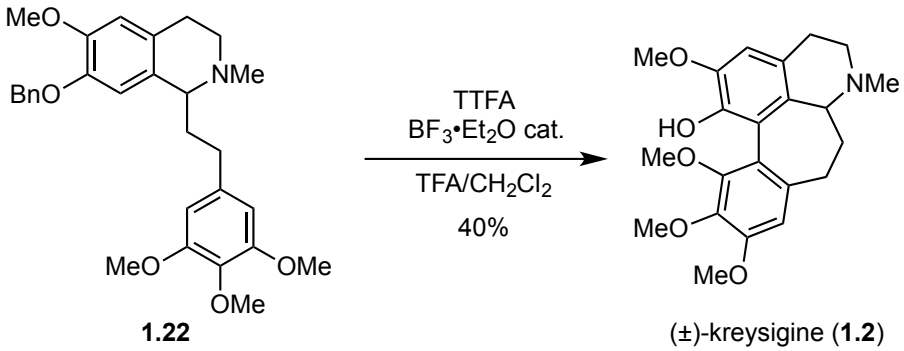

1.22 (±)-kreysigine (**1.2**) **(1.4)**

In a rather stark contrast to the previous example, when the bisbenzyloxy compound **1.23** was treated with TTFA, the oxidation occurred extremely rapidly (ca. three minutes for **1.23** vs. 28 hours for **1.22**). However, in this case, the monobenzyloxy-homoproaporphine **1.24** was isolated in 70% yield (Scheme 1.6). Tandem debenzylation and dienone-phenol rearrangement proceeded smoothly in concentrated sulfuric acid to give (±)-multifloramine (**1.3**) in 81% yield.[12]

Scheme 1.6. Synthesis of (±)-multifloramine (**1.3**) via thallium induced oxidative nonphenolic coupling

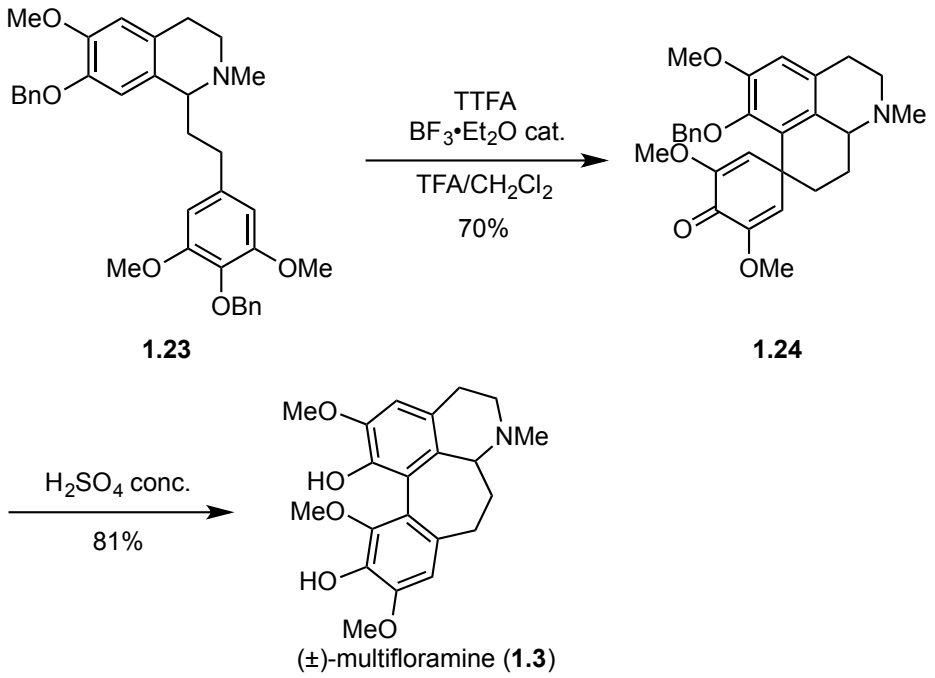

Synthesis of substrates **1.22** and **1.23** were reported to proceed via condensation of the requisite benzyloxy-phenethylamine and phenyl-3-propionic acid, followed by Bischler-Napieralski cyclization, methylation, and sodium borohydride reduction. The yields for these specific substrates were not given, thus an overall yield for these syntheses cannot be determined. In total, (±)-kreysigine (**1.2**) and (±)-multifloramine (**1.3**) were synthesized in at least five- and six-steps, respectively. The use of strong acids in these reactions to give tandem debenzylation ultimately limits the number of synthetic manipulations required in these syntheses.

1.3.1.4. Umezawa: p-Quinol Acetate Intermediates

One of the more unique approaches undertaken in the 1970's towards the synthesis of homoaporphine alkaloids, was Umezawa's use of the intermediate *p*-quinol acetates.[13–17] In these studies, he found that treatment of phenolic compounds with lead (IV) tetraacetate oxidized the phenol, and upon nucleophilic capture by acetic acid, formed the *p*-quinol acetate. When treated with strong acid, these intermediates underwent an electrophilic aromatic substitution reaction to give the resultant aporphine or homoaporphine.

Umezawa utilized this strategy in the total synthesis of (±)-kreysigine (**1.2**) (Scheme 1.7).[18,19] The phenethylisoquinoline **1.16** was constructed through standard conditions. Heating of phenethylamine **1.18** with propionic acid **1.19** gave amide **1.20** in 88% yield. Bischler-Napieralski cyclization of **1.20** afforded the dihydroisoquinoline **1.25** in 77% yield. The three-step sequence of methylation, reduction, and hydrogenolysis proceeded in 88% to give the phenethylisoquinoline **1.16**. Treatment of **1.16** with lead (IV) tetraacetate led to a brown amorphous substance that was "undoubtedly" the *p*-quinol acetate **1.26**, as characterized by IR.[18] Immediate treatment with concentrated sulfuric acid in acetic anhydride led to the formation of *O*-acetylkreysigine (**1.27**) in 18% yield. Finally, hydrolysis via hydrochloric acid gave (±)-kreysigine (**1.2**) in 56% yield.

Scheme 1.7. Umezawa's total synthesis of (±)-kreysigine (**1.2**)

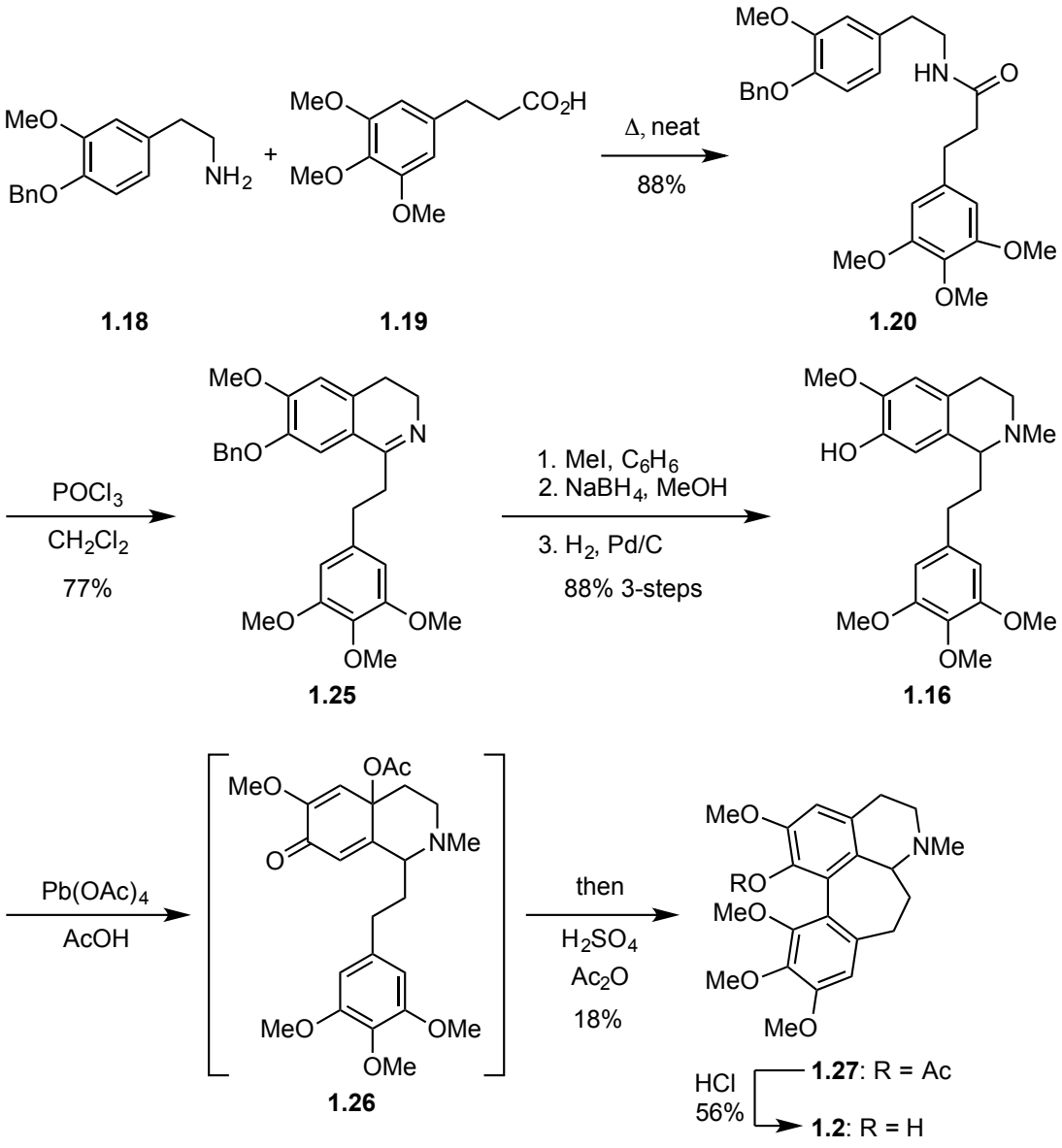

In a similar sequence, Umezawa synthesized (±)-multifloramine (**1.3**) utilizing another *p*-quinol acetate (Scheme 1.8).[20] In this synthesis, condensation of phenethylamine **1.28** and propionic acid **1.29** gave amide **1.30** in 59% yield. Subsequent

Bischler-Napieralski cyclization, reduction, and reductive amination led to the formation of isoquinoline **1.31** in 44% yield over three steps. Treatment of **1.31** with lead (IV) tetraacetate, followed by addition of trifluoroacetic acid led to the formation of benzylmultifloramine **1.32** in 27% yield. Finally, hydrogenolysis of the benzyl ether afforded (±)-multifloramine (**1.3**) in 87% yield.

Scheme 1.8. Umezawa's total synthesis of (±)-multifloramine (**1.3**)

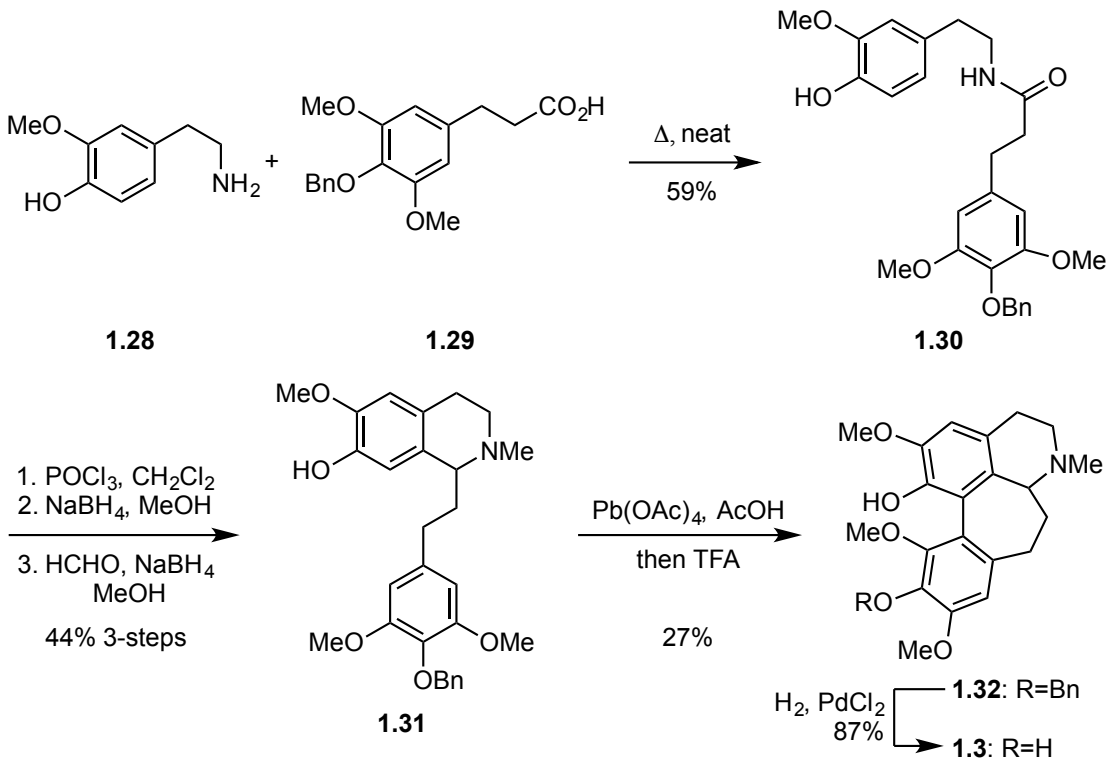

In these syntheses, Umezawa developed a strategy to effect an oxidative phenolic coupling by oxidizing the phenol into a suitable electrophile for an acid-catalyzed electrophilic aromatic substitution reaction. The yields of this key step were quite low

and the use of highly toxic lead (IV) tetracetate is far from ideal. Nonetheless, Umezawa was able to synthesize (±)-kreysigine (**1.2**) and (±)-multifloramine (**1.3**) in seven- and six-steps, respectively, with a 6% overall yield for both compounds.

1.3.2. Dehydroaporphine Ring Homologation Strategy

To date there is only a single strategy towards the synthesis of homoaporphine alkaloids that does not involve the late stage formation of the biaryl bond. Unfortunately, this synthesis started from the corresponding dehydroaporphine, which is a non-trivial starting material to synthesize. In this strategy, ring homologation was achieved through reduction of the dichlorocyclopropane, which resulted from the treatment of dehydroaporphines with dichlorocarbene.[21,22]

Scheme 1.9. Synthesis of unnatural homoaporphine **1.36** via *C*-ring homologation

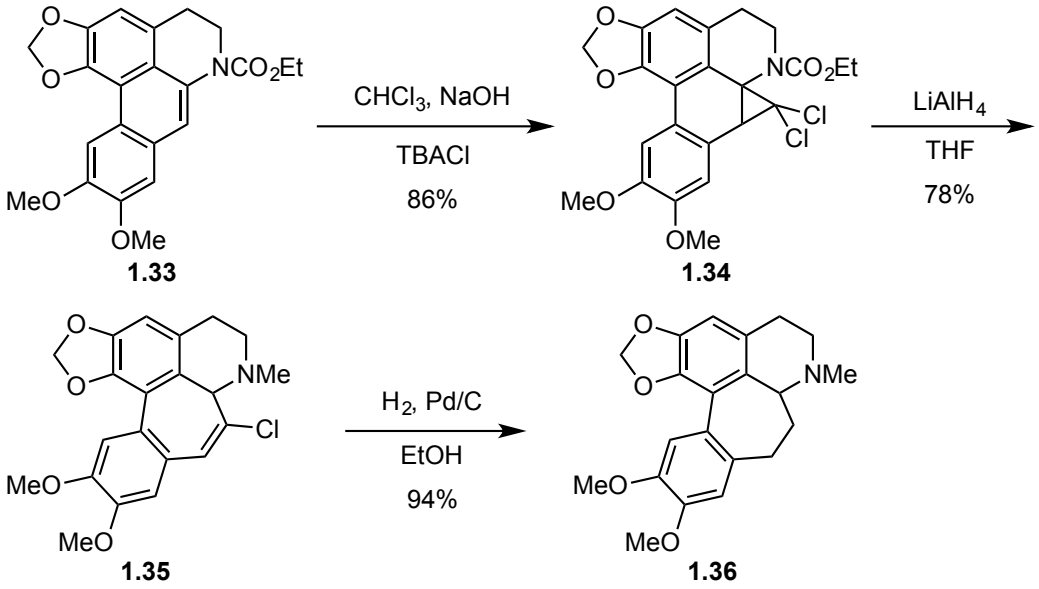

In one example, the dehydroaporphine **1.33** was treated with base in chloroform under phase transfer conditions to give the dichlorocyclopropane **1.34** in 86% yield (Scheme 1.9). Lithium aluminum hydride reduction of **1.34** led to ring homologation and concomitant reduction of the ethyl carbamate to form **1.35** in 78% yield. Finally, reduction of vinyl chloride **1.35** via hydrogenation gave the unnatural homoaporphine **1.36** in 94% yield. Even though this method formed the homoaporphine in just three steps, with an overall yield of 63%, the major drawback was that the starting material is not readily available. The authors do not comment on the synthesis of the starting dehydroaporphines. [21,22]

1.3.3. Direct Arylation Strategies

This section will review synthetic strategies in which the key step was a direct arylation reaction. This differs from the oxidative phenolic coupling strategies, in that this strategy requires functionalization of one of the aromatic moieties. Consequently, the formation of the biaryl bond is a redox neutral operation. This strategy, and thus the following examples, effectively span the chronology of homoaporphine syntheses from some of the oldest examples, to the most recently reported synthesis of homoaporphine alkaloids.

1.3.3.1. Kametani: Photocyclization and Photo-Pschorr Reaction

Throughout the late 1960's and into the early 1970's, Kametani was considered a pioneer in the synthesis of homoaporphine and related alkaloids. At the onset of his studies, Kametani focused a significant amount of effort to understanding the effects of substrate substitution patterns on the oxidative phenolic coupling.[23,24] Much of this work overlaps with that of Battersby, which has been previously described and is not subject to this discussion. Kametani also put significant effort into understanding the stereochemical bias of the dienone- and dienol-phenol rearrangements.[25–27] Additionally, he was able to resolve the enantiomers of a number of synthetic samples to verify the stereochemical assignments of the respective natural homoaporphine alkaloids.[28,29] Further studies into the synthesis of homoaporphine and related alkaloids led to the use of the photo-Pschorr and photolytic-cyclization reactions.[30,31]

Scheme 1.10. Total synthesis of (±)-multifloramine (**1.3**) via photolytic-cyclization

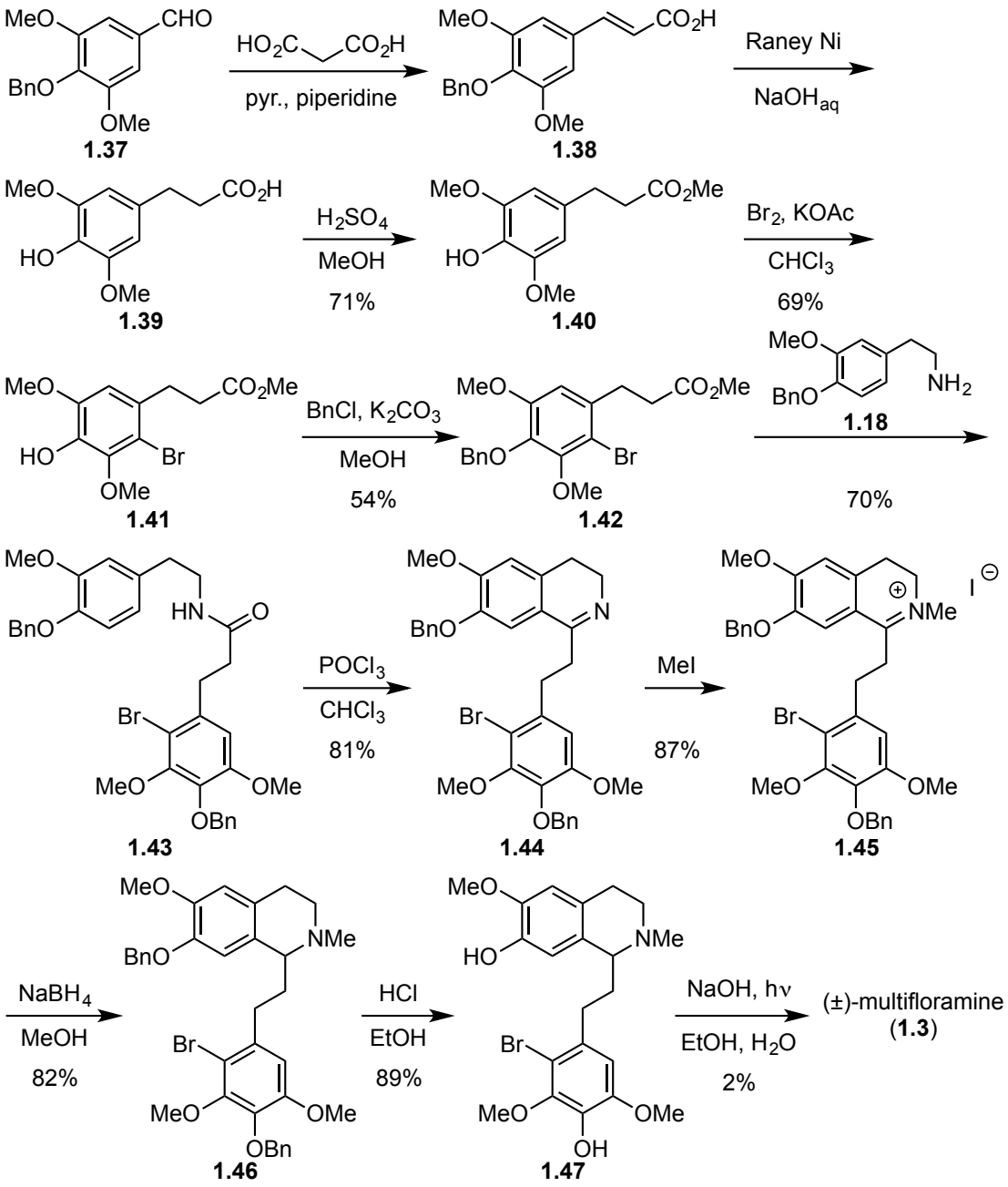

Utilizing this direct arylation strategy via photolytic cyclization from the tetrahydroisoquinoline **1.47**, (±)-multifloramine (**1.3**) was isolated in very poor 2% yield (Scheme 1.10).[32] Even though the synthesis was inefficient, historically it marked the first synthetic route to a homoaporphine alkaloid by direct coupling of two biaryl moieties, negating the formation of the corresponding homoproaporphine. The synthesis started from phenylpropionic acid **1.39**, which was synthesized in a previous study via condensation of malonic acid and **1.37** followed by reduction with Raney nickel to give **1.39**. Carboxylic acid **1.39** was esterified to the methyl ester **1.40** in 71% yield. Bromination of **1.40** and subsequent formation of the benzyl ether proceeded in 69% and 54% yields, respectively, to give ester **1.42**. Heating a neat mixture of **1.42** and **1.18** afforded amide **1.43** in 70% yield. Bischler-Napieralski cyclization gave the dihydroisoquinoline **1.44** in 81% yield. Dissolving **1.44** in neat iodomethane followed by reduction with sodium borohydride proceeded in 87% and 82% yields, respectively, to give the tetrahydroisoquinoline **1.46**. Finally, benzyl deprotection by heating in concentrated hydrochloric acid and ethanol gave the photocyclization precursor **1.47** in 89% yield. Photolytic cyclization occurred upon irradiation of **1.47** in an alkaline solution of ethanol and water. Despite the fact that 1.9 g of crude material (84% mass balance) was recovered, only 34 mg of (±)-multifloramine (**1.3**) was isolated upon chromatography.

In two related syntheses, Kametani synthesized (±)-kreysigine (**1.2**) via a photolytic cyclization and by a photo-Pschorr reaction. The tetrahydroisoquinoline **1.48**

was synthesized in an analogous fashion to **1.47**. The photolytic cyclization of **1.48** yielded only 3% of pure (±)-kreysigine (**1.2**) (Equation 1.5).[33] In another synthesis of (±)-kreysigine (**1.2**), diazonation of **1.49** followed by irradiation with light, induced a photo-Pschorr reaction to give (±)-kreysigine (**1.2**) in 5% yield and the hydroxy compound **1.50** in 32% yield (Equation 1.6).[34] In summary, the photolytic cyclizations to afford homoaporphines were quite inefficient. The total synthesis of (±)-multifloramine (**1.3**) proceeded in 11-steps with an overall yield of less than 0.2%.

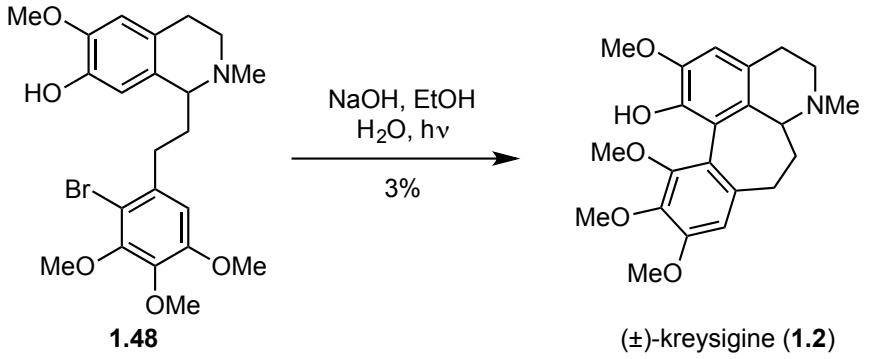

1.48 (±)-kreysigine (**1.2**) **(1.5)**

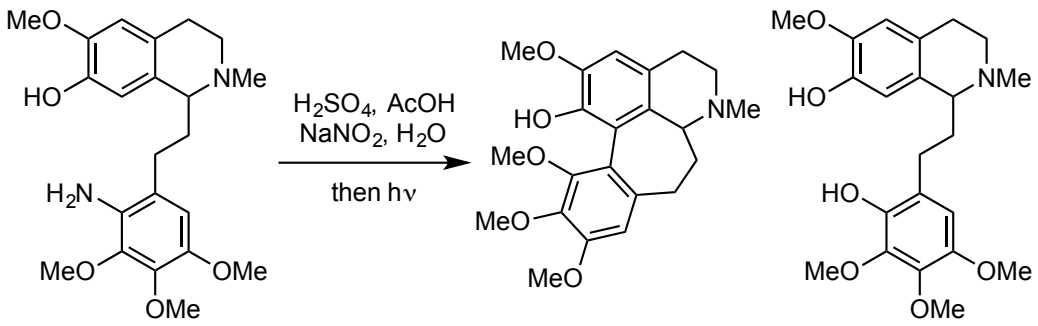

1.49 (±)-kreysigine (**1.2**) (5%) **1.50** (32%) **(1.6)**

1.3.3.2. $S_{RN}1$ Arylation

In a more recent example, the synthesis of unnatural homoaporphine **1.52** was achieved through a photostimulated radical nucleophilic substitution reaction of tetrahydroisoquinoline **1.51** (Equation 1.7). The reaction proceeded in 40% yield and was the only example of a homoaporphine-type compound to be synthesized in this report. The report did not make any comment as to how **1.51** was synthesized.[35]

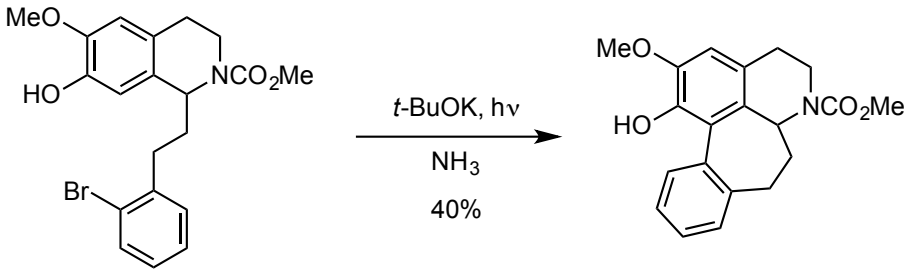

1.51 **1.52** **(1.7)**

1.3.3.3. Palladium-Catalyzed Direct Arylation

To date, the most recent synthesis of a homoaporphine alkaloid was the synthesis of (±)-homonantenine (**1.63**), which is an unnatural homoaporphine and the homologue of the naturally occurring aporphine (±)-nantenine.[36] This strategy relied on a late stage palladium-catalyzed arylation to form the key biaryl bond (Scheme 1.11). The synthesis started with the bromination of acid **1.53**, which proceeded in 87% yield, to give bromoacid **1.54**. Amide coupling of 3,4-dimethoxyphenethylamine (**1.55**) and **1.54** gave amide **1.56** in 77% yield. Bischler-Napieralski cyclization and subsequent sodium borohydride reduction led to the formation of phenethylisoquinoline **1.57** in 93% yield

over two steps. Formation of the ethyl carbamate proceeded in 92% yield to give **1.58**. Unfortunately, palladium-catalyzed direct arylation of **1.58** proved to be difficult. After optimization attempts, through screening of a number of bases, ligands, and stoichiometric ratios, the highest yield achieved for the conversion of **1.58** to carbamate protected homonantenine **1.59** was 36% yield, which was formed alongside the *des*-brominated starting material in 54% yield.

Scheme 1.11. Attempted synthesis of (±)-homonantenine (**1.63**)

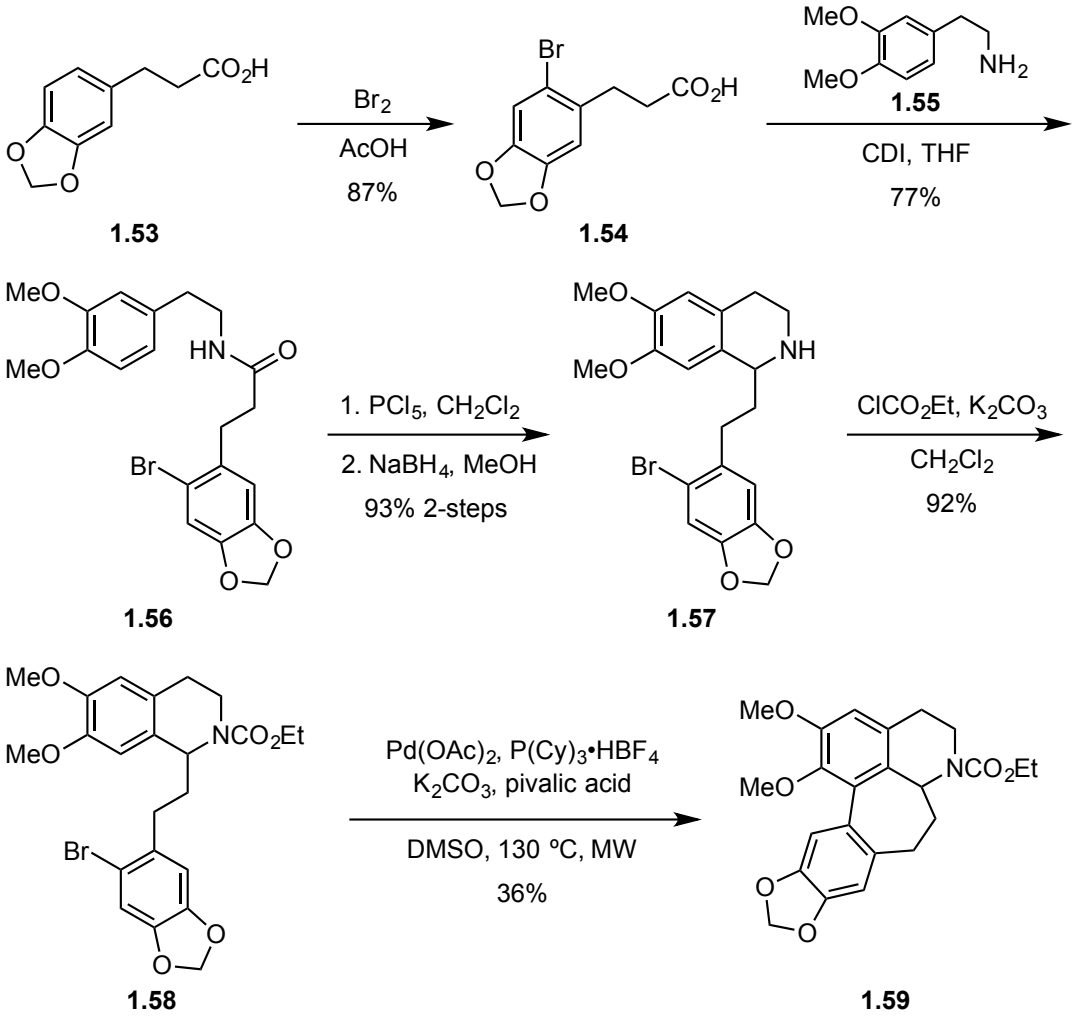

After these initial attempts, (±)-homonantenine (**1.63**) was synthesized from **1.60** in five steps (Scheme 1.12). The synthesis of **1.60** was achieved using "similar methods" to that of **1.58**, but the yields are unreported. The palladium-catalyzed arylation of **1.60** gave an inseparable mixture (~7:1) of the corresponding benzyloxyhomoaporphine (not shown) and the respective *des*-brominated starting material. It was found that arylation,

followed immediately by hydrogenolysis of the crude material, led to the isolation of homoaporphine **1.61** in 85% yield over two steps. No comment was made as to why the benzyloxy/*N*-Boc substrate **1.60** proceeded in significantly higher yield than that of **1.58**. following the arylation, *O*-methylation of **1.61** proceeded to give **1.62** in 83% yield. Finally, *N*-Boc deprotection and reductive amination of **1.62** gave (±)-homonantenine (**1.63**) in 66% yield over two steps.[36]

Scheme 1.12. Synthesis of (±)-homonantenine (**1.63**)

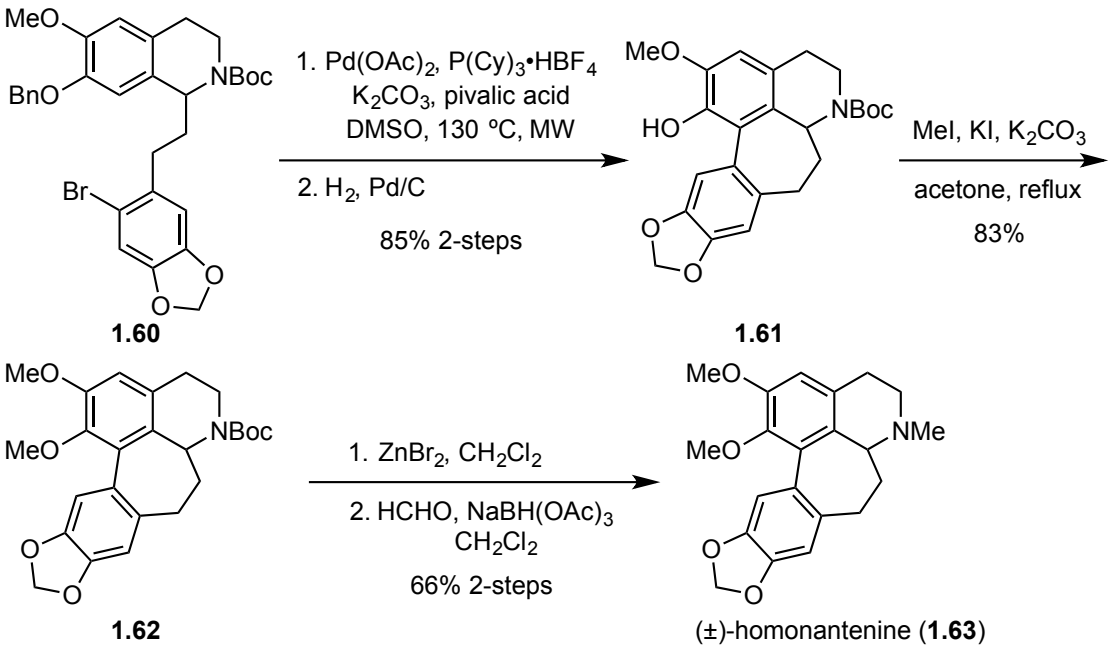

Though not explicitly stated, it appears that this direct arylation reaction was very sensitive to the aryl substitution patterns. In other examples, it was found that the substrates containing the benzyloxy or hydroxy substituent at C1 proceed in respectable yields (~70%), even when the nitrogen was protected as the ethyl carbamate. Since the

synthesis of substrate **1.60** was not given in the report or the cited references, an overall yield was not able to be determined. But using the sequence shown for substrate **1.58**, we can estimate that (±)-homonantenine (**1.63**) was synthesized in about 10-steps with an overall yield around 27%.

1.4. MAGNUS SYNTHETIC STRATEGY TOWARDS DIENONE-DERIVED ALKALOIDS

1.4.1. *para*-Phenolic *C*-Alkylation

A *p*-phenolic *C*-alkylation was first reported by Winstein and Baird in 1957. They found that heating a solution of the phenolic brosylate **1.64**, in a slight excess of potassium *tert*-butoxide, afforded the spirocyclic hexadienone **1.65** in roughly 50% yield (Equation 1.8).[37] Further mechanistic and synthetic studies have since been covered in reviews.[38]

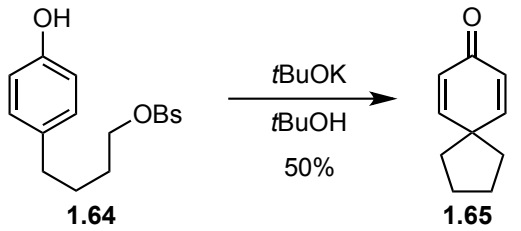

1.64 **1.65** **(1.8)**

Since the initial report, a number of terpenoid natural products have been synthesized utilizing this method. In a particularly elegant series of papers, Masamune cyclized phenol **1.66** to give dienone **1.67** in 90% yield.[39,40] Dienone **1.67** was then transformed into a divergent intermediate **1.68**, which was used to access a series of

natural products namely, garryine (**1.69**), atisine (**1.70**), and kaurene (**1.71**) (Scheme 1.13).[41–43]

Scheme 1.13. *p*-Phenolic *C*-alkylation in divergent total syntheses

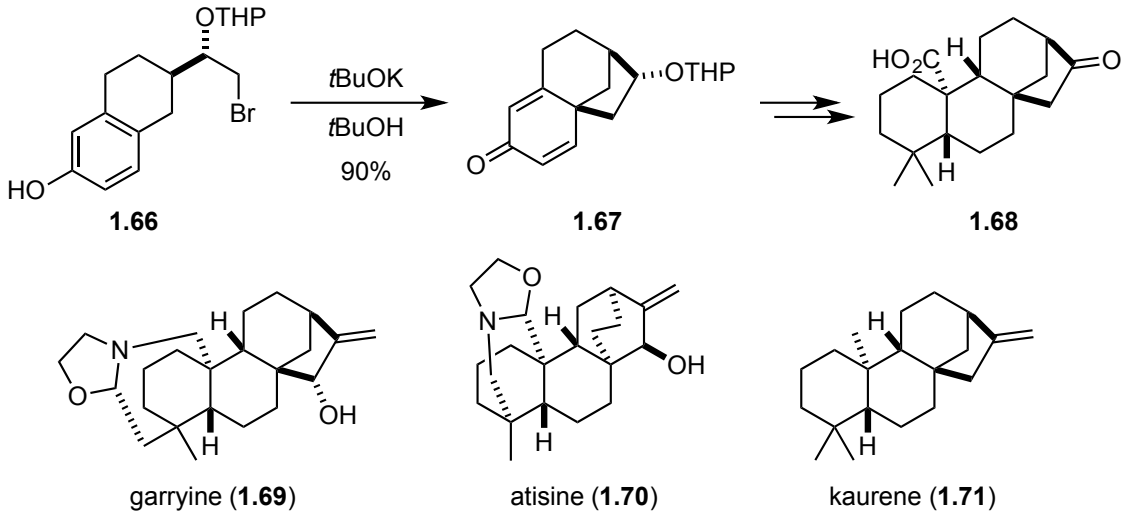

1.4.2. Previous Work in the Magnus Lab: *p*-Phenolic *C*-Alkylation

In developing new methodologies applicable towards the synthesis of complex natural products, the Magnus lab utilized the *p*-phenolic *C*-alkylation in the synthesis of (±)-narwedine (**1.74**) and (±)-codeine (**1.75**) (Scheme 1.14).[44] In this work, Magnus developed a novel synthetic strategy to ultimately effect the connectivity of the oxidative phenolic coupling, by reversing the order of bond formation. To this end, an early Suzuki cross coupling reaction established the key biaryl bond (shown in blue) of **1.72**, negating the necessity of the problematic oxidative phenolic coupling. Subsequent *p*-phenolic *C*-alkylation, which was induced via fluoride deprotection of phenolic silyl ether **1.72**, led

to the cross-conjugated cyclohexadienone **1.73** in 96% yield. This step formed the quaternary center (bond shown in red) and in-effect established the same skeletal carbon framework as the oxidative phenolic coupling, albeit in reverse order.[45,46]

Scheme 1.14. Magnus synthetic strategy to (±)-narwedine (**1.74**) and (±)-codeine (**1.75**)

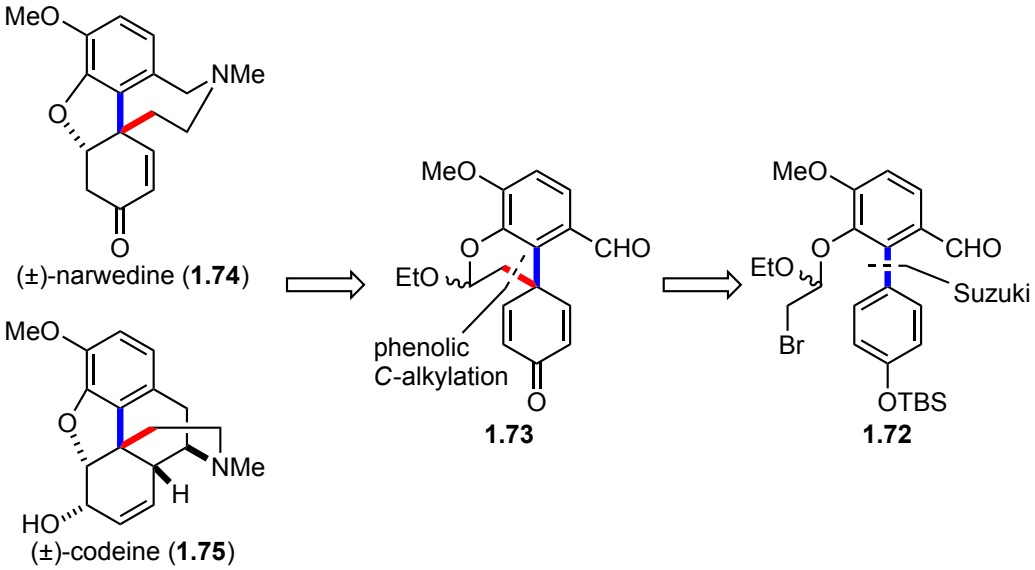

1.4.3. Magnus Total Synthesis of (±)-Narwedine and (±)-Codeine

The total synthesis of (±)-narwedine (**1.74**) and (±)-codeine (**1.75**) commenced with a Suzuki cross coupling between benzaldehyde **1.76** and the corresponding boroxime trimer, to give biaryl aldehyde **1.77** in 99% yield (Scheme 1.15). Alkylation of **1.77**, with *in situ* brominated ethylvinyl ether, led to the formation of bromoacetal **1.78** in 99% yield. The key *p*-phenolic *C*-alkylation of **1.78** proceeded smoothly to give cross-conjugated cyclohexadienone **1.73** in 96% yield. The *p*-phenolic *C*-alkylation efficiently

established the quaternary carbon in just three steps with high yields, circumventing the use of the inefficient oxidative phenolic coupling. At this point, the syntheses of (±)-narwedine (**1.74**) and (±)-codeine (**1.75**) diverge from intermediate dienone **1.73**.

Scheme 1.15. Synthesis of divergent intermediate **1.73**

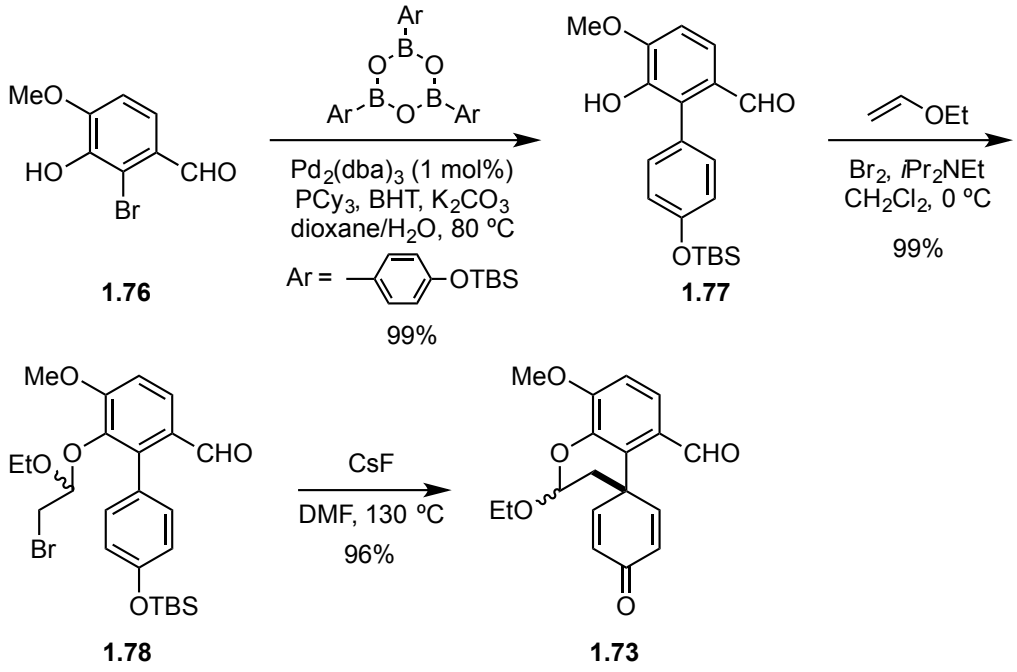

The synthesis of (±)-narwedine (**1.74**) was completed in three additional synthetic steps from intermediate **1.73**. Treatment of **1.73** with acid led to a tandem double conjugate addition and hemi-acetal formation to give **1.79** in 93% yield (Scheme 1.16). Reductive amination with methylamine hydrochloride gave the amino-boron adduct **1.80**, the structure of which was confirmed by X-ray crystallography. Finally, heating an acidic solution of **1.80** in 1,4-dioxane gave (±)-narwedine (**1.74**) in 72% yield over two steps.

Given that previous reports have shown that the treatment of (±)-narwedine (**1.74**) with L-Selectride leads to reduction and spontaneous resolution to give (-)-galanthamine (**1.81**) in near quantitative yield,[47] this study marks the formal synthesis of (-)-galanthamine (**1.81**) in eight steps with an overall yield of 63%, which is approximately five-fold greater yield than the current commercial process.[48–50]

Scheme 1.16. Total synthesis of (±)-narwedine (**1.74**) and formal synthesis of (-)-galanthamine (**1.81**)

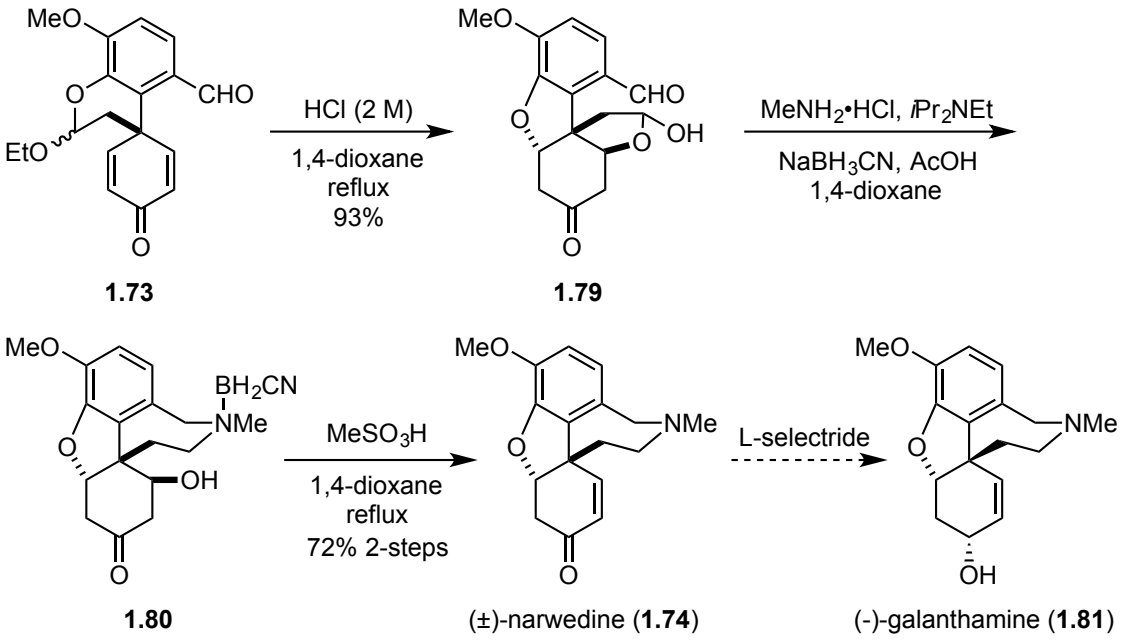

Upon completion of the total synthesis of (±)-narwedine (**1.74**), hexadienone **1.73** was then transformed into (±)-codeine (**1.75**). A Henry reaction of **1.73** led to the formation of cyclized nitrostyrene **1.82** in 97% yield (Scheme 1.17). Selective conjugate reduction of **1.82**, via treatment with acetic acid and sodium cyanoborohydride, gave **1.83**

in 88% yield. Exposure of **1.83** to lithium aluminum hydride afforded 1,2-reduction of the enone to give allylic alcohol **1.84** in 72% yield. Upon opening of the cyclic acetal with acid, **1.84** underwent a tandem conjugate substitution and intramolecular reductive amination to give **1.85** in 66% yield, which contains the carbon skeleton of (±)-codeine (**1.75**). Finally, protecting the amine as the ethyl carbamate formed **1.86** in 90% yield.

Scheme 1.17. Synthesis of the carbon skeleton of (±)-codeine (**1.75**)

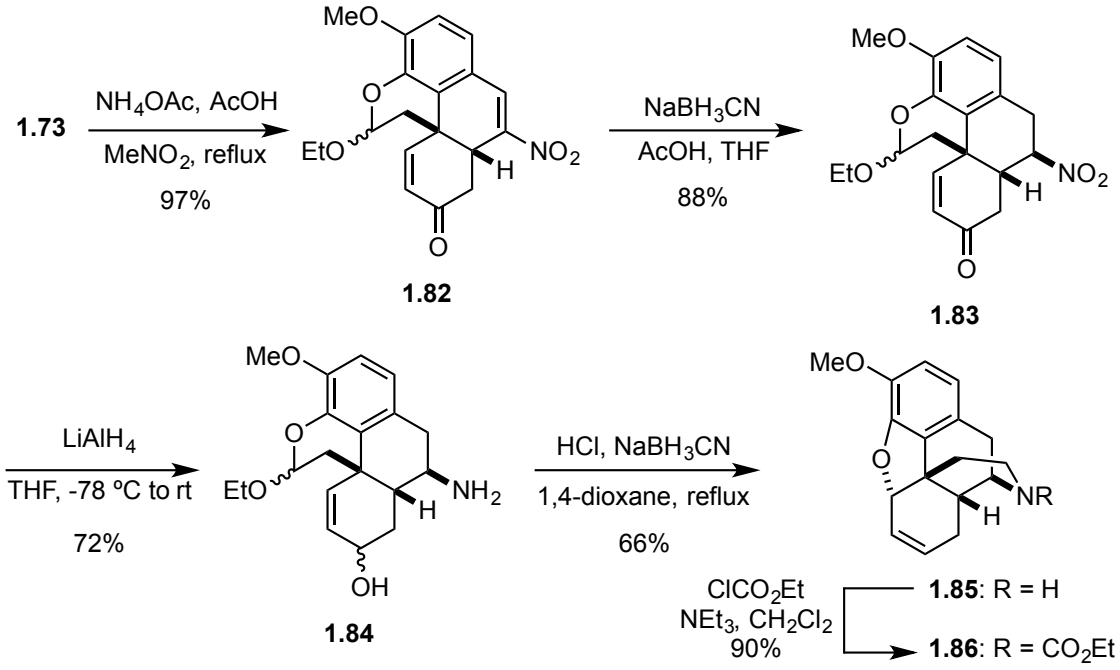

In the final sequence of the synthesis, it was found that conditions for direct epoxidation of the olefin in **1.86** consistently led to epoxide formation on the undesired β-face. Fortunately, upon forming the halohydrin **1.87**, by reacting **1.86** with 5,5-dimethyl-1,3-dibromohydantoin, exposure of **1.87** to base gave the desired epoxide **1.88**

in 91% over two steps (Scheme 1.18). Nucleophilic epoxide opening of **1.88** with sodium benzenethiolate gave sulfide **1.89** in nearly quantitative yield. Oxidation and subsequent sulfoxide elimination gave the desired allylic alcohol **1.91** in 76% yield over two steps. Finally, concomitant reduction of the ethyl carbamate and aryl bromide of **1.91** gave (±)-codeine (**1.75**) in 87% yield. In this study, (±)-codeine (**1.75**) was synthesized in a total of 13-steps with an overall yield of 20%.

Scheme 1.18. Total synthesis of (±)-codeine (**1.75**)

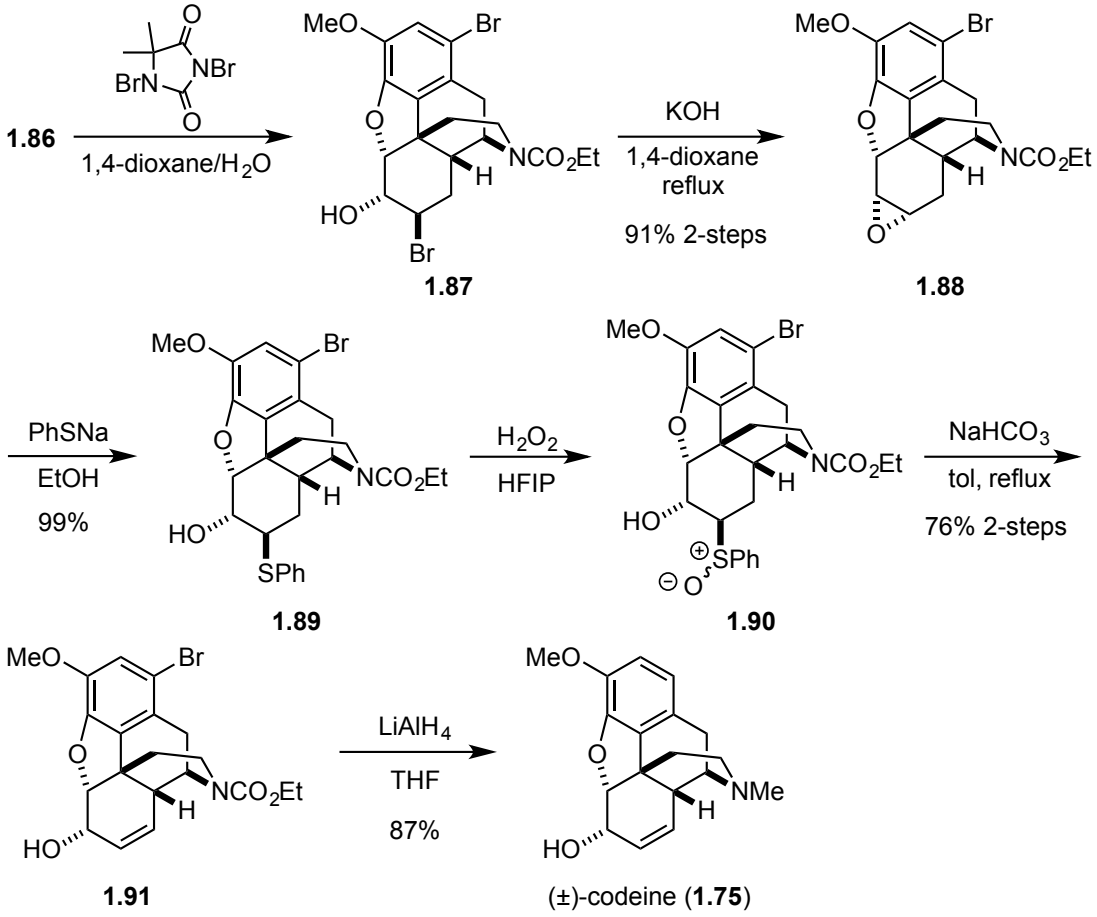

1.4.4. Magnus Total Synthesis of (±)-Cepharatine A

Scheme 1.19. Total synthesis of (±)-cepharatine A (**1.96**)

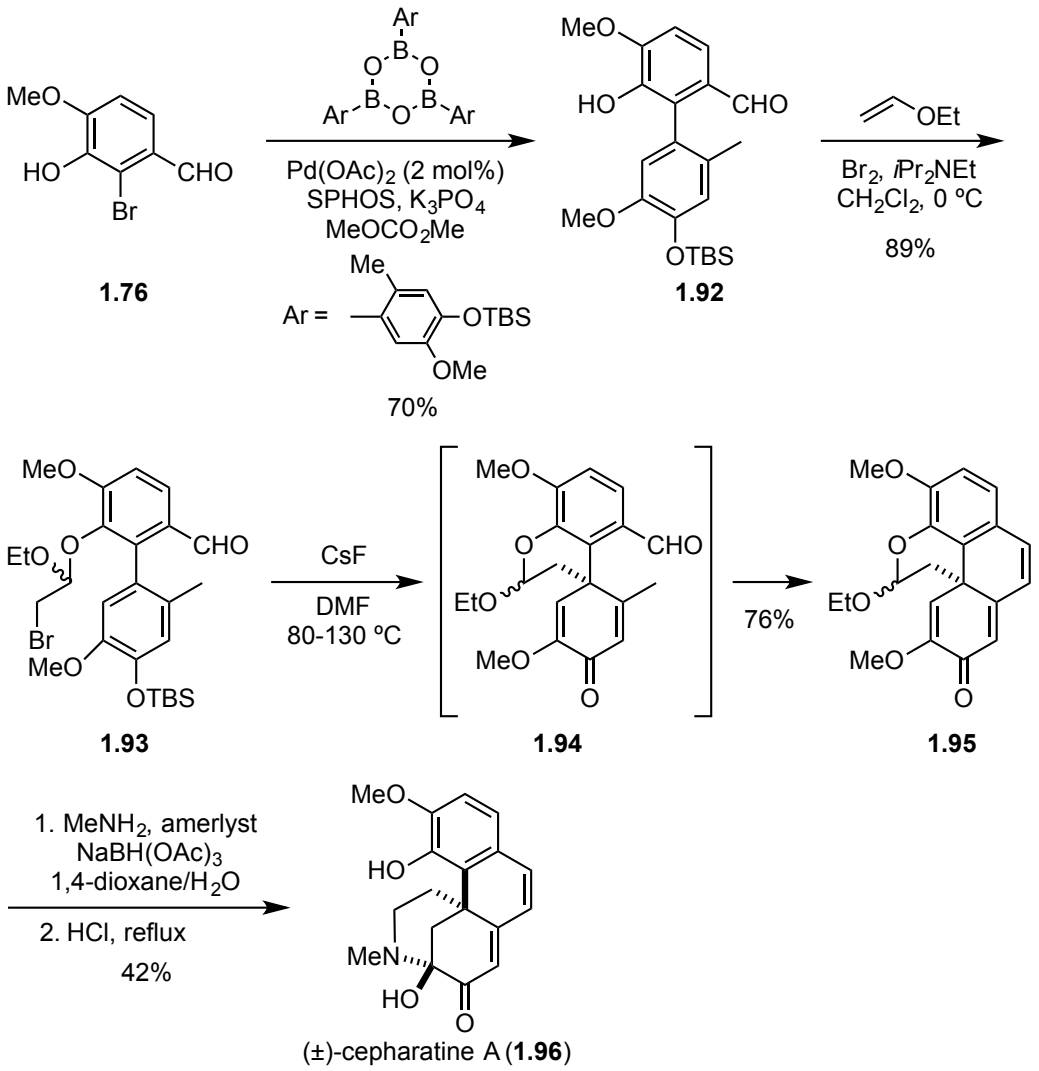

In a particularly elegant application of this synthetic strategy, the total synthesis of hasubanan alkaloid (±)-cepharatine A was completed in seven steps with a 16% overall yield (Scheme 1.19). The synthesis started with the Suzuki cross coupling of

benzaldehyde **1.76** and the corresponding boroxime trimer to give biaryl aldehyde **1.92** in 70% yield. Alkylation of **1.92** with *in situ* brominated ethylvinyl ether gave **1.93** in 89% yield. The key *p*-phenolic *C*-alkylation of **1.93** proceeded to give the corresponding cyclohexadienone **1.94**, which spontaneously underwent an intramolecular vinylogous aldol reaction to give cyclohexadienone **1.95** in 76% yield. Finally, a two-step procedure afforded reductive amination, vinyl ether hydrolysis, and addition of the resulting amine to give the title compound, (±)-cepharatine A (**1.96**), in 42% yield.

1.4.5. Summary of the Magnus Synthetic Strategy

Figure 1.2. Natural products accessed via the Magnus synthetic strategy

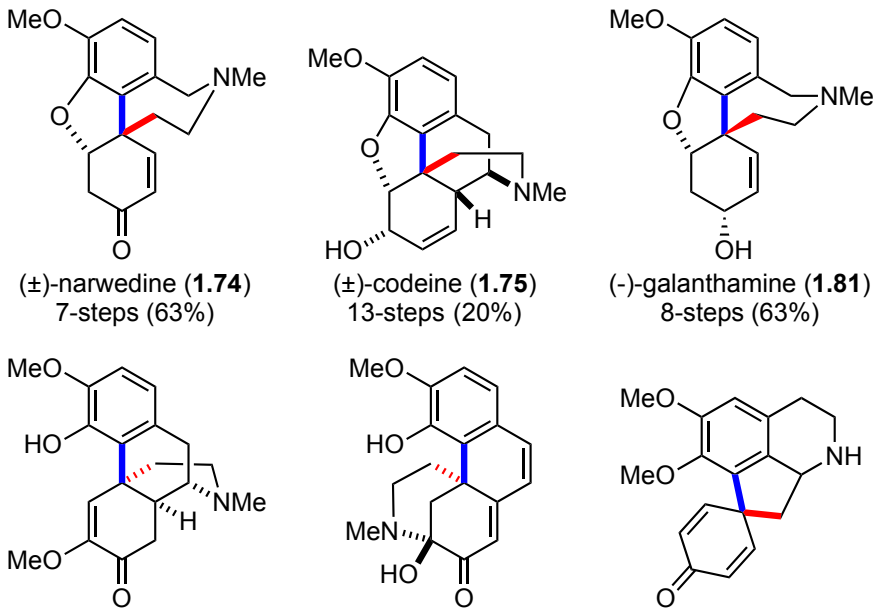

The utility of this synthetic strategy has been demonstrated through the efficient syntheses of multiple natural products, shown in Figure 1.2. As previously mentioned, (±)-narwedine (**1.74**) and (±)-codeine (**1.75**) were synthesized in seven-steps (63% overall yield) and 13-steps (20% overall yield), respectively.[44] In a related synthesis, 8,14-dihydromorphinandienone isosinomenine (**1.97**) was synthesized in 10-steps, 17% overall yield.[51] This synthetic strategy was also shown to be effective in the concise total synthesis of hasubanan alkaloids, culminating the total synthesis of (±)-cepharatine A (**1.96**) in seven-steps, 16% overall yield.[52] Finally, it is worth noting, that in the time since the following research was conducted, the synthesis of proaporphine alkaloid (±)-stepharine (**1.98**) was completed in eight steps and 29% overall yield.[53]

Though the previous syntheses nicely demonstrated the utility of the *p*-phenolic - *C*-alkylation towards the synthesis of morphinan and hasubanan alkaloids, this strategy has yet to be demonstrated on substrates with a nitrogen-containing substrate. Historically, this reaction found utility in the synthesis of terpene natural products, which inherently lack a nitrogen substituent. The recent Magnus syntheses performed the *p*-phenolic *C*-alkylation on substrates without a nitrogen atom, and subsequently introduced the nitrogen atom later in the syntheses. To truly create a generalizable and useful method towards the synthesis of alkaloid natural products, these potential shortcomings must be addressed. In addressing these current problems with the dienone synthetic strategy, we undertook studies towards the total synthesis of homoproaporphine and homoaporphine alkaloids.

Chapter 2: Total Synthesis of Homoaporphine-Type Alkaloids

2.1. Homoaporphine Synthetic Targets

The synthetic strategy discussed in the preceding chapter, in which the biomimetic oxidative phenolic coupling is circumvented through a Suzuki cross coupling and subsequent *p*-phenolic *C*-alkylation, has yet to be reported on a substrate with a nitrogen-atom. The goal of this work was to address this shortcoming and to expand the structural motifs accessible with this methodology, through the total synthesis of homoaporphine alkaloids containing a nitrogen substituent during the key *p*-phenolic *C*-alkylation. At the onset of the project, we planned to synthesize **2.1**, an unnatural homoaporphine with a simplified aryl substitution pattern, as a model system and proof of principle that this strategy is applicable for the synthesis of these alkaloids (Figure 2.1). Upon establishing the underlying efficacy of this methodology through the synthesis of **2.1**, subsequent studies will focus on synthesizing homoaporphine natural products that mapped onto our route namely, (±)-kreysigine (**2.2**) and (±)-multifloramine (**2.3**). By changing the aryl substitution patterns of the given starting materials, we will be able to access the corresponding natural homoaporphines alkaloids in an analogous sequence to that for **2.1**. However, due to the unexpected retirement of Dr. P. Magnus, the syntheses of (±)-kreysigine (**2.2**) and (±)-multifloramine (**2.3**) were unable to be attempted.

Figure 2.1. Homoaporphine model system (**2.1**) and target homoaporphine natural products (±)-kreysigine (**2.2**) and (±)-multifloramine (**2.3**)

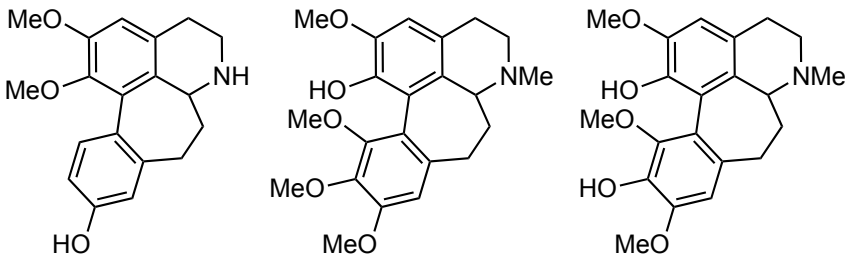

2.1 (±)-kreysigine (**2.2**) (±)-multifloramine (**2.3**)

2.2. RETROSYNTHETIC ANALYSIS

The retrosynthetic analysis of homoaporphine model system **2.1** is shown in Scheme 2.1. We intended to synthesize **2.1** via an acid-catalyzed dienone-phenol rearrangement from homoproaporphine **2.4**. We envisioned homoproaporphine **2.4** arising from the *p*-phenolic *C*-alkylation of phenethylisoquinoline **2.5**. For this key step, we were unsure if the 6-*exo*-tet cyclization (favored by Baldwin's rules[54,55]) would occur readily. For that reason, we anticipated the identity of both the nitrogen substituent (-R) and the leaving group (-X) would play a significant role in the efficiency of this transformation. Nonetheless, we planned to synthesize **2.5** in a classical manner, upon condensation of **2.6** with the appropriate aldehyde, Pictet-Spengler cyclization would yield **2.5**. After a Henry reaction of biaryl aldehyde **2.7**, phenethylamine **2.6** would arise from a reduction of the resulting β-nitrostyrene. Finally, biaryl aldehyde **2.7** would come from a Suzuki cross coupling of commercially available 5-bromoveratraldehyde (**2.8**) and the corresponding boronic acid.

Scheme 2.1. Retrosynthetic analysis of homoaporphine model system **2.1**

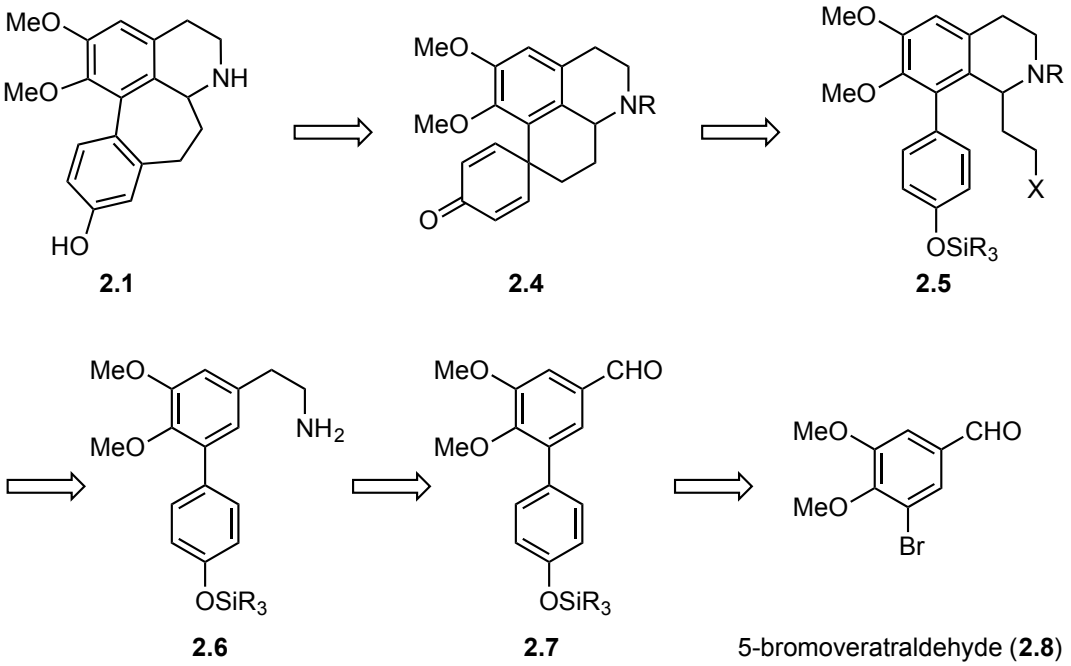

2.3. SYNTHESIS OF 5-BROMOVERATRALDEHYDE

Although 5-bromoveratraldehyde (**2.8**) is commercially available, this compound can be synthesized on large scale from vanillin (**2.9**), which is significantly cheaper (5-bromoveratraldehyde: $51/g vs. vanillin $0.02/g, Sigma-Aldrich, as of the time of this writing). In a very straightforward procedure, vanillin (**2.9**) was allowed to react with bromine in acetic acid to give crude 5-bromovanillin. Upon exposure of the crude material to iodomethane, 5-bromoveratraldehyde (**2.8**) was obtained in 81% yield over two steps (Equation 2.1).

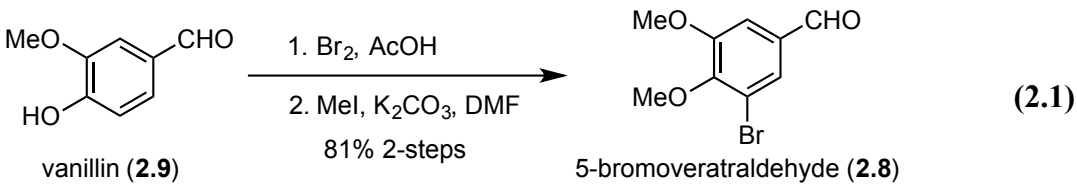

vanillin (**2.9**) 5-bromoveratraldehyde (**2.8**) **(2.1)**

2.4. SYNTHESIS OF β-NITROSTYRENE

With 5-bromoveratraldehyde (**2.8**) in hand, we focused our attention towards the synthesis of the boroxime coupling partner **2.12**. 4-Bromophenol (**2.10**) was protected as the *tert*-butyldimethylsilyl ether **2.11** in 92% yield (Scheme 2.2). Based on previous work in the Magnus lab, silyl ether **2.11** was treated successively with *n*-butyllithium, triisopropyl borate, and azeotropically dehydrated with toluene to give boroxime **2.12** in 81% yield.

Scheme 2.2. Synthesis of Suzuki coupling partner **2.12**

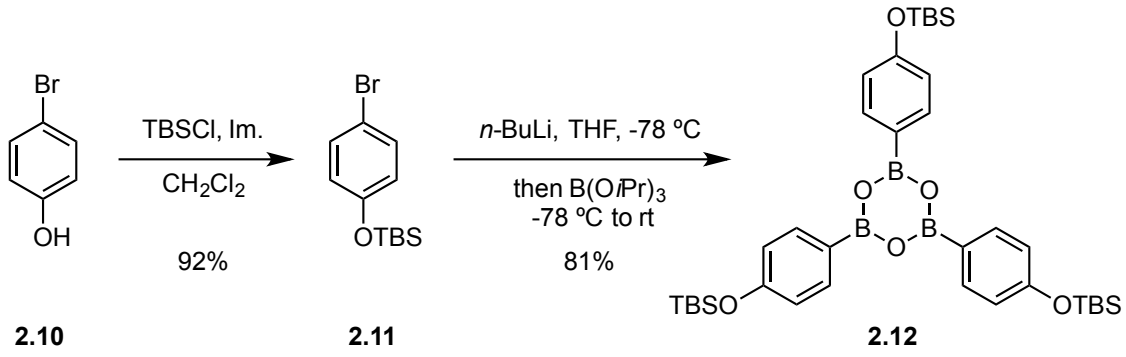

2.10 **2.11** **2.12**

We next attempted the Suzuki cross coupling of **2.8** and **2.12**. The initial set of conditions used for the Suzuki cross coupling were based on previous results within the Magnus lab.[56] To our delight, these conditions efficiently formed the biarylaldehyde **2.13**

in 96% yield (Scheme 2.3). Following the Suzuki cross coupling, **2.13** was subjected to a Henry reaction by heating in nitromethane in the presence of catalytic ammonium acetate to give β-nitrostyrene **2.14** in 77% yield.

Scheme 2.3. Synthesis of β-nitrostyrene **2.14**

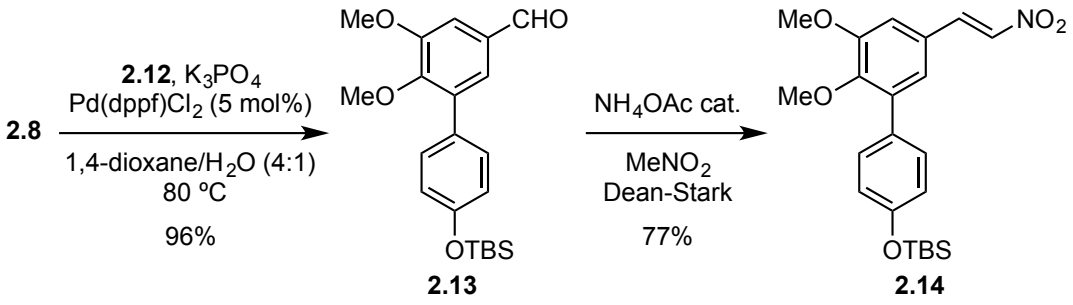

2.5. β-NITROSTYRENE REDUCTION: PART I.

Following the Henry reaction, reduction of **2.14** to the corresponding phenethylamine **2.15**, was surprisingly difficult (Equation 2.2). A wide range of conditions were attempted and ultimately failed to give satisfactory yields of **2.15**. We first attempted to reduce **2.15** using lithium aluminum hydride in THF under reflux.[57] While this method successfully reduced the β-nitrostyrene moiety, we also observed concomitant loss of the phenolic-TBS group. Additional attempts utilizing previously reported conditions including, borane with catalytic sodium borohydride,[58] superhydride,[58] and lithium borohydride with chlorotrimethylsilane[59] all gave intractable mixtures of unknown byproducts. On small scale, we found that hydrogenation with catalytic palladium on carbon in the presence of hydrochloric acid yielded primarily

2.15.[60] However, all attempts to perform this reaction on larger scale led to loss of the phenolic-TBS group.

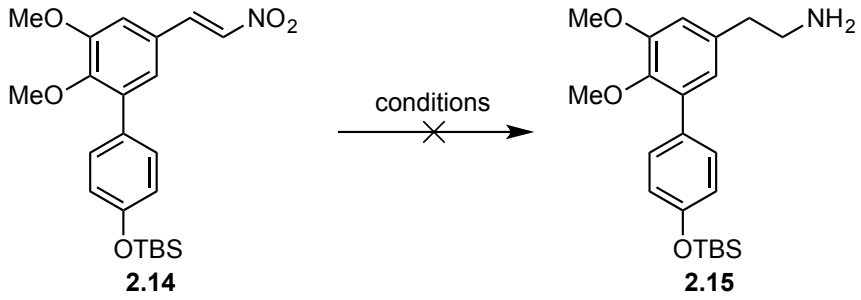

(2.2)

At this point, it had become clear that the phenolic-TBS group was too labile for the strongly reducing and/or acidic conditions necessary for β-nitrostyrene reduction. We decided a more robust silyl-based protecting group would be required, and thus, synthesized the analogous triisopropylsilyl ether.

2.6. *O*-TIPS β-NITROSTYRENE SYNTHESIS

The synthesis of the triisopropylsilyl ether protected β-nitrostyrene **2.19** proceeded in an analogous fashion to **2.14** (Scheme 2.4). From 4-bromophenol (**2.10**), silyl protection and formation of boroxime **2.17** proceeded in 98% and 89% yields, respectively. Subsequent Suzuki cross coupling of **2.8** and **2.17** gave the analogous *O*-TIPS aldehyde **2.18** in 91% yield. Henry reaction of **2.18** formed β-nitrostyrene **2.19** in 88% yield.

Scheme 2.4. Synthesis of *O*-TIPS protected β-nitrostyrene **2.19**

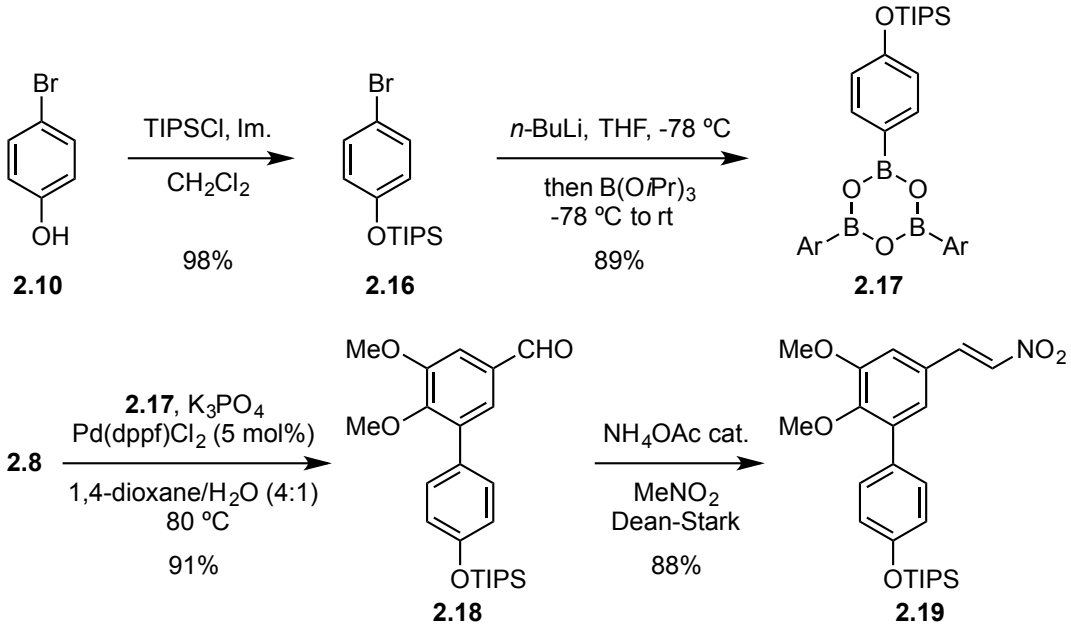

2.7. β-NITROSTYRENE REDUCTION: PART II.

With β-nitrostyrene **2.19** in hand, we once again turned our attention to the formation of the corresponding phenethylamine **2.20**. Initial attempts at catalytic hydrogenation in various alcoholic solvents with strong Brønsted acids[60,61] led to mainly intractable mixtures of byproducts with trace amounts of product formation. Literature conditions utilizing iron (0) in acidic alcoholic media also failed to yield more than trace amounts of **2.20**.[62] Finally, much to our delight, we found that dropwise addition of a solution of **2.19** in 1,4-dioxane into an excess of diisobutylaluminum hydride led to immediate formation of **2.20** in 94% yield (Equation 2.3).[63]

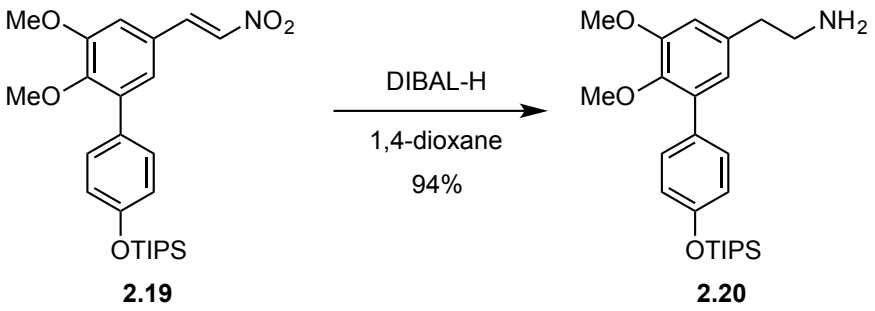

(2.3)

2.8. SYNTHESIS OF 3-BENZYLOXYPROPIONALDEHYDE

Following the reduction of β-nitrostyrene **2.19**, the next step in our synthesis was the Pictet-Spengler cyclization. Before any attempts at the Pictet-Spengler cyclization could be made, we first needed to synthesize the requisite 3-substituted propionaldehyde. Careful consideration as to the substituent at the 3-postion was taken. We required a substituent that would not only be unreactive towards our primary amine, but that we could also easily manipulate into a proper leaving group for the following *p*-phenolic *C*-alkylation. We decided that a protected alcohol should fit the aforementioned requirements. The benzyl ether was chosen as the protecting group because it afforded us the ability of orthogonal deprotection, with respect to the phenolic triisopropylsilyl ether. From 1,3-propane diol (**2.21**), monobenzylation via *in situ* Finkelstein reaction using catalytic tetrabutylammonium iodide with one equivalent of benzyl chloride and sodium hydride, proceeded to give alcohol **2.22** in 78% yield (Scheme 2.5). Swern oxidation of **2.22** yielded 93% of 3-benzyloxypropionaldehyde (**2.23**).[64]

Scheme 2.5. Synthesis of 3-benzyloxypropionaldehyde **2.23**

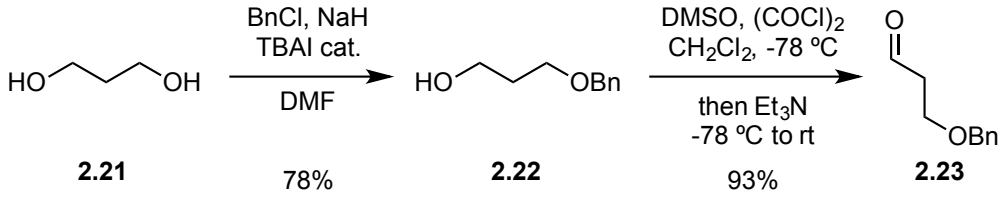

2.9. PICTET-SPENGLER CYCLIZATION: PART I.

The Pictet-Spengler cyclization has been utilized in a multitude of total syntheses and has been subject to a number of reviews.[65–67] All attempts made towards the Pictet-Spengler cyclization of **2.20** with aldehyde **2.23**, failed to yield any isolable quantities of desired product **2.24** (Equation 2.4). Of the conditions attempted, acids including, acetic acid, sulfuric acid, trifluoroacetic acid, triflic acid, and titanium (IV) chloride, all failed to give **2.24**.[68,69] Attempts at an acyl-Pictet-Spengler cyclization, through *in situ N*-acylation of **2.20** via treatment with acetyl chloride or trifluoroacetic anhydride, both failed. At this point in time, we were inspired by a recent report in which several aliphatic aldehydes were cyclized onto a carbamate protected phenethylamine in a mixture of concentrated sulfuric acid and acetic acid at room temperature.[70]

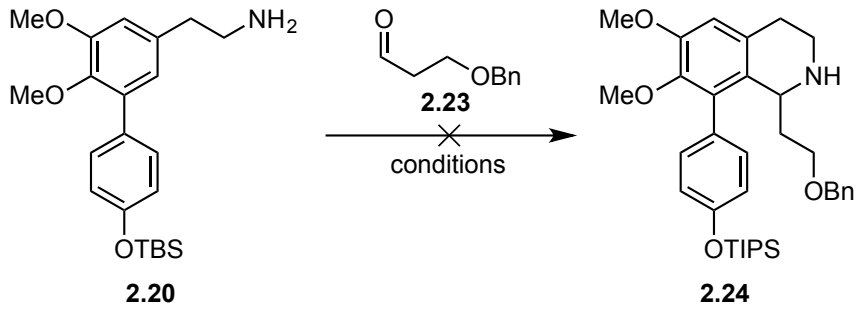

(2.4)

2.10. MONOARYL ETHYL CARBAMATE SYNTHESIS

We decided to initially test the recently reported carbamate cyclization conditions on the monoaryl carbamate **2.27** (Scheme 2.6) for two reasons. First, it is possible that the biaryl substituent at the 5-postion was too sterically demanding to allow for cyclization to occur at that position. Secondly, the monoaryl amine was easier and cheaper to synthesize in large quantities. Henry reaction of 5-bromoveratraldehyde (**2.8**) and subsequent diisobutylaluminum hydride reduction each proceeded in 97% yield, respectively, to give phenethylamine **2.26**. Treatment of **2.26** with ethyl chloroformate gave carbamate **2.27** in 76% yield.

Scheme 2.6. Synthesis of monoaryl carbamate **2.27**

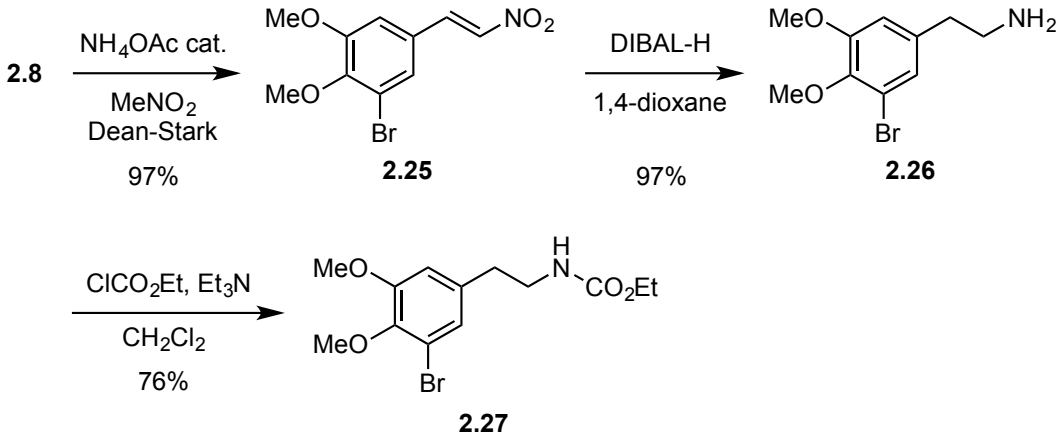

2.11. PICTET-SPENGLER CYCLIZATION: PART II. MONOARYL CARBAMATE

Representative results of the Pictet-Spengler cyclization and optimization studies are shown in Table 2.1. From carbamate **2.27**, attempts to replicate the aforementioned literature procedure resulted in only trace amounts of **2.28** (entry 1). We obtained similar results by stirring carbamate **2.27** and aldehyde **2.23** in hexafluoroisopropanol (HFIP) at room temperature (entry 2). However, we found that heating a solution of **2.27** and **2.23** in HFIP with catalytic amounts of trifluoroacetic acid led to a substantial increase in yield (entries 3-5). Given these results, we decided to test these conditions on the analogous biaryl derivative.

Table 2.1. Optimization of Pictet-Spengler cyclization on monoaryl carbamate **2.27**

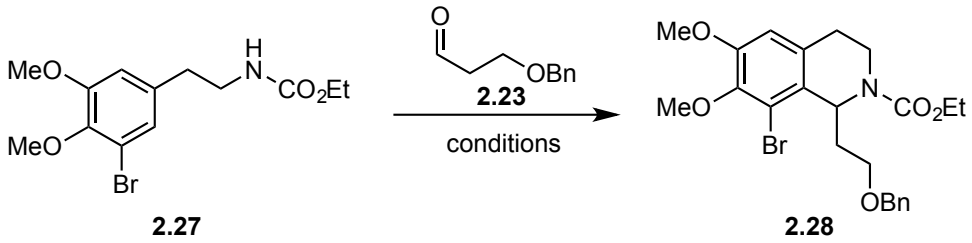

2.27 **2.28**

Entry	Acid	Solvent	Temperature	Yield of **2.28**
1	H_2SO_4	AcOH	rt	trace
2	-	HFIP	rt	trace
3	-	HFIP	50 ºC	30%
4	TFA cat.	HFIP	50 ºC	50%
5	TFA cat.	HFIP	60 ºC	68%

(HFIP = 1,1,1,3,3,3-hexafluoroisopropanol)

2.12. PICTET-SPENGLER CYCLIZATION: PART III. BIARYL CARBAMATE

Ethyl carbamate **2.29** was synthesized in 86% yield from **2.20** upon treatment with ethyl chloroformate. Following the isolation of **2.29**, the previously discovered Pictet-Spengler cyclization conditions were attempted and gave tetrahydroisoquinoline **2.30** in 65% yield (entry 1, Table 2.2). In attempts to further optimize the reaction, we first tested to see if trifluoroacetic acid was necessary for cyclization to occur. The use of catalytic acetic acid, in place of trifluoroacetic acid, yielded only trace amounts of **2.30** (entry 2). We next focused our attention on whether HFIP was necessary as the solvent. Given the toxicity and relatively expensive cost of HFIP, we hoped to find a safer and cheaper alternative. Attempts using isopropanol as the solvent gave only returned starting

materials **2.29** (entry 3). Finally, we found that the use of trifluoroethanol (TFE) was just as effective as HFIP, giving **2.30** in 85% yield (entry 4).

Table 2.2. Pictet-Spengler cyclization of biaryl carbamate **2.29**

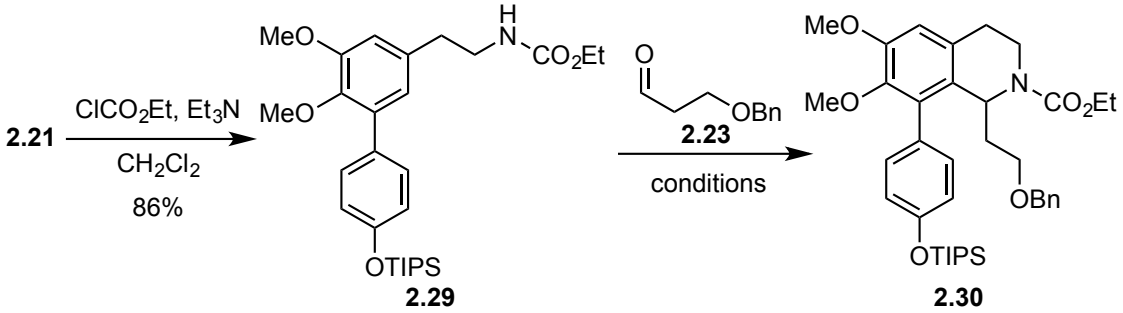

Entry	Acid	Solvent	Temperature	Yield of **2.30**
1	TFA cat.	HFIP (0.2 M)	60 ºC	65%
2	AcOH cat.	HFIP (0.2 M)	60 ºC	trace
3	TFA cat.	*i*PrOH (0.2M)	60 ºC	rsm
4	TFA cat.	TFE (0.2 M)	60 ºC	85%
5	TFA cat.	HFIP (0.4 M)	60 ºC	86%

HFIP = 1,1,1,3,3,3-hexafluoroisopropanol, TFE = 1,1,1-trifluoroethanol. Concentrations with respect to carbamate **2.29**

2.13. *P*-PHENOLIC *C*-ALKYLATION: PART I. ETHYL CARBAMATE

To set the stage for the key *p*-phenolic *C*-alkylation, we first needed to transform the benzyl ether of **2.30** into an appropriate leaving group. For our initial studies, we chose to use the mesylate leaving group. Hydrogenolysis of benzyl ether **2.30**, using catalytic palladium on carbon, gave alcohol **2.31** in 60% yield (Scheme 2.7). Subsequent treatment with mesyl chloride gave the mesyl alcohol **2.32** in 43% yield.

Scheme 2.7. Synthesis of *p*-phenolic *C*-alkylation substrate **2.32**

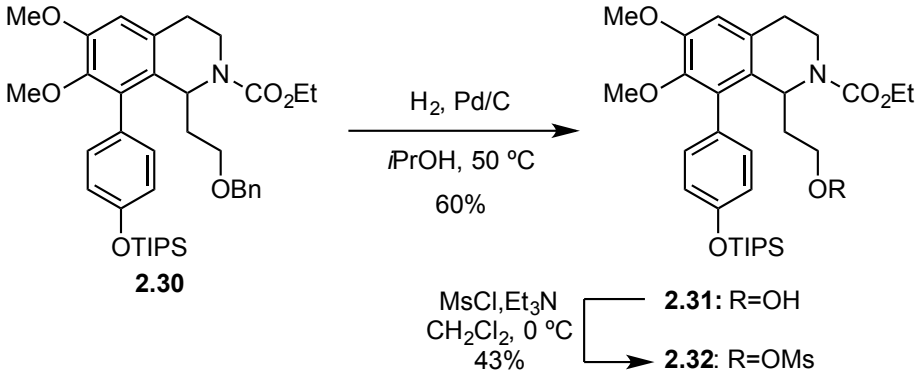

Conditions for the *p*-phenolic *C*-alkylation were chosen based on previous studies from the Magnus lab.[56,71] Heating a solution of **2.32** in DMF to 80 ºC followed by addition of flame-dried cesium fluoride, and subsequent heating to 120 ºC, led to a mixture of products (Figure 2.2). The desired homoproaporphine **2.33** was isolated in poor yield (< 20% in each attempt).

Figure 2.2. Initial attempt at *p*-phenolic *C*-alkylation

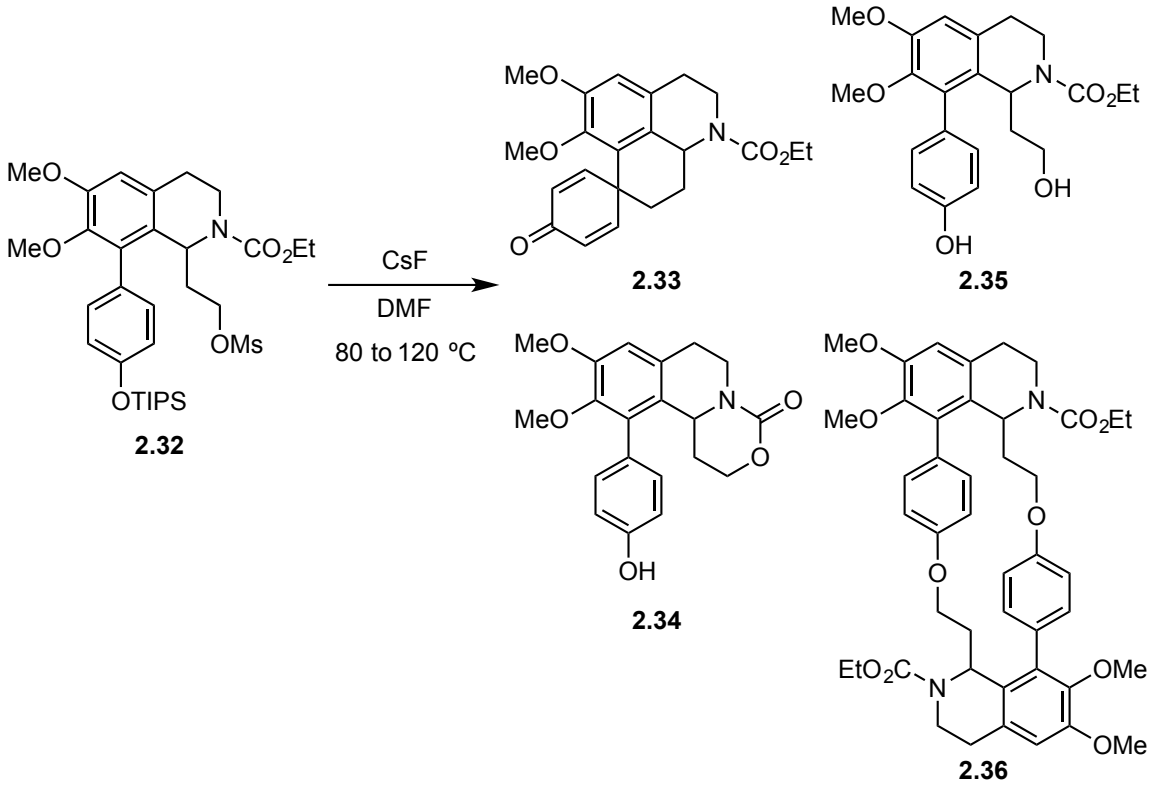

In analyzing the mixture of products and designing future experiments, we reasoned that the formation of dimer **2.36** could be mitigated by running the reaction under higher dilution. Initially, the formation of alcohol **2.35** and tetrahydrooxazinone **2.34** was perplexing. After careful consideration, we hypothesized that the carbonyl oxygen atom could be displacing the mesylate to form an imidate intermediate **2.37** (Scheme 2.8). Addition of water into **2.37** would lead to the formation of tetrahedral intermediate **2.38**, which upon leaving of the alkoxy group (red) or ethoxy group (blue) would form alcohol **2.35** or tetrahydrooxazinone **2.34**, respectively.

Scheme 2.8. Proposed mechanism of the formation of **2.34** and **2.35**

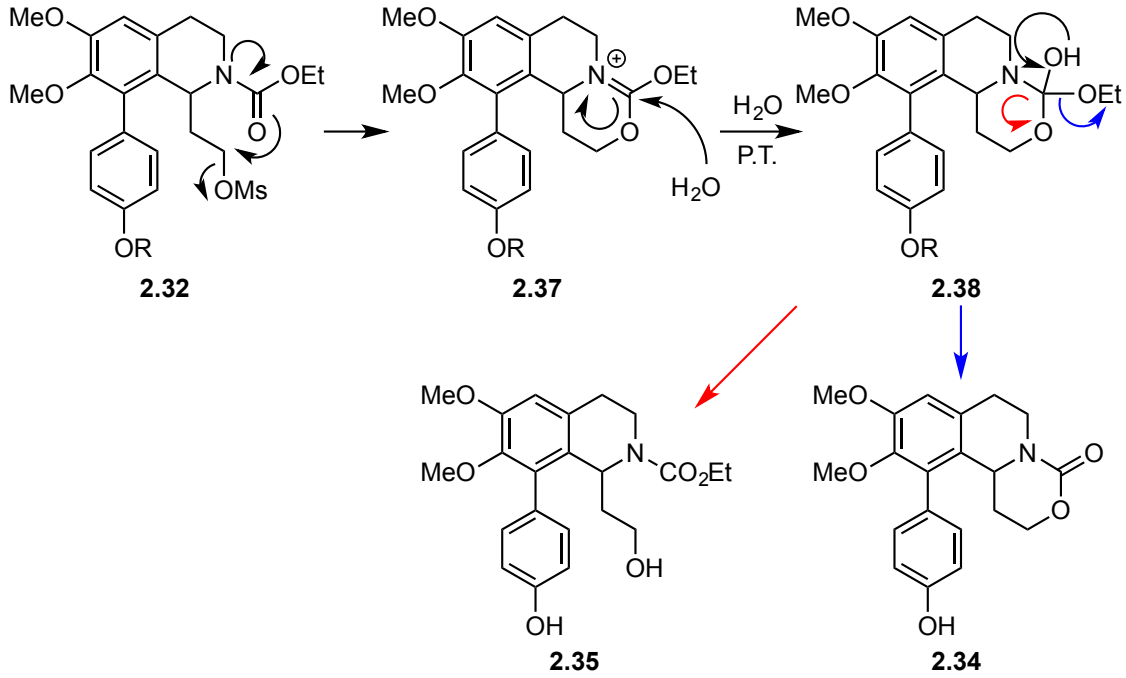

If the given side-reaction is proceeding through the proposed mechanism, then the formation of byproducts **2.34** and **2.35** would be mechanistically independent from the desired *p*-phenolic *C*-alkylation pathway. With this in mind, we ran a control experiment to determine whether or not the starting material was stable to the reaction conditions. Heating **2.32** in DMF followed by an aqueous work-up led to the exclusive formation of alcohol **2.39** and tetrahydrooxazinone **2.40**, thus indicating that these side reactions are likely happening before the desired *p*-phenolic *C*-alkylation can occur (Equation 2.5). Given the experimental evidence that the ethylcarbamate is likely displacing our alcohol before the desired transformation can occur, we decided that the *N*-protecting group needed to be changed.

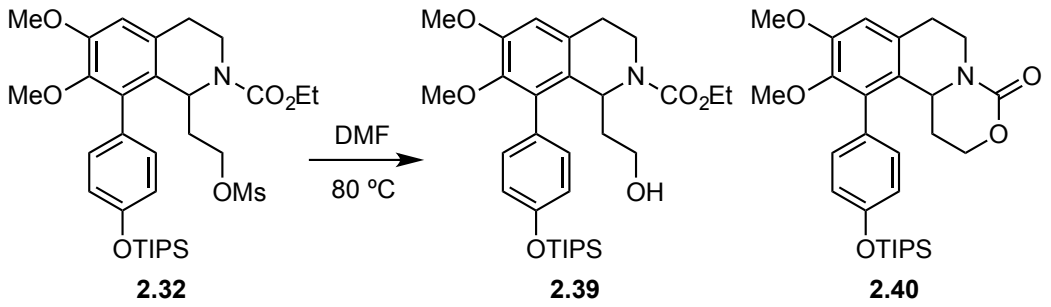

2.32 **2.39** **2.40**

(2.5)

2.14. NITROGEN PROTECTING GROUP STRATEGIES

In planning a new *N*-protecting group strategy, two possibilities immediately came to mind. The first idea was to perform the *p*-phenolic *C*-alkylation without a protecting group, i.e. from the N-H compound **2.41** (Figure 2.3). However, from our previous studies into the Pictet-Spengler cyclization, we know that the phenethylamine **2.20** will not cyclize. Given that the step immediately following the Pictet-Spengler cyclization is a hydrogenolysis, we reasoned that the use of a Cbz *N*-protecting group would allow for the Pictet-Spengler to occur analogously to previous examples to give **2.42**. Subsequent hydrogenolysis of **2.42** would afford a tandem benzyl and Cbz deprotection, yielding **2.41** without any additional synthetic steps.

The second potential *N*-protecting group strategy considered, was use of the *N*-tosyl sulfonamide **2.43**. The oxygen atoms on the *N*-sulfonamide are less nucleophilic, and thus less likely to participate in the displacement of the leaving group during the *p*-phenolic *C*-alkylation, as compared a carbamate oxygen atom. The biggest unknown with

respect to the use of the N-tosyl group in our synthesis, was whether the Pictet-Spengler cyclization would occur analogously to the carbamate substrates.

Figure 2.3. Potential nitrogen-protecting group strategies

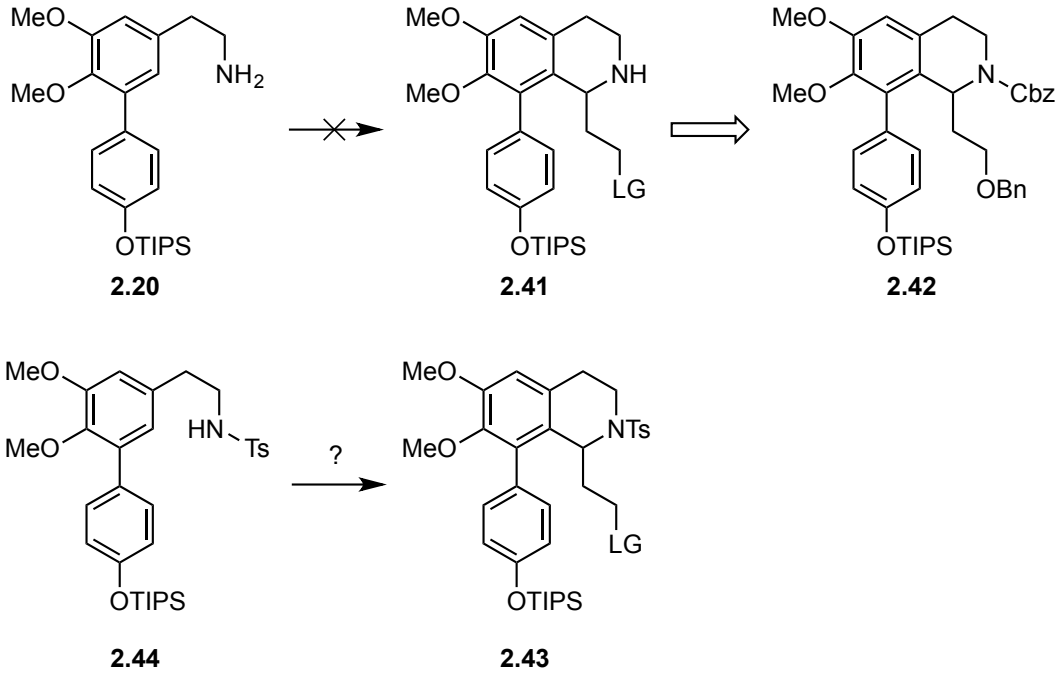

2.15. *P*-PHENOLIC *C*-ALKYLATION: PART II. SECONDARY AMINE

In preparation to attempt the *p*-phenolic *C*-alkylation without a nitrogen protecting group, we synthesized alkyl bromide **2.48** (Scheme 2.9). Protection of **2.20** as the Cbz carbamate proceeded in 79% yield to give **2.45**. Subsequent Pictet-Spengler cyclization using the dimethyl acetal **2.46** gave tetrahydroisoquinoline **2.42** in 91% yield. Concomitant benzyl and Cbz deprotection was achieved via hydrogenation with catalytic palladium on carbon to give secondary amino alcohol **2.47** in 63% yield. Given that

treatment of secondary amine **2.47** with methanesulfonyl chloride would likely lead to the *N*-mesyl compound, we synthesized the corresponding alkyl bromide **2.48**. Heating a solution of **2.47** in toluene under reflux in the presence of phosphorus tribromide gave quantitative conversion to bromide **2.48**.

Scheme 2.9. Synthesis of secondary amine **2.48**

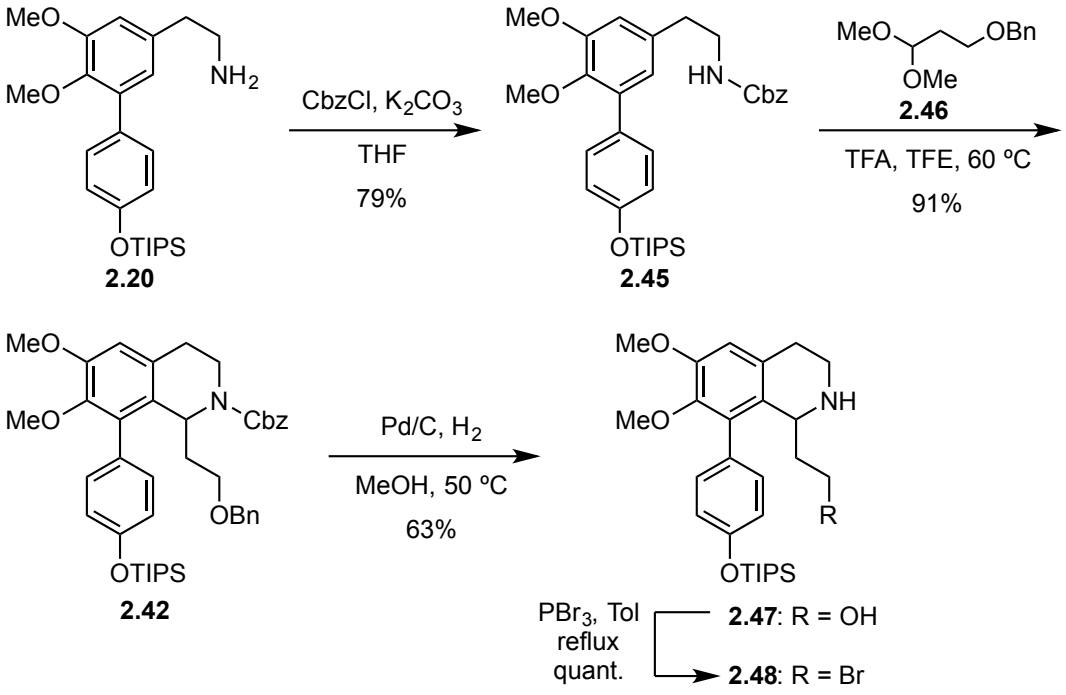

With the stage set, we attempted the key *p*-phenolic *C*-alkylation on **2.48**. Upon heating a solution of **2.48** in DMF and adding flame-dried cesium fluoride, we isolated 80% of elimination product **2.49** (Equation 2.6).

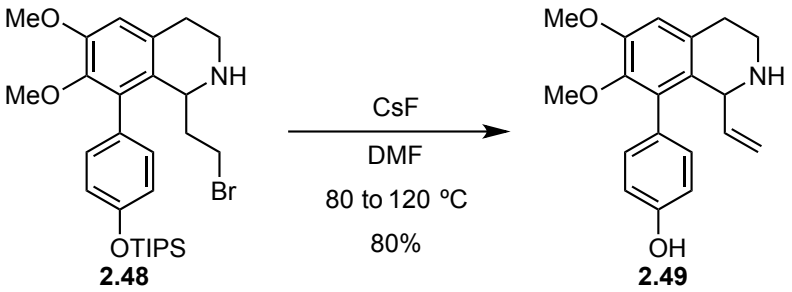

(2.6)

We reasoned that the elimination to form **2.49** likely occurs because of the basic nature of the secondary amine. Heating **2.48** in DMF as a control experiment led to the formation of olefin **2.50**, confirming that the starting material is not stable to the reaction conditions (Equation 2.7). Given these results, we focused our attention on synthesizing the corresponding *N*-tosyl protected amine.

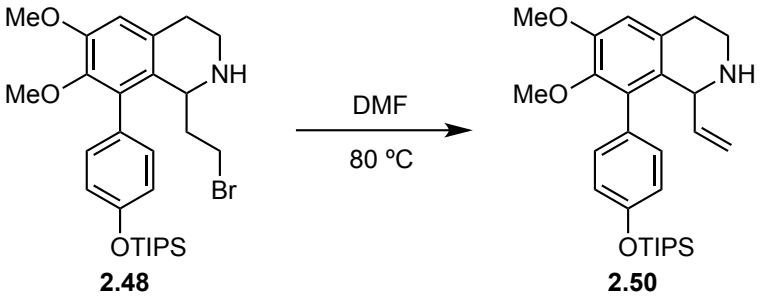

(2.7)

2.16. *P*-PHENOLIC *C*-ALKYLATION: PART III. N-TOSYL SULFONAMIDE

The synthesis of *N*-tosyl tetrahydroisoquinoline **2.51** was accomplished analogously to previous examples. Treatment of phenethylamine **2.20** with tosyl chloride gave the *N*-tosyl phenethylamine **2.44** in 80% yield (Scheme 2.10). Pictet-Spengler cyclization of **2.44** proceeded smoothly to give tetrahydroisoquinoline **2.51** in 87% yield. Palladium-catalyzed transfer hydrogenolysis of **2.51** gave alcohol **2.52** in 83% yield.

Alcohol **2.52** was transformed into the mesylate **2.53** via treatment with methanesulfonyl chloride in near quantitative yield.

Scheme 2.10. Synthesis of N-tosyl sulfonamide *p*-phenolic *C*-alkylation substrate **2.53**

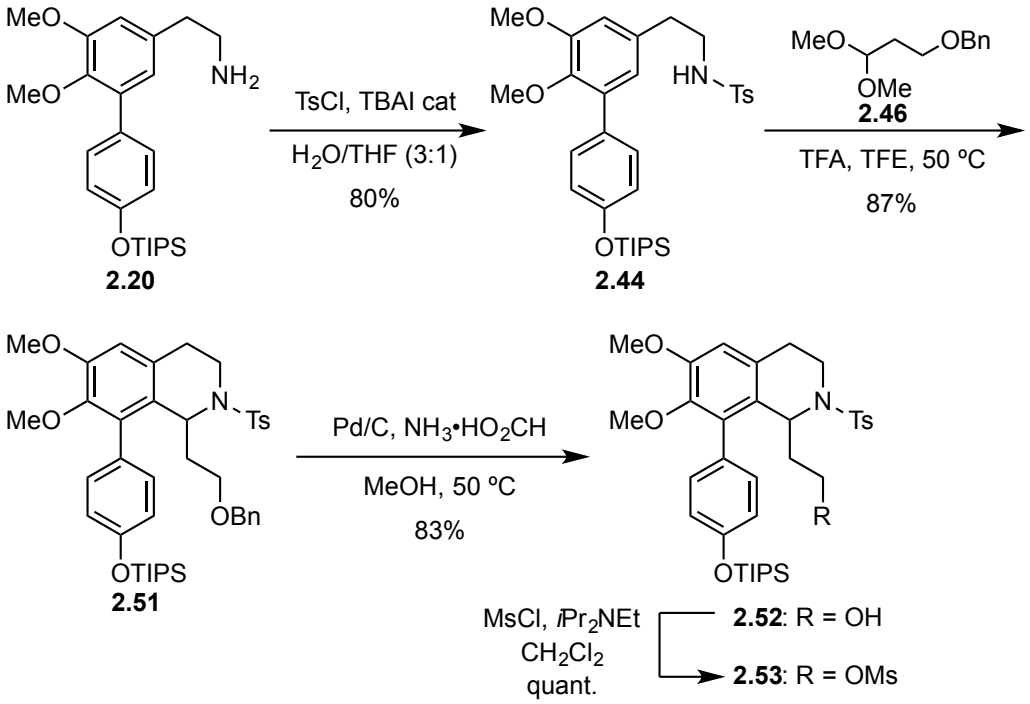

With mesylate **2.53** in hand, it was once again time to attempt the *p*-phenolic *C*-alkylation. Upon addition of flame-dried cesium fluoride to a solution of **2.53** in DMF at 80 ºC, followed by heating to 120 ºC, we were quite surprised to find that we not only isolated the desired homoproaporphine **2.54** in 22% yield, but we also isolated the formate ester **2.55** in 21% yield (Equation 2.8).

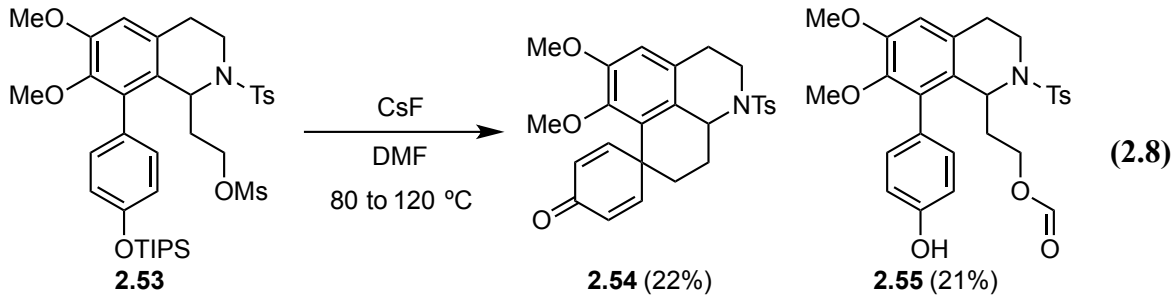

2.53 **2.54** (22%) **2.55** (21%) **(2.8)**

In these experiments, the formation of **2.55** coincided with the presence of trace amounts of the corresponding alcohol (analogous to **2.35**). However, unlike the previous *p*-phenolic *C*-alkylation attempts with ethyl carbamate **2.32**, the formation of **2.55** was a strong indication that the accompanying alcohol was not arising from neighboring group participation of the nitrogen protecting group. This led us to revise our mechanistic model to explain the formation of the alcohol byproduct. Given that DMF is known to act as a nucleophile in reactions such as the Vilsmeier-Haack,[72] it is possible that DMF is displacing our leaving group to give intermediate **2.56** (Scheme 2.11). Subsequent hydrolysis upon aqueous work-up would lead to **2.55**, and further hydrolysis would form the corresponding alcohol.

Scheme 2.11. Mechanistic rationale for the observation of formate byproduct **2.55**

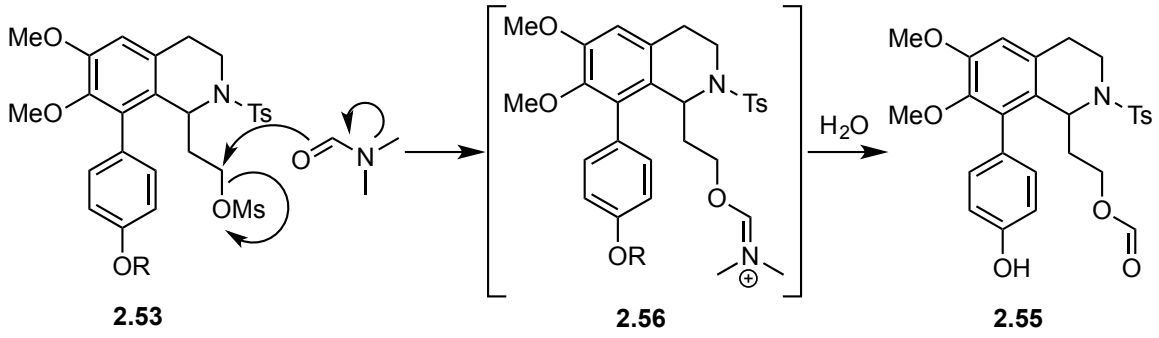

2.53 **2.56** **2.55**

In order to mitigate this side reaction, we attempted the *p*-phenolic *C*-alkylation on substrates possessing weaker leaving groups namely, bromide **2.57** and chloride **2.58**. We anticipated that the weaker leaving group ability would decrease the reactivity of our substrates towards the solvent, thus allowing intramolecular alkylation to occur. With this in mind, bromide **2.57** and chloride **2.58** were synthesized from an Appel reaction in 95% and 83% yields, respectively (Equation 2.9).

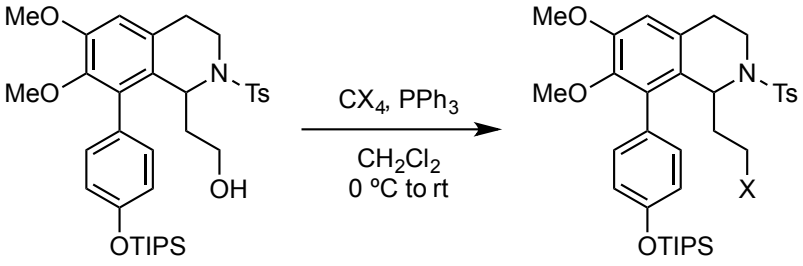

2.52

2.57: X=Br (95%)
2.58: X=Cl (83%)

(2.9)

From bromide **2.57**, *p*-phenolic *C*-alkylation under our previously reported conditions gave the homoproaporphine **2.54** in 57% yield (Equation 2.10). However, while the use of the bromide leaving group mitigated the deleterious side reaction to a significant degree, trace quantities of **2.55** were still observed. Previous studies have shown that the bromide exhibits a weaker leaving group ability, as compared to the mesylate leaving group, with respect to intermolecular substitution reactions.[73,74] Therefore, we postulated that the attenuated leaving group ability of the bromide lowers the rate of solvolysis, relative to the rate of intramolecular alkylation, leading to an increased yield of **2.54**. However, the 57% yield was not satisfactory for this key-step, so we decided to try this reaction in a number of different high-boiling aprotic solvents.

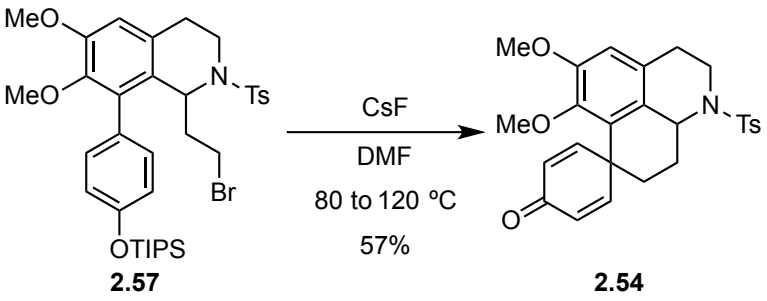

2.57 **2.54** **(2.10)**

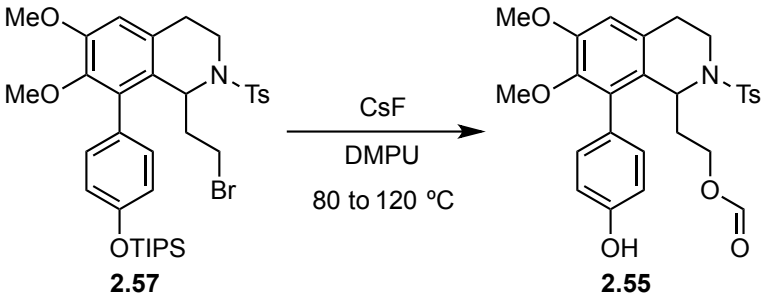

2.57 **2.55** **(2.11)**

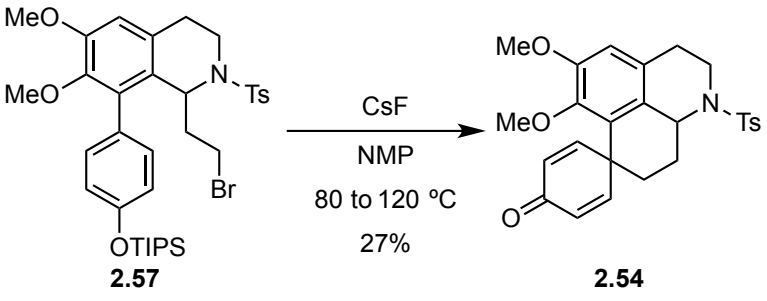

2.57 **2.54** **(2.12)**

The use of 1,3-dimethyl-3,4,5,6-tetrahydro-2-pyrimidinone (DMPU) as the solvent in the *p*-phenolic *C*-alkylation led to exclusive formation of formate **2.55** (Equation 2.11). The use of *N*-methyl pyrrolidinone (NMP) as solvent gave the desired homoproaporphine **2.54** in 27% yield (Equation 2.12), along with varying amounts of the corresponding alcohol. The quantities of byproducts formed during these reactions was found to be qualitatively dependent on the amount of time **2.57** was preheated at 80 ºC. Given our inability to completely shut down this side reaction, we considered that for

every substrate attempted, this side reaction occurred when heating the substrate before addition of the cesium fluoride. Based on previous work in our laboratory, this preheating was thought to be necessary for the success of the *p*-phenolic *C*-alkylation.[44–46,51,71,75] Nonetheless, we reasoned that reversing the order of addition, in adding a solution of our substrate to the reaction flask already containing cesium fluoride at the reaction temperature, would limit the amount of time that our substrate was heated before being able to react with the cesium fluoride, and thus minimize the formation of **2.55**.

Our initial experiment utilizing the inverse addition procedure was met with great success. Cannulating a solution of **2.57** in NMP into a flask with flame-dried cesium fluoride at 100 ºC gave **2.54** in 79% yield (Equation 2.13), the structural assignment of which was confirmed by X-ray crystallography (Figure 2.4). Given this result, we ran a number of similar experiments and found that the inverse addition protocol was far superior to the previous reaction conditions for our system. Using diglyme as the solvent at 100 ºC and 120 ºC yielded **2.54** in 53% and 71%, respectively (Equation 2.14). We also found the chloride leaving group to be particularly efficient, albeit at higher temperatures. In NMP at 100 ºC, the chloride **2.58** was unreactive and simply yielded the TIPS-deprotected phenol of the starting material. However, when **2.58** was heated to 150 ºC, we isolated the desired product **2.54** in 91% yield (Equation 2.15).

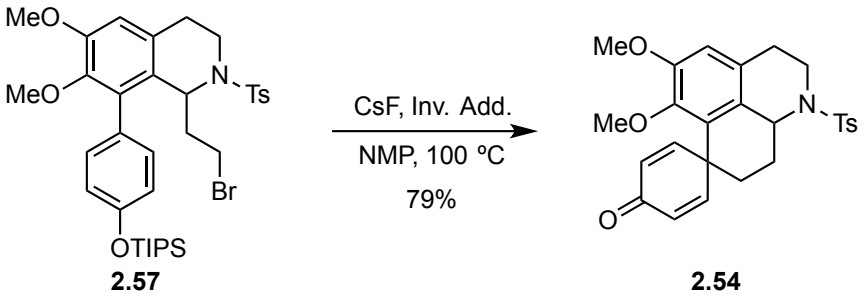

2.57 **2.54** **(2.13)**

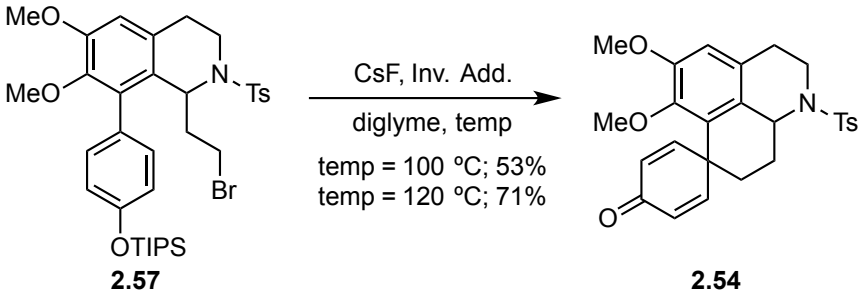

2.57 **2.54** **(2.14)**

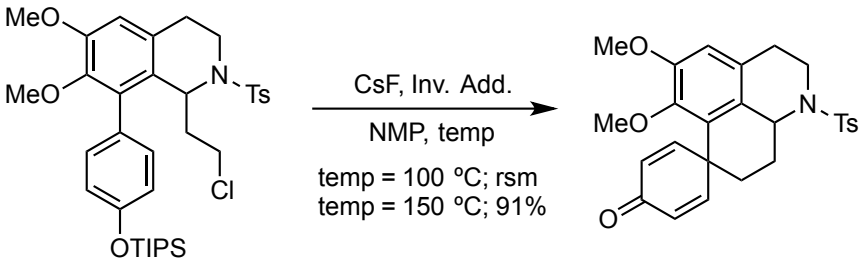

2.58 **2.54** **(2.15)**

Figure 2.4. X-ray crystal structure of homoproaporphine **2.54**

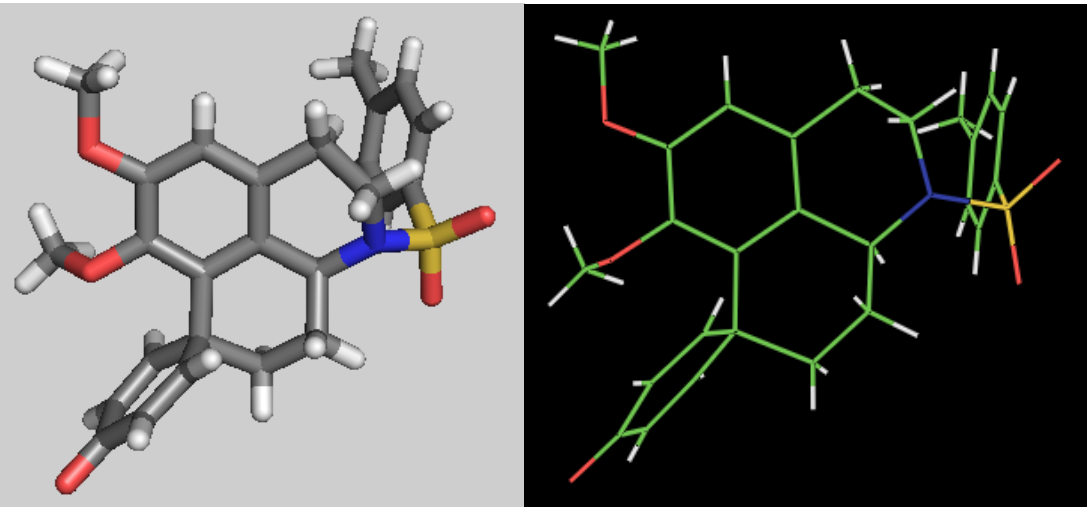

2.17. Dienone-Phenol Rearrangement and *N*-Tosyl Deprotection

Upon synthesis of the *N*-tosyl homoproaporphine **2.54**, we next turned our attention towards the dienone-phenol rearrangement. The dienone-phenol rearrangement of a homoproaporphine to form the corresponding homoaporphine has been reported almost as early as the discovery of these compounds.[5] We first attempted Battersby's procedure by stirring **2.54** in concentrated sulfuric acid.[26] However, this led to an intractable mixture of multiple byproducts. We then attempted a previously reported procedure using boron trifluoride etherate in dichloromethane.[12,76,77] This method gave the desired product in ~20% yield at most. We found significantly improved yields upon the use of Kametani's conditions,[78,79] thus stirring a solution of **2.54** in a mixture of acetic acid and concentrated hydrochloric acid at room temperature for two-days led to a 48% yield of the desired homoaporphine **2.59**. Slightly modifying Kametani's conditions, we

found that heating the reaction mixture to 50 ºC for 12 hours gave **2.59** in 79% yield (Equation 2.16), the structural assignment of which was confirmed by X-ray crystallography (Figure 2.5).

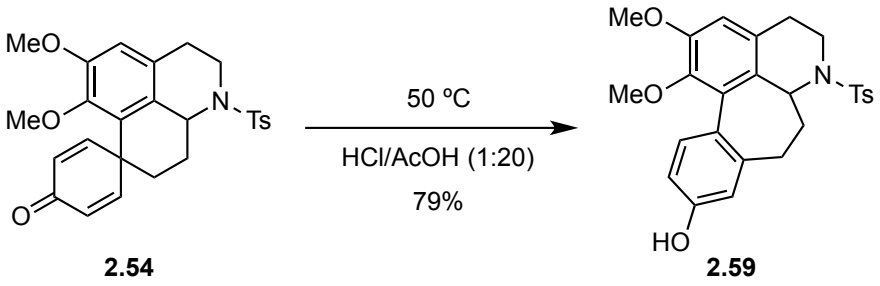

2.54 **2.59** **(2.16)**

Figure 2.5. X-ray crystal structure of *N*-tosyl homoaporphine **2.59**

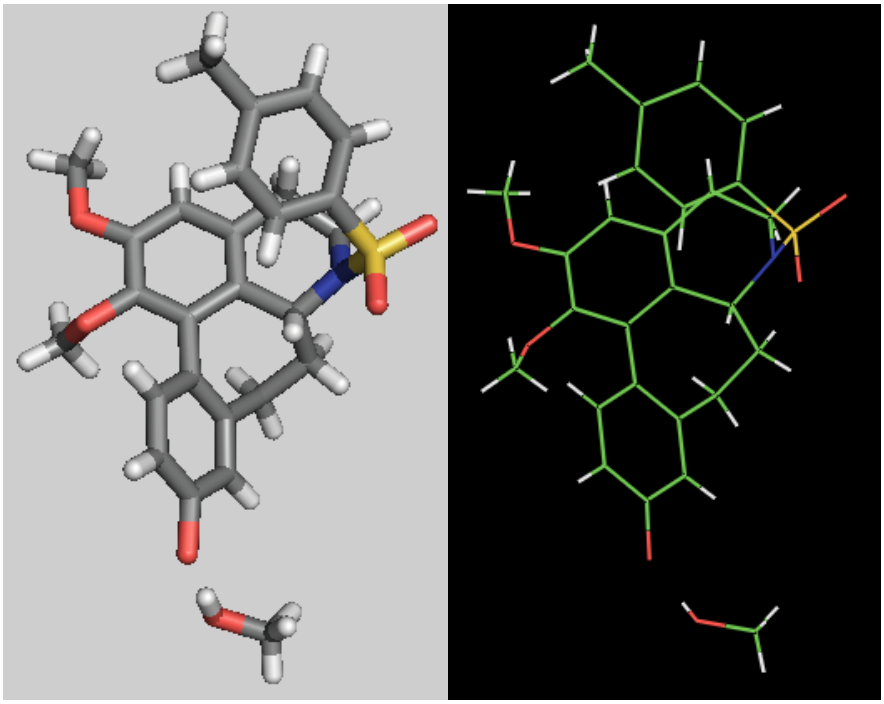

With the homoaporphine **2.59** in hand, we were able to deprotect our N-tosyl sulfonamide to access our target compound **2.1**. Treatment of **2.59** with sodium naphthalide in dimethoxyethane gave the final homoaporphine **2.1** in 58% yield (Equation 2.17). Due to a lack of material and a shortage on time, these reaction conditions were not optimized. Further difficulty was experienced with respect to the purification of **2.1**. Attempted purification via recrystallization failed to give satisfactory yields. Initial attempts at purification by column chromatography over silica gel were unable to yield the title compound without the presence of at least one unidentifiable byproduct. Finally, with material almost completely gone, the reaction was run one last time. Chromatography conditions previously reported by Kametani for the synthesis of an unnatural homoaporphine[79], in which chloroform-acetone-methanol (5:4:1) was used as the eluent, yielded 58% of pure homoaporphine **2.1**.

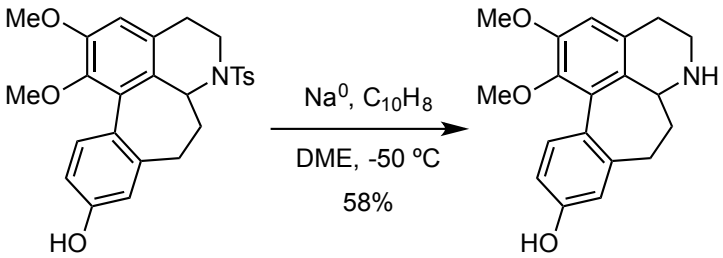

2.59 **2.1** **(2.17)**

2.18. SUMMARY AND CONCLUSION

In summary, unnatural homoaporphine **2.1** was synthesized in 10-steps from commerically available 5-bromoveratraldehyde (**2.8**), with an overall yield of 15% (Scheme 2.12). In the final sequence, the biaryl-phenethylamine **2.20** was synthesized

from **2.8** through a Suzuki cross coupling, Henry reaction, and reduction of the β-nitrostyrene proceeding in 75% over three steps. Formation of the key intermediates were achieved from **2.20** through a tosylation, Pictet-Spengler cyclization, hydrogenolysis, and Appel reactions in 55% and 48% yields over four steps to give **2.57** and **2.58**, respectively. From these two substrates, the key *p*-phenolic *C*-alkylation afforded homoproaporphine **2.54** in 79% and 91% yields from **2.57** and **2.58**, respectively. Finally, dienone-phenol rearrangement and subsequent *N*-tosyl deprotection gave the final homoaporphine **2.1** in 46% yield over two steps. The synthetic strategy of forming the biaryl bond through an efficient Suzuki cross coupling and subsequent formation of the homoproaporphine system via *p*-phenolic *C*-alkylation proceeded in high yields. This strategy allows access to the homoproaporphine motif in just eight steps with an overall yield of 33%. The use of the bromide and chloride leaving groups resulted in the same overall yield for each sequence.

Scheme 2.12. Summary of the total synthesis of homoaporphine **2.1**

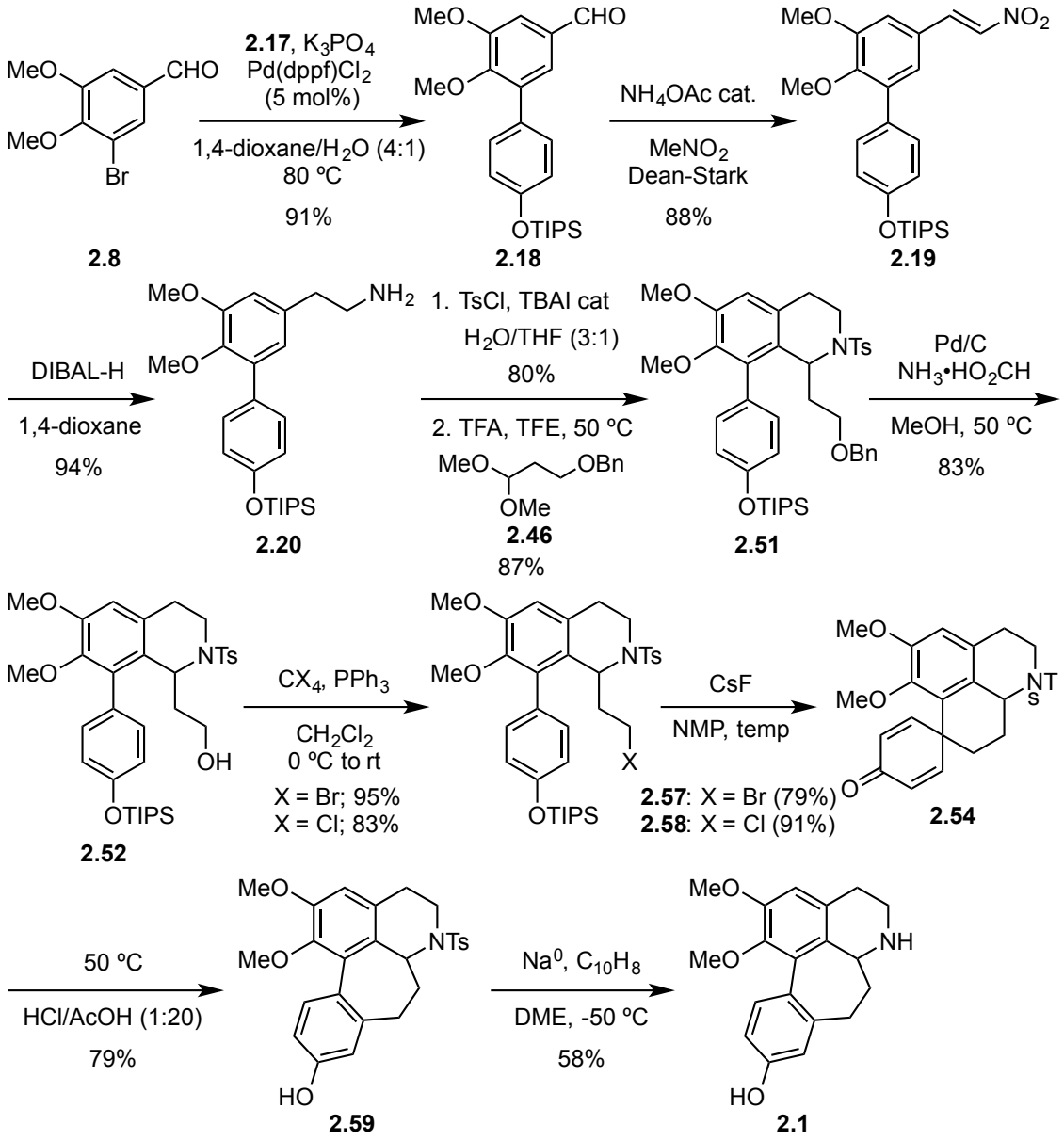

HUMAN AFRICAN TRYPANOSOMIASIS

Chapter 3: Treating Human African Trypanosomiasis: Current and Future Methods

3.1. HUMAN AFRICAN TRYPANOSOMIASIS

Human African trypanosomiasis (HAT), also known as African sleeping sickness, is a disease caused by the protozoan *Trypanosoma brucei*. Transmitted via the bite of the tsetse fly in Sub-Saharan Africa, HAT affects an estimated 10,000 - 30,000 individuals annually, with more than 60 million inhabitants at risk of infection.[80] There are two sub-species of the parasite that are known to infect humans, *Trypanosoma brucei gambiense* and *Trypanosoma brucei rhodesiense*. The former affects central and western Africa and accounts for between 95 - 98% of reported HAT cases.[81] The disease progresses through two stages, and if left untreated, it is uniformly fatal.

The early, hemolymphatic stage, occurs when the parasite is restricted to the blood and lymph system, and is characterized by symptoms including, fevers, headaches, itching, joint pain, and swollen lymph nodes. This stage can last anywhere from months to years after the initial infection by *T. brucei gambiense*. Conversely, the first stage of the disease arising from the infection of *T. brucei rhodesiense* only lasts a couple of weeks before progression to the second stage occurs. The second, meningoencephalitic stage, results from the parasite entering the central nervous system (CNS) and crossing the blood brain barrier.[82] This causes severe neurological symptoms including allodynia,

sensory-motor disruptions, sleep disturbances, and hyperalgesia. If left untreated this second stage will result in coma and ultimately, death.[83]

3.1.1. Current HAT Treatments

Current drug treatments for both early and late stage HAT are problematic. Given that diagnosis of the disease requires the microscopic analysis of an infected fluid or tissue sample and that rural areas are the most heavily affected, often times the disease is left undiagnosed and untreated until neurological symptoms of the second stage appear.[84] Due to the fact that second stage is caused by the parasite crossing the blood brain barrier, drugs that do not cross the blood brain barrier are completely ineffective at treating this stage of the infection. Furthermore, approved drug treatments for the second stage of the disease are either highly toxic or very expensive.

One of the earliest HAT treatments, suramin (**3.1**) was discovered in 1922 and is still used to treat the first stage of *T. brucei rhodesiense* infections (Figure 3.1). A typical treatment regimen consists of slow intravenous infusion every three to seven days over a month's time. Suramin (**3.1**) does not cross the blood brain barrier, and thus, is completely ineffective at treating second stage HAT infections. The mechanism of action towards *T. brucei* is currently unknown.[85]

Early stage infections due to *T. brucei gambiense* are most commonly treated with pentamidine (**3.2**) (Figure 3.1). Now considered to be the first line of treatment, one regimen of pentamidine (**3.2**) requires intramuscular injections once daily for 17 days. If

the disease is treated during the first stage, this drug is typically effective and relatively cheap. Notwithstanding, there are a few common side effects such as nephrotoxicity, hypoglycemia, hyperglycemia, and hypotension. The drug is thought to act through non-specific binding to DNA, resulting in disruption of mitochondrial function.[86] Pentamidine (**3.1**) does not cross the blood brain barrier, and thus, is ineffective for treatment of the disease in the second stage.

Figure 3.1. Current HAT drugs suramin (**3.1**), pentamidine (**3.2**), melarsoprol (**3.3**), eflornithine (**3.4**), and nifurtimox (**3.5**)

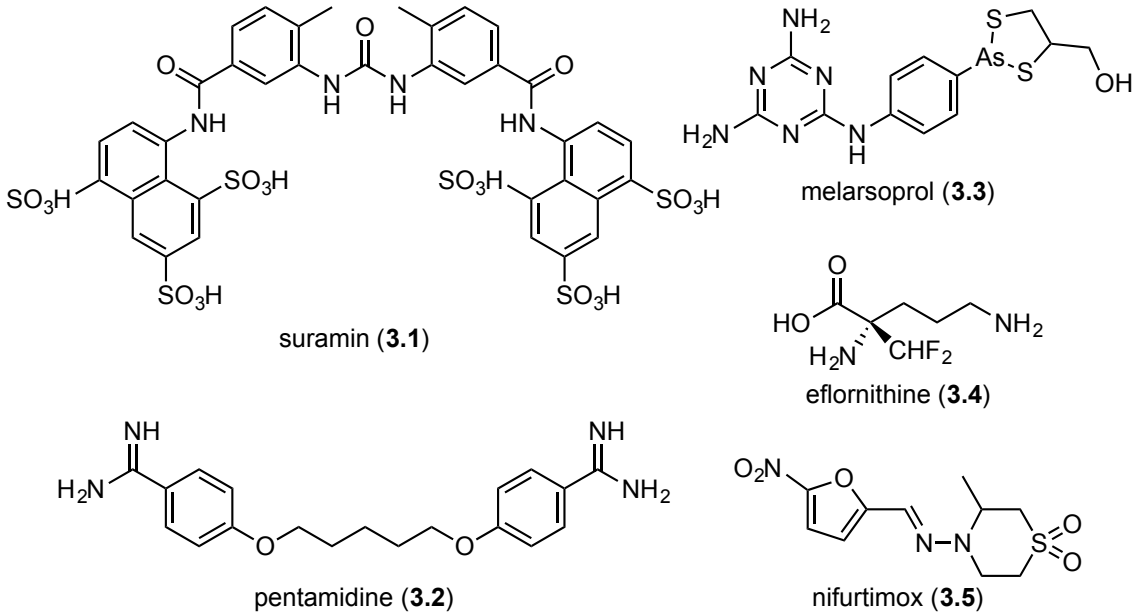

Currently there are only two drugs available to treat HAT in the second stage of the infection. Of these two drugs, Melarsoprol (**3.3**) is an organoarsenical drug that was introduced in 1949.[87] This drug is still the only treatment option for second stage HAT

caused by *T. brucei rhodesiense*. Melarsoprol (**3.3**) is highly toxic, with side effects typically mirroring that of arsenic poisoning, treatment leads to encephalopathy in 5-18% of patients with a mortality rate of 44-57% of said patients.[80] However, due to the high cost and distribution challenges associated with the only alternative, melarsoprol (**3.3**) was still being used to treat as much as 88% of the *gambiense* HAT cases as recently as 2003.[84] The mechanism of action has been found to proceed through uptake of the drug via P2 transporters. Once in the parasite, melarsoprol (**3.3**) disrupts the trypanothione protein, which in turn alters the cellular redox environment, killing the parasite.[88] Recently, drug resistant *T. brucei* strains have led to treatment failure rates upwards of 30% in some regions.[89]

The introduction of eflornithine (**3.4**) (Figure 3.1) in 1981 as a treatment for second stage HAT was a major breakthrough. Although eflornithine (**3.4**) only treats infections from *T. brucei gambiense*, it provides a much safer alternative to the arsenic based treatments. A repurposed drug, originally prescribed for the treatment of facial hair growth in women, eflornithine (**3.4**) acts through inhibition of ornithine decarboxylase, which plays an essential role in polyamine synthesis.[86] The major drawback with this drug is the intense treatment regimen, requiring multigram injections (dosed at 100 mg/kg) every six-hours for 14-days. This translates to roughly half a kilogram of the active drug per patient. Furthermore, the associated costs of a treatment regimen are very high, limiting availability in affected regions.[90] Recently, through support from the World

Health Organization (WHO), kits used to treat two 40 kg individuals were made available at a cost of $1,420 (US).[91]

A recent advancement, that has now become the first line of defense against second stage *T. brucei gambiense* HAT cases, is the use of nifurtimox (**3.5**) (Figure 3.1) eflornithine (**3.4**) combination therapy (NECT). Nifurtimox (**3.5**) is a drug currently used to treat Chagas disease (*Trypanosoma cruzi*), that failed clinical trials as a standalone treatment for HAT.[84] An NECT regimen consists of oral administration of nifurtimox (**3.5**) three times a day for 10-days in conjunction with intravenous eflornithine (**3.4**) administration. The major advantage to NECT is that it requires significantly smaller quantities of eflornithine (**3.4**) per regimen, only requiring IV injections every 12-hours for seven-days at 200 mg/kg.[86] This cut the total cost of a treatment regimen roughly in half, kits of four treatments for individuals weighing 36 kg are available through the WHO at a cost of $1,440 per kit.[91] The combination of these drugs toxic side effects, limited availability, and the ever-increasing prevalence of drug resistant parasite strains justify the desperate need for new, safer and cheaper HAT treatments.

3.1.2. Current HAT Drug Candidates

Currently, there are three drug candidates under clinical evaluation as potential HAT treatments. Originally discovered by Hoechst in the 1970s, fexinidazole (**3.6**) (Figure 3.2) was found to have trypanocidal activity.[92] However, fexinidazole (**3.6**) was not evaluated for clinical use until a rediscovery by the Drugs for Neglected Diseases initiative (DNDi) in 2006. The compound exhibited *in vitro* activity against a number of

laboratory and clinical *T. brucei* strains with an IC_{50} (50% inhibition concentration) ranging from 0.30 to 0.93 μg/mL. Though considerably less efficacious than melarsoprol (**3.3**) (IC_{50} = 0.003 μg/mL), fexinidazole (**3.6**) displayed a significant reduction in toxicity. Furthermore, it cured *in vivo* mouse models when dosed orally at 50 mg/kg twice a day or at 100 mg/kg once per day.[93] Fexinidazole (**3.6**) has since entered clinical trials in France, and if successful, it will become the first oral treatment for stage two HAT.[85]

In the early 2000s, Anacor Pharmaceuticals discovered that benzoxaborole-6-carboxamide compounds are potent inhibitors against *T. brucei* strains *in vitro*. Optimizing the pharmacokinetic properties through medicinal chemistry studies led to the discovery of SCXY-7158 (**3.7**) (Figure 3.2).[85] Subsequent *in vivo* studies showed a 100% cure rate in mice following a seven-day regimen of i.p. injections dosed at 25 mg/kg. These studies found that drug concentrations in the brain remained well above the minimum inhibitory concentration (MIC = 0.95 μg/mL) for 24 hours, indicating that SCYX-7158 (**3.7**) could be useful towards the treatment of stage two HAT. In 2012, SCYX-7158 (**3.7**) entered Phase II/III clinical trials, for evaluation of efficacy in humans.[86]

Figure 3.2. HAT treatments currently under clinical evaluation

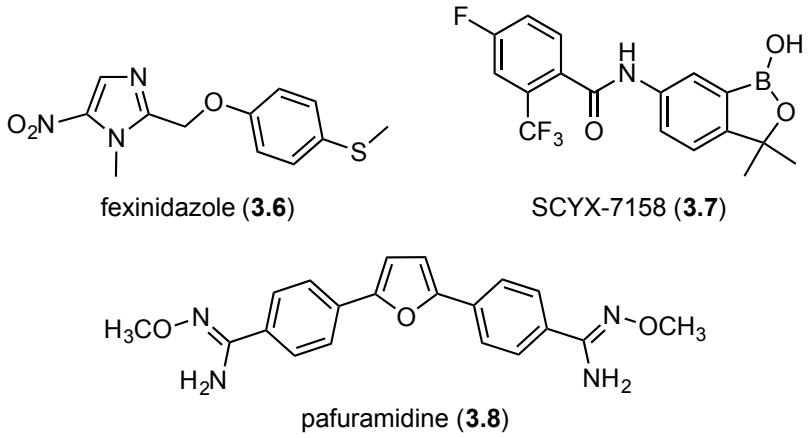

Bisamidine compounds, such as pentamidine (**3.2**), have long been known to treat HAT. Recently, phase III clinical trials of the bisamidine pafuramidine (**3.8**) have concluded (Figure 3.2).[94] This trial found that pafuramidine (**3.8**) was comparable to pentamidine (**3.2**) in treatment efficacy, curing 84% of patients, as compared to 89% cured for pentamidine (**3.2**). However, pafuramidine (**3.8**) exhibited lower levels of nephrotoxicity, with respect to pentamidine (**3.2**). Given the negative side-effects of pentamidine (**3.2**), pafuramidine (**3.8**) could provide a safer treatment alternative for first stage HAT infections.

3.2. AMINOACYL-TRNA SYNTHETASES AS DRUGGABLE TARGETS

A rapidly emerging method for the treatment of infectious diseases is the design of drugs that inhibit aminoacyl-tRNA synthetases (aaRS) of pathogenic organism. Due to the important role that aaRS play in protein synthesis, their inhibition is detrimental to

cell viability.[95] This makes aaRS enzymes particularly attractive drug targets for several reasons.[96]

1. The evolutionary divergence between prokaryotic and eukaryotic aaRS enzymes has led to significant structural differences, which allows for the ability to selectively inhibit prokaryotic aaRS.
2. Many aaRS enzymes are highly conserved across most pathogenic bacterial strains, leading to the potential design of compounds with broad-spectrum antibiotic activity profiles.
3. The 20 different aaRS enzymes found within most pathogenic bacteria lead to 20 different potentially druggable targets.
4. Most of these enzymes are soluble, stable, and easily purified on large scale from recombinant expression systems, thus allowing for easy *in vitro* evaluation.
5. X-ray structures for most of the aaRS enzymes have been solved, therefore allowing a platform for rational drug design approaches.

This approach has been validated through the success of the antibiotic mupirocin (**3.9**), which is currently used as a topical treatment against methicillin resistant *Staphylococcus aureus* (MRSA) (Figure 3.3). Mupirocin (**3.9**) selectively inhibits the isoleucyl-tRNA synthetase (IleRS) of archaea and bacteria, resulting in prokaryotic cell death, with no observable effect to eukaryotic IleRS.[97,98]

Figure 3.3. Antibiotic mupirocin (**3.9**), a selective aaRS inhibitor

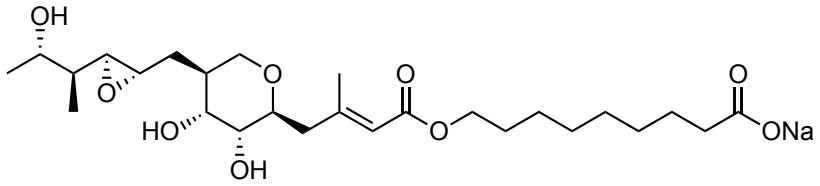

mupirocin (**3.9**)

3.2.1. Aminoacyl-tRNA Synthetases In Protein Translation

The major role of aaRS enzymes is to charge a specific tRNA with the respective amino acid for use in protein translation. This process occurs in two main steps. In the first step, the respective amino acid (AA) and a molecule of ATP bind to the aaRS (Equation 3.1). Attack of the amino acid carboxylate onto the α-phosphate of the proximal ATP, forms the aaRS bound amino acid-adenylate (aaRS•AA•AMP) with concomitant leaving of a molecule of pyrophosphate (PP_i). In the second step, the hydroxyl group of a terminal adenosine from the respective tRNA adds into the amino acid, resulting in 3'-esterification of the amino acid by the tRNA, and the displacement of a molecule of AMP (Equation 3.2). Finally, this charged $tRNA^{AA}$ molecule is released from the aaRS and can bind to the translation elongation factor for transport to the ribosome for subsequent translation.[99]

$$\boldsymbol{AA + ATP + aaRS \leftrightharpoons aaRS \bullet AA \bullet AMP + PP_i} \quad \textbf{(3.1)}$$

$$\boldsymbol{aaRS \bullet AA \bullet AMP + tRNA \leftrightharpoons aaRS + tRNA^{AA} + AMP} \quad \textbf{(3.2)}$$

3.2.2. Previously Reported Methionyl-tRNA Synthetase Inhibitors

In the design of antibiotics that possess novel mechanisms of actions, the selective inhibition of bacterial methionyl-tRNA synthetase (MetRS) is particularly attractive. The MetRS enzyme is unique, compared to other aaRS enzymes, in that MetRS is not only essential for translation elongation, but is also critical for translation initiation. Given that methionine is the first amino acid in protein synthesis, the disruption of a cells ability to charge $tRNA^{Met}$ has the potential to completely shut down protein synthesis within the cell.[100]

Through a series of a high throughput screening (HTS) experiments, it has been shown that the 1,3-diaminoquinolinone motif is quite effective at inhibiting bacterial MetRS. The potential value of this structural motif for MetRS inhibition, led Lee and coworkers pursue structure-activity relationship (SAR) studies towards optimizing these compounds. They discovered that compound **3.10** (Figure 3.4) efficiently inhibited *S. aureus* MetRS, with an IC_{50} = 1.09 nM. Subsequent cell assays showed that this compound possessed *in vitro* activity against MRSA with a 50% effective concentration (EC_{50}) of 16 nM, and was even more potent towards *Enterococcus faecalis* (MIC = 0.5-1 nM).[101]

A separate HTS experiment and subsequent SAR lead optimization studies, identified REP8839 (**3.11**) (Figure 3.4) as a potent MetRS inhibitor towards gram positive and gram negative bacteria. Currently, REP8839 (**3.11**) is being prepared for clinical trials as a topical antibiotic with particular interest in its activity against

mupirocin-resistant MRSA. Preclinical evaluations have found that REP8839 (**3.11**) exhibits a very good broad spectrum antibiotic profile. The MIC values for a number of bacterial strains were determined: *S aureus* strains ranged from 0.033 μM to 2.2 μM, a number of *Streptococcus* species (including *pneumoniae*) had a MIC from 0.015 μM to 2.2 μM, and *Enterococcus faecalis* as well as *Enterococcus faecium* had MIC from 0.033 μM to 0.26 μM.[98] Following reports of MetRS inhibition in novel antibiotics, and the power of the 1,3-diaminoquinolinone motif in this respect, it is not surprising that studies of these compounds towards their use for the treatment of neglected diseases would soon follow.

Figure 3.4. Examples of previous bacterial MetRS inhibitors

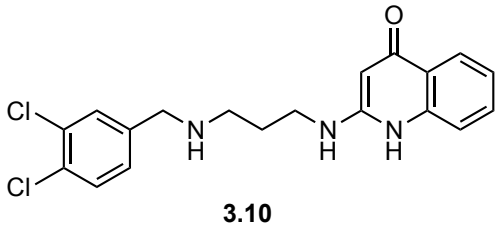

3.10

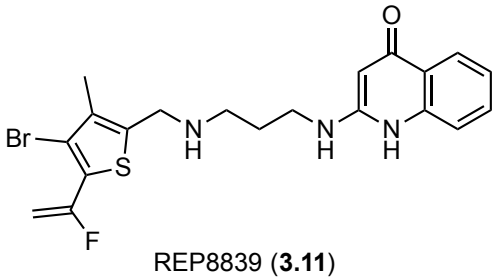

REP8839 (**3.11**)

3.2.3. *Trypanosoma brucei* MetRS Inhibition

Recent studies suggest that inhibition of MetRS in *T. brucei* could be a useful method to treat HAT. Shibata et. al. demonstrated, through RNAi knockdown of the single *T. brucei* methionyl-tRNA synthetase (*Tb*MetRS) enzyme, that inhibition of *Tb*MetRS is deadly to the parasite, and thus a potentially useful method to treat HAT.[102]

This group designed the first reported class of *Tb*MetRS selective inhibitors, coined the aminoquinolinone-based inhibitors (ABIs), which have the general structure shown in Figure 3.5. The most potent of these ABIs was **3.12** with an EC_{50} of 4 nM in *T. brucei* cell assays.[102,103] Unfortunately, due to the poor bioavailability of these ABIs, they were unable to cross the BBB, and would therefore be ineffective at treating late stage HAT.

Figure 3.5. General structures of aminoquinolinone-based (ABI) and urea-based (UBI) *Tb*MetRS inhibitors

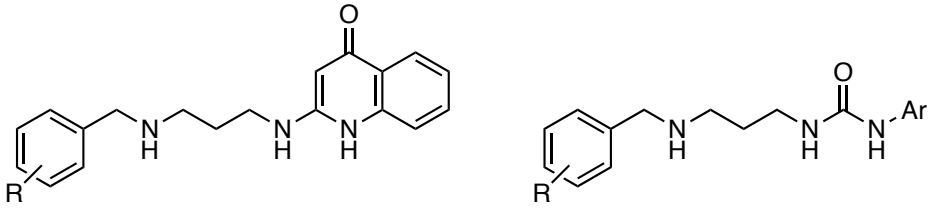

ABI
3.12: R = 3,5-dichloro

UBI
3.13: R = 3,5-dichloro
Ar = 3-thiophene

A related class of *Tb*MetRS inhibitors from the same group was the urea-based inhibitors (UBIs) (Figure 3.5). Of these inhibitors, the most efficacious was found to be **3.13** with an EC_{50} = 150 nM for *in vitro T. brucei* assays.[82,104] While the UBIs were less efficacious than the ABIs, with respect to *Tb*MetRS inhibition, the UBIs possessed more favorable pharmacokinetic properties such as a high oral bioavailability and the ability to cross the BBB. Unfortunately, infected mice treated with **3.13** only survived an average of one day longer than control subjects.[104]

Given the recent problems with drug resistant *T. brucei* strains, new HAT treatments must mitigate the potential for the development of drug resist parasites. In a

recent induced resistance study by Shibata, they found that *T. brucei* strains grown *in vitro*, in the presence of pentamidine (**3.2**), eflornithine (**3.4**), ABI **3.12**, and UBI **3.13,** respectively, developed resistance for pentamidine (**3.2**) and eflornithine (**3.4**) more than twice as quickly as **3.12** or **3.13**. In fact, the *T. brucei* strains grown in **3.12** were unable to reach the experimental threshold of resistance over a 130-day period. Furthermore, previous studies have shown that drug resistance towards pentamidine (**3.1**) and eflornithine (**3.4**) arises from a mutation to the respective membrane transport protein, thus impeding the uptake of each drug into the parasite.[105,106] However, resistance towards **3.12** and **3.13** was found to arise from an overexpression of *Tb*MetRS within the resistant *T. brucei* strains. The overexpression of *Tb*MetRS resulted in a diminished ability of the resistant parasite to grow *in vitro*, thereby greatly reducing the capability of these strains to infect mouse models.[107] This study showed that a HAT treatment, which inhibits *Tb*MetRS, could lead to the slower formation of drug resistant parasites with a weakened ability to infect a host, relative to the pentamidine (**3.1**) or eflornithine (**3.4**) resistant parasites. These findings have created an academic footrace towards the develop new HAT treatments targeting *Tb*MetRS.

3.3. Multicomponent Assembly Process (MCAP): A Combinatorial Approach to Drug Discovery

3.3.1. Diversity Oriented Synthesis

In the search for new medicines or drug lead compounds, the diversity oriented synthesis (DOS) approach is commonly used. In these studies, a wide range of structural

motifs are accessed through a short series of synthetic manipulations. Often used to develop libraries of structurally diverse compounds that can then undergo biological screening, this method has shown great utility in discovering new potential drug lead compounds.[108–112]

Typically, a DOS scheme will involve a reaction or sequence of reactions that can be used with a number of substrates tolerating a range of functional groups. Subsequent manipulations of these functional groups allows for the assembly of a wide range of different heterocyclic moieties. Finally, diversification of each unique scaffold using strategically placed functionalities, allows for the expedient synthesis of libraries of structurally diverse compounds. These synthetic strategies are referred to as "build, couple, pair" (Scheme 3.1).[112] Namely, the starting materials are "built" by installing the requisite functional groups for subsequent cyclizations and derivatization. This is followed by "coupling" of these materials to form the cyclization precursors. Finally, the functional groups on these precursors are "paired" in the sense that cyclization and/or derivatization of the chosen functional groups will lead a diverse set of structural motifs.[112,113]

Scheme 3.1. Schematic illustration of the "build, couple, pair" strategy in DOS studies

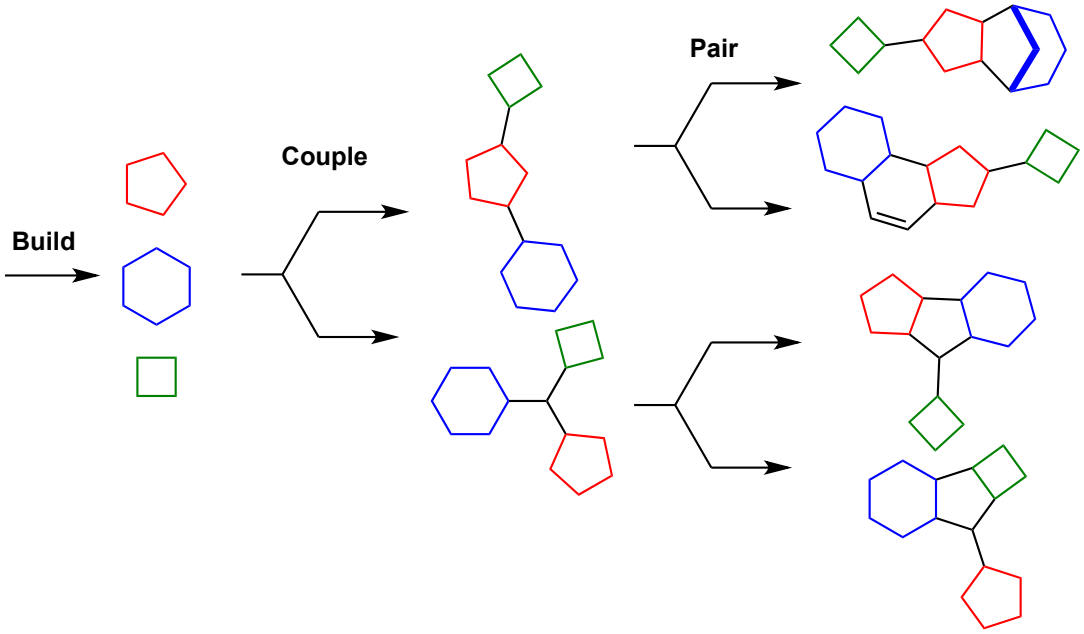

3.3.2. MCAP vs. MCR

In order to quickly access these chemically diverse libraries the use of multicomponent assembly processes (MCAP) and multicomponent reactions (MCR) is key. Multicomponent assembly processes (MCAP) refer to one-pot procedures in which three or more substrates and/or reagents are added in a specific sequence to carry out the given transformation(s).[114–118] In contrast to the sequential nature of the MCAP, multicomponent reactions (MCR) require the simultaneous addition of three or more substrates and/or reagents to perform the given transformation(s). These types of reactions utilize relatively simple building blocks to facilitate cyclization reactions of the paired functional groups. These powerful methods can quickly access chemical libraries

possessing a significant degree of molecular complexity, and have been extensively reviewed.[40–50]

3.4. Previous Work in the Martin Lab

3.4.1. Vinylogous Mannich Reaction: MCAP Inspiration

Early work in the Martin lab, focused on the synthesis of heteroyohimbine alkaloids (±)-tetrahydroalstonine (**3.14**), (±)-cathenamine (**3.15**) and the corynantheioid alkaloid (±)-geissoschizine (**3.16**) (Figure 3.6), eventually led to the development of a highly generalizable MCAP procedure. The synthesis of these natural products revolved around a key MCAP involving a vinylogous Mannich reaction to form a triene that underwent an intramolecular Diels-Alder cycloaddition.[130,131]

Figure 3.6. Natural products that inspired the Martin group MCAP procedure

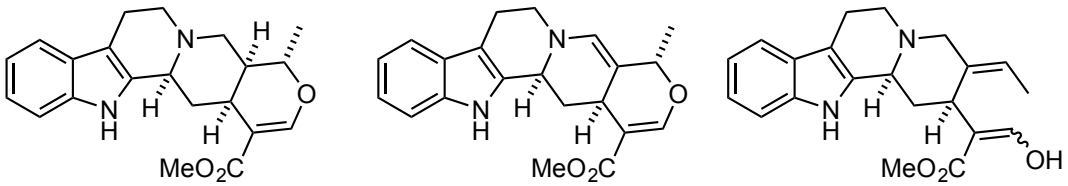

(±)-tetrahydroalstonine (**3.14**) (±)-cathenamine (**3.15**) (±)-geissoschizine (**3.16**)

In this study, dihydro-β-carboline **3.17** was treated sequentially with *trans*-crotonoyl chloride and 1-[(trimethylsilyl)oxy]butadiene to give triene **3.18** (Scheme 3.2). Holding a solution of **3.18** in mesitylene under reflux gave a mixture of cis:trans isomers (9:1, ring fusion) in 89% yield over two steps, with **3.19** as the major product. From **3.19**

a two-step procedure previously used in the Martin laboratory[132–134] installed the vinyl methyl ester moiety in 66% yield to give intermediate **3.20**.

Scheme 3.2. Martin synthesis of common intermediate **3.20**

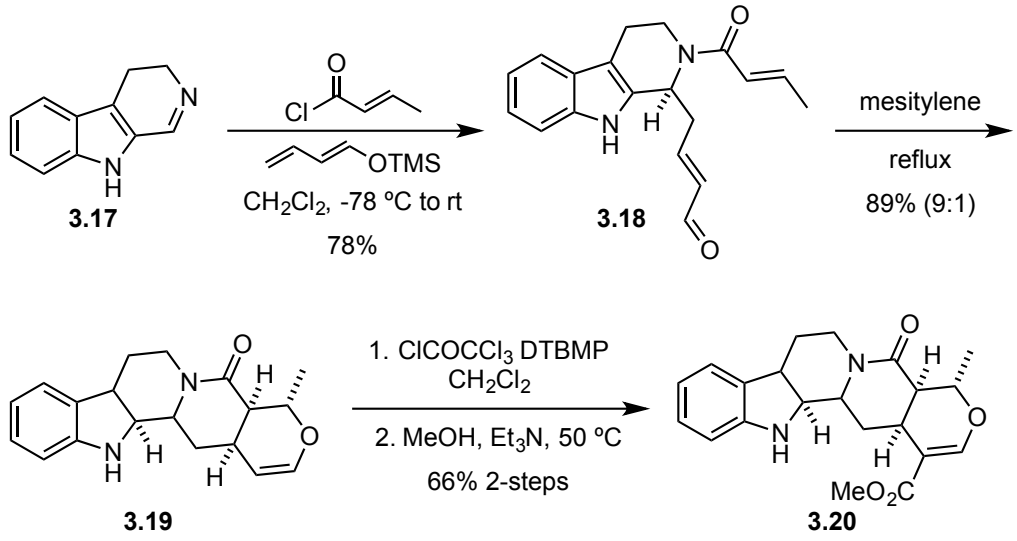

The synthesis of intermediate **3.20** elegantly set the stage for quick access to the heteroyohimbine and corynantheioid alkaloids. Treatment of **3.20** with alane followed by addition of 2% methanolic acetic acid and excess sodium cyanoborohydride gave (±)-tetrahydroalstonine (**3.14**) in 90% yield (Scheme 3.3). Alternatively, treatment of **3.20** with lithium diethoxyaluminum hydride gave (±)-cathenamine (**3.15**) in 70% yield. Finally, (±)-geissoschizine (**3.16**) was synthesized in a two-step procedure, by treating **3.20** with sodium amide, followed by the sequential addition of lithium hexamethyldisilazide, triethylaluminum, and diisobutylaluminum hydride, to give (±)-geissoschizine (**3.16**) in 35% yield.

Scheme 3.3. Synthesis of heteroyohimbine and corynantheioid alkaloids

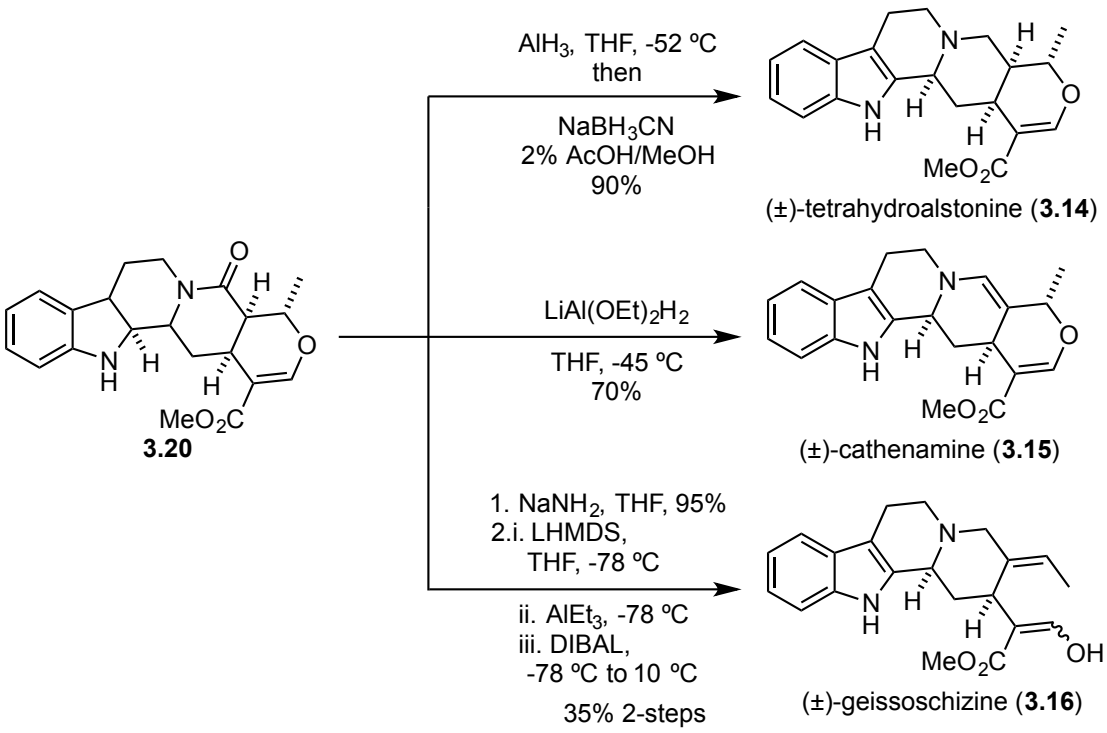

The total syntheses of the three title compounds were elegantly achieved in five- to six-steps from commercially available dihydro-β-carboline (**3.17**). The vinylogous Mannich reaction with *trans*-crotonoyl chloride and 1-[(trimethylsilyl)oxy]butadiene installed the requisite functionalities that underwent the intramolecular Diels-Alder cycloaddition, allowing access to the heteroyohimbine and corynantheioid cores in just two steps with high yield. This sequence was later generalized as a MCAP to synthesize a diverse library of small molecules with the goal of discovering new drug leads.[135]

3.4.2. MCAP and NIH Molecular Libraries Program

Scheme 3.4. Generalized Martin MCAP strategy

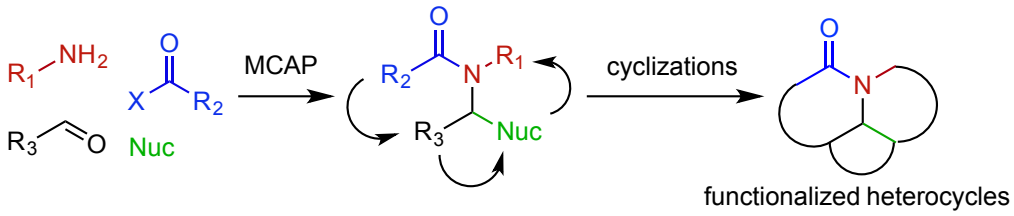

Almost two decades after the syntheses of heteroyohimbine and corynantheioid natural products, the same synthetic strategy was generalized to form an extensive library of small molecules. These compounds were then screened in a number of cell and enzyme based assays to identify new potential drug lead compounds. Scheme 3.4 shows the generalized strategy in which arylaldehydes (R_3CHO) were condensed with a primary amine (R_1NH_2) to form an imine *in situ*, and acylation (R_2COX) led to a transient acyl-iminium ion that was subsequently attacked by a nucleophile (Nuc). In each example of this MCAP procedure the substituents of each fragment were carefully selected to predispose the resulting motif to a variety of cyclizations and/or cycloadditions. The aforementioned cyclization reactions included, ring closing metathesis, intramolecular Heck coupling, Dieckmann condensation, intramolecular Diels-Alder cycloadditions, [3+2]-dipolar cycloadditions, and intramolecular Friedel-Crafts alkylations. A library of more than 1,000 functionalized heterocyclic compounds was synthesized throughout the course of this work.[136–148]

3.4.3. MCAP Leads to Trypanocidal Hit Compounds

Throughout the course of our MCAP based DOS program, a number of tetrahydro-β-carboline based small molecules were synthesized.[135,149] In one iteration of this sequence, dihydro-β-carboline (**3.17**) was treated with *trans*-crotonoyl chloride and TBS-silyl enol ether in the presence of TMS-triflate to give **3.21** (Scheme 3.5). Crude **3.21** was then heated with N-methylhydroxylamine hydrochloride and triethylamine in toluene to afford the [3+2]-dipolar cycloaddition adduct **3.22** in 60% yield over two steps. At this point, **3.22** was then reduced with lithium aluminum hydride to give **3.23** in 98% yield. Both **3.22** and **3.23** were treated with nickel boride to give β-amino alcohols **3.24** and **3.25** in 68% and 64% yields, respectively. Compounds **3.24** and **3.25** were further derivatized at the secondary amine position to form the corresponding amides, ureas, tertiary amines, and sulfonamides.

Scheme 3.5. Dihydro-β-carboline MCAP diversification

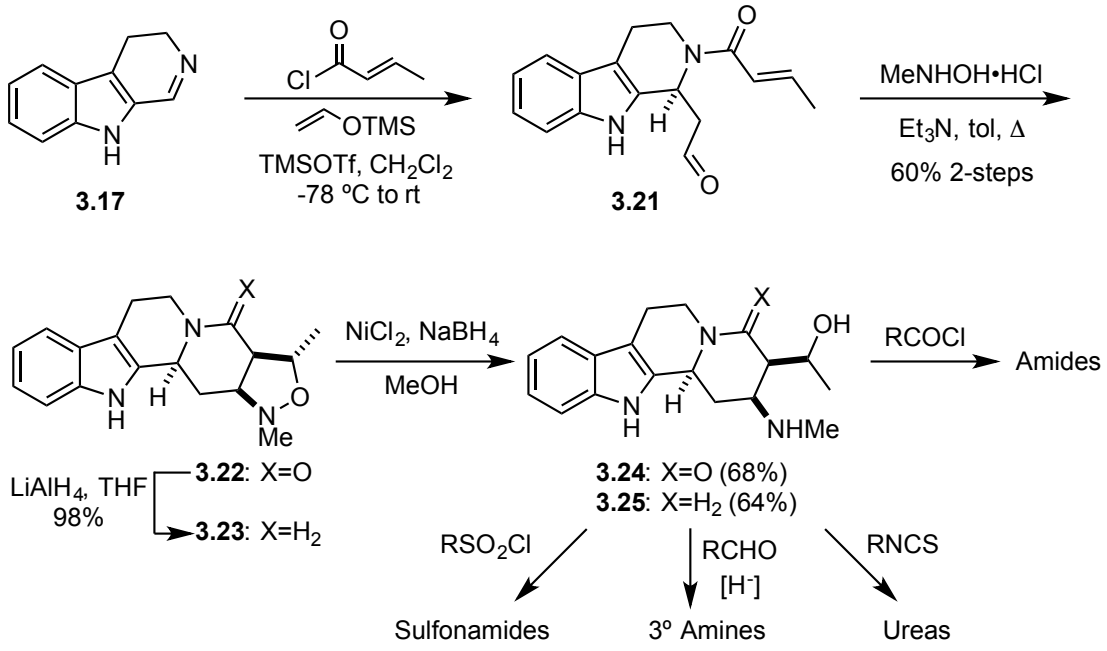

This approach provided a library of >180 of yohimbine- and corynantheioid-type compounds, which were screened for potential biological activities. These tests identified two compounds, **3.26** and **3.27**, that inhibited *Tb*MetRS in sub-micromolar concentrations with IC_{50} value of 586 nM and 297 nM, respectively (Figure 3.7). Further evaluation in *T. brucei* cell based assays, found that **3.26** and **3.27** displayed EC_{50} values of 2 μM and >10 μM, respectively. Given the recent success of aaRS inhibitors in disease treatment and the evidence supporting *Tb*MetRS as a viable drug target, we decided to undertake studies towards the optimization of **3.26** and **3.27** as potential drug leads for the treatment of human African trypanosomiasis.

Figure 3.7. Trypanocidal hit compounds from MCAP DOS

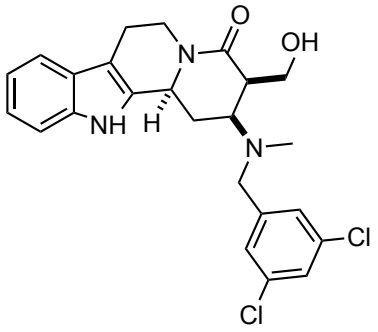

3.26
*Tb*MetRS IC_{50} = 586 nM
T. brucei EC_{50} = 2 μM

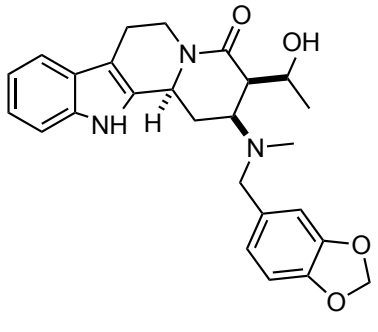

3.27
*Tb*MetRS IC_{50} = 297 nM
T. brucei EC_{50} >10 μM

In attempting to develop a more effective drug candidate for the treatment of HAT, our first objective was to design compounds with increased *Tb*MetRS inhibition. This is being accomplished through the systematic design of compounds that include or exclude given functionalities of the hit compounds. The resulting IC_{50} and EC_{50} values of these new compounds will reveal which functionalities are beneficial or detrimental towards *Tb*MetRS inhibition. A secondary objective is to simplify the molecular complexity of the new compounds, while maintaining biological activity. This will allow for a more efficient synthesis, thus improving the likelihood of the compound being economically viable for large-scale production. Given the low profit margins of drug candidates designed to treat neglected tropical diseases, a synthetically cheap and easy target is important.

Chapter 4: Studies Towards New Compounds with Trypanocidal Activity

4.1. Rational Drug Design: Lead Compound

At the onset of this project, we wanted to optimize our initial hit compounds that inhibited the *Tb*MetRS enzyme as well as improve their activity towards killing the parasite on a cellular level. To this end, we took careful consideration of the molecular features from our active compounds, as well as the molecular features of structurally similar compounds that were inactive towards *Tb*MetRS. We also analyzed previously reported crystal structures of inhibitor-bound *Tb*MetRS to aid in the design of our new inhibitors.

4.1.1. Previous Martin Group Compounds: What Works and What Doesn't

When designing new compounds with the goal of optimizing biological activity, it is arguably just as important to consider the molecular functionalities of inactive compounds, as it is the active compounds. To this end, there were a number of compounds structurally similar to our hit compounds **4.1** - **4.3** (Figure 4.1), that were synthesized and tested during the course of our MCAP based DOS program that informed the current project.

Figure 4.1. Initial hit compounds and relevant inactive compounds

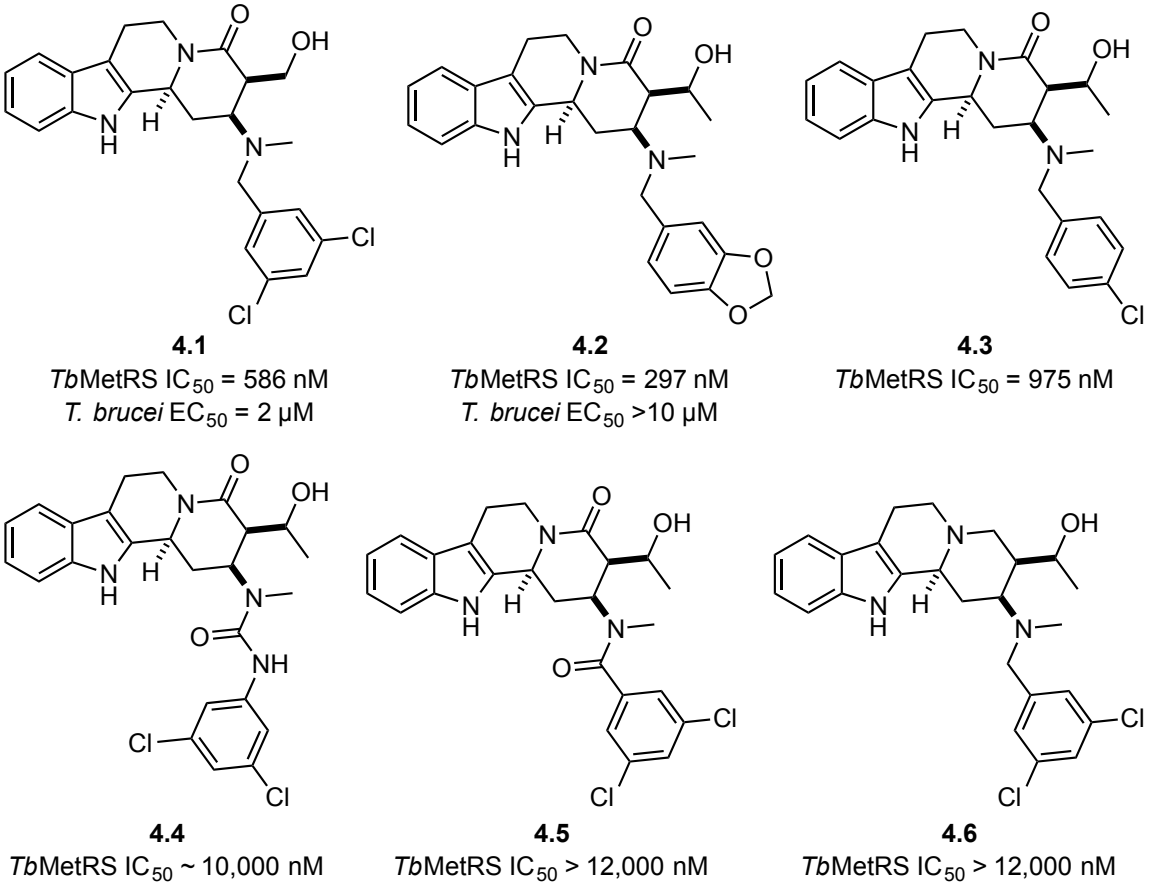

By considering the compounds shown in Figure 4.1, we started to get a preliminary idea of the structure activity relationship (SAR) of our scaffold relative to *Tb*MetRS inhibition. Compounds **4.1**, **4.2**, and **4.3** displayed inhibition of *Tb*MetRS at sub-micromolar concentrations. Each of these compounds possesses a 2-piperidinone motif with δ-benzylamino alcohol functionality. Interestingly, we found a large drop in activity towards *Tb*MetRS inhibition with compounds **4.4** - **4.6**. Compound **4.4** was the only compound of these three to show any activity against *Tb*MetRS, with an IC_{50} value

around 10 μM. Structurally, the only difference between the active compounds and **4.4**/**4.5** was the *N*-carbonyl moiety in the D-ring. Both the urea functionality in **4.4** and the amide functionality of **4.5** reduce the basicity of the nitrogen substituent and led to a steep drop in biological activity. Conversely, when the 2-piperidinone motif was reduced to the basic piperidine, as in **4.6**, we observed a complete loss of *Tb*MetRS inhibition up to 12 μM concentration. These results led to the hypothesis that the benzyl-substituted tertiary amine and the 2-piperidinone moieties were required for effective inhibition of *Tb*MetRS.

As a quick follow up to the previous set of compounds, the structurally simplified compounds **4.7** - **4.10** were synthesized and evaluated for inhibition of *Tb*MetRS (Figure 4.2). These compounds were designed to test whether a *N*-benzyl-4-amino-2-piperidinone core would retain biological activity. Unfortunately, all of these compounds were completely inactive towards *Tb*MetRS. There are two key molecular differences between compounds **4.7** - **4.10** and our active compounds **4.1** - **4.3**. The first, is that the *N*-indolylethyl moiety on the 2-piperidinone core was changed to an *N*-benzyl group. This benzyl group adds hydrophobicity to the compounds and lacks a hydrogen bond donor, which was present in the indole moiety, and could contribute to the observed loss in binding towards *Tb*MetRS. Secondly, the methylene hydroxy substituent at the α-position of the 2-piperdinone was omitted. This also removed a potential hydrogen bond donor from the core and could contribute to loss in binding affinity towards *Tb*MetRS.

Figure 4.2. Inactive 4-amino-2-benzylpiperidinone compounds

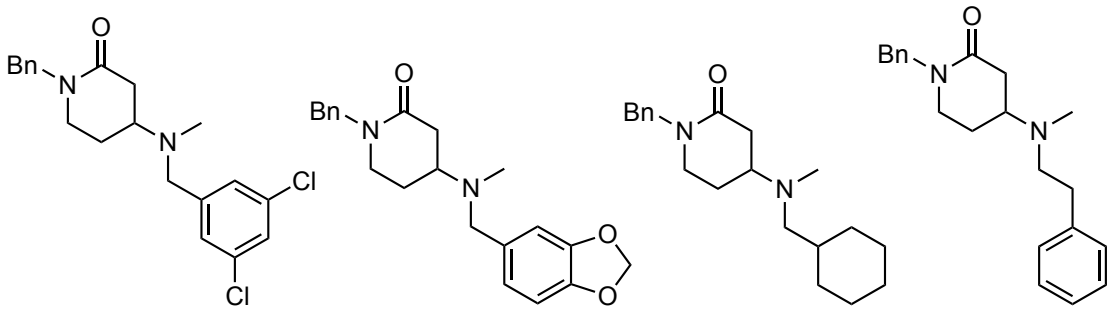

4.1.2. Crystallographic Data in the Design of Target Compound

With our follow up compounds showing no inhibition of *Tb*MetRS, we decided to look at crystallographic data from previously reported *Tb*MetRS inhibitors. The crystal structure of UBI inhibitor **4.11** bound to *Tb*MetRS is shown in Figure 4.3. The crystal structure shows **4.11** binding into two discrete pockets within the *Tb*MetRS active site. The 3,5-dichlorobenzyl moiety occupies the methionine binding pocket and inhibits *Tb*MetRS through competitive binding. Interestingly, the opposite termini of **4.11** contains a planar heteroaromatic moiety (3-thiophene), which binds in what is referred to as the "auxiliary binding pocket".[103] This auxiliary binding pocket was found to form upon complexation of **4.11** with *Tb*MetRS, thus leading to the proposal of an induced-fit mode of binding for this protein-ligand interaction. Based on the crystallographic data, Shibata suggested that a planar heteroaromatic moiety is required at the terminus of the inhibitor in order to fit into the auxiliary binding pocket. [82,103]

Figure 4.3. X-ray crystal structure of UBI inhibitor **4.11** bound to *Tb*MetRS (pdb: 4mvw)

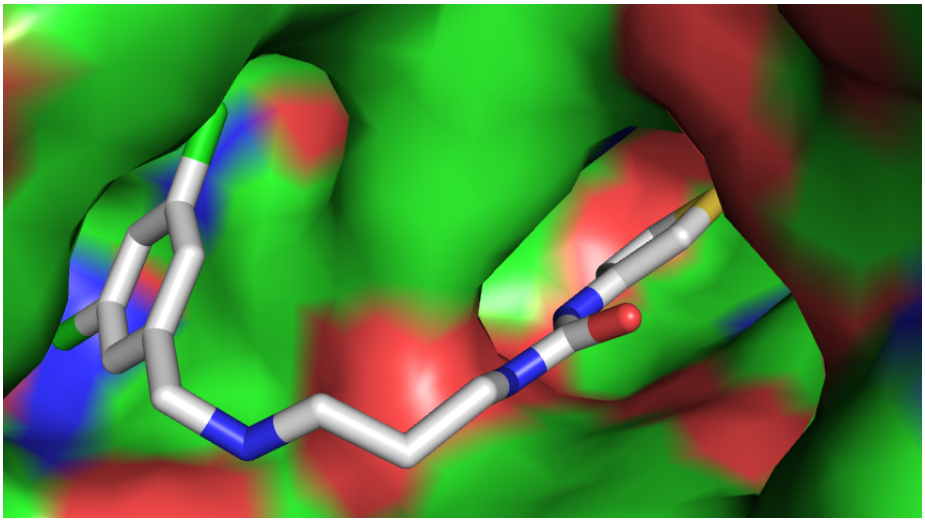

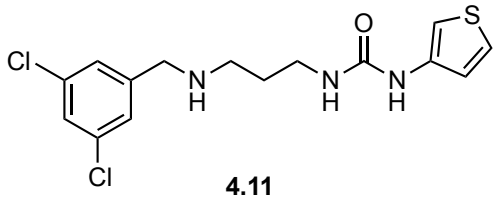

4.11

In the process of designing our first target compound, we considered how the active compound **4.1** might be binding to *Tb*MetRS. Given that **4.1** and **4.11** both possess a dichlorobenzylamine substituent on one terminus of the molecule and a heteroaromatic moiety at the other, we postulated that **4.1** could be binding to *Tb*MetRS in an analogous fashion to **4.11**. To obtain a graphical representation of how **4.1** might be binding to *Tb*MetRS, colleague Lance Lepovitz performed shape complementary-based molecular docking studies. Even though these docking studies did not predict binding energies, they provided a visual representation of how **4.1** might bind to *Tb*MetRS (A, Figure 4.4).

Figure 4.4. A) Shape complementary binding of **4.1** to *Tb*MetRS. B) Overlay of *Tb*MetRS bound to **4.11** (white) and predicted binding of **4.1** (pink)

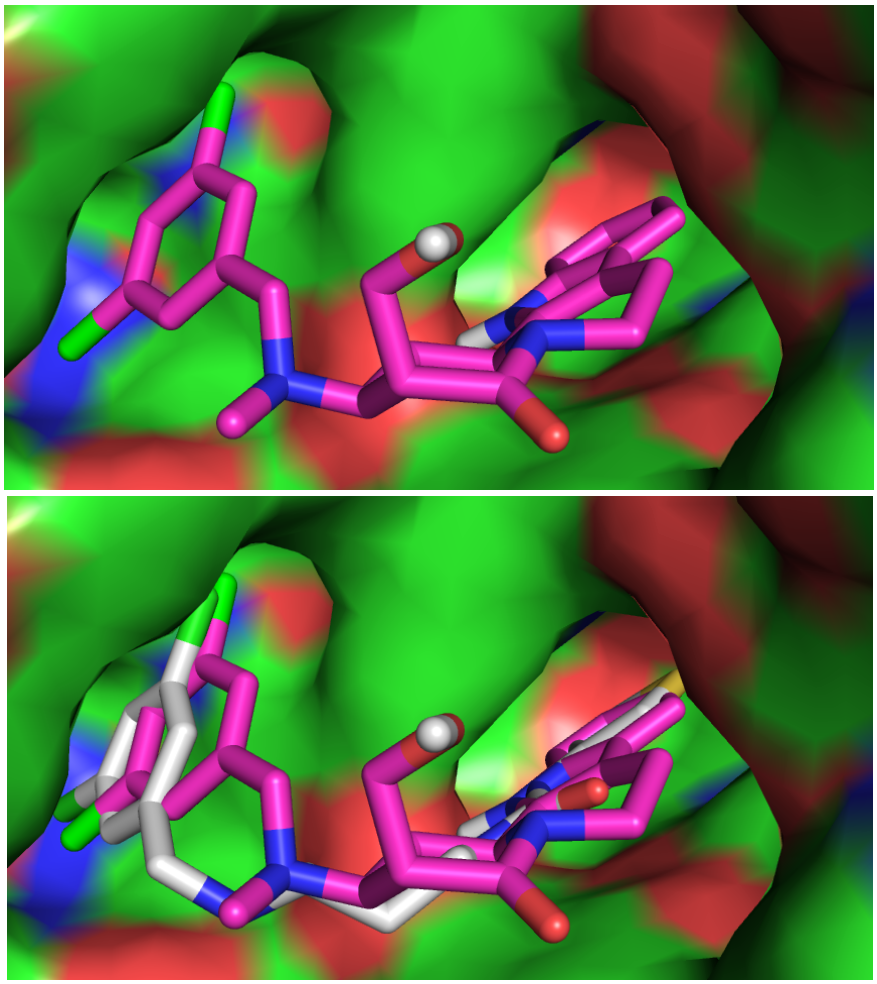

(A)

(B)

In analyzing the graphical representation of **4.1** bound to *Tb*MetRS, we also compared the predicted binding for **4.1** to the actual mode of binding for **4.11** (B, Figure 4.4). We immediately noticed that the tetracyclic yohimbine-like core of **4.1** is quite rigid and contains significantly fewer degrees of rotational freedom than **4.11**. With this notion, we hypothesized that a conceptual "opening" of the tetrahydro-β-carboline ring to

give the analogous tryptamine derivative (Figure 4.5), would increase the conformational flexibility and possibly lead to an increase in binding to *Tb*MetRS.

Figure 4.5. Conceptual "opening" of **4.1** to give our initial target compound **4.12**

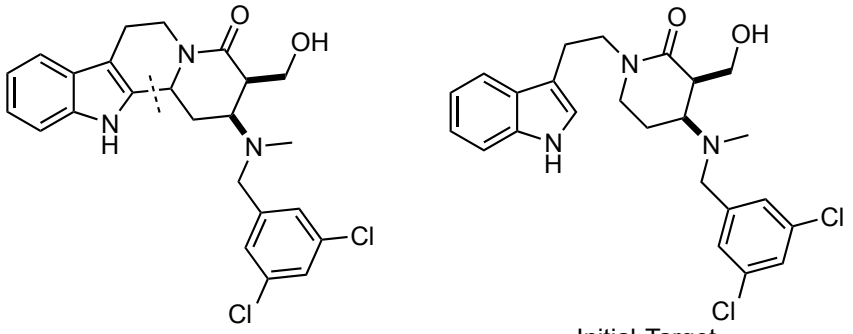

4.1 **4.12**

At this point, Lance Lepovitz performed an analogous set of docking studies to predict how **4.12** might bind to *Tb*MetRS. The shape complementary predicted binding of **4.12** to *Tb*MetRS is shown in Figure 4.6 (A), and an overlay of predicted binding poses of **4.1** and **4.12** is given in Figure 4.6 (B). In comparing the overlay of the predicted binding of **4.1** and **4.12**, it is clear that the two compounds could adopt significantly different conformations upon binding. Though these predicted binding modes are not quantitative representations, they did provide sufficient impetus to undertake studies towards the synthesis and evaluation of **4.12** as a new *Tb*MetRS inhibitor.

Figure 4.6. A) Shape complementary binding of **4.12** to *Tb*MetRS. B) Overlay of the predicted binding of **4.12** (orange) and **4.1** (pink)

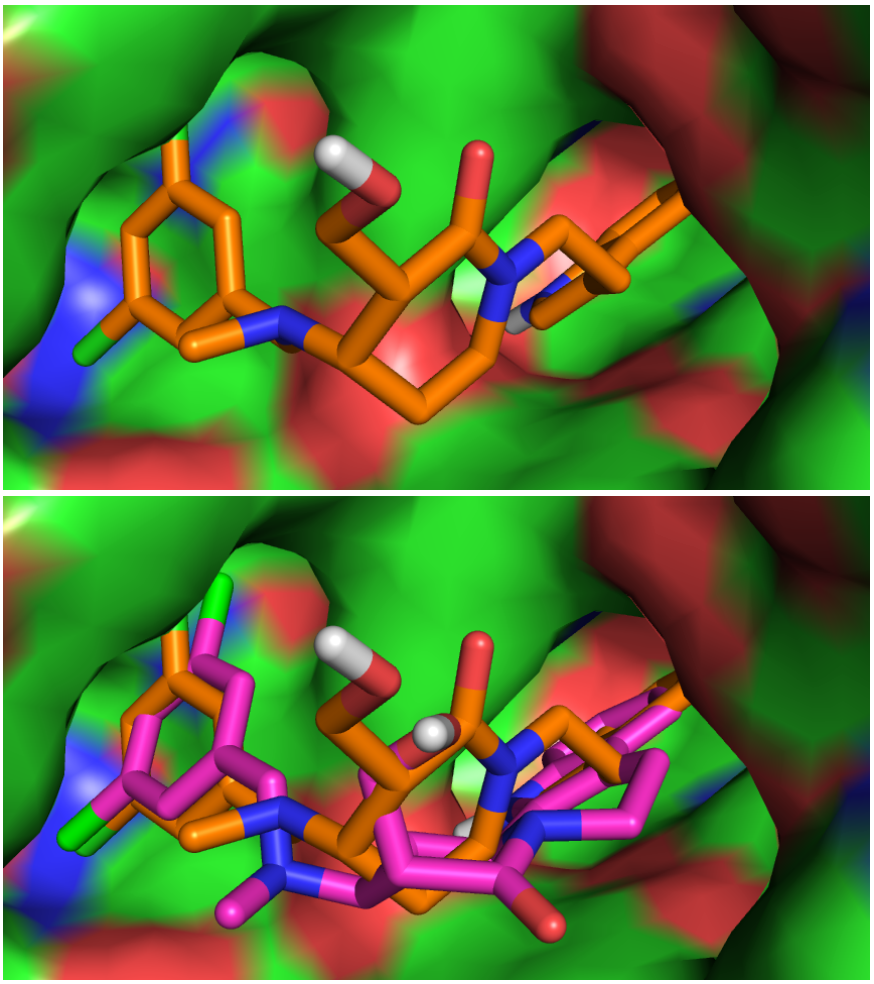

(A)

(B)

4.2. Synthesis of Initial Target Compound

4.2.1. Target Inhibitor: Retrosynthetic Analysis

The initial synthetic strategy to access our target compound **4.12** was designed to allow late stage functionalization of the heteroaromatic and benzylamine moieties, thereby allowing for easy access to diversification (Scheme 4.1). We envisioned that **4.12**

would arise from **4.13** through nucleophilic substitution of the 2-piperidinone nitrogen atom, followed by reductive *N*-*O* bond cleavage and reductive amination. Condensation of *N*-methylhydroxylamine onto **4.14** and subsequent 1,3-dipolar cycloaddition would lead to the isoxazolidine **4.13**. At this stage, we envisaged two potential routes to access aldehyde **4.14**.

Scheme 4.1. Retrosynthetic analysis of target compound **4.12**

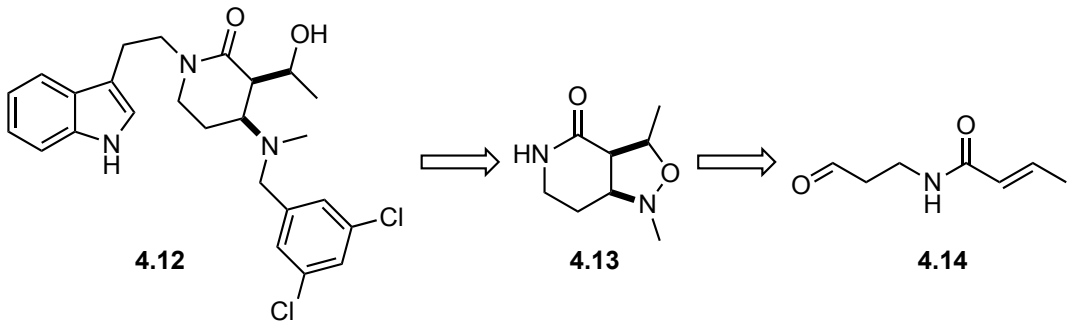

The retrosynthesis of the two proposed routes to access aldehyde **4.14** are shown in Scheme 4.2. In the first route (A), **4.14** would arise from an MCAP-type procedure utilizing crotonoyl chloride and a vinyl silyl enol ether with triazine **4.15**. This route would lead to an *N*-benzyl protected amine requiring an additional deprotection step. Notably, this route would establish the amide moiety and the free aldehyde in one step. In the second route (B), amination of 3-bromopropionaldehyde dimethyl acetal (**4.16**), followed by acylation and deprotection of the aldehyde would give **4.14** in three steps.

Scheme 4.2. Retrosynthetic analysis of intermediate aldehyde **4.14**

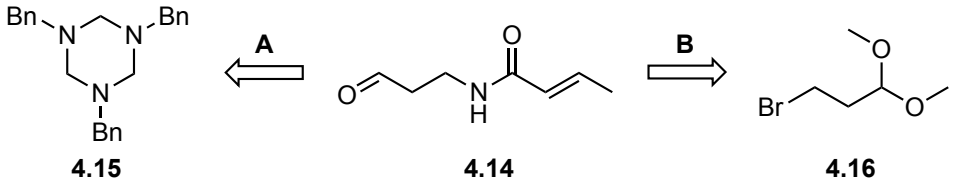

4.15 **4.14** **4.16**

4.2.2. Attempted Synthesis of Aldehyde Precursor

We first set out to synthesize aldehyde **4.14** through an MCAP-type procedure. Benzyl triazine **4.15** was synthesized by condensation of benzylamine and formaldehyde in 64% yield (Scheme 4.3). All attempts at *in situ* acylation of triazine **4.15** and enol ether addition into the resulting transient iminium ion failed to yield more than trace amounts of the desired product **4.17**.

Scheme 4.3. Attempted synthesis of aldehyde **4.17**

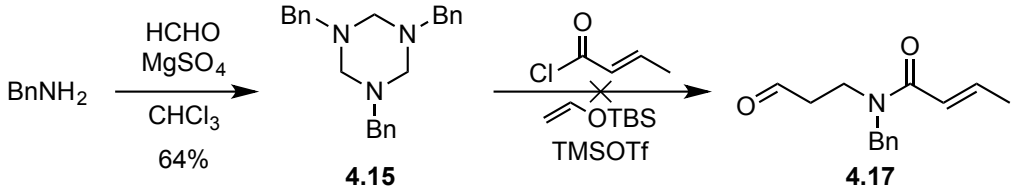

Attempts to access cycloaddition precursor **4.14** with the other proposed route also faced problems. Amination of **4.16** with methanolic ammonia in a sealed tube gave virtually quantitative conversion to hydrobromide **4.18** (Scheme 4.4). Subsequent acylation attempts using either crotonoyl chloride or acryloyl chloride (not shown) were low yielding. This transformation was plagued by two major problems. First, the desired

product **4.19** was water soluble, leading to the isolation of only trace quantities of **4.19** after aqueous work-up. Second, **4.19** was unstable to silica gel chromatography, leading to complex mixtures of **4.19**, free aldehyde **4.14**, and various aldol byproducts. After some experimentation, we were able to isolate **4.19** in 67% yield upon treatment of **4.18** with crotonoyl chloride in a mixture of pyridine and dichloromethane followed immediately by a quick silica plug. However, despite this success, we were unable to cleanly isolate the aldehyde **4.14** upon treatment with acid.

Scheme 4.4. Attempts towards the synthesis of aldehyde **4.14**

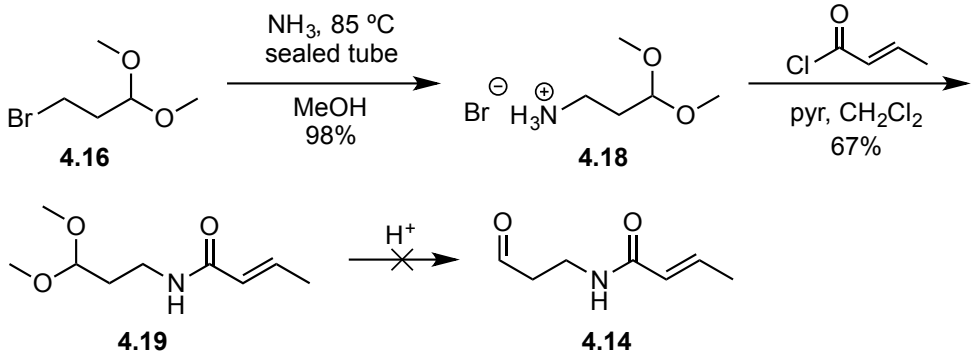

4.2.3. Target Inhibitor: Alternate Retrosynthetic Analysis

In the revised synthetic route towards inhibitor **4.12**, we decided to introduce the indole moiety earlier in the synthesis. While this tactic would limit our ability to diversify the heteroaromatic moiety late in the synthesis, we speculated that early incorporation of the indole might add enough hydrophobicity to the intermediates to limit their solubility in water, thus allowing us to purify via aqueous extraction.

In this route, **4.12** will be formed from reductive *N-O* bond cleavage and reductive alkylation of isoxazolidine **4.20**. Isoxazolidine **4.20** will be accessed via the 1,3-dipolar cycloaddition of **4.21** after aldehyde deprotection and condensation with N-methylhydroxylamine. Finally, **4.21** will be prepared by the reductive amination of **4.22** and **4.18**.

Scheme 4.5. Revised retrosynthetic analysis of target inhibitor **4.12**

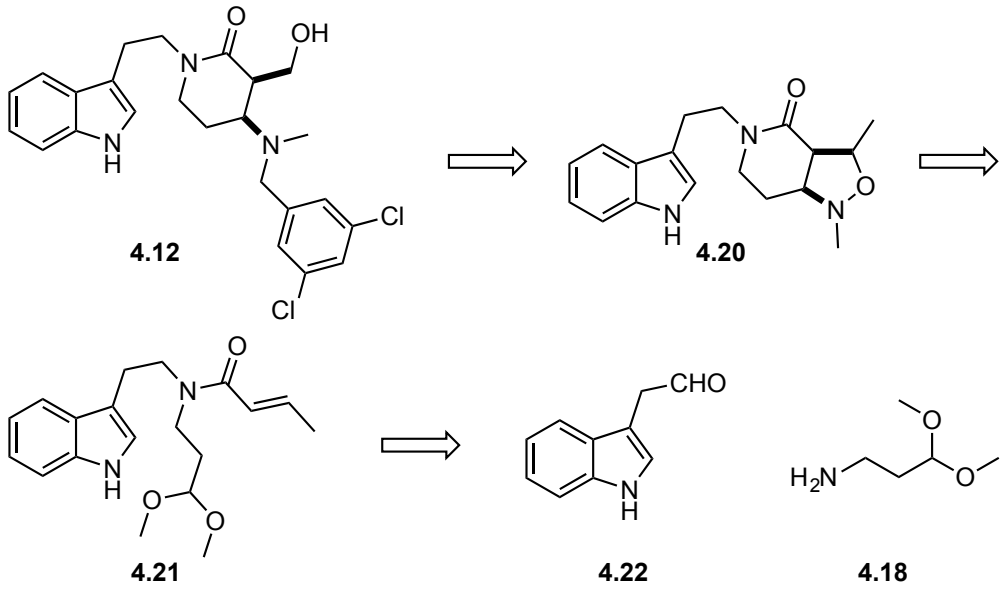

4.2.4. Synthesis Indole-3-Acetaldehyde

We first needed to synthesize indole-3-acetaldehyde (**4.22**), because of the surprisingly high cost ($206 / 100 mg, Sigma-Aldrich). A Fisher-esterification of indole-3-acetic acid (**4.23**) gave methyl indole-3-acetate (**4.24**) in essentially quantitative yield (Scheme 4.6). Subsequent reduction of **4.24** to indole-3-acetaldehyde (**4.22**) using

DIBAL proceeded in yields varying from 40% to 73%. We also found that the yield for this reaction dropped off precipitously on larger scales (>500 mg). The un-scalable and unpredictable nature of this reaction would lead to future studies directed towards circumventing this transformation. However, at the time, this reaction did provide sufficient quantities of **4.22** to pursue the route depicted in Scheme 4.5.

Scheme 4.6. Synthesis of indole-3-acetaldehyde (**4.22**)

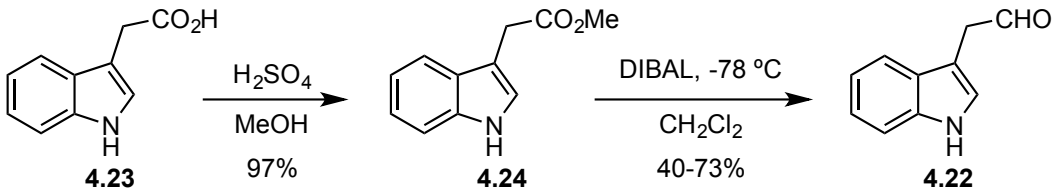

4.2.5. Synthesis of Secondary Amide *via* Reductive Amination

With indole-3-acetaldehyde **4.22** and ammonium bromide **4.18** in hand, we next focused on the synthesis of tertiary amide **4.21**. Reductive amination of **4.22** and **4.18** proceeded with sodium cyanoborohydride to give secondary amine **4.25** in 89% yield (Scheme 4.7). Initially, acylation of **4.25** with crotonoyl chloride and triethylamine at either -78 ºC or 0 ºC gave the desired product **4.21** in 38% and 41% yields, respectively. However, the use of Hünig's base in place of triethylamine at -78 ºC consistently gave **4.21** in 71% yield.

Scheme 4.7. Synthesis of tertiary amide **4.21**

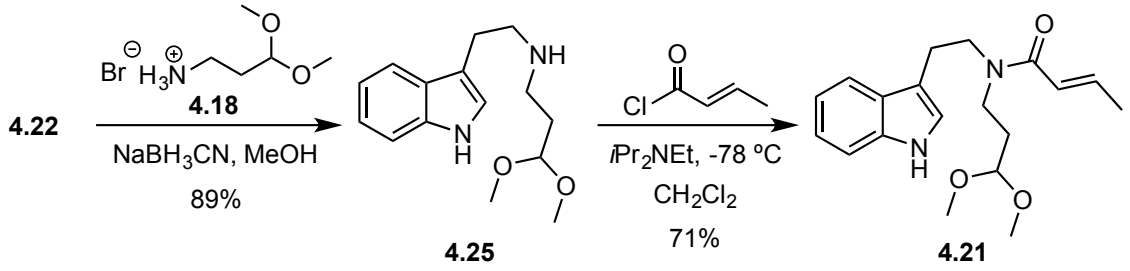

4.2.6. 1,3-Dipolar Cycloaddition

Previous attempts to remove the acetal of **4.19** revealed that the desired aliphatic aldehyde was likely to be unstable towards chromatographic conditions. With this in mind, we attempted a few procedures in which we tried to form aldehyde **4.26** in solution and isolate the crude material to carry onto the 1,3-dipolar cycloaddition. To this end, hydrochloric acid and oxalic acid in various solvents did not yield any quantifiable amounts of the desired aldehyde **4.26**. While pondering this reaction, we realized the dimethyl acetal deprotection was reminiscent of the Pictet-Spengler cyclization discussed in Chapter 2. In the final iteration of the Pictet-Spengler reaction, catalytic trifluoroacetic acid in 2,2,2-trifluoroethanol (TFE) led to the deprotection of a dimethyl acetal *in situ*, which subsequently participated in cyclization. Following this idea, we tried similar conditions and found that treating **4.21** with catalytic trifluoroacetic acid in a mixture of TFE and water (3:1) gave virtually quantitative conversion to **4.26** (as judged by crude ^{1}H-NMR) (Scheme 4.8). Immediately following the isolation of crude **4.26**, we subjected the material to 1,3-dipolar cycloaddition conditions. Heating a solution of crude **4.26**, *N*-

methylhydroxylamine hydrochloride, and triethylamine in ethanol under reflux, gave the desired isoxazolidine **4.20** in 30% yield.

Scheme 4.8. Synthesis of isoxazolidine **4.20**

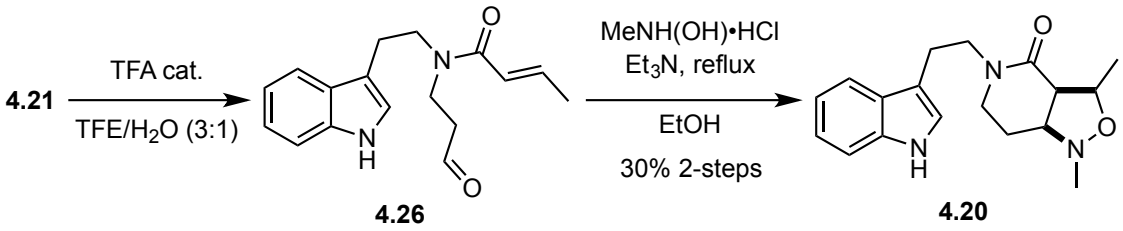

4.2.7. Synthesis of Secondary Amine via Glyoxylamide Reduction

Excited as we were to have isoxazolidine **4.20** in hand, the current synthetic route was not sufficiently scalable to meet our needs. In particular, the reduction of methyl indole-3-acetate (**4.24**) to indole-3-acetaldehyde (**4.22**) was a major bottleneck with respect to synthesizing gram-quantities of material. At the time, two approaches were attempted in parallel. First, we were attempting to synthesize **4.22** via oxidation of tryptophol. This transformation was only attempted twice and was quickly abandoned after positive results from our alternate approach (Scheme 4.9).

Scheme 4.9. Synthesis of amine **4.25** via glyoxylamide **4.27** reduction

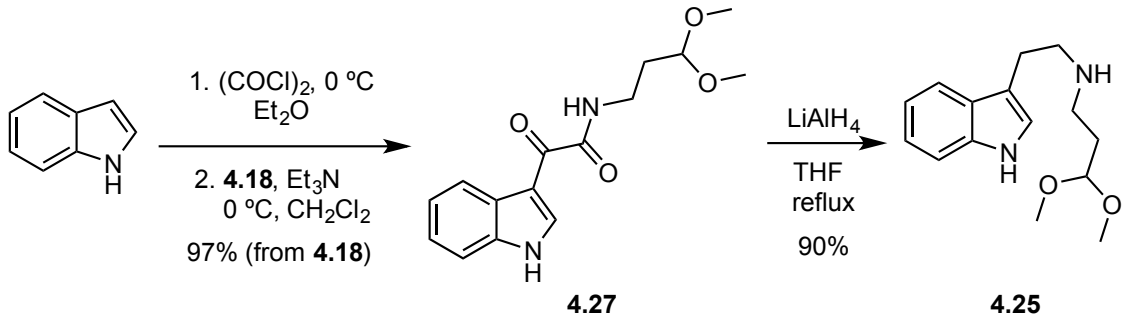

In attempting to develop a scalable synthesis to amine **4.25**, we found that the formation and reduction of glyoxylamide **4.27** was superior in terms of both yield and scalability. Treatment of indole with oxalyl chloride in ice-cold ether led to precipitation of the bright yellow indole-3-glyoxyl chloride. Adding a slurry of indole-3-glyoxyl chloride to an ice-cold solution of **4.18** and triethylamine gave clean conversion to glyoxylamide **4.27** in 97% yield (Scheme 4.9). Heating a solution of **4.27** and lithium aluminum hydride under reflux in tetrahydrofuran led to the formation of amine **4.25** in 90% yield. Despite the fact that the previous reductive amination route was one-step to convert **4.18** to **4.25**, this new route was far superior with respect to reproducibility, scalability, purification (no column chromatography required), and overall yield.

4.2.8. Synthesis of Target Inhibitor

With a scalable route to amide **4.21** in hand, we focused on improving the yield of the 1,3-dipolar cycloaddition. We found that conditions previously reported for the synthesis of **4.1** – **4.6** worked well for our system.[150,151] From amide **4.21**, acetal

deprotection followed immediately by 1,3-dipolar cycloaddition of crude **4.26** using *N*-methylhydroxylamine hydrochloride and triethylamine in toluene gave isoxazolidine **4.20** in 85% yield over two steps (Scheme 4.10). We then used previously reported conditions for reductive *N-O* bond cleavage via *in situ* generation of nickel boride.[140,144,150,151] However, all attempts failed to yield anything more than trace amounts of the desired product **4.28**. We then decided to try a more "classical" approach, and by heating a suspension of zinc dust and **4.20** in acetic acid, we obtained amino alcohol **4.28** in 91% yield. Finally, reductive alkylation of **4.28** and 3,5-dichlorobenzaldehyde with sodium cyanoborohydride and acetic acid gave the target compound **4.12** in 48% yield.

Scheme 4.10. Synthesis of new inhibitor **4.12**

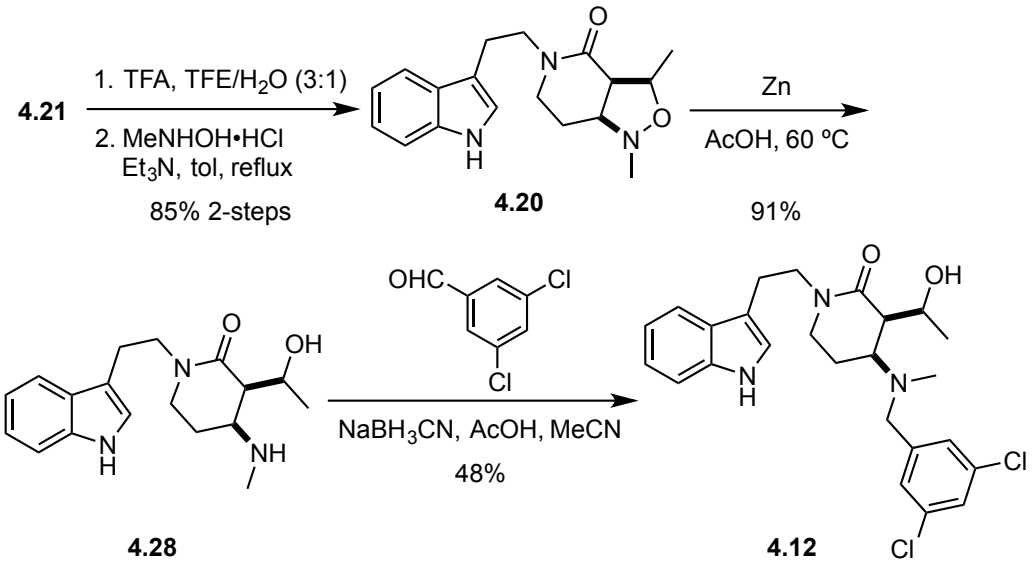

4.3. BIOLOGICAL ACTIVITY: NEW INHIBITOR

Before we can comment on the biological activity of the new inhibitor **4.12**, it must be noted that access to the previously utilized *Tb*MetRS enzyme assay was no longer at our disposal. We are greatly appreciative and indebted to what became our new cell biology collaboration with the lab of Dr. Kojo Mensa-Wilmont of the University of Georgia. At the time, the Mensa-Wilmont lab was conducting *T. brucei* cell-based growth inhibition assays. This assay compared the cell densities of *T. brucei* cultures grown in the presence of inhibitors after 48 h, to that of the representative control cultures. In order to get a baseline of comparison for our new inhibitor, we first needed to know how **4.1** performed in this growth inhibition assay. Compound **4.1** displayed a 50% growth inhibition (GI_{50}) of 25.3 ± 0.5 μM and our target inhibitor **4.12** exhibited a GI_{50} of 4.3 ± 0.4 μM (Figure 4.7). Upon determining the 5-fold increase in activity towards *T. brucei* growth inhibition of **4.12** with respect to **4.1**, we immediately undertook SAR studies to investigate the molecular functionalities conducive to *T. brucei* activity, with the goal of improving efficacy towards *T. brucei* growth inhibition.

Figure 4.7. *T. brucei* growth inhibition of **4.1** and **4.12**

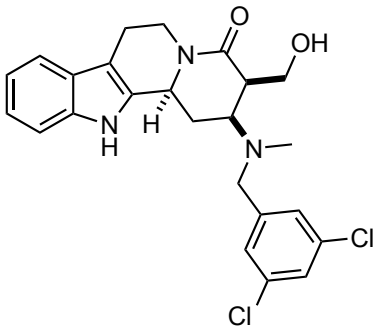

4.1

T. brucei GI_{50} = 25.3 ± 0.5 μM

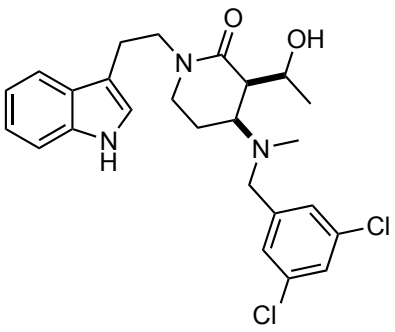

4.12

T. brucei GI_{50} = 4.3 ± 0.4 μM

4.4. Structure Activity Relationship

Figure 4.8. Sites of derivatization for initial SAR study

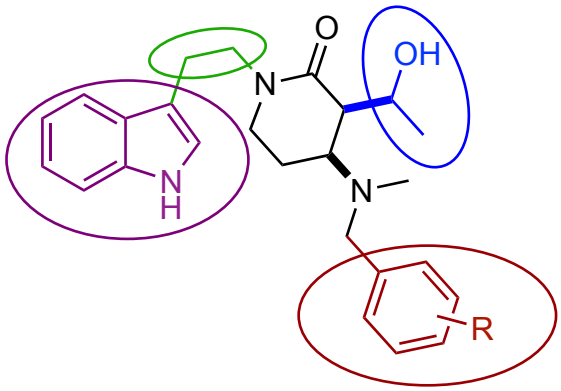

When considering how to study the SAR of this scaffold, we first identified four key regions of **4.12** that could be chemically modified. After individually modifying each region, the resulting growth inhibition data will allow us to identify the optimal substituents in each region. Incorporation of these optimal substituents into future inhibitors would hopefully allow access to significantly more potent *T. brucei* inhibitors.

The first and easiest region to diversify was the substitution of the benzyl amine substituent, shown in red (Figure 4.8). By substituting various benzaldehyde derivatives in the last step of the synthesis, we could quickly access a diverse array of aromatic substitution patterns at this position. Secondly, we wanted to determine the role of the ethylene hydroxy side chain (blue). The alcohol functionality is a potential hydrogen bond donor, and we reasoned that if hydrogen bonding at this position with the protein is important for binding, then removing the alcohol should lead to a decrease growth inhibition. Next, we wanted to test the effects of the carbon linker length between the indole and the 2-piperidinone moieties (green) towards binding to *Tb*MetRS. Given that the opposite termini of our inhibitors are possibly binding in two discrete pockets, we should be able to elucidate an optimal linker length to maximize binding affinity. Finally, we postulated that substitution of hydrogen bond donors and acceptors on the indole moiety (purple) might lead to increased hydrogen bonding interactions within the auxiliary binding pocket, which would improve binding to *Tb*MetRS.

4.4.1. Benzylamine Substitution: Part I. Synthesis

We first set out to synthesize a number of inhibitors with a variety of substitution patterns on the benzyl amine moiety. As shown in Figure 4.9, substituted benzylamine compounds **4.29** - **4.36** were synthesized utilizing the previous reductive alkylation protocol. The substituents were chosen for a few key reasons. First, we knew the 3,5-dichloro and 3,4-methylenedioxy substitution patterns should be active based on the

activity of compounds **4.1** and **4.2**. The unsubstituted benzylamine was chosen as a pseudo-negative control in that, according to previous reports,[103] an electronegative atom in the methionine binding pocket is required for binding to the enzyme. Using the same logic, a 3-thiomethylbenzyl group was chosen to mimic the natural thiomethyl substituent of methionine. We also wanted to test a number of benzyl groups incorporating various methoxy and chloride substitution patterns. Accordingly, we prepared compounds **4.29** – **4.36** for evaluation as *T. brucei* growth inhibitors (Figure 4.9).

Figure 4.9. Synthesis of benzylamine substituted compounds **4.29** - **4.36**

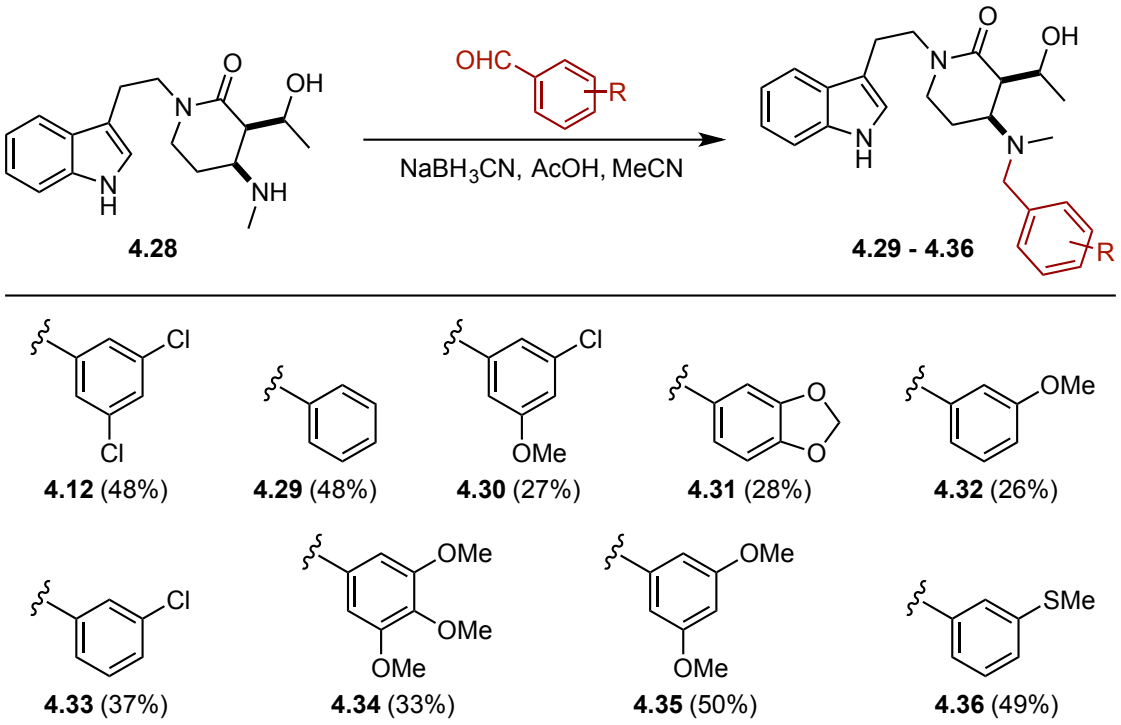

The yields for this reductive alkylation step were consistently low. The major reason for these poor yields was due to intramolecular trapping of the iminium ion by the proximal alcohol. As shown in Figure 4.10, condensation of **4.28** with the given benzaldehyde will give the iminium ion **4.28a**. The iminium ion can either be reduced to the desired tertiary amine **4.29 – 4.36** or the hydroxy substituent can add into the iminium ion to give the cyclic *N*-*O*-acetal **4.28b**. All attempts to reduce *N*-*O*-acetal **4.28b** failed to give the desired tertiary amines, thus the formation of **4.28b** effectively shut down the desired reductive alkylation pathway.

Figure 4.10. Reductive alkylation pathway and undesired side reaction

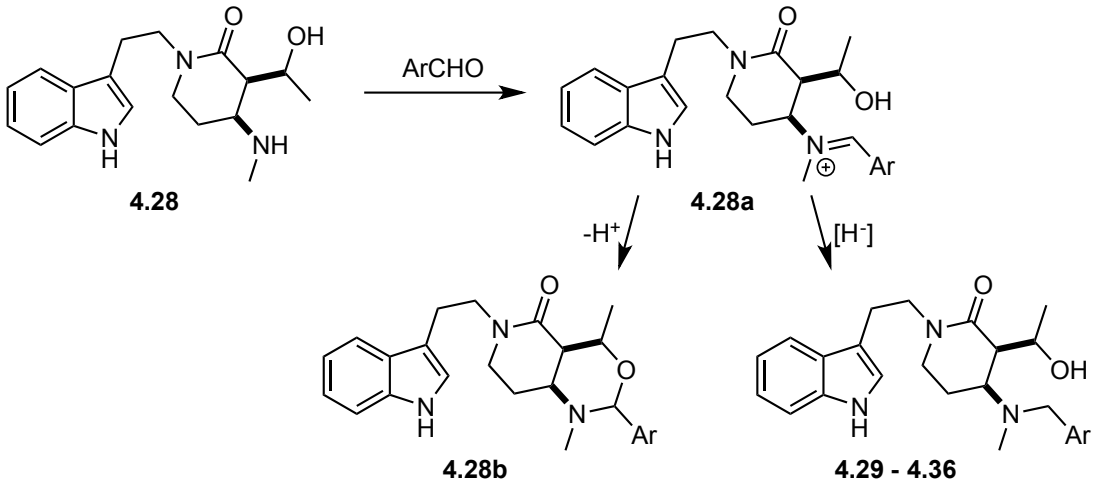

4.4.2. Benzylamine Substitution: Part II. Biological Activity

The results of the *T. brucei* growth inhibition assay for compounds **4.29** – **4.36** are shown in Table 4.1. Overall, there was not a significant difference in growth inhibition

between our initial target **4.12** and compounds **4.29** – **4.36**, with most of these compounds exhibiting less than a 2-fold difference in GI_{50} values relative to **4.12**. Compounds **4.29** and **4.35** were the two exceptions to this trend, with both compounds being completely inactive towards growth inhibition at the 10 μM threshold of this assay. Given that the 3-methoxy compound **4.32** and the 3,4,5-trimethoxy compound **4.34** were both single-digit micromolar growth inhibitors of *T. brucei*, the inactivity of the 3,5-dimethoxy compound **4.35** was quite puzzling. Conversely, the inactivity of the unsubstituted analogue **4.29** was expected. From an SAR perspective, this result fit our hypothesis that substitution of the benzylamine moiety with an electronegative atom was necessary for binding. However, with most of the compounds in this series being equipotent to our initial compound **4.12**, further conclusions about the SAR cannot be made.

Table 4.1. *T. brucei* growth inhibition data of substituted benzylamine derivatives **4.29** - **4.36**

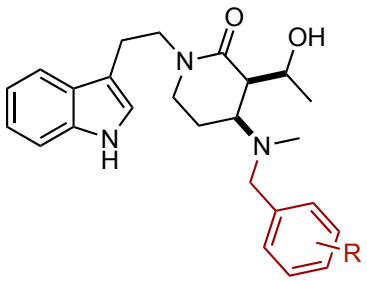

Compound	Substitution (R-)	GI_{50} (μM)
4.12	3,5-dichloro	4.3 ± 0.4
4.29	H	> 10
4.30	3-chloro-5-methoxy	4.8 ± 0.2
4.31	3,4-methylenedioxy	3.9 ± 0.7
4.32	3-methoxy	5.7 ± 0.4
4.33	3-chloro	2.1 ± 0.2
4.34	3,4,5-trimethoxy	8.1 ± 1.7
4.35	3,5-dimethoxy	> 10
4.36	3-thiomethyl	2.3 ± 0.6

4.4.3. Methylene Hydroxy Side Chain: Part I. Synthesis

To further understand the SAR of our compounds, we designed a set of derivatives to test the effects of the methylene hydroxy side chain towards *T. brucei* growth inhibition. To this end, we set out to synthesize the compounds shown in Figure 4.10. By comparing the growth inhibition of compounds **4.37** and **4.38** to our lead compound **4.12**, we hoped to develop an understanding of how the hydroxyl group might be participating in binding to *Tb*MetRS.

Figure 4.11. Target methylene hydroxy side chain derivatives

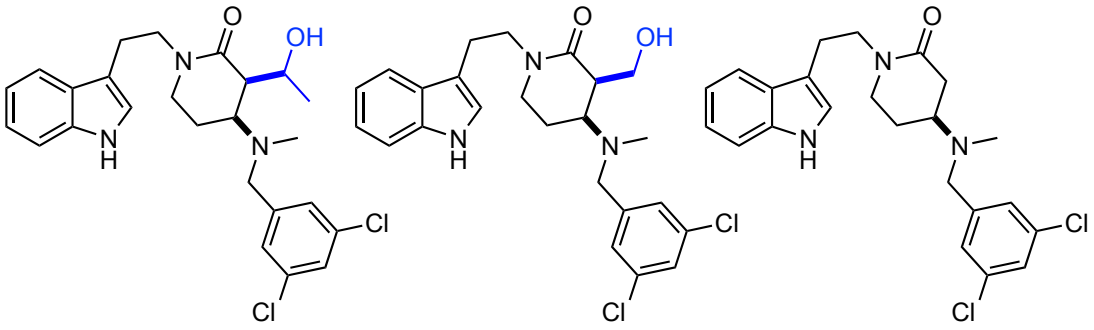

4.12 **4.37** **4.38**

The synthesis of methylene hydroxy inhibitor **4.37** is shown in Scheme 4.11 and commenced by the treatment of amine **4.25** with acryloyl chloride to give amide **4.39** in 54% yield. Subsequent removal of the dimethyl acetal protecting group and 1,3-dipolar cycloaddition gave isoxazolidine **4.40** in 73% yield over two steps. Reductive *N*-*O* bond cleavage with zinc metal in acetic acid gave amino alcohol **4.41** in 80% yield. Finally, reductive alkylation of **4.41** with 3,5-dichlorobenzaldehyde gave **4.37** in 42% yield.

Scheme 4.11. Synthesis of methylene hydroxy inhibitor **4.37**

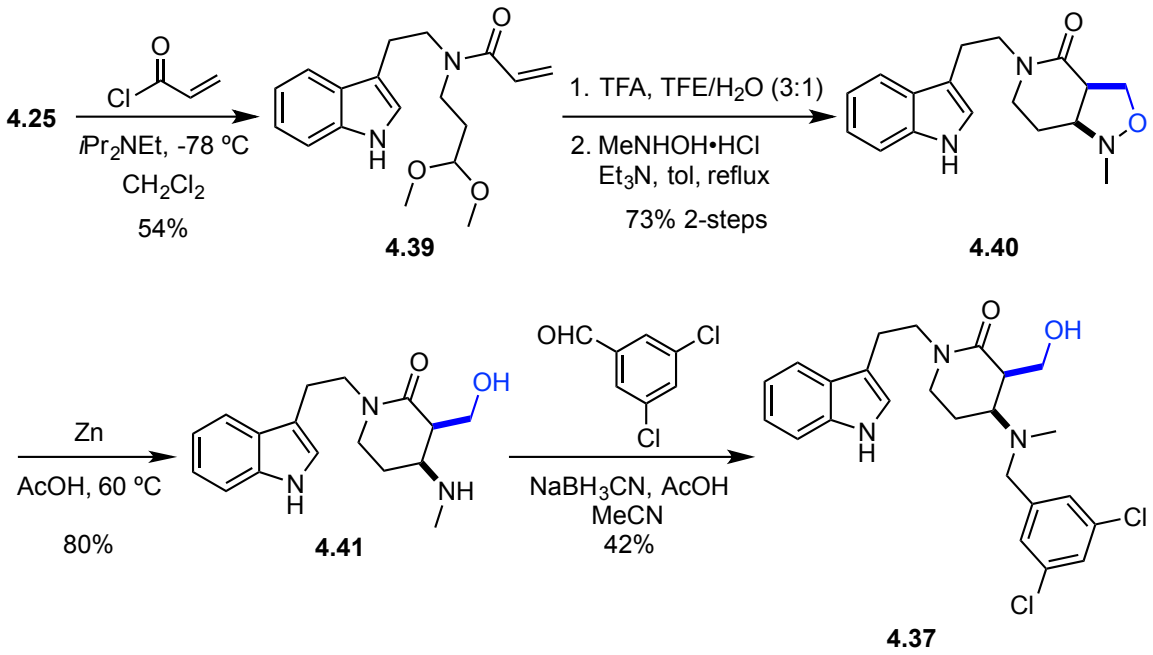

Simultaneous to the synthesis of compounds **4.29** - **4.36**, Lance Lepovitz synthesized an analogous series of nor-methylene hydroxy inhibitors, in which the α-position of the lactam was unsubstituted. The synthesis of these inhibitors started from the conjugate addition of tryptamine into ethyl acrylate to give **4.42** in 90% yield (Scheme 4.12). Amide coupling of **4.42** with monoethyl malonate utilizing EDCI-hydrochloride gave amide **4.43** in 88% yield. A one-pot, two-step procedure involving a Dieckmann cyclization and subsequent decarboxylation afforded β-keto-2-piperidinone **4.44** in 64% yield. Finally, sequential reductive aminations with methylamine hydrochloride and substituted benzaldehydes led to nor-methylene hydroxy inhibitors **4.38** and **4.45**-**4.51** in 50 - 80% yield.

Scheme 4.12. Synthesis of nor-methylene hydroxy compounds **4.38** and **4.45** – **4.51**

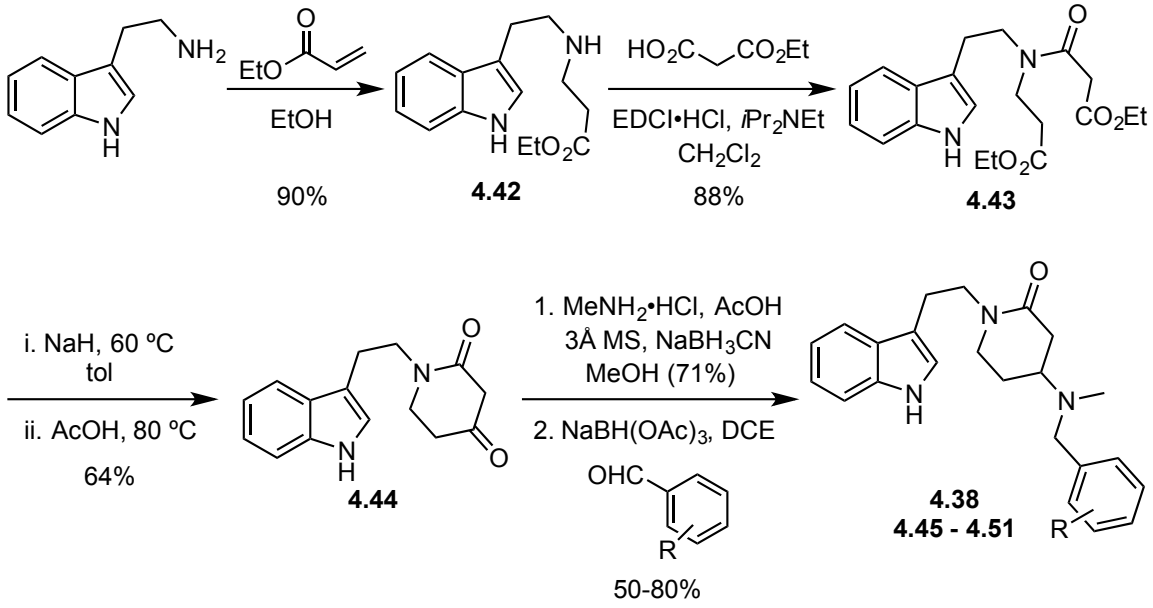

4.4.4. Methylene Hydroxy Side Chain: Part II. Biological Activity

The *T. brucei* growth inhibition assay results for compounds **4.37**, **4.38**, and **4.45** – **4.52** are shown in Table 4.2. In comparing the analogous 3,5-dichlorobenzyl compounds **4.12**, **4.37**, and **4.38**, we again found less than a two-fold difference in GI_{50} values. Conversely, we did observe a decrease in growth inhibition with compounds **4.47**, **4.48**, and **4.51**, relative to the ethylene hydroxy analogues **4.31**, **4.32**, **4.36**. From an SAR perspective, these results are inconclusive. If these compounds are indeed inhibiting *T. brucei* cell growth by inhibition of *Tb*MetRS, then the fact that **4.12**, **4.37**, and **4.38** are equipotent would indicate that the ethylene hydroxy side-chain does not play a major role in protein binding. However, because compounds **4.47**, **4.48**, and **4.51** do not inhibit *T.*

brucei growth, whereas the analogous compounds **4.31**, **4.32**, and **4.36** do inhibit growth, might suggest that this series of compounds could be acting through an alternative mechanism of action.

Table 4.2. *T. brucei* growth inhibition of methylene hydroxy and nor-methylene hydroxy analogues

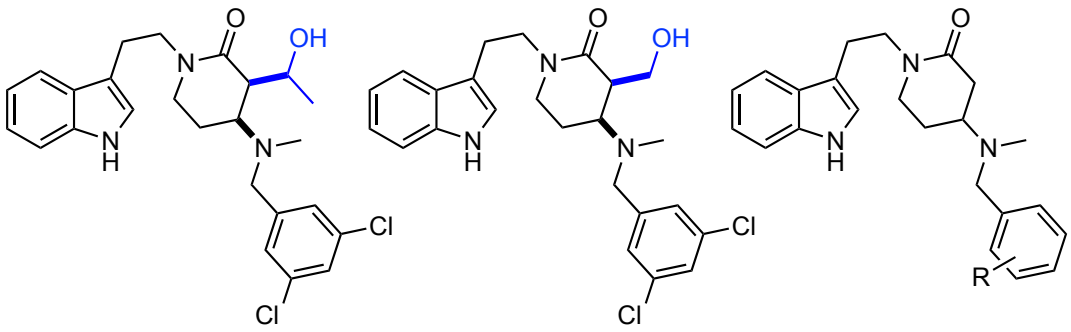

4.12 **4.37** **4.38**
4.45 - 4.51

Compound	Substitution (R-)	GI_{50} (μM)
4.12	3,5-dichloro	4.3 ± 0.4
4.37	3,5-dichloro	5.5 ± 0.4
4.38[a]	3,5-dichloro	7.1 ± 0.7
4.45[a]	H	>10
4.46[a]	3-chloro-5-methoxy	6.2 ± 0.2
4.47[a]	3,4-methylenedioxy	>10
4.48[a]	3-methoxy	>10
4.49[a]	3-chloro	9.0 ± 0.4
4.50[a]	3,5-dimethoxy	>10
4.51[a]	3-thiomethyl	>10

[a] Compounds synthesized by Lance Lepovitz

4.4.5. Carbon Linker Length: Part I. Synthesis

In continuing SAR studies of our compounds as *T. brucei* growth inhibitors, we turned our attention to synthesizing compounds with the goal of optimizing the carbon

linker length between the indole and 2-piperdinone moieties. Given the fact that known *Tb*MetRS inhibitors have been shown experimentally to bind into two distinct binding pockets, we designed compounds **4.52** and **4.53** to determine the optimal carbon linker length for binding (Figure 4.11).

Figure 4.12. Carbon linker length analogues **4.52** and **5.53**

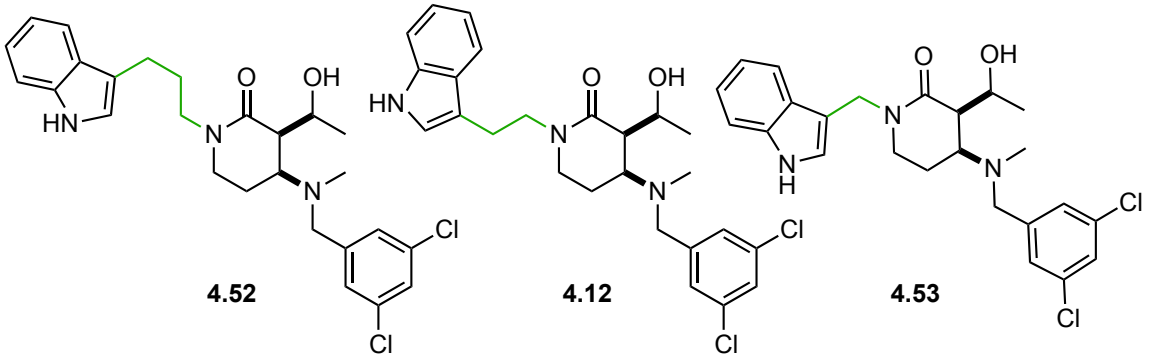

The synthesis of inhibitor **4.52**, which contains a three-carbon linker, was similar to the previous growth inhibitors. Treatment of indole-3-propionic acid (**4.54**) with thionyl chloride, followed by a reaction with amine **4.18** in the presence of triethylamine, gave amide **4.55** in 97% yield (Scheme 4.13). Lithium aluminum hydride reduction of **4.55** and subsequent acylation with crotonoyl chloride gave amine **4.56** and amide **4.57** in 87% and 62% yields, respectively. Removal of the dimethyl acetal protecting group and 1,3-dipolar cycloaddition proceeded smoothly to give isoxazolidine **4.58** in 68% yield over two steps. Treatment of **4.58** with zinc metal in acetic acid afforded amino alcohol

4.59 in 57% yield. Finally, reductive alkylation of **4.59** with 3,5-dichlorobenzaldehyde yielded **4.52** in 20% yield.

Scheme 4.13. Synthesis of three-carbon linker length inhibitor **4.52**

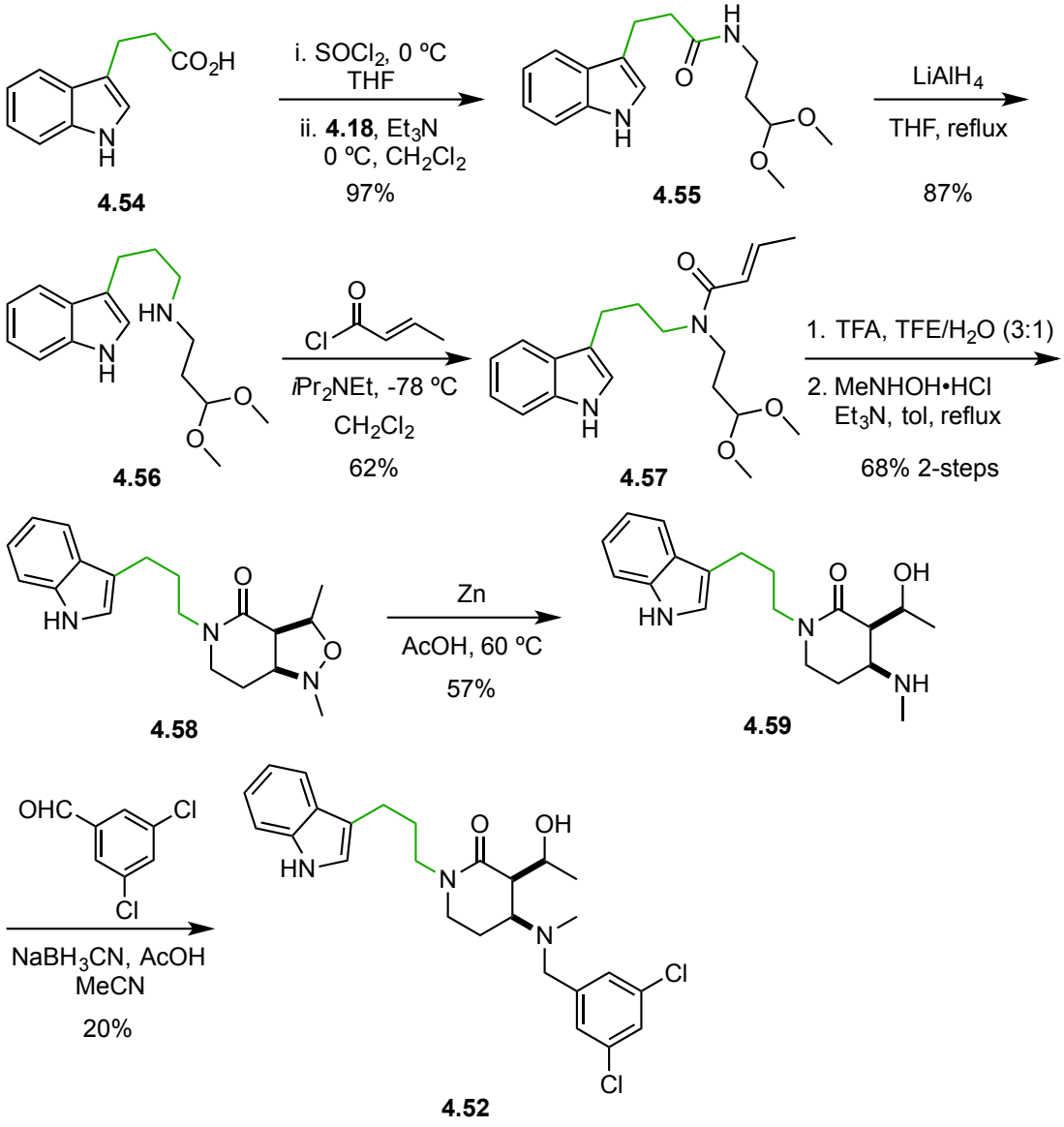

Synthesis of the one-carbon linker analogue **4.53** was achieved in an identical sequence to that of the three-carbon linker analogue **4.52**, with one noticeable difference in the removal of the dimethyl acetal protecting group. Treatment of indole-3-carboxylic acid (**4.60**) with thionyl chloride, followed by addition to **4.18**, gave amide **4.61** in 88% yield (Scheme 4.14). Upon reduction of **4.61** with lithium aluminum hydride, the resulting amine **4.62** was found to be unstable to silica gel column chromatography and aqueous acid extraction. However, when crude **4.62** was acylated, silica gel column chromatography provided amide **4.63** in 86% yield over two steps. When subjecting amide **4.63** to conditions for the removal of the dimethyl acetal protecting group in TFE, we were rather surprised when we exclusively isolated compound **4.66** (Scheme 4.15).

Scheme 4.14. Synthesis of one-carbon linked inhibitor **4.53**

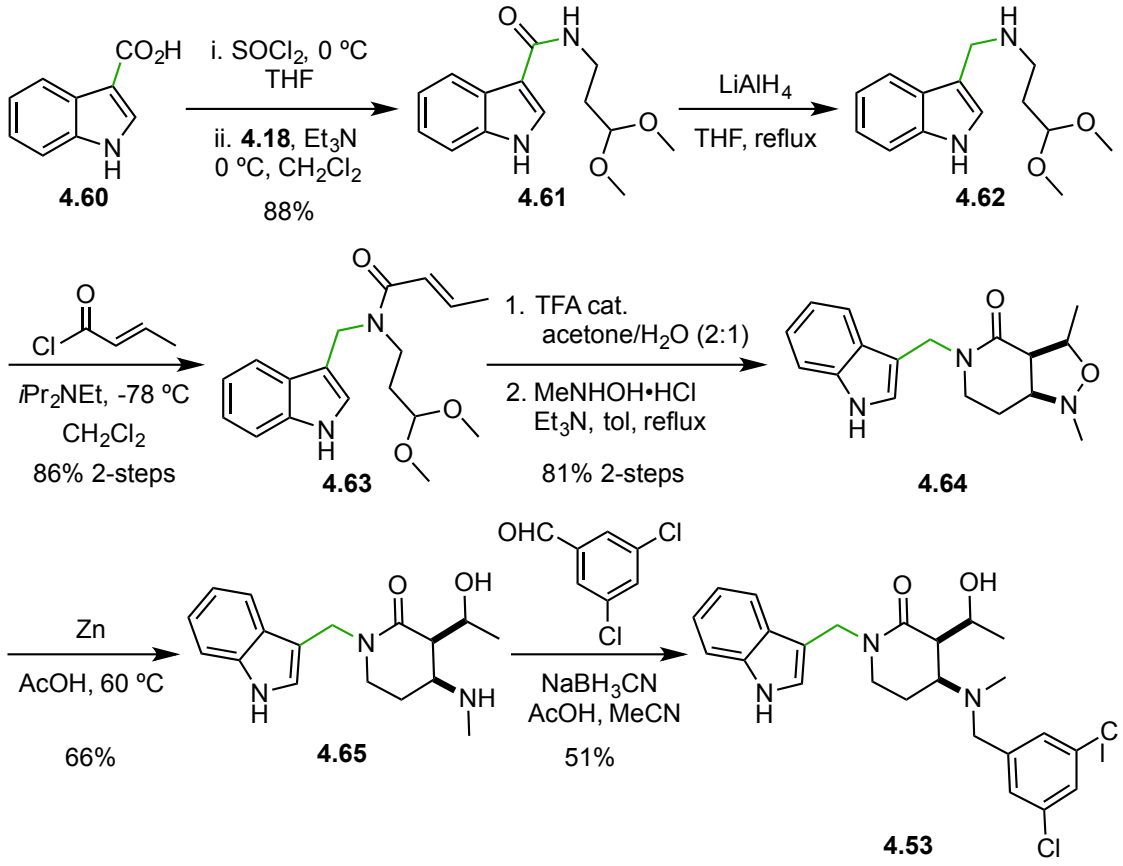

A mechanistic rationale for the formation of **4.66** is shown in Scheme 4.15. Upon formation of the oxonium ion **4.63a** (R = Me or H), the electrophilic carbon atom is five-atoms from the three-position of the indole. Nucleophilic attack from this position will form spirocyclic intermediate **4.63b**. Subsequent 1,2-alkyl migration followed by rearomatization forms the seven-membered ring and indole moieties in **4.63c**. Finally, acid-catalyzed elimination of methanol (or water) leads to the formation of **4.66**.

Scheme 4.15. Proposed mechanistic rationale for byproduct **4.66** formation (R = Me or H)

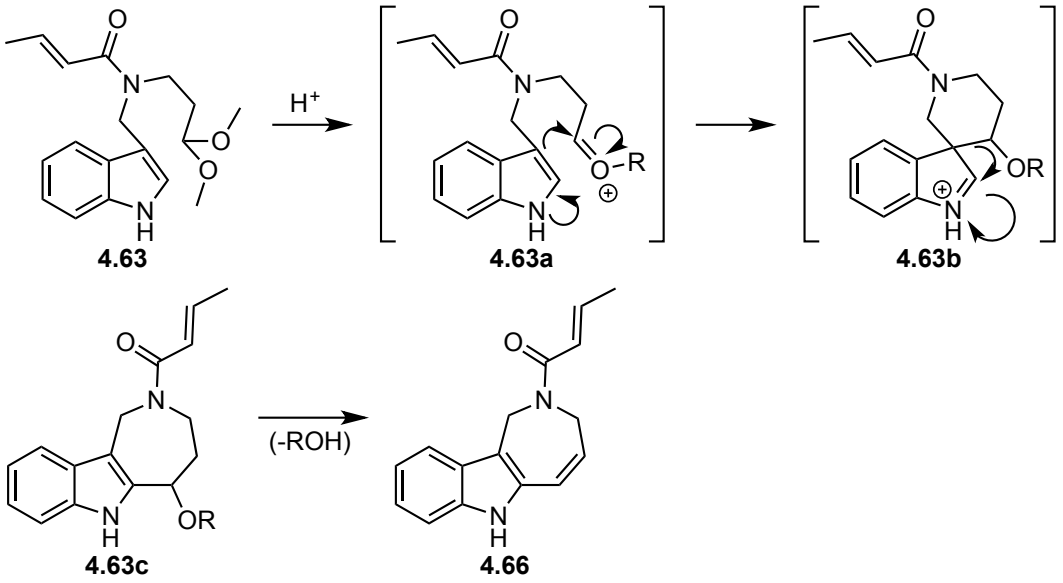

To mitigate the formation of **4.66**, we screened a number of solvents and found that a mixture of acetone and water (2:1) led to the formation of the desired aldehyde and only trace amounts of **4.66**. The crude mixture was subjected to 1,3-dipolar cycloaddition conditions, leading to the formation of isoxazolidine in **4.64** in 81% yield over two steps. Finally, reductive *N-O* bond cleavage of **4.64**, followed by reductive alkylation of **4.65** proceeded in 66% and 51% yields, respectively, to give analogue **4.53**.

4.4.6. Carbon Linker Length: Part II. Biological Activity

The growth inhibition data for compounds **4.52** and **4.53** are shown in Figure 4.12. We were quite surprised to find that the one-, two-, and three-carbon linked analogues were effectively equipotent *T. brucei* growth inhibitors. These results were

quite disconcerting. Based on our hypothesized mode of binding to *Tb*MetRS, we expected the linker length to have a significant effect on biological activity. Given that we observed no change in growth inhibition, we reasoned that two possible scenarios could be taking place: either our compounds were not binding to *Tb*MetRS or some type of cellular process (uptake, metabolism, ect.) was causing growth inhibition to be uncharacteristic of *Tb*MetRS inhibition. In order to elucidate any meaningful conclusions from the growth inhibition data gathered thus far, we needed to determine the enzyme inhibition of our compounds. Though not available to us when we started our work in this area, Lance Lepovitz eventually developed an in-house *Tb*MetRS enzyme inhibition assay to determine if our compounds inhibited *Tb*MetRS. Nevertheless, we continued to study the developing cell-based SAR of our compounds by synthesizing analogues containing substitution on the indole moiety.

Figure 4.13. Growth inhibition assay results as compared by carbon-chain linker-length

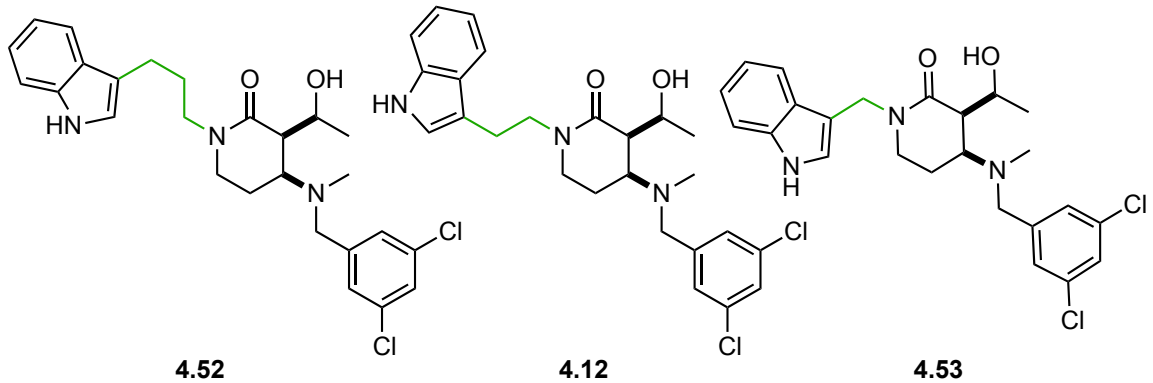

4.52
GI_{50} = 4.1 ± 0.6μM

4.12
GI_{50} = 4.3 ± 0.4μM

4.53
GI_{50} = 5.5 ± 0.2μM

4.4.7. Substituted Indole Analogues: Part I. Synthesis

When designing analogues containing substituents on the indole moiety, we wanted to incorporate hydrogen-bond donors and acceptors. The *Tb*MetRS inhibitors discussed in the preceding chapter all featured a heteroaromatic motif, namely an aminoquinolinone or a urea, that could act as both a hydrogen-bond donor and acceptor. We expected that adding the capability for hydrogen-bonding on the indole moiety would increase activity. To this end, we synthesized analogues containing 5-methoxyindole, 5-benzyloxyindole, 5-hydroxyindole, and 4-benzyloxyindole motifs.

Synthesis of the 5-methoxyindole analogue **4.73** followed the same protocol as previous analogues. Treatment of 5-methoxyindole (**4.67**) with oxalyl chloride in ether led to precipitation of the corresponding glyoxyl chloride. Addition of the glyoxyl chloride to a solution of **4.18** and triethylamine led to nearly quantitative formation of glyoxylamide **4.68** (Scheme 4.16). Lithium aluminum hydride reduction of **4.68** gave secondary amine **4.69** in 90% yield. Acylation of **4.69** with crotonoyl chloride proceeded smoothly to give crotyl amide **4.70** in 71% yield. Removal of the dimethyl acetal protecting group and subsequent 1,3-dipolar cycloaddition led to the formation of isoxazolidine **4.71** in 85% yield over two steps. Reductive *N*-*O* bond cleavage of **4.71** gave amino alcohol **4.72** in 85% yield. Finally, reductive alkylation of **4.72** gave the 5-methoxyindole analogue **4.73** in 89% yield.

Scheme 4.16. Synthesis of 5-methoxyindole inhibitor **4.73**

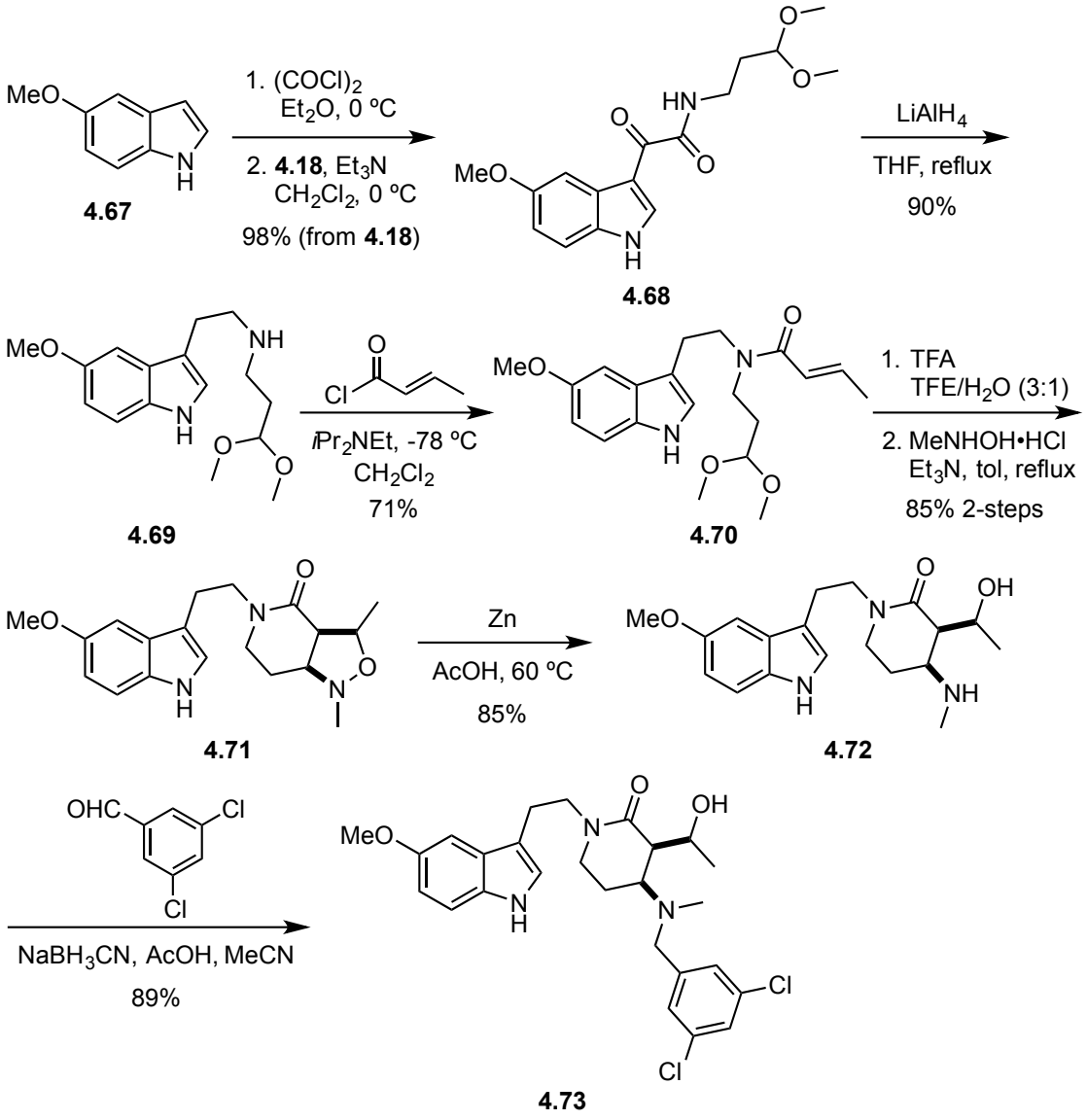

Synthesis of the 5-benzyloxyindole **4.80** and 5-hydroxyindole **4.81** analogues, started with the treatment of 5-benzyloxyindole (**4.74**) with oxalyl chloride to give the corresponding glyoxyl chloride (Scheme 4.17). Addition of the glyoxyl chloride to a

solution of **4.18** and triethylamine gave the glyoxylamide **4.75** in 95% yield. Reduction of **4.75** to the corresponding amine **4.76** was achieved in 94% yield. Treatment of **4.76** with crotonoyl chloride led to the formation of amide **4.77** in 61% yield. Removal of the dimethyl acetal protecting group and 1,3-dipolar cycloaddition of **4.77** proceeded to give isoxazolidine **4.78** in 68% yield over two steps. Treatment of **4.78** with zinc metal afforded *N-O* bond cleavage to give aminoalcohol **4.79** in 85% yield. The ensuing reductive alkylation of **4.79** with 3,5-dichlorobenzaldehyde gave the 5-benzyloxyindole analogue **4.80** in 37% yield. The 5-hydroxyindole analogue **4.81** was synthesized from **4.78** in two steps (Equation 4.1). First, palladium-catalyzed hydrogenolysis in acidic ethanol of **4.78** effected benzyl deprotection and *N-O* bond cleavage to give the crude 5-hydroxyindole amino alcohol (not shown), which was unstable. However, subjecting the crude 5-hydroxyindole amino alcohol directly to reductive alkylation conditions led to the formation of 5-hydroxyindole analogue **4.81** in 28% yield over two steps.

Scheme 4.17. Synthesis of 5-benzyloxyindole inhibitor **4.80**

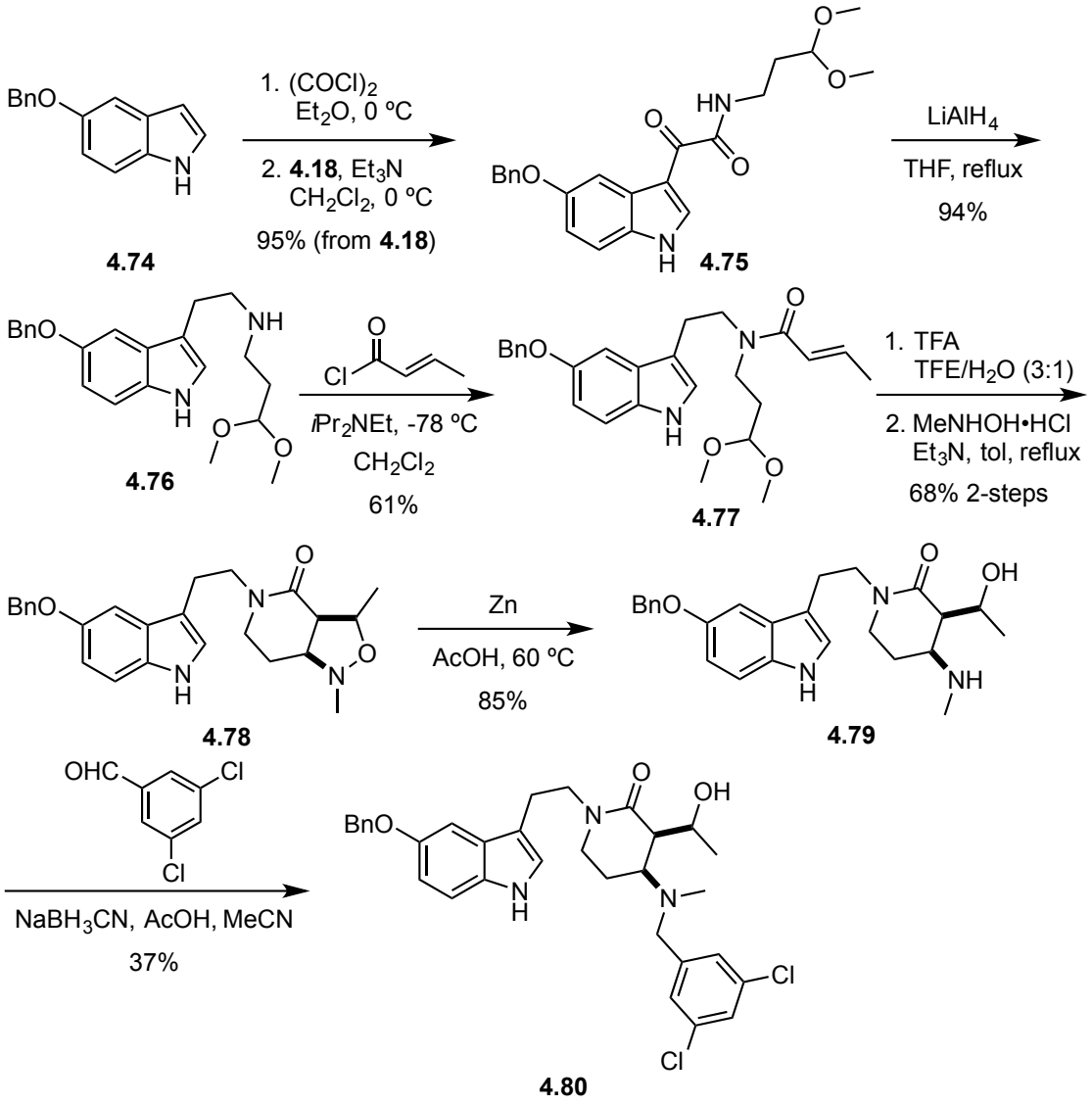

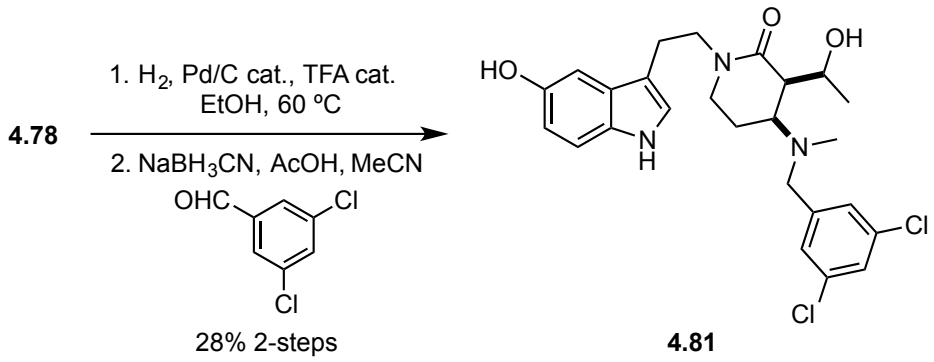

(4.1)

We next focused on the synthesis of the 4-benzyloxyindole analogue **4.89**, which was the most troublesome inhibitor to prepare. In contrast to every previous example, treatment of 4-benzyloxyindole (**4.82**) with oxalyl chloride did not lead to precipitation of the corresponding glyoxyl chloride. Rather a dark red solution formed, and over a relatively short period of time, the solution turned dark green. Even more frustrating was the fact that addition of either this red or green solution to **4.18** led to complex mixtures of starting material **4.82**, desired product **4.83**, and oxalyl-amide **4.84** (Equation 4.2). To further compound the problems with this reaction, we found that **4.82**, **4.83**, and **4.84** were inseparable by acid/base extraction and unstable to chromatography conditions, resulting in an intractable mixture of unidentifiable degradation products.

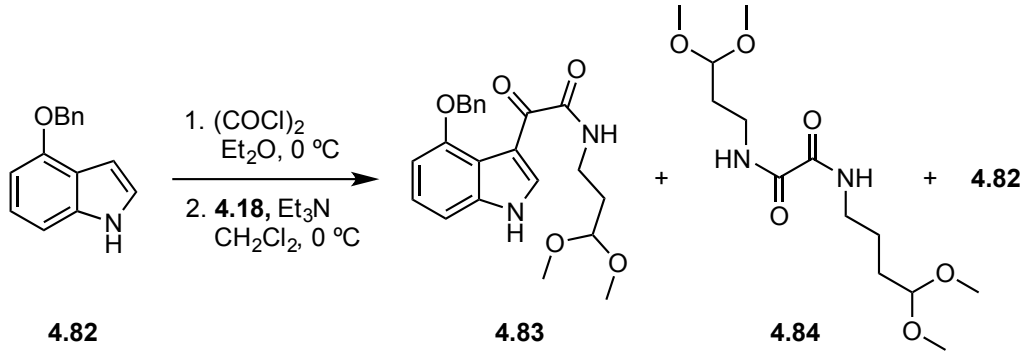

4.82 **4.83** **4.84**

(4.2)

Given the large number of problems with the formation and isolation of glyoxylamide **4.83**, an astonishingly simple solution was devised. We discovered that cannulating an ice-cold solution of a large excess of the glyoxyl chloride, which was formed using an equimolar ratio of **4.82** and oxalyl chloride, into an ice-cold solution of **4.18** with excess triethylamine minimized the formation of **4.84**. Upon a quick aqueous workup, the crude mixture was immediately subjected to a lithium aluminum hydride reduction, which enabled purification of the desired product by a simple acid/base extraction, to give pure **4.85** in 67% yield over two steps (Scheme 4.18). Acylation of **4.85** with crotonoyl chloride gave amide **4.86** in 86% yield. Unmasking of the aldehyde in **4.86** and subsequent 1,3-dipolar cycloaddition gave isoxazolidine **4.87** in 93% over two steps. Treatment of **4.87** with zinc metal afforded amino alcohol **4.88** in 57% yield. Finally, reductive alkylation of **4.88** with 3,5-dichlorobenzaldehyde gave the 4-benzyloxyindole analogue **4.89** in 19% yield. It should be noted that all attempts at benzyl deprotection of **4.87**, **4.88**, and **4.89** led to complex mixtures that quickly decomposed to unspecified byproducts.

Scheme 4.18. Synthesis of 4-benzyloxyindole inhibitor **4.89**

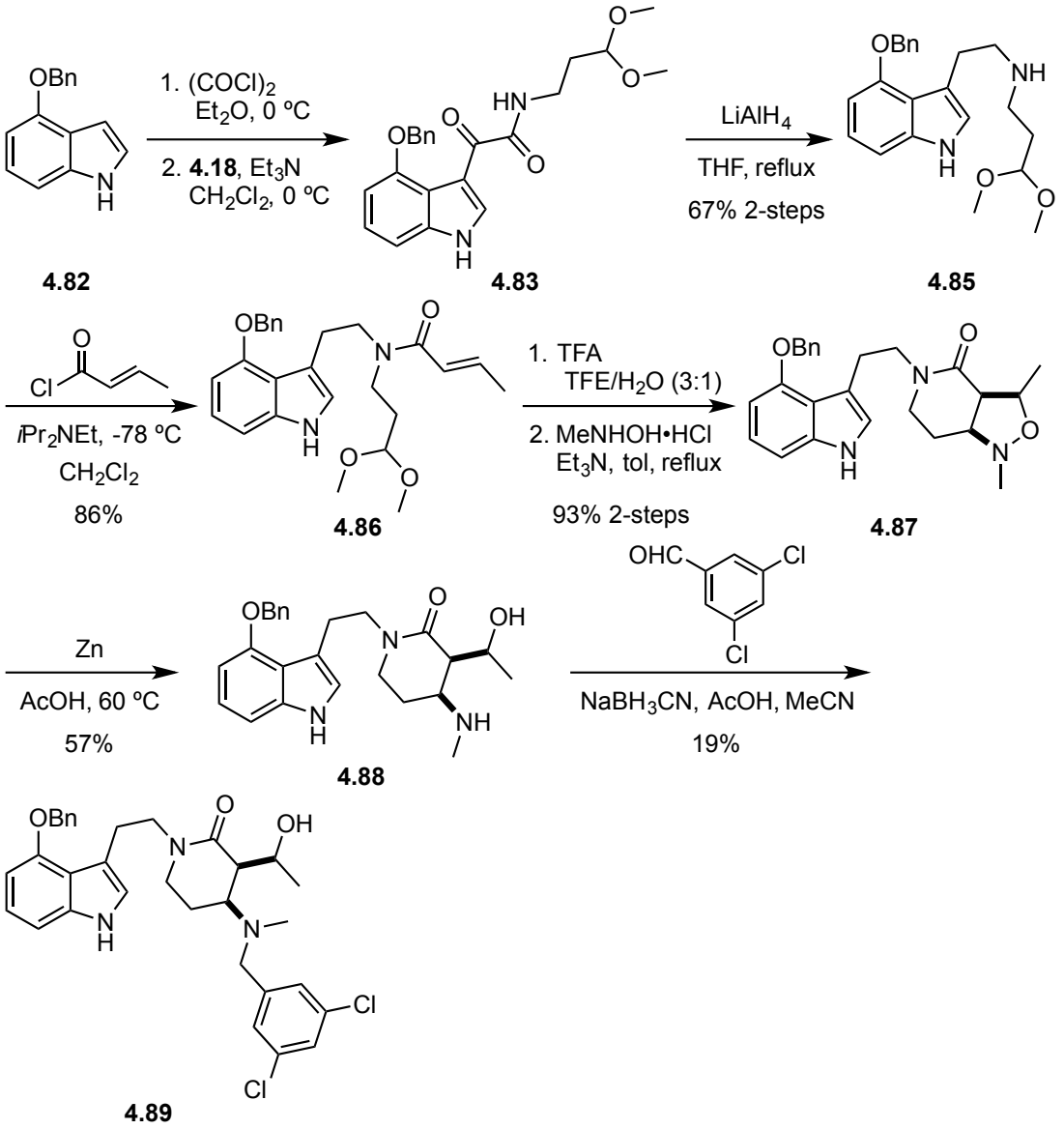

4.4.8. Substituted Indole Analogues: Part II. Biological Activity

Growth inhibition data for compounds **4.73**, **4.80**, **4.81**, and **4.89** are shown in Table 4.3. We were elated to find that the 5-methoxyindole analogue **4.73** exhibited sub-

micromolar growth inhibition of *T. brucei* (GI_{50} = 0.95 ± 0.04 μM), which to this day, is our most potent growth inhibitor. The benzyloxyindole and hydroxyindole compounds **4.80**, **4.81**, and **4.89** exhibited less than a two-fold difference in growth inhibition, with respect to compound **4.12**. As excited as we were to have finally achieved a significant increase in biological activity in compound **4.73**, it was undeniable that our library of compounds displayed a relatively flat SAR.

Table 4.3. *T. brucei* growth inhibition data of substituted indole derivatives

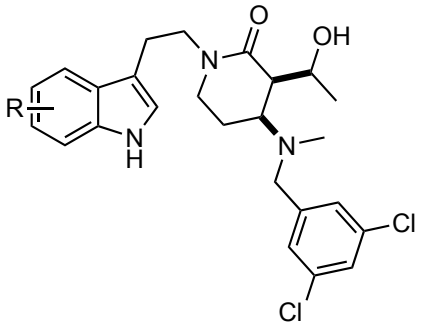

Compound	Substituent (R)	GI_{50} (μM)
4.12	H	4.3 ± 0.4
4.73	5-methoxy	0.95 ± 0.04
4.80	5-benzyloxy	2.1 ± 0.4
4.81	5-hydroxy	5.5 ± 0.6
4.89	4-benzyloxy	2.0 ± 0.2

4.5. *Tb*METRS ENZYME ASSAY RESULTS

After some experimentation Lance Lepovitz developed an in-house *Tb*MetRS enzyme inhibition assay. This assay utilized a colorimetric method to determine inhibition of the enzyme. This method is less sensitive than the radiolabeled *l*-methionine

competitive binding enzyme assay that was previously used to determine the IC_{50} values of compounds **4.1** – **4.6**. For this reason, we first obtained a baseline for comparison by determining the IC_{50} value of **4.1** in our enzyme assay. We found that **4.1** exhibited an IC_{50} value of 4.9 ± 1.5 μM, which is roughly an eight-fold decrease in value, as compared to of the radiolabeled *l*-methionine-based *Tb*MetRS inhibition assay (IC_{50} = 586 nm). With a proper baseline for comparing with **4.1**, we assayed our new compounds using this protocol, and the results are shown in Table 4.4. We were surprised to find that all of our new analogues were completely inactive towards inhibition of *Tb*MetRS at concentrations up to 200 μM. Hence, each new compound has an IC_{50} value greater than 200 μM. These results show that our new analogues, though better growth inhibitors of the parasite than **4.1** and **4.2**, are not acting through inhibition of *Tb*MetRS, but rather by some different mechanism of action.

4.6. BIOLOGICAL ACTIVITY

Table 4.4. Summary of the biological activity of 4-amino-2-piperidinone analogues towards *T. brucei* and *Tb*MetRS.

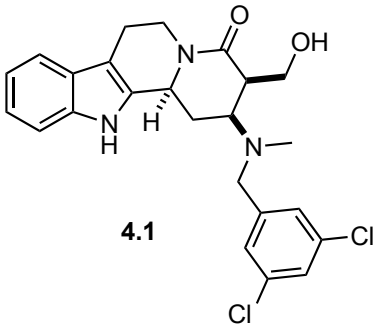

4.1

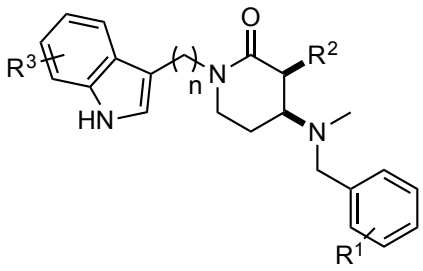

Compound	R^1	R^2	R^3	n	GI_{50} (μM)	*Tb*MetRS Inhib. (%)[a]
4.1	3,5-*di*Cl	CH_2OH	H	2	25.3 ± 0.5	4.9 ± 1.5 μM[c]
4.12	3,5-*di*Cl	$CH(OH)CH_3$	H	2	4.3 ± 0.4	28 ± 10
4.29	H	$CH(OH)CH_3$	H	2	>10	17 ± 3
4.30	3-Cl-5-OMe	$CH(OH)CH_3$	H	2	4.8 ± 0.2	17 ± 3
4.31	3,4-O_2CH_2	$CH(OH)CH_3$	H	2	3.9 ± 0.7	0
4.32	3-OMe	$CH(OH)CH_3$	H	2	5.7 ± 0.4	0
4.33	3-Cl	$CH(OH)CH_3$	H	2	2.1 ± 0.2	n/a
4.34	3,4,5-*triOMe*	$CH(OH)CH_3$	H	2	8.1 ± 1.7	10 ± 1
4.35	3,5-*di*OMe	$CH(OH)CH_3$	H	2	>10	0
4.36	3-SMe	$CH(OH)CH_3$	H	2	2.3 ± 0.6	0
4.37	3,5-*di*Cl	CH_2OH	H	2	5.5 ± 0.4	0
4.38[b]	3,5-*di*Cl	H	H	2	7.1 ± 0.7	17 ± 15
4.45[b]	H	H	H	2	>10	0
4.46[b]	3-Cl-5-OMe	H	H	2	6.2 ± 0.2	9 ± 7
4.47[b]	3,4-O_2CH_2	H	H	2	>10	0
4.48[b]	3-OMe	H	H	2	>10	7 ± 5
4.49[b]	3-Cl	H	H	2	9.0 ± 0.4	0
4.50[b]	3,5-*di*OMe	H	H	2	>10	4 ± 1
4.51[b]	3-SMe	H	H	2	>10	10 ± 1
4.52	3,5-*di*Cl	$CH(OH)CH_3$	H	3	5.5 ± 0.2	n/a
4.53	3,5-*di*Cl	$CH(OH)CH_3$	H	1	4.1 ± 0.6	n/a
4.73	3,5-*di*Cl	$CH(OH)CH_3$	5-OMe	2	0.95 ± 0.04	0
4.80	3,5-*di*Cl	$CH(OH)CH_3$	5-OBn	2	2.1 ± 0.4	0
4.81	3,5-*di*Cl	$CH(OH)CH_3$	5-OH	2	5.5 ± 0.6	27 ± 4
4.89	3,5-*di*Cl	$CH(OH)CH_3$	4-OBn	2	2.0 ± 0.2	0

[a] Percentage of *Tb*MetRS deactivation at 200 μM concentration. [b] Compounds synthesized by L. Lepovitz.
[c] Given value is the *Tb*MetRS inhibition constant (IC_{50}) using the in-house colorimetric enzyme assay.

4.7. SUMMARY

The synthetic efforts resulted in the synthesis of a library of indole containing 4-amino-2-piperidinone compounds. The generalized synthetic route developed, which is shown in Scheme 4.19, depicts the methods used to make the aforementioned library. This route allows access to these structural motifs in seven steps from amine **4.18** and indole (eight steps total). A major benefit of this route was the use of simple reaction protocols. Additionally, the purification of these reactions was quite simple. With the exception of the acylation and the final reductive alkylation step, these procedures did not require chromatography to afford material of >95% purity.

Scheme 4.19. Generalized synthetic scheme of 4-amino-2-piperidinone compounds

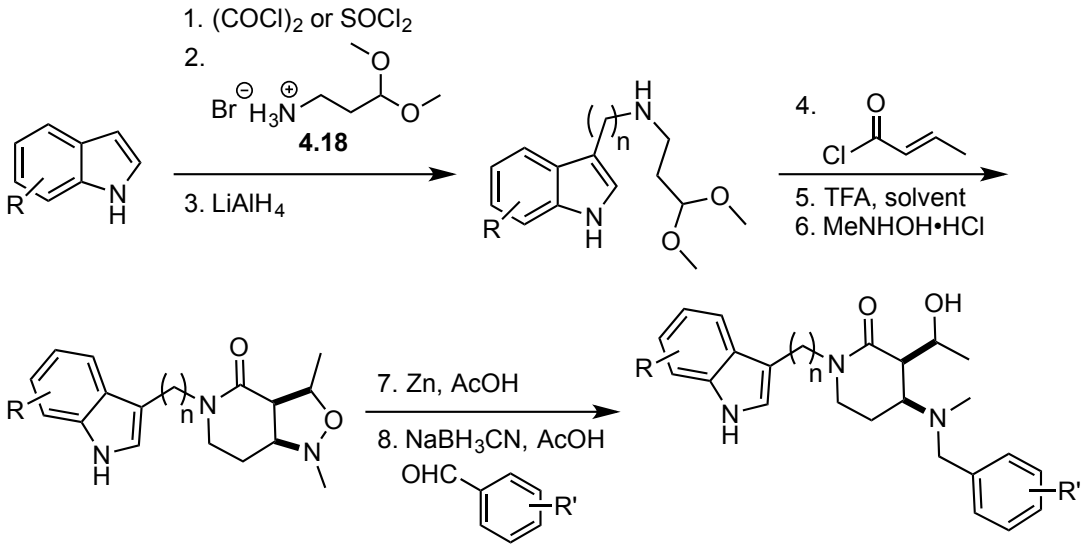

To summarize, we sought to develop an SAR that correlated specific molecular functionalities of our scaffold with the activity towards growth inhibition of *T. brucei*. We synthesized a library of analogues of our initial inhibitor **4.12** that were designed to test the effects upon inhibiting growth of *T. brucei* by varying the benzylamine substituent (shown in red, Figure 4.14), the ethylene hydroxy side-chain (shown in blue), the length of the carbon linker (shown in green), and substitution on the indole moiety (shown in purple). We thus discovered a very flat SAR between these sites of derivation and growth inhibition.

Figure 4.14. Inhibitor scaffold and derivatized functionalities

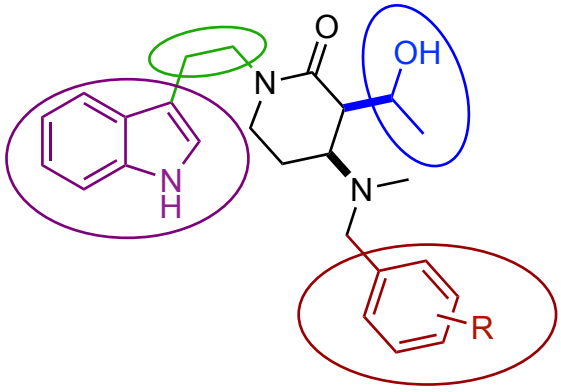

We originally thought the observed *T. brucei* growth inhibition of our compounds was due to the inhibition of *Tb*MetRS. This assumption was based upon the structural similarities between our compounds and the known *Tb*MetRS inhibitors **4.1** - **4.3**. However, during the course of our studies we discovered that the changes made to our scaffold, which we predicted would affect binding to *Tb*MetRS, did not lead to

appreciable changes in growth inhibition. For this reason, we undertook studies to develop an in-house *Tb*MetRS enzyme inhibition assay.

The entire collection of biological data for the compounds described is shown in Table 4.4. As previously described, our tryptamine-based analogues are generally more efficacious *T. brucei* growth inhibitors than the initial hit compound **4.1**. However, this increased activity at the cellular level is no longer acting through inhibition of *Tb*MetRS, as demonstrated by the lack of *Tb*MetRS inhibition in our in-house enzyme assay.

4.8. CONCLUSION

We have learned that our initial hypothesis that the flexible tryptamine analogues of our previous tetrahydro-β-carboline compounds **4.1** – **4.3** would be better *Tb*MetRS inhibitors was incorrect. When this study was initiated, access to a *Tb*MetRS enzyme inhibition assay was not available in our labs so we had to operate under the assumption that growth inhibition of *T. brucei* reflected *TbMetRS* inhibition. In fact, the in-house enzyme assays of our tryptamine analogues surprisingly showed that these compounds did not inhibit the activity of *Tb*MetRS at all.

Though the exact reason why our tryptamine analogues no longer bind to *Tb*MetRS is unclear, it is possible that the tetrahydro-β-carboline scaffold is preorganized into a conformation that positions the indole moiety, relative to the 2-piperidinone moiety, in an ideal orientation for binding to *Tb*MetRS. Conversely, even though the tryptamine analogues possess greater conformational flexibility, the indole moiety in this

scaffold physically cannot adopt the same conformation as in **4.1**, because of the steric repulsion that would develop between the hydrogen atom at the two-position of the indole and the hydrogen atoms in the three-position of the 2-piperidinone moieties.

Nevertheless, upon analyzing the enzyme inhibition assay data, the observed lack of an SAR between our analogues and growth inhibition of *T. brucei* is no longer surprising. With the knowledge that our compounds do not bind to *Tb*MetRS, there is no longer a logical argument for why the molecular changes made would lead to a change in biological activity.

Using a rational drug design approach, we synthesized a number of compounds that exhibited enhanced efficacy on a cellular level towards growth inhibition of the *T. brucei* parasite. However, we found that this enhanced activity on a cellular level was through a new mode of action relative to compounds **4.1** – **4.3**. These studies substantiate the importance of verifying the activity towards a proposed biochemical target when undertaking a rational drug design approach in drug discovery. Even though our tryptamine based analogues were no longer inhibiting the *Tb*MetRS enzyme, the increased efficacy towards *T. brucei* growth inhibition is intriguing. Future collaborative efforts to elucidate the new mechanism of action for these compounds is currently being considered. Nevertheless, the compounds described in this chapter add to the growing body of research towards finding a more effective cure for HAT.

NEURONS THAT MATTER: USING LIGHT TO TAG NEURONAL ENSEMBLES BASED ON FUNCTION

Chapter 5: Photolabile Protecting Groups

5.1. PHOTOLABILE PROTECTING GROUPS: GENERAL

Photolabile protecting groups (PPGs) are light reactive moieties that can render a given functional group chemically inert. Much like traditional protecting groups, the utility of a PPG is inherently tied to the ability to efficiently install/remove the group as well as the chemical stability towards various conditions. Unlike traditional protecting groups, the removal of PPGs is accomplished using light as the sole input, thus negating the need for chemical reagents. This characteristic of PPGs often translates to their utility within sensitive systems, especially in biological settings. While originally designed by synthetic chemists, the use of PPGs in chemical synthesis has been minimal.[152] However, the use of PPGs to study and manipulate biological systems has grown consistently since their early discovery. Often referred to as "cages" or "photocages", biological applications using photocaged compounds have found use in controlling protein functions, cellular stimulation, control over gene silencing, and neuronal stimulation or inhibition. These applications have been the subject of a multiple of reviews.[153–161]

When determining the photochemical efficiency of deprotection, quantum yield is often used as a quantitative metric. The quantum yield of substrate release (Φ_r) is equal to the rate constant of substrate release from the excited state (k_r) divided by the sum of all rate constants for every possible photochemical pathway from the excited state (Equation

5.1). To simplify, the quantum yield is the probability of substrate release upon promotion of a PPG-protected compound to the excited state upon irradiation of a given wavelength.

$$\Phi_r = \frac{k_r}{\sum k} \quad \textbf{(5.1)}$$

When considering absorption of light, the probability of a compound absorbing a photon is a function of molar absorptivity (ε). If we consider a compound with a quantum yield of unity ($\Phi_r = 1$), then every photon absorbed will lead to release of the given substrate. However, if this compound has a very low molar absorptivity at a given wavelength, it will require longer irradiation times (more photons) to be promoted to the excited state. This leads to the product of quantum yield and molar absorptivity ($\Phi_r \bullet \varepsilon$) being a better representative metric of photochemical efficiency of deprotection. This is especially true for visible light absorbing PPGs, where large absorptivities in the visible region are often attributed to the availability of multiple unproductive photochemical pathways.[162]

The first reported use of PPGs started to appear in the literature in the early 1960's. Early publications by Barltrop,[163] Barton,[164,165] Patchornik and Woodward[166] set the stage for what continues to be a large area of research today. In his seminal report, Barltrop described the first use of a photo-removable group as a new protecting group strategy. In this study, irradiation of Cbz-glycine (**5.1**) with UV-light (254 nm, mercury lamp) led to the isolation of benzyl alcohol (**5.2**) and glycine (**5.3**) in up to 75% yield

(Equation 5.2). Though unbeknownst at the time, the use of PPG-protected carbamates and carbonates to release free amines and alcohols upon decarboxylation, is still commonplace in PPG strategies today.[167,168]

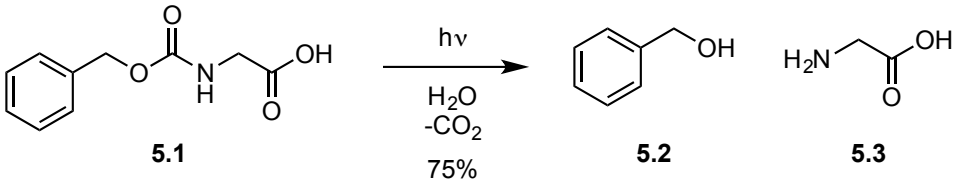

5.1 **5.2** **5.3** **(5.2)**

Though each individual application will necessitate a specific set of requirements, a general set of criteria should be met in the design of a useful PPG.[161]

1. The PPG-protected compound needs to be chemically and biologically inert to the system under investigation.
2. Photodeprotection should occur cleanly, in high chemical and quantum yields. With respect to biological systems, caging groups should decage at wavelengths > 350 nm to minimize cellular damage.
3. The photochemical byproducts should be inert within the system being studied. In the case of biological systems, these byproducts must also be non-toxic to mitigate potential interference with the given study.
4. The protected compound must be soluble in the target media. Given the prominent use of PPGs within biological studies, this often means the protected compounds must soluble in aqueous media.

5. The observed release rate of the target compound must exceed that of the response under investigation. This is particularly important for biological studies of very fast physiological events, such as electrophysiology.

A major reason for the continued development of novel PPGs is that no one group currently fulfills all of these given requirements for all potential applications. With literally hundreds of PPGs reported in the literature, we will highlight the most commonly used PPGs, grouped by common structural features.

5.2. *o*-NITROBENZYL-BASED PHOTOLABILE PROTECTING GROUPS

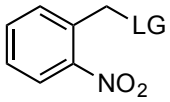

***o*-nitrobenzyl (NB)**

By far the most commonly used class of PPGs and photocages is the *o*-nitrobenzyl based family. One of the oldest known groups of PPGs, this class of compounds was pioneered by Barltrop[169] and Patchornik.[166] Over four decades of research has led to a profound understanding of how these groups react photochemically. However, despite their wide-spread use in biological and chemical applications, there are a number of disadvantages to the **NB**-based PPGs. These disadvantages can be understood by considering the mechanism of deprotection of **NB** groups.

5.2.1. *o*-Nitrobenzyl Mechanism of Deprotection

The mechanism of deprotection of *o*-nitrobenzyl PPG is shown in Scheme 5.1.[161,170] Upon irradiation, a molecule of **NB** will enter the exited state **5.4**. An intramolecular 1,5-hydrogen abstraction from the excited nitro group leads to the formation of the *aci*-nitro intermediate **5.5**. In aqueous media, the reactive *(E)-aci*-intermediate **5.5** is in rapid equilibrium with the unproductive *(Z)-aci*-intermediate (not shown). The irreversible cyclization of **5.5** to **5.6** occurs with a rate constant on the order of 10^2 - 10^4 s^{-1}. For moderate to good leaving groups, the decay of **5.5** is rate limiting. Ring opening of **5.6** leads to the formation of **5.7**. Hydrolysis of hemiacetal **5.7**, which can be rate-limiting for poor leaving groups or basic media, releases the leaving group and forms 2-nitrosobenzaldehyde (**5.8**).

Scheme 5.1. *o*-Nitrobenzyl PPG mechanism of deprotection

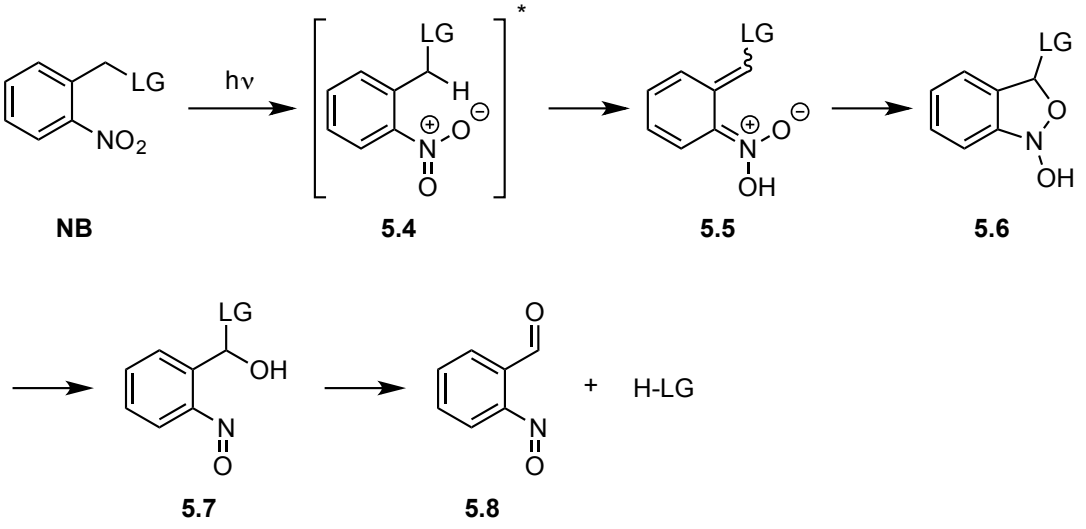

In considering the mechanism shown in Scheme 5.1, a number of problems arise from the use of these PPGs. First and foremost, is the formation of a 2-nitrosobenzaldehyde byproduct as **5.8**. Far from chemically inert, **5.8** can participate in a number side-reactions, the most troublesome of which is the condensation with primary amines.[171,172] Given that deprotection of an amino-containing compound generates equimolar amounts **5.8** and the released amine, subsequent condensation of **5.8** and the released amine will inhibit the amine from participating in the desired response, thus effectively diminishing the efficiency of deprotection. Additionally, Bayley and Givens found that **5.8** reacted with thiophosphotyrosine in photoreleased peptides, which inhibited the released peptide from binding to the respective protein.[173,174] Furthermore, the 2-nitrosobenzaldehyde byproducts can be toxic towards biological systems.[162] Finally, these byproducts exhibit a stronger absorbance of light at similar wavelengths to the parent *o*-nitrobenzyl protected compound, leading to the formation of dark colored solutions. This absorbance acts as an internal UV-filter, thus decreasing the rate of deprotection as a function of reaction progress.

An issue that is commonplace amongst many types of PPGs, including **NBs**, is the inability to efficiently release poor leaving groups, such as alcohols and amines (Equation 5.3). A common method used to circumvent this problem is to protect the given alcohol or amine as the PPG-carbonate or –carbamate **5.9**, respectively (Equation 5.4). In general, the carbonates and carbamates are good leaving groups and will lead to efficient deprotection. Upon departure of the carbonate or carbamate **5.10**, subsequent

decarboxylation will yield the free alcohol or amine (H-LG). As for **NB** specifically, the decarboxylation step often becomes rate limiting. This relatively slow effective rate of release largely negates the utility of these PPGs towards fast physiological applications.[162]

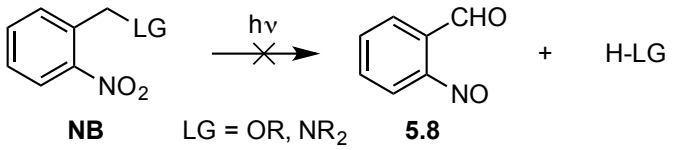

(5.3)

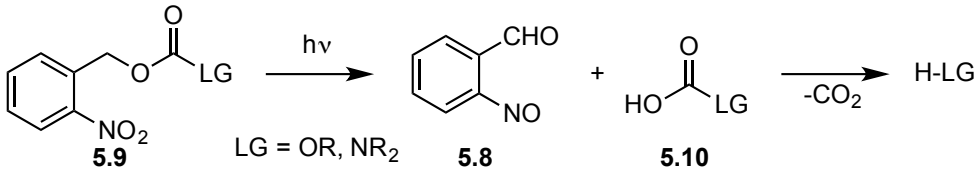

(5.4)

5.2.2. *o*-Nitrobenzyl-Based PPG Derivatives

Over the years, a plethora of **NB** derivatives have been designed with the goal of increasing the utility of these compounds as PPGs and caging groups. In order to circumvent the formation of **5.8**, early nitrobenzyl derivatives focused on substitution at the benzylic carbon. Patchornik demonstrated that the use of the 1-(2-nitrophenyl)ethyl group (**NPE**) (Figure 5.1) led to quantitative release of amino acids.[166] The addition of the methyl group at the benzylic position leads to the formation of the corresponding 2-nitrosoacetophenone, which is significantly less prone to imine formation than **5.8**. However, substitution at the α-substitution of these PPGs creates a new stereogenic center that can lead to the formation of diastereomers during synthesis, which can significantly complicate the synthesis of chiral and biological compounds.

An early PPG that was designed to increase efficiency of deprotection was the 2,6-dinitrobenzyl group (**DNB**) (Figure 5.1). It was found that the second nitro group on the aromatic ring led to an increase in quantum yield upon irradiation at 248, 254, and 313 nm relative to the analogous **NB** derivatives.[175,176] The rationale behind the observed increase in quantum efficiency was that, upon absorption of a photon, the second *o*-nitro group led to a statistical increase in the probability of 1,5-hydrogen abstraction to form the *aci*-intermediate analogous to **5.5** in the rate determining step. The **DNB** group was shown to release amino acids, as carbamates, in higher chemical yields, as compared to the **NB** counterpart.[175,177] However, later studies found that this increase in efficiency was not due to the additional hydrogen-abstracting group, but instead due to the resulting ketone byproduct being less prone to imine formation of the released amino acid.[178,179]

Figure 5.1. *o*-Nitrobenzyl photolabile protecting group derivatives

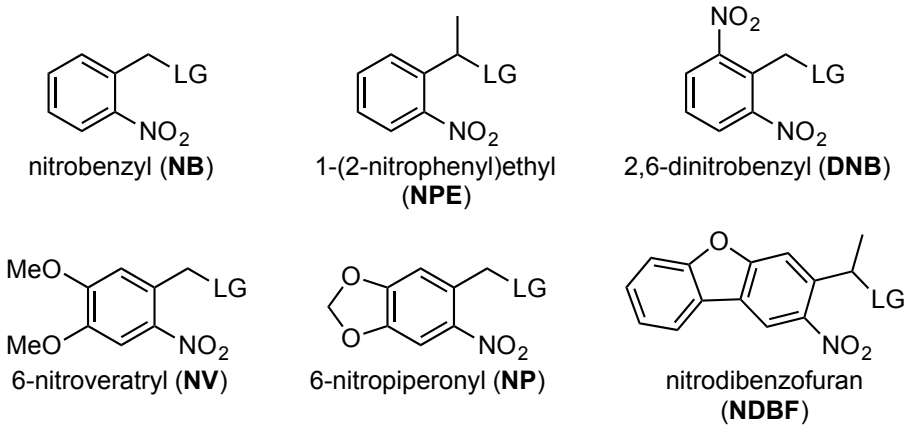

Finally, several analogues with various substitution patterns on the aromatic ring have been designed to alter the absorption properties. The 6-nitroveratryl (**NV**) and 6-

nitropiperonyl (**NP**) are amongst the most common PPGs and photocages in modern science.[162,170] The electron donating groups lead to a significant bathochromic shift and hyperchromic effect, which increased absorptivity at longer wavelengths. Interestingly, the **NB** group actually deprotects more efficiently than the **NV** group at 254 nm and is comparable in efficiency at 350-420 nm.[180] It is believed that the increased absorbance of the **NV** group is due to the availability of several new excited states that proceed through unproductive photochemical pathways.[179]

A recent example of an *o*-nitrobenzyl-based PPG that has found quick use in a variety of biological applications is the nitrodibenzofuran group (**NDBF**). Originally synthesized by Ellis-Davies for the photochemical release of calcium ions, **NDBF** undergoes photolysis between 16 – 160 times faster and more efficiently than previous **NB** derivatives.[181] With a very high molar absorptivity at 330 nm (ε = 18,400 M^{-1} cm^{-1}) and 350 nm (ε = 15,300 M^{-1} cm^{-1}), this group has quickly found use as a caging group in a number of biological applications, including cellular activation, peptide activation, and photoregulation of siRNA.[182–184]

5.3. NITROPHENPROPYL PHOTOLABILE PROTECTING GROUPS

First reported by Hasan in the late 1990s, the nitrophenpropyl PPG (**NPP**) is closely related to the **NB** PPG, although considerably fewer studies have been conducted using **NPP**.[177] The mechanism of deprotection of the **NPP**-based PPGs is shown in Scheme 5.2. Similar to the **NB**-based PPG, the first step upon excitation to **5.11** is a 1,5-

hydrogen abstraction to form the *aci*-nitro-intermediate **5.12**. Decomposition of the *aci*-intermediate occurs through elimination of the leaving group and formation of the 2-nitrostyrene byproduct **5.13**.

Scheme 5.2. Nitrophenpropyl PPG deprotection mechanism

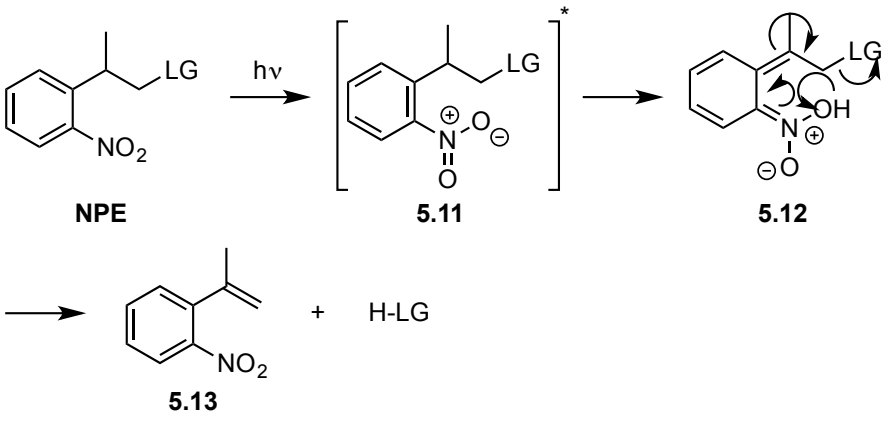

The **NPP**-based PPGs possess a few notable advantages over the **NB**-PPGs. First, **NPP** has been shown to release 5'-*O*-nucleoside carbonates about twice as fast as the analogous **NB**-caged nucleosides.[185] Furthermore, the **MNPPOC** (Figure 5.2) released carbonates at 365 nm with a five-fold increase in rate ($t_{1/2}$ = 11 s) relative to the analogous **αMe-NP** ($t_{1/2}$ = 54 s) and 20-fold faster than the **NV** group ($t_{1/2}$ = 216 s).[186] In addition to the increased photolysis efficiency, the **NPP**-based PPGs are also more suitable for the release of amine containing compounds, with respect to **NB** PPGs**,** because the photochemical byproduct **5.13** is unreactive towards amines.

Recently, a number of reports on the design and use of nitrobiphenyl compounds as efficient PPGs have been published.[162] The **ANBP** and **EANBP** groups (Figure 5.2)

have been shown to exhibit a strong absorbance in the visible region (λ_{max} = 400 nm, ε = 7,500 $M^{-1}cm^{-1}$).[187] These compounds have been used in a number of interesting applications including, live-cell fluorescence imaging, release of neurotransmitters, and photochemical DNA synthesis.[188–191]

Figure 5.2. *o*-Nitrophenpropyl PPG derivatives

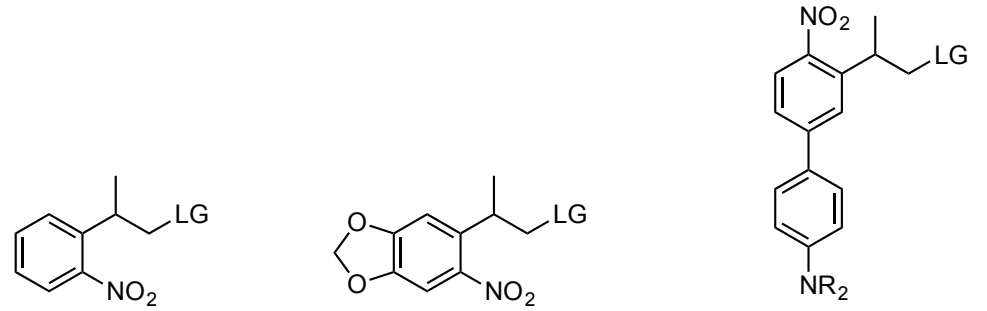

5.4. Arylcarbonylmethyl Photolabile Protecting Groups: Part I. Benzoin

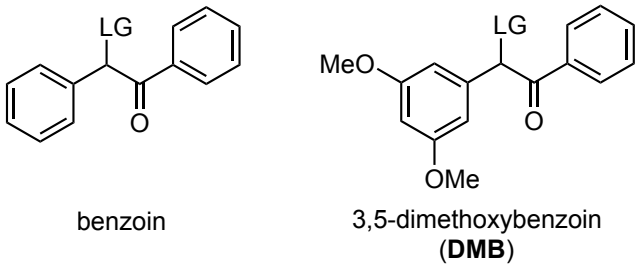

The use of benzoin-based compounds as PPGs was first reported by Sheehan and Wilson in the 1960s.[192] Early studies found that the use of the 3,5-dimethoxybenzoin (**DMB**) derivative significantly improved the efficiency of photolysis, these improved photochemical properties are believed to be due to what is known as the meta effect (see

Section 5.7.1). The deprotection of carboxylates and phosphates proceeds very quickly and cleanly to quantitatively yield the desired product and 2-phenyl-5,7-dimethoxybenzofuran (**DMBF**, **5.17**) (Scheme 5.3).[193] These reactions take place readily in both polar and nonpolar solvents. The photochemical mechanism of deprotection was found to be virtually independent of the identity of the leaving group, thus allowing for direct release of poor leaving groups such as amines.[168,194]

The **DMB** mechanism of deprotection has been subject to extensive studies and is shown in Scheme 5.3.[195–199] A number of time-resolved studies have shown that excitation of the parent **DMB**-protected compound yields a short-lived excited singlet state **5.14**. Initial studies suggested that the cyclohexadienyl cation **5.16** was formed directly from **5.14**. However, more recent pump-probe experiments with picosecond time resolution found that the preoxetane biradical **5.15** was formed with a rate constant ($k = 6 \times 10^{10}$ s^{-1}) from the excited singlet state, and decayed into **5.6** within 1-2 ns. Deprotonation of **5.16** yields the final protonated leaving group and **DMBF**.[198]

Scheme 5.3. 3,5-Dimethoxybenzoin (**DMB**) mechanism of deprotection

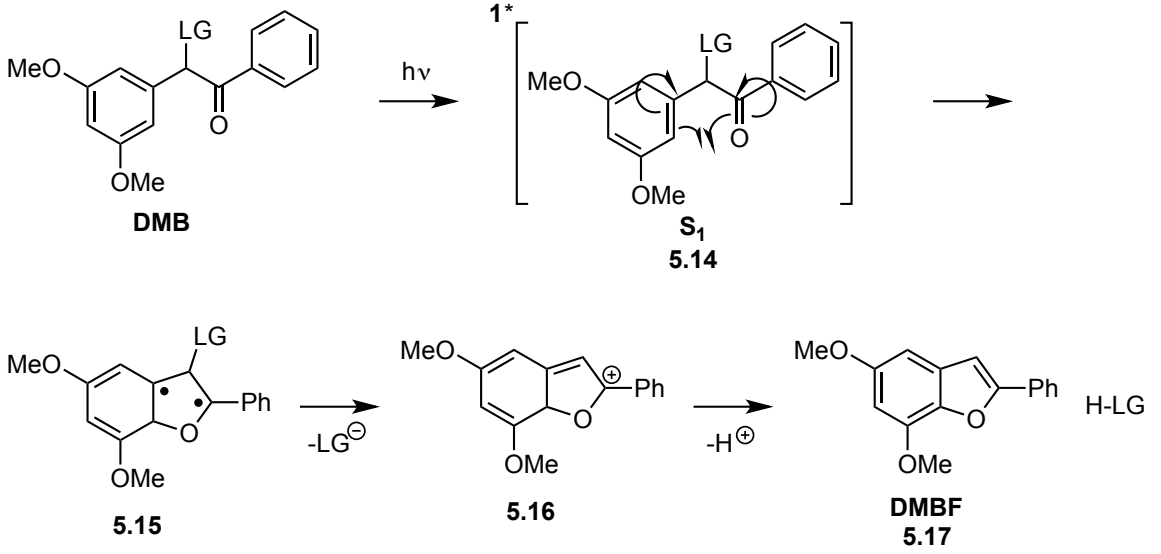

A major issue that has limited the use of **DMB** for protecting amines and alcohols as carbamates and carbonates are the potential side reactions that can occur during synthesis. Reacting **5.18** with phosgene or CDI leads to the formation of **5.19** (Scheme 5.4). Compound **5.19** can undergo an intramolecular cyclization to give **5.22**, which is unproductive towards PPG use. Furthermore, reacting **5.19** with a primary amine will give carbamate **5.20**, which can undergo a similar cyclization to give the photochemically inert **5.21**.[167] With respect to biological studies, the poor water solubility of **DMB**-caged compounds also limits the utility of this caging group. [162]

Scheme 5.4. Side-reactions upon **DMB**-protected substrate synthesis

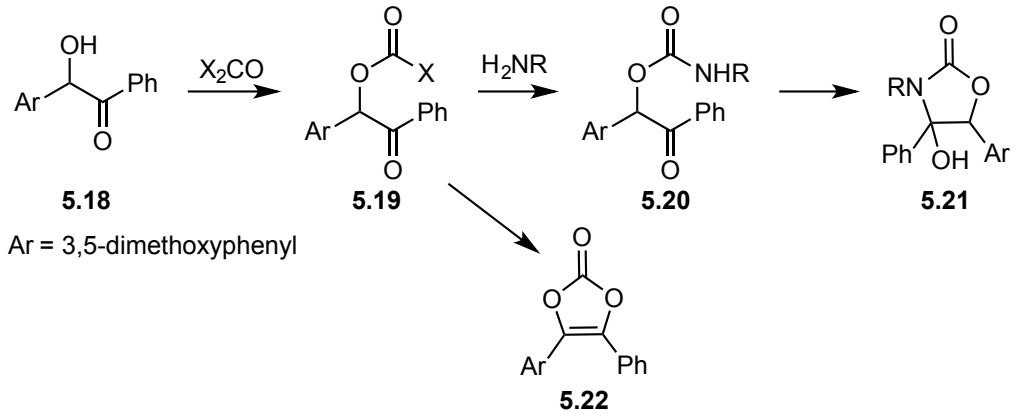

5.18 **5.19** **5.20** **5.21**

Ar = 3,5-dimethoxyphenyl

5.22

5.5. ARYLCARBONYLMETHYL PHOTOLABILE PROTECTING GROUPS: PART II. *P*-HYDROXYPHENACYL

Since the discovery of the *p*-hydroxyphenacyl PPG (**pHP**) (Scheme 5.5) a little over two decades ago, this group has since proven to be useful in numerous applications such as neurobiology and enzyme catalysis.[161,200,201] The **pHP** group has a number of advantageous properties compared to many other PPGs. First, the deprotection of most leaving groups proceeds cleanly to give the deprotected compound and *p*-hydroxyphenylacetic acid (**5.24**) in quantitative yields. Secondly, the rates of photolysis are very fast, with rate constants on the order of $k_r > 10^8$ s^{-1}. Finally, the hydrophilicity of the **pHP** chromophore leads to **pHP**-protected compounds that are soluble in aqueous media.[170] Interestingly, at neutral pH **pHP** has a λ_{max} at 278 nm. In aqueous base there is both a hypochromic and bathochromic effect to increase the absorptivity and red shift the maximum absorbance to λ_{max} = 325 nm.[162] Photolytic cleavage of the conjugate base of

pHP-protected compounds proceeds with comparable efficiencies to that of the neutral **pHP** species. In contrast to many other types of PPGs, there is no chiral center on the **pHP** chromophore, thus allowing for easier preparation and purification of chiral protected compounds.

Scheme 5.5. *p*-Hydroxyphenacyl PPG (**pHP**) mechanism of deprotection

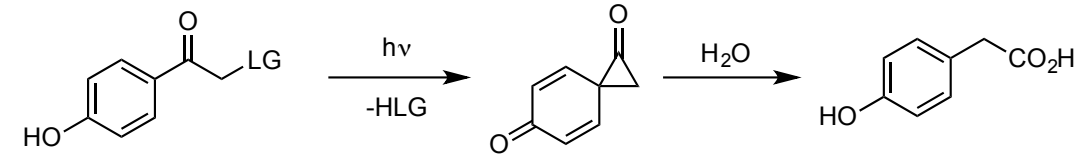

p-hydoxyphenacyl (**pHP**) **5.23** **5.24**

The mechanism of deprotection of **pHP** is unique and has been the focus of a number of studies.[202] As shown in Scheme 5.5, deprotection of **pHP** occurs via photochemical formation of the cyclopropanone intermediate **5.23** with simultaneous release of the leaving group.[203,204] Due to the structural similarity of **5.23** to that of the intermediate in the Favorskii rearrangement, this mechanism has been coined the photo-Favorskii rearrangement. The exact nature of the excited state formation of **5.23** has been subject to debate. Both excited singlet and short-lived excited triplet state pathways have been proposed.[205,206] Addition of water into **5.23** gives the sole photochemical byproduct, *p*-hydroxyphenylacetic acid (**5.24**).

A few key points can be made with regard to this mechanism of deprotection. First, the formation of the **5.23** as the sole photochemical byproduct is quite advantageous. *p*-Hydroxyphenylacetic acid (**5.23**) has a drastic change in absorbance and

does not interfere with parent **pHP** absorption.[153] Adding to the utility of the **pHP** group as a photocage in biological studies, **5.23** is biologically inert and photochemically stable.[207] The photochemical efficiency of deprotection is highly dependent on the identity of the leaving group. Good leaving groups, such as phosphates or sulfonates, typically release with quantum yields near unity and poor leaving groups, like phenolates, often proceed with low quantum yields ($\Phi_r < 0.1$).[208,209]

5.6. PHOTOENOLIZATION-BASED PHOTOLABILE PROTECTING GROUPS

Despite the structural similarities between **DMB** and **pHP** PPGs, the photoenolization PPGs are grouped based on their similar mechanism of deprotection. A number of interesting modifications to the photoenolization mechanism have led to the development of numerous photoenolization-based PPGs that will be discussed in the following sections.

5.6.1. 2-Methyl-Substituted Acetophenones

The most basic of the photoenolization-based PPGs is the 2-methylacetophenone PPG **5.25** (Scheme 5.6).[210–212] Upon irradiation, **5.25** is promoted to the singlet excited state **5.26**. Intersystem crossing (ISC) to the excited triplet state **5.27** allows for homolytic 1,5-hydrogen abstraction, leading to the triplet 1,4-diradical **5.28**. Biradical **5.28** will then form two isomeric photoenols *(Z)*-photoenol **5.29** and *(E)*-photoenol **5.30**. However, direct enolization from the singlet excited state **5.26** leads to the sole formation of the *(Z)*-

photoenol **5.29**, which is short lived and quickly undergoes a 1,5-sigmatropic rearrangement to give the parent compound **5.25**. The *(E)*-photoenol **5.30**, however, requires intermolecular hydrogen transfer to quench, and therefore persists long enough to undergo nucleophilic attack at the α-carbon to release the leaving group and form 1-indanone (**5.31**). Given that the leaving group is released through an S_N2 displacement, the efficiency of deprotection is directly correlated to the leaving group ability. Consequently, **5.25** is unsuitable for protection of poor leaving groups like phenols, thiols, alcohols, and amines.

Scheme 5.6. 2-Methylacetophenone PPG **5.25** mechanism of deprotection

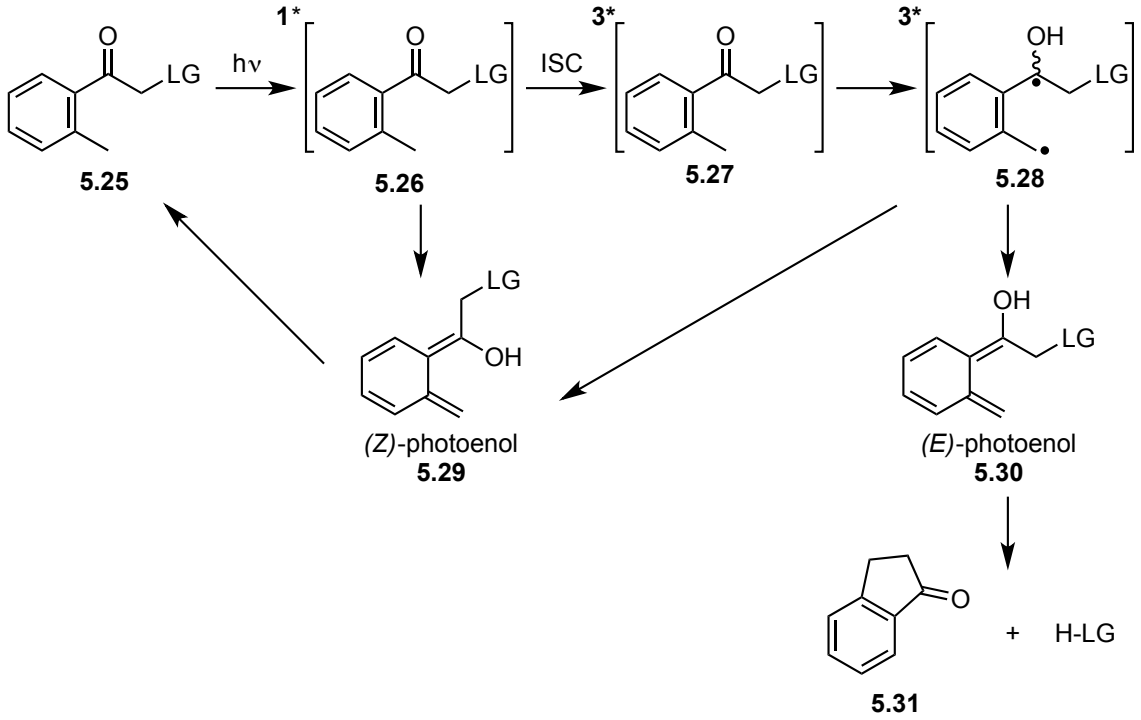

The 2-methyl-substituted acetophenones **5.25** release good leaving groups such as phosphates, carboxylates, and sulfonates.[170] However, there are numerous disadvantages of this PPG that have limited its application to a few examples of photoresponsive polymers.[213,214] The first of these disadvantages, is the poor photochemical efficiency of deprotection. Quantum yields and rates of release are typically very low for **5.25**-protected compounds relative to other PPGs. Furthermore, deprotection only occurs upon irradiation of UV-light, typically λ = 250 – 300 nm. In addition to the requirement of UV-light, the utility of **5.25**-caged compounds for biological applications is further hampered by the hydrophobicity of **5.25**, resulting in poor aqueous solubility.

Interestingly, the photochemical reactivity of this group was utilized in the syntheses of 1-indanone containing compounds, such as the Alzheimer's drug donepezil (**5.34**), pterosine B (**5.37**), and pterosine C (**5.40**), were achieved (Scheme 5.7). Benzoyl ester **5.32** was irradiated with a medium pressure mercury lamp to give 1-indanone **5.33** in 90% yield, thereby completing a formal synthesis of the acetylcholinesterase inhibitor donepezil (**5.34**) (A, Scheme 5.7).[215,216] In a separate study, Wessig irradiated α-mesylates **5.35** and **5.38** to form the 1-indanones **5.36** and **5.39** in 19% and 31% yield, respectively. Hydrolysis and α-methylation of **5.36** and **5.39** gave the natural products pterosine B (**5.37**) and pterosine C (**5.40**), respectively (C and D, Scheme 5.7).[217,218]

Scheme 5.7. 1-Indanone compounds accessed via photoenolization

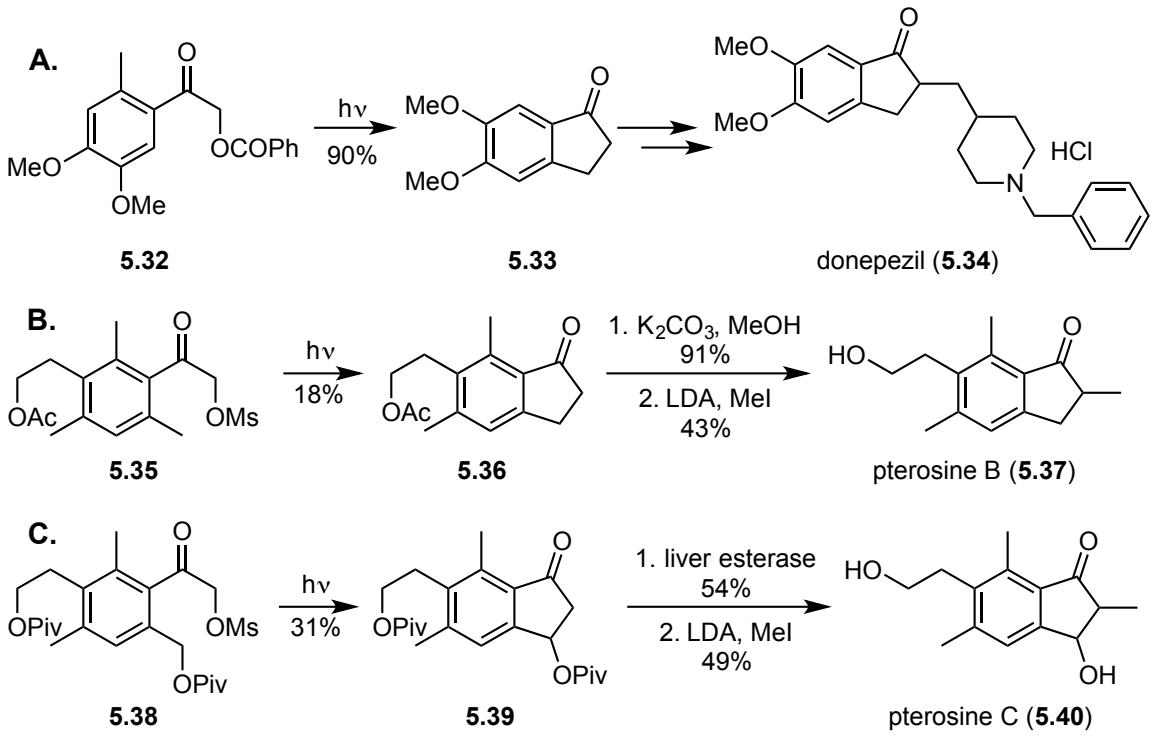

5.6.2. 2-Ethylene-Substituted Aryl Ketone Photolabile Protecting Groups

In the 1970s a new PPG was developed that utilized a 2-ethylene-substituted benzophenone core (**5.41**, R = Ph) (Scheme 5.8). Later reports proposed the use of related 2-ethylene-substituted acetophenones (**5.41**, R = Me).[219–221] The mechanism of deprotection of **5.41**-protected compounds is shown in Scheme 5.8. Excitation of **5.41** leads to the formation of *(E)*-photoenol **5.42**, which can undergo ketonization to eliminate the leaving the group and form the 2-styrene byproduct **5.43**. Due to the fact that protonation of **5.42** to reform the parent compound **5.41** is faster than elimination, these

PPGs release leaving groups with poor photochemical efficiency. Consequently, the use of these groups has been minimal since their initial discovery.[162]

Scheme 5.8. 2-Ethylene-substituted aryl ketone mechanism of deprotection

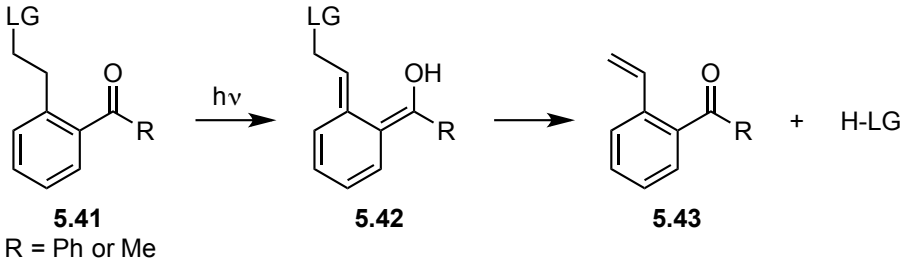

5.41
R = Ph or Me

5.42

5.43

5.6.3. Intramolecular Lactonization

A very interesting application of these reactive photoenols was reported by Gudmundsdottir in 2005.[222,223] In this report, excitation of protected alcohol **5.44** produced photoenol **5.45** via the triplet excited state (Scheme 5.9). Photoenol **5.45** then undergoes an electrocyclization to give benzocyclobutanol **5.46**, which positions the hydroxyl group proximal to the ester carbonyl. Subsequent lactonization of **5.46** leads to **5.47** and simultaneous release of the leaving group. In this report free alcohols were released in high chemical yields (90%).[224,225]

Scheme 5.9. Photodeprotection of **5.44** via lactone formation

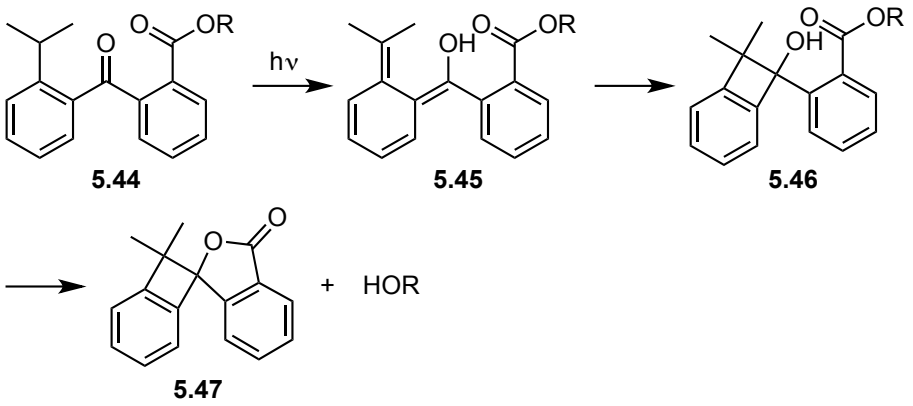

The direct release of free alcohols is a desired feature in PPGs. However, the low quantum yields of release and slow reaction rates of **5.44**, is likely the reason this group has not been utilized in any biological applications.

5.7. BENZYL BASED PHOTOLABILE PROTECTING GROUPS

A large class of PPGs is based on the photosolvolysis of benzyl substituted compounds. To generalize, a leaving group is attached to the benzylic carbon of an aromatic or heteroaromatic chromophore ($ArCH_2LG$) (Equation 5.5). Upon irradiation, excitation leads to heterolytic bond cleavage, or homolytic bond cleavage followed by immediate electron transfer, to give a benzyl cation ($ArCH_2^+$) and leaving group anion (LG^-) ion pair.[162] Trapping of the benzyl cation with a nucleophile, generally solvent (ROH), leads to the release of the leaving group. Given the necessity of a nucleophile, these photosolvolysis reactions are most efficient in polar protic solvents. In the absence

of nucleophilic trapping of the benzyl cation, recombination of the ion pair results in the formation of the original starting material.

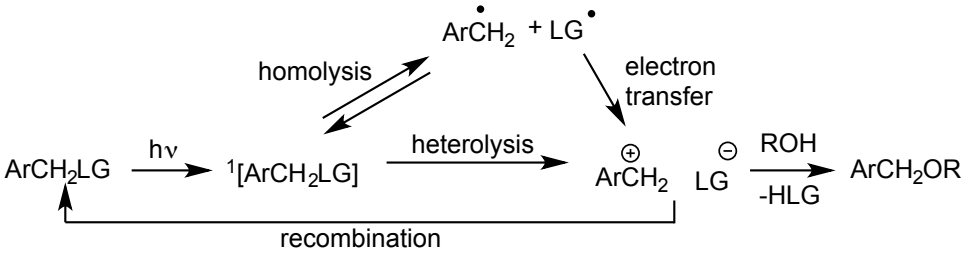

(5.5)

5.7.1. The Meta Effect

As mentioned in the discussion of the **DMB**, it is commonplace in PPG design to incorporate electron donating groups meta to the benzylic position. The rationale behind these substitution patterns is based on what is known as the meta effect.

In what is now considered a historic series of papers in photochemistry, Zimmerman discovered that electron donating groups in the meta-position actually stabilize benzylic carbocations in their excited states.[226–231] Through molecular orbital calculations of the excited state, he found that there is significant orbital overlap between the meta-positions within excited states of aromatic compounds. Experimental evidence was obtained through the photolysis of 4-methoxybenzylacetate (**5.48**) and 3-methoxybenzylacetate (**5.52**). Upon photolysis in aqueous dioxane, **5.48** gave **5.49** – **5.51**, the products of homolytic bond cleavage and subsequent radical chain reactions (Equation 5.6). However, upon photolysis of **5.52** in aqueous dioxane, the photosolvolysis product **5.53** was obtained as the major product, and radical byproducts

analogous to **5.49** – **5.51** were only observed in trace amounts (Equation 5.7). Furthermore, photolysis of 3,5-dimethoxybenzyl acetate (**5.54**) (Scheme 5.10) led to exclusive formation of the corresponding benzyl alcohol.

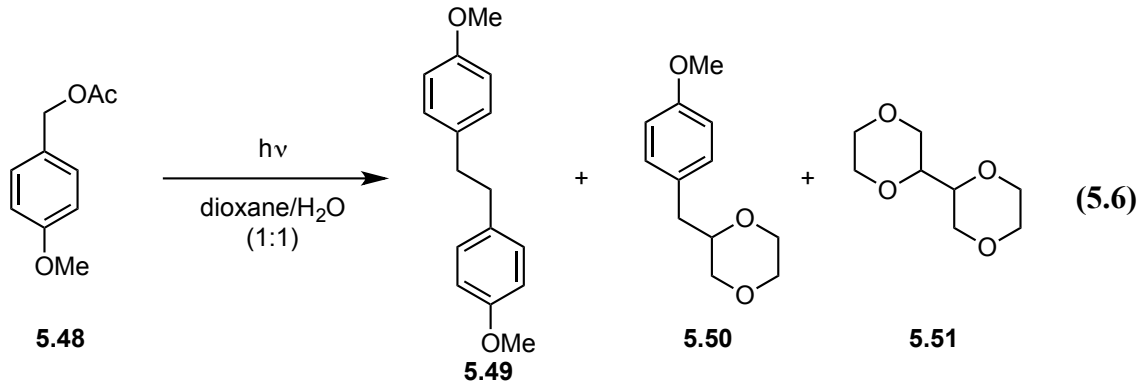

5.48 **5.49** **5.50** **5.51** **(5.6)**

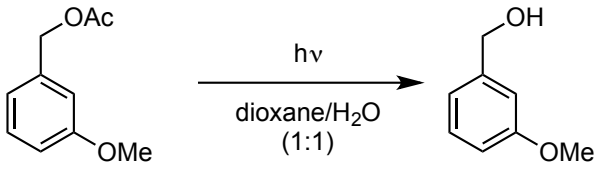

5.52 **5.53** **(5.7)**

Based on molecular orbital calculations of the excited state of **5.54**, Zimmerman describes the reaction mechanism shown in Scheme 5.10. Upon excitation of **5.54**, a $\pi \rightarrow \pi^*$ transition leads to an excited state that is best depicted as **5.54a**. Upon ionization of the acetate, the resulting excited state benzyl cation can be depicted as resonance structures **5.55a** and **5.55b**. The interconversion between **5.55a** and **5.55b** illustrates the stabilization of the excited-state benzyl cation by the meta effect.

Scheme 5.10. Mechanistic representation of the meta effect from M.O. calculations

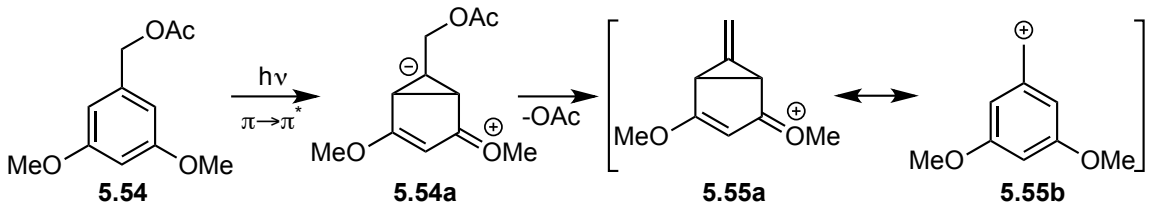

5.7.2. Benzyl Based PPG Examples

A select number of benzyl-based PPGs are shown in Figure 5.3. For this class of PPGs, release of the leaving group is dependent on nucleophilic capture of the resulting benzyl cation, thus weaker leaving groups tend to lead to faster rates of recombination, reducing the efficiency of deprotection. The 9-phenylxanthyl PPG (**Px**) has been shown to release alcohols directly upon irradiation of light at 254 – 300 nm in yields ranging from 78-97%.[232] Further improvements to **Px** led to the development of the 9-phenylthioxanthyl group (**S-Px**) and the corresponding meta-methoxy derivatives. In some of these examples, primary alcohols were released upon irradiation of light with wavelengths as long as 350 nm in varied yields (75-97%).[233]

The anthraquinone-2-yleth-2-yl (**Aqe**) group has also been shown to release alcohols, as the carbonate, and carboxylic acids. Applications in releasing carbohydrates and nucleosides upon irradiation at 350 nm has also been demonstrated.[234,235] While the yields of the **Aqe** deprotection again vary depending on the leaving group, this PPG has a distinct advantage within biological studies in that deprotection can occur with irradiation of visible light. Finally, the 3-(dimethylamino)trityl group (**DMATr**) was first reported

by Wang.[170,236] The **DMATr** PPG releases primary alcohols upon irradiation at 254 nm in good yields. Secondary alcohols as leaving groups led poor yields upon synthesis of the **DMATr**-protected compounds. Given that the trityl group has traditionally been used as an acid-labile protecting group in organic synthesis, the main concern with **DMATr** PPGs was their stability in acid. Wang demonstrated orthogonal deprotection between a standard trityl protected alcohol and a **DMATr**-protected alcohol.[237] In continuing their studies with trityl-based PPGs, Wang developed **5.56** for protection of ketones and aldehydes. Irradiation of various aldehydes and ketones with light ($\lambda < 320$ nm) led to efficient release of the corresponding aldehydes and ketones.[238,239] This class of PPGs has been used for a number of biological applications including, neural activation and photogeneration of bases for cellular imaging.[170,240,241]

Figure 5.3. Selected examples of benzyl-based photolabile protecting groups

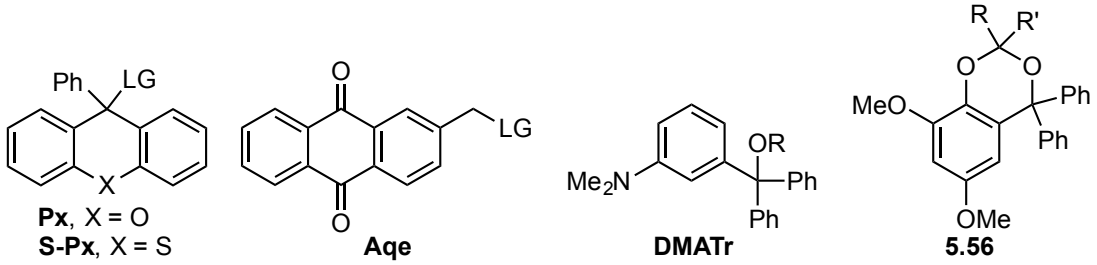

5.8. COUMARIN-BASED PHOTOLABILE PROTECTING GROUPS

Arguably, one of the most useful classes of PPGs are the coumarin-based PPGs. First discovered by Givens, who showed that phosphate esters were efficiently and

quickly released from the methoxycoumarin PPG (**MCM**) (Figure 5.4), this class of compounds has since been broadly investigated.[242] The coumarin-based PPGs have a number of distinct advantages over some of the previously discussed PPGs. First the coumarin chromophore has a very large absorption coefficient at longer wavelengths (λ_{max} = 350 – 475 nm), allowing derivatives to be reactive in visible light. Second, the coumarin chromophore is a strong fluorophore as well, allowing for the ability to monitor reaction progress through changes in fluorescence.[162] Finally, for good leaving groups, such as, phosphates, sulfonates, and carboxylates, this class of PPGs has some of the fastest rates of release for a PPG, making these PPGs useful for monitoring very fast physiological events, such as in electrophysiology studies.[152] However, due to the photosolvolytic mechanism of deprotection (Scheme 5.11), these groups do not efficiently release poor leaving groups like phenols, thiols, alcohols, or amines. Furthermore, decarboxylation becomes the rate limiting step in the release of carbonates and carbamates, which significantly reduces the apparent rates of release for alcohols and amines.[243–245]

Figure 5.4. Select coumarin photolabile protecting group examples

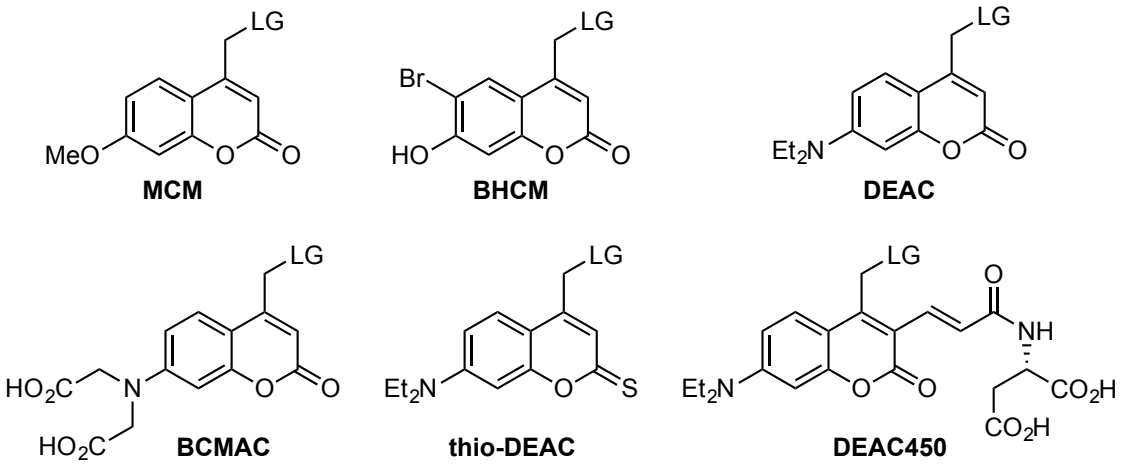

In recent years, a large number of coumarin PPG derivatives have been described, and reviews on the subject have been published.[200] An interesting development within the "first-generation" of coumarin-based PPGs was the 6-bromo-7-hydroxycoumarin-4-methyl group (**BHCM**) (Figure 5.4). The bromide substituent lowered the pKa of the proximal phenol by two-units, thus allowing full deprotonation of the phenol at physiological pH. Deprotonation of **BHCM** dramatically increased the aqueous solubility of **BHCM**-protected derivatives, and also resulted in a 50 nm redshift of the maximum absorbance (λ_{max} = 370 nm), as compared to **MCM** (λ_{max} = 320 nm).[246,247]

The "second-generation" coumarin PPGs are groups containing a 7-amino substituent, such as diethylaminocoumarin (**DEAC**). Addition of the 7-amino-substiuent was found to improve the efficiency of deprotection and further red shift the maximum absorbance (λ_{max} = 390 nm).[248,249] Shortly after the discovery of the improved

photochemical properties of **DEAC**, Ellis-Davis reported the synthesis of **DEAC450**, which has a maximum absorbance well into the visible region (λ_{max} = 450 nm), due to the extended conjugation of the enone moiety.[250,251] Finally, **thio-DEAC** has recently been reported and shown to possess a very high absorptivity in the visible region as well (λ_{max} = 470 nm). Furthermore, upon irradiation of green light (λ = 500 nm), the **thio-DEAC** group efficiently released a small molecule transcription inducer, cyclofen, in zebra fish embryos to induce protein expression.[252]

A major drawback to the coumarin-based PPGs is the hydrophobicity of the protected compounds. Given that most biological systems require aqueous media, this creates problems when attempting to use coumarin based cages for biological applications. To address this problem a number of coumarin-based PPGs containing polar functionalities have been designed, including **BCMAC** and **DEAC450**. Though the concentration of saturated aqueous solutions of **BCMAC**- and **DEAC450**-protected compounds were not given in these reports, biological studies were conducted at 1 mM concentrations without the addition of an organic co-solvent.

5.8.1. Coumarin Mechanism of Deprotection

Using **MCM** as an illustrative example, the mechanism of deprotection for the coumarin-based PPGs is shown in Scheme 5.11.[253–256] Upon irradiation, the parent compound is promoted to the excited singlet state, which is represented by the resonance structures **5.57a** and **5.57b**. From this excited singlet state, loss of a photon results in

fluorescence and gives the parent compound **MCM**. Alternatively, heterolytic bond cleavage of **5.57** leads to the formation of a tight ion pair **5.58**, which comprises the leaving group anion and the coumarin cation. This tight ion pair can either undergo recombination to give the parent compound **MCM**, or it can form a solvent-separated ion pair. From the solvent separated ion pair a nucleophile, typically solvent, can react with the cation to form **5.59**, and subsequent protonation of the leaving group anion gives the deprotected compound. It is worth noting that time-resolved absorption studies have shown the rate of heterolysis (for phosphate esters) is about 2 x 10^{10} s^{-1}, making this amongst the fastest measured photolysis rates for any PPG. However, due to the fact that the rate of recombination is about 10-fold faster than that of nucleophilic trapping, the actual observed rate of product formation is much lower.[257]

Coumarin-based PPGs and photocages have been extensively utilized in a range of biological applications, including small molecule gene regulation, siRNA gene regulation, small molecule neural activation, photochemical peptide synthesis, and embryonic cellular signal transduction.[153,162,243,248,250–252,258]

Scheme 5.11. Coumarin mechanism of deprotection

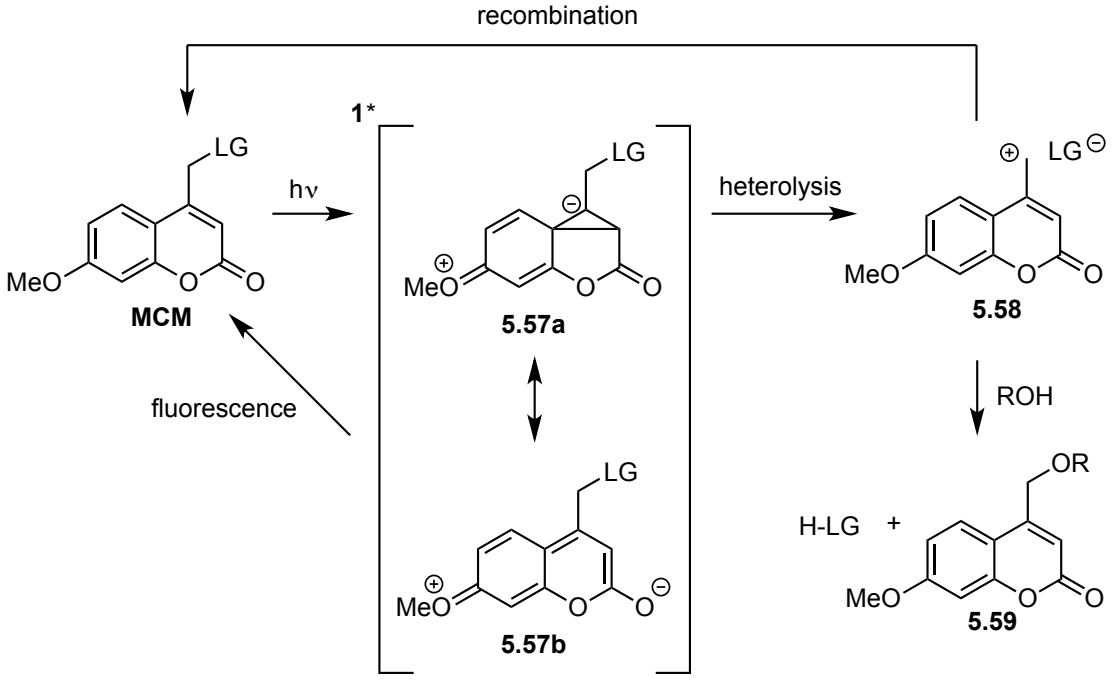

5.9. PHOTOCAGING: BIOLOGICAL APPLICATIONS OF PPGS

Though originally designed by synthetic chemists, the use of PPGs in biological settings has become a fertile field of research. One of the earliest examples of the use of a PPG-protected compound in biology was in 1977 by Engels, who synthesized **NB-cAMP** (Figure 5.5) and demonstrated *in vitro* decaging through activation of the **cAMP**-dependent protein kinase in rat glioma cells.[259] Shortly thereafter, Hoffman reported the use of **NB-ATP** to study Na/K ion pumps through the decaging of ATP in human red blood cells.[260] In this paper, Hoffman refers to the **NB-ATP** compound as "caged ATP".

From that point on, the use of PPGs to inactivate biological compounds has been known as “caging”.

Figure 5.5. First examples of photocaged biological compounds

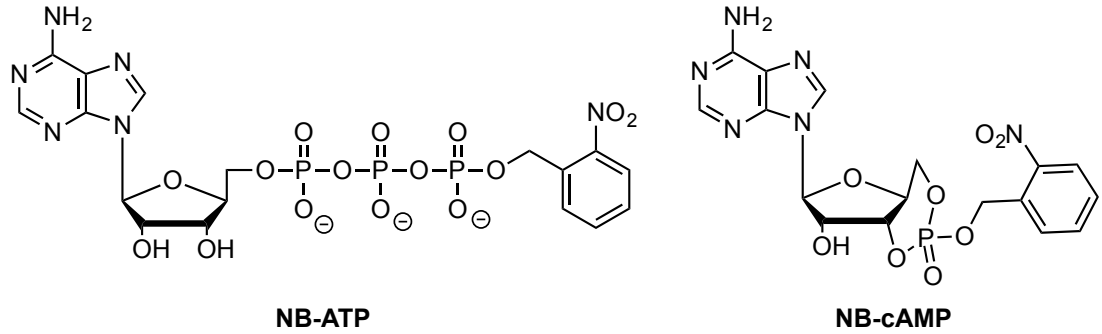

Though the term has stuck for nearly half-century, the use of “caging” to denote PPG-protected biological compounds has been met with scrutiny.[160] The term “caging” is often misinterpreted to mean a biological compound that is completely encompassed by a photoreactive molecule, which physically opens upon irradiation of light.[160] Consequently, over the past 40 years, a number of terms such as, photoactivatable, light-triggered, or photocaged, have been used interchangeably with the term “caged”. Nonetheless, an immense amount of research using photocaged compounds to study biological processes including, the control of gene expression, inhibition of mRNA, protein synthesis/folding, neuronal activation/inhibition, and cellular imaging, have been reported since the seminal report by Engles. In the following section, we will highlight a few examples that are directly applicable to the research at hand. A number of reviews

have previously covered the applications of photocaged compounds across multiple divisions of biology.[153–162,200,261]

5.9.1. Induced Gene Expression via Photocaged Small Molecules

A common application of photocaged small molecules, is the photochemical control of gene expression. Inducible heterologous gene expression is a fundamental process in synthetic biology.[262] Heterologous transgene expression systems, consisting of a specific group of genes (operon) that allows for the ability to "turn on" or "turn off" expression of a gene of interest, are activated by a specific small molecule. Commonly, these small molecules consist of clinically approved antibiotics, such as erythromycin A, doxycycline, or rapamycin.[154,263] Therefore, in these studies, control over when and for how long the small molecule is present, leads to the temporal control of gene expression. Recently, to increase the temporal resolution within these expression systems, the use of photocaged small molecules has allowed for control over gene expression through irradiation of light.[156,264] By releasing these small molecules *in vitro* or *in vivo* via decaging, temporal resolution on the order of the rate of deprotection is achievable.

In one example of the photochemical control of gene expression, Deiters used the nitropiperonyl-protected erythromycin-9-oxime (**NP-ERY**) (Figure 5.6) to induce expression of a fluorescent protein in bacteria.[265] In this study, the macrolide-inducible transgene expression system (E_{ON}), which activates transgene expression in the presence of erythromycin A, was utilized.[266] Unable to directly photocage erythromycin A (**ERY**),

Deiters first ran a positive control experiment to confirm that erythromycin-9-oxime initiated transcription of the fluorescent reporter. After confirmation, he demonstrated that irradiation of **NP-ERY** with UV-light (365 nm, 25 W) for five minutes, induced the same level of fluorescent protein expression as the positive control. Deiters further demonstrated spatial control over gene expression by seeding the bacterial cells onto an agar plate and covering half of the plate. Subsequent irradiation with UV light for five minutes led to fluorescent protein expression of only the exposed portion of the plate. While this study was an elegant demonstration of spatial resolution of bacterial gene expression, the use of UV-light was taxing on cell viability, leading to a decrease in fluorescence response with irradiation times greater than five minutes.

Figure 5.6. Erythromycin A (**ERY**) and nitropiperonyl-caged erythromycin-9-oxime (**NP-ERY**)

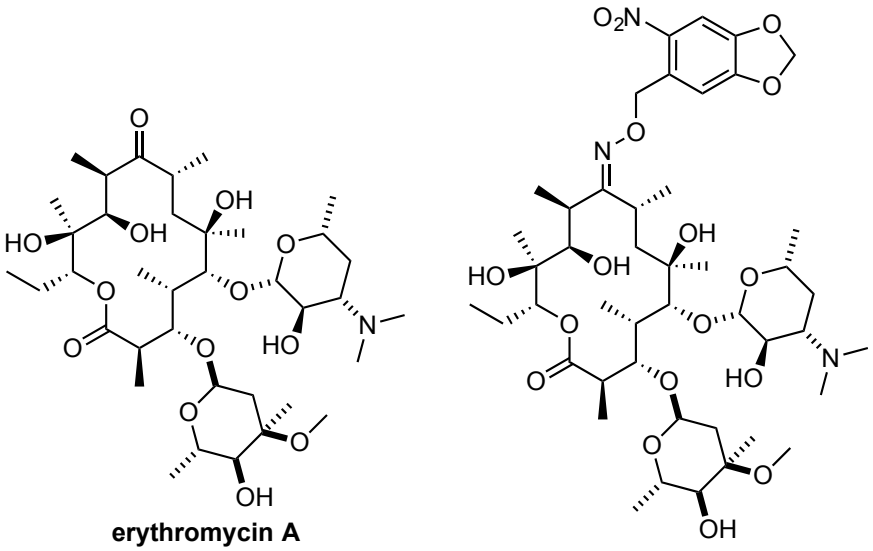

Another exciting advance in the field was reported by Cambridge in 2009. In this study, a nitroveratryl photocaged doxycycline derivative (**NV-DOX**) was used to induce the expression of a fluorescent reporter *in vivo* (Figure 5.7).[267] In this report, Cambridge used the tetracycline-inducible expression system (Tet_{ON}), which induces heterologous gene expression in the presence of tetracycline derivatives, like doxycycline (**DOX**).[268,269] Upon irradiation of transduced rat hippocampal brain slices at 330 – 350 nm for 15 seconds, they observed expression of the fluorescent reporter. Furthermore, an impressive degree of spatial resolution was achieved, demonstrating the ability to induce a fluorescence response in individual cells. Comically, this spatial resolution was also demonstrated by the creation of a fluorescent "smiley face" in one brain slice.

Furthering the potential applicability of light-dependent gene control methods, Cambridge also demonstrated photoactivated gene expression in live mouse embryos. Using a mouse whole-embryo culture system,[270,271] they infected mice embryos with the Tet_{ON} expression system. After 10.5 days, the embryos were removed, incubated with **NV-DOX**, and irradiated with light (330 nm, 15 s). They observed a fluorescence response in the irradiated embryos, thus demonstrating photoactivation of gene expression *in vivo*.

Figure 5.7. Doxycycline (**DOX**) and nitroveratryl caged doxycycline (**NV-DOX**)

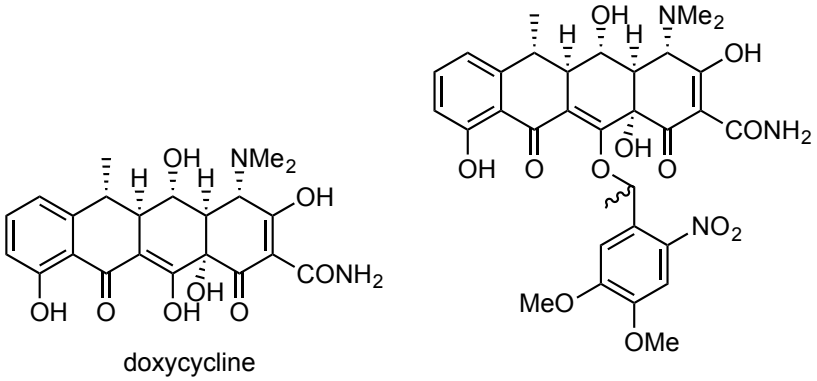

5.9.2. Photoinduced Muscle Contraction via Calcium Ion Release

Since the first reported use of a photocage in 1977, the overwhelming majority of *in vitro* studies have utilized the **NB** or **NV** caging groups, which require UVA-light for one-photon decaging and high-intensity near IR-light for two-photon decaging.[162] Consequently, the light required for these decaging processes can be damaging to cells and can also bleach endogenous chromophores, thus restricting these photocages from use *in vivo*. In addressing these shortcomings, Ellis-Davis designed the **NDBF** photocage, which improved photochemical properties such as, larger molar absorptivities, faster rates of release, and better quantum yields of release, with respect to the **NB** and **NV** photocages (Figure 5.8).[183]

For this study, Ellis-Davis designed **NDBF-EGTA** to photochemically release Ca^{2+} ions and demonstrated the efficient release of Ca^{2+} *in vitro*.[183] They found that the parent **NDBF-EGTA** was a strong binder of Ca^{2+} ($k_d = 1.4 \times 10^{-8}$), and upon photolysis, underwent a 140,000-fold decrease in binding to Ca^{2+} ($k_d = 10^{-3}$). Decaging in guinea pig cardiac muscle, via irradiation with a UV-laser at a power of 70 mJ, produced the

maximum force of muscle contraction. By comparison, under the same conditions, the **NB-EGTA** analogue produced < 10% of the maximum force of muscle contraction, due to the poor photochemical release of Ca^{2+} by **NB-EGTA**. Furthermore, decaging was found to be very efficient, proceeding with a rate constant of $k_r = 2 \times 10^4$ and a quantum yield of 0.7 ($\Phi_r \bullet \varepsilon = 1.8 \times 10^4$). Since this initial report of the **NDBF** cage, multiple studies have demonstrated the fast release of nucleotides,[184] thiols,[183] and amides.[181]

Figure 5.8. Structures of **NDBF-EGTA** and **NDBF**

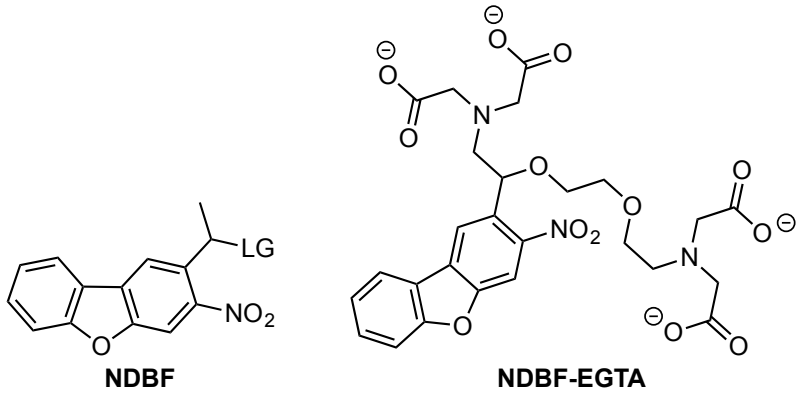

5.9.3. Photoactivation and Photoinhibition of Neurons

One of the most potentially impactful applications of photocaged small molecules, is the release of neurotransmitters to enable photoactivation or photoinhibition of neurons. The decaging of neurotransmitters such as, glutamate or GABA, allows for precise spatial and temporal control of neuron activation/inhibition using light. Furthermore, three-dimensional spatial resolution has been demonstrated through two-photon uncaging in living organisms.[208,244] However, the poor photochemical efficiencies of traditional nitrobenzyl-based caging groups has limited the *in vivo* applications of this

technique. To address these shortcomings, recent studies have focused on the design of novel caging compounds with better two-photon efficiencies

In 2012, Goeldner and Specht reported the use of **ANBP-GABA** to effect the photoactivation of neurons (Figure 5.9).[187] In these studies, they found that **ANBP-GABA** possessed a number of advantageous properties, compared to previous photocaged GABA examples. First, **ANBP-GABA** was found to be soluble in phosphate buffer up to 10 mM and hydrolytically stable at room temperature for 24 hours. Furthermore, the **ANBP** cage absorbed light in the visible region (λ_{max} = 397 nm) and displayed decent one-photon decaging efficiency ($\Phi_r \bullet \varepsilon$ = 1.1 x 10^3 M^{-1} cm^{-1}). However, the **ANBP** cage displayed an impressive two-photon rate of release, with a single nanosecond laser pulse leading to nearly complete photolysis in under 5 μs. Subsequent *in vitro* studies found that isolated rat cortical brain slices, incubated in a 1 mM solution of **ANBP-GABA**, quickly underwent two-photon decaging when irradiated at 800 nm, and showed almost immediate dendritic current spikes. The efficiency of two-photon decaging of **ANBP-GABA** *in vitro*, has sparked interest in the potential use of **ANBP**-caged neurotransmitters for *in vivo* photoactivation of neurons.

Figure 5.9. Examples of photocaged **GABA** and **cAMP**

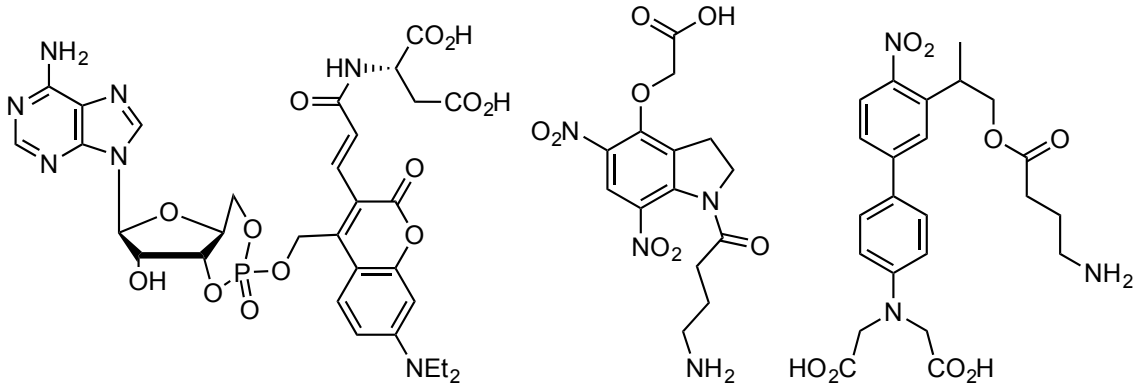

More recently, the ability to selectively excite and inhibit neurons, through the orthogonal decaging of **DEAC450-cAMP** and **CDNI-GABA** has been reported (Figure 5.9).[251] In designing the **DEAC450** photocage, Ellis-Davis discovered that **DEAC450** not only exhibited a large absorbance in the visible region (λ_{max} = 450 nm, ε = 43,000 M^{-1} cm^{-1}), but also displayed a relative minimum in absorbance at wavelengths commonly used for decaging (λ_{min} = 350 nm). He demonstrated orthogonal deprotection of **DEAC450-cAMP** and **CDNI-GABA** in striatal cholinergic interneurons, isolated from mouse brain slices. These neurons are known to spontaneously fire at a given frequency.[272] The firing rate is known to be upregulated in response to stimuli that produce **cAMP**, thus the presence of **cAMP** increases the frequency of action potential firing.[273] Conversely, action potential firing is inhibited by **GABA**, and thus the frequency of action potential firing decreases in response to the presence of **GABA**.[274] In this assay, a solution of **DEAC450-cAMP** (25 – 75 μM) and **CDNI-GABA** (1 mM) was

added to the cholinergic interneurons, which resulted in no change of the action potential frequency. Upon irradiation at 473 nm for 100 - 200 ms, a dramatic increase in action potential frequency that lasted for tens of seconds was observed. In the same solution, irradiation at 355 nm for 2 ms, led to an immediate decrease in the frequency of neuron firing. The design of new visible light reactive caging groups has allowed for the ability to orthogonally deprotect two photocaged compounds, which will undoubtedly lead to entirely new applications of photocaged compounds.

5.10. Summary of Photolabile Protecting Groups and The Future of Photocaging

Since the first report of the photolytic deprotection of Cbz-glycine, the field of photolabile protecting groups has grown dramatically.[153] To reiterate, a successful PPG must meet the five criteria discussed. The protected compounds must be inert to the system under investigation. Deprotection should proceed quickly and efficiently upon irradiation. Photochemical byproducts must be inert and non-toxic to the system at hand. The protected compounds must be soluble in the target media. The observed rate of release must be faster than the response under investigation (biological studies). Since no one PPG meets all of these criteria for every potential application, selection of an appropriate PPG is paramount to the success of a given application.

A wide variety of PPGs featuring unique structural and mechanistic properties have been reported over the past half-century. Some of the most commonly used PPGs, or photocages, are shown in Figure 5.10. By far the most commonly used groups for

photocaging applications are the **NV** and **NP** cages. Though the photochemical efficiencies of these groups are less than ideal, the ability to reliably uncage a wide range of functionalities, combined with the simple synthesis of caged substrates from commercially available materials, has led to the wide-spread use of the **NV** and **NP** caging groups.[170] New *ortho*-nitrobenzyl photocages, such as **NDBF**, have dramatically increased the photochemical efficiencies of decaging and will certainly be applied to future applications.[183]

The arylcarbonylmethyl photocages, namely, **DMB** and **pHP**, are especially useful in photochemical electrophysiology studies.[194,201] Due to the fast rates of release and the formation of biologically inert photochemical byproducts, **DMB** and **pHP** caged neurotransmitters have been extensively utilized to study photoactivation and photoinhibition of neurons. Unfortunately, despite many efforts, the design of new photocages related to **DMB** and **pHP** that decage in visible light, have not been successful.

Though mechanistically related to the *ortho*-nitrobenzyl photocages, the *ortho*-nitrophenpropyl photocages are particularly effective at two-photon decaging. One of the original *ortho*-nitrophenpropyl photocages, the **NPP** cage has been extensively used in photochemical gene silencing and photochemical activation/inhibition of enzymes, via the use of **NPP**-caged siRNA and peptides, respectively.[275] Red-shifting the wavelengths of decaging into the visible region, the **ANBP** photocage is remarkably efficient at two-

photon decaging, which will allow for unprecedented levels of spatial and temporal control in photocaging applications within living organisms.[187]

Figure 5.10. Summary of the most commonly used and advantageous PPGs

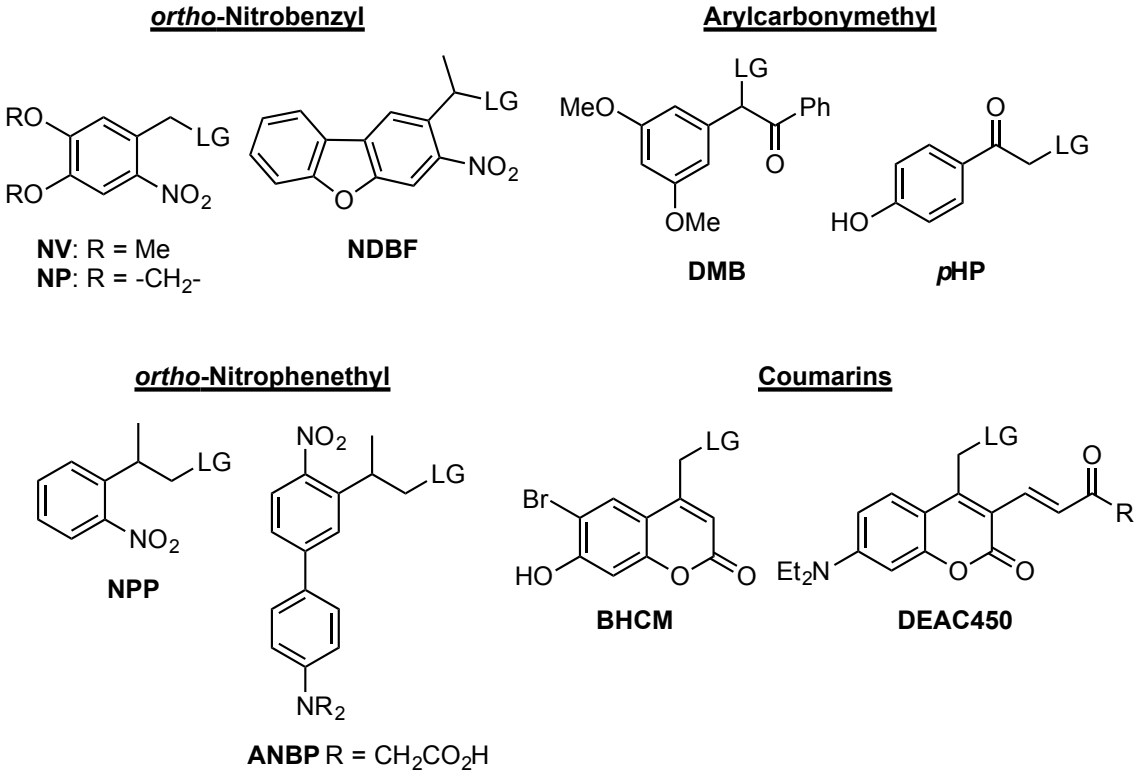

Finally, the coumarin-based cages are one of the most promising classes of new photocages is the coumarin-based cages. With fast rates of decaging, large absorbance in the visible region, and advantageous fluorescent properties, coumarin-based photocages are quickly becoming a favorite choice for many *in vitro* applications.[250] However, due to the photosolvolysis mechanism of deprotection, the coumarin caging groups are only applicable for the photocaging of good leaving groups. Nonetheless, many coumarin-

based derivatives have been designed for photocaging applications. As demonstrated by Ellis-Davis, the large absorbance at long wavelengths of **DEAC450**, allows for orthogonal deprotection between traditional photocages, like the *ortho*-nitrobenzyl cages.

To this day, research continues towards the development of novel photocages to further meet the needs of current applications. There is currently a need for better caging groups that fulfill the criteria previously discussed. Currently, we are conducting research into the design of new caging groups that can release poor leaving groups, like alcohols and amines, upon irradiation with visible light. The unique and advantageous properties of the most recent photocages, has instigated a paradigm shift in what is now believed to be possible through the application of photoactivated compounds. Research into novel applications of photocages will lead to exciting advances in the fields of drug delivery, molecular biology, synthetic biology, and neurobiology. In the latter field, we have commenced a chemical, genetic, and neurobiological collaborative effort to develop a functional neuronal tagging method that, if successful, will lead to an unprecedented understanding of how the brain functions on a cellular level.

Chapter 6: Studies Towards Neuronal Tagging Through Caged Small Molecule Repressor Ligands.

6.1. Studying Brain Function

In 1861, the French physiologist Paul Broca used the brain of Louis Leborgne, known in science folklore simply as "tan", to show that a small section in the frontal lobe of the human brain was responsible for speech production. The patient, who could only speak the syllable "tan" with altered volume and inflection, was found post-mortem to have damage to the ventral frontal lobe of the left hemisphere of his brain.[276] By correlating physiological symptoms to physical damage of the brain, Broca made an inference that this area of the brain, now known as Broca's area, is crucial in speech production. At the time, this pioneering work launched what is known today within neurobiology as the lesion method.[277]

The lesion method of studying the brain is the practice of observing symptoms of a subject upon, removal or damage to a given area of their brain. Correlations between damaged sections of the brain and the corresponding physiological consequences, allows one to infer the function of a given area of the brain. While seemingly archaic and arguably outdated, this method of neurobiological research has led to a great deal of knowledge on brain function in the areas of language comprehension,[278] long-term memory formation,[279] processing of emotions,[280,281] and visual perception.[282] However, this method has a number of limitations.

A major problem with lesion studies, is that this method inherently requires the destruction of neuronal circuitry, which means that conclusions based on this method are drawn from the lack of connectivity within the brain, as opposed to the study of a healthy intact brain. This relationship between a lack of function and the disruption of connectivity is further complicated by the ability of certain sections of the brain to change function in response to damaged circuitry.[283] Second, the lesion method lacks the capability for an experimental control. The inference of brain function, based on the location of a lesion and the resulting physiological symptoms assumes these functional areas of the brain are localized to the exact same position for all individuals. However, it has been well documented that the brain shows a relatively large degree of anatomical diversity between individuals.[284] Therefore, without proper experimental control subjects and a representative sample size, the results from an individual cannot be assumed to hold true for an entire population. Finally, this method assumes discrete anatomical modulation of cognitive function, also known as the "modularity" or "localization" assumption.[277] This assumption has proven problematic because it has been shown that many brain functions are distributed between a number of localities.[285] Though rich in history, many conclusions drawn from lesion studies have since been modified or disproven with the advent of modern functional brain imaging techniques, most notably functional magnetic resonance imaging (fMRI).

Since the discovery of functional magnetic resonance imaging (fMRI) in the early 1990's, this technique has revolutionized neurobiological research.[286,287] Most

commonly, blood-oxygen-level dependent (BOLD) contrast is utilized. This method takes advantage of the fact that oxygenated and deoxygenated blood have different magnetic properties,[288] which allows for images based on oxygenated blood flow within the brain to be produced. Since there is a direct relationship between blood flow within the brain and neural activity, these images have been shown to reflect brain activity.[289] This technique has led to remarkable gains in the understanding of how the human brain functions. However, there are also limitations to this technique, one of which is that the results are purely correlational. Because this method does not provide any information on brain function, it cannot be known if an activated area of the brain is necessary or even participates in a given task.[277] Furthermore, the spatial resolution is limited to about 1 mm^3. While this resolution has allowed researchers to learn a great deal about what areas of the brain are active during a given function, it provides little or no insight into how specific neuronal pathways are interconnected, nor how these pathways contribute to a given function.

6.2. New Method For Function-Based Neuronal Tagging

In addressing the shortcomings of these previous techniques, we are developing a novel method to tag or label neurons based on function. While early attempts to develop this method will focus on fluorescently labeling activated neurons within a live mouse host, successive iterations will feature the expression of cellular actuators within these activated neurons. This will allow for experimental manipulation of the given subsets of

neurons that have been identified based on function, thus allowing the ability to probe neuronal circuitry on a cellular level.

The genetic construct to achieve this neuronal labeling method is currently being designed and developed in the laboratory of Dr. Boris Zemelman. For *in vivo* studies, we plan to install the genetic sequence via transduction of a viral vector. The three main components of this construct are Promoter X, Operator X, and the reporter (A, Figure 6.1). Promoter X is a DNA sequence that acts as a binding site for a specific transcription factor (TF). The transcription factor responds to neuron activation by binding to the promoter and initiating transcription of downstream genes. For the purpose of this work, the reporter is green fluorescent protein (GFP). Operator X is a DNA sequence that acts as a binding site for the respective repressor protein. When bound to Operator X, the repressor protein blocks transcription downstream of Operator X, thus for a transduced neuron in the presence of the repressor, expression of the reporter is blocked or repressed irrespective of neuron activation (B, Figure 6.1). Finally, the repressor ligand is a small molecule with high-affinity for the repressor protein. When the repressor ligand is introduced, it binds to the repressor protein and the resulting protein-ligand complex detaches from Operator X. This allows for the reporter to be expressed whenever the transcription factor responds to neuron activation (C, Figure 6.1).

Figure 6.1. Proposed genetic construct to functionally tag activated neurons[a]

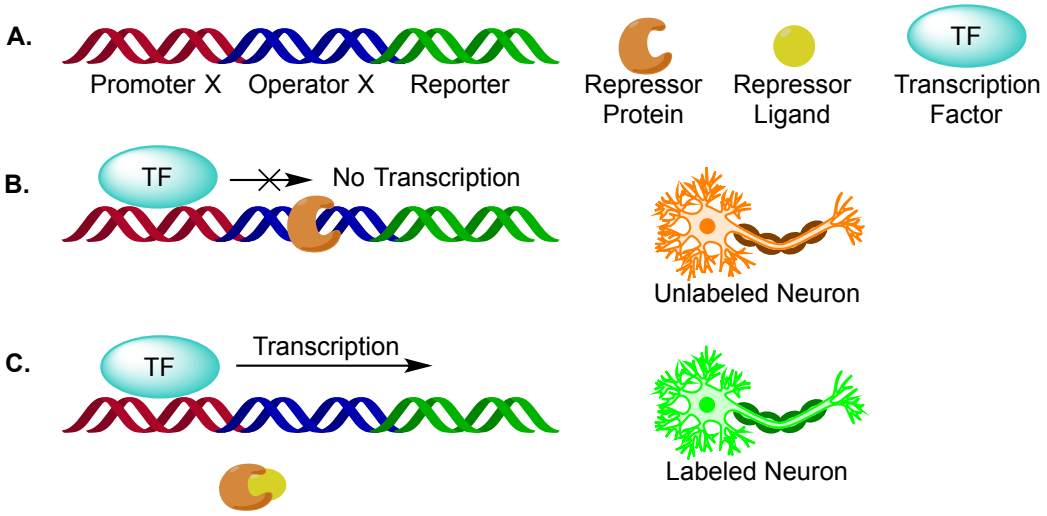

[a]**A)** Schematic representation of each component within the proposed genetic construct. **B)** In the absence of the repressor ligand, the repressor protein binds to the operator, thereby repressing expression of the reporter. Therefore, a transduced neuron will remain unlabeled irrespective of transcription factor activation due to neuron firing. **C)** Upon introduction of the repressor ligand, the repressor protein-ligand complex will dissociate from Operator X. Upon dissociation, neuron action potential will provoke a response from the transcription factor, which will initiate transcription of the reporter and lead to labeling of the neuron.

6.2.1. Promoter X

An elegant feature of the proposed genetic construct is the inherent modularity of the genetic components. While the basic nature of Promoter X, Operator X, and the reporter will fundamentally remain the same, we have the ability to use any number of specific genes for each component to best fit our goal. For instance, promoter X can be a number of different DNA sequences, or response elements, that act as binding sites for transcription factors, which respond to neuron activation. Previous studies have reported the use of transcription factors that respond to immediate early genes (IEGs), such as *c-fos* or *arc*, to induce gene expression reflective of neuronal activation.[290–295] However, for

our initial studies we plan to use the cAMP response element binding protein (CREB) as the transcription factor and the cAMP response element (CRE) as Promoter X. CREB is naturally found in all neurons and regulates gene expression, including IEG expression, based on neural activity. In the neuron signaling pathway, CREB-mediated gene expression occurs prior to the expression of IEGs, thus its use as the transcription factor should allow for a more responsive signaling method.

In nature, CREB activates gene transcription in response to a number of cellular signals, such as cAMP or Ca^{2+}, that arise from neuron activation. Found in all neurons and a near universal indicator of neuronal activation, CREB has been previously used to control exogenous expression in neurons.[296,297] The neuron signaling pathway for CREB-mediated gene expression is shown in Figure 6.2. Binding of a ligand (L), or neurotransmitter, to the G protein-coupled receptor (GPCR) activates G protein (G), which in turn induces adenylyl cyclase (AC) mediated cAMP production. The secondary messenger, cAMP, promotes the dissociation of the heterotetrameric protein kinase A (PKA), which consists of two pairs of catalytic- (C) and regulatory-subunits (R). Through passive diffusion, the catalytic subunit (C) will enter the nucleus and phosphorylate (p) CREB at a single serine residue (Ser133). The phosphorylated-CREB binds to the cAMP response element (CRE), which is a repeating palindromic DNA sequence (TGACGTCA) and CREB binding site. Upon binding to CRE, the phosphorylated-CREB associates with the co-activator, CREB-binding protein (CBP), which in turn coordinates with RNA polymerase II (POL II) and initiates transcription.[298] CREB-mediated gene

expression generally peaks about 30 min after neuronal stimulation, and subsequently decreases over the ensuing two – four hours, due to CREB dephosphorylation by the serine/threonine phosphatases PP-1 and PP-2A.

Figure 6.2. Neuron signaling pathway leading to CREB-mediated gene transcription[a]

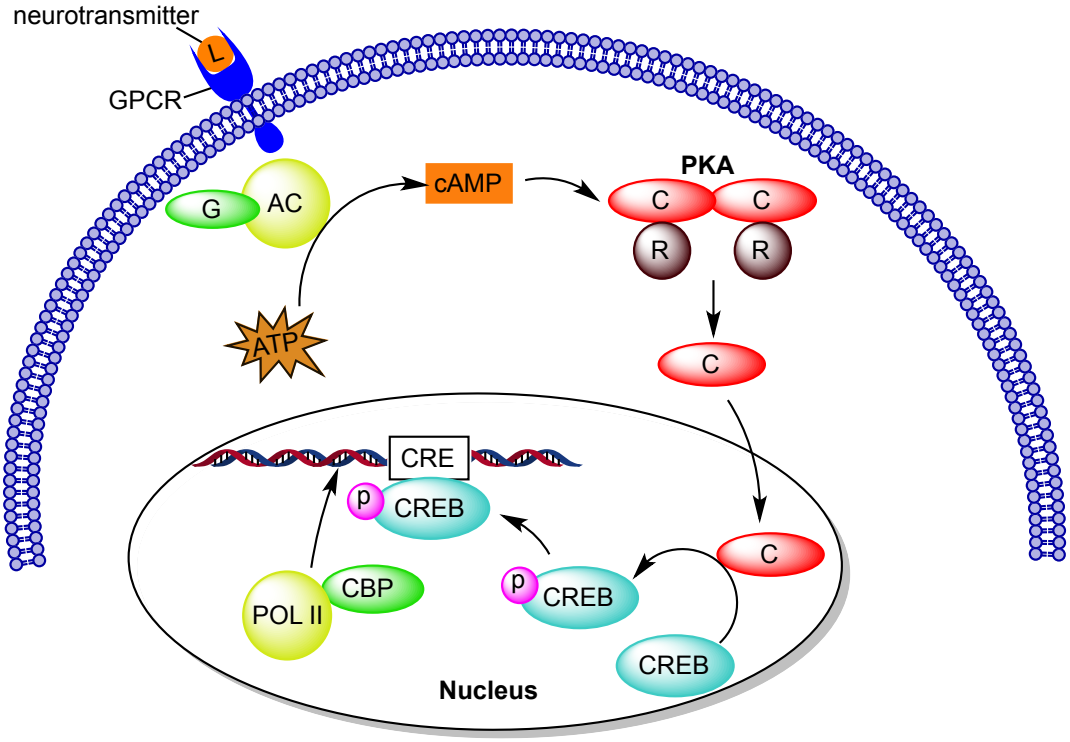

[a]Ligand (L) binding to G protein-coupled receptor (GPCR) activates the G protein (G), which induces adenylyl cyclase (AC) mediated cAMP production. cAMP promoted dissociation of protein kinase A (PKA) releases the catalytic-subunit (C), which enters the nucleus through passive diffusion. The catalytic-subunit phosphorylates CREB, which in turn binds to the response element CRE. Upon binding to CRE, phosphorylated CREB initiates transcription through the association of CREB binding protein (CBP), which coordinates with RNA polymerase II (POL II).

6.2.2. Operator/Repressor Systems

In order to label neurons based on function, during a given physiological event or stimulus, we need to restrict the expression of our reporter to a physiologically relevant

timeframe. Without this control, preliminary results have shown that over time, every transduced neuron will inevitably activate and express the reporter. Control of gene expression will be achieved through the inclusion of a heterologous transgene expression system. To date, a large number of eukaryotic transgene expression systems have been reported.[299]

Most heterologous transgene expression systems have been modified to both expression-ON and expression-OFF variants.[266,299] Although mechanisms can vary between specific expression systems, typically in an expression-ON system, the respective repressor protein binds directly to the operator DNA sequence. Since the operator is downstream of the promoter, this binding interaction sterically blocks RNA polymerase (RNA-Pol) from binding to the protomer, thereby repressing transcription (A, Figure 6.3). Introduction of the repressor ligand leads to a protein-ligand interaction between the repressor protein and the repressor ligand that causes the ligand-bound repressor to dissociate from the operator, known as derepression, thus allowing RNA polymerase to bind to the promoter and initiate transcription.

Conversely, expression-OFF systems are designed so that introduction of the repressor ligand leads to repression of gene transcription. In these systems, generally a reverse ligand-dependent transactivator (Activator) is expressed (B, Figure 6.3).[266,299] This transactivator contains a repressor protein domain and when this domain is unbound, the transactivator coordinates with RNA polymerase and binds to the operator, thus promoting gene expression. When the repressor ligand is introduced, the ligand binds to

the repressor protein domain of the transactivator. This binding interaction causes the transactivator and RNA polymerase to dissociate from the operator, thus repressing transcription.

Figure 6.3. Generalized heterologous gene expression schematic diagrams[a]

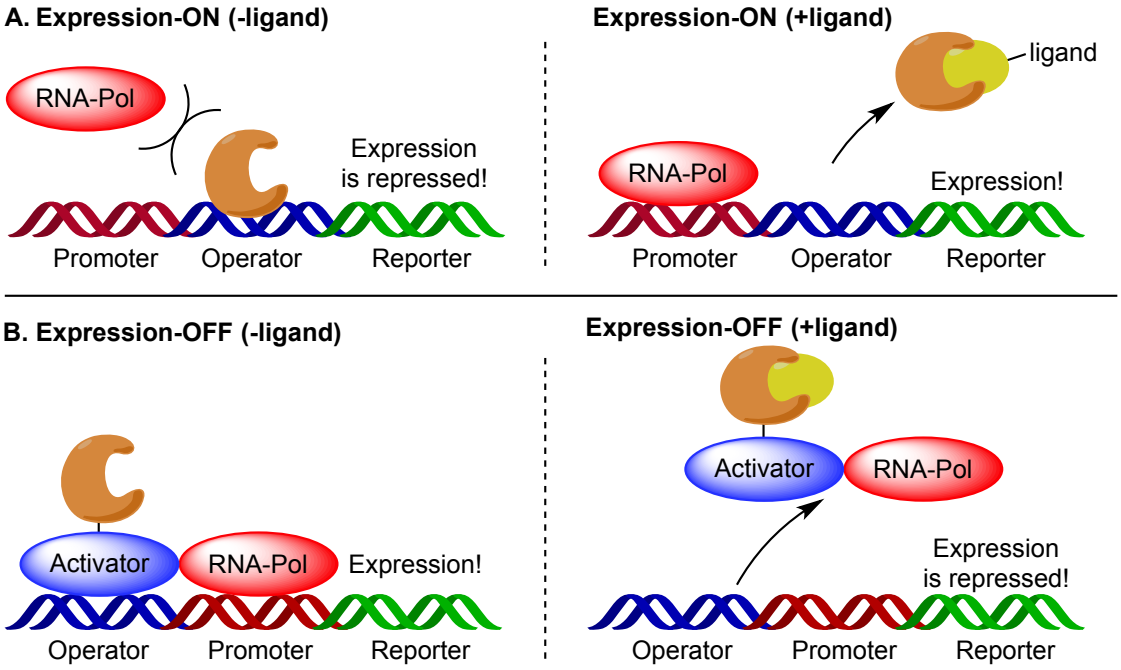

[a]**A)** Expression-ON: in the absence of the repressor ligand, gene expression is repressed. Upon addition of the repressor ligand, derepression allows for gene transcription. **B)** Expression-OFF: in the absence of the repressor ligand a transactivator (Activator) promotes the binding of RNA polymerase (RNA-pol) to the promoter and leads to gene expression. Addition of the repressor ligand leads to dissociation of the transactivator and RNA polymerase to represses gene expression.

Gene regulation systems that utilize clinically approved small molecules including, erythromycin A, tetracycline, pristinamycin, and rapamycin as repressor ligands have been previously described.[262,299] We have chosen the erythromycin-dependent inducible expression regulation system (E_{ON}), which has been modified from

the macrolide 2'-phosphotransfersae I (mph(A)) protein, the protein responsible for inactivation of macrolide antibiotics and consequently, macrolide antibiotic resistance in *E. coli*.[300] The expression of mph(A) in *E. coli* is regulated by the presence of the macrolide 2'-phosphotransferase repressor protein (MphR).[266] MphR binds to a 35-base pair operator sequence (ETR) and overlaps with the mph(A) promoter, sterically blocking RNA polymerase from binding to the promoter, thus repressing gene expression (A, Figure 6.3, left side). Binding of erythromycin A to MphR leads to derepression of mph(A) and concomitant inactivation of erythromycin A (A, Figure 6.3, right side).

6.2.3. Illustrative Example of the Proposed Method

The genetic construct described currently has two requirements for the tagging of transduced neurons. First, since CRE (Promoter X) is upstream of ETR (Operator X) in our construct, erythromycin A (repressor ligand) must be present to induce derepression. Second, during derepression, the neuron must fire to phosphorylate CREB, which will then bind to CRE and lead the expression of GFP.

A hypothetical example using this method to study the neuronal circuitry responsible for the feeling of hunger in mice, is given in Figure 6.4. Experimentally, we would first install our genetic construct into the brain of the mouse, via transduction of a viral vector. Upon transduction, we would expose the subjects to the physiological state or event under investigation, in this example, hunger. Administration of erythromycin A to both the hungry mice and a set of sated mice (control subjects) will induce

derepression, which will allow for CREB-mediated expression of GFP in neurons that are activated during this time. We would then maintain these physiological states for amount of time required to achieve quantifiable levels of reporter expression. At which point, *ex vivo* imaging of the brain will allow for a comparison of the neuronal ensembles that were active in both the experimental and control subjects. By comparing the neuronal ensembles activated in the hungry subjects to that of the control subjects, we can identify the ensembles responsible for the hunger signal. Once we have identified the neuronal ensembles that are potentially responsible for hunger, subsequent studies can target these ensembles through the expression of molecular actuators. This will allow us to independently manipulate these subsets of neurons in order to validate that stimulation or inhibition of these ensembles leads to the observed hunger signal.

Figure 6.4. Illustrative example of the proposed method[a]

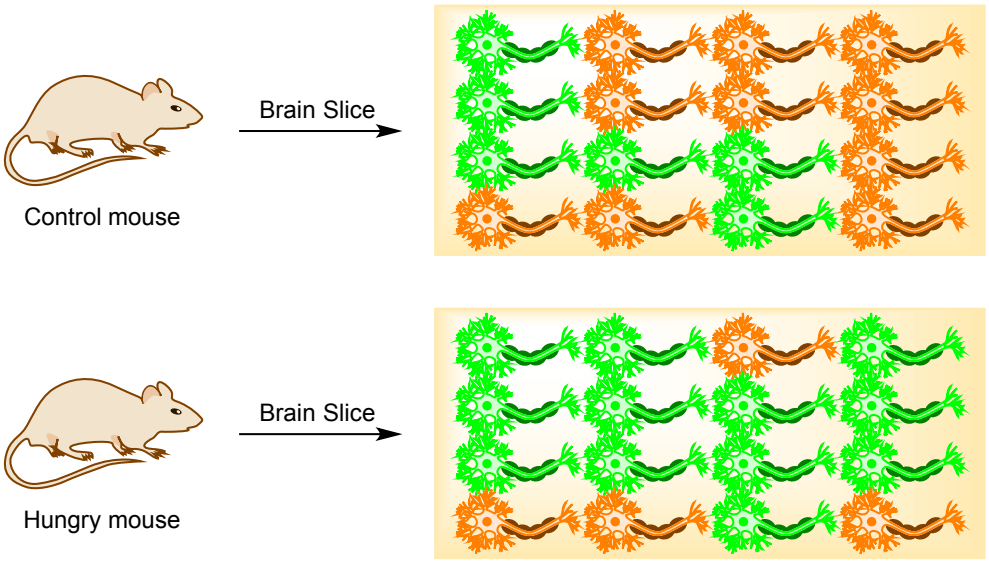

[a]The comparison of tagged neurons in the hungry mice to the tagged neurons in the control mice will allow identification of the neurons responsible for the hunger signal.

Though the methods described are well suited to study physiological events that can be maintained over a long period of time, such as hunger or addiction, the methods described will not allow for the study of very fast physiological events like memory formation or fear response. The major limitation in applying this method to very fast physiological events is that administration of erythromycin A, either orally or via injection, leads to the presence of the drug, and thus derepression, on the timescale of hours. To achieve the temporal resolution necessary for the study of fast physiological events, we will use light to quickly release erythromycin A in the brain from a photocaged-erythromycin derivative.

6.2.4. Proposed Method to Tag Neuronal Ensembles Based on Function

A summary of the proposed biochemical methods that will be used to achieve neuronal tagging are shown in Figure 6.5. First two expression cassettes will be transduced *in vivo* via a viral vector (A, Figure 6.5). Cassette (1) consists of the mouse synapsin promoter (mSyn promoter), which promotes constitutive transcription of downstream genes in mouse neurons, MphR will be continuously expressed. The second expression cassette (2) contains CRE, which is multimerized to adjust the sensitivity of gene expression, the ETR operator, and GFP. The expressed MphR protein will bind to ETR and repress transcription of GFP. Initially, administration of the photocaged erythromycin (caged-ERY) will not affect gene expression. However, following irradiation with visible light, released ERY will bind to MphR, and the MphR-ERY complex will dissociate from ETR (B, Figure 6.5). At this point, neuron action potential will lead to the phosphorylation of CREB, which will bind to CRE and initiate transcription of the reporter. By releasing erythromycin A from a photocage via irradiation with visible light, this system will achieve temporal resolution on the order of the rate of decaging. If decaging can be accomplished on the timescale of seconds to minutes, this method will be able to identify neuronal ensembles responsible for fast neurological events such as, memory formation or fear response.

Figure 6.5. The proposed biochemical construct and mechanism to effect tagging of activated neurons using visible light[a]

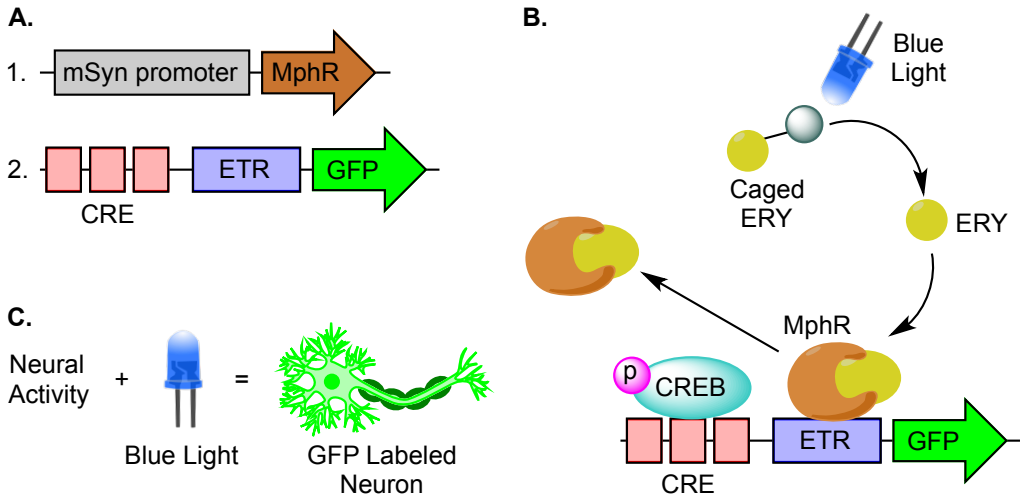

[a]**A)** Expression cassettes that will be transduced to install the genetic construct into mouse models. **B)** Irradiation of visible light will lead to the release of erythromycin, which will bind too and remove the MphR protein from the ETR operator. Subsequent phosphorylation of CREB, due to neural activity, will lead to the expression of the fluorescent reporter GFP. **C)** In summary, for a transduced neuron to express GFP as an output, neural activity and irradiation of light are required as inputs.

6.3. Visible Light Photocaged Erythromycin A

The ultimate goal of this project, is to develop a method to tag or label activated neurons within a living organism, and this necessitates that the caged-ERY derivative meets a strict set of criteria. Four requirements were identified in designing the caged-ERY derivative.

1. The caged-ERY must be water soluble. Given that we ultimately are developing a method to be used in the brain of a living organism, aqueous solubility is a necessity.

2. The caged compound must be inert in the biological system in the absence of light.
3. The caged-ERY needs to decage using visible light. The use of UV-light in decaging is commonplace in many applications, but UV-light damages living tissue. In our studies, neuronal damage will inherently disrupt the natural neuronal circuitry that we are attempting to study.
4. The caged-ERY derivative must decage on a timescale of seconds to minutes. The irradiation times required to decage ERY in suitable quantities, will directly affect the temporal resolution attainable with this method. Irradiation times greater than a few minutes will lead higher levels of neuron labeling due to background brain activity.

With the aforementioned requirements, we set out to design and validate a novel caged-ERY derivative that fit these criteria.

6.3.1. Erythromycin A Derivatives and Caging Groups

When considering how to photocage **ERY** (**6.1**) (Figure 6.6) with a suitable caging group, two factors were considered. First, we needed to use an **ERY** derivative that contained a suitable functional handle to append the photocage. Second, we needed to validate that this **ERY** derivative retains a high binding affinity to MphR. As mentioned previously (Chapter 5.9.1), Deiters had demonstrated that decaging of erythromycin A-9-oxime (**ERY-9-OX, 6.2**) allows for photoactivated derepression of

gene transcription using the E_{ON} expression system.[265] Furthermore, previous reports have shown that **ERY-9-OX** retains biological activity with respect to **ERY**.[301,302]

Figure 6.6. Erythromycin A (**ERY**, **6.1**) and erythromycin A-9-oxime (**ERY-9-OX, 6.2**)

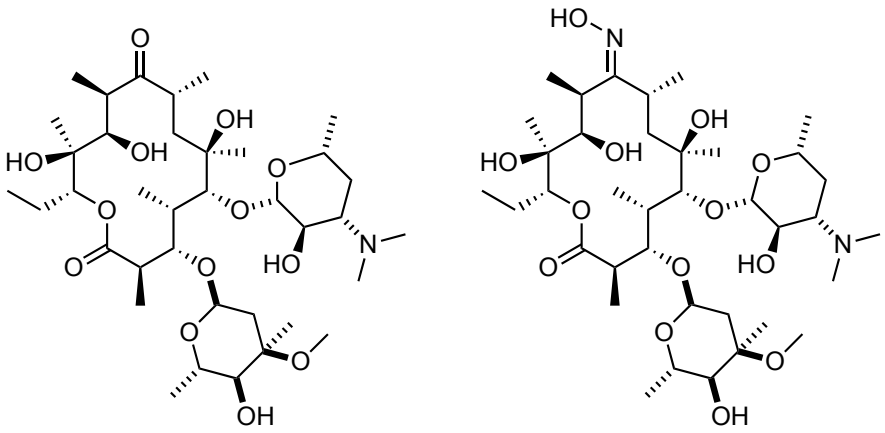

In view of the aforementioned precedent, it remained to determine which visible light caging group is best suited for our system. As described in Chapter 5, there are many potential caging groups. Based on the previously described criteria, we narrowed the number of options to two potential caging groups, the nitrodibenzofuran (**NDBF**, **6.3**) and diethylaminocoumarin 450 (**DEAC450**, **6.4**) groups (Figure 6.7). These groups stood out as promising caging candidates for **ERY-9-OX** based on previous reports of fast release rates and the successful applications of these caging groups in biological studies.[183,250,251]

Figure 6.7. Caging groups chosen for this study, **NDBF** (**6.3**) and **DEAC450** (**6.4**)

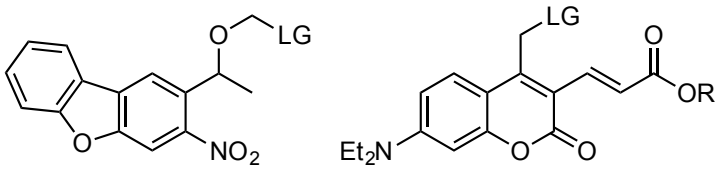

NDBF (6.3) **DEAC450 (6.4)**

As discussed in the preceding chapter (Section 5.9.2), the **NDBF** photocage has previously demonstrated efficient release of nucleotides,[181,184] peptides,[183] and calcium ions.[183] Notably, it was possible to quickly decage **NDBF** substrates with poor leaving groups like thiols[183] and amides.[181] Although the maximum absorbance is not in the visible region, the relatively large absorbance and efficient quantum yields of release (λ_{max} = 330 nm, ε = 18,400 M^{-1} cm^{-1}, $\varepsilon \bullet \Phi$ = 12,880)[183] provided promise for success of this caging group for our studies.

With a large absorbance well into the visible region (λ_{max} = 450 nm, ε = 43,000 M^{-1} cm^{-1}), the **DEAC450** photocage is also an attractive option for the caging of **ERY-9-OX**.[250] Furthermore, *in vitro* studies found that the decaging of cAMP from **DEAC450** proceeded in an impressive quantum yield of 0.78 ($\varepsilon \bullet \Phi$ = 33,500).[251] Though the decaging of coumarin-caged compounds with poor leaving is known to be inefficient, we anticipated that the low concentrations necessary for **ERY** induced gene expression (~1 μM),[266] would allow for the release of sufficient quantities of **ERY-9-OX**. With this in mind, we commenced studies towards the synthesis and evaluation of **NDBF-ERY** and **DEAC450-ERY**.

6.4. Synthesis of Erythromycin A-9-Oxime

The synthesis of **ERY-9-OX** proceeded smoothly according to literature precedent.[301] Stirring **ERY** at room temperature in pyridine with an excess of hydroxylamine hydrochloride for 72 hours, followed by extraction and recrystallization from ethanol gave **ERY-9-OX** in 74% yield on multi-gram scale (Equation 6.1).

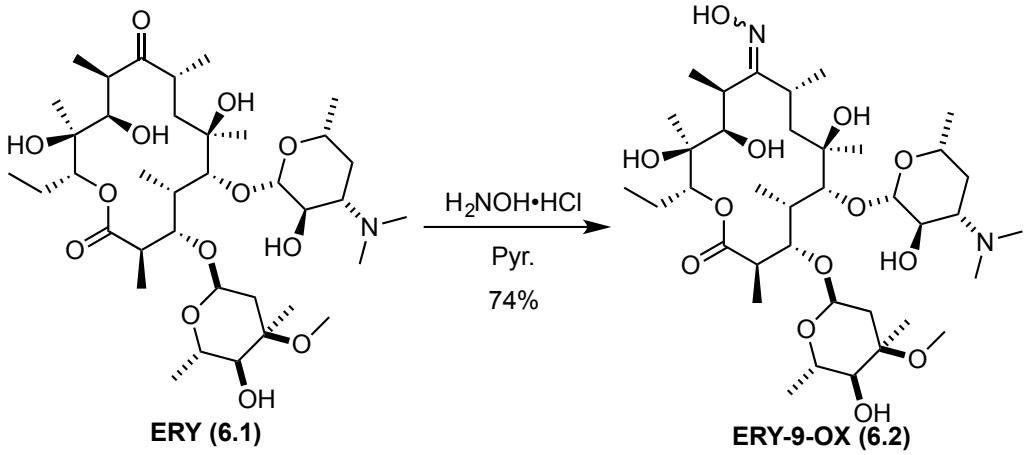

ERY (6.1) ERY-9-OX (6.2) **(6.1)**

6.5. Synthesis of NDBF Caging Group

The **NDBF** photocage was prepared according to previously reported methods.[181] However, our synthesis proceeded with higher yields for most steps and an overall yield of 31%, as compared to 19% overall yield in the previous report. Starting from 4-fluoro-2-nitrobenzaldehyde (**6.5**), an Ullman coupling with 2-iodophenol (**6.6**) gave biaryl ether **6.7** in 86% yield (Scheme 6.1). Allowing **6.7** to react with neat trimethylaluminum formed biaryl-alcohol **6.8** in nearly quantitative yield. Palladium-catalyzed arylation of **6.8** proceeded in 51% yield to give dibenzofuran **6.9**. Attempts to optimize this reaction

met with limited success. The use of different solvents, temperatures, reaction times, bases, and the addition of ligands failed to provide any appreciable gains in chemical yield. The major byproduct from this reaction was the dehalogenation of **6.8**. The poor reactivity of **6.8** towards palladium-catalyzed arylation is thought to arise from the poor reactivity of intermediate **6.10**, which is formed upon oxidative addition of palladium (0).[303,304] Intermediate **6.10** must undergo an electrophilic aromatic substitution onto the palladium center, which is followed by rearomatization and reductive elimination to give **6.9**. However, in this system the nitro substituent strongly deactivates that aromatic ring towards attack of the palladium center.

Scheme 6.1. Synthesis of nitrodibenzofuran alcohol **6.9**

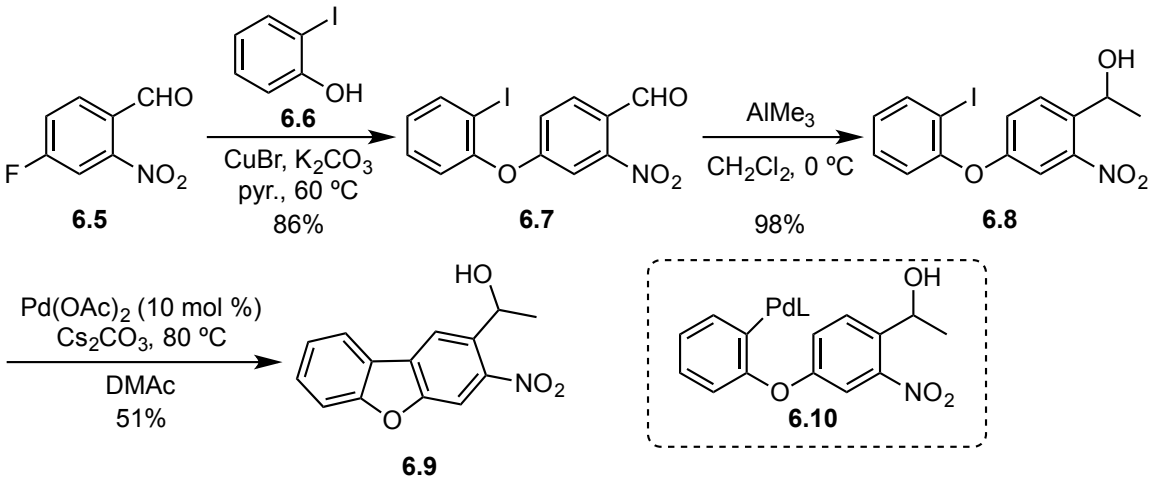

Synthesis of the **NDBF** caging group **6.12** from dibenzofuran **6.9** was completed in two additional steps (Scheme 6.2). Oxidation of dimethylsulfide led to the *in situ* formation of a Pummerer-type intermediate, and subsequent addition of **6.9** gave the

thioacetal **6.11** in 74% yield. Finally, allowing **6.11** to react with sulfuryl chloride gave the chloro-acetal **6.12** in nearly quantitative yield. It is worth noting that while compound **6.11** was benchtop stable, the alkylating agent **6.12** was quite unstable. Compound **6.12** is effectively an **NDBF**-caged chloride ion (good leaving group), so the reaction and work-up to isolate **6.12** needed to be carried out in the dark to avoid photochemical release of the chloride ion.

Scheme 6.2. Synthesis of **NDBF** caging group **6.12**

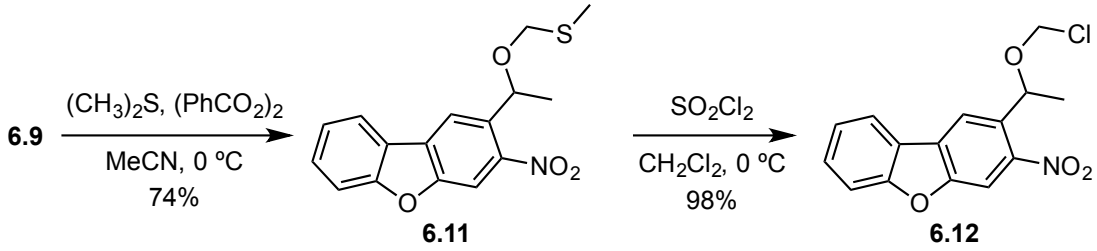

6.6. Synthesis of DEAC450 Caging Group

Synthesis of a **DEAC450** caging group commenced with the allylic oxidation of 7-diethylamino-4-methylcoumarin (**6.13**) to give the alcohol **6.14** in 29% yield (Scheme 6.3).[305] Though low yielding, this reaction was easily scaled to provide sufficient amounts of material to complete the synthesis. Protecting the alcohol **6.14** as the TBS silyl ether provided **6.15** in 77% yield. Ammonium acetate catalyzed aromatic bromination of **6.15** cleanly gave the bromide **6.16** in 86% yield. Heck cross coupling of **6.16** and *tert*-butyl acrylate gave **6.17** in 41% yield. All attempts to reproduce the literature yield (85%) and optimize this reaction failed to improve the isolated yield.[250]

Additionally, we were unable to replicate the literature yield (85%) for the TBS deprotection.[250] Using the reported protocol, treatment of **6.17** with TBAF consistently gave **6.18** in 30-40% yield. However, we found that the use of a 3HF•Et_3N solution in dichloromethane buffered with two equivalents of triethylamine afforded the free alcohol **6.18** in 92% yield. Finally, the transformation of **6.18** to the corresponding mesylate proceeded in nearly quantitative yield to give **6.19**.

Scheme 6.3. Synthesis of **DEAC450** caging group **6.19**

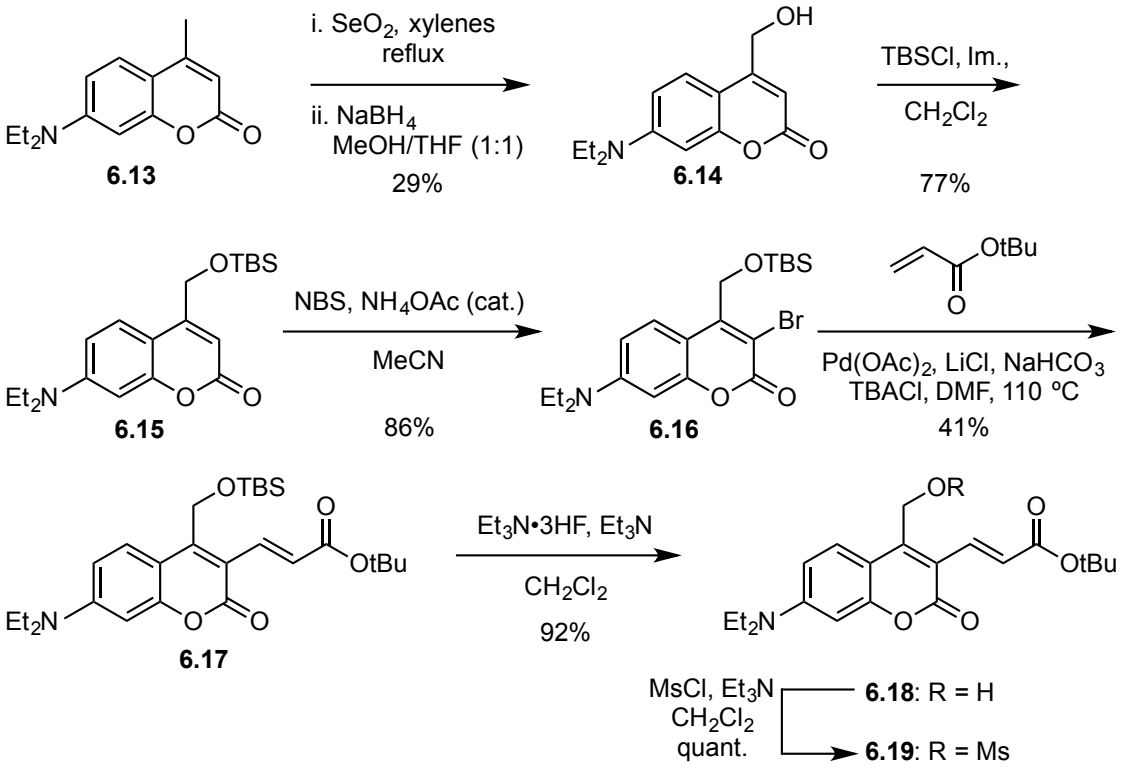

6.7. SYNTHESIS OF NDBF-ERY AND DEAC450-ERY

The final step in synthesizing our caged-**ERY** derivatives was the alkylation of **ERY-9-OX** with the respective caging group. We initially attempted this reaction by heating a solution of **ERY-9-OX**, **6.12**, and potassium carbonate in acetone under reflux, which consistently gave returned starting materials. We then found that treatment of **ERY-9-OX** with sodium hydride in a mixture of DMF and THF (1:1), followed by the addition of a solution of the respective alkylating agents, gave **NDBF-ERY** and **DEAC450-ERY** in 78% and 39% yields, respectively (Equation 6.2, 6.3). With **NDBF-ERY** and **DEAC450-ERY** in hand, we focused our attention on determining whether these compounds met the criteria necessary for the neuronal imaging studies.

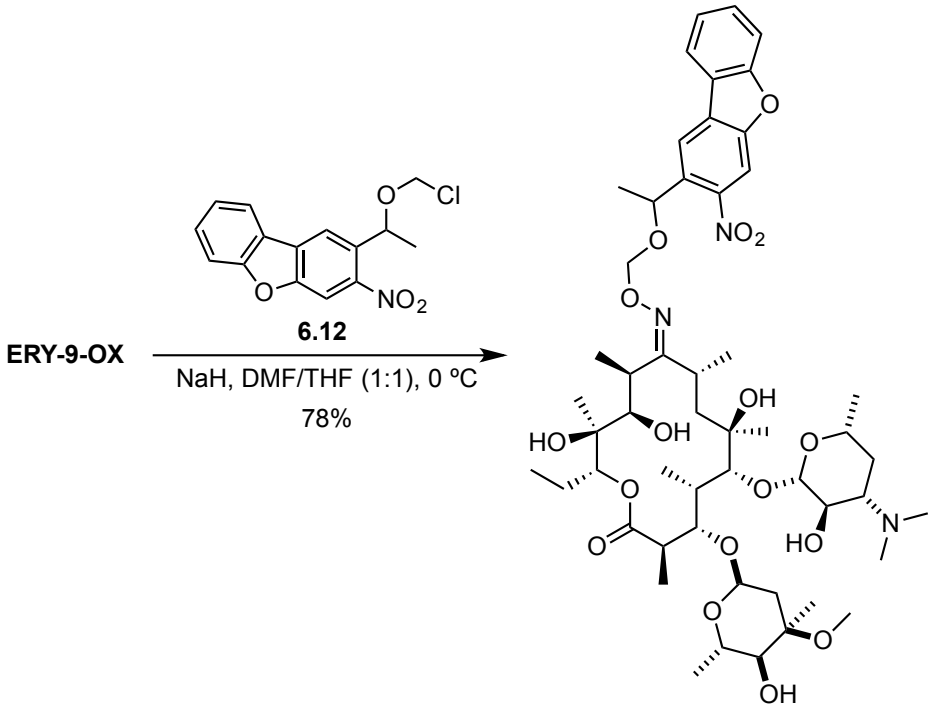
ERY-9-OX
6.12
NaH, DMF/THF (1:1), 0 ºC
78%
NDBF-ERY (6.20)

(6.2)

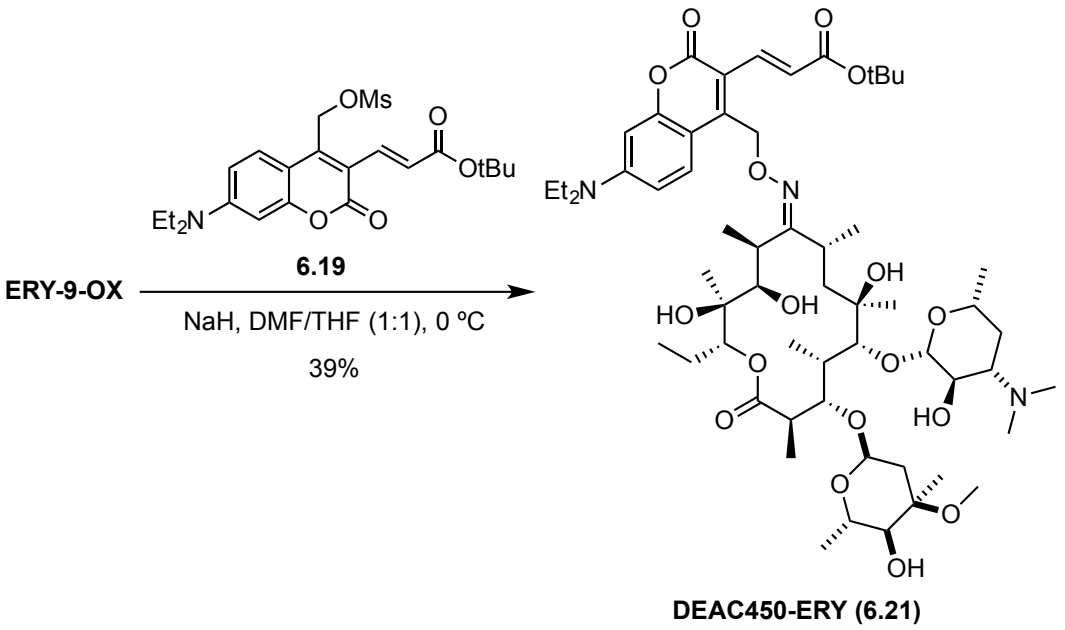
ERY-9-OX
6.19
NaH, DMF/THF (1:1), 0 ºC
39%
DEAC450-ERY (6.21)

(6.3)

6.8. Evaluating the Caged-ERY Criteria

As a quick summary, the criteria that our caged-**ERY** derivatives must fit are:

1. Water solubility.
2. Inert towards the biological system in the absence of light.
3. Uncaging with visible light.
4. Uncaging must occur on a timescale of seconds to minutes.

In evaluating the water solubility of **NDBF-ERY** and **DEAC450-ERY**, we utilized Beer's law to determine the concentration of a saturated solution of each compound. UV-vis spectroscopy was used with aqueous solutions of the caged-**ERY** derivatives to plot the absorbance at λ_{max} against concentration.

The Beer's law plots for **NDBF-ERY** and **DEAC450-ERY** are shown in Figure 6.8 and 6.9, respectively. We were pleased to find a linear relationship between absorbance and concentration in both cases at concentrations between ~10 – 100 μM. For **NDBF-ERY**, we found λ_{max} at 350 nm and determined the concentration of a saturated aqueous solution to be 115 μM. Although, the maximum absorbance occurs outside of the visible region, this does not innately mean that this compound is unsuitable for our purposes. In the UV-Vis plots (see S.I.) there is a trailing absorbance past 400 nm, which means that this compound could decage using visible light. Conversely, **DEAC450-ERY** displayed a strong absorbance between 440 – 470 nm with a λ_{max} at 460 nm. The Beer's law plot shows a near perfect linear relationship between absorbance at 461 nm and

concentrations from 8 to 100 µM. We determined the concentration of a saturated aqueous solution to be 100 µM.

Figure 6.8. Beer's law plot of **NDBF-ERY** at 350 nm

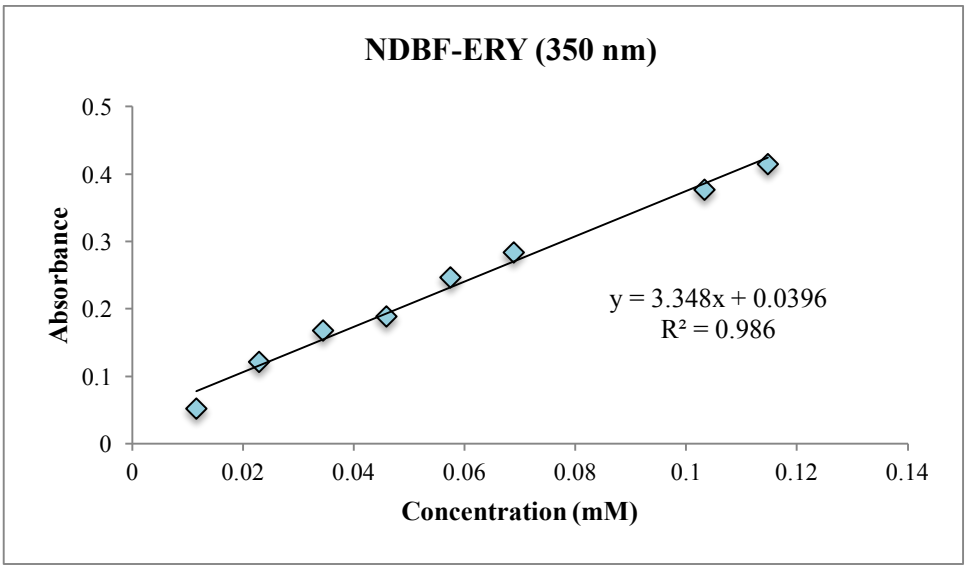

Figure 6.9. Beer's law plot of **DEAC450-ERY** at 461 nm

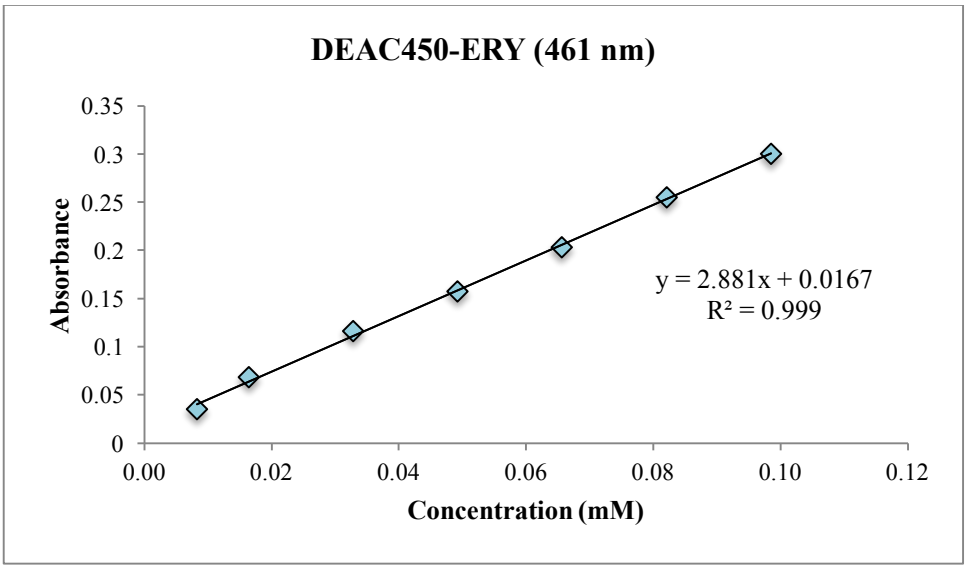

At this point, it was necessary to determine whether concentrations of 100 μM fit our criteria of water solubility. From a synthetic chemist perspective, these concentrations might not suggest that these molecules are "water soluble", because the saturated solutions equate to about 0.1 mg/mL. However, when reviewing previously reported literature on the use of MphR, we find that the E_{on} systems display induced gene expression with **ERY** concentrations ranging from 10 – 2,000 ng/mL, which equates to 0.013 – 2.7 μM.[266] This means, dependent on the yield of decaging, achieving final concentrations of **ERY** within a neuron at single or low double digit micromolar concentrations is feasible from a 100 μM solution of caged-**ERY**.

To determine the extent of decaging of **NDBF-ERY** and **DEAC450-ERY** with respect to time and wavelength, two key issues needed to be addressed. First, we needed to develop a method to quantitate micromolar concentrations of released **ERY-9-OX** in an aqueous solution. Typically, photolysis studies involve irradiation of the samples, followed by HPLC separation and quantitation using a UV detector. Because **ERY-9-OX** lacks a strongly absorbing chromophore this is challenging, and thus, **ERY-9-OX** is indiscernible on HPLC chromatograms with UV-vis detectors. Second, we needed to develop a method to irradiate our samples with discrete wavelengths of light at powers that were comparable to the fiber optics that will be used in the *in vivo* studies. Previous studies often relied on the use of lasers or powerful mercury lamps (~200-500 W) with a UV-filter to achieve irradiation at selected wavelengths. However, both methods provide light with a much greater intensity than the fiber optics.

We initially focused our attention towards developing an **ERY-9-OX** quantitation method. Initial attempts to quantify **ERY-9-OX** via HPLC chromatography were quickly found to be ineffective. The lack of an appreciable chromophore on **ERY-9-OX** meant that the micromolar concentrations used in these experiments were well below the instrumental detection limit. We next turned to the use of mass spectrometry as a method of quantitation. Subjection of a number of solutions of **ERY-9-OX** in concentrations ranging from 0.25 – 100 μM to LC/MS and subsequent plotting of concentration against a number of different signals (ion count, peak height, peak area), gave the data shown in Figure 6.10. We found a linear relationship between the mass spectrum peak area and **ERY-9-OX** concentrations from 6 – 100 μM. We observed that concentrations below 6 μM diverged from a linear relationship and approached zero in an exponential decay. The use of LC/MS, as opposed to direct injection MS, was chosen because the chromatographic separation will be advantageous when analyzing irradiated **NDBF-ERY** and **DEAC450-ERY** samples. This separation will allow us to not only determine the concentration of released **ERY-9-OX**, but also allow us to analyze the amounts of unreacted starting material and any potential photochemical decomposition byproducts.

Figure 6.10. LC/MS quantitation of **ERY-9-OX**

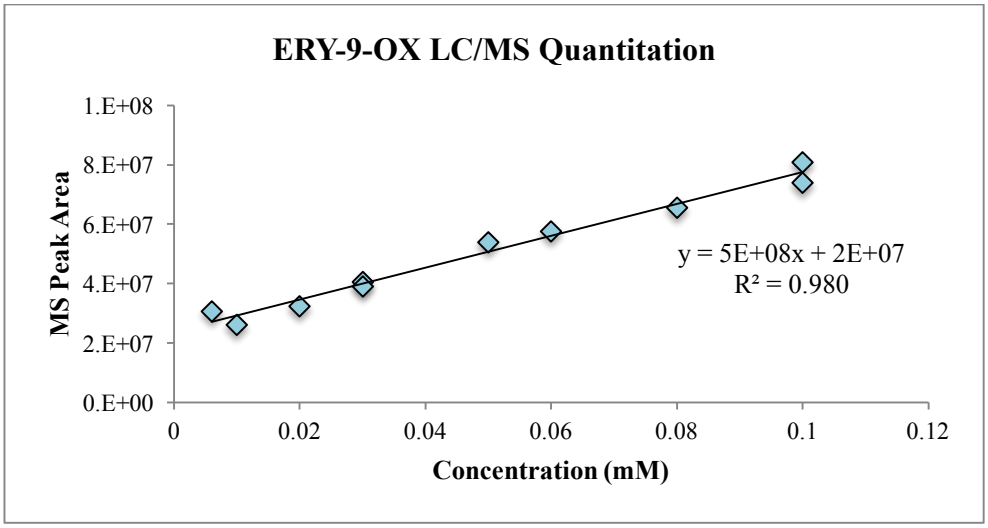

In the initial decaging studies, irradiation time was set as the variable. The purpose of this time-course study was to determine the feasibility of inducing **ERY-9-OX** release on a timescale of seconds to minutes. The following experiment was conducted using a UV-laser (λ = 340 nm, P = 100 mW). In this study, saturated aqueous solutions of **NDBF-ERY** in a vial were positioned directly beneath the laser. Each sample was irradiated for the given amount of time and immediately analyzed by the LC/MS quantitation method. The results are shown below (Figure 6.11).

Figure 6.11. Time-course decaging of **NDBF-ERY**

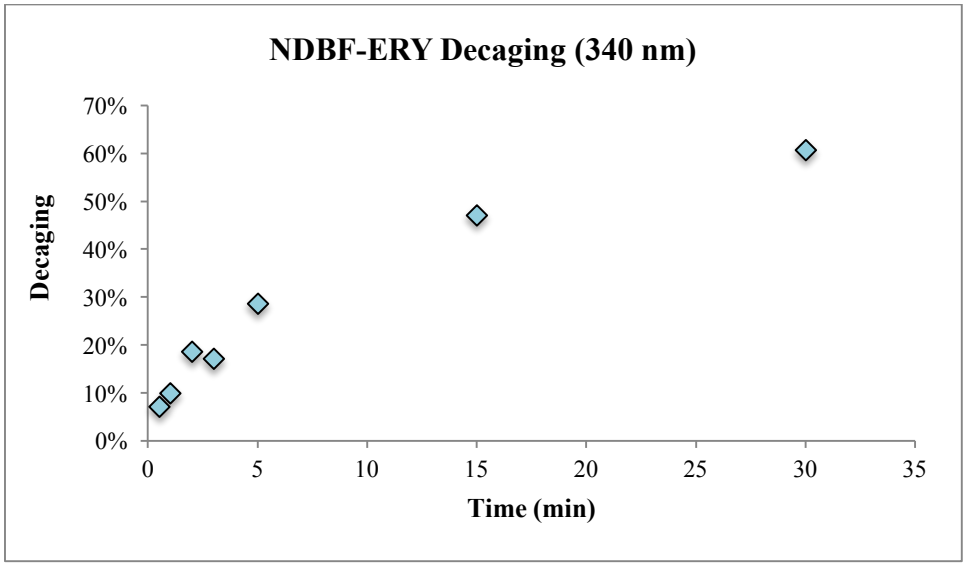

The results from this decaging study were encouraging. Decaging started rapidly (10% at 1 min) and proceeded to release **ERY-9-OX** in 30% yield after five minutes. Attempts to effect complete decaging of **ERY-9-OX** (15 min and 30 min) were unsuccessful. We postulated that that the inability to achieve complete decaging upon irradiation for 30 minutes, was in part due to the fact that the diameter of the laser beam was smaller than that of the vial used. Since that the samples were not irradiated homogenously, a fraction of the sample remained unreacted. Nonetheless, we were delighted to find that appreciable quantities of decaging (30%) were obtained after a reasonable amount of time (5 min). Under these conditions the concentration of **ERY-9-OX** is roughly 35 μM, which is well above the threshold necessary for induced transcription in the E_{ON} expression system found in previous studies.[266]

Though encouraged by these early results, there were multiple reasons for abandoning this decaging study. First, the laser used in this experiment was much more powerful than the light that would be available using fiber optics for the *in vivo* studies. Hence, these results were not a direct representation of the photochemical reactivity of **NDBF-ERY** within the *in vivo* system that would be used.

At this stage, we considered different ways we could select for specific wavelengths of light to irradiate our caged compounds. We decided a fluorometer could be an effective method to select specific wavelengths. Using a QuantaMaster Spectrofluorometer (PTI inc.), we irradiated saturated solutions of **NDBF-ERY** and **DEAC450-ERY** at wavelengths between 300 and 500 nm. The results from these wavelength-dependence decaging studies were both promising and disappointing.

Results of the wavelength-dependence decaging study of **NDBF-ERY** are shown below (Figure 6.12). In this study, 100 μL samples of aqueous **NDBF-ERY** solutions were irradiated for five minutes at the specified wavelength and analyzed by the LC/MS quantitation method discussed previously. Importantly, the dark control sample ($\lambda = 0$), which was keep in the dark for the entirety of the study, displayed no trace of **ERY-9-OX**. This indicates that **NDBF-ERY** is stable in an aqueous solution at room temperature for at least three hours. To avoid unwanted derepression in our biological studies, the stability of the caged-**ERY** compounds in aqueous media is paramount. Furthermore, we found that decaging was quite efficient at 325 nm, proceeding in an 80% yield of decaged **ERY-9-OX**. Though the yields of decaging declined as a function of wavelength, the

observed 37% yield at 400 nm demonstrated that **NDBF-ERY** meets the criteria for decaging under visible light on the order of seconds to minutes.

Figure 6.12. Wavelength-dependent decaging of **NDBF-ERY** (irradiation time = 5 min)

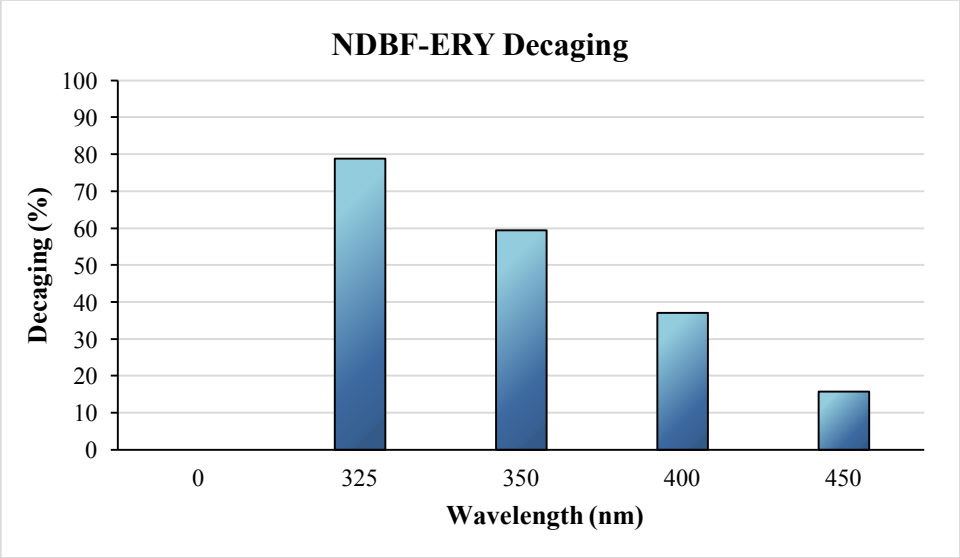

In almost direct contrast to the **NDBF-ERY** results, decaging of **DEAC450-ERY** was quite inefficient (Figure 6.13). Using the same protocol, we found that these conditions did not lead to an appreciable release of **ERY-9-OX**. At best, **ERY-9-OX** was released from **DEAC450-ERY** in 12% yield, upon irradiation at 400 nm. Furthermore, the dark control sample gave 2% decaging (or hydrolysis), which indicates that **DEAC450-ERY** is not stable in aqueous media at room temperature and could potentially be problematic. These results clearly indicate that, for the purposes of our studies, **DEAC450-ERY** does not fit the criteria of decaging using visible light on a timescale of seconds to minutes.

Figure 6.13. Wavelength-dependent decaging of **DEAC450-ERY**

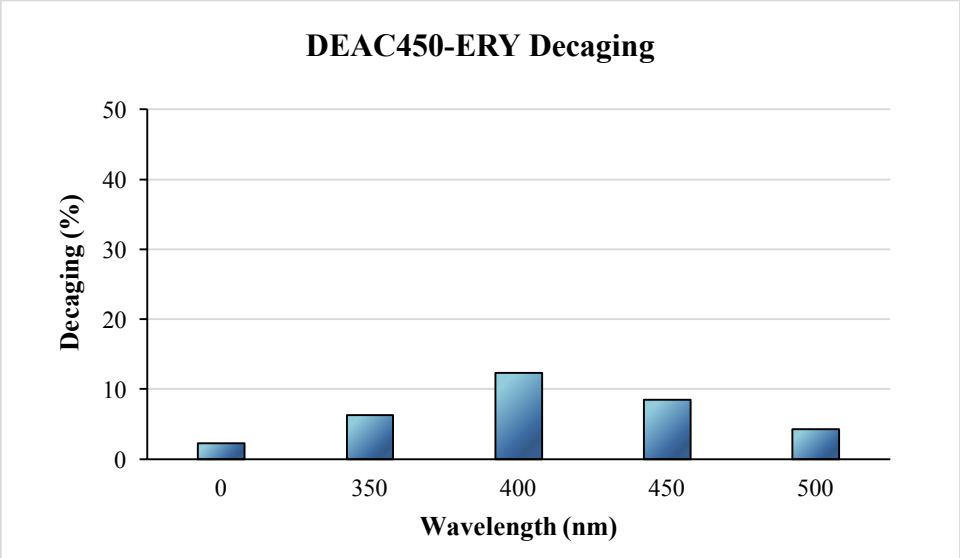

The slow decaging of **DEAC450-ERY** can likely be explained by considering the mechanism of decaging. As described in Chapter 5 (Section 5.8.1), release rates from coumarin-based photocages are highly dependent on the rate of heterolysis and the rate of ion-pair recombination. Namely, higher rates of recombination lead to lower rates of release. The rate of ion-pair recombination is directly related to the pKa of the conjugate acid for a given leaving group, so less acidic conjugate acids make poorer leaving groups. The conjugate acid of the leaving group in this instance, is **ERY-9-OX**. To our knowledge, studies to determine the pKa of **ERY-9-OX** have not been reported. However, the pKa values of alkyl-oximes have been reported and found to range from ~24-29 as exemplified by propanal oxime (pKa = 28.5 in DMSO).[306] For comparison sake, poor leaving groups, such as alcohols, exhibit similar pKa values (methanol, pKa =

29.0 in DMSO).[307] These relatively high pKa values indicate that the oxime functionality and by extension, **ERY-9-OX**, is not a satisfactory leaving group for the **DEAC450** caging group.

6.9. PENDING EXPERIMENTS: *IN VITRO* PROOF OF PRINCIPLE

A number of *in vitro* experiments are currently being conducted to establish proof of principle that our genetic construct will lead to the labeling activated neurons. First, we have to establish the optimal parameters for the neuron cell assay and tune the sensitivity of reporter response. In doing so, we are considering three variables namely, the number of repeating CRE sequences, the levels of MphR expression, and the concentration of **ERY-9-OX**. To determine the optimal number of CRE multimers, isolated mouse hippocampal neurons are being transduced with iterations of the genetic construct that not only omit the gene coding for MphR, but also vary in the number of CRE repeats. Upon chemical stimulation of the neurons using forskolin, we will determine the number of CRE repeats necessary for reporter expression.[308]

A second set of experiments is being performed to determine the required levels of MphR expression for full repression of the reporter, as well as the concentrations of **ERY-9-OX** required to achieve derepression. In these experiments, which are illustrated in Figure 6.14, transduced hippocampal mouse neurons are placed in each well of a microtiter plate. Expression levels of the MphR protein is increased in wells along the X-axis and concentration of **ERY-9-OX** was increased in wells along the Y-axis of the

plate. The first column the plate does not express any MphR and is thus a positive control to compare levels of reporter expression. Conversely, the bottom row, which contains no **ERY-9-OX**, is as a negative control to determine the minimum level of MphR expression required to achieve full repression of the reporter. By comparing the fluorescence intensity of each well to that of the positive control, we can determine the concentrations of **ERY-9-OX** required for derepression of a given level of MphR expression.

Figure 6.14. Illustrative representation of *in vitro* titration of MphR expression against **ERY-9-OX** concentration

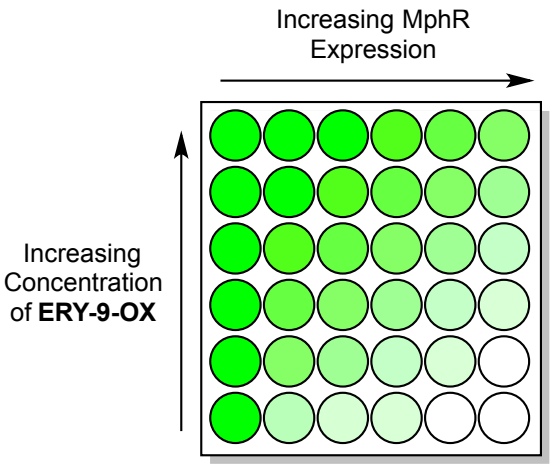

Once optimal cell assay parameters are established, *in vitro* studies will focus on demonstrating the utility of **NDBF-ERY** in the current system. First, transduced neurons will be incubated with increasing concentrations of **NDBF-ERY** to establish that **NDBF-ERY** is inert towards the biological system. Upon determining the concentrations at which **NDBF-ERY** is inert, neuron cultures containing **NDBF-ERY** will be irradiated

with visible light ($\lambda \sim 400$ nm), which will ideally lead to expression of the fluorescent reporter. If successful, these experiments will provide an adequate proof of principle to continue further studies in live mouse models.

6.10. Summary and Future Directions

We have synthesized two novel caged analogues of **ERY-9-OX**, although the caging groups themselves are known. To our knowledge, the use of visible-light caging groups on a molecule possessing the chemical complexity of **ERY-9-OX** has not been reported. We have demonstrated that irradiation of **NDBF-ERY** under a relatively low power of visible light (5-6 mW) efficiently releases **ERY-9-OX**. Conversely, we also found that the **DEAC450** caging group does not release **ERY-9-OX** under the same conditions.

Once the efficacy of **NDBF-ERY** towards the labeling of activated neurons *in vitro* is established, future studies will focus on two goals. The first goal will be to implement this method in live mouse models. Viral transduction of our genetic construct will circumvent the necessity for time-intensive transgenic animal models. Upon transduction, surgically implanted microsyringes flanked by fiber optic filaments will allow us to inject and irradiate **NDBF-ERY** inside of the brains of live mice. We anticipate that the release of **ERY-9-OX** in the brain will lead to expression of the fluorescent reporter in neurons that were activated during this time. Once this method has been established in mouse models, we can begin to expose the mouse subjects to

experimentally controlled physiological stimuli or conditioned responses and visualize the neural activity responsible for the given event.

The second aim of our future studies, is to introduce bidirectionality within our expression system. Given that the response element CRE is a palindromic DNA sequence, transcription of the antisense 3' to 5' direction will allow for the expression of a second reporter (Reporter Y) (Figure 6.15). Using a different operator/repressor pair (Operator Y and Repressor Y), we can then develop a caged derivative of the new repressor ligand (Ligand-PPG). One such possibility, is the use of the Tet_{ON} expression systems, for which the repressor protein (TetR) responds to the presence of tetracycline or doxycycline.[268,309] Photocaging of this ligand with an appropriate caging group could allow for orthogonal decaging between **NDBF-ERY** and new caged-ligand.

This bidirectional reporter system will allow for numerous experimental capabilities. First, in the absence of Repressor Y, the expression of Reporter Y will act as a positive internal standard to visualize transduced neurons. Secondly, the bidirectional reporter system will allow for the labeling of two distinct states of neuronal activation, thus allowing us to confirm that the same contextual stimuli leads to the activation of the same neuronal ensembles. Conversely, the bidirectional system will allow us to visualize the similarities and differences of neuronal ensembles activated by different contextual stimuli.

Figure 6.15. Future genetic construct to afford bidirectional neuronal tagging

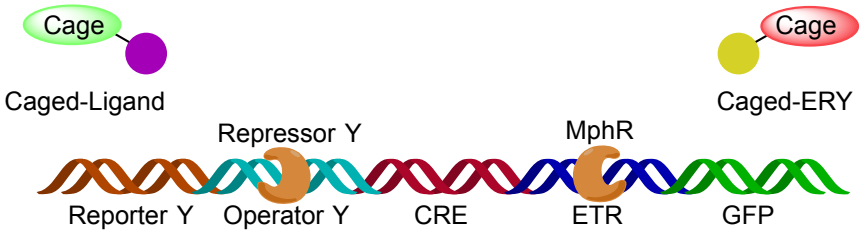

The potential applications of this function-based neuronal tagging technique are multifold. First, this method could allow for functional brain imaging with spatial resolution on the cellular level. This resolution would lead to tremendous gains in understanding what areas of the brain are responsible for given functions. Second, this tagging method could be used to express molecular actuators, such as channelrhodopsins, in subsets of neurons that have been specified based on neural function. By selecting for specific neuron populations by irradiating with light and subsequent neural activity, neurobiologists will have an unprecedented ability to experimentally target specific areas of the brain involved in a given physiological event. Finally, the use of this technique will have a profound impact on the medical community, specifically in the study of neurological disorders. Many neurological disorders are poorly understood and often difficult to treat. The use of this technique as an imaging method would not only permit studies of the neurological mechanisms responsible for these diseases, but could also lead to new diagnostic tools. Finally, the neurologist's holy grail, would be a method that could be used to treat neurological disorders by targeting, controlling, or manipulating selected populations of neurons that are responsible for the given disorder.

Chapter 7: Experimental Procedures

7.1. General Experimental Methods

Tetrahydrofuran and diethyl ether were dried by filtration through two columns of activated, neutral alumina according to the procedure described by Grubbs.[310] Methanol, acetonitrile and dimethylformamide were dried by filtration through two columns of activated molecular sieves, and toluene was dried by filtration through one column of activated, neutral alumina followed by one column of Q5 reactant. Benzene was distilled from sodium and benzophenone. Methylene chloride, diisopropylamine, triethylamine, and diisopropylethylamine were distilled from calcium hydride immediately prior to use. Pyridine was distilled from potassium hydroxide (KOH) and calcium hydride and stored over KOH pellets. All other reagents and solvents were reagent grade and were purchased and used as received unless otherwise noted. Reactions were performed under a nitrogen or argon atmosphere in round-bottom flasks sealed under rubber septa with magnetic stirring, unless otherwise noted. Water sensitive reactions were performed with flame- or oven-dried glassware, stir-bars, and steel needles. Reaction temperatures are reported as the temperatures of the bath surrounding the vessel. Sensitive reagents and solvents were transferred using plastic syringes and steel needles using standard techniques.

Proton nuclear magnetic resonance (^{1}H NMR) and carbon nuclear magnetic resonance (^{13}C NMR) spectra were acquired in $CDCl_3$ unless otherwise noted. Chemical shifts are reported in parts per million (ppm, δ), downfield from tetramethylsilane (TMS,

δ = 0.00 ppm) and are referenced to residual solvent ($CDCl_3$, δ = 7.26 ppm (^1H) and 77.16 ppm (^{13}C)). Coupling constants (*J*) are reported in hertz (Hz) and the resonance multiplicity abbreviations used are: s, singlet; d, doublet; t, triplet; q, quartet; p, pentet; sex, sextet; sep, septet; dt, doublet of triplets; dd, doublet of doublets; ddd, doublet of doublet of doublets; dddd, doublet of doublet of doublet of doublets; m, multiplet; comp, overlapping multiplets of magnetically non-equivalent protons. The abbreviations br and app stand for broad and apparent, respectively. Infrared (IR) spectra were obtained with a Thermo Scientific Nicolet IR-100 FT-IR series spectrometer as thin films on sodium chloride plates. Melting points were determined using a Thomas-Hoover Uni-melt capillary melting point apparatus. Thin-layer chromatography (TLC) was performed on EMD 60 F254 glass- backed pre-coated silica gel plates and were visualized using one or more of the following methods: UV light (254 nm) and staining with basic potassium permanganate (KMnO4) or acidic *p*-anisaldehyde (PAA). Flash chromatography was performed using glass columns and with Silicycle® SiliaFlash F60® (40-63 μm) silica gel eluting with the solvents indicated according to the procedure of Still.

7.2. EXPERIMENTAL PROCEDURES

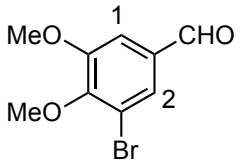

2.8

3-Bromo-4,5-dimethoxybenzaldehyde (2.8). ARMI23. Bromine (3.7 mL, 72.3 mmol) was added dropwise over 5 min to a solution of vanillin (10.0 g, 65.7 mmol) in acetic acid (100 mL), and the reaction was stirred at room temperature for 3 h. The mixture was poured over crushed ice (~200 g), and the solid was collected by filtration. Iodomethane (4.5 mL, 72.3 mmol) was added dropwise over 10 min to a solution of the isolated solid and K_3PO_4 (22.7 g, 164 mmol) in DMF (330 mL). The mixture was stirred for 14 h at room temperature, then diluted with water (300 mL), and extracted with *t*-butylmethyl ether (3 x 300 mL). The combined organic fractions were washed with brine (1 x 300 mL), dried (Na_2SO_4), filtered, and concentrated *in vacuo* to give crude **2.8** as an amorphous solid. Crystallization from boiling hexanes afforded 13.0 g (81%) of **2.8** as white crystals: M.p. 59-60 $^{\circ}$C. IR (thin film) 2945, 92836, 1692, 1587, 1566, 1486, 1281 cm^{-1}. ^{1}H NMR (400 MHz) δ 9.85 (s, 1 H), 7.66 (d, J = 2.0 Hz, 1 H), 7.39 (d, J = 2.0 Hz, 1 H), 3.95 (s, 3 H), 3.93 (s, 3 H). ^{13}C NMR (100 MHz) δ 189.9, 154.2, 151.8, 133.0, 128.8, 117.9, 110.0, 60.8, 56.2. HRMS calculated for $C_9H_9BrO_3$ (MH^+) 244.9813 and 246.9793 found 244.9815 and 246.9793.

NMR Assignment. ^{1}H NMR (400 MHz) δ 9.85 (s, 1 H, CHO), 7.66 (d, *J* = 2.0 Hz, 1 H, C2-H), 7.39 (d, *J* = 2.0 Hz, 1 H, C1-H), 3.95 (s, 3 H, OCH_3), 3.93 (s, 3 H, OCH_3).

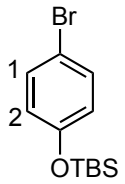

2.11

(4-Bromophenoxy)(*tert*-butyl)dimethylsilane (2.11). ARMVI21. A solution of 4-bromophenol (10.0 g, 57.8 mmol), TBSCl (9.5 g, 63.6 mmol), and imidazole (5.9 g, 86.7 mmol) in CH_2Cl_2 (150 mL) was stirred for 2.5 h at room temperature. the mixture was diluted with CH_2Cl_2 (100 mL), and washed successively with saturated aqueous NH_4Cl (100 mL) and water (100 mL). The organic fraction was dried (Na_2SO_4), filtered, and concentrated *in vacuo* to give crude **2.11** as a colorless oil. The crude material was purified via silica gel plug eluting with hexanes, to afford 15.28 g (92%) of **2.11** as a colorless oil: ^{1}H NMR (400 MHz) δ 7.33 (d, *J* = 8.8 Hz, 2 H), 6.73 (d, *J* = 8.8 Hz, 2 H), 1.00 (s, 9 H), 0.21 (s, 6 H).

NMR Assignment. ^{1}H NMR (400 MHz) δ 7.33 (d, *J* = 8.8 Hz, 2 H, C1-H), 6.73 (d, *J* = 8.8 Hz, 2 H, C2-H), 1.00 (s, 9 H, TBS), 0.21 (s, 6 H, TBS).

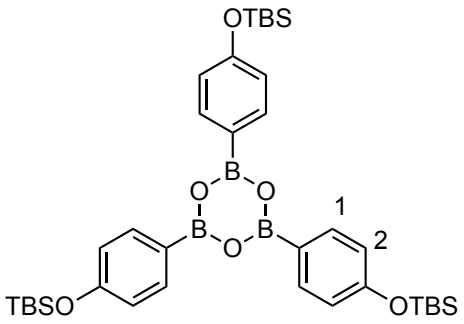

2.12

2,4,6-Tris(4-((*tert*-butyldimethylsilyl)oxy)phenyl)-1,3,5,2,4,6-trioxatriborinane (2.12). ARMI17. A solution of *n*-butyllithium (2.3 M, 3.7 mL, 8.7 mmol) was added dropwise to a solution of **2.11** (1.0 g, 3.5 mmol) in THF (8 mL) at -78 ºC, and stirred for 5 min at -78 ºC. Triisopropyl borate (3.3 g, 17.4 mmol) was added in one portion, and the reaction was slowly warmed to room temperature overnight. The mixture was diluted with water (50 mL) and saturated aqueous NH_4Cl (10 mL), and extracted with ethyl acetate (3 x 50 mL). The combined organic fractions were concentrated *in vacuo* to a total volume of roughly 20 mL, and refrigerated overnight. A white solid crashed out of solution, which was isolated by filtration to give 0.71 g (81%) of **2.12** as an amorphous white solid: ^{1}H NMR (400 MHz) δ 8.13 – 8.10 (m, 6 H), 6.97 – 6.94 (m, 6 H), 1.01 (s, 27 H), 0.26 (s, 18 H)

NMR Assignment. ^{1}H NMR (400 MHz) δ 8.13 – 8.10 (m, 6 H, C1-H), 6.97 – 6.94 (m, 6 H, C2-H), 1.01 (s, 27 H, TBS), 0.26 (s, 18 H, TBS)

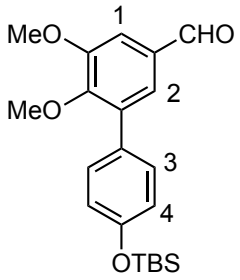

2.13

4'-((*tert*-Butyldimethylsilyl)oxy)-5,6-dimethoxy-[1,1'-biphenyl]-3-carbaldehyde (2.13). ARMI29. Solid $Pd(dppf)Cl_2 \bullet CH_2Cl_2$ (0.45 g, 0.5 mmol) was added to a degassed solution of K_3PO_4 (6.96 g, 32.8 mmol), **2.8** (2.67 g, 10.9 mmol), and **2.12** (3.31 g, 13.1 mmol) in 1,4-dioxane/water (4 : 1, 55 mL), and the heated to 80 ºC for 2.5 h. The reaction was cooled to room temperature, diluted with water (100 mL), and extracted with ethyl acetate (3 x 100 mL). The combined organic fractions were dried (Na_2SO_4), filtered, and concentrated *in vacuo* to give crude **2.13**. The crude material was purified via silica gel flash column chromatography eluting with hexanes : ethyl acetate (1 : 0 → 9 : 1 along a gradient) to give 3.9 g (96%) of **2.13** as an opaque oil: ^{1}H NMR (400 MHz) δ 9.98 (s, 1 H), 7.52 – 7.47 (comp, 4 H), 6.96 (d, J = 9.2 Hz, 2 H), 4.02 (s, 3 H), 3.72 (s, 3 H), 1.06 (s, 9 H), 0.29 (s, 6 H)

NMR Assignment. ^{1}H NMR (400 MHz) δ 9.98 (s, 1 H, CHO), 7.52 – 7.47 (comp, 4 H, C3-H, C2-H, C1-H), 6.96 (d, J = 9.2 Hz, 2 H, C4-H), 4.02 (s, 3 H, OCH_3), 3.72 (s, 3 H, OCH_3), 1.06 (s, 9 H, TBS), 0.29 (s, 6 H, TBS)

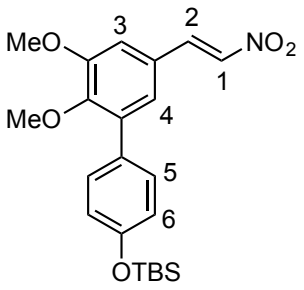

2.14

(*E*)-*tert*-Butyl((2',3'-dimethoxy-5'-(2-nitrovinyl)-[1,1'-biphenyl]-4-yl)oxy)dimethylsilane (2.14). ARMI33. A solution of **2.13** (3.60 g, 9.7 mmol) and ammonium acetate (0.55 g, 7.2 mmol) in nitromethane (74 mL) was heated for 12 h under reflux, with removal of water via Dean-Stark trap. The reaction was cooled to room temperature and the solvent removed *in vacuo*. The resulting residue was partitioned between ethyl acetate (100 mL) and water (100 mL). The layers were separated, and the aqueous layer was extracted with ethyl acetate (2 x 100 mL). The combined organic fractions were dried (Na_2SO_4), filtered, and concentrated *in vacuo* to give crude **2.14** as a viscous yellow oil. The crude material was purified via silica gel flash column chromatography eluting with hexanes : ethyl acetate (19 : 1) to give 3.11 g (77%) of **2.14** as a viscous yellow oil that slowly formed canary yellow crystals upon standing: ^{1}H NMR (400 MHz) δ 7.97 (d, *J* = 13.6 Hz, 1 H), 7.57 (d, *J* = 13.6 Hz, 1 H), 7.39 (d, *J* = 8.8 Hz, 2 H), 7.16 (d, *J* = 2.0 Hz, 1 H), 7.02 (d, *J* = 2.0 Hz, 1 H), 6.90 (d, *J* = 8.8 Hz, 2 H), 3.94 (s, 3 H), 3.64 (s, 3 H), 1.01 (s, 9 H), 0.25 (s, 6 H).

NMR Assignment. ^{1}H NMR (400 MHz) δ 7.97 (d, *J* = 13.6 Hz, 1 H, C2-H), 7.57 (d, *J* = 13.6 Hz, 1 H, C1-H), 7.39 (d, *J* = 8.8 Hz, 2 H, C5-H), 7.16 (d, *J* = 2.0 Hz, 1 H,

C4-H), 7.02 (d, J = 2.0 Hz, 1 H, C3-H), 6.90 (d, J = 8.8 Hz, 2 H, C6-H), 3.94 (s, 3 H, OCH_3), 3.64 (s, 3 H, OCH_3), 1.01 (s, 9 H, TBS), 0.25 (s, 6 H, TBS).

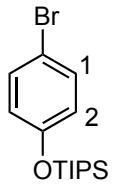

2.16

(4-Bromophenoxy)triisopropylsilane (2.16). ARMI59. A solution of 4-bromophenol (10.0 g, 57.8 mmol), TIPSCl (12.3 g, 63.6 mmol), and imidazole (5.9 g, 86.7 mmol) in CH_2Cl_2 (150 mL) was stirred for 2.5 h at room temperature. The mixture was diluted with CH_2Cl_2 (100 mL), and washed successively with saturated aqueous NH_4Cl (100 mL), and water (100 mL). The organic fraction was dried (Na_2SO_4), filtered, and concentrated *in vacuo* to give crude **2.16** as a colorless oil. The crude material was purified via silica gel plug eluting with hexanes to give 18.6 g (98%) of **2.16** as a colorless oil: ^{1}H NMR (400 MHz) δ 7.33 (d, J = 8.8 Hz, 2 H), 6.78 (d, J = 8.8 Hz, 2 H), 1.27 (sep, J = 6.8 Hz, 3 H), 1.12 (d, J = 6.8 Hz, 18 H).

NMR Assignment. ^{1}H NMR (400 MHz) δ 7.33 (d, J = 8.8 Hz, 2 H, C1-H), 6.78 (d, J = 8.8 Hz, 2 H, C2-H), 1.27 (sep, J = 6.8 Hz, 3 H, TIPS), 1.12 (d, J = 6.8 Hz, 18 H, TIPS).

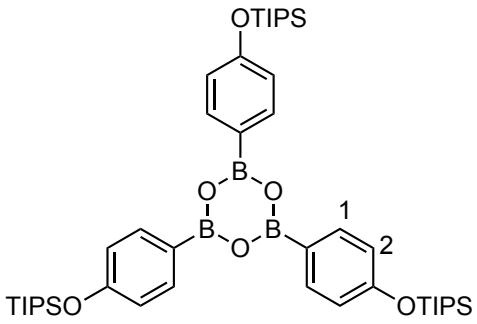

2.17

2,4,6-Tris(4-((triisopropylsilyl)oxy)phenyl)-1,3,5,2,4,6-trioxatriborinane (2.17). ARMI117. A solution of *n*-butyllithium (1.5 M, 50 mL, 75 mmol) was added dropwise to a solution of **2.16** (10.0 g, 30 mmol) in THF (100 mL) at -78 ºC. The reaction was stirred for 5 min at -78 ºC, whereupon triisopropyl borate (28.6 g, 150 mmol) was added in one portion, and the reaction was slowly warmed to room temperature overnight. The mixture was diluted with water (300 mL) and saturated aqueous NH_4Cl (100 mL), and extracted with ethyl acetate (3 x 300 mL). The combined organic fractions were dried (Na_2SO_4), filtered, and concentrated *in vacuo* to give crude **2.17** as a white paste. The crude material was purified via silica gel flash column chromatography eluting with hexanes : ethyl acetate (1 : 0 → 4 : 1 along a gradient) to give 7.99 g (89%) of **2.17** as a white amorphous solid: ^{1}H NMR (400 MHz) δ 8.10 (d, J = 8.8 Hz, 6 H), 6.98 (d, J = 8.8 Hz, 6 H), 1.31 (sep, J = 7.2 Hz, 9 H), 1.12 (d, J = 7.2 Hz, 54 H).

NMR Assignment. ^{1}H NMR (400 MHz) δ 8.10 (d, J = 8.8 Hz, 6 H, C1-H), 6.98 (d, J = 8.8 Hz, 6 H, C2-H), 1.31 (sep, J = 7.2 Hz, 9 H, TIPS), 1.12 (d, J = 7.2 Hz, 54 H, TIPS).

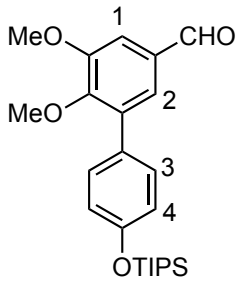

2.18

5,6-Dimethoxy-4'-((triisopropylsilyl)oxy)-[1,1'-biphenyl]-3-carbaldehyde (2.18). ARMII103. A solution of K_3PO_4 (16.1 g, 75.8 mmol), **2.17** (6.20 g, 25.3 mmol), **2.8** (8.38 g, 10.1 mmol) and $Pd(dppf)Cl_2 \bullet CH_2Cl_2$ (0.103 g, 0.13 mmol) in a degassed mixture of 1,4-dioxane/water (4 : 1, 125 mL) was heated to 80 ºC for 3 h. The reaction was cooled to room temperature, diluted with water (100 mL), and extracted with ethyl acetate (3 x 100 mL). The combined organic fractions were washed with brine (1 x 100 mL), dried (Na_2SO_4), and concentrated *in vacuo* to give crude **2.18** as a viscous oil. The crude material was purified via silica gel flash chromatography eluting with hexanes : ethyl acetate (1 : 0 → 85 : 15 along a gradient) to give 8.60 g (91%) of **2.18** as a white solid. Crystallization from methanol gave white needles: M.p. 75-76 ºC. IR (thin film) 2944, 2867, 2360, 1695, 1513, 1464, 1382, 1265 cm^{-1}. ^1H NMR (400 MHz) δ 9.92 (s, 1 H), 7.47 (d, J = 2.0 Hz, 1 H), 7.44 - 7.40 (m, 3 H), 6.65 (dt, J = 8.4, 2.0 Hz, 2 H), 3.96 (s, 3 H), 3.64 (s, 3 H), 1.29 (sep, J = 7.6 Hz, 3 H), 1.12 (d, J = 7.2 Hz, 18 H). ^{13}C NMR (100 MHz) δ 191.3, 155.9, 153.8, 151.9, 135.8, 132.3, 130.2, 129.6, 127.3, 119.8, 108.9, 60.5, 56.1, 17.9, 12.7. HRMS calculated for $C_{24}H_{34}O_4Si$ (MH^+) 415.2305, found 415.2305.

NMR Assignment. ^{1}H NMR (400 MHz) δ 9.92 (s, 1 H, CHO), 7.47 (d, *J* = 2.0 Hz, 1 H, C2-H), 7.44 - 7.40 (comp, 3 H, C1-H and C3-H), 6.65 (dt, *J* = 8.4, 2.0 Hz, 2 H, C4-H), 3.96 (s, 3 H, OCH_3), 3.64 (s, 3 H, OCH_3), 1.29 (sep, *J* = 7.6 Hz, 3 H, TIPS), 1.12 (d, *J* = 7.2 Hz, 18 H, TIPS).

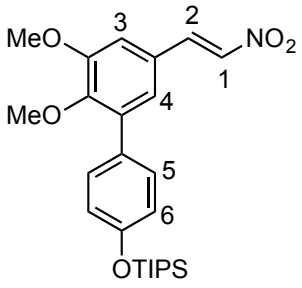

2.19

(*E*)-((2',3'-Dimethoxy-5'-(2-nitrovinyl)-[1,1'-biphenyl]-4-yl)oxy)triisopropylsilane (2.19). ARMIII41. A solution of **2.18** (3.08 g, 7.43 mmol) and ammonium acetate (0.43 g, 5.57 mmol) in nitromethane (56 mL) was heated under reflux for 12 h with removal of water via Dean-Stark trap. The reaction was cooled to room temperature, and concentrated *in vacuo* to give crude **2.19** as a viscous orange oil. The crude material was purified by silica gel column chromatography eluting with hexanes : ethyl acetate (19 : 1) to give 3.00 g (88%) of 2.19 as a viscous yellow oil that formed canary yellow crystals upon standing: M.p. 65-67 ºC. IR (thin film) 2944, 2867, 1512, 1335, 1264. ^{1}H NMR (400 MHz) δ 7.98 (d, *J* = 13.6 Hz, 1 H), 7.56 (d, *J* = 13.6 Hz, 1 H), 7.38 (d, *J* = 8.8 Hz, 2 H), 7.17 (d, *J* = 2.0 Hz, 1 H), 7.01 (d, *J* = 2.0 Hz, 1 H), 6.95 (d, *J* = 8.8 Hz, 2 H), 3.94 (s, 3 H), 3.61 (s, 3 H), 1.28 (sep, *J* = 7.2 Hz, 3 H), 1.13, (d, *J* = 7.2 Hz,

18 H). ^{13}C NMR (100 MHz) δ 155.9, 153.6, 150.1, 139.1, 136.5, 136.3, 130.1, 129.4, 125.6, 124.9, 119.8, 110.5, 60.6, 59.1, 17.9, 12.7. HRMS calculated for $C_{25}H_{35}NO_5Si$ $(M+Na)^+$ 480.21770, found 480.21750.

NMR Assignment. ^{1}H NMR (400 MHz) δ 7.98 (d, *J* = 13.6 Hz, 1 H, C2-H), 7.56 (d, *J* = 13.6 Hz, 1 H, C1-H), 7.38 (d, *J* = 8.8 Hz, 2 H, C5-H), 7.17 (d, *J* = 2.0 Hz, 1 H, C4-H), 7.01 (d, *J* = 2.0 Hz, 1 H, C3-H), 6.95 (d, *J* = 8.8 Hz, 2 H, C6-H), 3.94 (s, 3 H, OCH_3), 3.61 (s, 3 H, OCH_3), 1.28 (sep, *J* = 7.2 Hz, 3 H, TIPS), 1.13, (d, *J* = 7.2 Hz, 18 H, TIPS).

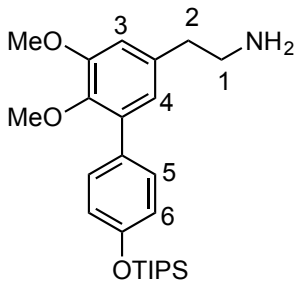

2.20

2-(5,6-Dimethoxy-4'-((triisopropylsilyl)oxy)-[1,1'-biphenyl]-3-yl)ethanamine (2.20). ARMI95. A solution of **2.19** (50 mg, 0.10 mmol) in 1,4-dioxane (1 mL, dried over 4Å mol sieves) was added dropwise to a solution of DIBAL-H (1 M in hexanes, 3 mL, 3.0 mmol) in 1,4-dioxane (1 mL) at room temperature. The reaction was stirred for 0.5 h at room temperature. The mixture was cooled to 0 ºC in an ice bath, and ethyl acetate (2 mL) followed by Rochelle's salt (3 mL) was carefully added. The mixture was stirred for 2 h at room temperature, whereupon layers were separated and the aqueous

layer was extracted with ethyl acetate (3 x 10 mL). The combined organic fractions were dried (Na_2SO_4), filtered, and concentrated *in vacuo* to give crude **2.20** as a viscous oil. The crude material was purified via silica gel column chromatography eluting with CH_2Cl_2 : methanol (1 : 0 → 9 : 1 along a gradient) to give 44 mg (94%) of **2.20** as a clear viscous oil: IR (thin film) 2944, 2867, 1607, 1512, 1263 cm^{-1}. ^1H NMR (400 MHz) δ 7.41 (d, *J* = 8.8 Hz, 2 H), 6.91, (d, *J* = 8.8 Hz, 2 H), 6.77 (d, *J* = 2.0 Hz, 1 H), 6.72 (d, *J* = 2.0 Hz, 1 H), 3.88 (s, 3 H), 3.50 (s, 3 H), 3.03 – 2.95 (comp, 4 H), 2.71 (t, *J* = 7.6 Hz, 2 H) 1.28 (sep, *J* = 8.0 Hz, 3 H), 1.12 (d, *J* = 7.2 Hz, 18 H). ^{13}C NMR (100 MHz) δ 155.3, 153.0, 144.9, 135.3, 134.8, 130.7, 130.2, 122.6, 119.6, 111.5, 60.3, 56.0, 43.0, 38.8, 17.9, 12.7. HRMS calculated for $C_{25}H_{39}NO_3Si$ $(M+Na)^+$ 452.24910 found 452.25840.

NMR Assignment. ^1H NMR (400 MHz) δ 7.41 (d, *J* = 8.8 Hz, 2 H, C5-H), 6.91, (d, *J* = 8.8 Hz, 2 H, C6-H), 6.77 (d, *J* = 2.0 Hz, 1 H, C4-H), 6.72 (d, *J* = 2.0 Hz, 1 H, C3-H), 3.88 (s, 3 H, OCH_3), 3.50 (s, 3 H, OCH_3), 3.03 – 2.95 (comp, 4 H, C1-H and NH_2), 2.71 (t, *J* = 7.6 Hz, 2 H, C2-H) 1.28 (sep, *J* = 8.0 Hz, 3 H, TIPS), 1.12 (d, *J* = 7.2 Hz, 18 H, TIPS).

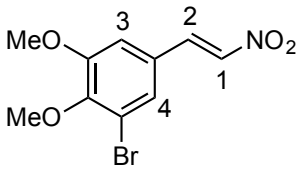

2.25

(*E*)-1-Bromo-2,3-dimethoxy-5-(2-nitrovinyl)benzene (2.25). ARMII23. A solution of **2.8** (3.00 g, 12.3 mmol) and ammonium acetate (0.72 g, 9.3 mmol) in nitromethane (98 mL) heated under reflux for 12 h, with removal of water via Dean-Stark trap. The reaction was cooled to room temperature and the solvent was removed *in vacuo*. The resulting residue was partitioned between ethyl acetate (100 mL) and water (100 mL), the layers were separated, and the aqueous layer was extracted with ethyl acetate (2 x 100 mL). The combined organic fractions were dried (Na_2SO_4), filtered, and concentrated *in vacuo* to give crude **2.25** as a viscous yellow oil. The crude material was purified via silica gel flash column chromatography eluting with hexanes : ethyl acetate (19 : 1) to give 3.42 g (97%) of **2.25** as a viscous yellow oil that slowly formed canary yellow crystals upon standing: ^{1}H NMR (400 MHz) δ 7.89 (d, *J* = 13.6 Hz, 1 H), 7.51 (d, *J* = 13.6 Hz, 1 H), 7.37 (d, *J* = 2.0 Hz, 1 H), 6.97 (d, *J* = 2.0 Hz, 1 H), 3.920 (s, 3 H), 3.917 (s, 3 H).

NMR Assignment. ^{1}H NMR (400 MHz) δ 7.89 (d, *J* = 13.6 Hz, 1 H, C2-H), 7.51 (d, *J* = 13.6 Hz, 1 H, C1-H), 7.37 (d, *J* = 2.0 Hz, 1 H, C4-H), 6.97 (d, *J* = 2.0 Hz, 1 H, C3-H), 3.920 (s, 3 H, OCH_3), 3.917 (s, 3 H, OCH_3).

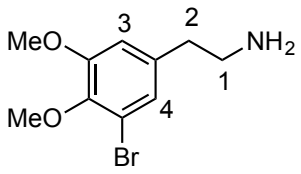

2.26

2-(3-Bromo-4,5-dimethoxyphenyl)ethan-1-amine (2.26). ARMII47. A solution of **2.25** (1.0 g, 3.4 mmol) in 1,4-dioxane (15 mL, dried over 4 Å MS) was added to a solution DIBAL-H (1 M in hexanes, 52 mL, 52 mmol) in 1,4-dioxane (15 mL). The reaction was warmed to room temperature, and stirred for 12 h. The reaction was cooled to 0 ºC, and excess DIBAL-H was quenched via slow addition of methanal (5 mL), followed by addition of Rochelle's salt (50 mL). The mixture was stirred at room temperature for 1 h, then extracted with ethyl acetate (3 x 50 mL). The combined organic fractions were washed with brine (1 x 100 mL), dried (Na_2SO_4), filtered, and concentrated *in vacuo* to give crude **2.26** as a viscous oil. The crude material was purified via silica gel flash column chromatography eluting with CH_2Cl_2 : methanol (1 : 0 → 9 : 1 along a gradient) to give 0.87 g (97%) of **2.26** as a viscous oil: ^{1}H NMR (400 MHz) δ 6.90 (d, *J* = 2.0 Hz, 1 H), 6.62 (d, *J* = 2.0 Hz, 1 H), 3.78 (s, 3 H), 3.75 (s, 3 H), 2.87 (t, *J* = 7.2 Hz, 2 H), 2.59 (t, *J* = 7.2 Hz, 2 H), 1.00 (brs, 2 H).

NMR Assignment. ^{1}H NMR (400 MHz) δ 6.90 (d, *J* = 2.0 Hz, 1 H, C4-H), 6.62 (d, *J* = 2.0 Hz, 1 H, C3-H), 3.78 (s, 3 H, OCH_3), 3.75 (s, 3 H, OCH_3), 2.87 (t, *J* = 7.2 Hz, 2 H, C1-H), 2.59 (t, *J* = 7.2 Hz, 2 H, C2-H), 1.00 (brs, 2 H, NH_2).

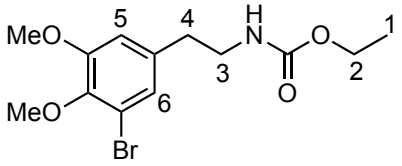

2.27

Ethyl (3-bromo-4,5-dimethoxyphenethyl)carbamate (2.27). ARMII33. Ethyl chloroformate (0.12 g, 1.1 mmol) was added to a solution of **2.26** (0.27 g, 1.0 mmol) and triethylamine (0.11 g, 1.1 mmol) in CH_2Cl_2 (3 mL) at 0 ºC. The reaction was stirred for 12 h, and warmed to room temperature. The reaction mixture was diluted with CH_2Cl_2 (50 mL), washed with water (50 mL), dried (Na_2SO_4), filtered, and concentrated *in vacuo* to give crude **2.27** as a viscous oil. The crude material was purified via silica gel flash column chromatography eluting with hexanes : ethyl acetate (7 : 3) to give 0.26 g (76%) of **2.27** as a viscous oil: ^{1}H NMR (400 MHz) δ 6.89 (d, *J* = 2.0 Hz, 1 H), 6.63 (d, *J* = 2.0 Hz, 1 H), 4.93 (brs, 1 H), 4.04 (q, *J* = 7.2 Hz, 2 H), 3.79 (s, 3 H), 3.76 (s, 3 H), 3.33 (q, *J* = 6.8 Hz, 2 H), 2.68 (t, *J* = 6.8 Hz, 2 H), 1.17 (t, *J* = 7.2 Hz, 3 H). ^{13}C NMR (100 MHz) δ 171.1, 156.5, 153.6, 144.9, 136.0, 124.6, 117.6, 112.2, 60.5, 56.1, 41.9, 35.7, 14.6.

NMR Assignment. ^{1}H NMR (400 MHz) δ 6.89 (d, *J* = 2.0 Hz, 1 H, C6-H), 6.63 (d, *J* = 2.0 Hz, 1 H, C5-H), 4.93 (brs, 1 H, NH), 4.04 (q, *J* = 7.2 Hz, 2 H, C2-H), 3.79 (s, 3 H, OCH_3), 3.76 (s, 3 H, OCH_3), 3.33 (q, *J* = 6.8 Hz, 2 H, C3-H), 2.68 (t, *J* = 6.8 Hz, 2 H, C4-H), 1.17 (t, *J* = 7.2 Hz, 3 H, C1-H).

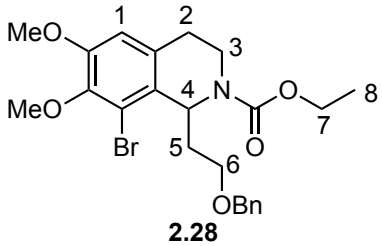

2.28

Ethyl 1-(2-(benzyloxy)ethyl)-8-bromo-6,7-dimethoxy-3,4-dihydroisoquinoline-2(1*H*)-carboxylate (2.28). ARMII125. A solution of **2.27** (66 mg, 0.2 mmol), **2.23** (66 mg, 0.4 mmol), and TFA (2 drops) in HFIP (1 mL) was heated to 60 ºC for 12 h, whereupon the solvent was removed *in vacuo* to give crude **2.28**. The crude mixture was purified via silica gel flash column chromatography eluting with CH_2Cl_2 with triethylamine (1%) to give 65 mg (68%) of **2.28** as a viscous oil: ^{1}H NMR (400 MHz) (rotamers 1 : 1) δ 7.27 – 7. 18 (comp, 5 H), 6.56 (s, 0.5 H), 6.54 (s, 0.5 H), 5.41 (dd, *J* = 10.4, 2.8 Hz, 0.5 H), 5.34 (dd, *J* = 10.4, 2.8 Hz, 0.5 H), 4.44 (s, 2 H), 4.12 – 3.99 (comp, 2.5 H), 3.94 – 3.88 (m, 0.5 H), 3.77 – 3.73 (comp, 6 H), 3.65 – 3.63 (m, 0.5 H), 3.58 – 3.54 (m, 1 H), 3.51 – 3.46 (m, 0.5 H), 3.38 – 3.31 (m, 0.5 H), 3.28 – 3.20 (m, 0.5 H), 2.90 – 2.78 (m, 1 H), 2.69 – 2.65 (m, 1 H), 2.24 (dtd, *J* = 14.8, 7.2, 3.2 Hz, 1 H), 1.91 – 1.80 (m, 1 H), 1.19 – 1.13 (comp, 3 H). ^{13}C NMR (100 MHz) (rotamers 1 : 1) δ 162.5, 155.7, 155.6, 152.0, 151.9, 145.0, 144.9, 138.6, 138.5, 131.4, 131.2, 130.0, 129.7, 128.3, 128.2, 127.5, 127.44, 127.36, 118.3, 118.0, 112.1, 111.8, 73.0, 68.2, 67.7, 61.6, 61.4, 60.5, 56.0, 52.2, 52.0, 37.6, 36.8, 33.9, 33.8, 28.2, 27.9, 14.7, 14.6.

NMR Assignment. ^{1}H NMR (400 MHz) (rotamers 1 : 1) δ 7.27 – 7. 18 (comp, 5 H, OBn), 6.56 (s, 0.5 H, C1-H), 6.54 (s, 0.5 H, C1-H), 5.41 (dd, *J* = 10.4, 2.8 Hz, 0.5 H,

C4-H), 5.34 (dd, J = 10.4, 2.8 Hz, 0.5 H, C4-H), 4.44 (s, 2 H, OBn), 4.12 – 3.99 (comp, 2.5 H, C7-H and C6-H), 3.94 – 3.88 (m, 0.5 H, C6-H), 3.77 – 3.73 (comp, 6 H, OCH_3 and OCH_3), 3.65 – 3.63 (m, 0.5 H, C6-H), 3.58 – 3.54 (m, 1 H, C3-H), 3.51 – 3.46 (m, 0.5 H, C6-H), 3.38 – 3.31 (m, 0.5 H, C3-H), 3.28 – 3.20 (m, 0.5 H, C3-H), 2.90 – 2.78 (m, 1 H, C2-H), 2.69 – 2.65 (m, 1 H, C2-H), 2.24 (dtd, J = 14.8, 7.2, 3.2 Hz, 1 H, C5-H), 1.91 – 1.80 (m, 1 H, C5-H), 1.19 – 1.13 (comp, 3 H, C8-H).

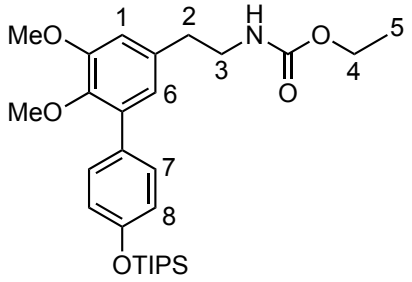

2.29

Ethyl (2-(5,6-dimethoxy-4'-((triisopropylsilyl)oxy)-[1,1'-biphenyl]-3-yl)ethyl)carbamate (2.29). ARMII131. Ethyl chloroformate (1.68 g, 15.5 mmol) was added over 20 min to a solution of **2.20** (4.43 g, 10.3 mmol) and triethylamine (1.57 g, 15.5 mmol) in CH_2Cl_2 (30 mL) at 0 ºC. The reaction was stirred for 12 h at 0 ºC, then warmed to room temperature. Water (50 mL) was added to the mixture, the two phases were separated, and the aqueous phase was extracted with CH_2Cl_2 (3 x 50 mL). The combined organic fractions were dried (Na_2SO_4), filtered, and concentrated *in vacuo* to give crude **2.29** as an opaque oil. The crude material was purified via silica gel column chromatography eluting with CH_2Cl_2 to give 4.47 g (86%) of **2.29** as a clear viscous oil:

^{1}H NMR (400 MHz) δ 7.41 (d, *J* = 8.8 Hz, 2 H), 6.91 (d, *J* = 8.8 Hz, 2 H), 6.76 (d, *J* = 2.0 Hz, 1 H), 6.70 (brs, 1 H), 4.71 (brs, 1 H), 4.11 (q, *J* = 7.2 Hz, 2 H), 3.89 (s, 3 H), 3.51 (s, 3 H), 3.45 (q, *J* = 6.8 Hz, 2 H), 2.79 (t, *J* = 6.8 Hz, 2 H), 1.38 – 1.21 (comp, 6 H), 1.12 (d, *J* = 7.2 Hz, 18 H).

NMR Assignment. ^{1}H NMR (400 MHz) δ 7.41 (d, *J* = 8.8 Hz, 2 H, C7-H), 6.91 (d, *J* = 8.8 Hz, 2 H, C8-H), 6.76 (d, *J* = 2.0 Hz, 1 H, C6-H), 6.70 (brs, 1 H, C1-H), 4.71 (brs, 1 H, NH), 4.11 (q, *J* = 7.2 Hz, 2 H, C4-H), 3.89 (s, 3 H, OCH_3), 3.51 (s, 3 H, OCH_3), 3.45 (q, *J* = 6.8 Hz, 2 H, C3-H), 2.79 (t, *J* = 6.8 Hz, 2 H, C2-H), 1.38 – 1.21 (comp, 6 H, C5-H and TIPS), 1.12 (d, *J* = 7.2 Hz, 18 H, TIPS).

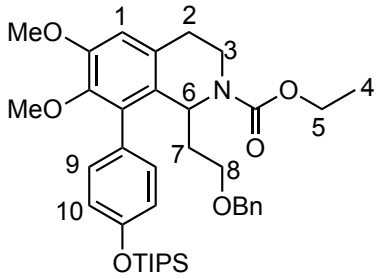

2.30

Ethyl 1-(2-(benzyloxy)ethyl)-6,7-dimethoxy-8-(4-((triisopropylsilyl)oxy)phenyl)-3,4-dihydroisoquinoline-2(1*H*)-carboxylate (2.30). ARMII145. A solution of **2.29** (200 mg, 0.40 mmol), **2.23** (131 mg, 0.80 mmol), and TFA (2 drops) in HFIP (1 mL) was heated to 60 ºC for 12 h. The reaction was cooled to room temperature, and the solvent removed *in vacuo* to give crude **2.30**. The crude material was purified via silica gel column chromatography eluting with hexanes : ethyl

acetate (1 : 0 → 9 :1 along a gradient) to give 223 mg (86%) of **2.30** as a clear viscous oil: ^{1}H NMR (400 MHz) (rotamers 1 : 1) δ 7.33 – 7.28 (comp, 2 H), 7.27 – 7.10 (comp, 5 H), 7.00 – 6.96 (comp, 2 H), 6.69 (s, 0.5 H), 6.66 (s, 0.5 H), 5.38 (dd, *J* = 10.8, 3.6 Hz, 0.5 H), 5.22 (dd, *J* = 10.8, 3.6 Hz, 0.5 H), 4.26 (s, 2 H), 4.15 – 4.02 (comp, 3 H), 3.87 (s, 1.5 H), 3.86 (s, 1.5 H), 3.43 – 3.37 (comp, 4 H), 3.28 – 3.19 (m, 1 H), 3.16 – 3.10 (m, 1 H), 3.04 – 2.93 (m, 1 H), 2.87 – 2.76 (m, 1 H), 1.87 – 1.77 (m, 1 H), 1.71 – 1.64 (m, 1 H), 1.34 – 1.23 (comp, 4.5 H), 1.19 – 1.12 (comp, 19.5 H).

NMR Assignment. ^{1}H NMR (400 MHz) (rotamers 1 : 1) δ 7.33 – 7.28 (comp, 2 H, C9-H), 7.27 – 7.10 (comp, 5 H, OBn), 7.00 – 6.96 (comp, 2 H, C9-H), 6.69 (s, 0.5 H, C1-H), 6.66 (s, 0.5 H, C1-H), 5.38 (dd, *J* = 10.8, 3.6 Hz, 0.5 H, C6-H), 5.22 (dd, *J* = 10.8, 3.6 Hz, 0.5 H, C6-H), 4.26 (s, 2 H, OBn), 4.15 – 4.02 (comp, 3 H, C5-H and C8-H), 3.87 (s, 1.5 H, OCH_3), 3.86 (s, 1.5 H, OCH_3), 3.43 – 3.37 (comp, 4 H, OCH_3 and C8-H), 3.28 – 3.19 (m, 1 H, C3-H), 3.16 – 3.10 (m, 1 H, C3-H), 3.04 – 2.93 (m, 1 H, C2-H), 2.87 – 2.76 (m, 1 H, C2-H), 1.87 – 1.77 (m, 1 H, C7-H), 1.71 – 1.64 (m, 1 H, C7-H), 1.34 – 1.23 (comp, 4.5 H, C4-H and TIPS), 1.19 – 1.12 (comp, 19.5 H, C4-H and TIPS).

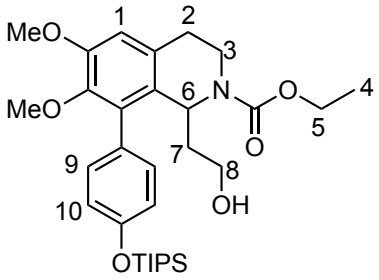

2.31

Ethyl 1-(2-hydroxyethyl)-6,7-dimethoxy-8-(4-((triisopropylsilyl)oxy)phenyl)-3,4-dihydroisoquinoline-2(1*H*)-carboxylate (2.31). ARMIII11. A solution of **2.30** (468 mg, 0.72 mmol) in 2-propanol (1 mL) was added to a suspension of Pd/C (10% w/w, 90 mg) in 2-propanol (15 mL) under a balloon of H_2 at 50 ºC. The reaction was stirred for 5 h at 50 ºC, whereupon the suspension was filtered through a pad of Celite and washed with methanol. The solution was concentrated *in vacuo* to give crude **2.31** as an opaque oil. The crude material was purified via silica gel flash column chromatography eluting with hexanes : ethyl acetate (9 : 1 → 3 : 1 along a gradient) to yield 240 mg (60%) of **2.31** as a clear viscous oil: ^{1}H NMR (400 MHz) δ 6.96 – 6.86 (comp, 2 H), 6.75 – 6.69 (comp, 2 H), 6.47 (s, 1 H), 5.06 – 5.02 (m, 1 H), 3.95 – 3.89 (comp, 2 H), 3.64 (s, 3 H), 3.61 – 3.55 (m, 1 H), 3.22 – 3.19 (comp, 4 H), 3.08 – 3.05 (comp, 2 H), 2.77 – 2.63 (comp, 2 H), 1.40 – 1.30 (comp, 2 H), 1.08 – 1.02 (comp, 6 H), 0.90 (d, J = 7.2 Hz, 18 H).

NMR Assignment. ^{1}H NMR (400 MHz) δ 6.96 – 6.86 (comp, 2 H, C9-H), 6.75 – 6.69 (comp, 2 H, C10-H), 6.47 (s, 1 H, C1-H), 5.06 – 5.02 (m, 1 H, C6-H), 3.95 – 3.89 (comp, 2 H, C5-H), 3.64 (s, 3 H, OCH_3), 3.61 – 3.55 (m, 1 H, C8-H), 3.22 – 3.19 (comp,

4 H, C8-H and OCH_3), 3.08 – 3.05 (comp, 2 H, C3-H), 2.77 – 2.63 (comp, 2 H, C2-H), 1.40 – 1.30 (comp, 2 H, C7-H), 1.08 – 1.02 (comp, 6 H, C4-H and TIPS), 0.90 (d, *J* = 7.2 Hz, 18 H, TIPS).

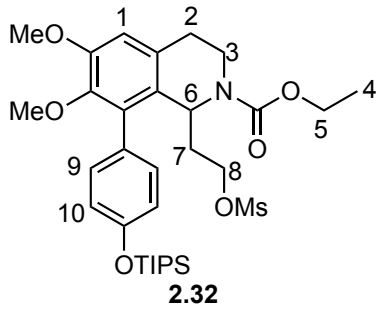

2.32

Ethyl 6,7-dimethoxy-1-(2-((methylsulfonyl)oxy)ethyl)-8-(4-((triisopropylsilyl)oxy)phenyl)-3,4-dihydroisoquinoline-2(1*H*)-carboxylate (2.32). ARMIII13. Mesyl chloride (23 mg, 0.20 mmol) was added to a solution of **2.31** (100 mg, 0.18 mmol) and triethylamine (27 mg, 0.27 mmol) in CH_2Cl_2 (1 mL) at 0 ºC, and the reaction was stirred for 0.5 h. The reaction was warmed to room temperature, and stirred for an additional 2.5 h. The mixture was diluted with CH_2Cl_2 (20 mL), and successively washed with water (10 mL), aqueous HCl (1 M, 10 mL), saturated aqueous $NaHCO_3$ (10 mL), and brine (10 mL). The combined organic fractions were dried (Na_2SO_4), filtered, and concentrated *in vacuo* to give crude **2.32** as an oil. The crude material was purified via silica gel flash column chromatography to give 49 mg (43%) of **2.32** as an oil: ^{1}H NMR (400 MHz)(rotamers 1 : 1) δ 6.96 – 6.85 (comp, 2 H), 6.75 (d, *J* = 8.4 Hz, 1 H), 6.70 (d, *J* = 8.4 Hz, 1H), 6.46 (s, 0.5 H), 6.44 (s, 0.5 H), 5.13 (td, *J* = 10.8, 2.8 Hz, 0.5 H),

5.01 (dd, *J* = 10.8, 2.8 Hz, 0.5 H), 3.93 – 3.85 (comp, 2.5 H), 3.78 – 3.74 (m, 0.5 H), 3.74 – 3.67 (m, 1 H), 3.63 (s, 3 H), 3.60 – 3.58 (m, 1 H), 3.23 – 3.17 (comp, 4 H), 3.12 – 3.06 (m, 1 H), 2.81 – 2.67 (m, 1 H), 2.62 – 2.59 (comp, 3 H), 1.73 – 1.64 (m, 1 H), 1.51 – 1.44 (m, 1 H), 1.08 – 1.01 (comp, 6 H), 0.89 (d, *J* = 7.2 Hz, 18 H).

NMR Assignment. ^{1}H NMR (400 MHz)(rotamers 1 : 1) δ 6.96 – 6.85 (comp, 2 H, C9-H), 6.75 (d, *J* = 8.4 Hz, 1 H, C10-H), 6.70 (d, *J* = 8.4 Hz, 1H, C10-H), 6.46 (s, 0.5 H, C1-H), 6.44 (s, 0.5 H, C1-H), 5.13 (td, *J* = 10.8, 2.8 Hz, 0.5 H, C6-H), 5.01 (dd, *J* = 10.8, 2.8 Hz, 0.5 H, C6-H), 3.93 – 3.85 (comp, 2.5 H, C5-H and C8-H), 3.78 – 3.74 (m, 0.5 H, C8-H), 3.74 – 3.67 (m, 1 H, C3-H), 3.63 (s, 3 H, OCH_3), 3.60 – 3.58 (m, 1 H, C3-H), 3.23 – 3.17 (comp, 3 H, OCH_3), 3.12 – 3.06 (m, 1 H, C2-H), 2.81 – 2.67 (m, 1 H, C2-H), 2.62 – 2.59 (comp, 3 H, OMs), 1.73 – 1.64 (m, 1 H, C7-H), 1.51 – 1.44 (m, 1 H, C7-H), 1.08 – 1.01 (comp, 6 H, C4-H and TIPS), 0.89 (d, *J* = 7.2 Hz, 18 H, TIPS).

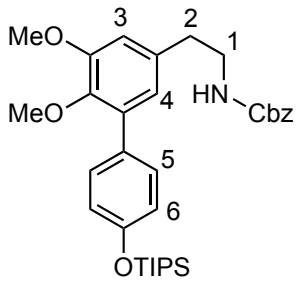

2.45

Benzyl (2-(5,6-dimethoxy-4'-((triisopropylsilyl)oxy)-[1,1'-biphenyl]-3-yl)ethyl)carbamate (2.45). ARMIII65. CbzCl (0.44 g, 2.59 mmol) was added dropwise over 5 min to a suspension of **2.20** (1.01 g, 2.35 mmol) and K_2CO_3 (0.39 g, 2.80 mmol)

in THF (15 mL). The reaction was stirred for 2 h at room temperature, at which point CbzCl (0.22 g, 1.80 mmol) was added. The reaction was stirred for an additional 2 h at room temperature, then diluted with CH_2Cl_2 (50 mL), and washed with saturated aqueous Na_2CO_3 (3 x 20 mL). The organic fraction was dried (Na_2SO_4), filtered, and concentrated *in vacuo* to give crude **2.45** as an oil. The crude material was purified via silica gel flash column chromatography eluting with CH_2Cl_2 to give 1.05 g (79%) of **2.45** as an oil: ^{1}H NMR (400 MHz) δ 7.41 (d, *J* = 8.0 Hz, 2 H), 7.35 – 7.29 (comp, 5 H), 6.92 (d, *J* = 8.0 Hz, 2 H), 6.76 (s, 1 H), 6.69 (s, 1 H), 5.10 (s, 2 H), 4.95 (brs, 1 H), 3.85 (s, 3 H), 3.52 (s, 3 H), 3.47 (q, *J* = 7.2 Hz, 2 H), 2.80 (t, *J* = 7.2 Hz, 2 H), 1.32 – 1.24 (sep, *J* = 7.2 Hz, 3 H), 1.13 (d, *J* = 7.2 Hz, 18 H).

NMR Assignment. ^{1}H NMR (400 MHz) δ 7.41 (d, *J* = 8.0 Hz, 2 H, C5-H), 7.35 – 7.29 (comp, 5 H, Cbz), 6.92 (d, *J* = 8.0 Hz, 2 H, C6-H), 6.76 (s, 1 H, C4-H), 6.69 (s, 1 H, C3-H), 5.10 (s, 2 H, Cbz), 4.95 (brs, 1 H, NH), 3.85 (s, 3 H, OCH_3), 3.52 (s, 3 H, OCH_3), 3.47 (q, *J* = 7.2 Hz, 2 H, C1-H), 2.80 (t, *J* = 7.2 Hz, 2 H, C2-H), 1.32 – 1.24 (sep, *J* = 7.2 Hz, 3 H, TIPS), 1.13 (d, *J* = 7.2 Hz, 18 H, TIPS).

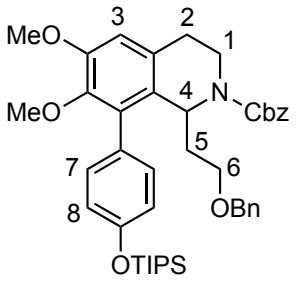

2.42

Benzyl 1-(2-(benzyloxy)ethyl)-6,7-dimethoxy-8-(4-((triisopropylsilyl)oxy)phenyl)-3,4-dihydroisoquinoline-2(1*H*)-carboxylate (2.42). **ARMIII95.** A solution of **2.45** (0.81 g, 1.40 mmol), **2.46** (0.61 g, 2.90 mmol), and TFA (0.25 g, 2.20 mmol) in TFE (17 mL) were heated to 60 ºC for 12 h, whereupon the solvent was removed *in vacuo* to give crude **2.42**. The crude material was purified via silica gel column chromatography eluting with hexanes : ethyl acetate (19 : 1 → 9 : 1 along a gradient) to give 0.94 g (91%) of **2.42** as an oil: ^{1}H NMR (400 MHz) (rotamers 3 : 7) δ 7.34 – 7.12 (comp, 11.7 H), 7.00 – 6.93 (comp, 2 H), 6.71 (dd, *J* = 8.4, 2.8 Hz, 0.7 H), 6.67 (s, 0.7 H), 6.65 (s, 0.3 H), 5.38 (dd, *J* = 10.8, 3.6 Hz, 0.3 H), 5.32 – 5.29 (comp, 1 H), 5.14 – 5.11 (comp, 1.3 H), 4.97 (d, *J* = 12.4 Hz, 0.7 H), 4.23 (s, 0.7 H), 4.15 (s, 1.3 H), 4.13 – 4.10 (m, 0.7 H), 4.06 – 4.01 (m, 0.3 H), 3.86 (s, 3 H), 3.45 – 3.35 (comp, 4 H), 3.24 – 2.92 (comp, 3 H), 2.80 (tt, *J* = 16.8, 4.8 Hz, 1 H), 1.85 – 1.60 (comp, 2 H), 1.31 – 1.23 (comp, 3 H), 1.13 – 1.10 (comp, 18 H).

NMR Assignment. ^{1}H NMR (400 MHz) (rotamers 3 : 7) δ 7.34 – 7.12 (comp, 11.3 H, Cbz and OBn), 7.00 – 6.93 (comp, 2 H, C8-H and OBn), 6.71 (dd, *J* = 8.4, 2.8 Hz, 0.7 H, OBn), 6.67 (s, 0.7 H, C3-H), 6.65 (s, 0.3 H, C3-H), 5.38 (dd, *J* = 10.8, 3.6 Hz,

0.3 H, C4-H), 5.32 – 5.29 (comp, 1 H, C4-H and Cbz), 5.14 – 5.11 (comp, 1.3 H, Cbz), 4.97 (d, *J* = 12.4 Hz, 0.7 H, Cbz), 4.23 (s, 0.7 H, OBn), 4.15 (s, 1.3 H, OBn), 4.13 – 4.10 (m, 0.7 H, C6-H), 4.06 – 4.01 (m, 0.3 H, C6-H), 3.86 (s, 3 H, OCH_3), 3.45 – 3.35 (comp, 4 H, C6-H and OCH_3), 3.24 – 2.92 (comp, 3 H, C1-H and C2-H), 2.80 (tt, *J* = 16.8, 4.8 Hz, 1 H, C2-H), 1.85 – 1.60 (comp, 2 H, C5-H), 1.31 – 1.23 (comp, 3 H, TIPS), 1.13 – 1.10 (comp, 18 H, TIPS).

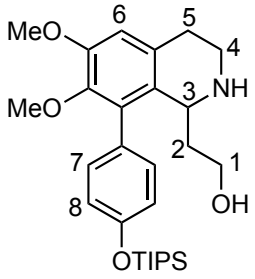

2.47

2-(6,7-Dimethoxy-8-(4-((triisopropylsilyl)oxy)phenyl)-1,2,3,4-tetrahydroisoquinolin-1-yl)ethan-1-ol (2.47). ARMIII87. A solution of **2.42** (227 mg, 0.32 mmol) in Methanol (1 mL) was added to a suspension of Pd/C (10% w/w, 320 mg) in degassed Methanol (10 mL) under a balloon of H_2 gas. The reaction was heated to 50 ºC for 3 h, whereupon the suspension was filtered through a pad of Celite, and washed with methanol. The crude reaction mixture was concentrated *in vacuo* to give crude **2.47** as a cloudy oil. The crude material was purified via silica gel flash column chromatography eluting with CH_2Cl_2 : methanol (1 : 0 → 19 : 1 along a gradient) to give 98 mg (63%) of **2.47** as an oil: ^{1}H NMR (400 MHz) δ 7.11 – 7. 05 (comp, 2 H), 6.97 –

6.91 (comp, 2 H), 6.64 (s, 1 H), 6.04 (brs, 1 H), 4.20 (d, *J* = 11.6, 1 H), 3.87 (s, 3 H), 3.50 (d, *J* = 5.6 Hz, 2 H), 3.43 (s, 3 H), 3.25 -3.21 (m, 1 H), 3.10 – 3.05 (m, 1 H), 2.82 – 2.71 (comp, 2 H), 1.83 – 1.75 (comp, 2 H), 1.31 – 1.21 (comp, 3 H), 1.12 (app dd, *J* = 7.2, 1.2 Hz, 18 H).

NMR Assignment. ^{1}H NMR (400 MHz) δ 7.11 – 7. 05 (comp, 2 H, C7-H), 6.97 – 6.91 (comp, 2 H, C8-H), 6.64 (s, 1 H, C6-H), 6.04 (brs, 1 H, NH), 4.20 (d, *J* = 11.6, 1 H, C3-H), 3.87 (s, 3 H, OCH_3), 3.50 (d, *J* = 5.6 Hz, 2 H, C1-H), 3.43 (s, 3 H, OCH_3), 3.25 -3.21 (m, 1 H, C4-H), 3.10 – 3.05 (m, 1 H, C4-H), 2.82 – 2.71 (comp, 2 H, C5-H), 1.83 – 1.75 (comp, 2 H, C2-H), 1.31 – 1.21 (comp, 3 H, TIPS), 1.12 (app dd, *J* = 7.2, 1.2 Hz, 18 H, TIPS).

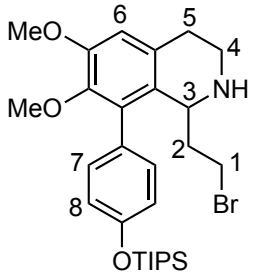

2.48

1-(2-Bromoethyl)-6,7-dimethoxy-8-(4-((triisopropylsilyl)oxy)phenyl)-1,2,3,4-tetrahydroisoquinoline (2.48). ARMIII99. Phosphorus tribromide (418 mg, 1.50 mmol) was added dropwise to a solution of **2.47** (75 mg, 0.15 mmol) in toluene (7.5 mL), and the reaction was heated under reflux for 3 h. The reaction was cooled to room temperature, followed by careful addition of methanol (1 mL) and water (2 mL). The

mixture was diluted with water (20 mL), and extracted with ether (3 x 20 mL). The combined organic fractions were successively washed with saturated aqueous $NaHCO_3$ (30 mL), water (30 mL), and brine (30 mL). The solution was dried (Na_2SO_4), filtered, and concentrated *in vacuo* to give crude **2.48** as an oil. The crude material was purified via silica gel flash column chromatography eluting with CH_2Cl_2 : methanol (1 : 0 → 19 : 1 along a gradient) to give 85 mg (quant.) of **2.48** as an oil: ^{1}H NMR (400 MHz) δ 7.01 (dd, *J* = 8.2, 2.0 Hz, 1 H), 6.91 – 6.85 (comp, 3 H), 6.68 (s, 1 H), 5.47 (q, *J* = 8.4 Hz, 1 H), 4.34 (pent, *J* = 8.4 Hz, 1 H), 3.84 (s, 3 H), 3.51 – 3.47 (m, 1 H), 3.40 (s, 3 H), 3.36 – 3.24 (comp, 2 H), 3.15 – 3.12 (comp, 2 H), 2.98 – 2.91 (m, 1 H), 2.25 – 2.14 (m, 1 H), 2.08 – 2.02 (m, 1 H), 1.23 (sept, *J* = 7.2 Hz, 3 H), 1.06 (d, *J* = 7.2 Hz, 18 H).

NMR Assignment. ^{1}H NMR (400 MHz) δ 7.01 (dd, *J* = 8.2, 2.0 Hz, 1 H, C7-H), 6.91 – 6.85 (comp, 3 H, C7-H and C8-H), 6.68 (s, 1 H, C6-H), 5.47 (q, *J* = 8.4 Hz, 1 H, C3-H), 4.34 (pent, *J* = 8.4 Hz, 1 H, NH), 3.84 (s, 3 H, OCH_3), 3.51 – 3.47 (m, 1 H, C4-H), 3.40 (s, 3 H, OCH_3), 3.36 – 3.24 (comp, 2 H, C4-H and C1-H), 3.15 – 3.12 (comp, 2 H, C1-H and C5-H), 2.98 – 2.91 (m, 1 H, C5-H), 2.25 – 2.14 (m, 1 H, C2-H), 2.08 – 2.02 (m, 1 H, C2-H), 1.23 (sept, *J* = 7.2 Hz, 3 H, TIPS), 1.06 (d, *J* = 7.2 Hz, 18 H, TIPS).

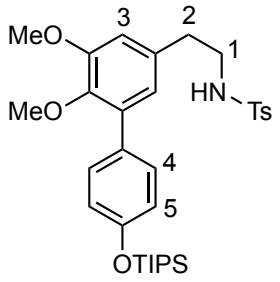

2.44

***N*-(2-(5,6-Dimethoxy-4'-((triisopropylsilyl)oxy)-[1,1'-biphenyl]-3-yl)ethyl)-4-methylbenzenesulfonamide (2.44). ARMVIII97.** A solution of **2.20** (0.687 g, 1.6 mmol), TsCl (0.366 g, 1.9 mmol), and TBAI (spatula tip), in THF (5 mL) and H_2O (15 mL) was stirred for 6 h at room temperature. The mixture was extracted with ethyl acetate (3 x 20 mL). The combined organic fractions were washed with brine (30 mL), dried (Na_2SO_4), and concentrated *in vacuo* to give crude **2.44** as an amorphous solid. The crude material was purified via silica gel flash column chromatography eluting with hexanes : ethyl acetate (19 : 1 → 9 : 1 along a gradient) to give 0.751 g (80%) of **2.44** as an off white solid: M.p. 99-100 ºC. IR (thin film) 2944, 2866, 1512, 1262. ^{1}H NMR (400 MHz) δ 7.68 (d, *J* = 8.4 Hz, 2 H), 7.36 (d, *J* = 8.4 Hz, 2 H), 7.26 (d, *J* = 8.0 Hz, 2 H), 6.91 (d, *J* = 8.8 Hz, 2 H), 6.59 (d, *J* = 4.8 Hz, 2 H), 4.39 (t, *J* = 6.0 Hz, 1 H), 3.84 (s, 3 H), 3.51 (s, 3 H), 3.24 (q, *J* = 6.8 Hz, 2 H), 2.74 (t, *J* = 6.8 Hz, 2 H), 2.41 (s, 3 H), 1.27 (sept, *J* = 6.8 Hz, 3 H), 1.13 (d, *J* = 6.8Hz, 18 H). ^{13}C NMR (100 MHz) δ 155.5, 153.2, 145.3, 143.4, 136.9, 135.7, 133.2, 130.5, 130.2, 129.7, 127.1, 122.4, 119.6, 111.3, 60.3, 55.9, 44.1, 35.6, 21.5, 17.9, 12.7. HRMS calculated for $C_{32}H_{45}NO_5SSi$ $(M)^+$ 583.2788 found 583.2795.

NMR Assignment. ^{1}H NMR (400 MHz) δ 7.68 (d, *J* = 8.4 Hz, 2 H, NTs), 7.36 (d, *J* = 8.4 Hz, 2 H, NTs), 7.26 (d, *J* = 8.8 Hz, 2 H, C4-H), 6.91 (d, *J* = 8.8 Hz, 2 H, C5-H), 6.59 (app d, *J* = 4.8 Hz, 2 H, C3-H and C4-H), 4.39 (t, *J* = 6.0 Hz, 1 H, NH), 3.84 (s, 3 H, OCH_3), 3.51 (s, 3 H, OCH_3), 3.24 (q, *J* = 6.8 Hz, 2 H, C1-H), 2.74 (t, *J* = 6.8 Hz, 2 H, C2-H), 2.41 (s, 3 H, NTs), 1.27 (sept, *J* = 6.8 Hz, 3 H, TIPS), 1.13 (d, *J* = 6.8Hz, 18 H, TIPS).

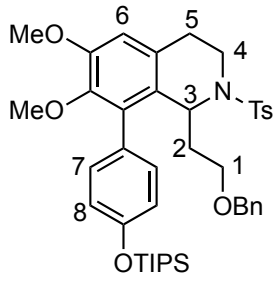

2.51

1-(2-(Benzyloxy)ethyl)-6,7-dimethoxy-2-tosyl-8-(4-((triisopropylsilyl)oxy)phenyl)-1,2,3,4-tetrahydroisoquinoline (2.51). ARM107. A solution of **2.44** (0.732 g, 1.25 mmol), **2.46** (0.395 g, 1.88 mmol), and TFA (0.14 mL, 1.88 mmol), in TFE (15 mL) was heated to 60 ºC for 24 h. The reaction was cooled to room temperature, and concentrated *in vacuo* to give crude **2.51**. The crude mixture was purified via silica gel flash column chromatography eluting with hexanes : ethyl acetate (19: 1 → 9 : 1 along a gradient) to 0.794 g (87%) of **2.51** as a clear viscous oil: IR (thin film) 2944, 2866, 1511, 1464, 1262 cm^{-1}. ^{1}H NMR (400 MHz) δ 7.60 (d, *J* = 8.0 Hz, 2 H), 7.32 - 6.95 (comp, 11 H), 6.51 (s, 1 H), 4.87 (dd, *J* = 10.4, 4.0 Hz, 1 H), 4.22 (s, 2 H),

3.89 - 3.80 (comp, 4 H), 3.61 - 3.53 (m, 1 H), 3.42 (s, 3 H), 3.26 (td, *J* = 9.2, 5.2 Hz, 1 H), 3.15 - 3.04 (m, 1 H), 2.95 - 2.81 (m, 1 H), 2.70 (dt, *J* = 16.8, 4.4 Hz, 1 H), 2.34 (s, 3 H), 1.85 – 1.69 (comp, 2 H), 1.30 (sept, *J* = 7.6 Hz, 3 H), 1.14 (d, *J* = 7.6 Hz, 18 H). ^{13}C NMR (100 MHz) δ 155.4, 151.4, 145.3, 143.0, 138.5, 137.3, 134.2, 131.8, 130.2, 129.2, 128.8, 128.2, 127.4, 127.3,120.1, 120.0, 111.7, 72.6, 67.7, 60.4, 55.7, 51.2, 38.8, 35.2, 27.0, 21.5, 17.9, 12.6. HRMS calculated for $C_{42}H_{55}NO_6SSi$ $(M+Na)^+$ 752.34120 found 752.33890.

NMR Assignment. ^{1}H NMR (400 MHz) δ 7.60 (d, *J* = 8.0 Hz, 2 H, NTs), 7.32 - 6.95 (comp, 11 H, OBn, NTs, C7-H, C8-H), 6.51 (s, 1 H, C6-H), 4.87 (dd, *J* = 10.4, 4.0 Hz, 1 H, C3-H), 4.22 (s, 2 H, OBn), 3.89 - 3.80 (comp, 4 H, OCH_3 and C1-H), 3.61 - 3.53 (m, 1 H, C1-H), 3.42 (s, 3 H, OCH_3), 3.26 (td, *J* = 9.2, 5.2 Hz, 1 H, C4-H), 3.15 - 3.04 (m, 1 H, C4-H), 2.95 - 2.81 (m, 1 H, C5-H), 2.70 (dt, *J* = 16.8, 4.4 Hz, 1 H, C5-H), 2.34 (s, 3 H, NTs), 1.85 – 1.69 (comp, 2 H, C2-H), 1.30 (sept, *J* = 7.6 Hz, 3 H, TIPS), 1.14 (d, *J* = 7.6 Hz, 18 H, TIPS).

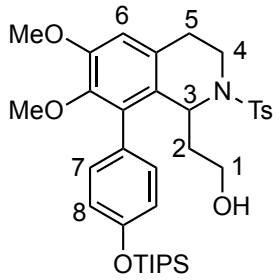

2.52

2-(6,7-Dimethoxy-2-tosyl-8-(4-((triisopropylsilyl)oxy)phenyl)-1,2,3,4-tetrahydroisoquinolin-1-yl)ethanol (2.52). ARMIII105. A suspension of **2.51** (0.396 g, 0.54 mmol), ammonium formate (0.171 g, 2.71 mmol) and Pd/C (10% w/w, 0.30 g) in methanol (20 mL) was heated to 50 ºC for 6 h. The suspension was filtered through a pad of Celite, washed with copious amounts of methanol, and concentrated *in vacuo* to give crude **2.52**. The crude material was purified via silica gel flash column chromatography eluting with hexanes : ethyl acetate (19 : 1 → 3 : 1 along a gradient) to give 0.287 g (83%) of **2.52** as a white solid. Recrystallization from methanol afforded white crystals: M.p. 105-107 ºC. IR (thin film) 3545, 2944, 2866, 2361, 2340, 1606, 1511, 1464, 1261 cm^{-1}. ^{1}H NMR (400 MHz) δ 7.53 (d, *J* = 7.6 Hz, 2 H), 7.18 (d, *J* = 8.2 Hz, 2 H), 7.12 (d, *J* = 7.6 Hz, 1 H), 6.99 (d, *J* = 8.2 Hz, 2 H), 6.86 (d, *J* = 7.2 Hz, 1 H), 6.53 (s, 1 H), 4.83 (dd, *J* = 8.4, 8 Hz, 1 H), 3.81 (s, 3 H), 3.62 – 3.50 (comp, 3 H), 3.47 - 3.41 (comp, 4 H), 2.70 - 2.78 (comp, 2 H), 2.37 (s, 3 H), 2.19 (t, *J* = 7.6 Hz, 1 H), 1.68 – 1.60 (comp, 2 H), 1.31 (sept, *J* = 7.6 Hz, 3 H), 1.14 (d, *J* = 7.6 Hz, 18 H). ^{13}C NMR (100 MHz) δ 155.6, 151.5, 145.4, 143.3, 136.3, 134.2, 131.4, 130.4, 129.4, 129.2, 128.3, 127.7, 127.3, 120.1,

119.9, 111.5, 60.5, 59.0, 55.7, 51.1, 40.5, 39.0, 27.3, 21.5, 17.9, 12.6. HRMS calculated for $C_{35}H_{49}NO_6SSi$ $(M+H)^+$ 640.3128 found 640.3107.

NMR Assignment. ^{1}H NMR (400 MHz) δ 7.53 (d, *J* = 7.6 Hz, 2 H, C7-H), 7.18 (d, *J* = 8.2 Hz, 2 H, NTs), 7.12 (d, *J* = 7.6 Hz, 1 H, C8-H), 6.99 (d, *J* = 8.2 Hz, 2 H, NTs), 6.86 (d, *J* = 7.6 Hz, 1 H, C8-H), 6.53 (s, 1 H, C6-H), 4.83 (dd, *J* = 8.4, 8 Hz, 1 H, C3-H), 3.81 (s, 3 H, OCH_3), 3.62 – 3.50 (comp, 3 H, C1-H and C4-H), 3.47 - 3.41 (comp, 4 H, OCH_3 and C4-H), 2.70 - 2.78 (comp, 2 H, C5-H), 2.37 (s, 3 H, NTs), 2.19 (t, *J* = 7.6 Hz, 1 H, OH), 1.68 – 1.60 (comp, 2 H, C2-H), 1.31 (sept, *J* = 7.6 Hz, 3 H, TIPS), 1.14 (d, *J* = 7.6 Hz, 18 H, TIPS).

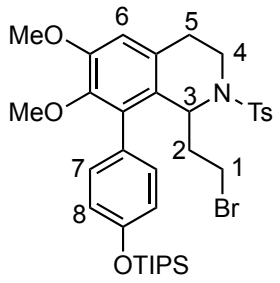

2.57

1-(2-Bromoethyl)-6,7-dimethoxy-2-tosyl-8-(4-((triisopropylsilyl)oxy)phenyl)-1,2,3,4-tetrahydroisoquinoline (2.57). ARMIV43. Triphenylphosphine (0.50 g, 1.92 mmol) was added to a solution of **2.52** (0.61 g, 0.96 mmol) and CBr_4 (0.64 g, 1.92 mmol) in CH_2Cl_2 (25 mL) at 0 ºC. The reaction was stirred for 15 min at 0 ºC, whereupon the cold bath was removed and the reaction stirred for 3 h at room temperature. The mixture was diluted with ether (100 mL), filtered, and concentrated *in vacuo* to give crude **2.57**.

The crude material was purified via silica gel flash column chromatography eluting with hexanes : ethyl acetate (9 : 1) to give 0.641 g (95%) of **2.57** as a white solid. The pure material was recrystallized from methanol to give white crystals: M.p. 112-113 ºC. IR (thin film) 2944, 2866, 1512, 1463, 1262 cm^{-1}. ^{1}H NMR (400 MHz) δ 7.62 (d, *J* = 8.0 Hz, 2 H), 7.19 (d, *J* = 8.0 Hz, 2 H), 7.15 - 7.05 (m, 1 H), 7.01 - 6.98 (comp, 3 H), 6.49 (s, 1 H), 4.80 (dd, *J* = 10.4, 3.2 Hz, 1 H), 3.81 – 3.74 (comp, 4 H), 3.48 (ddd, *J* = 15.6, 10.0, 5.6 Hz, 1 H), 3.42 (s, 3 H), 3.14 (td, *J* = 10.0, 4.4 Hz, 1 H), 2.90 - 2.77 (comp, 2 H), 2.67 (dt, *J* = 16.4, 5.2 Hz, 1 H), 2.37 (s, 3 H), 2.02 – 1.94 (m, 1 H), 1.87 – 1.79 (m, 1 H), 1.30 (sept, *J* = 6.8 Hz, 3 H), 1.14 (d, *J* = 6.8 Hz, 18 H). ^{13}C NMR (100 MHz) δ 155.5, 151.7, 145.4, 143.3, 137.0, 134.3, 131.6, 130.1, 129.4, 128.8, 127.7, 127.3, 127.1, 120.3, 120.0, 111.7, 105.0, 60.5, 55.7, 52.9, 39.0, 28.8, 27.0, 21.5, 17.9, 12.7. HRMS calculated for $C_{35}H_{48}BrNO_5SSi$ 724.20980 and 726.20840 found 724.20680 and 726.20690.

NMR Assignment. ^{1}H NMR (400 MHz) δ 7.62 (d, *J* = 8.0 Hz, 2 H, NTs), 7.19 (d, *J* = 8.0 Hz, 2 H, NTs), 7.15 - 7.05 (m, 1 H, C7-H), 7.01 - 6.98 (comp, 3 H, C7-H and C8-H), 6.49 (s, 1 H, C6-H), 4.80 (dd, *J* = 10.4, 3.2 Hz, 1 H, C3-H), 3.81 – 3.74 (comp, 4 H, OCH_3 and C4-H), 3.48 (ddd, *J* = 15.6, 10.0, 5.6 Hz, 1 H, C4-H), 3.42 (s, 3 H, OCH_3), 3.14 (td, *J* = 10.0, 4.4 Hz, 1 H, C1-H), 2.90 - 2.77 (comp, 2 H, C1-H and C5-H), 2.67 (dt, *J* = 16.4, 5.2 Hz, 1 H, C5-H), 2.37 (s, 3 H, NTs), 2.02 – 1.94 (m, 1 H, C2-H), 1.87 – 1.79 (m, 1 H, C2-H), 1.30 (sept, *J* = 6.8 Hz, 3 H, TIPS), 1.14 (d, *J* = 6.8 Hz, 18 H, TIPS).

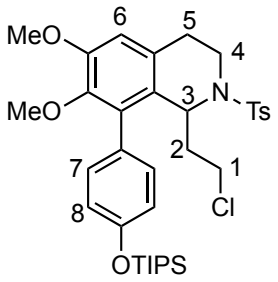

2.58

1-(2-Chloroethyl)-6,7-dimethoxy-2-tosyl-8-(4-((triisopropylsilyl)oxy)phenyl)-1,2,3,4-tetrahydroisoquinoline (2.58). ARMIV97. Triphenylphosphine (0.128 g, 0.49 mmol) was added to a solution of **2.52** (0.104 g, 0.16 mmol) and CCl_4 (0.075 g, 0.49 mmol) in CH_2Cl_2 (5 mL) at 0 ºC, and stirred for 15 min. The reaction was warmed to room temperature and stirred for an additional 5 h. The mixture was diluted with ether (30 mL), filtered, and concentrated *in vacuo* to give crude **2.58**. The crude material was purified via silica gel flash column chromatography eluting with hexanes : ethyl acetate (9 : 1) to give 0.088 g (83%) of **2.58** as a white solid. The purified material can be recrystallized from methanol to give white crystals: M.p. 115-118 ºC. IR (thin film) 2944, 2867, 1606, 1511, 1464, 1339,1263 cm^{-1}. ^1H NMR (400 MHz) δ 7.55 (d, *J* = 8.4 Hz, 2 H), 7.24 (d, *J* = 7.2 Hz, 1 H), 7.19 (d, *J* = 8.0 Hz, 2 H), 7.10 (d, *J* = 9.2 Hz, 1 H), 7.01 – 6.92 (comp, 2 H), 6.50 (s, 1 H), 4.77 (dd, *J* = 10.4, 3.2 Hz, 1 H), 3.73 (comp, 4 H), 3.49 (ddd, *J* = 15.2, 10.0, 5.6 Hz, 1 H), 3.42 (s, 3 H), 3.27 (ddd, *J* = 10.8, 9.6, 4.8 Hz, 1 H), 2.96 – 2.89 (m, 1 H), 2.82 – 2.74 (m, 1 H), 2.68 (dt, *J* = 15.2, 4.0 Hz, 1 H), 2.30 (s, 3 H), 1.92 – 1.85 (m, 1 H), 1.78 – 1.69 (m, 1 H), 1.31 (sept, *J* = 7.6 Hz, 3 H), 1.14 (d, *J* = 7.6 Hz, 18 Hz). ^{13}C NMR (100 MHz) δ 155.5, 151.6, 145.4, 143.3, 137.0, 134.3, 131.6,

130.1, 129.4, 128.8, 127.7, 127.3, 127.2, 120.2, 120.0, 111.7, 60.5, 55.7, 51.8, 41.0, 39.0, 38.5, 27.0, 21.5, 17.9, 12.7. HRMS calculated for $C_{35}H_{48}ClNO_5SSi$ $(M+Na)^+$ 680.26030 found 680.25790.

NMR Assignment. ^{1}H NMR (400 MHz) δ 7.55 (d, *J* = 8.4 Hz, 2 H, NTs), 7.24 (d, *J* = 7.2 Hz, 1 H, C7-H), 7.19 (d, *J* = 8.4 Hz, 2 H, NTs), 7.10 (d, *J* = 7.2 Hz, 1 H, C7-H), 7.01 – 6.92 (comp, 2 H, C8-H), 6.50 (s, 1 H, C6-H), 4.77 (dd, *J* = 10.4, 3.2 Hz, 1 H, C3-H), 3.73 (comp, 4 H, OCH_3 and C4-H), 3.49 (ddd, *J* = 15.2, 10.0, 5.6 Hz, 1 H, C4-H), 3.42 (s, 3 H, OCH_3), 3.27 (ddd, *J* = 10.8, 9.6, 4.8 Hz, 1 H, C1-H), 2.96 – 2.89 (m, 1 H, C1-H), 2.82 – 2.74 (m, 1 H, C5-H), 2.68 (dt, *J* = 15.2, 4.0 Hz, 1 H, C5-H), 2.30 (s, 3 H, NTs), 1.92 – 1.85 (m, 1 H, C2-H), 1.78 – 1.69 (m, 1 H, C2-H), 1.31 (sept, *J* = 7.6 Hz, 3 H, TIPS), 1.14 (d, *J* = 7.6 Hz, 18 Hz, TIPS).

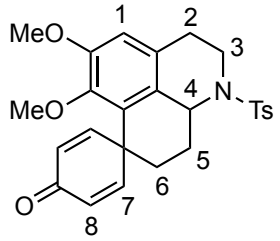

2.54

5,6-Dimethoxy-1-tosyl-1,2,3,8,9,9a-hexahydrospiro[benzo[*de*]quinoline-7,1'-cyclohexa[2,5]dien]-4'-one (2.54). ARMIV53. A solution of **2.57** (50 mg, 0.071 mmol) in NMP (14 mL) was added dropwise over 10 min via cannula, to flame-dried CsF (32 mg, 0.31 mmol) at 100 ºC. The resulting suspension was stirred for 2 h at 100 ºC. The

reaction was cooled to room temperature, diluted with water (30 mL), and extracted with toluene (4 x 30 mL). The combined organic fractions were washed with water (30 mL), brine (30 mL), dried ($MgSO_4$), and concentrated *in vacuo* to give crude **2.54**. The crude material was purified via silica gel flash column chromatography eluting with hexanes : ethyl acetate (4 : 1) to give 26 mg (79%) of **2.54** as a white solid. Crystals suitable for x-ray diffraction were grown via slow diffusion of hexanes into ethyl acetate: M.p. 174-175 ºC. IR (thin film) 2939, 2360, 2340, 1659, 1620, 1597, 1477, 1337, 1316. ^{1}H NMR (400 MHz) δ 7.75 (d, *J* = 8.0 Hz, 2 H), 7.31 (d, *J* = 8.0 Hz, 2 H), 7.02 (dd, *J* = 10.0, 3.2 Hz, 1 H), 6.92 (dd, *J* = 10.0, 3.2 Hz, 2 H), 6.52 (s, 1 H), 6.32 (dd, *J* = 10.0, 2.0 Hz, 1 H), 6.22 (dd, *J* = 10.0, 2.0 Hz, 1 H), 4.50 (dd, *J* = 11.6, 4.0 Hz, 1 H), 3.97 (dt, *J* = 13.6, 4.0 Hz, 1 H), 3.76 (s, 3 H), 3.58 (s, 3 H), 3.15 (ddd, *J* = 14.0, 11.6, 2.8 Hz, 1 H), 2.59 (dq, *J* = 12.8, 3.2 Hz, 1 H), 2.48 (dt, *J* = 15.6, 2.8 Hz, 1 H), 2.42 (s, 3 H), 2.33 (ddd, *J* = 15.2, 11.2, 4.0 Hz, 1 H), 2.20 (td, *J* = 14.0, 2.8 Hz, 1 H), 1.99 – 1.83 (m, 1 H), 1.79 (ddd, *J* = 14.0, 4.4, 2.8 Hz, 1 H). ^{13}C NMR (100 MHz) δ 186.0, 156.5, 153.5, 151.4, 143.6, 137.5, 131.4, 129.9, 129.1, 127.2, 126.4, 126.3, 124.4, 112.1, 105.0, 60.9, 55.6, 54.8, 43.7, 42.7, 35.7, 30.2, 29.3, 21.5. HRMS calculated $C_{26}H_{27}NO_5S$ $(M+H)^+$ 466.1688 found 466.1685.

NMR Assignment. ^{1}H NMR (400 MHz) δ 7.75 (d, *J* = 8.0 Hz, 2 H, NTs), 7.31 (d, *J* = 8.0 Hz, 2 H, NTs), 7.02 (dd, *J* = 10.0, 3.2 Hz, 1 H, C6-H), 6.92 (dd, *J* = 10.0, 3.2 Hz, 2 H, C6-H), 6.52 (s, 1 H, C1-H), 6.32 (dd, *J* = 10.0, 2.0 Hz, 1 H, C8-H), 6.22 (dd, *J* = 10.0, 2.0 Hz, 1 H, C8-H), 4.50 (dd, *J* = 11.6, 4.0 Hz, 1 H, C4-H), 3.97 (dt, *J* = 13.6, 4.0 Hz, 1 H, C3-H), 3.76 (s, 3 H, OCH_3), 3.58 (s, 3 H, OCH_3), 3.15 (ddd, *J* = 14.0, 11.6, 2.8

Hz, 1 H, C3-H), 2.59 (dq, *J* = 12.8, 3.2 Hz, 1 H, C2-H), 2.48 (dt, *J* = 15.6, 2.8 Hz, 1 H, C2-H), 2.42 (s, 3 H, NTs), 2.33 (ddd, *J* = 15.2, 11.2, 4.0 Hz, 1 H, C5-H), 2.20 (td, *J* = 14.0, 2.8 Hz, 1 H, C5-H), 1.99 – 1.83 (m, 1 H, C6-H), 1.79 (ddd, *J* = 14.0, 4.4, 2.8 Hz, 1 H, C6-H).

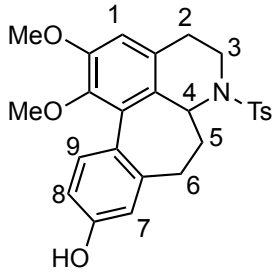

2.55

10,11-Dimethoxy-3-tosyl-1,2,3,3a,4,5-hexahydrobenzo[6,7]cyclohepta[1,2,3-*ij*]isoquinolin-7-ol (2.55). ARMIV87. Concentrated HCl (10 mL) was added dropwise to a solution of **2.54** (192 mg, 0.41 mmol) in glacial acetic acid (200 mL) at room temperature. The solution was heated to 50 ºC for 18 h, whereupon the reaction was cooled to room temperature, and the majority of solvent was removed *in vacuo* at 40 ºC (water bath). The resulting residue was diluted with CH_2Cl_2 (300 mL), and washed with water (2 x 200 mL), saturated aqueous $NaHCO_3$ (200 mL), brine (200 mL), dried ($MgSO_4$), and concentrated *in vacuo* to give crude **2.55**. The crude material was purified via silica gel flash column chromatography eluting with hexanes : ethyl acetate (9 : 1 → 82 : 18 along a gradient) to afford 152 mg (79%) of **2.55** as a white solid. Recrystallization by slow evaporation of methanol afforded x-ray quality crystals: M.p.

160 ºC. IR (thin film) 3418, 2937, 1597, 1452, 1245. ^{1}H NMR (400 MHz) δ 7.48 (d, *J* = 8.0 Hz, 2 H), 7.36 (d, *J* = 8.4 Hz, 1 H), 7.10 (d, *J* = 8.0 Hz, 2 H), 6.79 (dd, *J* = 8.4, 2.6 Hz, 1 H), 6.74 (d, *J* = 2.6 Hz, 1 H), 6.46 (s, 1 H), 5.12 (brs, 1 H), 4.58 (dd, *J* = 10.4, 6.4 Hz, 1 H), 3.95 (dd, *J* = 14.0, 6.4 Hz, 1 H), 3.82 (s, 3 H), 3.42 – 3.36 (comp, 4 H), 2.66 (td, *J* = 12.0, 6.8 Hz, 1 H), 2.56 (dd, *J* = 16.8, 3.6 Hz, 1 H), 2.45 – 2.40 (m, 1 H), 2.31-2.19 (comp, 5 H), 2.15 – 2.03 (m, 1 H). ^{13}C NMR (100 MHz) 155.4, 151.7, 144.2, 142.9, 140.3, 137.9, 131.7, 131.7, 129.3, 127.7, 126.8, 126.4, 125.6, 114.9, 113.4, 111.1, 60.3, 55.8, 52.4, 38.6, 37.7, 30.5, 27.5, 21.4. HRMS calculated for $C_{26}H_{27}NO_5S$ $(M+Na)^+$ 488.15020 found 488.14

NMR Assignment. ^{1}H NMR (400 MHz) δ 7.48 (d, *J* = 8.0 Hz, 2 H, NTs), 7.36 (d, *J* = 8.4 Hz, 1 H, C9-H), 7.10 (d, *J* = 8.0 Hz, 2 H, NTs), 6.79 (dd, *J* = 8.4, 2.6 Hz, 1 H, C8-H), 6.74 (d, *J* = 2.6 Hz, 1 H, C7-H), 6.46 (s, 1 H, C1-H), 5.12 (brs, 1 H, OH), 4.58 (dd, *J* = 10.4, 6.4 Hz, 1 H, C4-H), 3.95 (dd, *J* = 14.0, 6.4 Hz, 1 H, C3-H), 3.82 (s, 3 H, OCH_3), 3.42 – 3.36 (comp, 4 H, OCH_3 and C3-H), 2.66 (td, *J* = 12.0, 6.8 Hz, 1 H, C2-H), 2.56 (dd, *J* = 16.8, 3.6 Hz, 1 H, C2-H), 2.45 – 2.40 (m, 1 H, C5-H), 2.31- 2.19 (comp, 5 H, OCH_3, C5-H, and C6-H), 2.15 – 2.03 (m, 1 H, C6-H).

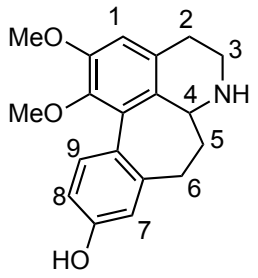

2.1

10,11-Dimethoxy-1,2,3,3a,4,5-hexahydrobenzo[6,7]cyclohepta[1,2,3-*ij*]isoquinolin-7-ol (2.1). ARMIV105. Sodium naphthalide was prepared by the addition of sodium metal (64 mg, 2.81 mmol), portionwise over 10 min, to a solution of naphthalene (458 mg, 3.58 mmol) in dry DME (2.5 mL), and stirring for 1 h at room temperature. The sodium naphthalide solution was added dropwise to a solution of **2.55** (119 mg, 0.26 mmol) in DME (10.4 mL) at -50 ºC, until a green color persisted. Water (1 mL) was added to the reaction, and the mixture was diluted with aqueous HCl (1 M, 80 mL), washed with ether (2 x 40 mL), and neutralized with solid $NaHCO_3$. The neutral aqueous solution was extracted with ether (4 x 100 mL), and the combined organic fractions were washed with brine (100 mL), dried ($MgSO_4$), and concentrated *in vacuo* to give crude **2.1**. The crude material was purified via silica gel flash column chromatography eluting with CH_2Cl_2 : acetone : methanol (5 : 4 : 1) to afford 46 mg (58%) of **2.1** as a white solid. Homoaporphine **2.1** is not bench-top stable, turning brown within hours, and must be stored in a freezer: M.p. 189-191 ºC. IR (thin film) 2917, 2849, 1454, 1427, 1243 cm^{-1}. ^1H NMR (400 MHz, CD_3OD) δ 7.20 (d, J = 9.2 Hz, 1 H), 6.76 (s, 1 H), 6.70 – 6.62 (comp, 2 H), 3.86 (s, 3 H), 3.53 (dd, J = 11.2, 6.8 Hz, 1 H), 3.41 (s, 3

H), 3.16 (td, *J* = 12.0, 4.4 Hz, 1 H), 3.00 (dd, *J* = 13.2, 6.4 Hz, 1 H), 2.88 (ddd, *J* = 17.6, 12.0, 6.4 Hz, 1 H), 2.74 (dd, *J* = 16.4, 2.4 Hz, 1 H), 2.48 (dd, *J* = 12.8, 6.0 Hz, 1 H), 2.35 (td, *J* = 12.8, 7.2 Hz, 1 H), 2.25 – 2.18 (m, 1 H), 2.11 – 2.01 (m, 1 H). ^{13}C NMR (125 MHz, $(CD_3)_2SO$) δ 156.5, 150.8, 143.3, 140.6, 131.2, 130.9, 129.7, 128.7, 125.4, 114.3, 112.5, 111.8, 59.7, 55.5, 50.2, 37.4, 30.5, 29.1. HRMS calculated for $C_{19}H_{21}NO_3$ $(M+H)^+$ 312.15940 found 312.15950.

NMR Assignment. ^{1}H NMR (400 MHz, CD_3OD) δ 7.20 (d, *J* = 9.2 Hz, 1 H, C9-H), 6.76 (s, 1 H, C1-H), 6.70 – 6.62 (comp, 2 H, C8-H and C7-H), 3.86 (s, 3 H, OCH_3), 3.53 (dd, *J* = 11.2, 6.8 Hz, 1 H, C4-H), 3.41 (s, 3 H, OCH_3), 3.16 (td, *J* = 12.0, 4.4 Hz, 1 H, C3-H), 3.00 (dd, *J* = 13.2, 6.4 Hz, 1 H, C3-H), 2.88 (ddd, *J* = 17.6, 12.0, 6.4 Hz, 1 H, C2-H), 2.74 (dd, *J* = 16.4, 2.4 Hz, 1 H, C2-H), 2.48 (dd, *J* = 12.8, 6.0 Hz, 1 H, C5-H), 2.35 (td, *J* = 12.8, 7.2 Hz, 1 H, C5-H), 2.25 – 2.18 (m, 1 H, C6-H), 2.11 – 2.01 (m, 1 H, C6-H).

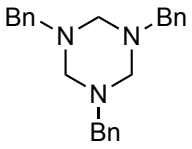

4.15

1,3,5-Tribenzyl-1,3,5-triazinane (4.11). Prepared according to previous literature reports.[311,312]

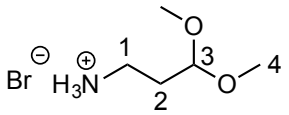

4.18

3,3-Dimethoxypropan-1-ammonium bromide (4.18). ARMV93. 3-Bromopropionaldehyde dimethyl acetal (1.34 g, 7.33 mmol) was added to a solution of methanolic ammonia (7 N, 100 mL) in a glass pressure vessel. The vessel was sealed and the reaction was heated at 85 ºC overnight. The reaction was cooled to room temperature, the pressure was carefully released, and the solvent was removed *in vacuo* to give 1.42 g (98%) of **4.18** as a white crystalline solid that formed an orange gum upon exposure to air; ^{1}H NMR (400 MHz, CD_3CN) δ 4.54 (t, J = 5.2 Hz, 1 H), 3.36 (s, 6 H), 3.05 (t, J = 5.2 Hz, 2 H), 2.41 (brs, 3 H), 2.04 (q, J = 5.2 Hz, 2 H); ^{13}C NMR (100 MHz, CD_3CN) δ 104.3, 54.5, 36.7, 30.4; IR (thin film) 2915, 2025, 1628 cm^{-1}; HRMS (ESI) *m/z* calcd for $C_5H_{13}NO_2$ $(M+1)^+$, 120.1019; found, 120.1018

NMR Assignments. ^{1}H NMR (400 MHz, CD_3OD) δ 4.54 (t, J = 5.2 Hz, 1 H, C3-H), 3.36 (s, 6 H, C4-H), 3.05 (t, J = 5.2 Hz, 2 H, C1-H), 2.41 (brs, 3 H, N-H), 2.04 (q, J = 5.2 Hz, 2 H, C2-H)

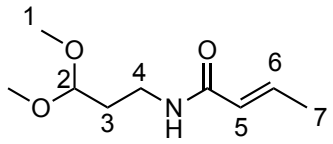

4.19

(*E*)-*N*-(3,3-Dimethoxypropyl)but-2-enamide (4.19). ARMV65. A solution of crotonoyl chloride (709 mg, 2.0 mmol) in pyridine (5 mL) was added dropwise over 10 min to a solution of **4.18** (200 mg, 1.0 mmol) in pyridine (5 mL) at 0 ºC. The reaction was stirred for 3 h at 0 ºC, whereupon the solvent was removed *in vacuo* to give crude **4.19**. The crude material was purified via silica gel plug eluting with ether to give 125 mg (67%) of **4.19** as an oil: ^{1}H NMR (400 MHz) δ 6.78 (qd, *J* = 15.2, 6.8 Hz, 1 H), 6.14 (brs, 1 H), 5.75 (dq, *J* = 15.2, 1.6 Hz, 1 H), 4.41 (t, *J* = 5.2 Hz, 1 H), 3.36 (q, *J* = 5.2 Hz, 2 H), 3.32 (s, 6 H), 1.83 – 1.78 (comp, 5 H).

NMR Assignment. ^{1}H NMR (400 MHz) δ 6.78 (qd, *J* = 15.2, 6.8 Hz, 1 H, C6-H), 6.14 (brs, 1 H, NH), 5.75 (dq, *J* = 15.2, 1.6 Hz, 1 H, C5-H), 4.41 (t, *J* = 5.2 Hz, 1 H, C2-H), 3.36 (q, *J* = 5.2 Hz, 2 H, C4-H), 3.32 (s, 6 H, C1-H), 1.83 – 1.78 (comp, 5 H, C3-H and C7-H).

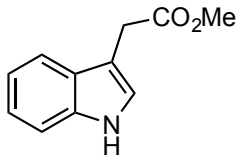

4.24

Methyl indole-3-ethanoate (4.24). Synthesized according to previous literature procedure.[313]

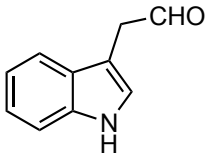

4.22

Indole-3-acetaldehyde (4.22). Synthesized according to previous literature procedure.[313]

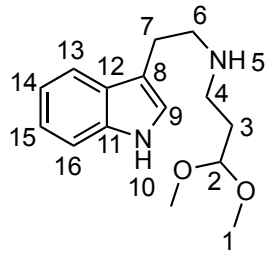

4.25

***N*-(2-(1*H*-Indol-3-yl)ethyl)-3,3-dimethoxypropan-1-amine (4.25). ARMV77**. Sodium cyanoborohydride (84 mg, 1.34 mmol) was added to a solution of **4.22** (170 mg, 1.07 mmol) and **4.18** (178 mg, 0.89 mmol) in methanol (5 mL). The reaction was stirred overnight at room temperature, whereupon the solvent was removed *in vacuo*, and the resulting residue was purified via silica gel flash column chromatography eluting with

CH_2Cl_2 : methanol (99 : 1 → 19 : 1 along a gradient) to give 208 mg (89%) of **4.25** as an off white oil: ^{1}H NMR (400 MHz) δ 8.61 (brs, 1 H), 7.57 (d, *J* = 7.2 Hz, 1 H), 7.42 (dt, *J* = 8.0, 1.2 Hz, 1 H), 7.27 – 7.20 (m, 1 H), 7.17 (dd, *J* = 8.0, 1.2 Hz, 1 H), 7.14 (ddd, *J* = 8.0, 7.2, 1.2 Hz, 1 H), 4.25 (t, *J* = 4.0 Hz, 1 H), 3.20 - 3.18 (comp, 4 H), 3.03 (t, *J* = 5.6 Hz, 2 H), 3.00 (s, 6 H), 1.88 (tt, *J* = 7.2, 4.0 Hz, 2 H). ^{13}C NMR (100 MHz) δ 134.0, 123.8, 121.5, 120.0, 117.4, 115.6, 109.2, 105.8, 101.3, 52.3, 45.6, 41.1, 25.8, 19.6. IR (neat) 3411, 2337, 2173, 1640, 1458 cm^{-1}; HRMS (CI) *m/z* calcd for $C_{15}H_{23}N_2O_2$ $(M+1)^+$, 263.1760; found, 263.1760.

NMR Assignment. ^{1}H NMR (400 MHz) δ 8.61 (brs, 1 H, N10-H), 7.57 (d, *J* = 7.2 Hz, 1 H, C13-H), 7.42 (dt, *J* = 8.0, 1.2 Hz, 1 H, C16-H), 7.27 – 7.20 (m, 1 H, C15-H), 7.17 (dd, *J* = 8.0, 1.2 Hz, 1 H, C14-H), 7.14 (ddd, *J* = 8.0, 7.2, 1.2 Hz, 1 H, C9-H), 4.25 (t, *J* = 4.0 Hz, 1 H, C2-H), 3.20-3.18 (comp, 4 H, C4-H and C6-H), 3.03 (t, *J* = 5.6 Hz, 2 H, C7-H), 3.00 (s, 6 H, C1-H), 1.88 (tt, *J* = 7.2, 4.0 Hz, 2 H, C3-H)

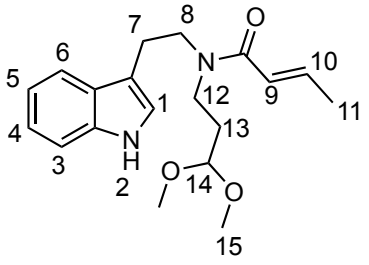

4.21

(*E*)-*N*-(2-(1*H*-Indol-3-yl)ethyl)-*N*-(3,3-dimethoxypropyl)but-2-enamide (4.21). ARMV95. A solution of crotonoyl chloride (51 mg, 0.48 mmol) in CH_2Cl_2 (1

mL) was added dropwise to a solution of triethylamine (82 mg, 0.81 mmol) and **4.25** (106 mg, 0.40 mmol) in CH_2Cl_2 (1 mL) at – 78 ºC. The reaction was stirred for 2 h at –78 ºC, whereupon saturated aqueous $NaHCO_3$ (5 mL) was added. The phases were separated, and the aqueous phase was extracted with CH_2Cl_2 (3 x 10 mL). The combined organic fractions were dried (Na_2SO_4), filtered, and the was solvent removed *in vacuo.* The resulting residue was purified via silica gel flash column chromatography eluting with CH_2Cl_2 : methanol (99 : 1 → 97 : 1 along a gradient) to give 94 mg (71%) of **4.21** as a clear oil: ^{1}H NMR (400 MHz) (1 : 1 rotamer mixture) δ 9.24 (brs, 0.5 H), 9.20 (brs, 0.5 H), 7.65 (d, *J* = 8.0 Hz, 0.5 H), 7.58 (d, *J* = 8.0 Hz, 0.5 H), 7.42 (d, *J* = 3.6 Hz, 0.5 H), 7.40 (d, *J* = 3.6 Hz, 0.5 H), 7.17 – 7.14 (comp, 1 H), 7.10 – 7.06 (comp, 2 H), 6.87 (dq, *J* = 14.8, 7.2 Hz, 0.5 H), 6.64 (dq, *J* = 14.8, 7.2 Hz, 0.5 H), 6.40 (dd, *J* = 14.8, 1.6 Hz, 0.5 H), 6.16 (dd, *J* = 14.8, 1.6 Hz, 0.5 H), 4.38 – 4.34 (comp, 1 H), 3.63 (t, *J* = 6.4 Hz, 1 H), 3.61 (t, *J* = 6.4 Hz, 1 H), 3.39 – 3.35 (comp, 2 H), 3.27 (s, 6 H), 3.00 (t, *J* = 8.0 Hz, 1 H), 2.98 (t, *J* = 8.0 Hz, 1 H), 1.99 (dd, *J* = 6.8, 1.6 Hz, 1.5 H), 1.83 – 1.79 (comp, 2 H), 1.69 (dd, *J* = 6.8, 1.6 Hz, 1.5 H); ^{13}C NMR (1:1 rotamer mixture) (100 MHz, CD_3CN) δ 166.2, 166.0, 140.9, 140.1, 136.8, 127.8, 127.7, 123.4, 122.7, 122.6, 122.6, 121.8, 121.7, 119.1, 119.0, 118.9, 118.5, 112.9, 111.9, 111.7, 111.6, 103.1, 102.6, 52.8, 52.5, 48.8, 47.5, 44.0, 42.5, 32.7, 31.1, 25.3, 23.7, 17.5, 17.3; HRMS (ESI) *m/z* calcd for $C_{19}H_{26}N_2O_3$ $(M+Na)^+$, 353.1836; found, 353.1836.

NMR Assignment. ^{1}H NMR (400 MHz) (1 : 1 rotamer mixture) δ 9.24 (brs, 0.5 H, N2-H), 9.20 (brs, 0.5 H, N2-H), 7.65 (d, *J* = 8.0 Hz, 0.5 H, C6-H), 7.58 (d, *J* = 8.0 Hz,

0.5 H, C6-H), 7.42 (d, *J* = 3.6 Hz, 0.5 H, C3-H), 7.40 (d, *J* = 3.6 Hz, 0.5 H, C3-H), 7.17 – 7.14 (comp, 1 H, C4-H), 7.10 – 7.06 (comp, 2 H, C5-H and C1-H), 6.87 (dq, *J* = 14.8, 7.2 Hz, 0.5 H, C10-H), 6.64 (dq, *J* = 14.8, 7.2 Hz, 0.5 H, C10-H), 6.40 (dd, *J* = 14.8, 1.6 Hz, 0.5 H, C9-H), 6.16 (dd, *J* = 14.8, 1.6 Hz, 0.5 H, C9-H), 4.38 – 4.34 (comp, 1 H, C14-H), 3.63 (t, *J* = 6.4 Hz, 1 H, C8-H), 3.61 (t, *J* = 6.4 Hz, 1 H, C8-H), 3.39 – 3.35 (comp, 2 H C12-H), 3.27 (s, 6 H, C15-H), 3.00 (t, *J* = 8.0 Hz, 1 H, C7-H), 2.98 (t, *J* = 8.0 Hz, 1 H, C7-H), 1.99 (dd, *J* = 6.8, 1.6 Hz, 1.5 H, C11-H), 1.83 – 1.79 (comp, 2 H, C13-H), 1.69 (dd, *J* = 6.8, 1.6 Hz, 1.5 H, C11-H).

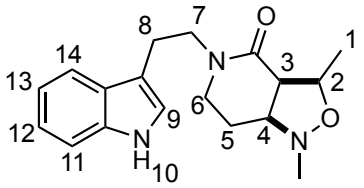

4.20

(3*S*,3a*R*,7a*S*)-5-(2-(1*H*-Indol-3-yl)ethyl)-1,3-dimethylhexahydroisoxazolo[4,3-*c*]pyridin-4(1*H*)-one (4.20). ARMV88/ARMV89. A solution of trifluoroacetic acid (230 mg, 2.02 mmol) and **4.21** (65 mg, 0.20 mmol) in trifluoroethanol/water (3 : 1, 2 mL) was stirred for 1.5 h at room temperature, whereupon saturated aqueous $NaHCO_3$ (5 mL) was added. The layers were separated, and the aqueous layer was extracted with CH_2Cl_2 (3 x 10 mL). The combined organic fractions were dried (Na_2SO_4), filtered, and the solvent was removed *in vacuo*. The resulting residue was dissolved in ethanol (4 mL). N-methylhydroxylamine hydrochloride (18 mg, 0.22 mmol) and triethylamine (22 mg, 0.22

mmol) were added to the mixture, and the reaction was heated under reflux for 48 h. the reaction was cooled to room temperature, the solvent was removed *in vacuo*, and the crude mixture was purified via silica gel flash column chromatography eluting with CH_2Cl_2 : methanol (97 : 3) to give 19 mg (30%) of **4.20** as a clear oil: ^{1}H NMR (500 MHz) δ 8.26 (brs, 1 H), 6.62 (d, *J* = 8.1 Hz, 1 H), 7.32 (d, *J* = 8.1 Hz, 1 H), 7.16 (t, *J* = 7.1 Hz, 1 H), 7.09 (t, *J* = 7.1 Hz, 1 H), 6.99 (d, *J* = 1.7 Hz, 1 H), 3.89 (pent, *J* = 6.1 Hz, 1 H), 3.73 – 3.68 (m, 1 H), 3.64 – 3.58 (m, 1 H), 3.53 (td, *J* = 12.0, 2.9 Hz, 1 H), 2.99 - 2.95 (comp, 3 H), 2.81 – 2.76 (comp, 2 H), 2.63 (s, 3 H), 1.75 (ddt, *J* = 14.5, 11.2, 4.1 Hz, 1 H) 1.59 (dq, *J* = 14.5, 3.2 Hz, 1 H), 1.44 (d, *J* = 5.9 Hz, 3 H); ^{13}C NMR (125 MHz) δ 169.0, 136.3, 127.4, 122.0, 121.9, 119.3, 118.7, 112.8, 111.2, 77.4, 66.1, 55.3, 48.5, 44.0, 43.1, 25.2, 23.4, 19.2; HRMS (CI) *m/z* calcd for $C_{18}H_{23}N_3O_2$ $(M+1)^+$, 314.1869; found, 314.1867.

NMR Assignment. ^{1}H NMR (500 MHz) δ 8.26 (brs, 1 H, N10-H), 6.62 (d, *J* = 8.1 Hz, 1 H, C14-H), 7.32 (d, *J* = 8.1 Hz, 1 H, C11-H), 7.16 (t, *J* = 7.1 Hz, 1 H, C12-H), 7.09 (t, *J* = 7.1 Hz, 1 H, C13-H), 6.99 (d, *J* = 1.7 Hz, 1 H, C9-H), 3.89 (pent, *J* = 6.1 Hz, 1 H, C2-H), 3.73 – 3.68 (m, 1 H, C7-H), 3.64 – 3.58 (m, 1 H, C7-H), 3.53 (td, *J* = 12.0, 2.9 Hz, 1 H, C6-H), 2.99 - 2.95 (comp, 3 H, C8-H and C6-H), 2.81 – 2.76 (comp, 2 H, C3-H and C4-H), 2.63 (s, 3 H, N-CH_3), 1.75 (ddt, *J* = 14.5, 11.2, 4.1 Hz, 1 H, C5-H) 1.59 (dq, *J* = 14.5, 3.2 Hz, 1 H, C5-H), 1.44 (d, *J* = 5.9 Hz, 3 H, C1-H).

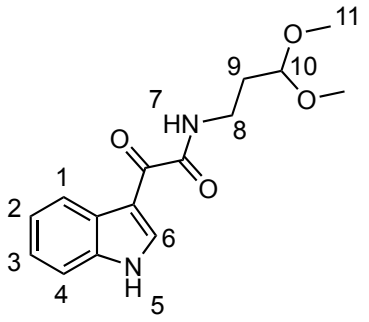

4.27

***N*-(3,3-Dimethoxypropyl)-2-(1*H*-indol-3-yl)-2-oxoacetamide (4.27).** **ARMVII132-ARMVII133.** A solution of oxalyl chloride (1.52 g, 12.0 mmol) in ether (1 mL) was added dropwise over 5 min to a solution of indole (1.41 g, 12.0 mmol) in ether (24 mL) at 0 ºC. The reaction was stirred at 0 ºC for 1 h, then warmed to room temperature, and stirred for an additional 1 h. The yellow precipitate was collected via vacuum filtration and dried *in vacuo* to give 2.28 g (87%) of indole-3-glyoxal chloride. A suspension of indole-3-glyoxal chloride (1.91 g, 8.7 mmol) in CH_2Cl_2 (20 mL) was added dropwise over 30 min to a solution of **4.18** (1.47 g, 7.3 mmol) and triethylamine (3.70 g, 36.5 mmol) in CH_2Cl_2 (75 mL) at 0 ºC. The reaction was stirred at 0 ºC for 0.5 h, then warmed to room temperature and stirred for an additional 1 h. Saturated aqueous $NaHCO_3$ (100 mL) was added to the reaction and stirred for 15 min. The mixture was extracted with CH_2Cl_2 (3 x 100 mL), and the combined organic extracts were washed with aqueous NaOH (1 M, 2 x 100 mL), water (100 mL), and brine (100 mL), dried (Na_2SO_4), filtered, and concentrated *in vacuo* to give 2.23 g (97%) of crude **4.27**. The crude material was >90% purity, and was further purified by dissolving in CH_2Cl_2 (300

mL) and successively with saturated aqueous NH_4Cl (200 mL), saturated aqueous $NaHCO_3$ (200 mL), water (200 mL), and brine (200 mL). The organic fraction was dried (Na_2SO_4), and concentrated *in vacuo* to give 1.91 g (90%) of **4.27** as a pale yellow solid (>95% purity, ^{1}H NMR): ^{1}H NMR (400 MHz) δ 9.99 (brs, 1 H), 9.01 (d, *J* = 3.2 Hz, 1 H), 8.41 (d, *J* = 7.2 Hz, 1 H), 7.97 (t, *J* = 6.0 Hz, 1 H), 7.40 – 7.38 (m, 1 H), 7.31 (ddd, *J* = 8.4, 7.2, 1.2 Hz, 1 H), 7.25 (ddd, *J* = 8.4, 7.2, 1.2 Hz, 1 H), 4.48 (t, *J* = 6.4 Hz, 1 H), 3.47 (q, *J* = 6.4 Hz, 2 H), 3.36 (s, 6 H), 1.91 (q, *J* = 6.4 Hz, 2 H). ^{13}C NMR (100 MHz, CD_3CN) δ 181.6, 163.0, 139.1, 136.5, 126.9, 124.0, 123.1, 121.9, 112.8, 112.5, 103.7, 53.1, 35.1, 32.3. HRMS (ESI) *m/z* calcd for $C_{15}H_{18}N_2O_4$ $(M+Na)^+$, 313.1159; found, 313.1166.

NMR Assignment. ^{1}H NMR (400 MHz) δ 9.99 (brs, 1 H, N5-H), 9.01 (d, *J* = 3.2 Hz, 1 H, C6-H), 8.41 (d, *J* = 7.2 Hz, 1 H, C1-H), 7.97 (t, *J* = 6.0 Hz, 1 H, N7-H), 7.40 – 7.38 (m, 1 H, C4-H), 7.31 (ddd, *J* = 8.4, 7.2, 1.2 Hz, 1 H, C3-H), 7.25 (ddd, *J* = 8.4, 7.2, 1.2 Hz, 1 H, C2-H), 4.48 (t, *J* = 6.4 Hz, 1 H, C10-H), 3.47 (q, *J* = 6.4 Hz, 2 H, C8-H), 3.36 (s, 6 H, C11-H), 1.91 (q, *J* = 6.4 Hz, 2 H, C9-H).

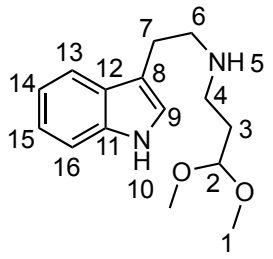

4.25

***N*-(2-(1*H*-Indol-3-yl)ethyl)-3,3-dimethoxypropan-1-amine (4.25).**

ARMVII137. A solution of **4.27** (0.50 g, 1.70 mmol) in THF (5 mL) was added dropwise over 15 min to a stirred suspension of lithium aluminum hydride (0.65 g, 17.0 mmol) in THF (40 mL) at 0 ºC. The reaction was heated at 65 ºC for 14 h. The reaction was cooled to 0 ºC and the Fieser work-up was carefully performed by successive addition of water (0.6 mL), aqueous sodium hydroxide (15% w/v, 0.6 mL), and water (3 mL). The suspension was warmed to room temperature and $MgSO_4$ was added. The solution was filtered through a fritted funnel, and the solids were washed with excess CH_2Cl_2. The filtrate was concentrated *in vacuo* to give crude **4.25** as an opaque viscous oil. The crude material was taken up in aqueous HCl (0.2 M, 150 mL) and washed with ether (2 x 100 mL). The aqueous fraction was basified with aqueous NaOH (40% w/v) to pH 12-14, as judged by pH paper. The basic solution was extracted with CH_2Cl_2 (3 x 200 mL). The combined organic extracts were dried (Na_2SO_4), filtered, and concentrated to give 0.41 g (90%) of **4.25** as a viscos oil (>95% purity, ^{1}H NMR); ^{1}H NMR (400 MHz) δ 8.61 (brs, 1 H), 7.57 (d, J = 7.2 Hz, 1 H), 7.42 (dt, J = 8.0, 1.2 Hz, 1 H), 7.27 – 7.20 (m, 1 H), 7.17 (dd, J = 8.0, 1.2 Hz, 1 H), 7.14 (ddd, J = 8.0, 7.2, 1.2 Hz, 1 H), 4.25 (t, J = 4.0 Hz, 1 H),

3.20 - 3.18 (comp, 4 H), 3.03 (t, J = 5.6 Hz, 2 H), 3.00 (s, 6 H), 1.88 (tt, J = 7.2, 4.0 Hz, 2 H); ^{13}C NMR (100 MHz) δ 134.0, 123.8, 121.5, 120.0, 117.4, 115.6, 109.2, 105.8, 101.3, 52.3, 45.6, 41.1, 25.8, 19.6; IR (neat) 3411, 2337, 2173, 1640, 1458 cm^{-1}; HRMS (CI) *m/z* calcd for $C_{15}H_{23}N_2O_2$ $(M+1)^+$, 263.1760; found, 263.1760.

NMR Assignment. ^{1}H NMR (400 MHz) δ 8.61 (brs, 1 H, N10-H), 7.57 (d, J = 7.2 Hz, 1 H, C13-H), 7.42 (dt, J = 8.0, 1.2 Hz, 1 H, C16-H), 7.27 – 7.20 (m, 1 H, C15-H), 7.17 (dd, J = 8.0, 1.2 Hz, 1 H, C14-H), 7.14 (ddd, J = 8.0, 7.2, 1.2 Hz, 1 H, C9-H), 4.25 (t, J = 4.0 Hz, 1 H, C2-H), 3.20-3.18 (comp, 4 H, C4-H and C6-H), 3.03 (t, J = 5.6 Hz, 2 H, C7-H), 3.00 (s, 6 H, C1-H), 1.88 (tt, J = 7.2, 4.0 Hz, 2 H, C3-H)

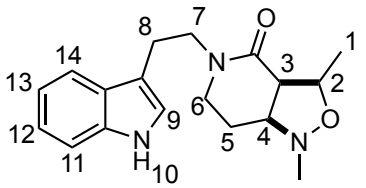

4.20

(3*S*,3a*R*,7a*S*)-5-(2-(1*H*-Indol-3-yl)ethyl)-1,3-dimethylhexahydroisoxazolo[4,3-*c*]pyridin-4(1*H*)-one (4.20). ARMVII146-ARMVII147. A solution of trifluoroacetic acid (5 drops) and **4.21** (110 mg, 0.33 mmol) in TFE/water (3 : 1, 7 mL) was stirred for 1 h at room temperature. Saturated aqueous $NaHCO_3$ (20 mL) was added, and the aqueous layer extracted with CH_2Cl_2 (3 x 20 mL). The combined organic fractions were dried (Na_2SO_4), filtered, and concentrated *in vacuo*. The crude mixture was dissolved in toluene (5 mL), followed by addition of N-methylhydroxylamine hydrochloride (41 mg,

0.50 mmol) and triethylamine (83 mg, 0.83 mmol). The reaction was heated under reflux for 1 h, then cooled to room temperature, and partitioned between saturated aqueous $NaHCO_3$ (20 mL), ethyl acetate (20 mL), and methanol (2 mL). The layers were separated, and the aqueous layer was extracted with ethyl acetate (3 x 20 mL). The combined organic fractions were washed with water (30 mL), brine (30 mL), dried (Na_2SO_4), filtered, and concentrated *in vacuo* to give 88 mg (85%) of **4.20** as an oil (>90% purity, ^{1}H NMR); ^{1}H NMR (500 MHz) δ 8.26 (brs, 1 H), 6.62 (d, *J* = 8.1 Hz, 1 H), 7.32 (d, *J* = 8.1 Hz, 1 H), 7.16 (t, *J* = 7.1 Hz, 1 H), 7.09 (t, *J* = 7.1 Hz, 1 H), 6.99 (d, *J* = 1.7 Hz, 1 H), 3.89 (p, *J* = 6.1 Hz, 1 H), 3.73 (m, 1 H), 3.64 (m, 1 H), 3.53 (td, *J* = 12.0, 2.9 Hz, 1 H), 2.99 - 2.95 (comp, 3 H), 2.81 – 2.76 (comp, 2 H), 2.63 (s, 3 H), 1.75 (ddt, *J* = 14.5, 11.2, 4.1 Hz, 1 H) 1.59 (dq, *J* = 14.5, 3.2 Hz, 1 H), 1.44 (d, *J* = 5.9 Hz, 3 H); ^{13}C NMR (125 MHz) δ 169.0, 136.3, 127.4, 122.0, 121.9, 119.3, 118.7, 112.8, 111.2, 77.4, 66.1, 55.3, 48.5, 44.0, 43.1, 25.2, 23.4, 19.2; HRMS (CI) *m/z* calcd for $C_{18}H_{23}N_3O_2$ $(M+1)^+$, 314.1869; found, 314.1867.

NMR Assignment. ^{1}H NMR (500 MHz) δ 8.26 (brs, 1 H, N10-H), 6.62 (d, *J* = 8.1 Hz, 1 H, C14-H), 7.32 (d, *J* = 8.1 Hz, 1 H, C11-H), 7.16 (t, *J* = 7.1 Hz, 1 H, C12-H), 7.09 (t, *J* = 7.1 Hz, 1 H, C13-H), 6.99 (d, *J* = 1.7 Hz, 1 H, C9-H), 3.89 (p, *J* = 6.1 Hz, 1 H, C2-H), 3.73 (m, 1 H, C7-H), 3.64 (m, 1 H, C7-H), 3.53 (td, *J* = 12.0, 2.9 Hz, 1 H, C6-H), 2.99 - 2.95 (comp, 3 H, C8-H and C6-H), 2.81 – 2.76 (comp, 2 H, C3-H and C4-H), 2.63 (s, 3 H, N-CH_3), 1.75 (ddt, *J* = 14.5, 11.2, 4.1 Hz, 1 H, C5-H) 1.59 (dq, *J* = 14.5, 3.2 Hz, 1 H, C5-H), 1.44 (d, *J* = 5.9 Hz, 3 H, C1-H)

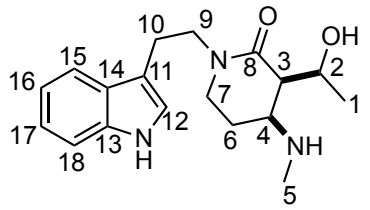

4.28

(±)-(3*R*,4*S*)-1-(2-(1*H*-Indol-3-yl)ethyl)-3-((*R*)-1-hydroxyethyl)-4-(methylamino)piperidin-2-one (4.28). ARMVII152. Zinc (powder, 530 mg, 8.14 mmol) was added in three portions over 1.5 h to a solution of **4.20** (85 mg, 0.27 mmol) in acetic acid (aq 80%, 20 mL) at 60 ºC, and stirred at 60 ºC for an additional 1 h. The reaction was cooled to room temperature, whereupon excess zinc was filtered and washed with ethyl acetate. Ethyl acetate (100 mL) was added to the filtrate and zinc acetate immediately precipitated out of solution as a fluffy white solid. The zinc acetate was filtered, and washed with excess ethyl acetate. The solvent was removed *in vacuo* to give crude **4.28**. the crude material was taken up in aqueous HCl (1 M, 30 mL) and washed with ether (2 x 30 mL). The aqueous fraction was basified with aqueous NaOH (40% w/v) to pH ~ 14. The basic solution was extracted with CH_2Cl_2 (4 x 50 mL). The combined organic fractions were washed with saturated aqueous $NaHCO_3$ (100 mL), water (100 mL), brine (1 x 100 mL), dried (Na_2SO_4), filtered, and concentrated *in vacuo* to give 78 mg (91%) of **4.28** as an oil (>95% purity, ^{1}H NMR); ^{1}H NMR (500 MHz, CD_3OD) δ 7.58 (dt, *J* = 7.8, 0.7 Hz, 1 H), 7.32 (dt, *J* = 7.8, 0.7 Hz, 1 H), 7.09 – 7.05 (comp, 2 H), 7.00 (td, *J* = 7.1, 1.0 Hz, 1 H), 4.37 (pent, *J* = 6.3 Hz, 1 H), 3.67 – 3.60 (m, 1 H), 3.56 – 3.49 (m, 1 H), 3.33 – 3.17 (comp, 1 H), 3.15 (pent, *J* = 3.9 Hz, 1 H), 3.11 –

3.04 (comp, 3 H), 2.40 (dd, *J* = 6.1, 4.2 Hz, 1 H), 2.34 (s, 3 H), 1.97 (app sex, *J* = 7.8 Hz, 1 H), 1.74 (dtd, *J* = 13.9, 7.1, 3.2 Hz, 1 H), 1.23 (d, *J* = 6.4 Hz, 3 H); ^{13}C NMR (125 MHz, CD_3OD) δ 171.0, 138.1, 128.9, 123.6, 122.4, 119.7, 119.3, 113.1, 112.3, 67.5, 56.1, 51.4, 45.7, 33.5, 30.8, 24.8, 23.7, 22.5; HRMS (ESI) *m/z* calcd for $C_{18}H_{25}N_3O_2$ $(M+1)^+$, 316.2020; found, 316.2024.

NMR Assignment. ^{1}H NMR (500 MHz, CD_3OD) δ 7.58 (dt, *J* = 7.8, 0.7 Hz, 1 H, C15-H), 7.32 (dt, *J* = 7.8, 0.7 Hz, 1 H, C18-H), 7.09 – 7.05 (comp, 2 H, C17-H and C12-H), 7.00 (td, *J* = 7.1, 1.0 Hz, 1 H, C16-H), 4.37 (pent, *J* = 6.3 Hz, 1 H, C2-H), 3.67 – 3.60 (m, 1 H, C-9H), 3.56 – 3.49 (m, 1 H, C9-H), 3.33 – 3.17 (comp, 1 H, C7-H and solvent), 3.15 (pent, *J* = 3.9 Hz, 1 H, C4-H), 3.11 – 3.04 (comp, 3 H, C7-H and C10-H), 2.40 (dd, *J* = 6.1, 4.2 Hz, 1 H, C3-H), 2.34 (s, 3 H, C5-H), 1.97 (app sex, *J* = 7.8 Hz, 1 H, C6-H), 1.74 (dtd, *J* = 13.9, 7.1, 3.2 Hz, 1 H, C6-H), 1.23 (d, *J* = 6.4 Hz, 3 H, C1-H); ^{13}C NMR (125 MHz, CD_3OD) δ 171.0 (C8), 138.1 (C13), 128.9 (C14), 123.6 (C12), 122.4 (C17), 119.7 (C16), 119.3 (C15), 113.1 (C11), 112.3 (C18), 67.5 (C2), 56.1 (C4), 51.4 (C3), 45.7 (C9), 33.5 (C7), 30.8 (C5), 24.8 (C6), 23.7 (C10), 22.5 (C1).

Representative Procedure for the Reductive Amination of Amino-Alcohols

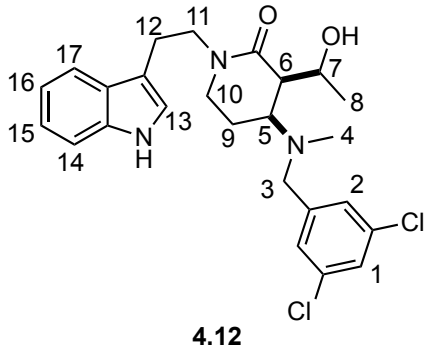

4.12

(3*R*,4*S*)-1-(2-(1*H*-Indol-3-yl)ethyl)-4-((3,5-dichlorobenzyl)(methyl)amino)-3-((*R*)-1-hydroxyethyl)piperidin-2-one (4.12). ARMV171. A solution of **4.28** (50 mg, 0.16 mmol) and 3,5-dichlorobenzaldehyde (45 mg, 0.26 mmol) in acetonitrile (1 mL) was heated under reflux for 2 h. The reaction was cooled to room temperature, at which time $NaBH_3CN$ (22 mg, 0.35 mmol) and acetic acid (53 μL, 0.89 mmol) were added. The reaction was stirred at room temperature for 20 h. The mixture was partitioned between saturated aqueous $NaHCO_3$ (6.5 mL), ethyl acetate (6.5 mL), and methanol (0.5 mL). The two phases were separated, and the aqueous phase was extracted with ethyl acetate (2 x 6.5 mL). The combined organic fractions were washed with brine (6.5 mL), dried (Na_2SO_4), filtered, and concentrated *in vacuo* to give crude **4.12** as an opaque viscous oil. The crude material was purified via flash column chromatography eluting with a gradient of hexanes : ethyl acetate (1 : 1) → ethyl acetate : methanol (20 : 1), to give 36 mg (48%) of **4.12** as a white solid; ^{1}H NMR (600 MHz) δ 8.15 (d, J = 1.9 Hz, 1 H), 7.55 (d, J = 8.2 Hz, 1 H), 7.34 (dt, J = 8.1, 0.8 Hz, 1 H), 7.27 (t, J = 1.9 Hz, 1 H), 7.18 (ddd, J = 8.1, 7.1,

1.1 Hz, 1 H), 7.12 – 7.08 (comp, 3 H), 7.02 (d, *J* = 1.9 Hz, 1 H), 4.35 (dq, *J* = 6.5, 6.2 Hz, 1 H), 3.74 - 3.78 (m, 1 H), 3.64 - 3.69 (m, 1 H), 3.41 - 3.26 (comp, 3 H), 3.24 (dt, *J* = 13.4, 5.4 Hz, 1 H), 3.12 (dt, *J* = 16.9, 9.2 Hz, 1 H), 3.04 - 2.99 (m, 1 H), 2.97 - 2.92 (m, 1 H), 2.31 (t, *J* = 5.2 Hz, 1H), 2.03 (s, 3 H), 1.83 - 1.87 (comp, 3 H), 1.15 (d, *J* = 6.5 Hz, 3 H); ^{13}C NMR (150 MHz) δ 171.7, 140.6, 136.3, 135.2, 128.1, 127.6, 127.3, 122.4, 122.1, 119.4, 118.4, 112.3, 111.5, 66.2, 58.9, 48.0, 47.4, 44.9, 37.3, 29.7, 23.2, 21.7, 20.1; HRMS (ESI) *m/z* calcd for $C_{25}H_{29}Cl_2N_3O_2$ $(M+1)^+$, 474.1710 and 476.1686; found, 474.1712 and 476.1690.

NMR Assignment. ^{1}H NMR (600 MHz) δ 8.15 (d, *J* = 1.9 Hz, 1 H, NH), 7.55 (d, *J* = 8.2 Hz, 1 H, C17-H), 7.34 (dt, *J* = 8.1, 0.8 Hz, 1 H, C14-H), 7.27 (t, *J* = 1.9 Hz, 1 H, C1-H), 7.18 (ddd, *J* = 8.1, 7.1, 1.1 Hz, 1 H, C15-H), 7.12 – 7.08 (comp, 3 H, C16-H and C2-H), 7.02 (d, *J* = 1.9 Hz, 1 H, C13-H), 4.35 (dq, *J* = 6.5, 6.2 Hz, 1 H, C7-H), 3.75 – 3.70 (m, 1 H, C11-H), 3.66 – 3.60 (m, 1 H, C11-H), 3.41 - 3.26 (comp, 3 H, C3-H and C5-H), 3.24 (dt, *J* = 13.4, 5.4 Hz, 1 H, C10-H), 3.12 (dt, *J* = 16.9, 9.2 Hz, 1 H, C10-H), 3.09 – 2.99 (m, 1 H, C12-H), 2.95 – 2.86 (m, 1 H, C12-H), 2.31 (t, *J* = 5.2 Hz, 1 H, C6-H), 2.03 (s, 3 H, C4-H), 1.93 – 1.80 (comp, 3 H, C9-H and OH), 1.15 (d, *J* = 6.5 Hz, 3 H, C8-H).

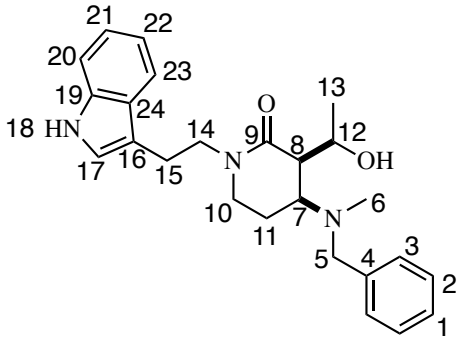

4.29

(±)-(3*R*,4*S*)-1-(2-(1*H*-Indol-3-yl)ethyl)-4-(benzyl(methyl)amino)-3-((*R*)-1-hydroxyethyl)piperidin-2-one (4.29). ARMV174. Prepared according to representative procedure for compound **4.12**. The crude material was purified via flash column chromatography eluting with a gradient with hexanes : ethyl acetate (1 : 1) → ethyl acetate : methanol (20 : 1). To give 31 mg (48%) of **4.29** as an off white solid; ^{1}H NMR (500 MHz) δ 8.13 (brs, 1 H), 7.58 (d, *J* = 7.9 Hz, 1 H), 7.35 (d, *J* = 7.9 Hz, 1 H), 7.33 – 7.26 (comp, 3 H), 7.21 (d, *J* = 6.6 Hz, 2 H), 7.19 (t, *J* = 7.1 Hz, 1 H), 7.11 (t, *J* = 7.1 Hz, 1 H), 7.03 (d, *J* = 2.2 Hz, 1 H), 4.34 (p, *J* = 6.1 Hz, 1 H), 3.76 (p, *J* = 7.6 Hz, 1 H), 3.64 (p, *J* = 6.4 Hz, 1 H), 3.52, 3.47 (ABq, J_{AB} = 12.7 Hz, 2 H), 3.42 (q, *J* = 7.6 Hz, 1 H), 3.26 (ddd, *J* = 13.7, 6.6, 3.4 Hz, 1 H), 3.16 - 3.10 (m, 1 H), 3.04 - 2.93 (comp, 2 H), 2.35 (t, *J* = 5.6 Hz, 1 H), 2.06 (s, 3 H), 1.96 - 1.90 (comp, 2 H), 1.16 (d, *J* = 6.4 Hz, 3 H); ^{13}C NMR (125 MHz) δ 171.7, 136.7, 136.3, 129.3, 128.7, 127.9, 127.3, 122.3, 122.1, 119.4, 118.4, 112.4, 111.4, 66.4, 60.0, 48.3, 47.4, 45.1, 37.2, 29.7, 23.2, 21.9, 20.1; HRMS (ESI) *m/z* calcd for $C_{25}H_{31}N_3O_2$ $(M+1)^+$, 406.2489; found, 406.2490.

NMR Assignment. ^{1}H NMR (500 MHz) δ 8.13 (brs, 1 H, N18-H), 7.58 (d, *J* = 7.9 Hz, 1 H, C23-H), 7.35 (d, *J* = 7.9 Hz, 1 H, C20-H), 7.33 – 7.26 (comp, 3 H, C1-H and C2-H), 7.21 (d, *J* = 6.6 Hz, 2 H, C3-H), 7.19 (t, *J* = 7.1 Hz, 1 H, C21-H), 7.11 (t, *J* = 7.1 Hz, 1 H, C22-H), 7.03 (d, *J* = 2.2 Hz, 1 H, C17-H), 4.34 (p, *J* = 6.1 Hz, 1 H, C12-H), 3.76 (p, *J* = 7.6 Hz, 1 H, C14-H), 3.64 (p, *J* = 6.4 Hz, 1 H, C14-H), 3.52, 3.47 (ABq, J_{AB} = 12.7 Hz, 2 H, C5-H), 3.42 (q, *J* = 7.6 Hz, 1 H, C7-H), 3.26 (ddd, *J* = 13.7, 6.6, 3.4 Hz, 1 H, C10-H), 3.16 – 3.10 (m, 1 H, C10-H), 3.04 – 2.93 (m, 2 H, C15-H), 2.35 (t, *J* = 5.6 Hz, 1 H, C8-H), 2.06 (s, 3 H, C6-H), 1.96 – 1.90 (comp, 2 H, C11-H), 1.16 (d, *J* = 6.4 Hz, 3 H, C13-H).

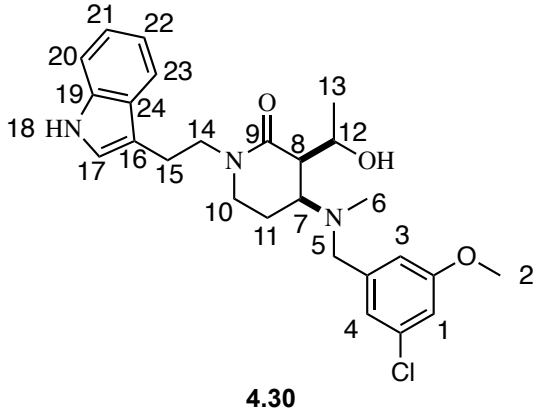

4.30

(±)-(3*R*,4*S*)-1-(2-(1*H*-Indol-3-yl)ethyl)-4-((3-chloro-5-methoxybenzyl)(methyl)amino)-3-((*R*)-1-hydroxyethyl)piperidin-2-one (4.30). **ARMV175.** Prepared according to representative procedure for compound **4.12**. The crude material was purified via flash column chromatography eluting with a gradient with hexanes : ethyl acetate (1 : 1) → ethyl acetate : methanol (20 : 1). To give 30 mg (27%)

of **4.30** as a white solid: ^{1}H NMR (400 MHz) δ 8.24 (s, 1 H), 7.57 (d, *J* = 7.6 Hz, 1 H), 7.33 (d, *J* = 7.6 Hz, 1 H), 7.18 (td, *J* = 7.2, 1.2 Hz, 1 H), 7.10 (td, *J* = 8.0, 1.2 Hz, 1 H), 7.01 (d, *J* = 2.4 Hz, 1 H), 6.80 (t, *J* = 1.6 Hz, 1 H), 6.78 (t, *J* = 1.6 Hz, 1 H), 6.67 (t, *J* = 1.6 Hz, 1 H), 4.33 (p, *J* = 6.4 Hz, 1 H), 3.79 - 3.72 (comp, 4 H), 3.61 (p, *J* = 6.4 Hz, 1 H), 3.47 – 3.30 (comp, 3 H), 3.23 (dt, *J* = 12.4, 4.8 Hz, 1 H), 3.10 (dt, *J* = 12.4, 9.2 Hz, 1 H), 3.02 - 2.90 (comp, 2 H), 2.38 (t, *J* = 6.0 Hz, 1 H), 2.06 (s, 3 H), 1.91 - 1.85 (comp, 2 H), 1.18 (d, *J* = 6.4 Hz, 3 H); ^{13}C NMR (100 MHz) δ 170.9, 160.5, 139.6, 136.2, 135.0, 127.3, 122.3, 122.1, 121.4, 119.3, 118.4, 113.6, 113.4, 112.4, 111.4, 66.3, 59.0, 58.0, 55.6, 48.5, 47.4, 45.0, 37.5, 23.1, 22.1, 20.5; HRMS (ESI) *m/z* calcd for $C_{26}H_{32}ClN_3O_3$ $(M+1)^+$, 470.2205; found, 470.2207.

NMR Assignment. ^{1}H NMR (400 MHz) δ 8.24 (s, 1 H, N18-H), 7.57 (d, *J* = 7.6 Hz, 1 H, C23-H), 7.33 (d, *J* = 7.6 Hz, 1 H, C20-H), 7.18 (td, *J* = 7.2, 1.2 Hz, 1 H, C21-H), 7.10 (td, *J* = 8.0, 1.2 Hz, 1 H, C22-H), 7.01 (d, *J* = 2.4 Hz, 1 H, C17-H), 6.80 (t, *J* = 1.6 Hz, 1 H, C4-H), 6.78 (t, *J* = 1.6 Hz, 1 H, C3-H), 6.67 (t, *J* = 1.6 Hz, 1 H, C1-H), 4.33 (p, *J* = 6.4 Hz, 1 H, C12-H), 3.79 – 3.72 (comp, 4 H, C2-H and C14-H), 3.61 (p, *J* = 6.4 Hz, 1 H, C14-H), 3.47 – 3.30 (comp, 3 H, C5-H and C7-H), 3.23 (dt, *J* = 12.4, 4.8 Hz, 1 H, C10-H), 3.10 (dt, *J* = 12.4, 9.2 Hz, 1 H, C10-H), 3.02 – 2.90 (comp, 2 H, C15-H), 2.38 (t, *J* = 6.0 Hz, 1 H, C8-H), 2.06 (s, 3 H, C6-H), 1.91 – 1.85 (comp, 2 H, C11-H), 1.18 (d, *J* = 6.4 Hz, 3 H, C13-H).

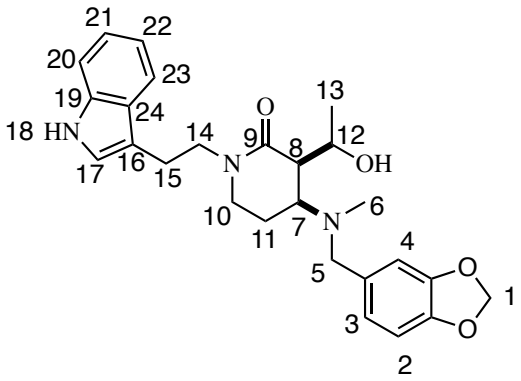

4.31

(3*R*,4*S*)-1-(2-(1*H*-Indol-3-yl)ethyl)-4-((benzo[*d*][1,3]dioxol-5-ylmethyl)(methyl)amino)-3-((*R*)-1-hydroxyethyl)piperidin-2-one (4.31). ARMV184. Prepared according to representative procedure for compound **4.12**. The crude material was purified via flash column chromatography eluting with a gradient with hexanes : ethyl acetate (3 : 1 → 0 : 1) to give 30 mg (28%) of **4.31** as an off white solid; ^{1}H NMR (400 MHz) δ 8.35 (s, 1 H), 7.63 (d, *J* = 7.6 Hz, 1 H), 7.35 (d, *J* = 8.0 Hz, 1 H), 7.19 (t, *J* = 7.2 Hz, 1 H), 7.12 (t, *J* = 7.6 Hz, 1 H), 7.02 (d, *J* = 2.0 Hz, 1 H), 6.74 – 6.72 (comp, 2 H), 6.67 (d, *J* = 8.0 Hz, 1 H), 4.28 (dq *J* = 6.4, 6.0 Hz, 1 H), 3.81 (p, *J* = 7.6 Hz, 1 H), 3.54 (p, *J* = 6.4 Hz, 1 H), 3.48, 3.37 (ABq, J_{AB} = 12.4 Hz, 2 H), 3.28 - 3.23 (m, 1 H), 3.16 - 3.10 (comp, 2 H), 3.07 - 2.98 (comp, 2 H), 2.65 (dd, *J* = 8.8, 5.2 Hz, 1 H), 2.10 (s, 3 H), 1.99 - 1.96 (comp, 2 H), 1.32 (d, *J* = 6.0 Hz, 3 H); ^{13}C NMR (100 MHz) δ 170.1, 148.0, 147.1, 136.4, 131.2, 127.5, 122.4, 122.2, 122.1, 119.4, 118.7, 112.8, 111.4, 109.4, 108.3, 101.1, 66.8, 59.8, 58.6, 50.1, 47.6, 45.6, 38.0, 23.3, 22.8, 21.6; HRMS (ESI) *m/z* calcd for $C_{26}H_{31}N_3O_4$ $(M+1)^+$, 450.2387; found, 450.2394.

NMR Assignment. ^{1}H NMR (400 MHz) δ 8.35 (s, 1 H, N18-H), 7.63 (d, *J* = 7.6 Hz, 1 H, C23-H), 7.35 (d, *J* = 8.0 Hz, 1 H, C20-H), 7.19 (t, *J* = 7.2 Hz, 1 H, C21-H), 7.12 (t, *J* = 7.6 Hz, 1 H, C22-H), 7.02 (d, *J* = 2.0 Hz, 1 H, C17-H), 6.74 – 6.72 (comp, 2 H, C3-H and C4-H), 6.67 (d, *J* = 8.0 Hz, 1 H, C2-H), 4.28 (dq *J* = 6.4, 6.0 Hz, 1 H, C12-H), 3.81 (p, *J* = 7.6 Hz, 1 H, C14-H), 3.54 (p, *J* = 6.4 Hz, 1 H, C14-H), 3.48, 3.37 (ABq, J_{AB} = 12.4 Hz, 2 H, C5-H), 3.28 – 3.23 (m, 1 H, C7-H), 3.16 – 3.10 (comp, 2 H, C10-H), 3.07 – 2.98 (comp, 2 H, C15-H), 2.65 (dd, *J* = 8.8, 5.2 Hz, 1 H, C8-H), 2.10 (s, 3 H, C6-H), 1.99 – 1.96 (comp, 2 H, C11-H), 1.32 (d, *J* = 6.0 Hz, 3 H, C13-H).

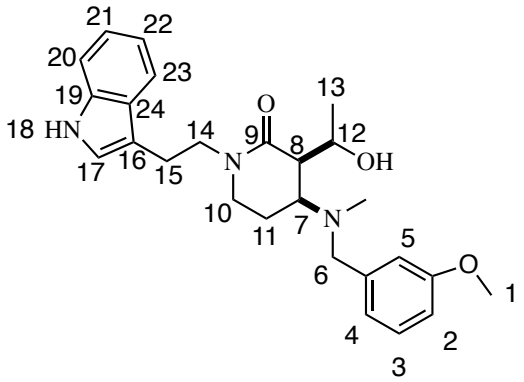

4.32

(3*R*,4*S*)-1-(2-(1*H*-Indol-3-yl)ethyl)-3-((*R*)-1-hydroxyethyl)-4-((3-methoxybenzyl)(methyl)amino)piperidin-2-one (4.32). ARMV198. Prepared according to representative procedure for compound **4.12**. The crude material was purified via flash column chromatography eluting with a gradient with hexanes : ethyl acetate (1 : 1) → ethyl acetate : methanol (20 : 1) to give 18 mg (26%) of **4.32** as an off white solid; ^{1}H NMR (400 MHz) δ 8.19 (s, 1 H), 7.58 (d, *J* = 8.0 Hz, 1 H), 7.34 (d, *J* =

8.0 Hz, 1 H), 7.24 – 7.16 (comp, 2 H), 7.10 (td, *J* = 8.0, 1.2 Hz, 1 H), 7.03 (d, *J* = 2.4 Hz, 1 H), 6.82 (d, *J* = 2.0 Hz, 1 H), 6.80 (d, *J* = 2.0 Hz, 1 H), 6.77 (t, *J* = 2.0 Hz, 1 H), 4.33 (p, *J* = 6.4 Hz, 1 H), 3.81 - 3.74 (comp, 4 H), 3.60 (p, *J* = 6.4 Hz, 1 H), 3.50, 3.43 (ABq, J_{AB} = 12.8 Hz, 2 H), 3.37 - 3.32 (m, 1 H), 3.24 (dt, *J* = 12.0, 4.4 Hz, 1 H), 3.11 (dt, *J* = 12.0, 8.0 Hz, 1 H), 3.04 - 2.92 (comp, 2 H), 2.41 (t, *J* = 7.2 Hz, 1 H), 2.07 (s, 3 H), 1.95 - 1.89 (comp, 2 H), 1.19 (d, *J* = 6.4 Hz, 3 H); ^{13}C NMR (100 MHz, CD_3OD) δ 171.8, 161.4, 140.3, 137.6, 130.6, 128.9, 123.7, 122.4, 122.3, 119.7, 119.3, 115.5, 114.2, 112.8, 112.3, 68.0, 61.2, 59.6, 55.6, 50.9, 46.6, 38.3, 24.0, 22.9, 22.3; HRMS (ESI) *m/z* calcd for $C_{26}H_{33}N_3O_3$ $(M+1)^+$, 436.2595; found, 436.2599.

NMR Assignment. ^{1}H NMR (400 MHz) δ 8.19 (s, 1 H, N18-H), 7.58 (d, *J* = 8.0 Hz, 1 H, C23-H), 7.34 (d, *J* = 8.0 Hz, 1 H, C20-H), 7.24 – 7.16 (comp, 2 H, C3-H and C21-H), 7.10 (td, *J* = 8.0, 1.2 Hz, 1 H, C22-H), 7.03 (d, *J* = 2.4 Hz, 1 H, C17-H), 6.82 (d, *J* = 2.0 Hz, 1 H, C4-H), 6.80 (d, *J* = 2.0 Hz, 1 H, C2-H), 6.77 (t, *J* = 2.0 Hz, 1 H, C5-H), 4.33 (p, *J* = 6.4 Hz, 1 H, C12-H), 3.81 – 3.74 (comp, 4 H, C1-H and C14-H), 3.60 (p, *J* = 6.4 Hz, 1 H, C14-H), 3.50, 3.43 (ABq, J_{AB} = 12.8 Hz, 2 H, C6-H), 3.37 – 3.32 (m, 1 H, C7-H), 3.24 (dt, *J* = 12.0, 4.4 Hz, 1 H, C10-H), 3.11 (dt, *J* = 12.0, 8.0 Hz, 1 H, C10-H), 3.04 – 2.92 (comp, 2 H, C15-H), 2.41 (t, *J* = 7.2 Hz, 1 H, C8-H), 2.07 (s, 3 H, NCH_3), 1.95 – 1.89 (comp, 2 H, C11-H), 1.19 (d, *J* = 6.4 Hz, 3 H, C13-H).

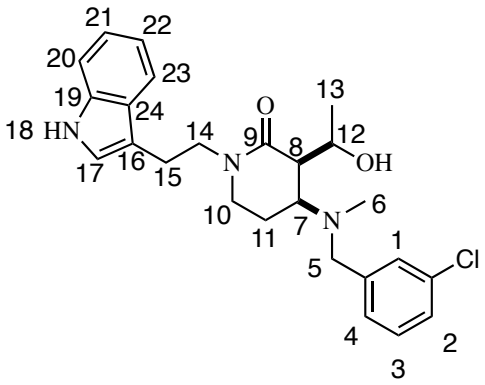

4.33

(3*R*,4*S*)-1-(2-(1*H*-Indol-3-yl)ethyl)-4-((3-chlorobenzyl)(methyl)amino)-3-((*R*)-1-hydroxyethyl)piperidin-2-one (4.33). ARMV199. Prepared according to representative procedure for compound **4.12**. The crude material was purified via flash column chromatography eluting along a gradient with hexanes : ethyl acetate (3 : 1 → 0 : 1) to give 26 mg (37%) of **4.33** as a white solid; ^{1}H NMR (400 MHz, CD_3OD) δ 7.58 (d, *J* = 7.6 Hz, 1 H), 7.33 (d, *J* = 7.4 Hz, 1 H), 7.31 – 7.26 (comp, 3 H), 7.18 (dt, *J* = 6.8, 1.6 Hz, 1 H), 7.11 – 7.07 (comp, 2 H), 7.02 (ddd, *J* = 7.6, 6.8, 0.8 Hz, 1 H), 4.22 (dq, *J* = 8.8, 6.0 Hz, 1 H), 3.77 (dt, *J* = 13.2, 7.2 Hz, 1 H), 3.57 – 3.51 (comp, 2 H), 3.44 (d, *J* = 12.8 Hz, 1 H), 3.35 - 3.32 (m, 1 H), 3.18 – 2.90 (comp, 4 H), 2.59 (dd, *J* = 8.4, 5.2 Hz, 1 H), 2.07 (s, 3 H), 2.04 - 1.98 (m, 1 H), 1.94 - 1.87 (m, 1 H), 1.20 (d, *J* = 6.4 Hz, 3 H); ^{13}C NMR (100 MHz, CD_3OD) δ 171.8, 141.6, 138.1, 135.5, 131.1, 130.0, 128.9, 128.5, 123.7, 122.4, 119.7, 119.3, 112.8, 112.3, 67.9, 61.2, 58.9, 51.0, 46.6, 38.3, 24.0, 22.8, 22.4; HRMS (ESI) *m/z* calcd for $C_{25}H_{30}ClN_3O_2$ $(M+1)^+$, 440.2099; found, 440.2099.

NMR Assignment. ^{1}H NMR (400 MHz, CD_3OD) δ 7.58 (d, *J* = 7.6 Hz, 1 H, C23-H), 7.33 (d, *J* = 7.4 Hz, 1 H, C20-H), 7.31 – 7.26 (comp, 3 H, C1-H, C3-H, C4-H), 7.18 (dt, *J* = 6.8, 1.6 Hz, 1 H, C2-H), 7.11 – 7.07 (comp, 2 H, C17-H and C21-H), 7.02 (ddd, *J* = 7.6, 6.8, 0.8 Hz, 1 H, C22-H), 4.22 (dq, *J* = 8.8, 6.0 Hz, 1 H, C12-H), 3.77 (dt, *J* = 13.2, 7.2 Hz, 1 H, C14-H), 3.57 – 3.51 (comp, 2 H, C5-H and C14-H), 3.44 (d, *J* = 12.8 Hz, 1 H, C5-H), 3.35 – 3.32 (m, 1 H, C7-H), 3.18 – 2.90 (comp, 4 H, C10-H, C15-H), 2.59 (dd, *J* = 8.4, 5.2 Hz, 1 H, C8-H), 2.07 (s, 3 H, C6-H), 2.04 – 1.98 (m, 1 H, C11-H), 1.94 – 1.87 (m, 1 H, C11-H), 1.20 (d, *J* = 6.4 Hz, 3 H, C13-H)

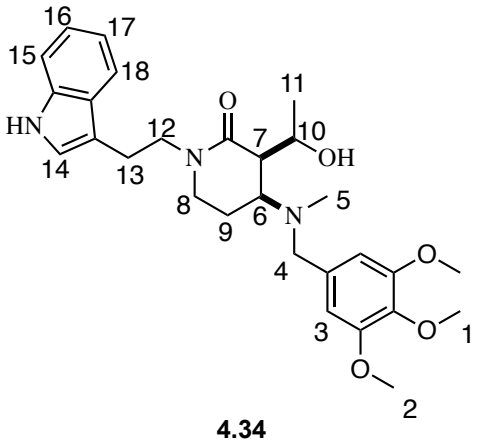

4.34

(3*R*,4*S*)-1-(2-(1*H*-Indol-3-yl)ethyl)-3-((*R*)-1-hydroxyethyl)-4-(methyl(3,4,5-trimethoxybenzyl)amino)piperidin-2-one (4.34). ARMV202. Prepared according to representative procedure for compound **4.12**. The crude material was purified via flash column chromatography eluting with a gradient with hexanes : ethyl acetate (1 : 1 → 0 : 1) to give 26 mg (33%) of **4.34** as a an off white solid; ^{1}H NMR (400 MHz, CD_3OD)

δ 7.59 (dt, *J* = 8.0, 1.2 Hz, 1 H), 7.33 (dt, *J* = 8.4, 1.2 Hz, 1 H), 7.11 – 7.07 (comp, 2 H), 7.02 (ddd, *J* = 8.0, 7.2, 1.2 Hz, 1 H), 6.58 (s, 2 H), 4.23 (dq, *J* = 9.2, 6.4 Hz, 1 H), 3.82 (s, 6 H), 3.81 - 3.76 (m, 1 H), 3.75 (s, 3 H), 3.64 – 3.54 (comp, 3 H), 3.59 - 3.49 (m, 1 H), 3.22 – 3.14 (comp, 2 H), 3.10 – 2.92 (comp, 2 H), 2.61 (dd, *J* = 9.2, 5.6 Hz, 1 H), 2.16 (s, 3 H), 2.10 - 2.04 (m, 1 H), 2.00 - 1.93 (m, 1 H), 1.20 (d, *J* = 6.0 Hz, 3 H); ^{13}C NMR (125 MHz, CD_3OD) δ 169.8, 152.7, 136.7, 136.2, 127.0, 121.8, 120.5, 117.8, 117.3, 110.9, 110.4, 105.4, 66.0, 59.2, 59.1, 57.9, 54.7, 48.9, 44.6, 36.4, 22.0, 21.0, 20.3; HRMS (ESI) *m/z* calcd for $C_{28}H_{37}N_3O_5$ $(M+1)^+$, 496.2806; found, 496.2803

NMR Assignment. ^{1}H NMR (400 MHz, CD_3OD) δ 7.59 (dt, *J* = 8.0, 1.2 Hz, 1 H, C18-H), 7.33 (dt, *J* = 8.4, 1.2 Hz, 1 H, C15-H), 7.11 – 7.07 (comp, 2 H, C16-H and C14-H), 7.02 (ddd, *J* = 8.0, 7.2, 1.2 Hz, 1 H, C17-H), 6.58 (s, 2 H, C3-H), 4.23 (dq, *J* = 9.2, 6.4 Hz, 1 H, C10-H), 3.82 (s, 6 H, C2-H), 3.81 – 3.76 (m, 1 H, C12-H), 3.75 (s, 3 H, C1-H), 3.64 – 3.45 (comp, 3 H, C12-H and C4-H), 3.59 – 3.49 (m, 1 H, C6-H), 3.22 – 3.14 (comp, 2 H, C8-H), 3.10 – 2.92 (comp, 2 H, C13-H), 2.61 (dd, *J* = 9.2, 5.6 Hz, 1 H, C7-H), 2.16 (s, 3 H, C5-H), 2.10 – 2.04 (m, 1 H, C9-H), 2.00 – 1.93 (m, 1 H, C9-H), 1.20 (d, *J* = 6.0 Hz, 3 H, C11-H)

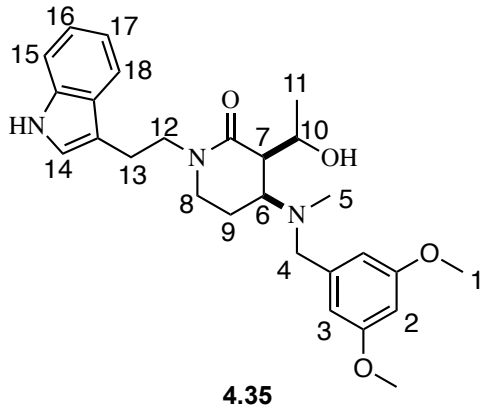

4.35

(3*R*,4*S*)-1-(2-(1*H*-Indol-3-yl)ethyl)-4-((3,5-dimethoxybenzyl)(methyl)amino)-3-((*R*)-1-hydroxyethyl)piperidin-2-one (4.35). ARMV203. Prepared according to representative procedure for compound **4.12**. The crude material was purified via flash column chromatography eluting with a gradient with hexanes : ethyl acetate (1 : 1 → 0 : 1) to give 37 mg (50%) of **4.35** as a white solid; ^{1}H NMR (400 MHz, CD_3OD) δ 7.58 (dt, J = 8.0, 0.8 Hz, 1 H), 7.33 (dt, J = 8.0, 0.8 Hz, 1 H), 7.11 - 7.07 (comp, 2 H), 7.01 (td, J = 8.0, 6.8, 1.2 Hz, 1 H), 6.42 (d, J = 2.4 Hz, 2 H), 6.38 (t, J = 2.4 Hz, 1 H), 4.23 (dq, J = 14.0, 6.0 Hz, 1 H), 3.81 - 3.71 (comp, 7 H), 3.57 - 3.51 (m, 1 H), 3.47, 3.41 (ABq, J_{AB} = 12.8 Hz, 2 H), 3.34 - 3.30 (m, 1 H), 3.17 - 2.93 (comp, 4 H), 2.58 (dd, J = 8.8, 5.6 Hz, 1 H), 2.09 (s, 3 H), 2.04 - 1.98 (m, 1 H), 1.95 - 1.85 (m, 1 H), 1.19 (d, J = 6.0 Hz, 3 H); ^{13}C NMR (100 MHz, CD_3OD) δ 171.9, 162.5, 141.4, 138.1, 128.9, 123.7, 122.4, 119.7, 119.3, 112.8, 112.3, 107.8, 100.3, 68.0, 61.0, 59.8, 55.7, 50.9, 46.7, 38.4, 24.0, 22.8, 22.3; HRMS (ESI) *m/z* calcd for $C_{27}H_{35}N_3O_4$ $(M+1)^+$, 466.2700; found, 466.2701.

NMR Assignment. ^{1}H NMR (400 MHz, CD_3OD) δ 7.58 (dt, *J* = 8.0, 0.8 Hz, 1 H, C18-H), 7.33 (dt, *J* = 8.0, 0.8 Hz, 1 H, C15-H), 7.11 – 7.07 (comp, 2 H, C14-H and C16-H), 7.01 (td, *J* = 8.0, 6.8, 1.2 Hz, 1 H, C17-H), 6.42 (d, *J* = 2.4 Hz, 2 H, C3-H), 6.38 (t, *J* = 2.4 Hz, 1 H, C2-H), 4.23 (dq, *J* = 14.0, 6.0 Hz, 1 H, C10-H), 3.81 – 3.71 (comp, 7 H, C1-H and C12-H), 3.57 – 3.51 (m, 1 H, C12-H), 3.47, 3.41 (ABq, J_{AB} = 12.8 Hz, 2 H, C4-H), 3.34 – 3.30 (m, 1 H, C6-H), 3.17 – 2.93 (comp, 4 H, C8-H and C13-H), 2.58 (dd, *J* = 8.8, 5.6 Hz, 1 H, C7-H), 2.09 (s, 3 H, C5-H), 2.04 – 1.98 (m, 1 H, C9-H), 1.95 – 1.85 (m, 1 H, C9-H), 1.19 (d, *J* = 6.0 Hz, 3H, C11-H).

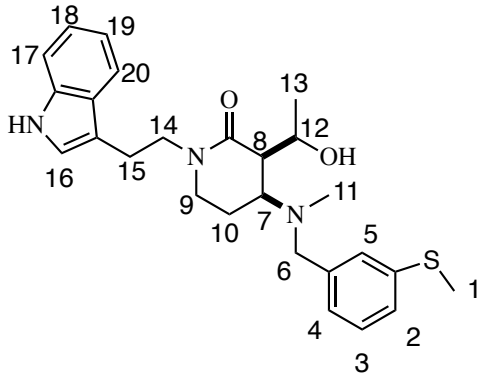

4.36

(3*R*,4*S*)-1-(2-(1*H*-Indol-3-yl)ethyl)-3-((*R*)-1-hydroxyethyl)-4-(methyl(3-(methylthio)benzyl)amino)piperidin-2-one (4.36). ARMV214. Prepared according to representative procedure for compound **4.12**. The crude material was purified via flash column chromatography eluting with a gradient with hexanes : ethyl acetate (1 : 1 → 0 : 1) to give 45 mg (49%) of **4.36** as a fluffy white solid; ^{1}H NMR (400 MHz, CD_3OD)

δ 7.58 (d, *J* = 7.6 Hz, 1 H), 7.33 (d, *J* = 8.0 Hz, 1 H), 7.26 (td, *J* = 7.6, 0.8 Hz, 1 H), 7.17 - 7.15 (comp, 2 H), 7.09 (ddd, *J* = 8.0, 7.6, 0.8 Hz, 1 H), 7.07 (s, 1 H), 7.03 - 6.99 (comp, 2 H), 4.22 (dq, *J* = 8.8, 6.0 Hz, 1 H), 3.77 (dt, *J* = 13.2, 7.6 Hz, 1 H), 3.56 - 3.49 (comp, 2 H), 3.43 (d, *J* = 12.8, 1 H), 3.34 - 3.28 (m, 1 H), 3.17 - 2.92 (comp, 4 H), 2.58 (dd, *J* = 8.8, 5.6 Hz, 1 H), 2.45 (s, 3 H), 2.07 (s, 3 H), 2.02 - 1.86 (comp, 2 H), 1.19 (d, *J* = 6.4 Hz, 3 H); ^{13}C NMR (100 MHz, CD_3OD) δ 171.8, 140.6, 139.7, 138.1, 130.0, 128.8, 127.8, 126.7, 125.4, 123.7, 122.4, 119.7, 119.3, 112.8, 112.3, 67.9, 61.1, 59.4, 50.9, 46.5, 38.3, 24.0, 22.9, 22.3, 15.5; HRMS (ESI) *m/z* calcd for $C_{26}H_{33}N_3O_2S$ $(M+Na)^+$, 474.2186; found, 474.2187.

NMR Assignment. ^{1}H NMR (400 MHz, CD_3OD) δ 7.58 (d, *J* = 7.6 Hz, 1 H, C20-H), 7.33 (d, *J* = 8.0 Hz, 1 H, C17-H), 7.26 (td, *J* = 7.6, 0.8 Hz, 1 H, C18-H), 7.17 – 7.15 (comp, 2 H, C2-H and C5-H), 7.09 (ddd, *J* = 8.0, 7.6, 0.8 Hz, 1 H, C19-H), 7.07 (s, 1 H, C16-H), 7.03 – 6.99 (comp, 2 H, C3-H and C4-H), 4.22 (dq, *J* = 8.8, 6.0 Hz, 1 H, C12-H), 3.77 (dt, *J* = 13.2, 7.6 Hz, 1 H, C14-H), 3.56 – 3.49 (comp, 2 H, C6-H and C14-H), 3.43 (d, *J* = 12.8, 1 H, C6-H), 3.34 – 3.28 (m, 1 H, C7-H), 3.17 – 2.92 (comp, 4 H, C9-H and C15-H), 2.58 (dd, *J* = 8.8, 5.6 Hz, 1 H, C8-H), 2.45 (s, 3 H, C1-H), 2.07 (s, 3 H, C11-H), 2.02 – 1.86 (comp, 2 H, C10-H), 1.19 (d, *J* = 6.4 Hz, 3 H, C13-H).

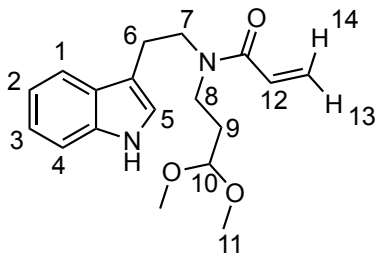

4.39

***N*-(2-(1*H*-Indol-3-yl)ethyl)-*N*-(3,3-dimethoxypropyl)acrylamide (4.39).** **ARMV217.** Acryloyl chloride (0.42 g, 4.7 mmol) was added dropwise over 5 min to a solution of **4.25** (0.94 g, 3.6 mmol) and Hünig's base (1.20 g, 9.3 mmol) in CH_2Cl_2 (40 mL) at -78 ºC. The solution was stirred for 2 h at -78 ºC, then partitioned between saturated aqueous $NaHCO_3$ (40 mL) and CH_2Cl_2 (40 mL). The two phases were separated, and the aqueous phase was extracted with CH_2Cl_2 (3 x 40 mL). The combined organic fractions were washed with water (40 mL), brine (40 mL), dried (Na_2SO_4), filtered, and concentrated *in vacuo* to give crude **4.39** as a clear oil. The crude material was purified via silica gel flash column chromatography eluting with hexanes : ethyl acetate (3 : 1 → 1 : 1 along a gradient) to give 0.63 g (54%) of **4.39** as a clear oil; ^{1}H NMR (500 MHz) (1 : 1 rotamer mixture) δ 8.76 (brs, 0.5 H), 8.63 (brs, 0.5 H), 7.70 (d, *J* = 6.4 Hz, 0.5 H), 7.56 (d, *J* = 8.0 Hz, 0.5 H), 7.35 (app t, *J* = 8.0 Hz, 1 H), 7.21 – 7.01 (comp, 2 H), 6.98 (d, *J* = 2.5 Hz, 0.5 H), 6.92 (d, *J* = 2.5 Hz, 0.5 H), 6.64 (dd, *J* = 16.7, 10.4 Hz, 0.5 H), 6.45 (dd, *J* = 16.7, 2.0 Hz, 0.5 H), 6.40 (dd, *J* = 16.7, 10.4 Hz, 0.5 H), 6.27 (dd, *J* = 16.7, 2.0 Hz, 0.5 H), 5.73 (dd, *J* = 10.4, 2.0 Hz, 0.5 H), 5.52 (dd, *J* = 10.4, 2.0 Hz, 0.5 H), 4.42 (t, *J* = 5.6 Hz, 0.5 H), 4.32 (t, *J* = 5.6 Hz, 0.5 H), 3.71 (app t, *J* = 7.2

Hz, 1 H), 3.64 (app t, *J* = 7.2 Hz, 1 H), 3.49 (t, *J* = 7.2 Hz, 0.5 H), 3.39 (t, *J* = 7.2 Hz, 0.5 H), 3.33 (s, 3 H), 3.30 (s, 3 H), 3.08 (t, *J* = 7.2 Hz, 1 H), 3.02 (t, *J* = 7.2 Hz, 1 H), 1.97 – 1.93 (m, 1 H), 1.83 (dt, *J* = 7.2, 5.6 Hz, 1 H); ^{13}C NMR (125 MHz) (1 : 1 rotamer mixture) δ 166.5, 166.3, 136.43, 136.39, 128.2, 127.7, 127.6, 127.5, 127.4, 127.1, 122.5, 122.2, 122.1, 121.9, 119.4, 119.2, 118.8, 118.1, 112.9, 111.6, 111.5, 111.3, 102.9, 102.1, 53.3, 53.1, 49.0, 47.9, 44.2, 43.0, 32.5, 30.9, 25.5, 23.7; HRMS (ESI) *m/z* calcd for $C_{18}H_{24}N_2O_3$ $(M+Na)^+$, 339.1679; found, 339.1662.

NMR Assignment. ^{1}H NMR (500 MHz) (1 : 1 rotamer mixture) δ 8.76 (brs, 0.5 H, NH), 8.63 (brs, 0.5 H, NH), 7.70 (d, *J* = 6.4 Hz, 0.5 H, C1-H), 7.56 (d, *J* = 8.0 Hz, 0.5 H, C1-H), 7.35 (app t, *J* = 8.0 Hz, 1 H, C4-H), 7.21 – 7.01 (comp, 2 H, C2-H and C3-H), 6.98 (d, *J* = 2.5 Hz, 0.5 H, C5-H), 6.92 (d, *J* = 2.5 Hz, 0.5 H, C5-H), 6.64 (dd, *J* = 16.7, 10.4 Hz, 0.5 H, C12-H), 6.45 (dd, *J* = 16.7, 2.0 Hz, 0.5 H, H-14), 6.40 (dd, *J* = 16.7, 10.4 Hz, 0.5 H, C12-H), 6.27 (dd, *J* = 16.7, 2.0 Hz, 0.5 H, H-14), 5.73 (dd, *J* = 10.4, 2.0 Hz, 0.5 H, H-13), 5.52 (dd, *J* = 10.4, 2.0 Hz, 0.5 H, H-13), 4.42 (t, *J* = 5.6 Hz, 0.5 H, C10-H), 4.32 (t, *J* = 5.6 Hz, 0.5 H, C10-H), 3.71 (app t, *J* = 7.2 Hz, 1 H, C8-H), 3.64 (app t, *J* = 7.2 Hz, 1 H, C8-H), 3.49 (t, *J* = 7.9 Hz, 1 H, C7-H), 3.39 (t, *J* = 7.9 Hz, 1 H, C7-H), 3.33 (s, 3 H, C11-H), 3.30 (s, 3 H, C11-H), 3.08 (t, *J* = 7.9 Hz, 1 H, C6-H), 3.02 (t, *J* = 7.9 Hz, 1 H, C6-H), 1.97 – 1.93 (m, 1 H, C9-H), 1.83 (dt, *J* = 7.2, 5.6 Hz, 1 H, C9-H).

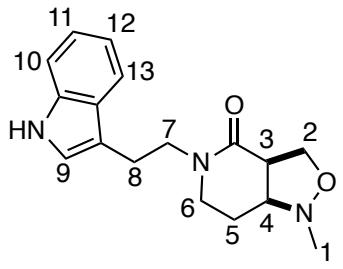

4.40

(3a*R*,7a*S*)-5-(2-(1*H*-Indol-3-yl)ethyl)-1-methylhexahydroisoxazolo[4,3-*c*]pyridin-4(1*H*)-one (4.40). ARMVII92/ARMVII93. A solution of trifluoroacetic acid (45 mg, 0.40 mmol) and **4.39** (250 mg, 0.79 mmol) in TFE/water (3 : 1, 16 mL) was stirred for 1 h at room temperature. Saturated aqueous $NaHCO_3$ (20 mL) was added and the aqueous layer was extracted with CH_2Cl_2 (3 x 20mL). The combined organic fractions were dried (Na_2SO_4), filtered, and concentrated *in vacuo*. The crude mixture was dissolved in toluene (12 mL). N-Methylhydroxylamine hydrochloride (99 mg, 1.19 mmol) and triethylamine (200 mg, 1.98 mmol) were added to the reaction mixture, and the reaction was heated at reflux for 1.5 h. The reaction was cooled to room temperature, and partitioned between saturated aqueous $NaHCO_3$ (20 mL), ethyl acetate (20 mL), and methanol (2 mL). The layers were separated, and the aqueous layer was extracted with ethyl acetate (3 x 20 mL). The combined organic fractions were washed with water (40 mL), brine (40 mL), dried (Na_2SO_4), filtered, and concentrated *in vacuo* to give 173 mg (73%) of **4.40** as a clear oil (>95% purity, by ^{1}H NMR); ^{1}H NMR (500 MHz) δ 8.29 (s, 1 H), 7.64 (d, J = 7.8 Hz, 1 H), 7.36 (d, J = 8.0 Hz, 1 H), 7.18 (td, J = 8.0, 1.0 Hz, 1 H), 7.11 (td, J = 7.8, 1.0 Hz, 1 H), 7.02 (d, J = 2.2 Hz, 1 H), 4.34 (t, J = 9.0 Hz, 1 H), 3.80 (t,

J = 8.0 Hz, 1 H), 3.69 - 3.65 (comp, 2 H), 3.45 (td, *J* = 12.9, 3.4 Hz, 1 H), 3.39 (td, *J* = 9.0, 6.8 Hz, 1 H), 3.07 – 3.00 (comp, 3 H), 2.86 (s, 1 H), 2.66 (s, 3 H), 1.83 (ddt, *J* = 13.9, 9.8, 4.1 Hz, 1 H), 1.65 (dq, *J* = 13.9, 5.1 Hz, 1 H); ^{13}C NMR (125 MHz) δ 169.3, 136.3, 127.4, 122.1, 122.0, 119.3, 118.7, 112.9, 111.3, 69.3, 65.2, 48.8, 48.6, 44.3, 43.2, 25.4, 23.4; HRMS (ESI) *m/z* calcd for $C_{17}H_{21}N_3O_2$ $(M+Na)^+$, 322.1526; found, 322.1529.

NMR Assignment. ^{1}H NMR (500 MHz) δ 8.29 (s, 1 H, N-H), 7.64 (d, *J* = 7.8 Hz, 1 H, C13-H), 7.36 (d, *J* = 8.0 Hz, 1 H, C10-H), 7.18 (td, *J* = 8.0, 1.0 Hz, 1 H, C11-H), 7.11 (td, *J* = 7.8, 1.0 Hz, 1 H, C12-H), 7.02 (d, *J* = 2.2 Hz, 1 H, C9-H), 4.34 (t, *J* = 9.0 Hz, 1 H, C2-H), 3.80 (t, *J* = 8.0 Hz, 1 H, C2-H), 3.69 – 3.65 (comp, 2 H, C7-H), 3.45 (td, *J* = 12.9, 3.4 Hz, 1 H, C6-H), 3.39 (td, *J* = 9.0, 6.8 Hz, 1 H, C3-H), 3.07 – 3.00 (comp, 3 H, C6-H and C8-H), 2.86 (brs, 1 H, C4-H), 2.66 (s, 3 H, N-CH_3), 1.83 (ddt, *J* = 13.9, 9.8, 4.1 Hz, 1 H, C5-H), 1.65 (dq, *J* = 13.9, 5.1 Hz, 1 H, C5-H).

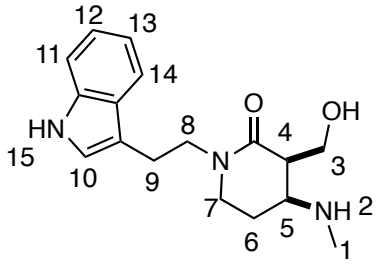

4.41

(3*R*,4*S*)-1-(2-(1*H*-Indol-3-yl)ethyl)-3-(hydroxymethyl)-4-(methylamino)piperidin-2-one (4.41). ARMV229. Zinc (dust, 2.00 g, 30 mmol) was added in three portions over 1 h to a solution of **4.40** (293 mg, 1.0 mmol) in acetic acid

(aq 80%, 60 mL) at 65 ºC, and stirred for an additional 1 h. The reaction was cooled to room temperature, excess zinc was filtered and washed with ethyl acetate. Hexanes (100 mL) was added to the filtrate, whereupon zinc acetate immediately precipitated out of solution as a fluffy white solid. The zinc acetate was removed by vacuum filtration and washed with excess ethyl acetate. The combined filtrate and washes were concentrated *in vacuo*. The resulting residue was taken up in HCl (aq 1 M, 100 mL), and washed with ether (100 mL). The aqueous fraction was basified to pH ~14 with solid NaOH. The resulting basic solution was extracted with CH_2Cl_2 (3 x 150 mL). The combined organic fractions were washed with brine (200 mL), dried (Na_2SO_4), filtered, and concentrated *in vacuo*. The crude mixture was purified via flash column chromatography eluting with CH_2Cl_2 : methanol (98 : 2 → 9 : 1 along a gradient) to give 240 mg (80%) of **4.41** as a yellow oil; ^{1}H NMR (600 MHz, CD_3OD) δ 7.57 (dt, *J* = 7.9, 1.0 Hz, 1 H), 7.33 (dt, *J* = 8.1, 0.9 Hz, 1 H), 7.10 – 7.07 (comp, 2 H), 7.01 (ddd, *J* = 8.0, 7.0, 1.0 Hz, 1 H), 3.95 (qd, *J* = 11.3, 7.7 Hz, 2 H), 3.66 (ddd, *J* = 13.3, 7.2, 6.2 Hz, 1 H), 3.54 (ddd, *J* = 13.3, 8.0, 6.7 Hz, 1 H), 3.24 (ddd, *J* = 10.2, 5.2, 3.3 Hz, 1 H), 3.16 - 3.10 (m, 1 H), 3.09 - 3.02 (m, 1 H), 3.01 - 2.90 (comp, 2 H), 2.87 (dt, *J* = 7.7, 4.3 Hz, 1 H), 2.54 (s, 3 H), 2.02 – 1.96 (m, 1 H), 1.90 - 1.84 (m, 1 H); ^{13}C NMR (150 MHz, CD_3OD) δ 169.8, 138.1, 128.9, 123.7, 122.4, 119.7, 119.25, 113.0, 112.4, 61.4, 57.1, 50.0, 47.2, 46.4, 32.8, 23.7, 23.4; HRMS (ESI) *m/z* calcd for $C_{17}H_{23}N_3O_2$ $(M+1)^+$, 302.1863; found, 302.1864.

NMR Assignment. ^{1}H NMR (600 MHz, CD_3OD) δ 7.57 (dt, *J* = 7.9, 1.0 Hz, 1 H, C14-H), 7.33 (dt, *J* = 8.1, 0.9 Hz, 1 H, C11-H), 7.10 – 7.07 (comp, 2 H, C10-H and C12-

H), 7.01 (ddd, *J* = 8.0, 7.0, 1.0 Hz, 1 H, C13-H), 3.95 (qd, *J* = 11.3, 7.7 Hz, 2 H, C3-H), 3.66 (ddd, *J* = 13.3, 7.2, 6.2 Hz, 1 H, C8-H), 3.54 (ddd, *J* = 13.3, 8.0, 6.7 Hz, 1 H, C8-H), 3.24 (ddd, *J* = 10.2, 5.2, 3.3 Hz, 1 H, C5-H), 3.16 – 3.10 (m, 1 H, C7-H), 3.09 – 3.02 (m, 1 H, C7-H), 3.01 – 2.90 (comp, 2 H, C9-H), 2.87 (dt, *J* = 7.7, 4.3 Hz, 1 H, C4-H), 2.54 (s, 3 H, C1-H), 2.02 – 1.96 (m, 1 H, C6-H), 1.90 – 1.84 (m, 1 H, C6-H).

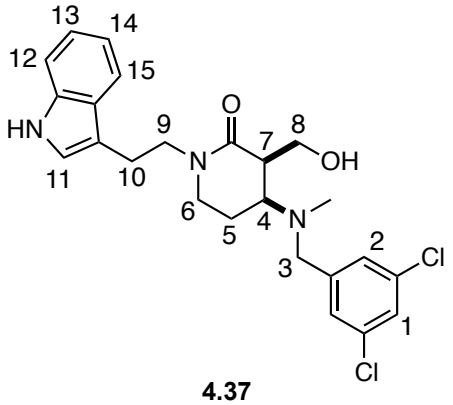

4.37

(3*R*,4*S*)-1-(2-(1*H*-Indol-3-yl)ethyl)-4-((3,5-dichlorobenzyl)(methyl)amino)-3-(hydroxymethyl)piperidin-2-one (4.37). ARMV250. A solution of **4.41** (50 mg, 0.17 mmol) and 3,5-dichlorobenzaldehyde (87 mg, 0.50 mmol) in acetonitrile (1 mL) was heated under reflux for 2 h. The solution was cooled to room temperature, at which time $NaBH_3CN$ (31 mg, 0.5 mmol) and acetic acid (glacial, 58 μL, 1.0 mmol) were added. The reaction was stirred for 20 h at room temperature, then partitioned between aqueous NaOH (1 M, 10 mL) and CH_2Cl_2 (10 mL). The two phases were separated, and the aqueous phase extracted with CH_2Cl_2 (2 x 10 mL). The combined organic fractions were washed with brine (10 mL) and dried (Na_2SO_4), filtered, and concentrated *in vacuo* to

give crude **4.37** as an opaque viscous oil. The crude material was purified via silica gel flash column chromatography eluting with a gradient of hexanes : ethyl acetate (1 : 1) → ethyl acetate : methanol (20 : 1). To give 32 mg (42%) of **4.37** as a white solid: ^{1}H NMR (500 MHz, CD_3OD) δ 7.57 (d, *J* = 7.8 Hz, 1 H), 7.32 (dt, *J* = 8.3, 0.7 Hz, 1 H), 7.28 (t, *J* = 2.0 Hz, 1 H), 7.23 (s, 2 H), 7.09 - 7.06 (comp, 2 H), 6.99 (ddd, *J* = 8.1, 7.1, 1.0 Hz, 1 H), 3.98 (d, *J* = 5.9 Hz, 2 H), 3.68 - 3.64 (comp, 2 H), 3.46 (d, *J* = 14.2 Hz, 1 H), 3.40 (d, *J* = 14.2 Hz, 1 H), 3.23 - 3.02 (comp, 3 H), 2.98 (p, *J* = 7.1 Hz, 2 H), 2.74 (brs, 1 H), 2.04 (s, 3 H), 1.86 - 1.81 (comp, 2 H); ^{13}C NMR (125 MHz, CD_3OD) δ 173.5, 145.0, 138.1, 136.0, 128.8, 128.0, 128.0, 123.7, 122.4, 119.7, 119.3, 112.9, 112.4, 61.3, 60.4, 58.4, 47.5, 38.7, 24.0, 23.2; HRMS (ESI) *m/z* calcd for $C_{24}H_{27}Cl_2N_3O_2$ $(M+Na)^+$, 482.1373 and 484.1348; found, 482.1379 and 484.1354.

NMR Assignment. ^{1}H NMR (500 MHz, CD_3OD) δ 7.57 (d, *J* = 7.8 Hz, 1 H, C15-H), 7.32 (dt, *J* = 8.3, 0.7 Hz, 1 H, C12-H), 7.28 (t, *J* = 2.0 Hz, 1 H, C1-H), 7.23 (s, 2 H, C2-H), 7.09 - 7.06 (comp, 2 H, C14-H and C11-H), 6.99 (ddd, *J* = 8.1, 7.1, 1.0 Hz, 1 H, C13-H), 3.98 (d, *J* = 5.9 Hz, 2 H, C8-H), 3.68 - 3.64 (comp, 2 H, C9-H), 3.46 (d, *J* = 14.2 Hz, 1 H, C3-H), 3.40 (d, *J* = 14.2 Hz, 1 H, C3-H), 3.23 - 3.02 (comp, 3 H, C4-H and C6-H), 2.98 (p, *J* = 7.1 Hz, 2 H, C10-H), 2.74 (brs, 1 H, C7-H), 2.04 (s, 3 H, N-CH_3), 1.86 - 1.81 (comp, 2 H, C5-H).

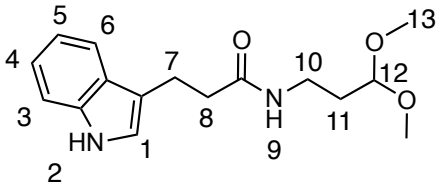

4.55

***N*-(3,3-Dimethoxypropyl)-3-(1*H*-indol-3-yl)propanamide (4.55).**

ARMVI45-ARMVI46. Thionyl chloride (1.14 g, 9.6 mmol) was added dropwise over 10 min to a solution of indole-3-propionic acid (1.51 g, 8.0 mmol) and DMF (3 drops) in THF (40 mL) at 0 ºC. The reaction was stirred for 2 h at 0 ºC, whereupon all volatiles were removed *in vacuo.* The crude material was dissolved in CH_2Cl_2 (20 mL) and added dropwise over 20 min to a solution of **4.18** (1.46 g, 7.3 mmol) and triethylamine (3.30 g, 32.8 mmol) in CH_2Cl_2 (120 mL) at 0 ºC. The reaction was stirred for 1 h at 0 ºC, followed by stirring for 2 h at room temperature. The solution was diluted with CH_2Cl_2 (300 mL) and washed successively with saturated aqueous NH_4Cl (150 mL), aqueous Na_2CO_3 (5% w/v, 150 mL), and brine (150 mL). The organic fraction was dried (Na_2SO_4), filtered, and concentrated *in vacuo* to give crude **4.55** as a viscous yellow oil. The crude material was purified via silica gel flash column chromatography eluting with hexanes : ethyl acetate (1 : 1 → 1 : 3 along a gradient) to give 2.05 g (97%) of **4.55** as a viscous yellow oil: ^{1}H NMR (400 MHz) δ 8.42 (brs, 1 H), 7.59 (d, J = 8.0 Hz, 1 H), 7.33 (d, J = 8.0 Hz, 1 H), 7.18 (td, J = 8.0, 1.2 Hz, 1 H), 7.11 (ddd, J = 8.0, 7.2, 0.8 Hz, 1 H), 6.96 (d, J = 2.4 Hz, 1 H), 5.94 (brs, 1 H), 4.26 (t, J = 5.2 Hz, 1 H), 3.30 - 3.25 (comp, 8 H), 3.10 (t, J = 7.2 Hz, 2 H), 2.55 (t, J = 7.2 Hz, 2 H), 1.69 (q, J = 7.2 Hz, 2H); ^{13}C NMR

(100 MHz) δ 172.7, 136.4, 127.1, 121.9, 121.8, 119.2, 118.6, 114.7, 111.3, 103.9, 53.3, 37.4, 35.3, 31.9, 21.4; HRMS (ESI) *m/z* calcd for $C_{16}H_{22}N_2O_3$ $(M+Na)^+$, 313.1523; found, 313.1524.

NMR Assignment. ^{1}H NMR (400 MHz) δ 8.42 (brs, 1 H, N2-H), 7.59 (d, *J* = 8.0 Hz, 1 H, C6-H), 7.33 (d, *J* = 8.0 Hz, 1 H, C3-H), 7.18 (td, *J* = 8.0, 1.2 Hz, 1 H, C4-H), 7.11 (ddd, *J* = 8.0, 7.2, 0.8 Hz, 1 H, C5-H), 6.96 (d, *J* = 2.4 Hz, 1 H, C1-H), 5.94 (brs, 1 H, N9-H), 4.26 (t, *J* = 5.2 Hz, 1 H, C12-H), 3.30 - 3.25 (comp, 8 H, C10-H and C13-H), 3.10 (t, *J* = 7.2 Hz, 2 H, C7-H), 2.55 (t, *J* = 7.2 Hz, 2 H, C8-H), 1.69 (q, *J* = 7.2 Hz, 2H, C11-H).

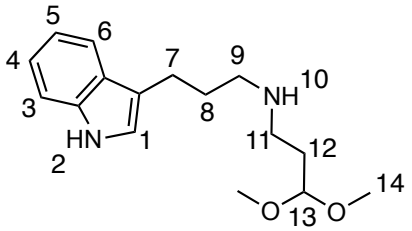

4.56

***N*-(3-(1*H*-Indol-3-yl)propyl)-3,3-dimethoxypropan-1-amine (4.56).** **ARMVII150.** A solution of **4.55** (400 mg, 1.4 mmol) in THF (5 mL) was added dropwise over 15 min to a suspension of lithium aluminum hydride (115 mg, 3.0 mmol) in THF (30 mL) at 0 ºC. The reaction was heated at 65 ºC for 14 h, at which point the reaction was cooled to 0 ºC, and the Fieser work-up was carefully performed by successive addition of water (0.1 mL), aqueous NaOH (15% w/v, 0.1 mL), and water (1

mL). The suspension was warmed to room temperature and $MgSO_4$ was added. The solids were removed by filtration through a fritted funnel, and washed with copious amounts of CH_2Cl_2. The filtrate was concentrated *in vacuo* to give crude **4.56** as an opaque viscous oil. The crude material was taken up into aqueous HCl (0.2 M, 150 mL) and washed with ether (2 x 100 mL). The aqueous fraction was basified to pH ~ 12-14 by dropwise addition of aqueous NaOH (40% w/v), and extracted with CH_2Cl_2 (4 x 150 mL). The combined organic fractions were successively washed with saturated aqueous $NaHCO_3$ (200 mL), water (200 mL), and brine (200 mL). The organic fraction was dried (Na_2SO_4), filtered, and concentrated *in vacuo* to give 331 mg (87%) of **4.56** as an oil (>95% purity, by ^{1}H NMR): ^{1}H NMR (400 MHz) δ 8.43 (brs, 1 H), 7.60 (d, *J* = 7.6 Hz, 1 H), 7.33 (dt, *J* = 8.0, 1.2 Hz, 1 H), 7.18 (td, *J* = 6.8, 1.2 Hz, 1 H), 7.10 (td, *J* = 6.8, 1.2 Hz, 1 H), 6.94 (d, *J* = 2.0 Hz, 1 H), 4.46 (t, *J* = 5.6 Hz, 1 H), 3.33 (s, 6 H), 2.80 (t, *J* = 7.6 Hz, 2 H), 2.72 - 2.68 (comp, 4 H), 1.92 (p, *J* = 7.6 Hz, 2 H), 1.82 (q, *J* = 6.0 Hz, 2 H); ^{13}C NMR (100 MHz) δ 136.4, 127.5, 121.8, 121.2, 119.0, 118.8, 116.1, 111.1, 103.6, 52.9, 49.9, 45.5, 32.8, 30.4, 22.9; HRMS (ESI) *m/z* calcd for $C_{16}H_{24}N_2O_2$ $(M+1)^+$, 277.1911; found 277.1912.

NMR Assignment. ^{1}H NMR (400 MHz) δ 8.43 (brs, 1 H, N2-H), 7.60 (d, *J* = 7.6 Hz, 1 H, C6-H), 7.33 (dt, *J* = 8.0, 1.2 Hz, 1 H, C3-H), 7.18 (td, *J* = 6.8, 1.2 Hz, 1 H, C4-H), 7.10 (td, *J* = 6.8, 1.2 Hz, 1 H, C5-H), 6.94 (d, *J* = 2.0 Hz, 1 H, C1-H), 4.46 (t, *J* = 5.6 Hz, 1 H, C13-H), 3.33 (s, 6 H, C14-H), 2.80 (t, *J* = 7.6 Hz, 2 H, C9-H), 2.72 - 2.68

(comp, 4 H, C7-H and C11-H), 1.92 (p, *J* = 7.6 Hz, 2 H, C8-H), 1.82 (q, *J* = 6.0 Hz, 2 H, C12-H).

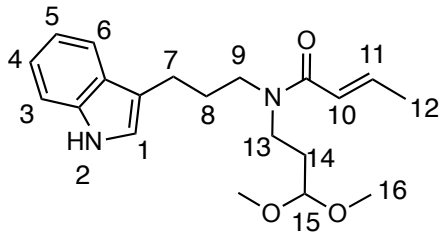

4.57

(*E*)-*N*-(3-(1*H*-Indol-3-yl)propyl)-*N*-(3,3-dimethoxypropyl)but-2-enamide (4.57). ARMV257. Crotonoyl chloride (200 mg, 1.9 mmol) was added dropwise over 10 min to a stirred solution of **4.56** (440 mg, 1.6 mmol) and Hünig's base (496 mg, 3.8 mmol) in CH_2Cl_2 (16 mL) at -78 ºC. The solution was stirred for 2 h at -78 ºC, then partitioned between saturated aqueous $NaHCO_3$ solution (50 mL) and CH_2Cl_2 (50 mL). The two phases were separated and the aqueous phase extracted with CH_2Cl_2 (2 x 50 mL). The combined organic fractions were successively washed with water (50 mL), brine (50 mL), dried (Na_2SO_4), filtered, and concentrated *in vacuo* to give crude **4.57** as a colorless oil. The crude material was purified via silica gel flash column chromatography eluting with a gradient hexanes : ethyl acetate (3 : 1 → 1 : 1 along a gradient) to give 340 mg (62%) of **4.57** as an opaque viscous oil: ^{1}H NMR (400 MHz) (1:1 rotamer mixture) δ 8.69 (brs, 0.5 H), 8.54 (brs, 0.5 H), 7.57 (dd, *J* = 8.0, 0.4 Hz, 1 H), 7.35 (d, *J* = 8.0 Hz, 0.5 H), 7.32 (d, *J* = 8.0 Hz, 0.5 H), 7.20 - 7.06 (comp, 2 H), 7.00 - 6.95 (comp,

1.5 H), 6.85 (dq, *J* = 14.2, 6.8 Hz, 0.5 H), 6.32 (dd, *J* = 14.2, 1.6 Hz, 0.5 H), 5.98 (dd, *J* = 14.2, 1.6 Hz, 0.5 H), 4.38 (t, *J* = 6.0 Hz, 0.5 H), 4.33 (t, *J* = 6.0 Hz, 0.5 H), 3.50 - 3.39 (comp, 3 H), 3.36 - 3.28 (comp, 7 H), 2.77 (app q, *J* = 7.2 Hz, 2 H), 2.01 (q, *J* = 7.2 Hz, 2 H), 1.90 - 1.83 (comp, 3.5 H), 1.68 (dd, *J* = 6.8, 1.6 Hz, 1.5 H); ^{13}C NMR (400 MHz) (1:1 rotamer mixture) δ 166.5, 166.4, 141.8, 141.5, 136.6, 136.4, 127.4, 127.2, 121.9, 121.8, 121.6, 121.5, 119.1, 118.9, 118.7, 118.6, 115.3, 114.6, 111.3, 111.2, 102.9, 102.2, 53.2, 53.0, 48.0, 46.5, 43.6, 42.3, 32.5, 31.0, 29.6, 28.0, 22.6, 22.3, 18.3, 18.0; HRMS (ESI) *m/z* calcd for $C_{20}H_{28}N_2O_2$ $(M+Na)^+$, 367.1992; found, 367.1994.

NMR Assignment. ^{1}H NMR (400 MHz) (1:1 rotamer mixture) δ 8.69 (brs, 0.5 H, N2-H), 8.54 (brs, 0.5 H, N2-H), 7.57 (dd, *J* = 8.0, 0.4 Hz, 1 H, C6-H), 7.35 (d, *J* = 8.0 Hz, 0.5 H, C3-H), 7.32 (d, *J* = 8.0 Hz, 0.5 H, C3-H), 7.20 - 7.06 (comp, 2 H, C5-H and C4-H), 7.00 - 6.95 (comp, 1.5 H, C11-H and C1-H), 6.85 (dq, *J* = 14.2, 6.8 Hz, 0.5 H, C11-H), 6.32 (dd, *J* = 14.2, 1.6 Hz, 0.5 H, C10-H), 5.98 (dd, *J* = 14.2, 1.6 Hz, 0.5 H, C10-H), 4.38 (t, *J* = 6.0 Hz, 0.5 H, C15-H), 4.33 (t, *J* = 6.0 Hz, 0.5 H, C15-H), 3.50 - 3.39 (comp, 3 H, C13-H and C9-H), 3.36 - 3.28 (comp, 7 H, C16-H and C13-H), 2.77 (app q, *J* = 7.2 Hz, 2 H, C7-H), 2.01 (q, *J* = 7.2 Hz, 2 H, C14-H), 1.90 - 1.83 (comp, 3.5 H, C12-H and C8-H), 1.68 (dd, *J* = 6.8, 1.6 Hz, 1.5 H, C12-H).

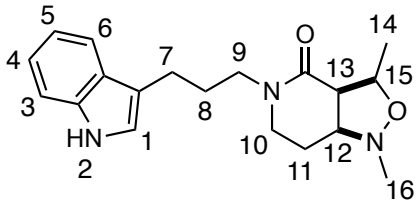

4.58

(3*R*,3a*R*,7a*S*)-5-(3-(1*H*-Indol-3-yl)propyl)-1,3-dimethylhexahydroisoxazolo[4,3-*c*]pyridin-4(1*H*)-one (4.58). ARMVII156-ARMVII157. A solution of trifluoroacetic acid (5 drops) and **4.57** (50 mg, 0.14 mmol) in TFE/water (3 : 1, 4 mL) was stirred for 1 h at room temperature. Saturated aqueous $NaHCO_3$ (10 mL) was added, the layers were separated, and the aqueous layer was extracted with CH_2Cl_2 (3 x 20 mL). The combined organic fractions were dried (Na_2SO_4), filtered, and concentrated *in vacuo*. The crude mixture was dissolved in toluene (2 mL), followed by the addition of N-methylhydroxylamine hydrochloride (18 mg, 0.22 mmol) and triethylamine (37 mg, 0.36 mmol). The reaction was heated under reflux for 1.5 h. After cooling the to room temperature, the reaction was partitioned between saturated aqueous $NaHCO_3$ (10 mL), ethyl acetate (20 mL), and methanol (1 mL). The layers were separated, and the aqueous layer was extracted with ethyl acetate (3 x 20 mL). The combined organic fractions were washed successively with water (40 mL) and brine (40 mL), dried (Na_2SO_4), filtered, and concentrated *in vacuo* to give 49 mg (quant) of **4.58** as an oil of ~80 - 90% purity, as judged by ^{1}H NMR. The crude material was taken up in aqueous HCl (1 M, 10 mL), and washed with ether (2 x 10 mL). The aqueous fraction was basified to pH 12-14 by dropwise addition of aqueous NaOH (40%

w/v), as judged by pH paper. The basic solution was extracted with CH_2Cl_2 (2 x 30 mL) and ethyl acetate (2 x 30 mL). The combined organic fractions were dried (Na_2SO_4), filtered, and concentrated *in vacuo* to give 33 mg (68%) of **4.58** as a colorless oil: ^{1}H NMR (400 MHz) δ 8.24 (brs, 1 H), 7.57 (d, *J* = 7.6 Hz, 1 H), 7.35 (dt, *J* = 8.4, 1.2 Hz, 1 H), 7.18 (ddd, *J* = 8.4, 7.2, 1.2, 1 H), 7.10 (ddd, *J* = 8.0, 7.2, 1.2 Hz, 1 H), 7.03 (d, *J* = 2.0 Hz, 1 H), 3.94 (dq, *J* = 7.2, 6.0 Hz, 1 H), 3.68 - 3.55 (comp, 2 H), 3.44 - 3.37 (m, 1 H), 3.07 (dt, *J* = 12.4, 4.0 Hz, 1 H), 2.91 - 2.87 (m, 1 H), 2.84 - 2.70 (comp, 3 H), 2.69 (s, 3 H), 2.00 - 1.85 (comp, 3 H), 1.71 (dq, *J* = 14.4, 3.6 Hz, 1 H), 1.47 (d, *J* = 6.0 Hz, 3 H); ^{13}C NMR (100 MHz) δ 169.0, 136.4, 127.3, 121.8, 121.5, 119.1, 118.7, 115.4, 111.1, 77.6, 66.1, 55.4, 47.3, 46.0, 43.2, 27.6, 25.2, 22.4, 19.2; HRMS (ESI) *m/z* calcd for $C_{19}H_{25}N_3O_2$ $(M+Na)^+$, 350.1839; found, 350.1845.

NMR Assignment. ^{1}H NMR (400 MHz) δ 8.24 (brs, 1 H, N2-H), 7.57 (d, *J* = 7.6 Hz, 1 H, C6-H), 7.35 (dt, *J* = 8.4, 1.2 Hz, 1 H, C3-H), 7.18 (ddd, *J* = 8.4, 7.2, 1.2, 1 H, C4-H), 7.10 (ddd, *J* = 8.0, 7.2, 1.2 Hz, 1 H, C5-H), 7.03 (d, *J* = 2.0 Hz, 1 H, C1-H), 3.94 (dq, *J* = 7.2, 6.0 Hz, 1 H, C15-H), 3.68 - 3.55 (comp, 2 H, C9-H), 3.44 - 3.37 (m, 1 H, C10-H), 3.07 (dt, *J* = 12.4, 4.0 Hz, 1 H, C10-H), 2.91 - 2.87 (m, 1 H, C12-H), 2.84 - 2.70 (comp, 3 H, C13-H and C7-H), 2.69 (s, 3 H, C16-H), 2.00 - 1.85 (comp, 3 H, C11-H and C8-H), 1.71 (dq, *J* = 14.4, 3.6 Hz, 1 H, C11-H), 1.47 (d, *J* = 6.0 Hz, 3 H, C14-H).

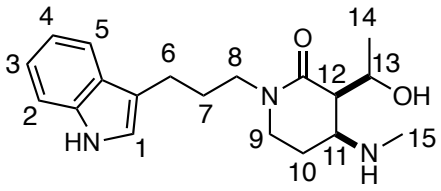

4.59

(3*R*,4*S*)-1-(3-(1*H*-Indol-3-yl)propyl)-3-((*R*)-1-hydroxyethyl)-4-(methylamino)piperidin-2-one (4.59). **ARMVI55.** A suspension of zinc (dust, 7.0 g, 84 mmol) and **4.58** (1.37 g, 4.2 mmol) in acetic acid (aq 80%, 200 mL) was stirred for 3 h at 65 ºC, at which point the reaction was cooled to room temperature. Excess zinc was removed via vacuum filtration and washed with ethyl acetate (200 mL), whereupon zinc acetate immediately precipitated out of solution as a fluffy white solid. The zinc acetate was removed by vacuum filtration and washed with ethyl acetate. The combined filtrate and washes were concentrated *in vacuo*. The resulting residue was dissolved in aqueous HCl (1 M, 300 mL), and washed with ether (150 mL). The aqueous fraction was carefully basified to pH ~14 with solid NaOH, and extracted with CH_2Cl_2 (3 x 300 mL). The combined organic fractions were washed with brine (200 mL), dried (Na_2SO_4), filtered, and concentrated *in vacuo* to give crude **4.59**. The crude mixture was purified via silica gel flash column chromatography eluting with CH_2Cl_2 : methanol (98 : 2 → 9 : 1 along a gradient) to give 791 mg (57%) of **4.59** as a yellow oil: ^{1}H NMR (500 MHz, CD_3OD) δ 7.51 (dt, *J* = 8.0, 1.5 Hz, 1 H), 7.30 (dt, *J* = 8.5, 1.0 Hz, 1 H), 7.06 (ddd, *J* = 8.5, 7.0, 1.5 Hz, 1 H), 7.03 (s, 1 H), 6.97 (ddd, *J* = 8.0, 7.0, 1.5 Hz, 1 H), 4.41 (t, *J* = 6.2 Hz, 1 H), 3.54 (ddd, *J* = 13.4, 8.4, 6.8 Hz, 1 H), 3.38 (ddd, *J* = 12.7, 7.5, 6.3 Hz, 1 H), 3.28 - 3.20

(comp, 2 H), 3.16 (p, *J* = 3.8 Hz, 1 H), 2.75 (t, *J* = 7.4 Hz, 2 H), 2.37 (s, 3 H), 2.34 (dd, *J* = 5.9, 4.1 Hz, 1 H), 2.09 - 2.02 (m, 1 H), 1.99 - 1.93 (comp, 2 H), 1.79 (dtd, *J* = 14.3, 7.4, 3.6 Hz, 1 H), 1.25 (d, *J* = 6.2 Hz, 3 H); ^{13}C NMR (125 MHz, CD_3OD) δ 171.2, 138.2, 128.7, 122.8, 122.2, 119.4, 119.3, 115.7, 112.2, 67.4, 56.1, 51.4, 48.3, 45.0, 33.7, 28.4, 25.2, 23.7, 22.3; HRMS (ESI) *m/z* calcd for $C_{19}H_{27}N_3O_2$ $(M+Na)^+$, 352.1995; found, 352.2000.

NMR Assignment. ^{1}H NMR (500 MHz, CD_3OD) δ 7.51 (dt, *J* = 8.0, 1.5 Hz, 1 H, C5-H), 7.30 (dt, *J* = 8.5, 1.0 Hz, 1 H, C2-H), 7.06 (ddd, *J* = 8.5, 7.0, 1.5 Hz, 1 H, C3-H), 7.03 (s, 1 H, C1-H), 6.97 (ddd, *J* = 8.0, 7.0, 1.5 Hz, 1 H, C4-H), 4.41 (t, *J* = 6.2 Hz, 1 H, C13-H), 3.54 (ddd, *J* = 13.4, 8.4, 6.8 Hz, 1 H, C8-H), 3.38 (ddd, *J* = 12.7, 7.5, 6.3 Hz, 1 H, C9-H), 3.28 - 3.20 (comp, 2 H, C9-H and C8-H), 3.16 (p, *J* = 3.8 Hz, 1 H, C11-H), 2.75 (t, *J* = 7.4 Hz, 2 H, C6-H), 2.37 (s, 3 H, C15-H), 2.34 (dd, *J* = 5.9, 4.1 Hz, 1 H, C12-H), 2.09 - 2.02 (m, 1 H, C10-H), 1.99 - 1.93 (comp, 2 H, C7-H), 1.79 (dtd, *J* = 14.3, 7.4, 3.6 Hz, 1 H, C10-H), 1.25 (d, *J* = 6.2 Hz, 3 H, C14-H).

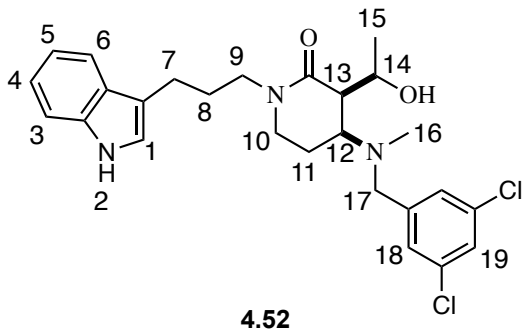

4.52

(3*R*,4*S*)-1-(3-(1*H*-Indol-3-yl)propyl)-4-((3,5-dichlorobenzyl)(methyl)amino)-3-((*R*)-1-hydroxyethyl)piperidin-2-one (4.52). ARMVI56. A solution of **4.56** (100 mg, 0.30 mmol) and 3,5-dichlorobenzaldehyde (159 mg, 0.91 mmol) in acetonitrile (2 mL) was heated under reflux for 2 h. The reaction was cooled to room temperature, at which time $NaBH_3CN$ (22 mg, 0.35 mmol) and acetic acid (glacial, 53 μL, 0.89 mmol) were added. The reaction was stirred for 20 h at room temperature, then partitioned between aqueous NaOH (1 M, 15 mL) and CH_2Cl_2 (30 mL). The two phases were separated, and the aqueous phase was extracted with CH_2Cl_2 (2 x 15 mL). The combined organic fractions were washed with brine (15 mL), dried (Na_2SO_4), filtered, and concentrated *in vacuo* to give crude **4.52** as an opaque viscous oil. The crude material was purified via silica gel flash column chromatography eluting with hexanes : ethyl acetate (1 : 1 → 0 : 1 along a gradient) to give 30 mg (20%) of **4.52** as a white solid: ^{1}H NMR (400 MHz) δ 8.10 (brs, 1 H), 7.57 (d, *J* = 7.6 Hz, 1 H), 7.36 (dt, *J* = 8.4, 0.8 Hz, 1 H), 7.27 (t, *J* = 2.0 Hz, 1 H), 7.21 - 7.17 (m, 1 H), 7.14 (d, *J* = 2.0 Hz, 2 H), 7.11 (ddd, *J* = 8.0, 7.2, 0.8 Hz, 1 H), 7.04 (d, *J* = 2.0 Hz, 1 H), 7.33 (dq, *J* = 8.8, 6.4 Hz, 1 H), 3.62 - 3.55 (comp, 2 H), 3.45 (d, *J* = 13.2 Hz, 1 H), 3.39 - 3.24 (comp, 3 H), 3.14 (dt, *J* = 10.4, 5.6 Hz, 1 H), 2.77

(t, J = 7.2 Hz, 2 H), 2.70 (dd, J = 8.4, 5.6 Hz, 1 H), 2.16 (s, 3 H), 2.13 - 2.05 (comp, 2 H), 1.99 - 1.92 (comp, 2 H), 1.34 (d, J = 6.0 Hz, 3 H); ^{13}C NMR (100 MHz, $CDCl_3$) δ 169.9, 141.2, 136.3, 135.2, 127.8, 127.3, 127.1, 121.9, 121.4, 119.2, 118.7, 115.4, 111.2, 66.5, 60.3, 57.9, 50.2, 46.6, 44.9, 39.5, 27.5, 22.5, 22.5, 21.8; HRMS (ESI) *m/z* calcd for $C_{26}H_{31}Cl_2N_3O_2$ $(M+Na)^+$, 510.1686 and 512.1662; found, 510.1690 and 512.1695.

NMR Assignment. ^{1}H NMR (400 MHz) δ 8.10 (brs, 1 H, N2-H), 7.57 (d, J = 7.6 Hz, 1 H, C6-H), 7.36 (d, J = 8.4 Hz, 1 H, C3-H), 7.27 (t, J = 2.0 Hz, 1 H, C19-H), 7.19 (dt, J = 7.2, 1.2 Hz, 1 H, C4-H), 7.14 (d, J = 2.0 Hz, 2 H, C18-H), 7.11 (ddd, J = 8.0, 7.2, 0.8 Hz, 1 H, C5-H), 7.04 (d, J = 2.0 Hz, 1 H, C1-H), 4.33 (dq, J = 8.8, 6.4 Hz, 1 H, C14-H), 3.62 - 3.55 (comp, 2 H, C17-H and C12-H), 3.45 (d, J = 13.2 Hz, 1 H, C17-H), 3.39 - 3.24 (comp, 3 H, C10-H and C9-H), 3.14 (dt, J = 10.4, 5.6 Hz, 1 H, C10-H), 2.77 (t, J = 7.2 Hz, 2 H, C7-H), 2.70 (dd, J = 8.4, 5.6 Hz, 1 H, C13-H), 2.16 (s, 3H, C16-H), 2.13 - 2.05 (comp, 2 H, C11-H), 1.99 - 1.92 (comp, 2 H, C8-H), 1.34 (d, J = 6.0 Hz, 3 H, C15-H).

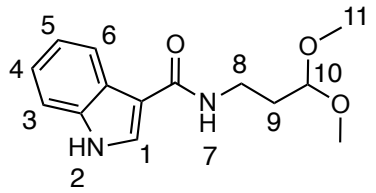

4.61

***N*-(3,3-Dimethoxypropyl)-1*H*-indole-3-carboxamide (4.61). ARMVII143.** Freshly distilled thionyl chloride (0.37 g, 3.2 mmol) was added dropwise over 10 min, followed by addition of DMF (3 drops), to a solution of indole-3-carboxylic acid (0.42 g, 2.6 mmol) in THF (13 mL) at 0 ºC. The reaction was stirred for 1.5 h at 0 ºC and for an additional 0.5 h at room temperature. The solvent was removed *in vacuo*, whereupon the crude material was taken up in CH_2Cl_2 (5 mL), and added dropwise over 10 min to a solution of **4.18** (0.52 g, 2.6 mmol) and triethylamine (0.79 g, 7.8 mmol) in CH_2Cl_2 (50 mL) at 0 ºC. The reaction was stirred for 1 h at 0 ºC, then warmed to room temperature and stirred for an additional 1 h. The mixture was diluted with CH_2Cl_2 (100 mL), and successively washed with saturated aqueous NH_4Cl (100 mL), saturated aqueous Na_2CO_3 (100 mL), water (100 mL) and brine (100 mL). The organic fraction was dried (Na_2SO_4), filtered, and concentrated *in vacuo* to give 0.60 g (88%) of **4.61** as a viscous oil (>95% purity, by ^{1}H NMR): ^{1}H NMR (400 MHz) δ 9.94 (brs, 1 H), 7.95 - 7.93 (m, 1 H), 7.72 (d, J = 2.9 Hz, 1 H), 7.44 - 7.42 (m, 1 H), 7.25 - 7.20 (comp, 2 H), 6.85 (t, J = 4.9 Hz, 1 H), 4.54 (t, J = 5.4 Hz, 1 H), 3.64 (q, J = 5.4 Hz, 2 H), 3.40 (s, 6 H), 1.98 (q, J = 5.4 Hz, 2 H); ^{13}C NMR (100 MHz) δ 165.7, 136.8, 128.9, 124.5, 122.7, 121.5, 119.5, 112.4, 112.2,

104.9, 53.8, 35.6, 32.2; HRMS (ESI) *m/z* calcd for $C_{14}H_{18}N_2O_3$ $(M+Na)^+$, 285.1210; found, 285.1212.

NMR Assignment. ^{1}H NMR (400 MHz) δ 9.94 (brs, 1 H, N2-H), 7.95 - 7.93 (m, 1 H, C3-H), 7.72 (d, *J* = 2.9 Hz, 1 H, C1-H), 7.44 - 7.42 (m, 1 H, C6-H), 7.25 - 7.20 (comp, 2 H, C5-H and C4-H), 6.85 (t, *J* = 4.9 Hz, 1 H, N7-H), 4.54 (t, *J* = 5.4 Hz, 1 H, C10-H), 3.64 (q, *J* = 5.4 Hz, 2 H, C8-H), 3.40 (s, 6 H, C11-H), 1.98 (q, *J* = 5.4 Hz, 2 H, C9-H)

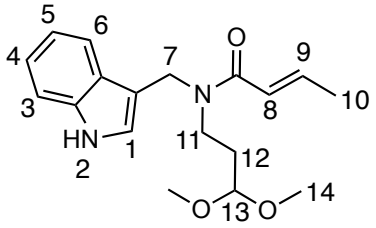

4.63

(*E*)-*N*-((1*H*-Indol-3-yl)methyl)-*N*-(3,3-dimethoxypropyl)but-2-enamide (4.63). **ARMV255/ARMV260**. A solution of **4.61** (140 mg, 0.53 mmol) in THF (3 mL) was added dropwise over 10 min to a stirred suspension of lithium aluminum hydride (101 mg, 2.7 mmol) in THF (10 mL) at 0 ºC. The reaction heated to 65 ºC for 48 h, then cooled to 0 ºC, and the Fieser work-up was carefully performed by successive addition of water (0.1 mL), aqueous NaOH (15%, 0.1 mL), and water (1 mL). The suspension was warmed to room temperature and $MgSO_4$ was added, followed by removal of solids by vacuum filtration through a fritted funnel, and washing with copious amounts of ether and CH_2Cl_2. The filtrate was concentrated *in vacuo* to give 132 mg (quant.) of crude **4.62**

as an opaque viscous oil. Due to the instability of **4.62** towards acid/base extraction and chromatographic conditions, the crude material was immediately carried on to the next step without further purification.

Crotonoyl chloride (66 mg, 0.64 mmol) was added dropwise over 5 min to a stirred solution of crude **4.62** (132 mg, 0.53 mmol) and Hünig's base (165 mg, 1.28 mmol) in CH_2Cl_2 (5 mL) at -78 ºC. The solution was stirred for 2 h at -78 ºC, then partitioned between saturated aqueous $NaHCO_3$ (10 mL) and CH_2Cl_2 (10 mL). The phases were separated, and the aqueous phase extracted with CH_2Cl_2 (2 x 10 mL). The combined organic fractions were successively washed with water (10 mL) and brine (10 mL), dried (Na_2SO_4), filtered, and concentrated *in vacuo* to give crude **4.63** as a viscous yellow oil. The crude material was purified via silica gel flash column chromatography eluting with hexanes : ethyl acetate (2 : 1 → 1 : 1 along a gradient) to give 141 mg (86%, two-steps) of **4.63** as a yellow solid: ^{1}H NMR (400 MHz) (1:1 rotamer mixture) δ 9.04 (brs, 0.5 H), 8.85 (brs, 0.5 H), 7.69 (d, *J* = 7.8 Hz, 0.5 H), 7.53 (d, *J* = 7.8 Hz, 0.5 H), 7.38 (d, *J* = 8.1 Hz, 0.5 H), 7.34 (d, *J* = 8.1 Hz, 0.5 H), 7.23 - 6.96 (comp, 4 H), 6.41 (dd, *J* = 14.9, 1.2 Hz, 0.5 H), 6.34 (dd, *J* = 14.9, 1.2 Hz, 0.5 H), 4.85 (s, 1 H), 4.75 (s, 1 H), 4.40 (t, *J* = 5.5 Hz, 0.5 H), 4.30 (t, *J* = 5.5 Hz, 0.5 H), 3.53 (t, *J* = 7.4 Hz, 1 H), 3.40 (t, *J* = 7.4 Hz, 1 H) 3.28 (s, 6 H), 1.97 - 1.81 (comp, 5 H); ^{13}C NMR (100 MHz) (1 : 1 rotamer mixture) δ 166.0, 165.4, 141.0, 140.9, 135.7, 135.3, 125.9, 124.9, 123.2, 121.5, 121.3, 121.1, 121.1, 120.9, 118.6, 118.2, 117.3, 111.0, 110.6, 110.2, 101.9, 101.3, 52.2,

51.9, 43.5, 41.5, 41.0, 38.9, 31.1, 29.8, 17.3, 17.2; HRMS (ESI) *m/z* calcd for $C_{18}H_{24}N_2O_3$ $(M+Na)^+$, 339.1679; found, 339.1680.

NMR Assignment. ^{1}H NMR (400 MHz) (1:1 rotamer mixture) δ 9.04 (brs, 0.5 H, N2-H), 8.85 (brs, 0.5 H, N2-H), 7.69 (d, *J* = 7.8 Hz, 0.5 H, C6-H), 7.53 (d, *J* = 7.8 Hz, 0.5 H, C6-H), 7.38 (d, *J* = 8.1 Hz, 0.5 H, C3-H), 7.34 (d, *J* = 8.1 Hz, 0.5 H, C3-H), 7.23 - 6.96 (comp, 4 H, C9-H, C5-H, C4-H, and C1-H), 6.41 (dd, *J* = 14.9, 1.2 Hz, 0.5 H, C8-H), 6.34 (dd, *J* = 14.9, 1.2 Hz, 0.5 H, C8-H), 4.85 (s, 1 H, C7-H), 4.75 (s, 1 H, C7-H), 4.40 (t, *J* = 5.5 Hz, 0.5 H, C13-H), 4.30 (t, *J* = 5.5 Hz, 0.5 H, C13-H), 3.53 (t, *J* = 7.4 Hz, 1 H, C11-H), 3.40 (t, *J* = 7.4 Hz, 1 H, C11-H) 3.28 (s, 6 H, C14-H), 1.97 - 1.81 (comp, 5 H, C12-H and C10-H)

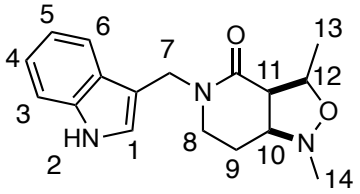

4.64

(3*R*,3a*R*,7a*S*)-5-((1*H*-Indol-3-yl)methyl)-1,3-dimethylhexahydroisoxazolo[4,3-*c*]pyridin-4(1*H*)-one (4.64). ARMV285/ARMV287. A solution of trifluoroacetic acid (36 mg, 0.32 mmol) and **4.63** (100 mg, 0.32 mmol) in a mixture of acetone/water (2 : 1, 6 mL) was stirred for 3 h at room temperature. Saturated aqueous $NaHCO_3$ (20 mL) was added, the layers were separated, and the aqueous layer was extracted with CH_2Cl_2 (3 x 30 mL). The combined organic fractions were dried (Na_2SO_4), filtered, and concentrated

in vacuo. The resulting residue was dissolved in toluene (5 mL), followed by the addition of N-methylhydroxylamine hydrochloride (40 mg, 0.47 mmol) and triethylamine (81 mg, 0.80 mmol). The resulting solution was heated under reflux for 1 h, at which point the solution was cooled to room temperature, and partitioned between saturated aqueous $NaHCO_3$ (20 mL), ethyl acetate (20 mL) and methanol (1 mL). The phases were separated, and the aqueous phase was extracted with ethyl acetate (3 x 20 mL). The combined organic fractions were washed successively with water (50 mL) and brine (50 mL), dried (Na_2SO_4), filtered, and concentrated *in vacuo* to give 76 mg (81%, two-steps) of **4.64** as a colorless oil (>95% purity, by ^{1}H NMR): ^{1}H NMR (400 MHz, CD_3OD) δ 7.57 (dt, *J* = 8.0, 1.0 Hz, 1 H), 7.35 (dt, *J* = 8.2, 0.8 Hz, 1 H), 7.26 (s, 1 H), 7.11 (ddd, *J* = 8.2, 7.1, 1.2 Hz, 1 H), 7.00 (ddd, *J* = 8.0, 7.1, 1.0 Hz, 1 H), 4.78 (s, 2 H), 3.93 - 3.87 (m, 1 H), 3.40 - 3.33 (m, 1 H), 3.20 (dt, *J* = 12.8, 4.3 Hz, 1 H), 2.97 - 2.88 (comp, 2 H), 2.62 (s, 3 H), 1.79 (tt, *J* = 14.4, 4.0 Hz, 1 H), 1.63 (dq, *J* = 14.4, 3.9 Hz, 1 H), 1.45 (d, *J* = 6.0 Hz, 3 H); ^{13}C NMR (100 MHz, CD_3OD) δ 169.2, 136.9, 126.5, 124.5, 121.4, 118.7, 118.4, 111.0, 109.8, 77.3, 66.2, 54.9, 41.4, 41.1, 24.1, 24.1, 18.1; HRMS (ESI) *m/z* calcd for $C_{17}H_{21}N_3O_2$ $(M+Na)^+$, 322.1526; found, 322.1529.

NMR Assignment. ^{1}H NMR (400 MHz, CD_3OD) δ 7.57 (dt, *J* = 8.0, 1.0 Hz, 1 H, C6-H), 7.35 (dt, *J* = 8.2, 0.8 Hz, 1 H, C3-H), 7.26 (s, 1 H, C1-H), 7.11 (ddd, *J* = 8.2, 7.1, 1.2 Hz, 1 H, C4-H), 7.00 (ddd, *J* = 8.0, 7.1, 1.0 Hz, 1 H, C5-H), 4.78 (s, 2 H, C7-H), 3.93 - 3.87 (m, 1 H, C12-H), 3.40 - 3.33 (m, 1 H, C10-H), 3.20 (dt, *J* = 12.8, 4.3 Hz, 1 H, C8-H), 2.97 - 2.88 (comp, 2 H, C11-H and C8-H), 2.62 (s, 3 H, C14-H), 1.79 (tt, *J* = 14.4,

4.0 Hz, 1 H, C9-H), 1.63 (dq, *J* = 14.4, 3.9 Hz, 1 H, C9-H), 1.45 (d, *J* = 6.0 Hz, 3 H, C13-H).

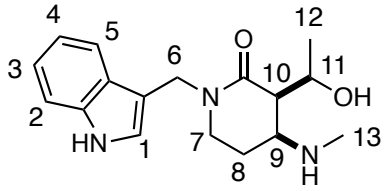

4.65

(3*R*,4*S*)-1-((1*H*-Indol-3-yl)methyl)-3-((*R*)-1-hydroxyethyl)-4-(methylamino)piperidin-2-one (4.65). ARMV298. A mixture of **4.64** (104 mg, 0.35 mmol) and zinc (dust, 680 mg, 10.4 mmol) in acetic acid (aq 80%, 21 mL) was stirred for 48 h at room temperature. Excess zinc was removed via vacuum filtration, and washed with ethyl acetate (150 mL), whereupon zinc acetate immediately precipitated out of solution as a fluffy white solid. The zinc acetate was removed by vacuum filtration and washed with ethyl acetate. The combined filtrate and washes were concentrated *in vacuo*, and the residue dissolved in aqueous HCl (1 M, 50 mL). The resulting solution was washed with ether (50 mL), and carefully basified to pH ~14 with solid NaOH. The basic solution was extracted with CH_2Cl_2 (3 x 75 mL). The combined organic fractions were washed with brine (100 mL), dried (Na_2SO_4), filtered, and concentrated *in vacuo* to give 150 mg (quant) of crude **4.65** as the acetate salt with residual acetic acid. The crude material was taken up in aqueous HCl (1 M, 50 mL) and washed with ether (2 x 50 mL). The aqueous fraction was basified to pH ~14 with solid NaOH, and extracted with

CH_2Cl_2 (3 x 75 mL). The combined organic fractions were successively washed with aqueous NaOH (1 M, 100 mL), saturated aqueous $NaHCO_3$ (100 mL), water (100 mL), and brine (100 mL). The organic fraction was dried (Na_2SO_4), filtered, and concentrated *in vacuo* to give 69 mg (66%) of pure **4.65** as an off white solid: ^{1}H NMR (400 MHz, CD_3OD) δ 7.59 (dt, *J* = 7.9, 0.9 Hz, 1 H), 7.35 (dt, *J* = 8.1, 0.9 Hz, 1 H), 7.24 (s, 1 H), 7.09 (ddd, *J* = 8.1, 7.0, 1.1 Hz, 1 H), 6.98 (ddd, *J* = 7.9, 7.0, 1.0 Hz, 1 H), 4.89 (d, *J* = 14.4 Hz, 1 H), 4.56 (d, *J* = 14.4, 1 H), 4.42 (p, *J* = 6.4 Hz, 1 H), 3.38 (dt, *J* = 12.9, 6.6 Hz, 1 H), 3.28 - 3.21 (comp, 2 H), 2.55 (dd, *J* = 6.5, 4.1 Hz, 1 H), 2.43 (s, 3 H), 2.10 - 2.02 (m, 1 H), 1.88 - 1.83 (m, 1 H), 1.33 (d, *J* = 6.4 Hz, 3 H); ^{13}C NMR (100 MHz, CD_3OD) δ 169.7, 136.8, 126.7, 124.4, 121.3, 118.7, 118.4, 110.9, 110.1, 66.3, 54.8, 50.1, 42.1, 40.8, 32.4, 23.8, 21.0; HRMS (ESI) *m/z* calcd for $C_{17}H_{23}N_3O_2$ $(M+Na)^+$, 324.1682; found, 324.1686.

NMR Assignment. ^{1}H NMR (400 MHz, CD_3OD) δ 7.59 (dt, *J* = 7.9, 0.9 Hz, 1 H, C5-H), 7.35 (dt, *J* = 8.1, 0.9 Hz, 1 H, C2-H), 7.24 (s, 1 H, C1-H), 7.09 (ddd, *J* = 8.1, 7.0, 1.1 Hz, 1 H, C3-H), 6.98 (ddd, *J* = 7.9, 7.0, 1.0 Hz, 1 H, C4-H), 4.89 (d, *J* = 14.4 Hz, 1 H, C6-H), 4.56 (d, *J* = 14.4, 1 H, C6-H), 4.42 (p, *J* = 6.4 Hz, 1 H, C11-H), 3.38 (dt, *J* = 12.9, 6.6 Hz, 1 H, C7-H), 3.28 - 3.21 (comp, 2 H, C9-H and C7-H), 2.55 (dd, *J* = 6.5, 4.1 Hz, 1 H, C10-H), 2.43 (s, 3 H, C13-H), 2.10 - 2.02 (m, 1 H, C8-H), 1.88 - 1.83 (m, 1 H, C8-H), 1.33 (d, *J* = 6.4 Hz, 3 H, C12-H).

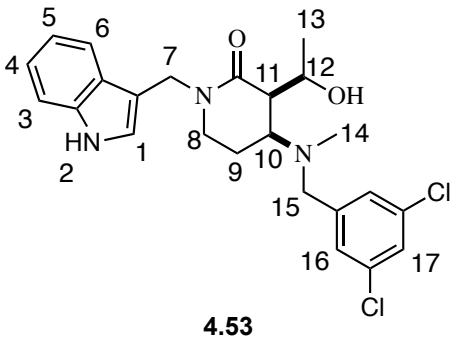

4.53

(3*R*,4*S*)-1-((1*H*-Indol-3-yl)methyl)-4-((3,5-dichlorobenzyl)(methyl)amino)-3-((*R*)-1-hydroxyethyl)piperidin-2-one (4.53). ARMVI41. A solution of **4.65** (75 mg, 0.25 mmol) and 3,5-dichlorobenzaldehyde (131 mg, 0.75 mmol) in acetonitrile (2 mL) was heated under reflux for 5 h. The reaction was cooled to room temperature, and sodium borohydride (28 mg, 0.75 mmol) was added. The solution was stirred at room temperature for 14 h, at which point, LC/MS analysis showed no trace of the desired product. Methanol (1 mL) and acetic acid (0.2 mL) were added, and the solution was stirred for 24 h at room temperature, no product detected by LC/MS. Acetic acid (0.1 mL) and $NaBH_3CN$ (62 mg, 1.0 mmol) were added, and the solution was stirred for an additional 24 h at room temperature. LC/MS analysis showed complete conversion to product and the reaction mixture was partitioned between aqueous NaOH (1 M, 20 mL) and CH_2Cl_2 (25 mL). The two phases were separated, and the aqueous phase extracted with CH_2Cl_2 (2 x 25 mL). The combined organic fractions were washed with water (50 mL), brine (50 mL), dried (Na_2SO_4), filtered, and concentrated *in vacuo* to give crude **4.53** as an amorphous solid. The crude material was purified via silica gel flash column chromatography eluting with CH_2Cl_2 : methanol (1 : 0 → 95 : 5 along a gradient) to give

59 mg (51%) of **4.53** as a white solid: ^{1}H NMR (400 MHz) δ 8.54 (brs, 1 H), 7.68 (d, *J* = 8.0 Hz, 1 H), 7.38 (d, *J* = 8.4 Hz, 1 H), 7.25 - 7.18 (comp, 3 H), 7.09 (ddd, *J* = 8.0, 7.2, 0.8 Hz, 1 H), 7.06 (d, *J* = 2.0 Hz, 2 H), 4.96 (d, *J* = 14.4 Hz, 1 H), 4.51 (d, *J* = 14.4 Hz, 1 H), 4.36 (dq, *J* = 8.4, 5.6 Hz, 1 H), 3.42 - 3.35 (comp, 3 H), 3.23 - 3.11 (comp, 2 H), 2.75 (dd, *J* = 8.8, 6.0 Hz, 1 H), 2.06 (s, 3 H), 1.99 - 1.92 (m, 1 H), 1.86 - 1.78 (m, 1 H), 1.41 (d, *J* = 6.0 Hz, 3 H); ^{13}C NMR (100 MHz) δ 169.7, 141.2, 136.3, 135.1, 127.7, 127.0, 126.8, 124.3, 122.4, 119.9, 119.3, 111.5, 111.3, 66.5, 60.4, 57.5, 50.3, 43.5, 40.8, 38.6, 22.6, 21.6; HRMS (ESI) *m/z* calcd for $C_{26}H_{31}Cl_2N_3O_3$ $(M+Na)^+$, 482.1373 and 484.1348; found, 482.1373 and 484.1349.

NMR Assignment. ^{1}H NMR (400 MHz) δ 8.54 (brs, 1 H, N2-H), 7.68 (d, *J* = 8.0 Hz, 1 H, C6-H), 7.38 (d, *J* = 8.4 Hz, 1 H, C3-H), 7.25 - 7.18 (comp, 3 H, C17-H, C4-H, and C1-H), 7.09 (ddd, *J* = 8.0, 7.2, 0.8 Hz, 1 H, C5-H), 7.06 (d, *J* = 2.0 Hz, 2 H, C16-H), 4.96 (d, *J* = 14.4 Hz, 1 H, C7-H), 4.51 (d, *J* = 14.4 Hz, 1 H, C7-H), 4.36 (dq, *J* = 8.4, 5.6 Hz, 1 H, C12-H), 3.42 - 3.35 (comp, 3 H, C15-H and C10-H), 3.23 - 3.11 (comp, 2 H, C8-H), 2.75 (dd, *J* = 8.8, 6.0 Hz, 1 H, C11-H), 2.06 (s, 3 H, C14-H), 1.99 - 1.92 (m, 1 H, C9-H), 1.86 - 1.78 (m, 1 H, C9-H), 1.41 (d, *J* = 6.0 Hz, 3 H, C13-H).

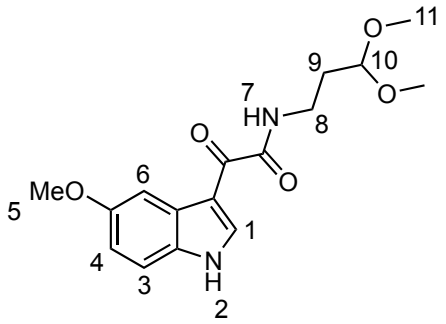

4.68

***N*-(3,3-Dimethoxypropyl)-2-(5-methoxy-1*H*-indol-3-yl)-2-oxoacetamide (4.68). ARMV233/ARMV236.** Oxalyl chloride (0.95 g, 7.5 mmol) was added dropwise over 10 min to a solution of 5-methoxyindole (1.00 g, 6.8 mmol) in ether (15 mL) at 0 ºC, whereupon a red precipitate immediately crashed out of solution and the resulting suspension was stirred for 1 h at room temperature. The precipitate was collected via vacuum filtration, and dried *in vacuo* to give 1.21 g (75%) of 5-methoxyindole-3-glyoxal chloride as a red powder. A slurry of 5-methoxyindole-3-glyoxal chloride (1.21 g, 5.1 mmol) in CH_2Cl_2 (10 mL) was added dropwise over 10 min to a solution of **4.18** (1.02 g, 5.1 mmol) and triethylamine (1.29 g, 12.8 mmol) in CH_2Cl_2 (50 mL) at 0 ºC, and the reaction was stirred for 2 h at room temperature. Saturated aqueous $NaHCO_3$ (50 mL) was added, the two phases were separated, and the aqueous phase extracted with CH_2Cl_2 (3 x 100 mL). The combined organic fractions were washed with water (100 mL), brine (100 mL), dried (Na_2SO_4), filtered, and concentrated *in vacuo* to give 1.59 g (98%) of **4.68** as a light pale yellow solid of (>95% purity, by ^{1}H NMR): ^{1}H NMR (400 MHz) δ 9.10 (brs, 1 H), 9.03 (d, J = 3.2 Hz, 1 H), 7.93 (d, J = 2.5 Hz, 1 H), 7.87 (t, J = 5.3 Hz, 1

H), 7.32 (d, *J* = 8.8 Hz, 1 H), 6.93 (dd, *J* = 8.8, 2.5 Hz, 1 H) 4.50 (t, *J* = 5.4 Hz, 1 H), 3.90 (s, 3 H), 3.49 (t, *J* = 6.1 Hz, 2 H), 3.39 (s, 6 H), 1.92 (q, *J* = 5.8 Hz, 2 H); ^{13}C NMR (125 MHz) δ 180.6, 162.5, 156.9, 138.2, 130.4, 127.6, 114.3, 113.2, 112.4, 103.9, 103.6, 55.8, 53.4, 35.2, 31.8; HRMS (ESI) *m/z* calcd for $C_{16}H_{20}N_2O_5$ $(M+Na)^+$, 343.1264; found, 343.1264.

NMR Assignment. ^{1}H NMR (400 MHz) δ 9.10 (brs, 1 H, N2-H), 9.03 (d, *J* = 3.2 Hz, 1 H, C1-H), 7.93 (d, *J* = 2.5 Hz, 1 H, C6-H), 7.87 (t, *J* = 5.3 Hz, 1 H, N7-H), 7.32 (d, *J* = 8.8 Hz, 1 H, C3-H), 6.93 (dd, *J* = 8.8, 2.5 Hz, 1 H, C4-H) 4.50 (t, *J* = 5.4 Hz, 1 H, C10-H), 3.90 (s, 3 H, C5-H), 3.49 (t, *J* = 6.1 Hz, 2 H, C8-H), 3.39 (s, 6 H, C11-H), 1.92 (q, *J* = 5.8 Hz, 2 H, C9-H).

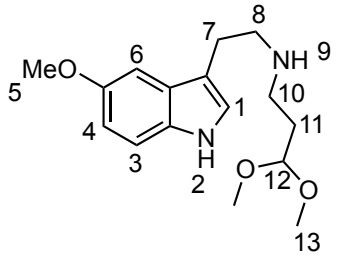

4.69

3,3-Dimethoxy-*N*-(2-(5-Methoxy-1*H*-indol-3-yl)ethyl)propan-1-amine (4.69). **ARMVII110.** A solution of **4.68** (200 mg, 0.62 mmol) in THF (5 mL) was added dropwise over 5 min to a suspension of lithium aluminum hydride (231 mg, 6.2 mmol) in THF (15 mL) at 0 ºC. The reaction heated to 65 ºC for 14 h. The reaction was then cooled to 0 ºC, and the Fieser work-up was carefully performed by successive addition of water

(0.25 mL), aqueous NaOH (15%, 0.25 mL), and water (1 mL). The suspension was warmed to room temperature and $MgSO_4$ was added. The solids were removed by vacuum filtration through a fritted funnel and washed with copious amounts of CH_2Cl_2. The filtrate was concentrated *in vacuo* to give crude **4.69** as an opaque viscous oil. The crude material was purified via acid/base extraction. The crude oil was taken up into aqueous HCl (0.2 M, 100 mL) and washed with ether (2 x 75 mL). The aqueous fraction was basified to pH 12 - 14 by dropwise addition of aqueous NaOH (40% w/v). The basic solution was extracted with CH_2Cl_2 (4 x 100 mL). The combined organic fractions were washed with saturated aqueous $NaHCO_3$ (200 mL), water (200 mL), brine (200 mL), dried (Na_2SO_4), filtered, and concentrated *in vacuo* to give 164 mg (90%) of **4.69** as an oil (>95% purity, by ^{1}H NMR): ^{1}H NMR (400 MHz) δ 8.58 (brs, 1 H), 7.23 (dd, *J* = 8.0, 0.5 Hz, 1 H), 7.05 (d, *J* = 2.4 Hz, 1 H), 6.99 (d, *J* = 2.4 Hz, 1 H), 6.83 (dd, *J* = 8.0, 2.4 Hz, 1 H), 4.38 (t, *J* = 5.6 Hz, 1 H), 3.85 (s, 3 H), 3.24 (s, 6 H), 2.95 (app s, 4 H), 2.72 (t, *J* = 7.2 Hz, 2 H), 1.80 (td, *J* = 7.2, 5.6 Hz, 2 H); ^{13}C NMR (100 MHz) δ 153.8, 131.6, 127.7, 123.0, 113.0, 112.1, 111.9, 103.6, 100.6, 55.9, 53.0, 49.8, 45.2, 32.5, 25.4; HRMS (ESI) *m/z* calcd for $C_{16}H_{24}N_2O_3$ $(M+1)^+$, 293.1860; found, 293.1870.

NMR Assignment. ^{1}H NMR (400 MHz) δ 8.58 (brs, 1 H, N2-H), 7.23 (dd, *J* = 8.0, 0.5 Hz, 1 H, C3-H), 7.05 (d, *J* = 2.4 Hz, 1 H, C1-H), 6.99 (d, *J* = 2.4 Hz, 1 H, C6-H), 6.83 (dd, *J* = 8.0, 2.4 Hz, 1 H, C4-H), 4.38 (t, *J* = 5.6 Hz, 1 H, C12-H), 3.85 (s, 3 H, C5-H), 3.24 (s, 6 H, C13-H), 2.95 (app s, 4 H, C7-H and C8-H), 2.72 (t, *J* = 7.2 Hz, 2 H, C10-H), 1.80 (td, *J* = 7.2, 5.6 Hz, 2 H, C11-H).

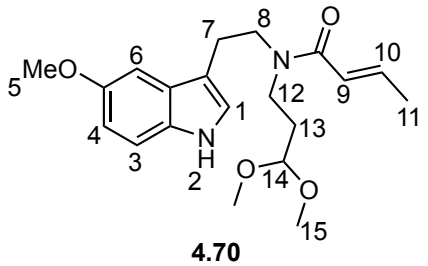

4.70

(*E*)-*N*-(3,3-Dimethoxypropyl)-*N*-(2-(5-methoxy-1*H*-indol-3-yl)ethyl)but-2-enamide (4.70). ARMVII109. Crotonoyl chloride (0.53 g, 5.1 mmol) was added dropwise over 5 min to a solution of **4.69** (1.24 g, 4.2 mmol) and Hünig's base (1.32 g, 10.8 mmol) in CH_2Cl_2 (42 mL) at -78 ºC. The reaction was stirred for 2 h at -78 ºC. Saturated aqueous $NaHCO_3$ (40 mL) was added and the mixture was stirred for 20 min at room temperature. The phases were separated, and the aqueous phase was extracted with CH_2Cl_2 (3 x 40 mL). The combined organic fractions were washed with saturated aqueous NH_4Cl (100 mL), water (100 mL), brine (100 mL), dried (Na_2SO_4), filtered, and concentrated *in vacuo* to give crude **4.70** as an opaque oil. The crude material was purified via silica gel flash column chromatography eluting with hexanes : ethyl acetate (1 : 1 → 1 : 2 along a gradient) to give 1.08 g (71%) of **4.70** as an oil: ^{1}H NMR (400 MHz) (1:1 mixture of rotamers) δ 8.78 (brs, 0.5 H), 8.65 (brs, 0.5 H), 7.21 (app t, *J* = 8.9 Hz, 1H), 7.11 (d, *J* = 2.2 Hz, 0.5 H), 7.05 - 6.74 (comp, 3.5 H), 6.30 (dd, *J* = 14.9, 1.6 Hz, 0.5 H), 6.02 (dd, *J* = 14.9, 1.6 Hz, 0.5 H), 4.39 (t, *J* = 5.6 Hz, 0.5 H), 4.31 (t, *J* = 5.6 Hz, 0.5 H), 3.87 (s, 1.5 H), 3.84 (s, 1.5 H), 3.66 (t, *J* = 7.1 Hz, 1 H), 3.61 (t, *J* = 7.1 Hz, 1 H), 3.44 (t, *J* = 7.3 Hz, 1 H), 3.35 (t, *J* = 7.3 Hz, 1 H), 3.30 (s, 3 H), 3.28 (s, 3 H), 3.01 (t, *J* = 7.1 Hz, 1 H), 2.96 (t, *J* = 7.1 Hz, 1 H) 1.94 - 1.79 (comp, 3.5 H), 1.66 (dd, *J* = 6.8, 1.4

Hz, 1.5 H); ^{13}C NMR (100 MHz) (1:1 mixture of rotamers) δ 166.7, 166.5, 154.0, 153.8, 141.9, 141.0, 131.6, 131.5, 127.8, 127.5, 123.3, 122.9, 121.8, 121.7, 112.7, 112.2, 112.1, 112.0, 111.4, 102.9, 102.1, 100.5, 100.1, 55.9, 55.9, 53.1, 53.0, 48.6, 47.7, 44.2, 42.9, 32.5, 30.9, 25.4, 23.7, 18.3, 18.0; HRMS (ESI) *m/z* calcd for $C_{20}H_{28}N_2O_4$ $(M+Na)^+$, 383.1941; found, 383.1943.

NMR Assignment. ^{1}H NMR (400 MHz) (1:1 mixture of rotamers) δ 8.78 (brs, 0.5 H, N2-H), 8.65 (brs, 0.5 H, N2-H), 7.21 (app t, *J* = 8.9 Hz, 1H, C3-H), 7.11 (d, *J* = 2.2 Hz, 0.5 H, C6-H), 7.05 - 6.74 (comp, 3.5 H, C10-H, C6-H, and C4-H), 6.30 (dd, *J* = 14.9, 1.6 Hz, 0.5 H, C9-H), 6.02 (dd, *J* = 14.9, 1.6 Hz, 0.5 H, C9-H), 4.39 (t, *J* = 5.6 Hz, 0.5 H, C14-H), 4.31 (t, *J* = 5.6 Hz, 0.5 H, C14-H), 3.87 (s, 1.5 H, C5-H), 3.84 (s, 1.5 H, C5-H), 3.66 (t, *J* = 7.1 Hz, 1 H, C8-H), 3.61 (t, *J* = 7.1 Hz, 1 H, C8-H), 3.44 (t, *J* = 7.3 Hz, 1 H, C16-H), 3.35 (t, *J* = 7.3 Hz, 1 H, C16-H), 3.30 (s, 3 H, C15-H), 3.28 (s, 3 H, C15-H), 3.01 (t, *J* = 7.1 Hz, 1 H, C7-H), 2.96 (t, *J* = 7.1 Hz, 1 H, C7-H) 1.94 - 1.79 (comp, 3.5 H, C13-H and C11-H), 1.66 (dd, *J* = 6.8, 1.4 Hz, 1.5 H, C11-H).

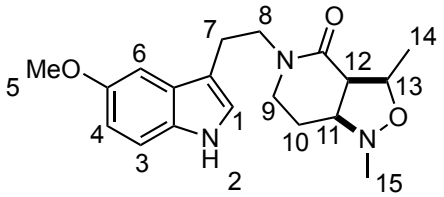

4.71

(3*R*,3a*R*,7a*S*)-5-(2-(5-Methoxy-1*H*-indol-3-yl)ethyl)-1,3-dimethylhexahydroisoxazolo[4,3-*c*]pyridin-4(1*H*)-one (4.71). ARMVII113-ARMVII114. A solution of **4.70** (250 mg, 0.69 mmol) and TFA (5 drops) in a mixture of TFE/water (3 : 1, 12 mL) was stirred for 1 h at room temperature. The reaction was poured into saturated aqueous $NaHCO_3$ (30 mL), and extracted with CH_2Cl_2 (3 x 50 mL). The combined organic fractions were washed with water (50 mL), dried (Na_2SO_4), filtered, and concentrated *in vacuo*. The resulting residue was dissolved in toluene (10 mL), followed by the addition of N-methylhydroxylamine hydrochloride (86 mg, 1.04 mmol) and triethylamine (175 mg, 1.73 mmol). The reaction was heated under reflux for 2 h, whereupon the mixture was cooled to room temperature, and partitioned between saturated aqueous $NaHCO_3$ (50 mL), ethyl acetate (50 mL) and methanol (2 mL). The phases were separated, and the aqueous phase was extracted with ethyl acetate (3 x 50 mL). The combined organic fractions were washed with water (100 mL), brine (100 mL), dried (Na_2SO_4), filtered, and concentrated *in vacuo* to give 202 mg (85%) of **4.71** as a viscous oil (>95% purity, by ^{1}H NMR): ^{1}H NMR (400 MHz) δ 8.11 (brs, 1 H), 7.25 (d, *J* = 8.8 Hz, 1 H), 7.07 (d, *J* = 2.4 Hz, 1 H), 7.01 (d, *J* = 2.1 Hz, 1 H), 6.85 (dd, *J* = 8.8, 2.4 Hz, 1 H), 3.92 - 3.87 (comp, 4 H), 3.76 (dt, *J* = 13.3, 7.7 Hz, 1 H), 3.65 (dt, *J* = 13.3, 7.0

Hz, 1 H), 3.56 (td, *J* = 11.8, 3.0 Hz, 1 H), 3.01 - 2.95 (comp, 3 H), 2.87 - 2.79 (comp, 2 H), 2.66 (s, 3 H), 1.79 (tt, *J* = 11.2, 4.2 Hz, 1 H), 1.61 (dq, *J* = 11.2, 3.4 Hz, 1 H), 1.46 (d, *J* = 6.1 Hz, 3 H); ^{13}C NMR (100 MHz) δ 169.1, 154.0, 131.6, 127.8, 123.0, 112.5, 112.13, 112.06, 100.7, 77.5, 66.2, 56.1, 55.4, 48.5, 44.1, 43.3, 25.1, 23.5, 19.4; HRMS (ESI) *m/z* calcd for $C_{19}H_{25}N_3O_3$ $(M+Na)^+$, 366.1788; found, 266.1794.

NMR Assignment. ^{1}H NMR (400 MHz) δ 8.11 (brs, 1 H, N2-H), 7.25 (d, *J* = 8.8 Hz, 1 H, C3-H), 7.07 (d, *J* = 2.4 Hz, 1 H, C6-H), 7.01 (d, *J* = 2.1 Hz, 1 H, C1-H), 6.85 (dd, *J* = 8.8, 2.4 Hz, 1 H, C4-H), 3.92 - 3.87 (comp, 4 H, C13-H and C5-H), 3.76 (dt, *J* = 13.3, 7.7 Hz, 1 H, C8-H), 3.65 (dt, *J* = 13.3, 7.0 Hz, 1 H, C8-H), 3.56 (td, *J* = 11.8, 3.0 Hz, 1 H, C11-H), 3.01 - 2.95 (comp, 3 H, C12-H and C9-H), 2.87 - 2.79 (comp, 2 H, C7-H), 2.66 (s, 3 H, C15-H), 1.79 (tt, *J* = 11.2, 4.2 Hz, 1 H, C10-H), 1.61 (dq, *J* = 11.2, 3.4 Hz, 1 H, C10-H), 1.46 (d, *J* = 6.1 Hz, 3 H, C14-H)

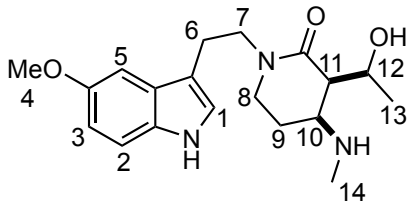

4.72

(3*R*,4*S*)-3-((*R*)-1-Hydroxyethyl)-1-(2-(5-methoxy-1*H*-indol-3-yl)ethyl)-4-(methylamino)piperidin-2-one (4.72). ARMVII129. Zinc (powder, 588 mg, 9.00 mmol) was added in three portions over 1.5 h to a solution of **4.71** (100 mg, 0.30 mmol) in acetic acid (aq 80%, 20 mL) at 60 ºC. The reaction was stirred for 1 h at 60 ºC. The

suspension was cooled to room temperature, excess zinc was filtered and washed with ethyl acetate. To the filtrate was added ethyl acetate (100 mL), upon which zinc acetate immediately precipitated out of solution as a fluffy white solid. The zinc acetate was filtered and washed with ethyl acetate. The solvent was removed *in vacuo* to give crude **4.72**. the crude material was taken up in aqueous HCl (1 M, 30 mL), and washed with ether (2 x 30 mL). The aqueous fraction was basified to pH ~14 with aqueous NaOH (40% w/v), and extracted with CH_2Cl_2 (4 x 50 mL). The organic fractions were washed with saturated aqueous $NaHCO_3$ (100 mL), water (100 mL), and brine (1 x 100 mL). The organic fractions were dried (Na_2SO_4), filtered, and concentrated *in vacuo* to give 86 mg (85%) of **4.72** as an oil (>95% purity, by ^{1}H NMR): ^{1}H NMR (400 MHz, CD_3OD) δ 7.22 (d, *J* = 8.8 Hz, 1 H), 7.08 (d, *J* = 2.3 Hz, 1 H), 7.04 (s, 1 H), 6.75 (dd, *J* = 8.8, 2.3 Hz, 1 H), 4.40 (p, *J* = 6.2 Hz, 1 H), 3.83 (s, 3 H), 3.71 - 3.65 (m, 1 H), 3.52 (dt, *J* = 13.2, 7.2 Hz, 1 H), 3.14 - 2.92 (comp, 5 H), 2.38 (dd, *J* = 5.8, 4.1 Hz, 1 H), 2.33 (s, 3 H), 1.97 (dq, *J* = 13.7, 6.1 Hz, 1 H), 1.70 (dtd, *J* = 13.7, 6.9, 3.5 Hz, 1 H), 1.23 (d, *J* = 6.4 Hz, 3 H); ^{13}C NMR (100 MHz, CD_3OD) δ 169.7, 135.6, 131.9, 127.8, 123.0, 111.6, 111.4, 111.2, 99.9, 66.1, 54.9, 54.6, 50.0, 48.2, 44.3, 32.2, 23.6, 22.3, 21.0; HRMS (ESI) *m/z* calcd for $C_{19}H_{27}N_3O_3$ $(M+H)^+$, 346.2125; found, 346.2124.

NMR Assignment. ^{1}H NMR (400 MHz, CD_3OD) δ 7.22 (d, *J* = 8.8 Hz, 1 H, C2-H), 7.08 (d, *J* = 2.3 Hz, 1 H, C5-H), 7.04 (s, 1 H, C1-H), 6.75 (dd, *J* = 8.8, 2.3 Hz, 1 H, C3-H), 4.40 (p, *J* = 6.2 Hz, 1 H, C12-H), 3.83 (s, 3 H, C4-H), 3.71 -3.65 (m, 1 H, C7-H), 3.52 (dt, *J* = 13.2, 7.2 Hz, 1 H, C7-H), 3.14 - 2.92 (comp, 5 H, C10-H, C8-H, and C6-H),

2.38 (dd, *J* = 5.8, 4.1 Hz, 1 H, C11-H), 2.33 (s, 3 H, C14-H), 1.97 (dq, *J* = 13.7, 6.1 Hz, 1 H, C9-H), 1.70 (dtd, *J* = 13.7, 6.9, 3.5 Hz, 1 H, C9-H), 1.23 (d, *J* = 6.4 Hz, 3 H, C13-H).

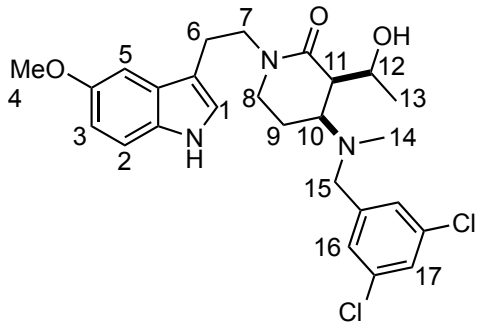

4.73

(3*R*,4*S*)-4-((3,5-Dichlorobenzyl)(methyl)amino)-3-((*R*)-1-hydroxyethyl)-1-(2-(5-methoxy-1*H*-indol-3-yl)ethyl)piperidin-2-one (4.73). ARMV252. Prepared according to the representative procedure for compound **4.12**; scaled to **4.72** (75 mg, 0.22 mmol). The crude material was purified via silica gel flash column chromatography eluting with hexanes : ethyl acetate (3 : 1 → 1 : 3 along a gradient) to give 97 mg (89%) of **4.73** as a white solid: ^{1}H NMR (600 MHz, CD_3OD) δ 7.34 (t, *J* = 1.9 Hz, 1 H), 7.22 - 7.21 (comp, 3 H), 7.07 (d, *J* = 2.1 Hz, 1 H), 7.04 (s, 1 H), 6.76 (ddd, *J* = 8.7, 2.4, 0.3 Hz, 1 H), 4.22 (dq, *J* = 8.7, 6.1, 1 H), 3.82 (s, 3 H), 3.76 (dt, *J* = 13.3, 7.6 Hz, 1 H), 3.55 (ddd, *J* = 13.4, 7.7, 5.8 Hz, 1 H), 3.50 (d, *J* = 13.4 Hz, 1 H), 3.41 (d, *J* = 13.4 Hz, 1 H), 3.36 - 3.32 (m, 1 H), 3.17 - 3.08 (comp, 2 H), 3.02 (p, *J* = 7.2 Hz, 1 H), 2.93 (ddd, *J* = 13.7, 7.8, 5.9 Hz, 1 H), 2.58 (dd, *J* = 8.4, 5.7 Hz, 1 H), 2.07 (s, 3 H), 1.99 (dt, *J* = 12.3, 5.7 Hz, 1 H), 1.96 - 1.91 (m, 1 H), 1.21 (d, *J* = 6.1 Hz, 3 H); ^{13}C NMR (150 MHz, CD_3OD) δ

172.0, 155.0, 143.7, 136.2, 133.4, 129.2, 128.5, 128.5, 124.5, 113.0, 112.6, 112.6, 101.5, 67.7, 61.2, 58.4, 56.4, 51.2, 48.8, 46.6, 38.5, 24.0, 22.8, 22.5; HRMS (ESI) *m/z* calcd for $C_{26}H_{31}Cl_2N_3O_3$ $(M+H)^+$, 504.1815 and 506.1792; found, 504.1815 and 506.1795.

NMR Assignment. ^{1}H NMR (600 MHz, CD_3OD) δ 7.34 (t, *J* = 1.9 Hz, 1 H, C17-H), 7.22 - 7.21 (comp, 3 H, C16-H and C2-H), 7.07 (d, *J* = 2.1 Hz, 1 H, C5-H), 7.04 (s, 1 H, C1-H), 6.76 (ddd, *J* = 8.7, 2.4, 0.3 Hz, 1 H, C3-H), 4.22 (dq, *J* = 8.7, 6.1, 1 H, C12-H), 3.82 (s, 3 H, C4-H), 3.76 (dt, *J* = 13.3, 7.6 Hz, 1 H, C7-H), 3.55 (ddd, *J* = 13.4, 7.7, 5.8 Hz, 1 H, C7-H), 3.50 (d, *J* = 13.4 Hz, 1 H, C15-H), 3.41 (d, *J* = 13.4 Hz, 1 H, C15-H), 3.36 - 3.32 (m, 1 H, C8-H), 3.17 - 3.08 (comp, 2 H, C10-H and C8-H), 3.02 (dt, *J* = 14.5, 7.2 Hz, 1 H, C6-H), 2.93 (ddd, *J* = 13.7, 7.8, 5.9 Hz, 1 H, C6-H), 2.58 (dd, *J* = 8.4, 5.7 Hz, 1 H, C11-H), 2.07 (s, 3 H, C14-H), 1.99 (dt, *J* = 12.3, 5.7 Hz, 1 H, C9-H), 1.96 - 1.91 (m, 1 H, C9-H), 1.21 (d, *J* = 6.1 Hz, 3 H, C13-H).

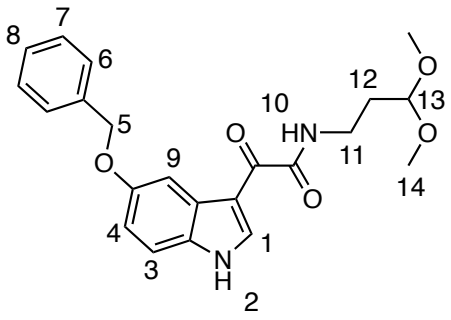

4.75

2-(5-(Benzyloxy)-1*H*-indol-3-yl)-*N*-(3,3-dimethoxypropyl)-2-oxoacetamide (4.75). ARMV281/ARMV237. Oxalyl chloride (1.25 g, 9.9 mmol) was added dropwise over 10 min to a solution of 5-benzyloxyindole (2.0 g, 9.0 mmol) in ether (18 mL) at 0 ºC. The solution was stirred for 2 h at 0 ºC, whereupon a red precipitate was isolated via vacuum filtration, and dried *in vacuo* to give 2.37 g (84%) of 5-benzyloxyindole-3-glyoxal chloride. A suspension of 5-benzyloxyindole-3-glyoxal chloride (0.97 g, 3.1 mmol) in CH_2Cl_2 (10 mL) was added dropwise over 10 min to a solution of **4.18** (0.62 g, 3.1 mmol) and triethylamine (0.78 g, 7.8 mmol) in CH_2Cl_2 (30 mL) at 0 ºC. The reaction was stirred for 2 h at 0 ºC. The reaction was poured into saturated aqueous $NaHCO_3$ (40 mL), the phases were separated, and the aqueous phase was extracted with CH_2Cl_2 (3 x 40 mL). The combined organic fractions were washed with water (100 mL) and brine (100 mL), dried (Na_2SO_4), filtered, and concentrated *in vacuo* to give 1.16 (95%) of **4.75** as a yellow solid (>95% purity, by ^{1}H NMR): ^{1}H NMR (400 MHz) δ 9.16 (brs, 1 H), 9.03 (d, *J* = 2.8 Hz, 1 H), 8.05 (d, *J* = 2.5 Hz, 1 H), 7.88 (t, *J* = 5.6 Hz, 1 H), 7.50 (d, *J* = 7.1 Hz, 2 H), 7.40 (t, *J* = 7.1 Hz, 2 H), 7.35 - 7.32 (comp, 2 H), 7.02 (dd, *J* = 8.7, 2.5 Hz, 1

H), 5.16 (s, 2 H), 4.51 (t, *J* = 5.4 Hz, 1 H), 3.59 (q, *J* = 6.7 Hz, 2 H), 3.39 (s, 6 H), 1.93 (q, *J* = 6.7 Hz, 2 H); ^{13}C NMR (100 MHz, CD_3CN) δ 181.5, 162.9, 155.9, 139.2, 138.0, 131.3, 128.7, 128.1, 127.9, 126.3, 114.4, 113.4, 112.7, 105.2, 103.7, 70.3, 53.0, 35.1, 32.3; HRMS (ESI) *m/z* calcd for $C_{22}H_{24}N_2O_5$ $(M+Na)^+$, 419.1577; found, 419.1575.

NMR Assignment. ^{1}H NMR (400 MHz) δ 9.16 (brs, 1 H, N2-H), 9.03 (d, *J* = 2.8 Hz, 1 H, C1-H), 8.05 (d, *J* = 2.5 Hz, 1 H, C9-H), 7.88 (t, *J* = 5.6 Hz, 1 H, N10-H), 7.50 (d, *J* = 7.1 Hz, 2 H, C6-H), 7.40 (t, *J* = 7.1 Hz, 2 H, C7-H), 7.35 - 7.32 (comp, 2 H, C8-H and C3-H), 7.02 (dd, *J* = 8.7, 2.5 Hz, 1 H, C4-H), 5.16 (s, 2 H, C5-H), 4.51 (t, *J* = 5.4 Hz, 1 H, C13-H), 3.59 (q, *J* = 6.7 Hz, 2 H, C11-H), 3.39 (s, 6 H, C14-H), 1.93 (q, *J* = 6.7 Hz, 2 H, C12-H).

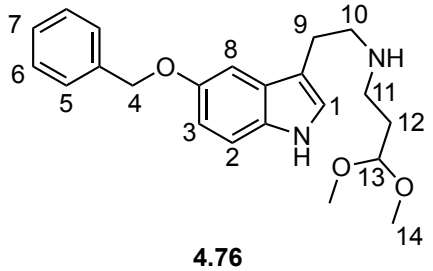

4.76

***N*-(2-(5-(Benzyloxy)-1*H*-indol-3-yl)ethyl)-3,3-dimethoxypropan-1-amine (4.76). ARMV256.** A solution of **4.75** (1.16 g, 2.93 mmol) in THF (15 mL) was added dropwise over 20 min to a suspension of lithium aluminum hydride (1.10 g, 29.3 mmol) in THF (70 mL) at 0 ºC. The reaction heated under reflux for 14 h, whereupon the reaction was cooled to 0 ºC, and the Fieser work-up was carefully performed by

successive addition of water (1.1 mL), aqueous NaOH (15%, 1.1 mL), and water (3.3 mL). The suspension was warmed to room temperature and $MgSO_4$ was added. The solids were removed by vacuum filtered through a fritted funnel, and washed with copious amounts of CH_2Cl_2. The filtrate was concentrated *in vacuo* to give crude **4.76** as an opaque viscous oil. The crude oil was taken up into aqueous HCl (0.2 M, 200 mL) and washed with ether (2 x 150 mL). The aqueous fraction was basified to pH 12-14 by addition of solid NaOH, as judged by pH paper. The basic solution was extracted with CH_2Cl_2 (4 x 200 mL). The combined organic fractions were washed with saturated aqueous $NaHCO_3$ (400 mL), water (400 mL), brine (400 mL), dried (Na_2SO_4), filtered, and concentrated *in vacuo* to give 1.02 g (94%) of **4.76** as an oil (>95% purity, by ^{1}H NMR): ^{1}H NMR (400 MHz) δ 8.41 (brs, 1 H), 7.49 (d, *J* = 7.2 Hz, 2 H), 7.34 (td, *J* = 7.2, 1.6 Hz, 2 H), 7.33 (tt, *J* = 7.2, 1.6 Hz, 1 H), 7.23 (d, *J* = 8.8 Hz, 1 H), 7.16 (d, *J* = 2.4 Hz, 1 H), 6.97 (d, *J* = 2.0 Hz, 1 H), 6.94 (dd, *J* = 8.8, 2.4 Hz, 1 H), 5.11 (s, 2 H), 4.41 (t, *J* = 5.6 Hz, 1 H), 3.28 (s, 6 H), 2.94 (app s, 4 H), 2.72 (t, *J* = 7.2 Hz, 2 H), 1.82 (td, *J* = 7.2, 5.6 Hz, 2 H); ^{13}C NMR (100 MHz) δ 153.0, 137.7, 131.8, 128.5, 127.82, 127.77 127.6, 123.0, 113.5, 112.8, 111.9, 103.6, 102.5, 71.0, 52.9, 49.9, 45.3, 32.8, 25.7; HRMS (CI) *m/z* calcd for $C_{22}H_{28}N_2O_3$ $(M+H)^+$, 369.2178; found, 369.2181.

NMR Assignment. ^{1}H NMR (400 MHz) δ 8.41 (brs, 1 H, NH), 7.49 (d, *J* = 7.2 Hz, 2 H, C5-H), 7.34 (td, *J* = 7.2, 1.6 Hz, 2 H, C6-H), 7.33 (tt, *J* = 7.2, 1.6 Hz, 1 H, C7-H), 7.23 (d, *J* = 8.8 Hz, 1 H, C2-H), 7.16 (d, *J* = 2.4 Hz, 1 H, C8-H), 6.97 (d, *J* = 2.0 Hz, 1 H, C1-H), 6.94 (dd, *J* = 8.8, 2.4 Hz, 1 H, C3-H), 5.11 (s, 2 H, C4-H), 4.41 (t, *J* = 5.6

Hz, 1 H, C13-H), 3.28 (s, 6 H, C14-H), 2.94 (app s, 4 H, C9-H and C10-H), 2.72 (t, *J* = 7.2 Hz, 2 H, C11-H), 1.82 (td, *J* = 7.2, 5.6 Hz, 2 H, C12-H).

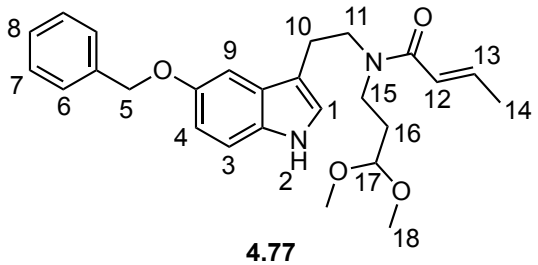

4.77

(*E*)-*N*-(2-(5-(Benzyloxy)-1*H*-indol-3-yl)ethyl)-*N*-(3,3-dimethoxypropyl)but-2-enamide (4.77). ARMV259. Crotonoyl chloride (0.35 g, 3.3 mmol) was added dropwise over 5 min to a solution of **4.76** (1.02 g, 2.8 mmol) and Hünig's base (0.85 g, 6.6 mmol) in CH_2Cl_2 (30 mL) at -78 ºC. The reaction was stirred for 2 h at –78 ºC, whereupon saturated aqueous $NaHCO_3$ (30 mL) was added, and the resulting solution was stirred for 20 min at room temperature. The phases were separated, and the aqueous phase was extracted with CH_2Cl_2 (3 x 30 mL). The combined organic fractions were washed with, water (50 mL), brine (50 mL), dried (Na_2SO_4), filtered, and concentrated *in vacuo* to give crude **4.77** as an opaque oil. The crude material was purified via silica gel flash column chromatography eluting with hexanes : ethyl acetate (2 : 1 → 1 : 1 along a gradient) to give 0.73 g (61%) of **4.77** as an oil: ^{1}H NMR (400 MHz) (1:1 mixture of rotamers) δ 8.65 (brs, 0.5 H), 8.53 (brs, 0.5), 7.50 - 7.48 (comp, 2 H), 7.41 - 7.37 (comp, 2 H), 7.34 - 7.30 (m ,1 H), 7.26 - 7.23 (comp, 1.5 H), 7.11 (d, *J* = 2.2 Hz, 0.5), 7.02 (dq, *J* = 13.8, 6.9 Hz, 0.5 H), 6.96 - 6.88 (comp, 2 H), 6.78 (dq, *J* = 13.8, 6.9 Hz, 0.5 H), 6.32 (dd, *J* = 14.9,

1.6 Hz, 0.5 H), 5.98 (dd, *J* = 14.9, 1.6 Hz, 0.5 H), 5.13 (s, 1 H), 5.10 (s, 1 H), 4.41 (t, *J* = 5.6 Hz, 0.5 H), 4.33 (t, *J* = 5.6 Hz, 0.5 H), 3.67 (t, *J* = 7.3 Hz, 1 H), 3.60 (t, *J* = 7.3 Hz, 1 H), 3.45 (t, *J* = 7.5 Hz, 1 H), 3.37 - 3.30 (comp, 7 H), 3.03 (t, *J* = 7.3 Hz, 1 H), 2.96 (t, *J* = 7.3 Hz, 1 H), 1.96 - 1.90 (comp, 2 H), 1.85 - 1.80 (comp, 1.5 H), 1.66 (dd, *J* = 6.8, 1.5 Hz, 1.5); ^{13}C NMR (100 MHz) (1:1 mixture of rotamers) δ 166.7, 166.6, 153.1, 153.1, 141.9, 141.0, 137.7, 137.6, 131.8, 131.7, 128.5, 128.5, 127.8, 127.7, 127.6, 127.5, 123.4, 123.0, 121.8, 121.8, 112.9, 112.8, 112.7, 112.0, 111.4, 102.9, 102.1, 102.0, 71.1, 70.9, 53.2, 53.0, 48.6, 47.8, 44.2, 42.9, 32.5, 31.0, 25.4, 23.7, 18.3, 18.1; HRMS (ESI) *m/z* calcd for $C_{26}H_{32}N_2O_4$ $(M+Na)^+$, 459.2254; found, 459.2253.

NMR Assignment. ^{1}H NMR (400 MHz) (1:1 mixture of rotamers) δ 8.65 (brs, 0.5 H, N2-H), 8.53 (brs, 0.5, N2-H), 7.50 -7.48 (comp, 2 H, C6-H), 7.41 - 7.37 (comp, 2 H, C7-H), 7.34 - 7.30 (m, 1 H, C8-H), 7.26 - 7.23 (comp, 1.5 H, C9-H and C3-H), 7.11 (d, *J* = 2.2 Hz, 0.5, C9-H), 7.02 (dq, *J* = 13.8, 6.9 Hz, 0.5 H, C13-H), 6.96 - 6.88 (comp, 2 H, C4-H and C1-H), 6.78 (dq, *J* = 13.8, 6.9 Hz, 0.5 H, C13-H), 6.32 (dd, *J* = 14.9, 1.6 Hz, 0.5 H, C12-H), 5.98 (dd, *J* =14.9, 1.6 Hz, 0.5 H, C12-H), 5.13 (s, 1 H, C5-H), 5.10 (s, 1 H, C5-H), 4.41 (t, *J* = 5.6 Hz, 0.5 H, C17-H), 4.33 (t, *J* = 5.6 Hz, 0.5 H, C17-H), 3.67 (t, *J* = 7.3 Hz, 1 H, C11-H), 3.60 (t, *J* = 7.3 Hz, 1 H, C11-H), 3.45 (t, *J* = 7.5 Hz, 1 H, C15-H), 3.37 - 3.30 (comp, 7 H, C18-H and C15-H), 3.03 (t, *J* = 7.3 Hz, 1 H, C10-H), 2.96 (t, *J* = 7.3 Hz, 1 H, C10-H), 1.96 - 1.90 (comp, 2 H, C16-H and C14-H), 1.85 - 1.80 (m, 1.5 H, C16-H), 1.66 (dd, *J* = 6.8, 1.5 Hz, 1.5 H, C14-H).

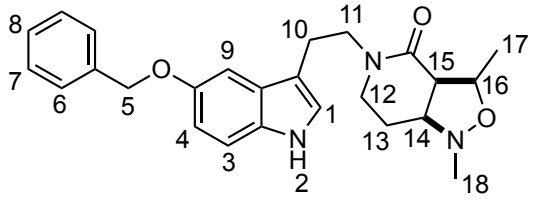

4.78

(3*R*,3a*R*,7a*S*)-5-(2-(5-(Benzyloxy)-1*H*-indol-3-yl)ethyl)-1,3-dimethylhexahydroisoxazolo[4,3-*c*]pyridin-4(1*H*)-one (4.78). ARMV296-ARMV297. A solution of **4.77** (250 mg, 0.57 mmol) and TFA (65 mg, 0.57 mmol) in TFE/water (3 : 1, 12 mL) was stirred for 1 h at room temperature. The reaction was poured into saturated aqueous $NaHCO_3$ (30 mL), and extracted with CH_2Cl_2 (3 x 50 mL). The combined organic fractions were washed with water (50 mL), dried (Na_2SO_4), filtered, and concentrated *in vacuo*. The resulting residue was dissolved in toluene (8 mL), followed by addition of N-methylhydroxylamine hydrochloride (71 mg, 0.86 mmol) and triethylamine (127 mg, 1.30 mmol). The reaction was heated under reflux for 2 h, then cooled to room temperature, and partitioned between saturated aqueous $NaHCO_3$ (50 mL), ethyl acetate (50 mL) and methanol (2 mL). The phases were separated, and the aqueous phase was extracted with ethyl acetate (3 x 50 mL). The combined organic fractions were washed with water (100 mL), brine (100 mL), dried (Na_2SO_4), filtered, and concentrated *in vacuo* to give crude **4.78**. The crude material was purified via silica gel flash column chromatography eluting with hexanes : ethyl acetate (1 : 1 → 0 : 1 along a gradient) to give 163 mg (68%, two-steps) of **4.78** as a viscous oil: ^{1}H NMR (400 MHz) δ 8.52 (brs, 1 H), 7.50 - 7.48 (comp, 2 H), 7.41 - 7.35 (comp, 2 H), 7.32 (tt, J = 7.2, 1.4

Hz, 1 H), 7.22 (d, *J* = 8.8 Hz, 1 H), 7.16 (d, *J* = 2.3 Hz, 1 H), 6.95 (s, 1 H), 5.11 (s, 2 H), 3.93 (p, *J* = 6.2 Hz, 1 H), 3.74 (dt, *J* = 13.3, 7.5 Hz, 1 H), 3.61 (dt, *J* = 13.3, 7.2 Hz, 1 H), 3.52 (td, *J* = 11.6, 2.5 Hz, 1 H), 2.99 - 2.92 (comp, 3 H), 2.83 - 2.79 (comp, 2 H), 2.66 (s, 3 H), 1.76 (tt, *J* = 11.1, 4.0 Hz, 1 H), 1.58 (dq, *J* = 11.1, 2.9 Hz, 1 H), 1.47 (d, *J* = 6.0 Hz, 3 H); ^{13}C NMR (100 MHz) δ 169.0, 153.0, 137.7, 131.7, 128.5, 127.8, 127.7, 127.7, 123.1, 112.7, 112.4, 112.0, 102.3, 77.5, 71.0, 66.1, 55.3, 48.4, 44.0, 43.2, 25.1, 23.5, 19.3; HRMS (ESI) *m/z* calcd for $C_{25}H_{29}N_3O_3$ $(M+Na)^+$, 442.2101; found, 442.2106.

NMR Assignment. ^{1}H NMR (400 MHz) δ 8.52 (brs, 1 H, N2-H), 7.50 - 7.48 (comp, 2 H, C6-H), 7.41 - 7.35 (comp, 2 H, C7-H), 7.32 (tt, *J* = 7.2, 1.4 Hz, 1 H, C8-H), 7.22 (d, *J* = 8.8 Hz, 1 H, C3-H), 7.16 (d, *J* = 2.3 Hz, 1 H, C9-H), 6.95 (s, 1 H, C1-H), 5.11 (s, 2 H, C5-H), 3.93 (p, *J* = 6.2 Hz, 1 H, C16-H), 3.74 (dt, *J* = 13.3, 7.5 Hz, 1 H, C11-H), 3.61 (dt, *J* = 13.3, 7.2 Hz, 1 H, C11-H), 3.52 (td, *J* = 11.6, 2.5 Hz, 1 H, C14-H), 2.99 - 2.92 (comp, 3 H, C12-H and C10-H), 2.83 - 2.79 (comp, 2 H, C15-H and C10-H), 2.66 (s, 3 H, C18-H), 1.76 (tt, *J* = 11.1, 4.0 Hz, 1 H, C13-H), 1.58 (dq, *J* = 11.1, 2.9 Hz, 1 H, C13-H), 1.47 (d, *J* = 6.0 Hz, 3 H, C17-H).

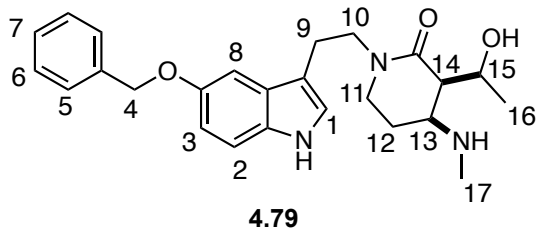

4.79

(3*R*,4*S*)-1-(2-(5-(Benzyloxy)-1*H*-indol-3-yl)ethyl)-3-((*R*)-1-hydroxyethyl)-4-(methylamino)piperidin-2-one (4.79). ARMV293. Zinc (dust, 586 mg, 9.0 mmol) was slowly added to a solution of **4.78** (126 mg, 0.30 mmol) in acetic acid (aq, 80%, 18 mL), and the mixture was stirred for 48 h at room temperature. Excess zinc was filtered, and washed with ethyl acetate. To the filtrate was added ethyl acetate (200 mL), at which point zinc acetate immediately precipitated out of solution as a fluffy white solid. The zinc acetate was removed by vacuum filtration, and the solvent was removed *in vacuo*. The resulting residue was dissolved in aqueous HCl (1 M, 30 mL), and washed with ether (30 mL). The aqueous fraction was basified to pH ~12-14 by addition of solid NaOH, as judged by pH paper. The basic solution was extracted with CH_2Cl_2 (3 x 50 mL), and the combined organic fractions were washed with brine (100 mL), dried (Na_2SO_4), filtered, and concentrated *in vacuo* to give crude **4.79** as an off white solid. The crude material was purified via silica gel flash column chromatography eluting with CH_2Cl_2 : methanol (1 : 0 → 9 : 1 along a gradient) to give 106 mg (85%) of **4.79** as an off white solid: ^{1}H NMR (400 MHz, CD_3OD) δ 7.48 - 7.46 (comp, 2 H), 7.38 - 7.34 (comp, 2 H), 7.29 (tt, *J* = 7.4, 1.4 Hz, 1 H), 7.24 (dd, *J* = 8.8, 0.4 Hz, 1 H), 7.17 (d, *J* = 2.1 Hz, 1 H), 7.04 (s, 1 H), 6.85 (dd, *J* = 8.8, 2.1 Hz, 1 H), 5.09 (s, 2 H), 4.27 (dq, *J* = 7.3, 6.4 Hz, 1 H), 3.62 -

3.52 (comp, 2 H), 3.31 - 3.26 (comp, 2 H), 3.14 - 3.06 (m, 1 H), 3.03 - 2.88 (comp, 2 H), 2.54 (dd, *J* = 6.8, 3.4 Hz, 1 H), 2.50 (s, 3 H), 2.07 - 2.01 (m, 1 H), 1.91 - 1.81 (m, 1 H), 1.24 (d, *J* = 6.3 Hz, 3H); ^{13}C NMR (100 MHz, CD_3OD) δ 169.4, 154.0, 139.4, 133.6, 129.4, 129.1, 128.7, 124.6, 113.4, 113.1, 112.6, 103.3, 72.1, 67.2, 56.6, 51.0, 49.3, 45.5, 32.5, 23.6, 23.0, 23.0; HRMS (ESI) *m/z* calcd for $C_{25}H_{31}N_3O_3$ $(M+H)^+$, 422.2438; found, 422.2447.

NMR Assignment. ^{1}H NMR (400 MHz, CD_3OD) δ 7.48 - 7.46 (comp, 2 H, C5-H), 7.38 - 7.34 (comp, 2 H, C6-H), 7.29 (tt, *J* = 7.4, 1.4 Hz, 1 H, C7-H), 7.24 (dd, *J* = 8.8, 0.4 Hz, 1 H, C2-H), 7.17 (d, *J* = 2.1 Hz, 1 H, C8-H), 7.04 (s, 1 H, C1-H), 6.85 (dd, *J* = 8.8, 2.1 Hz, 1 H, C3-H), 5.09 (s, 2 H, C4-H), 4.27 (dq, *J* = 7.3, 6.4 Hz, 1 H, C15-H), 3.62 - 3.52 (comp, 2 H, C10-H), 3.31 - 3.26 (comp, 2 H, C11-H), 3.14 - 3.06 (m, 1 H, C13-H), 3.03 - 2.88 (comp, 2 H, C9-H), 2.54 (dd, *J* = 6.8, 3.4 Hz, 1 H, C14-H), 2.50 (s, 3 H, C17-H), 2.07 - 2.01 (m, 1 H, C12-H), 1.91 - 1.81 (m, 1 H, C12-H), 1.24 (d, *J* = 6.3 Hz, 3H, C16-H).

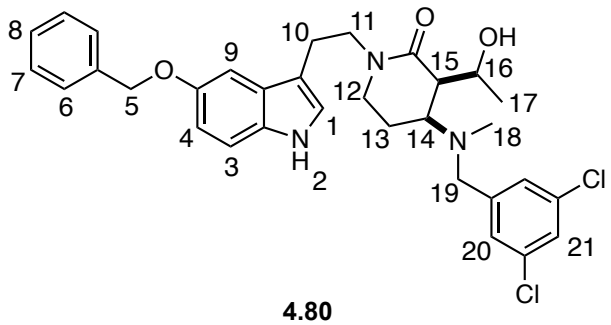

4.80

(3*R*,4*S*)-1-(2-(5-(Benzyloxy)-1*H*-indol-3-yl)ethyl)-4-((3,5-dichlorobenzyl)(methyl)amino)-3-((*R*)-1-hydroxyethyl)piperidin-2-one (4.80). **ARMVI98.** Prepared according to representative procedure for compound **4.12**; scaled to **4.79** (100 mg, 0.24 mmol). The crude material was purified via silica gel flash column chromatography eluting with hexanes : ethyl acetate (2 : 1 → 0 : 1 along a gradient) to give 50 mg (37%) of **4.80** as a white solid: ^{1}H NMR (600 MHz) δ 8.07 (brs, 1 H), 7.47 (d, *J* = 7.5 Hz, 2 H), 7.38 - 7.35 (comp, 2 H), 7.31 - 7.28 (m, 1 H), 7.25 - 7.23 (comp, 2 H), 7.13 (d, *J* = 2.4 Hz, 1 H), 7.08 (d, *J* = 1.9 Hz, 2 H), 6.99 (d, *J* = 2.3 Hz, 1 H), 6.93 (dd, *J* = 8.7, 2.3 Hz, 1 H), 5.11 (s, 2 H), 4.26 (dq, *J* = 8.8, 6.1 Hz, 1 H), 3.77 (dt, *J* = 13.4, 7.7 Hz, 1 H), 3.49 (dq, *J* = 7.8, 6.1 Hz, 1 H), 3.42 (d, *J* = 13.3, 1 H), 3.34 (d, *J* = 13.3, 1 H), 3.21 (ddd, *J* = 12.8, 6.7, 2.3 Hz, 1 H), 3.12 - 3.03 (comp, 2 H), 2.99 (p, *J* = 7.3 Hz, 1 H), 2.91 (p, *J* = 7.3 Hz, 1 H) 2.65 (dd, *J* = 8.7, 5.8 Hz, 1 H), 2.07 (s, 3 H), 1.96 - 1.84 (comp, 2 H), 1.31 (d, *J* = 6.1 Hz, 3 H); ^{13}C NMR (150 MHz) δ 169.8, 153.1, 141.2, 137.6, 135.1, 131.6, 128.5, 127.8, 127.8, 127.7, 127.6, 127.1, 123.0, 112.7, 112.5, 111.9, 102.4, 71.0, 66.5, 60.3, 57.6, 50.1, 47.2, 45.3, 38.6, 23.1, 22.5, 21.8; HRMS (ESI) *m/z* calcd for $C_{32}H_{35}Cl_2N_3O_3$ $(M+Na)^+$, 602.1948 and 604.1927; found, 602.1950 and 604.1931.

NMR Assignment. ^{1}H NMR (600 MHz) δ 8.07 (brs, 1 H, N2-H), 7.47 (d, *J* = 7.5 Hz, 2 H, C6-H), 7.38 - 7.35 (comp, 2 H, C7-H), 7.31 - 7.28 (m, 1 H, C8-H), 7.25 - 7.23 (m, 2 H, C3-H), 7.13 (d, *J* = 2.4 Hz, 1 H, C21-H), 7.08 (d, *J* = 1.9 Hz, 2 H, C20-H), 6.99 (d, *J* = 2.3 Hz, 1 H, C9-H), 6.93 (dd, *J* = 8.7, 2.3 Hz, 1 H, C4-H), 5.11 (s, 2 H, C5-H), 4.26 (dq, *J* = 8.8, 6.1 Hz, 1 H, C16-H), 3.77 (dt, *J* = 13.4, 7.7 Hz, 1 H, C11-H), 3.49 (dq, *J* = 7.8, 6.1 Hz, 1 H, C11-H), 3.42 (d, *J* = 13.3, 1 H, C19-H), 3.34 (d, *J* = 13.3, 1 H, C19-H), 3.21 (ddd, *J* = 12.8, 6.7, 2.3 Hz, 1 H, C14-H), 3.12 - 3.03 (comp, 2 H, C12-H), 2.99 (p, *J* = 7.3 Hz, 1 H, C20-H), 2.91 (p, *J* = 7.3 Hz, 1 H, C20-H) 2.65 (dd, *J* = 8.7, 5.8 Hz, 1 H, C15-H), 2.07 (s, 3 H, C18-H), 1.96 - 1.84 (comp, 2 H, C13-H), 1.31 (d, *J* = 6.1 Hz, 3 H, C17-H)

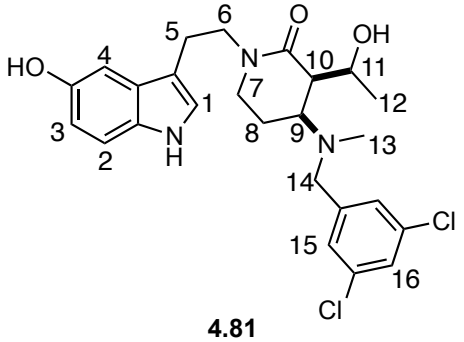

4.81

(3*R*,4*S*)-4-((3,5-Dichlorobenzyl)(methyl)amino)-1-(2-(5-hydroxy-1*H*-indol-3-yl)ethyl)-3-((*R*)-1-hydroxyethyl)piperidin-2-one (4.81). ARMVI58/ARMVI60. A solution of **4.78** (150 mg, 0.36 mmol) in ethanol (2 mL) was added over 5 min to a degassed of ethanol (12 mL) and Pd/C (10% w/w, 150 mg) at room temperature. A

balloon of hydrogen gas was bubbled through the suspension, followed immediately by addition of TFA (3 drops), and the reaction was stirred for 5 h at 60 ºC. The suspension was then cooled to room temperature, and filtered through a pad of Celite washing with copious amounts of methanol. The solvent was removed *in vacuo,* followed by azeotropic removal of water with toluene. The crude mixture was dissolved in acetonitrile (10 mL), and 3,5-dichlorobenzaldehyde (189 mg, 1.1 mmol) was added in one portion. The reaction was held under reflux for 2 h, after which the solution was cooled to room temperature. $NaBH_3CN$ (68 mg, 1.1 mmol) and acetic acid (glacial, 129 μL, 2.2 mmol) were added, and the reaction was stirred for 14 h at room temperature. Saturated aqueous $NaHCO_3$ (30 mL) was added to the mixture, followed by extraction with CH_2Cl_2 (3 x 30 mL). The combined organic fractions were washed with water (30 mL), dried (Na_2SO_4), filtered, and concentrated *in vacuo* to give crude **4.81**. The crude material was purified via flash column chromatography eluting with hexanes : ethyl acetate (1 : 1 → 0 : 1 along a gradient) to give 48 mg (28%, two-steps) of **4.81** as a white solid: ^{1}H NMR (600 MHz, CD_3OD) δ 7.32 (t, *J* = 1.9 Hz, 1 H), 7.20 (d, *J* = 1.9 Hz, 1 H), 7.15 (dd, *J* = 8.6, 0.4 Hz, 1 H), 7.00 (s, 1 H), 6.94 (d, *J* = 2.0 Hz, 1 H), 6.67 (dd, *J* = 8.6, 2.3 Hz, 1 H), 4.20 (dq, *J* = 8.6, 6.1 Hz, 1 H), 3.67 (dt, *J* = 13.2, 7.6 Hz, 1 H), 3.52 (ddd, *J* = 13.3, 7.6, 5.8 Hz, 1 H), 3.46 (d, *J* = 13.4 Hz, 1 H), 3.36 (d, *J* = 13.4 Hz, 1 H), 3.28 - 3.25 (m, 1 H), 3.09 - 3.01 (comp, 2 H), 2.96 (p, *J* = 7.1 Hz, 1 H), 2.88 - 2.84 (m, 1 H), 2.57 (dd, *J* = 8.0, 5.2 Hz, 1 H), 2.03 (s, 3 H), 1.94 - 1.91 (m, 1 H), 1.86 - 1.80 (m, 1 H), 1.21 (d, *J* = 6.1 Hz, 3 H); ^{13}C NMR (150 MHz, CD_3OD) δ 171.9, 151.3, 143.7, 136.2, 133.0, 129.6, 128.5, 128.4,

124.5, 112.8, 112.5, 112.1, 103.5, 67.7, 61.2, 58.4, 51.1, 49.8, 46.6, 38.5, 24.0, 22.8, 22.5; HRMS (ESI) *m/z* calcd for $C_{25}H_{29}Cl_2N_3O_3$ $(M+H)^+$, 512.1478 and 514.1455; found, 512.1483 and 514.1459.

NMR Assignment. ^{1}H NMR (600 MHz, CD_3OD) δ 7.32 (t, *J* = 1.9 Hz, 1 H, C16-H), 7.20 (d, *J* = 1.9 Hz, 1 H, C15-H), 7.15 (dd, *J* = 8.6, 0.4 Hz, 1 H, C2-H), 7.00 (s, 1 H, C1-H), 6.94 (d, *J* = 2.0 Hz, 1 H, C4-H), 6.67 (dd, *J* = 8.6, 2.3 Hz, 1 H, C3-H), 4.20 (dq, *J* = 8.6, 6.1 Hz, 1 H, C11-H), 3.67 (dt, *J* = 13.2, 7.6 Hz, 1 H, C6-H), 3.52 (ddd, *J* = 13.3, 7.6, 5.8 Hz, 1 H, C6-H), 3.46 (d, *J* = 13.4 Hz, 1 H, C14-H), 3.36 (d, *J* = 13.4 Hz, 1 H, C14-H), 3.28 - 3.25 (m, 1 H, C7-H), 3.09 - 3.01 (comp, 2 H, C9-H and C7-H), 2.96 (p, *J* = 7.1 Hz, 1 H, C5-H), 2.88 - 2.84 (m, 1 H, C5-H), 2.57 (dd, *J* = 8.0, 5.2 Hz, 1 H, C10-H), 2.03 (s, 3 H, C13-H), 1.94 - 1.91 (m, 1 H, C8-H), 1.86 - 1.80 (m, 1 H, C8-H), 1.21 (d, *J* = 6.1 Hz, 3 H, C12-H).

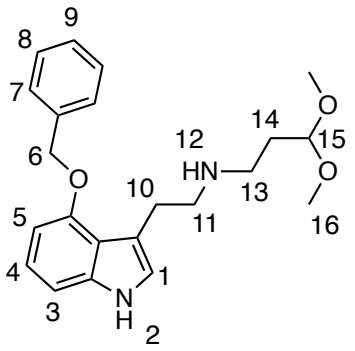

4.85

***N*-(2-(4-(Benzyloxy)-1*H*-indol-3-yl)ethyl)-3,3-dimethoxypropan-1-amine (4.85). ARMVII128/ARMVII149.** A solution of oxalyl chloride (0.57 g, 4.5 mmol) in ether (1 mL) was added dropwise over 20 min to a solution of 4-benzyloxyindole (1.40 g, 4.5 mmol) in ether (10 mL) at 0 ºC. The reaction was stirred for 2 h at 0 ºC, at which point the solution was transferred dropwise over 20 min via cannula into a solution of **4.18** (0.73 g, 3.7 mmol) and triethylamine (1.9 g, 18.5 mmol) in CH_2Cl_2 (50 mL) at 0 ºC. During the transfer, HCl gas was removed from the reaction through intermittent ventilation with a stream of nitrogen. The reaction was warmed to room temperature, and stirred for 1 h. Saturated aqueous $NaHCO_3$ (100 mL) was added, and the solution was stirred for 20 min at room temperature. The mixture was extracted with CH_2Cl_2 (3 x 100 mL). The combined organic fractions were washed with aqueous NaOH (1 M, 100 mL), water (100 mL), brine (100 mL), dried (Na_2SO_4), filtered, and concentrated *in vacuo* to give crude **4.83** as a thick orange semi-solid, which was carried onto the next step without further purification.

A solution of crude **4.83** (0.37 g, 0.93 mmol) in THF (5 mL) was added dropwise over 10 min to a suspension of lithium aluminum hydride (0.35 g, 9.30 mmol) in THF (20 mL) at 0 ºC. The reaction was heated to 60 ºC for 14 h. The reaction was then cooled to 0 ºC, and the Fieser work-up was carefully performed by successive addition of water (0.3 mL), aqueous NaOH (15%, 0.3 mL), and water (1 mL). The suspension was warmed to room temperature, and $MgSO_4$ was added. The solids were removed by vacuum filtration through a fritted funnel, and washed with copious amounts of CH_2Cl_2. The filtrate was concentrated *in vacuo* to give crude **4.85** as an opaque viscous oil. The crude residue was taken up into aqueous HCl (0.2 M, 100 mL), and washed with ether (2 x 50 mL). The aqueous fraction was basified to pH 12-14 by dropwise addition of aqueous NaOH (40% w/v), as judged by pH paper. The basic solution was extracted with CH_2Cl_2 (4 x 100 mL). The combined organic fractions were washed with saturated aqueous $NaHCO_3$ (100 mL), water (100 mL), brine (100 mL), dried (Na_2SO_4), filtered, and concentrated *in vacuo* to give 230 mg (67%) of **4.85** as a viscous oil (>95% purity, by ^{1}H NMR): ^{1}H NMR (400 MHz) δ 8.31 (brs, 1 H), 7.51 (d, J = 6.8 Hz, 2 H), 7.40 (td, J = 6.8, 1.4 Hz, 2 H), 7.34 (tt, J = 6.8, 1.4 Hz, 1 H), 7.06 (t, J = 7.8 Hz, 1 H), 6.98 (dd, J = 7.8 Hz, 0.7 Hz, 1 H), 6.91 (d, J = 2.1 Hz, 1 H), 6.55 (dd, J = 7.8, 0.7 Hz, 1 H), 5.17 (s, 2 H), 4.38 (t, J = 5.6 Hz, 1 H), 3.27 (s, 6 H), 3.06 (t, J = 6.8 Hz, 2 H), 2.89 (t, J = 6.8 Hz, 2 H), 2.58 (t, J = 7.2 Hz, 2 H), 1.71 (td, J = 7.2, 5.6 Hz, 2 H); ^{13}C NMR (100 MHz) δ 153.8, 138.4, 137.5, 128.5, 127.8, 127.4, 122.7, 121.0, 117.4, 114.5, 104.7, 103.5, 100.4, 69.8, 52.7,

51.1, 45.1, 33.0, 27.4; HRMS (CI) *m/z* calcd for $C_{22}H_{28}N_2O_3$ $(M+H)^+$, 369.2178 found, 369.2180.

NMR Assignment. ^{1}H NMR (400 MHz) δ 8.31 (brs, 1 H, N2-H), 7.51 (d, *J* = 6.8 Hz, 2 H, C7-H), 7.40 (td, *J* = 6.8, 1.4 Hz, 2 H, C8-H), 7.34 (tt, *J* = 6.8, 1.4 Hz, 1 H, C9-H), 7.06 (t, *J* = 7.8 Hz, 1 H, C4-H), 6.98 (dd, *J* = 7.8 Hz, 0.7 Hz, 1 H, C3-H), 6.91 (d, *J* = 2.1 Hz, 1 H, C1-H), 6.55 (dd, *J* = 7.8, 0.7 Hz, 1 H, C5-H), 5.17 (s, 2 H, C6-H), 4.38 (t, *J* = 5.6 Hz, 1 H, C15-H), 3.27 (s, 6 H, C16-H), 3.06 (t, *J* = 6.8 Hz, 2 H, C11-H), 2.89 (t, *J* = 6.8 Hz, 2 H, C10-H), 2.58 (t, *J* = 7.2 Hz, 2 H, C13-H), 1.71 (td, *J* = 7.2, 5.6 Hz, 2 H, C14-H).

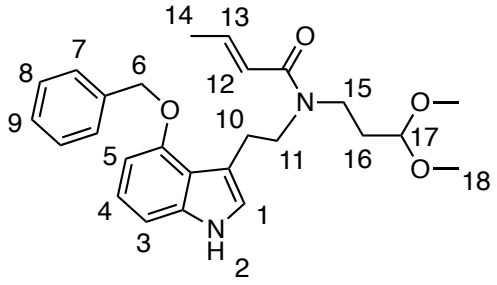

4.86

(*E*)-*N*-(2-(4-(Benzyloxy)-1*H*-indol-3-yl)ethyl)-*N*-(3,3-dimethoxypropyl)but-2-enamide (4.86). ARMVI32. Crotonoyl chloride (200 mg, 1.90 mmol) was added dropwise over 5 min to a solution of **4.85** (588 mg, 1.60 mmol) and Hünig's base (495 mg, 3.80 mmol) in CH_2Cl_2 (16 mL) at -78 ºC. The reaction was stirred for 1 h at –78 ºC. Saturated aqueous $NaHCO_3$ (20 mL) was added, and the resulting solution was stirred for 20 min at room temperature. The aqueous phase was extracted with CH_2Cl_2 (3 x 20 mL).

The combined organic fractions were washed with water (25 mL), brine (25 mL), dried (Na_2SO_4), filtered, and concentrated *in vacuo* to give crude **4.86** as an opaque oil. The crude material was purified via silica gel flash column chromatography eluting with hexanes : ethyl acetate (2 : 1 → 1 : 1 along a gradient) to give 590 mg (86%) of **4.86** as an oil: ^{1}H NMR (400 MHz) (1:1 mixture of rotamers) δ 8.51 (brs, 1 H), 7.50 - 7.47 (comp, 2 H), 7.39 (app td, *J* = 7.0, 1.4 Hz, 2 H), 7.35 - 7.31 (m, 1 H), 7.06 - 7.02 (comp, 1 H), 6.98 - 6.94 (comp, 1 H), 6.84 (d, *J* = 1.9 Hz, 0.5), 6.73 (d, *J* = 1.9 Hz, 0.5 H), 6.64 (dq, *J* = 13.6, 6.7 Hz, 1 H), 6.57 - 6.53 (comp, 1 H), 6.26 (dd, *J* = 13.6, 1.6 Hz, 0.5 H), 5.92 (dd, *J* = 13.6, 1.6 Hz, 0.5 H), 5.25 (s, 1 H), 5.22 (s, 1 H), 4.32 (t, *J* = 5.7 Hz, 0.5 H), 4.09 (t, *J* = 5.7 Hz, 0.5 H), 3.63 - 3.59 (comp, 2 H), 3.31 - 3.27 (comp, 4 H), 3.19 (s, 3 H), 3.17 - 3.04 (comp, 3 H), 1.88 (dd, *J* = 6.8, 1.5 Hz, 1.5 H), 1.82 (q, *J* = 7.0 Hz, 1 H), 1.58 (q, *J* = 7.0 Hz, 1 H), 1.50 (dd, *J* = 6.8, 1.5 Hz, 1.5 H); ^{13}C NMR (100 MHz) (1 : 1 mixture of rotamers) δ 166.8, 166.3, 153.6, 153.5, 141.3, 140.3, 138.3, 138.2, 137.5, 137.3, 128.6, 128.6, 127.9, 127.9, 127.5, 127.3, 122.8, 122.5, 121.8, 121.8, 117.4, 117.3, 113.4, 112.3, 105.0, 102.8, 101.9, 100.6, 100.4, 70.0, 69.9, 52.9, 52.8, 49.7, 48.8, 43.8, 42.7, 32.2, 30.8, 27.0, 25.2, 18.3, 18.2, 17.8; HRMS (ESI) *m/z* calcd for $C_{26}H_{32}N_2O_4$ $(M+Na)^+$, 459.2254; found, 459.2262

NMR Assignment. ^{1}H NMR (400 MHz) (1:1 mixture of rotamers) δ 8.51 (brs, 1 H, N2-H), 7.50 - 7.47 (comp, 2 H, C7-H), 7.39 (app td, *J* = 7.0, 1.4 Hz, 2 H, C8-H), 7.35 - 7.31 (m, 1 H, C9-H), 7.06 - 7.02 (comp, 1 H, C4-H), 6.98 - 6.94 (comp, 1 H, C3-H), 6.84 (d, *J* = 1.9 Hz, 0.5, C1-H), 6.73 (d, *J* = 1.9 Hz, 0.5 H, C1-H), 6.64 (dq, *J* = 13.6, 6.7

Hz, 1 H, C13-H), 6.57 - 6.53 (comp, 1 H, C5-H), 6.26 (dd, *J* = 13.6, 1.6 Hz, 0.5 H, C12-H), 5.92 (dd, *J* = 13.6, 1.6 Hz, 0.5 H, C12-H), 5.25 (s, 1 H, C6-H), 5.22 (s, 1 H, C6-H), 4.32 (t, *J* = 5.7 Hz, 0.5 H, C17-H), 4.09 (t, *J* = 5.7 Hz, 0.5 H, C17-H), 3.63 - 3.59 (comp, 2 H, C11-H), 3.31 - 3.27 (comp, 4 H, C18-H and C15-H), 3.19 (s, 3 H, C18-H), 3.17 - 3.04 (comp, 3 H, C15-H and C10-H), 1.88 (dd, *J* = 6.8, 1.5 Hz, 1.5 H, C14-H), 1.82 (q, *J* = 7.0 Hz, 1 H, C16-H), 1.58 (q, *J* = 7.0 Hz, 1 H, C16-H), 1.50 (dd, *J* = 6.8, 1.5 Hz, 1.5 H, C14-H).

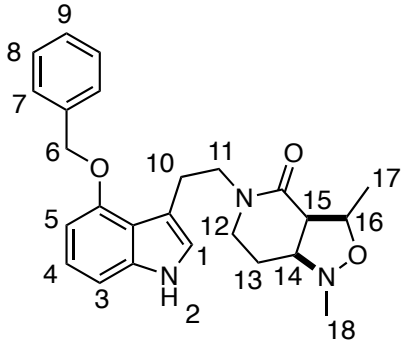

4.87

(3*R*,3a*R*,7a*S*)-5-(2-(4-(Benzyloxy)-1*H*-indol-3-yl)ethyl)-1,3-dimethylhexahydroisoxazolo[4,3-*c*]pyridin-4(1*H*)-one (4.87). ARMVII158-ARMVII159. A solution of **4.86** (149 mg, 0.34 mmol) and TFA (5 drops) in TFE/water (3 : 1, 6 mL) was stirred for 1 h at room temperature. The reaction was poured into saturated aqueous $NaHCO_3$ (20 mL), and extracted with CH_2Cl_2 (3 x 20 mL). The combined organic fractions were washed with water (20 mL), dried (Na_2SO_4), filtered, and concentrated *in vacuo*. The resulting residue was dissolved in toluene (4 mL),

followed by addition of N-methylhydroxylamine hydrochloride (34 mg, 0.41 mmol) and triethylamine (70 mg, 0.69 mmol). The reaction was heated under reflux for 1 h, at which point the reaction was cooled to room temperature, and portioned between saturated aqueous $NaHCO_3$ (20 mL), ethyl acetate (20 mL) and methanol (1 mL). The phases were separated, and the aqueous phase was extracted with ethyl acetate (3 x 20 mL). The combined organic fractions were washed with water (40 mL), brine (40 mL), dried (Na_2SO_4), filtered, and concentrated *in vacuo* to give 133 mg (93%) of **4.87** as an oil (>95% purity, by ^1H NMR): ^1H NMR (600 MHz) δ 8.12 (brs, 1 H), 7.49 - 7.47 (comp, 2 H), 7.40 - 7.38 (comp, 2 H), 7.32 (tt, *J* = 7.4, 1.3 Hz, 1 H), 7.06 (t, *J* = 8.0 Hz, 1 H), 6.98 (dd, *J* = 8.0, 0.6 Hz, 1 H), 6.90 (d, *J* = 2.3 Hz, 1 H), 5.57 (d, *J* = 8.0 Hz, 1 H), 5.14 (s, 2 H), 3.94 (p, *J* = 6.2 Hz, 1 H), 3.62 (ddd, *J* = 12.9, 9.7, 5.9 Hz, 1 H), 3.45 (ddd, *J* = 12.9, 9.7, 5.6 Hz, 1 H), 3.09 - 3.02 (comp, 2 H), 2.95 (ddd, *J* = 13.7, 9.5, 5.8 Hz, 1 H), 2.78 - 2.69 (comp, 2 H), 2.62 (s, 3 H), 2.41 (dt, *J* = 12.9, 4.2 Hz, 1 H), 1.57 - 1.52 (m, 1 H), 1.41 (d, *J* = 6.1 Hz, 3 H), 1.29 (dq, *J* = 14.3, 3.6 Hz, 1 H); ^{13}C NMR (150 MHz) δ 168.7, 153.8, 138.2, 137.2, 128.6, 128.4, 128.0, 122.7, 121.6, 117.2, 113.3, 104.9, 100.3, 77.5, 77.4, 70.2, 66.2, 55.2, 49.7, 43.2, 25.1, 25.0, 19.2; HRMS (ESI) *m/z* calcd for $C_{25}H_{29}N_3O_3$ $(M+H)^+$, 420.2282; found, 420.2289

NMR Assignment. ^1H NMR (600 MHz) δ 8.12 (brs, 1 H, N2-H), 7.49 - 7.47 (comp, 2 H, C7-H), 7.40 - 7.38 (comp, 2 H, C8-H), 7.32 (tt, *J* = 7.4, 1.3 Hz, 1 H, C9-H), 7.06 (t, *J* = 8.0 Hz, 1 H, C4-H), 6.98 (dd, *J* = 8.0, 0.6 Hz, 1 H, C3-H), 6.90 (d, *J* = 2.3 Hz, 1 H, C1-H), 5.57 (d, *J* = 8.0 Hz, 1 H, C5-H), 5.14 (s, 2 H, C6-H), 3.94 (p, *J* = 6.2 Hz, 1

H, C16-H), 3.62 (ddd, *J* = 12.9, 9.7, 5.9 Hz, 1 H, C11-H), 3.45 (ddd, *J* = 12.9, 9.7, 5.6 Hz, 1 H, C1-H), 3.09 - 3.02 (comp, 2 H, C12-H and C10-H), 2.95 (ddd, *J* = 13.7, 9.5, 5.8 Hz, 1 H, C10-H), 2.78 - 2.69 (comp, 2 H, C15-H and C14-H), 2.62 (s, 3 H, C18-H), 2.41 (dt, *J* = 12.9, 4.2 Hz, 1 H, C12-H), 1.57 - 1.52 (m, 1 H, C13-H), 1.41 (d, *J* = 6.1 Hz, 3 H, C17-H), 1.29 (dq, *J* = 14.3, 3.6 Hz, 1 H, C13-H).

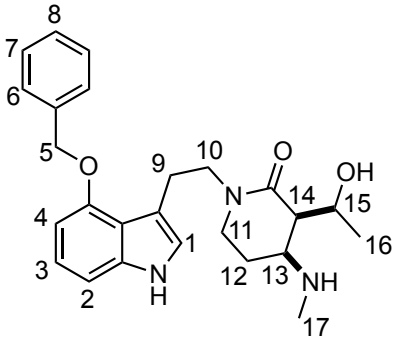

4.88

(3*R*,4*S*)-1-(2-(4-(Benzyloxy)-1*H*-indol-3-yl)ethyl)-3-((*R*)-1-hydroxyethyl)-4-(methylamino)piperidin-2-one (4.88). ARMVII163. Zinc (powder, 584 mg, 9.00 mmol) was added in three portions over 1.5 h to a solution of **4.87** (125 mg, 0.30 mmol) in acetic acid (aq 80%, 18 mL) at 60 ºC. The suspension was stirred for 1 h at 60 ºC. The suspension was cooled to room temperature, followed by the removal of excess zinc by filtration. Ethyl acetate (100 mL) was added to the filtrate, upon which zinc acetate immediately precipitated out of solution as a fluffy white solid. The zinc acetate was filtered and washed with ethyl acetate. The filtrate was concentrated *in vacuo* to give crude **4.88**. the crude material was taken up in aqueous HCl (1 M, 30 mL), and washed

with ether (2 x 30 mL). The aqueous fraction was basified to pH ~14 with aqueous NaOH (40% w/v). The basic solution was extracted with CH_2Cl_2 (4 x 50 mL). The combined organic fractions were washed with saturated aqueous $NaHCO_3$ (100 mL), water (100 mL), and brine (1 x 100 mL). The organic fractions were dried (Na_2SO_4), filtered, and concentrated *in vacuo* to give 72 mg (57%) of **4.88** as an oil (>95% purity, by ^{1}H NMR): ^{1}H NMR (500 MHz, CD_3OD) δ 7.47 (d, *J* = 7.0 Hz, 2 H) 7.39 – 7.33 (comp, 3 H), 7.03 (t, *J* = 8.0 Hz, 1 H), 6.98 (dd, *J* = 8.0, 0.5 H, 1 H), 6.90 (s, 1 H), 6.55 (dd, *J* = 8.0, 0.5 Hz, 1 H), 5.13 (s, 2 H), 4.39 (p, *J* = 6.0 Hz, 1 H), 3.48 – 3.44 (comp, 2 H), 3.03 – 2.98 (comp, 3 H), 2.80 – 2.78 (m, 1 H), 2.63 – 2.58 (m, 1 H), 2.27 – 2.23 (comp, 4 H), 1.73 (dq, *J* = 13.5, 6.0 Hz, 1 H), 1.46 – 1.40 (m, 1 H), 1.20 (d, *J* = 6.0 Hz, 3 H); ^{13}C NMR (125 MHz, CD_3OD) δ 169.5, 153.6, 138.3, 137.3, 128.5, 128.3, 128.0, 122.2, 122.0, 117.1, 112.2, 105.1, 99.9, 70.1, 66.4, 54.4, 50.0, 43.6, 33.3, 24.4, 23.3, 20.9; HRMS (ESI) *m/z* calcd for $C_{25}H_{31}N_3O_3$ $(M+H)^+$, 422.2438; found, 422.2442.

NMR Assignment. ^{1}H NMR (500 MHz, CD_3OD) δ 7.47 (d, *J* = 7.0 Hz, 2 H, C6-H) 7.39 – 7.33 (comp, 3 H, C7-H and C8-H), 7.03 (t, *J* = 8.0 Hz, 1 H, C3-H), 6.98 (dd, *J* = 8.0, 0.5 H, 1 H, C2-H), 6.90 (s, 1 H, C1-H), 6.55 (dd, *J* = 8.0, 0.5 Hz, 1 H, C4-H), 5.13 (s, 2 H, C5-H), 4.39 (p, *J* = 6.0 Hz, 1 H, C15-H), 3.48 – 3.44 (comp, 2 H, C10-H), 3.03 – 2.98 (comp, 3 H, C11-H and C13-H), 2.80 – 2.78 (m, 1 H, C9-H), 2.63 – 2.58 (m, 1 H, C9-H), 2.27 – 2.23 (comp, 4 H, C17-H and C14-H), 1.73 (dq, *J* = 13.5, 6.0 Hz, 1 H, C12-H), 1.46 – 1.40 (m, 1 H, C12-H), 1.20 (d, *J* = 6.0 Hz, 3 H, C16-H).

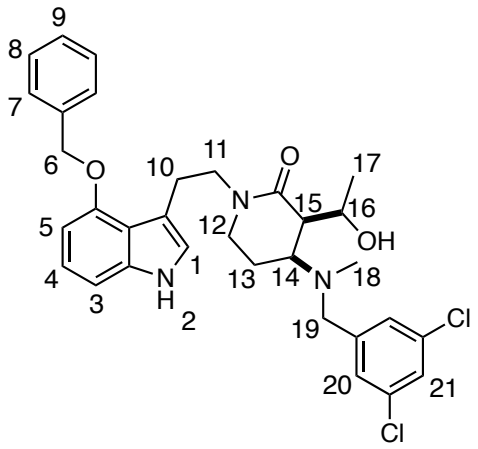

4.89

(3*R*,4*S*)-1-(2-(4-(Benzyloxy)-1*H*-indol-3-yl)ethyl)-4-((3,5-dichlorobenzyl)(methyl)amino)-3-((*R*)-1-hydroxyethyl)piperidin-2-one (4.89). **ARMVI76.** Prepared according to the representative procedure for compound **4.12** scaled to **4.88** (100 mg, 0.24 mmol). The crude material was purified via flash column chromatography eluting with CH_2Cl_2 : acetone : methanol (9 : 1 : 0 → 5 : 4 : 1 along a gradient) to give 26 mg (19%) of **4.89** as a white solid: ^{1}H NMR (400 MHz) δ 9.14 (brs, 1 H), 7.38 (dd, *J* = 8.4, 1.6 Hz, 2 H), 7.30 - 7.28 (comp, 2 H), 7.23 (d, *J* = 7.2 Hz, 1 H), 7.13 (s, 1 H), 7.01 (s, 2 H), 6.94 - 6.87 (comp, 2 H), 6.77 (d, *J* = 2.4 Hz, 1 H), 6.44 (dd, *J* = 7.2, 0.8 Hz, 1 H), 5.01 (s, 2 H), 4.09 (dq, *J* = 9.2, 6.8 Hz, 1 H), 3.55 - 3.48 (m, 1 H), 3.36 (d, *J* = 12.4 Hz, 1 H), 3.28 - 3.1 (comp, 2 H), 2.90 - 2.84 (comp, 3 H), 2.59 - 2.54 (m, 1 H), 1.97 (s, 3 H), 1.55 - 1.50 (comp, 2 H), 1.22 (d, *J* = 6.0 Hz, 3 H); ^{13}C NMR (125 MHz) δ 169.6, 153.8, 141.4, 138.2, 137.3, 135.2, 128.6, 128.5, 128.1, 127.8, 126.6, 122.8, 121.6, 117.2, 113.1, 105.0, 100.3, 70.2, 66.4, 60.4, 57.7, 50.1, 48.7, 44.6, 24.7,

22.5, 21.9; HRMS (ESI) *m/z* calcd for $C_{32}H_{35}Cl_2N_3O_3$ $(M+Na)^+$, 602.1948 and 604.1945; found, 602.1927 and 604.1954.

NMR Assignment. ^{1}H NMR (400 MHz) δ 9.41 (brs, 1 H, N2-H), 7.38 (dd, *J* = 8.4, 1.6 Hz, 2 H, C7-H), 7.30 - 7.28 (comp, 2 H, C8-H), 7.23 (d, *J* = 7.2 Hz, 1 H, C9-H), 7.13 (s, 1 H, C21-H), 7.01 (s, 2 H, C20-H), 6.94 - 6.87 (comp, 2 H, C4-H and C3-H), 6.77 (d, *J* = 2.4 Hz, 1 H, C1-H), 6.44 (dd, *J* = 7.2, 0.8 Hz, 1 H, C5-H), 5.01 (s, 2 H, C6-H), 4.09 (dq, *J* = 9.2, 6.8 Hz, 1 H, C16-H), 3.55 - 3.48 (m, 1 H, C11-H), 3.36 (d, *J* = 12.4 Hz, 1 H, C19-H), 3.28 - 3.1 (comp, 2 H, C19-H and C11-H), 2.90 - 2.84 (comp, 3 H, C14-H and C12-H), 2.59 - 2.54 (m, 1 H, C15-H), 1.97 (s, 3 H, C18-H), 1.55 - 1.50 (comp, 2 H, C13-H), 1.22 (d, *J* = 6.0 Hz, 3 H, C17-H).

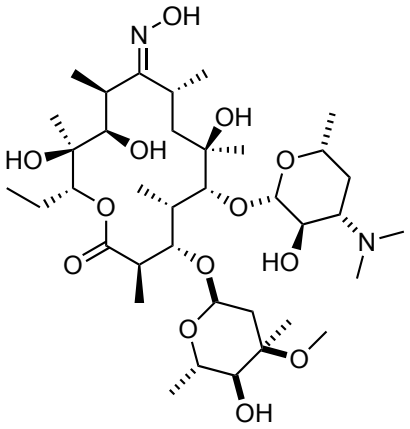

ERY-9-OX (6.2)

Erythromycin A-9-oxime (ERY-9-OX, 6.2). ARMVI151. A solution of erythromycin A (15.0 g, 20.4 mmol) and hydroxylamine hydrochloride (14.0 g, 204.0 mmol) in pyridine (100 mL) was stirred at room temperature for 72 h. The solvent was

removed *in vacuo*, whereupon the resulting slurry was taken up into aqueous NaOH (1 M, 200 mL) and extracted with CH_2Cl_2 (3 x 250 mL). The combined organic fractions were washed with brine (400 mL), dried (Na_2SO_4), filtered, and concentrated *in vacuo* to give 15.7 g (quant.) of crude **6.2**. The crude material was dissolved in boiling ethanol (~100 mL) then allowed to cool to room temperature, whereupon water (~5 mL) was added, the beaker was scratched, and placed in the refrigerator. The crystalline precipitate was isolated via vacuum filtration to give 7.56 g (49%) of **6.2**. The mother liquor was boiled down to ~1/2 the total volume, and placed in the refrigerator. The second crop of crystals isolated via vacuum filtration, which yielded an additional 3.81 g (25%) of **6.2**, to give a total of 11.36 g (74%) of **6.2** as a fine white crystalline solid. Spectral data matched that for previous reports:[301] ^{1}H NMR (400 MHz, DMSO-d_6) δ 10.62 (s, 1 H), 5.10 (dd, *J* = 11.1, 2.3 Hz, 1 H), 4.71 (d, *J* = 4.9 Hz, 1 H), 4.37 (d, *J* = 7.3 Hz, 1 H), 4.29 (d, *J* = 7.4 Hz, 1 H), 4.10 (d, *J* = 2.2 Hz, 1 H), 4.00 (d, *J* = 8.7 Hz, 2 H), 3.84 (d, *J* = 9.4 Hz, 1 H), 3.64 (dd, *J* = 11.0, 6.0 Hz, 1 H), 3.49 (s, 1 H), 3.45 (d, *J* = 7.0 Hz, 1 H), 3.19 (s, 3 H), 3.02 (t, *J* = 8.1 Hz, 1 H), 2.88 (dd, *J* = 9.4, 7.4 Hz, 1 H), 2.76 (t, *J* = 8.1 Hz, 1 H), 2.65 (q, *J* = 7.2 Hz, 1 H), 2.43 (d, *J* = 11.6 Hz, 1 H), 2.25 (d, *J* = 15.5 Hz, 1 H), 2.21 (s, 6 H), 1.87 (t, *J* = 7.3 Hz, 1 H), 1.83 – 1.73 (m, 1 H), 1.51 (ddd, *J* = 31.1, 14.3, 9.9 Hz, 3 H), 1.30 (s, 3 H), 1.13 (d, *J* = 6.1 Hz, 3 H), 1.10 (s, 3 H), 1.08 – 1.04 (comp, 11 H), 1.00 - 0.94 (comp, 10 H), 0.72 (t, *J* = 7.4 Hz, 3 H).

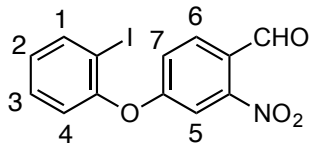

6.7

4-(2-Iodophenoxy)-2-nitrobenzaldehyde (6.7). ARMVI177. A solution of 4-fluoro-2-nitrobenzaldehyde (1.50 g, 8.9 mmol), 2-iodophenol (1.95 g, 8.9 mmol), copper (I) bromide (1.27 g, 8.9 mmol), and K_2CO_3 (2.45 g, 17.7 mmol) in pyridine (30 mL) was heated at 60 ºC for 12 h. The mixture was cooled to room temperature and filtered. The filtrate was diluted with ether (300 mL) and washed successively with aqueous NaOH (1 M, 2 x 200 mL), water (2 x 200 mL), and brine (200 mL). The organic fraction was dried (Na_2SO_4), filtered, and concentrated *in vacuo* to give crude **6.7** as an opaque viscous oil. The crude material was purified via silica gel flash column chromatography eluting with hexanes : ethyl acetate (92 : 8). To give 2.80 g (86%) of **6.7** as slightly yellow viscous oil: Spectral data matched that of previous reports:[181] ^{1}H NMR (400 MHz) δ 10.31 (d, *J* = 0.7 Hz, 1 H), 7.97 (d, *J* = 8.6 Hz, 1 H), 7.71 (dd, *J* = 8.0, 1.6 Hz, 1 H), 7.49 (d, *J* = 2.4 Hz, 1 H), 7.43 (td, *J* = 7.8, 1.6 Hz, 1 H), 7.25 - 7.17 (comp, 3 H)

NMR Assignment. ^{1}H NMR (400 MHz) δ 10.31 (d, *J* = 0.7 Hz, 1 H, CHO), 7.97 (d, *J* = 8.6 Hz, 1 H, C6-H), 7.71 (dd, *J* = 8.0, 1.6 Hz, 1 H, C1-H), 7.49 (d, *J* = 2.4 Hz, 1 H, C5-H), 7.43 (td, *J* = 7.8, 1.6 Hz, 1 H, C3-H), 7.25 - 7.17 (comp, 3 H, C7-H, C2-H, and C4-H)

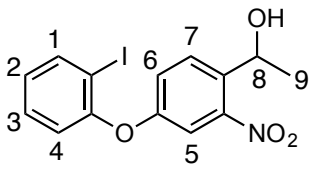

6.8

1-(4-(2-Iodophenoxy)-2-nitrophenyl)ethan-1-ol (6.8). ARMVI160. Trimethylaluminum (neat, 1.40 g, 20.0 mmol) was added dropwise over 20 min to a degassed solution of **6.7** (2.00 g, 13.2 mmol) in CH_2Cl_2 (90 mL) at 0 ºC. The reaction was stirred for 1 h at 0 ºC, whereupon cold water (~3 mL) was carefully added to quench excess trimethylaluminum. The mixture was warmed to room temperature, Rochelle's salt (100 mL) was added, and the mixture was stirred for 30 min. The phases were separated and the aqueous phase was extracted with CH_2Cl_2 (2 x 100 mL). The combined organic fractions were washed successively with aqueous NaOH (1 M, 200 mL) and brine (200 mL). The organic fraction was dried (Na_2SO_4), filtered, and concentrated *in vacuo* to give 2.11 g (98%) of **6.8** as a viscous yellow oil (>95% purity, by ^{1}H NMR). Spectral data matched that of previous reports:[181] ^{1}H NMR (400 MHz) δ 7.90 (dd, *J* = 7.9, 1.5 Hz, 1 H), 7.78 (d, *J* = 8.7 Hz, 1 H), 7.41 (d, *J* = 2.6 Hz, 1 H), 7.40 - 7.35 (m, 1 H), 7.21 (dd, *J* = 8.7, 2.6 Hz, 1 H), 7.02 - 6.96 (comp, 2 H), 5.36 (q, *J* = 6.3 Hz, 1 H), 1.56 (d, *J* = 6.3 Hz, 3 H)

NMR Assignment. ^{1}H NMR (400 MHz) δ 7.90 (dd, *J* = 7.9, 1.5 Hz, 1 H, C1-H), 7.78 (d, *J* = 8.7 Hz, 1 H, C7-H), 7.41 (d, *J* = 2.6 Hz, 1 H, C5-H), 7.40 - 7.35 (m, 1 H, C3-

H), 7.21 (dd, *J* = 8.7, 2.6 Hz, 1 H, C6-H), 7.02 - 6.96 (comp, 2 H, C2-H and C4-H), 5.36 (q, *J* = 6.3 Hz, 1 H, C8-H), 1.56 (d, *J* = 6.3 Hz, 3 H, C9-H)

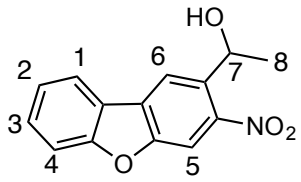

6.9

1-(3-Nitrodibenzo[*b*,*d*]furan-2-yl)ethan-1-ol (6.9). ARMVI164. A degassed solution of **6.8** (0.31 g, 0.80 mmol), $Pd(OAc)_2$ (18 mg, 0.08 mmol), and Cs_2CO_3 (0.52 g, 1.60 mmol) in DMAc (4 mL) was heated at 80 ºC for 6 h. The reaction was cooled to room temperature, then partitioned between water (50 mL) and ethyl acetate (50 mL). The two phases were separated and the aqueous phase was extracted with ethyl acetate (2 x 50 mL). The combined organic fractions were washed successively with water (100 mL) and brine (100 mL). The organic fractions were dried (Na_2SO_4), filtered, and concentrated *in vacuo* to give crude **6.9** as a viscous oil. The crude material was purified via silica gel flash column chromatography eluting with hexanes : ethyl acetate (19 : 1 → 17 : 3 along a gradient) to give 104 mg (51%) of **6.9** as a viscous oil. Spectra data matched that for previous reports:[181] ^{1}H NMR (400 MHz) δ 8.40 (s, 1 H), 8.15 (s, 1 H), 8.03 (d, *J* = 7.7 Hz, 1 H), 7.64 - 7.56 (comp, 2 H), 7.45 - 5.41 (m, 1 H), 5.58 (q, *J* = 6.2 Hz, 1 H), 2.46 (brs, 1 H), 1.67 (d, *J* = 6.3 Hz, 3 H)

NMR Assignment. ^{1}H NMR (400 MHz) δ 8.40 (s, 1 H, C5-H), 8.15 (s, 1 H, C6-H), 8.03 (d, *J* = 7.7 Hz, 1 H, C1-H), 7.64 - 7.56 (comp, 2 H, C3-H and C4-H), 7.45 - 5.41 (m, 1 H, C2-H), 5.58 (q, *J* = 6.2 Hz, 1 H, C7-H), 2.46 (brs, 1 H, OH), 1.67 (d, *J* = 6.3 Hz, 3 H, C8-H)

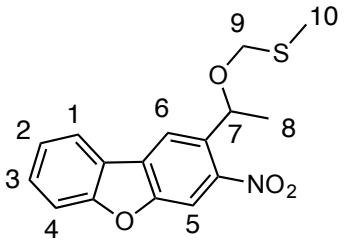

6.11

2-(1-((Methylthio)methoxy)ethyl)-3-nitrodibenzo[*b*,*d*]furan (6.11). **ARMVI194.** Solid benzoyl peroxide (0.74 g, 3.0 mmol) was added portion-wise over 30 min to a solution of **6.9** (0.20 g, 0.76 mmol) and dimethylsulfide (0.38 g, 6.1 mmol) in acetonitrile (4 mL) at 0 ºC. The solution was stirred for 5 h at 0 ºC, whereupon aqueous KOH (2 M, 25 mL) was added, and the mixture was stirred for 12 h at room temperature. The mixture was extracted with ethyl acetate (3 x 50 mL), and the combined organic fractions were washed successively with water (100 mL) and brine (100 mL), dried (Na_2SO_4), filtered, and concentrated *in vacuo* to give crude **6.11** as a viscous dark oil. The crude material was purified via silica gel flash column chromatography eluting with hexanes : ethyl acetate (10 : 1) to give 0.18 g (74%) of **6.11** as a light brown solid. Spectral data matched that of previous reports:[181] ^{1}H NMR (400 MHz) δ 8.32 (s, 1 H),

8.17 (s, 1 H), 8.04 (d, *J* = 7.4 Hz, 1 H), 7.63 (d, *J* = 8.1 Hz, 1 H), 7.58 (td, *J* = 7.4, 1.2 Hz, 1 H), 7.46 - 7.42 (m, 1 H), 5.55 (q, *J* = 6.3 Hz, 1 H), 4.69 (d, *J* = 11.5 Hz, 1 H), 4.37 (d, *J* = 11.5 Hz, 1 H), 2.16 (s, 3 H), 1.65 (d, *J* = 6.3 Hz, 3 H)

NMR Assignment. ^{1}H NMR (400 MHz) δ 8.32 (s, 1 H, C5-H), 8.17 (s, 1 H, C6-H), 8.04 (d, *J* = 7.4 Hz, 1 H, C1-H), 7.63 (d, *J* = 8.1 Hz, 1 H, C4-H), 7.58 (td, *J* = 7.4, 1.2 Hz, 1 H, C2-H), 7.46 - 7.42 (m, 1 H, C3-H), 5.55 (q, *J* = 6.3 Hz, 1 H, C7-H), 4.69 (d, *J* = 11.5 Hz, 1 H, C9-H), 4.37 (d, *J* = 11.5 Hz, 1 H, C9-H), 2.16 (s, 3 H, C10-H), 1.65 (d, *J* = 6.3 Hz, 3 H, C8-H)

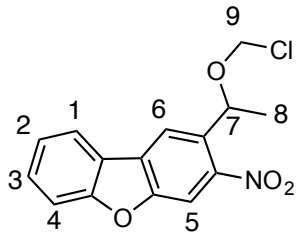

6.12

2-(1-(Chloromethoxy)ethyl)-3-nitrodibenzo[*b*,*d*]furan (6.12). ARMVI147. Sulfuryl chloride (31 mg, 0.23 mmol) was added dropwise to a solution of **6.11** (51 mg, 0.19 mmol) in CH_2Cl_2 (1 mL) at 0 ºC. The solution was stirred at 0 ºC for 30 min, at which point all volatiles were removed *in vacuo* to give 48 mg (98%) of **6.12** as an oil (>95% purity, by ^{1}H NMR). Spectral data matched that of previous reports:[181] ^{1}H NMR (400 MHz) δ 8.25 (s, 1 H), 8.22 (s, 1 H), 8.04 (d, *J* = 7.2 Hz, 1 H), 7.64 (d, *J* = 8.2 Hz, 1

H), 7.60 (td, *J* = 7.2, 1.2 Hz, 1 H), 7.46 - 7.42 (m, 1 H), 5.67 (q, *J* = 6.3 Hz, 1 H), 5.59 (d, *J* = 6.0 Hz, 1 H), 5.31 (d, *J* = 6.0 Hz, 1 H), 1.69 (d, *J* = 6.3 Hz, 1 H)

NMR Assignment. ^{1}H NMR (400 MHz) δ 8.25 (s, 1 H, C5-H), 8.22 (s, 1 H, C6-H), 8.04 (d, *J* = 7.2 Hz, 1 H, C1-H), 7.64 (d, *J* = 8.2 Hz, 1 H, C4-H), 7.60 (td, *J* = 7.2, 1.2 Hz, 1 H, C2-H), 7.46 - 7.42 (m, 1 H, C3-H), 5.67 (q, *J* = 6.3 Hz, 1 H, C7-H), 5.59 (d, *J* = 6.0 Hz, 1 H, C9-H), 5.31 (d, *J* = 6.0 Hz, 1 H, C9-H), 1.69 (d, *J* = 6.3 Hz, 1 H, C8-H)

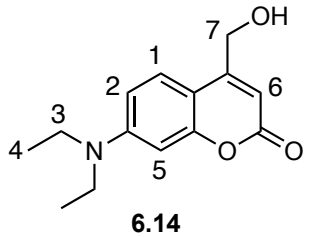

6.14

7-(Diethylamino)-4-(hydroxymethyl)-2*H*-chromen-2-one (6.14). ARMVI130. A suspension of **6.13** (5.00 g, 21.6 mmol) in xylenes (50 mL) was heated until complete dissolution was observed. Solid SeO_2 (3.36 g, 30.3 mmol) was added to the reaction, which was then heated under reflux for 16 h. The mixture was cooled to room temperature and all solids were removed by filtration. The filtrate was concentrated *in vacuo*, and the resulting residue was dissolved in methanol/THF (1:1, 50 mL). Sodium borohydride (0.82 g, 21.6 mmol) was slowly added to minimize effervescence, and the reaction was stirred for 4 h at room temperature. Aqueous HCl (1 M, 5 mL) was carefully added, and the volatiles were removed *in vacuo*. The resulting slurry was taken up in CH_2Cl_2 (300 mL), and washed with saturated aqueous K_2CO_3 (3 x 100 mL), dried

(Na_2SO4), filtered, and concentrated *in vacuo* to give crude **6.14** as a dark red oil. The crude material was purified via flash column chromatography eluting with CH_2Cl_2 : acetone (5 : 1) to give 1.53 g (29%) of **6.14** as a viscous oil. Spectral data matched that of previous reports:[250,251] ^{1}H NMR (400 MHz) δ 7.30 (d, *J* = 9.0 Hz, 1 H), 6.55 (dd, *J* = 9.0, 2.6 Hz, 1 H), 6.48 (d, *J* = 2.6 Hz, 1 H), 6.26 (t, *J* = 1.3 Hz, 1 H), 4.82 (s, 2 H), 3.39 (q, *J* = 7.1 Hz, 4 H), 2.49 (brs, 1 H), 1.19 (t, *J* = 7.1 Hz, 6 H)

NMR Assignment. ^{1}H NMR (400 MHz) δ 7.30 (d, *J* = 9.0 Hz, 1 H, C1-H), 6.55 (dd, *J* = 9.0, 2.6 Hz, 1 H, C2-H), 6.48 (d, *J* = 2.6 Hz, 1 H, C5-H), 6.26 (t, *J* = 1.3 Hz, 1 H, C6-H), 4.82 (s, 2 H, C7-H), 3.39 (q, *J* = 7.1 Hz, 4 H, C3-H), 2.49 (brs, 1 H, OH), 1.19 (t, *J* = 7.1 Hz, 6 H, C4-H).

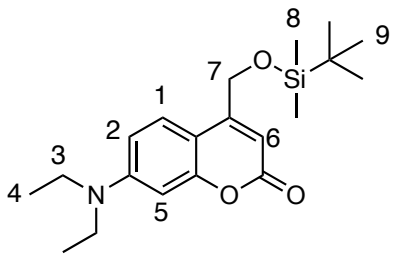

6.15

4-(((*tert*-Butyldimethylsilyl)oxy)methyl)-7-(diethylamino)-2*H*-chromen-2-one (6.15). ARMVI162. A solution of **6.14** (0.51 g, 2.1 mmol), TBSCl (0.34 g, 2.3 mmol), and imidazole (0.21 g, 3.1 mmol) in CH_2Cl_2 (20 mL) was stirred for 12 h at room temperature. The solution was diluted with CH_2Cl_2 (100 mL) and washed successively with saturated aqueous NH_4Cl (100 mL), water (100 mL), and brine (100 mL). The

organic fraction was dried (Na_2SO_4), filtered, and concentrated *in vacuo* to give crude **6.15** as a viscous oil. The crude material was purified via silica gel flash column chromatography eluting with hexanes : ethyl acetate (9 : 1) to give 0.58 g (77%) of **6.15** as a yellow solid. Spectral data matched that of previous reports:[250,251] ^{1}H NMR (400 MHz) δ 7.24 (d, *J* = 8.9 Hz, 1 H), 6.54 (dd, *J* = 8.9, 2.6 Hz, 1 H), 6.50 (d, *J* = 2.6 Hz, 1 H), 6.28 (t, *J* = 1.3 Hz, 1 H), 4.81 (d, *J* = 1.3 Hz, 2 H), 3.39 (q, *J* = 7.1 Hz, 4 H), 1.20 (t, *J* = 7.1 Hz, 6 H), 0.95 (s, 9 H), 0.14 (s, 6 H)

NMR Assignment. ^{1}H NMR (400 MHz) δ 7.24 (d, *J* = 8.9 Hz, 1 H, C1-H), 6.54 (dd, *J* = 8.9, 2.6 Hz, 1 H, C2-H), 6.50 (d, *J* = 2.6 Hz, 1 H, C5-H), 6.28 (t, *J* = 1.3 Hz, 1 H, C6-H), 4.81 (d, *J* = 1.3 Hz, 2 H, C7-H), 3.39 (q, *J* = 7.1 Hz, 4 H, C3-H), 1.20 (t, *J* = 7.1 Hz, 6 H, C4-H), 0.95 (s, 9 H, C9-H), 0.14 (s, 6 H, C8-H)

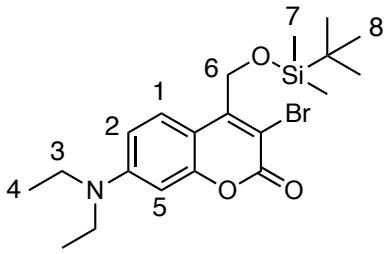

6.16

3-Bromo-4-(((*tert*-butyldimethylsilyl)oxy)methyl)-7-(diethylamino)-2*H*-chromen-2-one (6.16). ARMVI172. Solid NBS (1.19 g, 6.7 mmol) was added to a solution of **6.15** (2.21 g, 6.1 mmol) and NH_4OAc (0.047 g, 0.61 mmol) in acetonitrile (40 mL), and the reaction was stirred for 1 h at room temperature. The solution was poured

into water (150 mL) and extracted with ethyl acetate (3 x 150 mL). The combined organic fractions were dried (Na_2SO_4), filtered, and concentrated *in vacuo* to give crude **6.16**. The crude material was purified via silica gel flash column chromatography eluting with hexanes : ethyl acetate (9 :1) to give 2.32 g (86%) of **6.16** as a yellow solid. Spectral data matched that of previous reports:[250,251] ^{1}H NMR (400 MHz) δ 7.70 (d, *J* = 9.2 Hz, 1 H), 6.58 (dd, *J* = 9.2, 2.6 Hz, 1 H), 6.42 (d, *J* = 2.6 Hz, 1 H), 4.95 (s, 2 H), 3.38 (q, *J* = 7.1 Hz, 4 H), 1.18 (t, *J* = 7.1 Hz, 6 H), 0.87 (s, 9 H), 0.11 (s, 6 H)

NMR Assignment. ^{1}H NMR (400 MHz) δ 7.70 (d, *J* = 9.2 Hz, 1 H, C1-H), 6.58 (dd, *J* = 9.2, 2.6 Hz, 1 H, C2-H), 6.42 (d, *J* = 2.6 Hz, 1 H, C5-H), 4.95 (s, 2 H, C6-H), 3.38 (q, *J* = 7.1 Hz, 4 H, C3-H), 1.18 (t, *J* = 7.1 Hz, 6 H, C4-H), 0.87 (s, 9 H, C8-H), 0.11 (s, 6 H, C7-H)

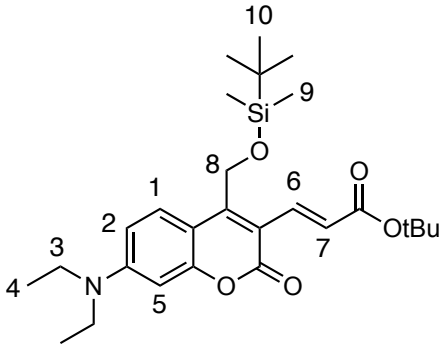

6.17

***tert*-Butyl (*E*)-3-(4-(((*tert*-butyldimethylsilyl)oxy)methyl)-7-(diethylamino)-2-oxo-2*H*-chromen-3-yl)acrylate (6.17). ARMVI187.** Solid lithium chloride (29 mg, 0.69 mmol), $NaHCO_3$ (102 mg, 1.22 mmol), and $Pd(OAc)_2$ (18 mg, 0.08 mmol) were

sequentially added to a degassed solution of **6.16** (179 mg, 0.41 mmol) and *t*-butyl acrylate (156 mg, 1.22 mmol) in DMF (4 mL), and the reaction was stirred for 30 min at 110 ºC. The reaction was cooled to room temperature and poured into water (20 mL). The mixture was extracted with ether (3 x 20 mL), followed by ethyl acetate (20 mL). The combined organic fractions were washed with brine (50 mL), dried (Na_2SO_4), filtered, and concentrated *in vacuo* to give crude **6.17** as a yellow oil. The crude material was purified via silica gel flash column chromatography eluting with hexanes : ethyl acetate (9 : 1) to give 81 mg (41%) of **6.17** as a yellow solid and 17 mg (9%) of returned starting material (**6.16**) as a yellow solid. Spectral data matched that of previous reports:[250,251] ^{1}H NMR (400 MHz) δ 7.74 (d, *J* = 15.6 Hz, 1 H), 7.63 (d, *J* = 9.2 Hz, 1 H), 6.98 (d, *J* = 15.6 Hz, 1 H), 6.61 (dd, *J* = 9.2, 2.6 Hz, 1 H), 6.45 (d, *J* = 2.6 Hz, 1 H), 4.89 (s, 2 H), 3.42 (q, *J* = 7.1 Hz, 4 H), 1.51 (s, 9 H), 1.21 (t, *J* = 7.1 Hz, 6 H), 0.89 (s, 9 H), 0.15 (s, 6 H)

NMR Assignment. ^{1}H NMR (400 MHz) δ 7.74 (d, *J* = 15.6 Hz, 1 H, C6-H), 7.63 (d, *J* = 9.2 Hz, 1 H, C1-H), 6.98 (d, *J* = 15.6 Hz, 1 H, C7-H), 6.61 (dd, *J* = 9.2, 2.6 Hz, 1 H, C2-H), 6.45 (d, *J* = 2.6 Hz, 1 H, C5-H), 4.89 (s, 2 H, C8-H), 3.42 (q, *J* = 7.1 Hz, 4 H, C3-H), 1.51 (s, 9 H, O*t*Bu), 1.21 (t, *J* = 7.1 Hz, 6 H, C4-H), 0.89 (s, 9 H, C10-H), 0.15 (s, 6 H, C9-H)

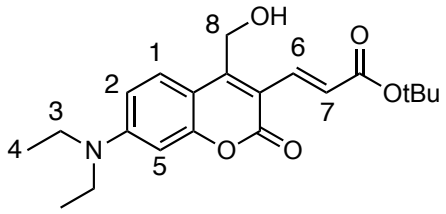

6.18

***tert*-Butyl (*E*)-3-(7-(diethylamino)-4-(hydroxymethyl)-2-oxo-2*H*-chromen-3-yl)acrylate (6.18). ARMVI246.** 3HF•Et_3N (108 mg, 0.67 mmol) was added dropwise to a solution of **6.17** (30 mg, 0.067 mmol) and triethylamine (67 mg, 0.67 mmol) in CH_2Cl_2 (2 mL), and the reaction was stirred for 2 h at room temperature. Ice cold water (5 mL) was added, and the resulting mixture was extracted with CH_2Cl_2 (3 x 10 mL). The combined organic fractions were dried (Na_2SO_4), filtered, and concentrated *in vacuo* to give 21 mg (92%) of **6.18** as an oil (>95% purity, by ^{1}H NMR): ^{1}H NMR (400 MHz) δ 7.78 (d, *J* = 15.6 Hz, 1 H), 7.67 (d, *J* = 9.2 Hz, 1 H), 7.07 (d, *J* = 15.6 Hz, 1 H), 6.62 (dd, *J* = 9.2, 2.6 Hz, 1 H), 6.46 (d, *J* = 2.6 Hz, 1 H), 4.95 (s, 2 H), 3.42 (q, *J* = 7.0 Hz, 4 H), 1.50 (s, 9 H), 1.25 - 1.19 (comp, 7 H).

NMR Assignment. ^{1}H NMR (400 MHz) δ 7.78 (d, *J* = 15.6 Hz, 1 H, C6-H), 7.67 (d, *J* = 9.2 Hz, 1 H, C1-H), 7.07 (d, *J* = 15.6 Hz, 1 H, C7-H), 6.62 (dd, *J* = 9.2, 2.6 Hz, 1 H, C2-H), 6.46 (d, *J* = 2.6 Hz, 1 H, C5-H), 4.95 (s, 2 H, C8-H), 3.42 (q, *J* = 7.0 Hz, 4 H, C3-H), 1.50 (s, 9 H, O*t*Bu), 1.25 - 1.19 (comp, 7 H, C4-H and OH).

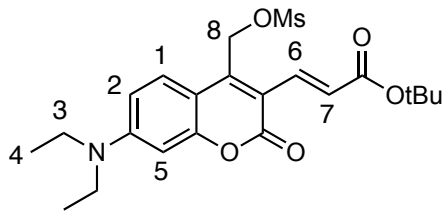

6.19

***tert*-Butyl (*E*)-3-(7-(diethylamino)-4-(((methylsulfonyl)oxy)methyl)-2-oxo-2*H*-chromen-3-yl)acrylate (6.19). ARMVI191.** A solution of MsCl (45 mg, 0.39 mmol) in CH_2Cl_2 (1 mL) was added dropwise to a solution of **6.18** (97 mg, 0.26 mmol) and triethylamine (53 mg, 0.52 mmol) in CH_2Cl_2 (15 mL) at 0 ºC, and the reaction was stirred for 20 min at 0 ºC. The mixture was poured into water (30 mL), and extracted with CH_2Cl_2 (3 x 30 mL). The combined organic fractions were washed with water (1 x 30 mL), dried (Na_2SO_4), filtered, and concentrated *in vacuo* to give 113 mg (96%) of **6.19** as an oil (>95% purity, by ^{1}H NMR): ^{1}H NMR (400 MHz) δ 7.68 (d, *J* = 15.5 Hz, 1 H), 7.62 (d, *J* = 9.3 Hz, 1 H), 7.08 (d, *J* = 15.5 Hz, 1 H), 6.66 (dd, *J* = 9.3, 2.6 Hz, 1 H), 6.49 (d, *J* =2.6 Hz, 1 H), 5.48 (s, 2 H), 3.44 (q, *J* = 7.1 Hz, 4 H), 3.10 (s, 3 H), 1.52 (s, 9 H), 1.23 (t, *J* = 7.1 Hz, 6 H).

NMR Assignment. ^{1}H NMR (400 MHz) δ 7.68 (d, *J* = 15.5 Hz, 1 H, C6-H), 7.62 (d, *J* = 9.3 Hz, 1 H, C1-H), 7.08 (d, *J* = 15.5 Hz, 1 H, C7-H), 6.66 (dd, *J* = 9.3, 2.6 Hz, 1 H, C2-H), 6.49 (d, *J* =2.6 Hz, 1 H, C5-H), 5.48 (s, 2 H, C8-H), 3.44 (q, *J* = 7.1 Hz, 4 H, C3-H), 3.10 (s, 3 H, OMs), 1.52 (s, 9 H, O*t*Bu), 1.23 (t, *J* = 7.1 Hz, 6 H, C4-H).

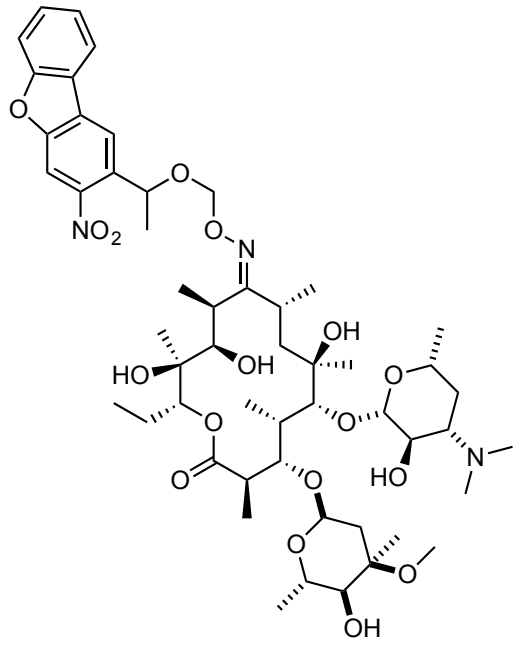

NDBF-ERY (6.20)

Nitrodibenzofuran-caged erythromycin A-9-oxime (NDBF-ERY, 6.20). ARMVI203. Solid sodium hydride (60% oil dispersion, 8.4 mg, 0.21 mmol) was added to a solution of **6.2** (104 mg, 0.14 mmol) in DMF/THF (1:1, 3 mL) at 0 ºC, and the suspension was stirred for 30 min at 0 ºC. A solution of **6.12** (86 mg, 0.28 mmol) in DMF/THF (1:1, 2 mL) was added, and the reaction was stirred for 30 min at 0 ºC. The reaction was warmed to room temperature, and stirred for 12 h, whereupon water (~1 mL) was carefully added. The mixture was diluted with CH_2Cl_2 (50 mL), and was washed with saturated aqueous $NaHCO_3$ (3 x 50 mL), dried (Na_2SO_4), filtered, and concentrated *in vacuo* to give crude **6.20**. The crude material was purified via silica gel flash column chromatography eluting along a gradient with hexanes : ethyl acetate : Et_3N (9 : 1 : 1%) → CH_2Cl_2 (1% Et_3N) to give 110 mg (78%) of **6.20** as a white solid: ^1H

NMR (400 MHz) δ 8.38 (d, *J* = 7.8 Hz, 1 H), 8.15 (d, *J* = 11.4 Hz, 1 H), 7.65 – 7.52 (comp, 3 H), 7.47 – 7.35 (m, 1 H), 5.52 (q, *J* = 6.2 Hz, 0.5 H), 5.44 (q, *J* = 6.3 Hz, 0.5 H), 5.25 – 5.19 (m, 1 H), 5.14 (d, *J* = 6.6 Hz, 1 H), 5.10 – 5.05 (m, 1 H), 5.02 (dd, *J* = 6.7, 2.7 Hz, 1 H), 4.86 (d, *J* = 4.7 Hz, 1 H), 4.45 – 4.38 (m, 1 H), 4.35 (d, *J* = 10.5 Hz, 0.5 H), 4.22 (d, *J* = 11.4 Hz, 0.5 H), 4.15 – 4.08 (m, 1 H), 4.01 (dd, *J* = 9.4, 6.1 Hz, 1 H), 3.97 – 3.93 (m, 1 H), 3.77 (d, *J* = 18.7 Hz, 1 H), 3.66 – 3.55 (m, 1 H), 3.53 – 3.39 (comp, 2 H), 3.33 (s, 3 H), 3.28 (s, 1 H) 3.21 (ddd, *J* = 9.9, 7.3, 2.6 Hz, 1 H), 3.10 (s, 1 H), 3.00 (t, *J* = 9.4 Hz, 1 H), 2.96 – 2.82 (comp, 3 H), 2.67 (q, *J* = 7.1 Hz, 1 H), 2.37 - 2.31 (comp, 4 H), 2.28 (s, 6 H), 2.03 – 1.85 (comp, 2 H), 1.69 – 1.56 (comp, 4 H), 1.56 – 1.38 (comp, 6 H), 1.30 (dd, *J* = 9.1, 6.2 Hz, 2 H), 1.27 – 1.13 (comp, 12 H), 1.14 – 1.06 (comp, 6 H), 0.92 – 0.76 (m, 4 H), 0.69 (d, *J* = 6.9 Hz, 1 H). ^{13}C NMR (100 MHz) δ 175.2, 174.0, 158.3, 154.0, 153.8, 135.1, 134.2, 130.2, 129.6, 129.4, 129.4, 123.7, 122.7, 122.6, 122.4, 121.9, 120.1, 119.9, 119.8, 119.6, 117.7, 112.1, 112.0, 108.4, 107.9, 103.0, 96.4, 96.3, 96.1, 95.4, 80.2, 77.9, 77.3, 77.2, 77.0, 76.8, 76.7, 75.1, 75.1, 74.3, 72.7, 71.6, 70.8, 70.4, 70.3, 68.5, 65.5, 65.4, 56.0, 49.4, 49.4, 44.7, 44.6, 40.1, 38.9, 37.7, 35.0, 33.1, 29.7, 29.3, 27.1, 27.0, 26.9, 24.4, 23.6, 22.7, 21.5, 21.3, 21.1, 18.6, 18.2, 16.3, 16.2, 16.1, 14.5, 14.4, 14.1, 10.7, 10.6, 9.2.

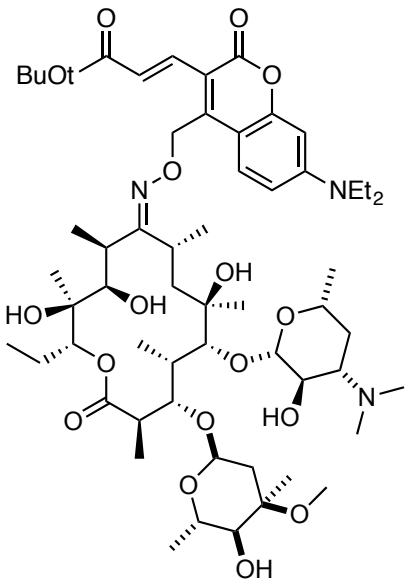

DEAC450-ERY (6.21)

Diethylaminocoumarin 450-caged erythromycin A-9-oxime (DEAC450-ERY, 6.21). ARMVI193. Solid sodium hydride (60% oil dispersion, 6.0 mg, 0.15 mmol) was added to a solution of **6.2** (75 mg, 0.10 mmol) in DMF/THF (1:1, 3 mL) at 0 ºC, and the resulting suspension was stirred for 30 min at 0 ºC. A solution of **6.19** (113 mg, 0.25 mmol) in DMF/THF (1:1, 2 mL) was added, and the reaction was stirred for 30 min at 0 ºC. The ice bath was removed and the reaction was stirred for 12 h at room temperature, whereupon water (~1 mL) was carefully added. The mixture was diluted with CH_2Cl_2 (50 mL), and washed with saturated aqueous $NaHCO_3$ (3 x 50 mL), dried (Na_2SO_4), filtered, and concentrated *in vacuo* to give crude **6.21**. The crude material was purified via silica gel flash column chromatography eluting along a gradient hexanes : CH_2Cl_2 : Et_3N (1 : 1 : 1% → 0 : 1 : 1%) to give 43 mg (39%) of **6.21** as a yellow solid: ^{1}H NMR (400 MHz) δ 7.78 (d, *J* = 15.7 Hz, 1 H), 7.56 (t, *J* = 9.6 Hz, 1 H), 6.97 (d, *J* = 15.6 Hz, 1 H), 6.66 (dd, *J*

= 9.3, 2.6 Hz, 1 H), 6.47 (d, *J* = 2.7 Hz, 1 H), 5.35 (d, *J* = 11.7 Hz, 1 H), 5.24 (dd, *J* = 11.9, 9.1 Hz, 1 H), 5.10 (dt, *J* = 11.1, 2.5 Hz, 1 H), 4.87 (d, *J* = 5.0 Hz, 1 H), 4.38 (dd, *J* = 11.1, 7.2 Hz, 1 H), 4.20 (d, *J* = 6.2 Hz, 1 H), 3.97 (t, *J* = 7.9 Hz, 2 H), 3.74 (d, *J* = 15.2 Hz, 1 H), 3.61 - 3.57 (m, 1 H), 3.55 – 3.35 (comp, 7 H), 3.29 (s, 3 H), 3.18 (dd, *J* = 10.3, 7.1 Hz, 1 H), 3.09 (s, 1 H), 2.98 (t, *J* = 9.7 Hz, 1 H), 2.92 – 2.87 (m, 1 H), 2.64 (q, *J* = 7.3 Hz, 1 H), 2.46 – 2.30 (comp, 2 H), 2.31 – 2.13 (comp, 7 H), 2.02 – 1.84 (comp, 3 H), 1.64 (d, *J* = 11.4 Hz, 1 H), 1.60 - 1.45 (comp, 12 H), 1.32 (s, 2 H), 1.29 – 1.12 (comp, 20 H), 1.22 - 1.14 (comp, 10 H), 0.90 (d, *J* = 7.0 Hz, 2 H), 0.83 (t, *J* = 7.3 Hz, 3 H).

Determination of aqueous solubility. NDBF-ERY (6.20). UV-Vis spectra were collected on a DU series 730 UV/Vis scanning spectrophotometer (Beckman Coulter). The spectra were collected with a wavelength range 200 – 500 nm, in 0.5 nm increments. Samples were places in a quartz cuvette with a 1 cm pathlength. The samples were prepared from by adding aqueous phosphate buffer (0.1 M, pH 7.4, 10 mL) to a sample of **NDBF-ERY** (1.17 mg, 1.15 μmol) and sonicating for 15 min. Serial dilutions were performed by taking aliquots of the previous solution (0.9 mL, 0.8 mL, 0.7 mL…) and diluting each aliquot with phosphate buffer to a final volume of 1 mL. Each sample was immediately analyzed by UV-Vis spectrophotometry. The saturated aqueous sample was prepared by sonicating a suspension of **NDBF-ERY** (1.9 mg, 1.9 μmol) in phosphate buffer (10 mL) for 30 min and passing the resulting suspension through a syringe filter. The UV/Vis spectroscopy results are shown below. For each sample, absorbance (350 nm) was plotted against concentration to give the Beer's law plot shown below.

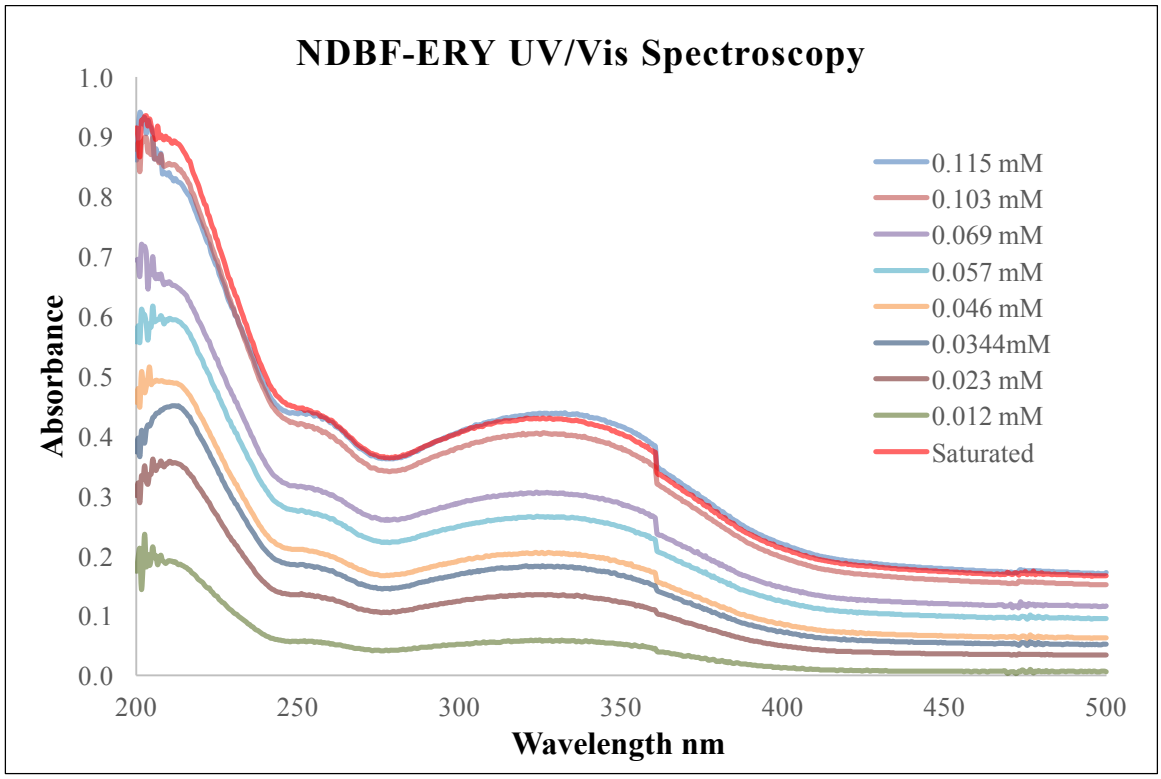
NDBF-ERY UV/Vis Spectroscopy
Absorbance
Wavelength nm
0.115 mM
0.103 mM
0.069 mM
0.057 mM
0.046 mM
0.0344mM
0.023 mM
0.012 mM
Saturated

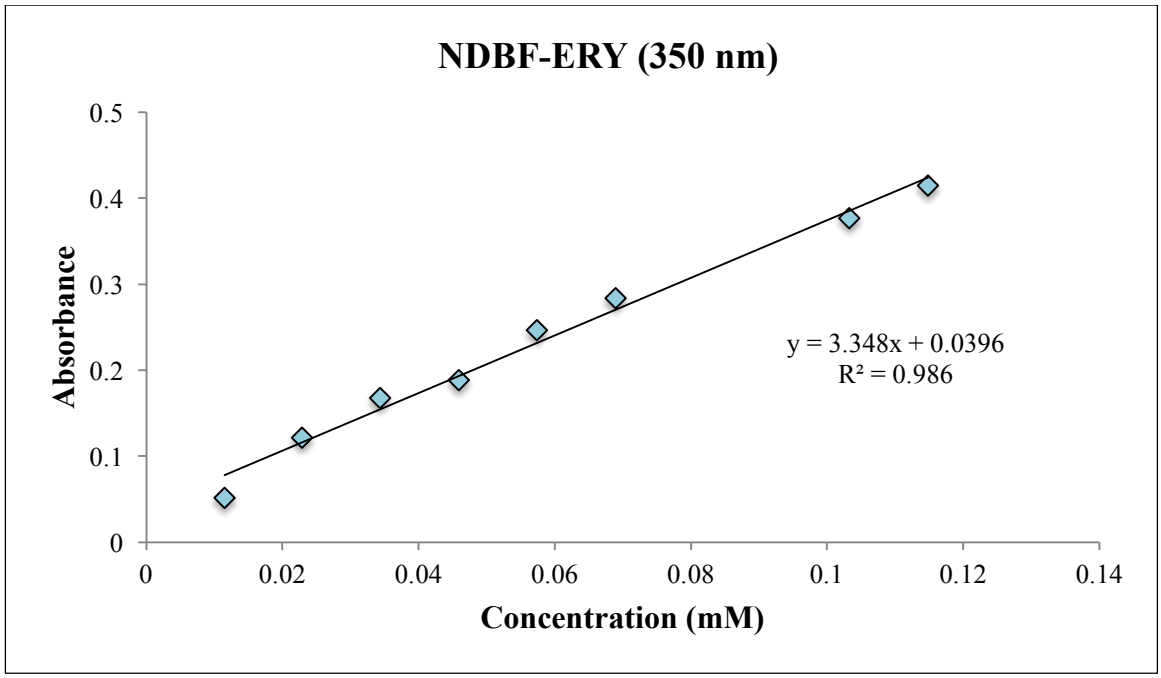
NDBF-ERY (350 nm)
Absorbance
Concentration (mM)
y = 3.348x + 0.0396
R² = 0.986

Determination of aqueous solubility. DEAC450-ERY (6.21). UV-Vis spectra were collected on a DU series 730 UV/Vis scanning spectrophotometer (Beckman Coulter). The spectra were collected with a wavelength range 200 – 700 nm, in 1 nm increments. Samples were places in a quartz cuvette with a 1 cm pathlength. The samples were prepared from by adding aqueous phosphate buffer (0.1 M, pH 7.4, 10 mL) to a sample of **DEAC450-ERY** (1.27 mg, 1.15 μmol) and sonicating for 15 min. Serial dilutions were performed by taking aliquots of the previous solution (0.9 mL, 0.8 mL, 0.7 mL…) and diluting each aliquot with phosphate buffer to a final volume of 1 mL. Each sample was immediately analyzed by UV-Vis spectrophotometry. The saturated aqueous sample was prepared by sonicating a suspension of **DEAC450-ERY** (2.1 mg, 1.8 μmol) in phosphate buffer (10 mL) for 30 min and passing the resulting suspension through a syringe filter. The UV/Vis spectroscopy results are shown below. For each sample, absorbance (461 nm) was plotted against concentration to give the Beer's law plot shown below.

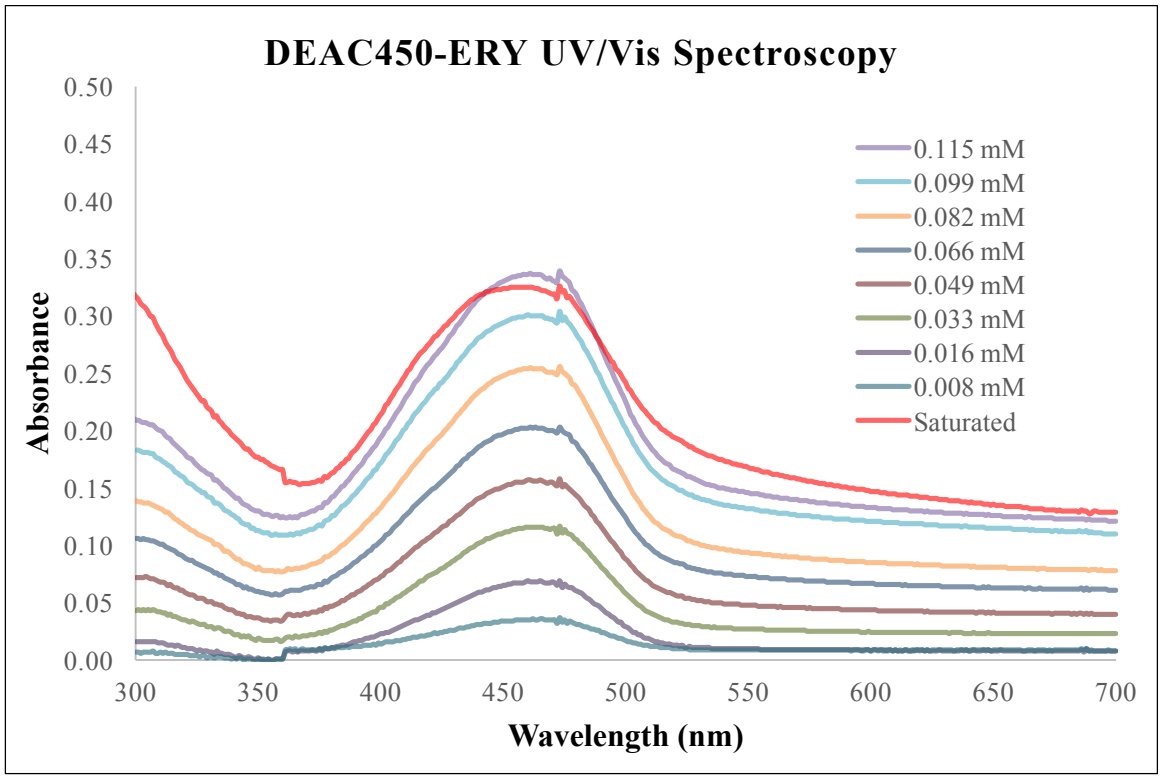
DEAC450-ERY UV/Vis Spectroscopy
Absorbance
Wavelength (nm)
0.115 mM
0.099 mM
0.082 mM
0.066 mM
0.049 mM
0.033 mM
0.016 mM
0.008 mM
Saturated

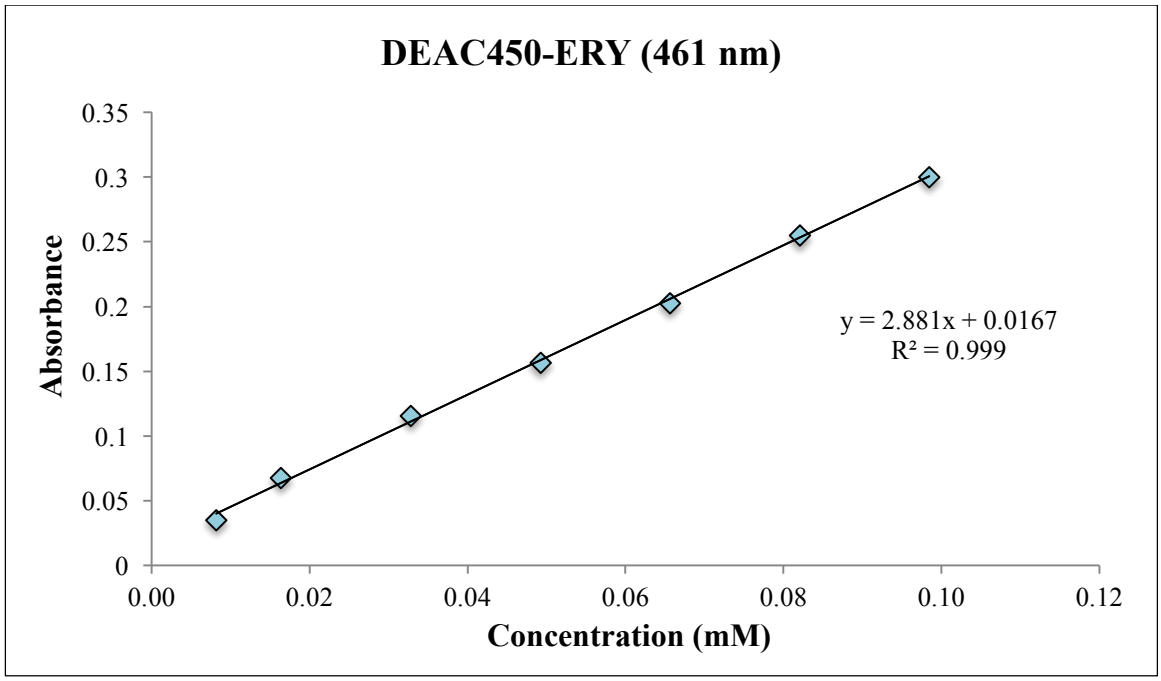
DEAC450-ERY (461 nm)
Absorbance
Concentration (mM)
y = 2.881x + 0.0167
R² = 0.999

Decaging Studies. Samples were irradiated in a QuantaMaster™ 500 Spectrofluorometer (PTI Inc.), with a 75 W xenon arc lamp light source and a bandpass filter of 20 nm. The power output of light at wavelengths of 325 – 500 (± 20) nm was measured to be 5-6 mW. Each sample was run in duplicate. Aqueous stock solutions (100 µM) were prepared by placing solid **NDBF-ERY** (0.41 mg, 0.4 µmol) and **DEAC450-ERY** (0.44 mg, 0.4 µmol), respectively, into water (4 mL) and sonicating for 30 min. The negative control sample (100 µL) was placed in a LC/MS vial and kept in the dark for the entirety of the study. Aliquots (100 µL) of the stock solution were placed in a quartz cuvette (volume = 100 µL, pathlength = 1 cm), which was placed in the spectrofluorometer and irradiated at the specified wavelength for 5 min. The sample was transferred via a fresh syringe into an LC/MS vial, and the cuvette was rinsed with water (3 x 100 µL) before adding the next sample. Each sample was analyzed by LC/MS, and the MS trace (example below) of each sample was quantified by peak area of **ERY-9-OX** and compared to area of the respective starting material peak.

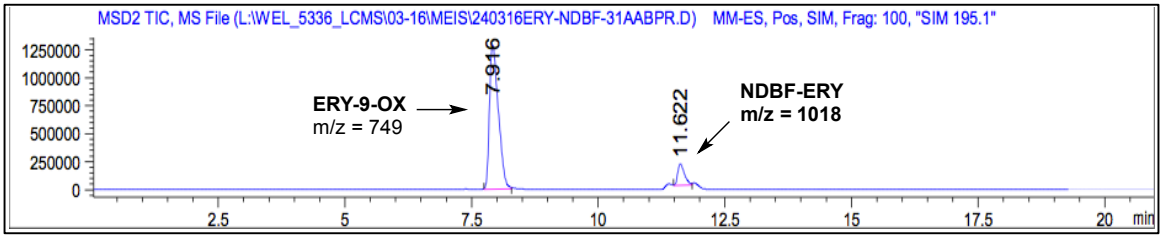

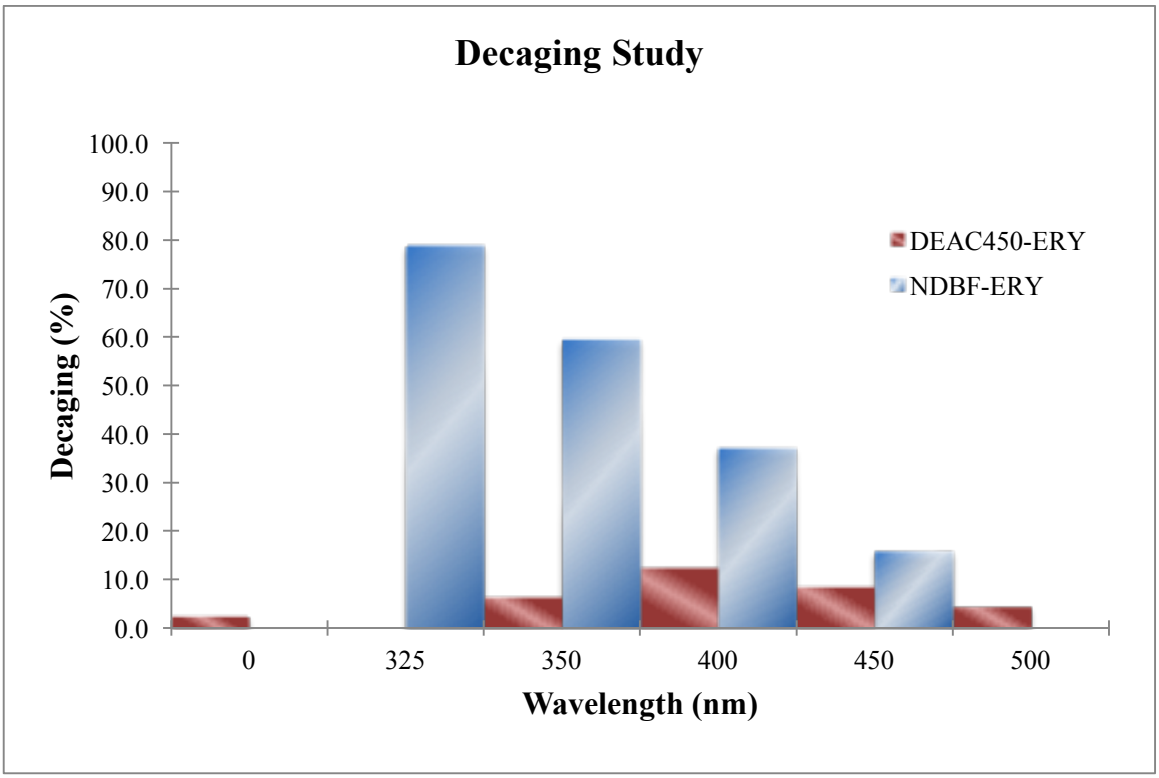
Decaging Study
100.0
90.0
80.0
70.0
60.0
50.0
40.0
30.0
20.0
10.0
0.0
Decaging (%)
0
325
350
400
450
500
Wavelength (nm)
DEAC450-ERY
NDBF-ERY

Appendix A:

Figure A.1. Crystal structure of **2.54** showing the atom labeling scheme. Displacement ellipsoids are scaled to the 50% probability level.

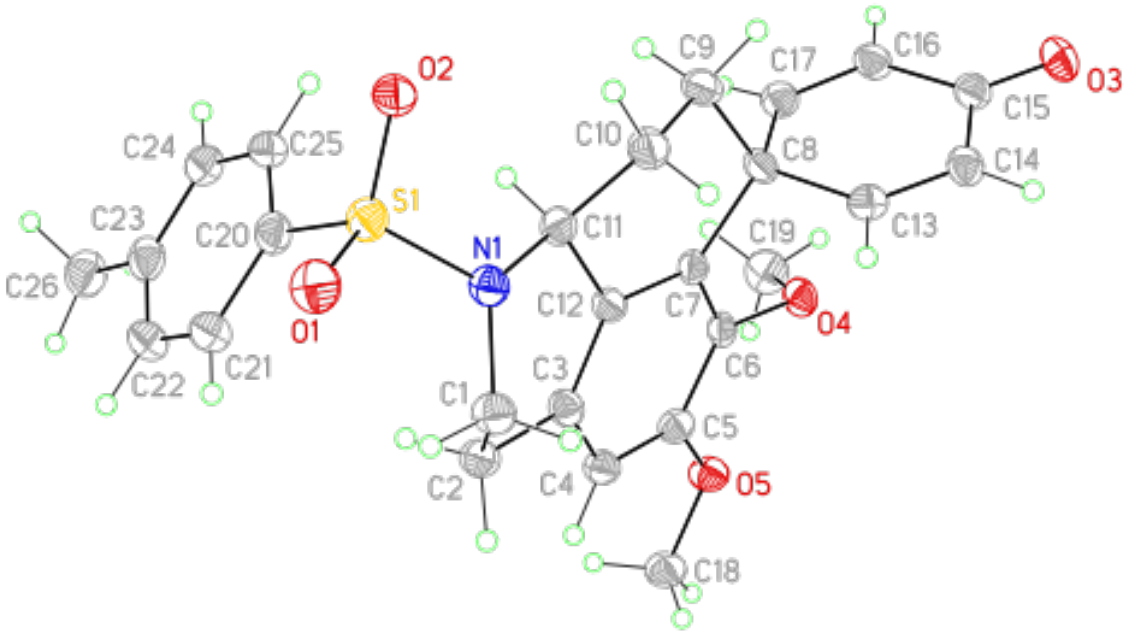

X-ray Experimental for $C_{26}H_{27}NO_5S$: Crystals grew as clusters of colorless prisms by slow diffusion of hexanes into ethyl acetate. The data crystal was cut from a larger crystal and had approximate dimensions; 0.20 x 0.18 x 0.12 mm. The data were collected on a Rigaku SCX-Mini diffractometer with a Mercury 2 CCD using a graphite monochromator with MoKα radiation (λ = 0.71075Å). A total of 481 frames of data were collected using ω-scans with a scan range of 1° and a counting time of 60 seconds per frame. The data were collected at 163 K using a Rigaku XStream low temperature

device. Details of crystal data, data collection and structure refinement are listed in Table 1. Data reduction were performed using the Rigaku Americas Corporation's Crystal Clear version 1.40.[314] The structure was solved by direct methods using SIR97[315] and refined by full-matrix least-squares on F^2 with anisotropic displacement parameters for the non-H atoms using SHELXL-97.[316] Structure analysis was aided by use of the programs PLATON98[317] and WinGX.[318] The hydrogen atoms on carbon were calculated in ideal positions with isotropic displacement parameters set to 1.2xUeq of the attached atom (1.5xUeq for methyl hydrogen atoms).

The function, $\Sigma w(|F_o|^2 - |F_c|^2)^2$, was minimized, where $w = 1/[(\sigma(F_o))^2 + (0.0418*P)^2 + (1.55*P)]$ and $P = (|F_o|^2 + 2|F_c|^2)/3$. $R_w(F^2)$ refined to 0.110, with R(F) equal to 0.0475 and a goodness of fit, S, = 0.922. Definitions used for calculating R(F), $R_w(F^2)$ and the goodness of fit, S, are given below.[319] The data were corrected for secondary extinction effects. The correction takes the form: $F_{corr} = kF_c/[1 + (2.3(6)x10^{-6})* F_c^2 \lambda^3/(\sin 2\theta)]^{0.25}$ where k is the overall scale factor. Neutral atom scattering factors and values used to calculate the linear absorption coefficient are from the International Tables for X-ray Crystallography (1992).[320] All figures were generated using SHELXTL/PC.[321] Tables of positional and thermal parameters, bond lengths and angles, torsion angles and figures are found in the proceeding sections.

Table A.1. Crystal data and structure refinement for **2.54**.

Empirical formula	C26 H27 N O5 S	
Formula weight	465.54	
Temperature	100(2) K	
Wavelength	0.71073 Å	
Crystal system	monoclinic	
Space group	C c	
Unit cell dimensions	a = 10.8751(14) Å	α= 90°.
	b = 23.420(3) Å	b= 99.649(6)°.
	c = 9.0337(12) Å	γ= 90°.
Volume	2268.2(5) $Å^3$	
Z	4	
Density (calculated)	1.363 Mg/m^3	
Absorption coefficient	0.182 mm^{-1}	
F(000)	984	
Crystal size	0.200 x 0.180 x 0.120 mm	
Theta range for data collection	2.089 to 27.483°.	
Index ranges	-14<=h<=14, -30<=k<=30, -11<=l<=11	
Reflections collected	10697	
Independent reflections	4726 [R(int) = 0.0576]	

Completeness to theta = 25.242°	99.9 %
Absorption correction	Semi-empirical from equivalents
Max. and min. transmission	1.00 and 0.761
Refinement method	Full-matrix least-squares on F^2
Data / restraints / parameters	4726 / 2 / 303
Goodness-of-fit on F^2	0.922
Final R indices [I>2sigma(I)]	R1 = 0.0475, wR2 = 0.1031
R indices (all data)	R1 = 0.0581, wR2 = 0.1101
Absolute structure parameter	0.02(12)
Extinction coefficient	$2.3(6)x10^{-6}$
Largest diff. peak and hole	0.270 and -0.256 e.$Å^{-3}$

Table A.2. Atomic coordinates ($x10^4$) and equivalent isotropic displacement parameters ($Å^2x10^3$) for **2.54**

U(eq) is defined as one third of the trace of the orthogonalized U^{ij} tensor.

	x	y	z	U(eq)
C1	1155(4)	2845(2)	2004(5)	24(1)
C2	558(4)	3429(2)	2013(5)	24(1)
C3	1554(4)	3883(2)	2135(5)	20(1)
C4	1259(4)	4412(2)	1455(5)	22(1)
C5	2170(4)	4830(2)	1520(5)	21(1)
C6	3403(3)	4703(2)	2191(4)	18(1)
C7	3713(4)	4172(2)	2842(4)	17(1)
C8	5106(4)	4023(2)	3322(5)	20(1)
C9	5261(4)	3476(2)	4308(5)	25(1)
C10	4352(4)	3008(2)	3716(5)	25(1)
C11	3045(3)	3219(2)	3777(5)	20(1)
C12	2761(4)	3762(2)	2860(4)	19(1)
C13	5623(4)	3897(2)	1914(5)	21(1)
C14	6704(4)	4101(2)	1627(5)	23(1)
C15	7470(4)	4495(2)	2659(5)	23(1)
C16	6972(4)	4662(2)	4008(5)	23(1)
C17	5864(4)	4476(2)	4255(5)	24(1)

C18	704(4)	5480(2)	195(5)	28(1)
C19	4276(4)	5601(2)	3026(6)	32(1)
C20	838(4)	2784(2)	5738(5)	24(1)
C21	-446(4)	2832(2)	5218(5)	28(1)
C22	-1152(4)	3182(2)	5989(5)	30(1)
C23	-621(4)	3487(2)	7252(5)	28(1)
C24	651(4)	3425(2)	7769(5)	26(1)
C25	1381(4)	3077(2)	7015(5)	25(1)
C26	-1418(4)	3879(2)	8037(6)	34(1)
N1	2106(3)	2757(1)	3344(4)	22(1)
O1	989(3)	1906(1)	4021(4)	30(1)
O2	2907(3)	2247(1)	5705(4)	26(1)
O3	8473(3)	4676(1)	2388(4)	31(1)
O4	4332(3)	5098(1)	2108(3)	24(1)
O5	1959(3)	5365(1)	924(3)	25(1)
S1	1756(1)	2366(1)	4716(1)	23(1)

Table A.3. Bond lengths [Å] and angles [°] for **2.54**

C1-N1	1.469(6)	C9-H9A	0.99
C1-C2	1.515(6)	C9-H9B	0.99
C1-H1A	0.99	C10-C11	1.515(5)
C1-H1B	0.99	C10-H10A	0.99
C2-C3	1.509(5)	C10-H10B	0.99
C2-H2A	0.99	C11-N1	1.494(5)
C2-H2B	0.99	C11-C12	1.521(5)
C3-C4	1.397(5)	C11-H11	1.0000
C3-C12	1.394(5)	C13-C14	1.334(5)
C4-C5	1.386(6)	C13-H13	0.95
C4-H4	0.95	C14-C15	1.468(6)
C5-O5	1.368(5)	C14-H14	0.95
C5-C6	1.407(6)	C15-O3	1.232(5)
C6-O4	1.382(4)	C15-C16	1.466(6)
C6-C7	1.393(5)	C16-C17	1.335(5)
C7-C12	1.413(5)	C16-H16	0.95
C7-C8	1.544(5)	C17-H17	0.95
C8-C13	1.503(5)	C18-O5	1.438(5)
C8-C17	1.512(6)	C18-H18A	0.98

C8-C9	1.553(5)	C18-H18B	0.98
C9-C10	1.513(6)	C18-H18C	0.98
C19-O4	1.446(5)	C23-C24	1.391(6)
C19-H19A	0.98	C23-C26	1.518(6)
C19-H19B	0.98	C24-C25	1.392(6)
C19-H19C	0.98	C24-H24	0.95
C20-C25	1.387(6)	C25-H25	0.95
C20-C21	1.401(6)	C26-H26A	0.98
C20-S1	1.765(4)	C26-H26B	0.98
C21-C22	1.388(6)	C26-H26C	0.98
C21-H21	0.95	N1-S1	1.635(3)
C22-C23	1.388(7)	O1-S1	1.442(3)
C22-H22	0.95	O2-S1	1.438(3)
N1-C1-C2	111.4(3)	H2A-C2-H2B	108.2
N1-C1-H1A	109.3	C4-C3-C12	121.0(4)
C2-C1-H1A	109.3	C4-C3-C2	118.9(4)
N1-C1-H1B	109.3	C12-C3-C2	120.0(3)
C2-C1-H1B	109.3	C5-C4-C3	119.8(4)
H1A-C1-H1B	108.0	C5-C4-H4	120.1
C1-C2-C3	109.5(3)	C3-C4-H4	120.1

C1-C2-H2A	109.8	O5-C5-C4	123.9(4)
C3-C2-H2A	109.8	O5-C5-C6	116.6(3)
C1-C2-H2B	109.8	C4-C5-C6	119.5(4)
C3-C2-H2B	109.8	O4-C6-C7	119.6(3)
O4-C6-C5	119.2(3)	N1-C11-C10	111.0(3)
C7-C6-C5	121.1(3)	N1-C11-C12	113.4(3)
C6-C7-C12	119.0(3)	C10-C11-C12	111.1(3)
C6-C7-C8	118.5(3)	N1-C11-H11	107.0
C12-C7-C8	122.0(3)	C10-C11-H11	107.0
C13-C8-C17	111.3(3)	C12-C11-H11	107.0
C13-C8-C7	107.2(3)	C3-C12-C7	119.4(4)
C17-C8-C7	114.5(3)	C3-C12-C11	121.0(3)
C13-C8-C9	107.7(3)	C7-C12-C11	119.4(3)
C17-C8-C9	105.2(3)	C14-C13-C8	124.1(4)
C7-C8-C9	110.8(3)	C14-C13-H13	117.9
C10-C9-C8	113.1(3)	C8-C13-H13	117.9
C10-C9-H9A	109.0	C13-C14-C15	121.8(4)
C8-C9-H9A	109.0	C13-C14-H14	119.1
C10-C9-H9B	109.0	C15-C14-H14	119.1
C8-C9-H9B	109.0	O3-C15-C16	122.4(4)

H9A-C9-H9B	107.8	O3-C15-C14	121.1(4)
C11-C10-C9	108.2(3)	C16-C15-C14	116.4(3)
C11-C10-H10A	110.1	C17-C16-C15	121.5(4)
C9-C10-H10A	110.1	C17-C16-H16	119.3
C11-C10-H10B	110.1	C15-C16-H16	119.3
C9-C10-H10B	110.1	C16-C17-C8	124.0(4)
H10A-C10-H10B	108.4	C16-C17-H17	118.0
C8-C17-H17	118.0	C22-C23-C26	120.3(4)
O5-C18-H18A	109.5	C24-C23-C26	121.4(4)
O5-C18-H18B	109.5	C23-C24-C25	120.9(4)
H18A-C18-H18B	109.5	C23-C24-H24	119.5
O5-C18-H18C	109.5	C25-C24-H24	119.6
H18A-C18-H18C	109.5	C20-C25-C24	119.9(4)
H18B-C18-H18C	109.5	C20-C25-H25	120.0
O4-C19-H19A	109.5	C24-C25-H25	120.0
O4-C19-H19B	109.5	C23-C26-H26A	109.5
H19A-C19-H19B	109.5	C23-C26-H26B	109.5
O4-C19-H19C	109.5	H26A-C26-H26B	109.5
H19A-C19-H19C	109.5	C23-C26-H26C	109.5
H19B-C19-H19C	109.5	H26A-C26-H26C	109.5

C25-C20-C21	120.0(4)	H26B-C26-H26C	109.5
C25-C20-S1	120.7(3)	C1-N1-C11	118.0(3)
C21-C20-S1	119.2(3)	C1-N1-S1	118.8(3)
C22-C21-C20	118.9(4)	C11-N1-S1	116.2(3)
C22-C21-H21	120.5	C6-O4-C19	114.4(3)
C20-C21-H21	120.5	C5-O5-C18	115.9(3)
C21-C22-C23	121.9(4)	O2-S1-O1	120.36(18)
C21-C22-H22	119.1	O2-S1-N1	106.90(18)
C23-C22-H22	119.1	O1-S1-N1	106.25(18)
C22-C23-C24	118.4(4)	O2-S1-C20	107.0(2)
O1-S1-C20	107.75(19)	N1-S1-C20	108.10(17)

Table A.4. Anisotropic displacement parameters ($Å^2x10^3$) for **2.54**.

The anisotropic displacement factor exponent takes the form: $-2\pi^2[h^2 a^{*2}U^{11} + ... + 2 h k a^* b^* U^{12}]$

	U^{11}	U^{22}	U^{33}	U^{23}	U^{13}	U^{12}
C1	25(2)	20(2)	26(2)	0(2)	2(2)	-4(2)
C2	22(2)	24(2)	24(2)	2(2)	1(2)	-2(2)
C3	19(2)	20(2)	22(2)	-2(2)	4(2)	-2(2)
C4	20(2)	26(2)	20(2)	-1(2)	2(2)	3(2)
C5	24(2)	19(2)	19(2)	1(2)	3(2)	2(2)
C6	17(2)	22(2)	18(2)	-2(2)	6(2)	-2(2)
C7	17(2)	20(2)	16(2)	-2(1)	5(2)	-2(2)
C8	14(2)	25(2)	22(2)	-2(2)	2(2)	0(2)
C9	19(2)	28(2)	27(2)	5(2)	0(2)	0(2)
C10	23(2)	23(2)	28(2)	5(2)	5(2)	2(2)
C11	21(2)	19(2)	21(2)	1(2)	4(2)	-4(2)
C12	17(2)	20(2)	18(2)	-1(2)	2(2)	0(1)
C13	22(2)	20(2)	20(2)	-1(2)	1(2)	2(2)
C14	21(2)	22(2)	25(2)	0(2)	6(2)	3(2)
C15	19(2)	24(2)	26(2)	4(2)	3(2)	1(2)
C16	19(2)	27(2)	23(2)	-4(2)	1(2)	-1(2)
C17	23(2)	28(2)	21(2)	-2(2)	2(2)	1(2)

C18	27(2)	26(2)	29(2)	7(2)	0(2)	4(2)
C19	36(3)	25(2)	36(3)	-5(2)	4(2)	-8(2)
C20	23(2)	23(2)	27(2)	6(2)	7(2)	0(2)
C21	22(2)	33(2)	29(3)	5(2)	1(2)	-2(2)
C22	19(2)	39(3)	33(3)	6(2)	4(2)	1(2)
C23	27(2)	24(2)	34(3)	9(2)	10(2)	4(2)
C24	26(2)	27(2)	26(2)	5(2)	5(2)	0(2)
C25	20(2)	28(2)	25(2)	6(2)	2(2)	0(2)
C26	32(3)	34(2)	38(3)	6(2)	12(2)	7(2)
N1	22(2)	19(2)	24(2)	1(1)	3(2)	-2(1)
O1	35(2)	19(1)	36(2)	2(1)	4(2)	-7(1)
O2	22(2)	27(2)	30(2)	8(1)	4(1)	5(1)
O3	20(2)	38(2)	36(2)	0(1)	7(1)	-5(1)
O4	22(1)	23(2)	27(2)	0(1)	5(1)	-7(1)
O5	25(2)	21(1)	27(2)	6(1)	0(1)	-1(1)
S1	24(1)	20(1)	26(1)	4(1)	5(1)	0(1)

Table A.5. Hydrogen coordinates ($x10^4$) and isotropic displacement parameters ($Å^2x10^3$) for **2.54**.

	x	y	z	U(eq)
H1A	504	2547	1964	29
H1B	1545	2806	1094	29
H2A	105	3459	2873	29
H2B	-49	3484	1077	29
H4	436	4486	950	26
H9A	6122	3330	4365	30
H9B	5143	3577	5339	30
H10A	4434	2912	2670	30
H10B	4529	2660	4338	30
H11	3016	3320	4846	24
H13	5150	3658	1182	25
H14	6985	3988	731	27
H16	7449	4907	4721	28
H17	5531	4639	5066	29
H18A	480	5219	-654	41
H18B	646	5875	-168	41
H18C	130	5425	912	41
H19A	3574	5840	2577	49

H19B	5055	5817	3086	49
H19C	4163	5485	4037	49
H21	-827	2629	4352	34
H22	-2024	3213	5643	36
H24	1026	3623	8648	32
H25	2249	3041	7375	30
H26A	-1077	4267	8074	51
H26B	-1420	3741	9061	51
H26C	-2274	3882	7483	51

Table A.6. Torsion angles [°] for **2.54**

N1-C1-C2-C3	56.8(5)	C13-C8-C9-C10	-73.8(4)
C1-C2-C3-C4	148.7(4)	C17-C8-C9-C10	167.5(3)
C1-C2-C3-C12	-28.5(5)	C7-C8-C9-C10	43.2(5)
C12-C3-C4-C5	-1.1(6)	C8-C9-C10-C11	-63.9(5)
C2-C3-C4-C5	-178.2(4)	C9-C10-C11-N1	-174.6(3)
C3-C4-C5-O5	-178.1(4)	C9-C10-C11-C12	58.3(4)
C3-C4-C5-C6	3.9(6)	C4-C3-C12-C7	-3.2(6)
O5-C5-C6-O4	-5.1(5)	C2-C3-C12-C7	173.9(4)
C4-C5-C6-O4	173.0(3)	C4-C3-C12-C11	171.8(4)
O5-C5-C6-C7	179.4(3)	C2-C3-C12-C11	-11.1(6)
C4-C5-C6-C7	-2.4(6)	C6-C7-C12-C3	4.6(6)
O4-C6-C7-C12	-177.3(3)	C8-C7-C12-C3	-166.9(4)
C5-C6-C7-C12	-1.8(6)	C6-C7-C12-C11	-170.4(3)
O4-C6-C7-C8	-5.5(5)	C8-C7-C12-C11	18.0(5)
C5-C6-C7-C8	170.0(4)	N1-C11-C12-C3	22.4(5)
C6-C7-C8-C13	-74.5(4)	C10-C11-C12-C3	148.1(4)
C12-C7-C8-C13	97.1(4)	N1-C11-C12-C7	-162.6(3)
C6-C7-C8-C17	49.5(5)	C10-C11-C12-C7	-36.9(5)
C12-C7-C8-C17	-139.0(4)	C17-C8-C13-C14	8.5(6)

C6-C7-C8-C9	168.3(3)	C7-C8-C13-C14	134.5(4)
C12-C7-C8-C9	-20.2(5)	C9-C8-C13-C14	-106.3(4)
C8-C13-C14-C15	-2.8(6)	C10-C11-N1-C1	-117.7(4)
C13-C14-C15-O3	179.3(4)	C12-C11-N1-C1	8.1(5)
C13-C14-C15-C16	-1.2(6)	C10-C11-N1-S1	91.7(4)
O3-C15-C16-C17	177.7(4)	C12-C11-N1-S1	-142.5(3)
C14-C15-C16-C17	-1.9(6)	C7-C6-O4-C19	-113.1(4)
C15-C16-C17-C8	8.9(6)	C5-C6-O4-C19	71.4(5)
C13-C8-C17-C16	-11.7(6)	C4-C5-O5-C18	-0.2(6)
C7-C8-C17-C16	-133.4(4)	C6-C5-O5-C18	177.9(3)
C9-C8-C17-C16	104.7(4)	C1-N1-S1-O2	167.5(3)
C25-C20-C21-C22	0.8(6)	C11-N1-S1-O2	-42.2(3)
S1-C20-C21-C22	-177.1(3)	C1-N1-S1-O1	37.8(3)
C20-C21-C22-C23	0.5(6)	C11-N1-S1-O1	-171.9(3)
C21-C22-C23-C24	-1.7(6)	C1-N1-S1-C20	-77.7(3)
C21-C22-C23-C26	178.2(4)	C11-N1-S1-C20	72.7(3)
C22-C23-C24-C25	1.8(6)	C25-C20-S1-O2	19.6(4)
C26-C23-C24-C25	-178.1(4)	C21-C20-S1-O2	-162.5(3)
C21-C20-C25-C24	-0.8(6)	C25-C20-S1-O1	150.4(3)
S1-C20-C25-C24	177.1(3)	C21-C20-S1-O1	-31.8(4)

C23-C24-C25-C20	-0.5(6)	C25-C20-S1-N1	-95.2(4)
C2-C1-N1-C11	-47.8(5)	C21-C20-S1-N1	82.7(4)
C2-C1-N1-S1	102.0(3)		

Figure A.2. View of *N*-tosyl *p*-phenolic *C*-alkylation dimer showing the atom labeling scheme. Displacement ellipsoids are scaled to the 50% probability level.

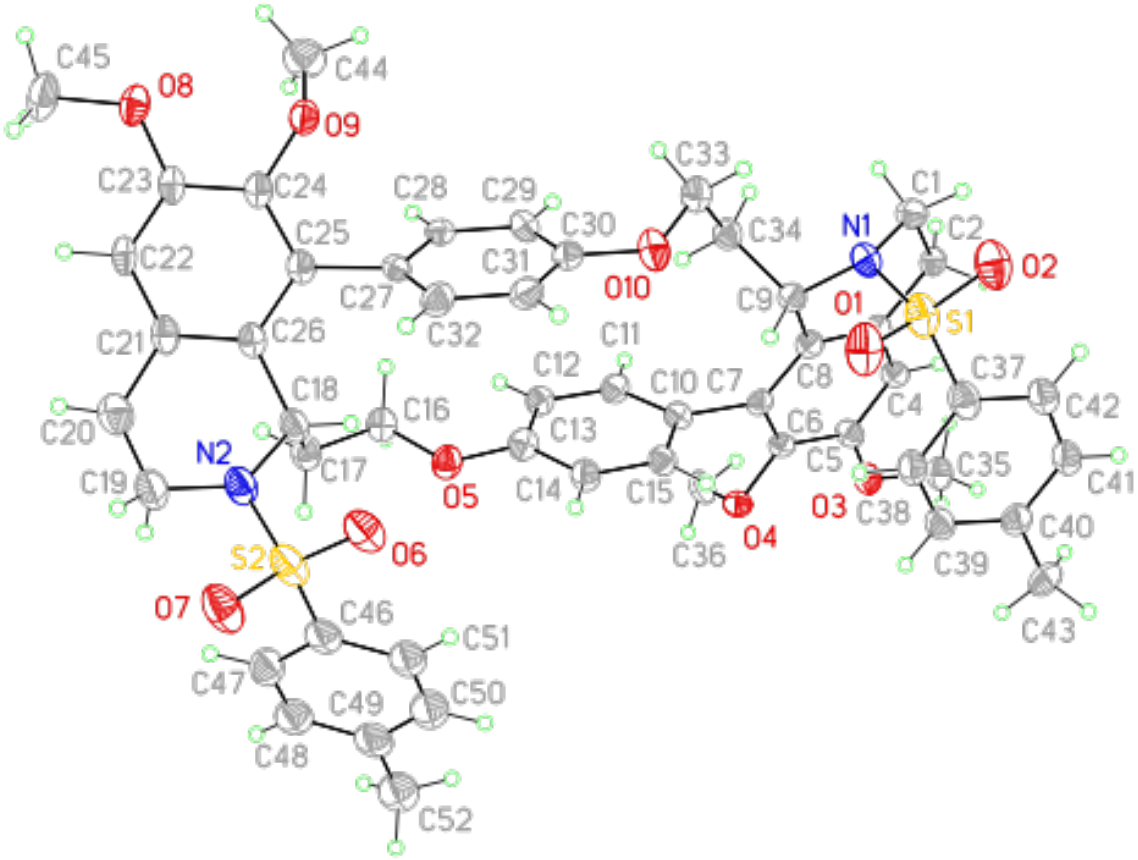

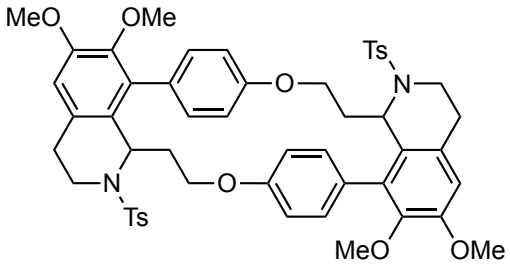

X-ray Experimental for $C_{52}H_{54}N_2O_{10}S_2$: Crystals grew as thin colorless plates by slow diffusion of hexanes into ethyl acetate. The data crystal was cut from a cluster of crystals and had approximate dimensions; 0.28 x 0.10 x 0.04 mm. The data were collected on a Rigaku AFC12 diffractometer with a Saturn 724+ CCD using a graphite

monochromator with MoKα radiation (λ = 0.71073Å). A total of 868 frames of data were collected using ω-scans with a scan range of 0.5° and a counting time of 60 seconds per frame. The data were collected at 153 K using an Oxford Cryostream low temperature device. Details of crystal data, data collection and structure refinement are listed in Table 1. Data reduction were performed using the Rigaku Americas Corporation's Crystal Clear version 1.40.[314] The structure was solved by direct methods using SIR97[315] and refined by full-matrix least-squares on F^2 with anisotropic displacement parameters for the non-H atoms using SHELXL-97.[316] Structure analysis was aided by use of the programs PLATON98[317] and WinGX.[318] The hydrogen atoms on carbon were calculated in ideal positions with isotropic displacement parameters set to 1.2xUeq of the attached atom (1.5xUeq for methyl hydrogen atoms).

The function, $\Sigma w(|F_o|^2 - |F_c|^2)^2$, was minimized, where $w = 1/[(\sigma(F_o))^2 + (0.063*P)^2 + (3.6294*P)]$ and $P = (|F_o|^2 + 2|F_c|^2)/3$. $R_w(F^2)$ refined to 0.245, with R(F) equal to 0.131 and a goodness of fit, S, = 1.05. Definitions used for calculating R(F), $R_w(F^2)$ and the goodness of fit, S, are given below.[319] The data were checked for secondary extinction effects but no correction was necessary. Neutral atom scattering factors and values used to calculate the linear absorption coefficient are from the International Tables for X-ray Crystallography (1992).[320] All figures were generated using SHELXTL/PC.[321] Tables of positional and thermal parameters, bond lengths and angles, torsion angles and figures are found elsewhere.

Table A.7. Crystal data and structure refinement for *N*-tosyl *p*-phenolic *C*-alkylation dimer

Empirical formula	C52 H54 N2 O10 S2	
Formula weight	931.09	
Temperature	100(2) K	
Wavelength	0.71073 Å	
Crystal system	orthorhombic	
Space group	P c a 21	
Unit cell dimensions	a = 17.728(7) Å	α= 90°.
	b = 17.893(7) Å	β= 90°.
	c = 14.312(6) Å	γ = 90°.
Volume	4540(3) $Å^3$	
Z	4	
Density (calculated)	1.362 Mg/m^3	
Absorption coefficient	0.181 mm^{-1}	
F(000)	1968	
Crystal size	0.280 x 0.100 x 0.040 mm	
Theta range for data collection	3.066 to 24.967°.	
Index ranges	-20<=h<=21, -21<=k<=21, -16<=l<=16	
Reflections collected	37604	
Independent reflections	7904 [R(int) = 0.2231]	

Completeness to theta = 25.242°	96.6 %
Absorption correction	Semi-empirical from equivalents
Max. and min. transmission	1.00 and 0.293
Refinement method	Full-matrix least-squares on F^2
Data / restraints / parameters	7904 / 553 / 602
Goodness-of-fit on F^2	1.054
Final R indices [I>2sigma(I)]	R1 = 0.1308, wR2 = 0.1942
R indices (all data)	R1 = 0.2518, wR2 = 0.2446
Absolute structure parameter	-0.1(3)
Extinction coefficient	n/a
Largest diff. peak and hole	0.266 and -0.271 e.$Å^{-3}$

Table A.8. Atomic coordinates ($x10^4$) and equivalent isotropic displacement parameters ($Å^2x10^3$) for *N*-tosyl *p*-phenolic *C*-alkylation dimer

U(eq) is defined as one third of the trace of the orthogonalized U^{ij} tensor.

	x	y	z	U(eq)
C1	-961(8)	4480(8)	5344(11)	47(4)
C2	-1723(7)	4780(7)	5076(11)	39(4)
C3	-1791(8)	5633(7)	5030(9)	34(3)
C4	-2476(9)	5963(7)	4841(10)	35(3)
C5	-2571(9)	6732(7)	4822(10)	38(3)
C6	-1935(8)	7174(8)	4933(9)	30(3)
C7	-1238(8)	6872(7)	5120(9)	31(3)
C8	-1155(8)	6093(8)	5219(10)	37(3)
C9	-422(8)	5736(7)	5536(10)	36(3)
C10	-562(8)	7394(7)	5166(10)	36(3)
C11	-243(8)	7683(8)	4369(10)	41(4)
C12	351(8)	8181(7)	4375(10)	38(4)
C13	663(9)	8392(8)	5254(11)	43(4)
C14	349(9)	8125(8)	6056(10)	46(4)
C15	-251(8)	7639(8)	6010(10)	39(4)
C16	1638(8)	9138(8)	4495(10)	46(4)
C17	2238(8)	9651(8)	4785(11)	50(4)

C18	2832(9)	9254(8)	5417(11)	47(4)
C19	3713(10)	10326(9)	5726(12)	65(5)
C20	4114(11)	10131(9)	4902(14)	81(6)
C21	4096(9)	9325(8)	4603(11)	45(4)
C22	4706(8)	8995(8)	4115(10)	43(4)
C23	4679(8)	8251(8)	3904(10)	38(3)
C24	4084(9)	7815(8)	4172(10)	41(3)
C25	3462(9)	8118(8)	4641(9)	39(3)
C26	3490(8)	8886(8)	4886(10)	38(3)
C27	2822(8)	7599(7)	4933(11)	38(3)
C28	2376(8)	7262(7)	4249(11)	41(4)
C29	1840(9)	6734(8)	4502(12)	49(4)
C30	1746(8)	6552(8)	5417(12)	45(4)
C31	2197(8)	6886(8)	6120(11)	50(4)
C32	2738(9)	7412(8)	5867(11)	48(4)
C33	950(9)	5491(8)	5145(12)	57(4)
C34	186(8)	5705(8)	4786(11)	45(4)
C35	-3923(8)	6617(8)	4711(11)	48(4)
C36	-2143(8)	8234(8)	3979(10)	48(4)
C37	-1612(9)	5330(8)	7321(11)	55(4)
C38	-1679(10)	6124(8)	7347(11)	52(4)

C39	-2392(10)	6438(8)	7385(11)	52(4)
C40	-3038(10)	6001(9)	7447(10)	52(4)
C41	-2965(10)	5234(9)	7446(10)	51(4)
C42	-2257(9)	4884(9)	7376(10)	50(4)
C43	-3819(10)	6345(9)	7511(12)	66(5)
C44	4099(11)	6792(10)	3106(12)	73(6)
C45	5914(9)	8331(10)	3178(13)	75(6)
C46	1961(10)	10412(9)	6990(9)	55(4)
C47	1990(11)	11099(9)	6594(12)	66(5)
C48	1327(12)	11519(10)	6460(12)	68(5)
C49	632(12)	11248(11)	6793(11)	67(5)
C50	612(11)	10549(10)	7185(12)	70(5)
C51	1251(11)	10132(10)	7290(10)	62(4)
C52	-78(11)	11710(10)	6673(13)	82(6)
N1	-524(7)	4983(6)	5957(9)	45(3)
N2	3195(7)	9778(7)	6088(9)	57(3)
O1	-164(7)	5390(7)	7555(7)	74(4)
O2	-776(6)	4160(6)	7320(9)	71(3)
O3	-3256(5)	7071(5)	4692(7)	44(3)
O4	-2031(5)	7949(5)	4906(7)	41(3)
O5	1247(6)	8895(5)	5330(7)	49(3)

O6	2588(7)	9148(5)	7431(7)	68(3)
O7	3316(8)	10304(6)	7658(8)	81(4)
O8	5265(6)	7904(6)	3437(8)	53(3)
O9	4124(5)	7044(5)	4053(7)	48(3)
O10	1264(6)	6011(6)	5780(8)	61(3)
S1	-705(3)	4932(3)	7098(3)	58(1)
S2	2794(3)	9875(2)	7113(3)	63(1)

Table A.9. Bond lengths [Å] and angles [°] for *N*-tosyl *p*-phenolic *C*-alkylation dimer

C1-N1	1.476(17)	C10-C11	1.374(18)
C1-C2	1.503(18)	C10-C15	1.399(18)
C1-H1A	0.99	C11-C12	1.380(18)
C1-H1B	0.99	C11-H11	0.95
C2-C3	1.533(17)	C12-C13	1.424(19)
C2-H2A	0.99	C12-H12	0.95
C2-H2B	0.99	C13-C14	1.363(18)
C3-C4	1.376(18)	C13-O5	1.377(16)
C3-C8	1.421(18)	C14-C15	1.376(19)
C4-C5	1.387(17)	C14-H14	0.95
C4-H4	0.95	C15-H15	0.95
C5-O3	1.370(16)	C16-O5	1.449(16)
C5-C6	1.386(18)	C16-C17	1.465(18)
C6-C7	1.375(17)	C16-H16A	0.99
C6-O4	1.397(15)	C16-H16B	0.99
C7-C8	1.410(17)	C17-C18	1.56(2)
C7-C10	1.520(18)	C17-H17A	0.99
C8-C9	1.518(18)	C17-H17B	0.99
C9-N1	1.488(17)	C18-N2	1.489(17)

C9-C34	1.522(19)	C18-C26	1.54(2)
C9-H9	1.00	C18-H18	1.00
C19-C20	1.42(2)	C30-O10	1.393(16)
C19-N2	1.440(18)	C30-C31	1.42(2)
C19-H19A	0.99	C31-C32	1.392(19)
C19-H19B	0.99	C31-H31	0.95
C20-C21	1.506(19)	C32-H32	0.95
C20-H20A	0.99	C33-O10	1.414(17)
C20-H20B	0.99	C33-C34	1.499(19)
C21-C26	1.390(18)	C33-H33A	0.99
C21-C22	1.42(2)	C33-H33B	0.99
C22-C23	1.367(19)	C34-H34A	0.99
C22-H22	0.95	C34-H34B	0.99
C23-C24	1.366(19)	C35-O3	1.434(15)
C23-O8	1.382(17)	C35-H35A	0.98
C24-O9	1.392(16)	C35-H35B	0.98
C24-C25	1.400(19)	C35-H35C	0.98
C25-C26	1.420(18)	C36-O4	1.435(16)
C25-C27	1.524(19)	C36-H36A	0.98
C27-C32	1.39(2)	C36-H36B	0.98

C27-C28	1.395(19)	C36-H36C	0.98
C28-C29	1.388(19)	C37-C42	1.397(19)
C28-H28	0.95	C37-C38	1.43(2)
C29-C30	1.36(2)	C37-S1	1.787(17)
C29-H29	0.95	C38-C39	1.38(2)
C38-H38	0.95	C46-C51	1.42(2)
C39-C40	1.39(2)	C46-S2	1.771(18)
C39-H39	0.95	C47-C48	1.41(2)
C40-C41	1.38(2)	C47-H47	0.95
C40-C43	1.52(2)	C48-C49	1.41(2)
C41-C42	1.41(2)	C48-H48	0.95
C41-H41	0.95	C49-C50	1.37(2)
C42-H42	0.95	C49-C52	1.51(3)
C43-H43A	0.98	C50-C51	1.36(2)
C43-H43B	0.98	C50-H50	0.95
C43-H43C	0.98	C51-H51	0.95
C44-O9	1.428(18)	C52-H52A	0.98
C44-H44A	0.98	C52-H52B	0.98
C44-H44B	0.98	C52-H52C	0.98
C44-H44C	0.98	N1-S1	1.667(13)

C45-O8	1.430(17)	N2-S2	1.640(13)
C45-H45A	0.98	O1-S1	1.421(11)
C45-H45B	0.98	O2-S1	1.423(11)
C45-H45C	0.98	O6-S2	1.427(10)
C46-C47	1.35(2)	O7-S2	1.433(12)
N1-C1-C2	114.0(11)	C2-C1-H1A	108.8
N1-C1-H1A	108.8	N1-C1-H1B	108.8
C2-C1-H1B	108.8	C7-C8-C3	118.0(13)
H1A-C1-H1B	107.7	C7-C8-C9	122.4(13)
C1-C2-C3	115.9(12)	C3-C8-C9	119.6(12)
C1-C2-H2A	108.3	N1-C9-C8	113.4(11)
C3-C2-H2A	108.3	N1-C9-C34	109.9(11)
C1-C2-H2B	108.3	C8-C9-C34	114.2(12)
C3-C2-H2B	108.3	N1-C9-H9	106.2
H2A-C2-H2B	107.4	C8-C9-H9	106.2
C4-C3-C8	119.3(13)	C34-C9-H9	106.2
C4-C3-C2	120.3(12)	C11-C10-C15	115.8(13)
C8-C3-C2	120.4(13)	C11-C10-C7	121.4(13)
C3-C4-C5	122.4(14)	C15-C10-C7	122.7(13)
C3-C4-H4	118.8	C10-C11-C12	123.6(14)

C5-C4-H4	118.8	C10-C11-H11	118.2
O3-C5-C6	118.9(12)	C12-C11-H11	118.2
O3-C5-C4	123.4(13)	C11-C12-C13	118.2(14)
C6-C5-C4	117.7(14)	C11-C12-H12	120.9
C7-C6-C5	121.9(13)	C13-C12-H12	120.9
C7-C6-O4	120.3(12)	C14-C13-O5	118.1(14)
C5-C6-O4	117.7(13)	C14-C13-C12	119.5(14)
C6-C7-C8	120.2(13)	O5-C13-C12	122.3(13)
C6-C7-C10	118.4(12)	C13-C14-C15	119.8(14)
C8-C7-C10	121.4(13)	C13-C14-H14	120.1
C15-C14-H14	120.1	C20-C19-H19A	108.1
C14-C15-C10	123.0(14)	N2-C19-H19A	108.1
C14-C15-H15	118.5	C20-C19-H19B	108.1
C10-C15-H15	118.5	N2-C19-H19B	108.1
O5-C16-C17	107.5(12)	H19A-C19-H19B	107.3
O5-C16-H16A	110.2	C19-C20-C21	117.4(15)
C17-C16-H16A	110.2	C19-C20-H20A	108.0
O5-C16-H16B	110.2	C21-C20-H20A	108.0
C17-C16-H16B	110.2	C19-C20-H20B	108.0
H16A-C16-H16B	108.5	C21-C20-H20B	108.0

C16-C17-C18	111.7(12)	H20A-C20-H20B	107.2
C16-C17-H17A	109.3	C26-C21-C22	119.9(14)
C18-C17-H17A	109.3	C26-C21-C20	118.4(15)
C16-C17-H17B	109.3	C22-C21-C20	121.5(14)
C18-C17-H17B	109.3	C23-C22-C21	119.2(14)
H17A-C17-H17B	107.9	C23-C22-H22	120.4
N2-C18-C26	105.1(12)	C21-C22-H22	120.4
N2-C18-C17	112.3(12)	C22-C23-C24	121.4(16)
C26-C18-C17	114.8(13)	C22-C23-O8	121.2(14)
N2-C18-H18	108.1	C24-C23-O8	117.4(14)
C26-C18-H18	108.1	C23-C24-O9	119.5(14)
C17-C18-H18	108.1	C23-C24-C25	121.4(15)
C20-C19-N2	116.8(15)	O9-C24-C25	118.9(13)
C24-C25-C26	117.7(14)	C26-C25-C27	123.2(14)
C24-C25-C27	118.9(13)	C21-C26-C25	120.2(15)
C21-C26-C18	119.2(13)	C31-C32-H32	120.4
C25-C26-C18	120.6(13)	O10-C33-C34	114.0(12)
C32-C27-C28	120.7(14)	O10-C33-H33A	108.7
C32-C27-C25	119.4(14)	C34-C33-H33A	108.7
C28-C27-C25	119.5(14)	O10-C33-H33B	108.7

C29-C28-C27	119.9(15)	C34-C33-H33B	108.7
C29-C28-H28	120.0	H33A-C33-H33B	107.6
C27-C28-H28	120.0	C33-C34-C9	114.0(13)
C30-C29-C28	119.9(16)	C33-C34-H34A	108.7
C30-C29-H29	120.1	C9-C34-H34A	108.7
C28-C29-H29	120.1	C33-C34-H34B	108.7
C29-C30-O10	126.9(15)	C9-C34-H34B	108.7
C29-C30-C31	120.9(15)	H34A-C34-H34B	107.6
O10-C30-C31	112.1(14)	O3-C35-H35A	109.5
C32-C31-C30	119.3(15)	O3-C35-H35B	109.5
C32-C31-H31	120.4	H35A-C35-H35B	109.5
C30-C31-H31	120.4	O3-C35-H35C	109.5
C27-C32-C31	119.2(16)	H35A-C35-H35C	109.5
C27-C32-H32	120.4	H35B-C35-H35C	109.5
H36A-C36-H36C	109.5	C40-C43-H43C	109.5
H36B-C36-H36C	109.5	H43A-C43-H43C	109.5
C42-C37-C38	119.9(16)	H43B-C43-H43C	109.5
C42-C37-S1	121.3(12)	O9-C44-H44A	109.5
C38-C37-S1	118.5(12)	O9-C44-H44B	109.5
C39-C38-C37	118.8(15)	H44A-C44-H44B	109.5

C39-C38-H38	120.6	O9-C44-H44C	109.5
C37-C38-H38	120.6	H44A-C44-H44C	109.5
C38-C39-C40	121.8(15)	H44B-C44-H44C	109.5
C38-C39-H39	119.1	O8-C45-H45A	109.5
C40-C39-H39	119.1	O8-C45-H45B	109.5
C41-C40-C39	118.9(17)	H45A-C45-H45B	109.5
C41-C40-C43	119.3(15)	O8-C45-H45C	109.5
C39-C40-C43	121.8(15)	H45A-C45-H45C	109.5
C40-C41-C42	121.8(15)	H45B-C45-H45C	109.5
C40-C41-H41	119.1	C47-C46-C51	118.7(18)
C42-C41-H41	119.1	C47-C46-S2	120.1(15)
C37-C42-C41	118.7(15)	C51-C46-S2	121.1(13)
C37-C42-H42	120.6	C46-C47-C48	120.6(18)
C41-C42-H42	120.6	C46-C47-H47	119.7
C40-C43-H43A	109.5	C48-C47-H47	119.7
C40-C43-H43B	109.5	C49-C48-C47	120.1(18)
H43A-C43-H43B	109.5	C49-C48-H48	120.0
C47-C48-H48	120.0	C19-N2-S2	121.7(11)
C50-C49-C48	118(2)	C18-N2-S2	117.2(10)
C50-C49-C52	121(2)	C5-O3-C35	118.5(11)

C48-C49-C52	120.1(18)	C6-O4-C36	113.3(10)
C51-C50-C49	122(2)	C13-O5-C16	119.4(11)
C51-C50-H50	119.2	C23-O8-C45	119.4(13)
C49-C50-H50	119.2	C24-O9-C44	115.3(12)
C50-C51-C46	120.5(17)	C30-O10-C33	117.4(13)
C50-C51-H51	119.7	O1-S1-O2	121.2(7)
C46-C51-H51	119.7	O1-S1-N1	106.8(7)
C49-C52-H52A	109.5	O2-S1-N1	106.8(7)
C49-C52-H52B	109.5	O1-S1-C37	107.1(8)
H52A-C52-H52B	109.5	O2-S1-C37	105.5(7)
C49-C52-H52C	109.5	N1-S1-C37	109.0(7)
H52A-C52-H52C	109.5	O6-S2-O7	118.7(7)
H52B-C52-H52C	109.5	O6-S2-N2	107.4(7)
C1-N1-C9	112.0(12)	O7-S2-N2	105.3(7)
C1-N1-S1	116.7(10)	O6-S2-C46	108.3(8)
C9-N1-S1	118.0(9)	O7-S2-C46	107.6(7)
C19-N2-C18	118.2(13)	N2-S2-C46	109.3(7)

Table A.10. Anisotropic displacement parameters ($Å^2x10^3$) for *N*-tosyl *p*-phenolic *C*-alkylation dimer

The anisotropic displacement factor exponent takes the form: $-2\pi^2[h^2 a^{*2}U^{11} + ... + 2 h k a^* b^* U^{12}]$

	U^{11}	U^{22}	U^{33}	U^{23}	U^{13}	U^{12}
C1	34(8)	45(7)	61(9)	-11(7)	-5(7)	0(6)
C2	24(7)	44(6)	49(10)	-5(6)	0(7)	-6(5)
C3	34(6)	42(6)	25(8)	-4(5)	-3(6)	-6(5)
C4	35(7)	43(6)	28(8)	-11(6)	-11(6)	-6(5)
C5	33(6)	40(6)	42(9)	-7(6)	-15(6)	-4(5)
C6	36(6)	43(6)	12(7)	-11(5)	-7(5)	-5(4)
C7	38(6)	43(6)	13(7)	-2(5)	2(5)	-4(4)
C8	33(6)	44(6)	34(8)	-5(5)	-3(6)	-3(4)
C9	33(6)	39(6)	35(7)	-4(5)	-4(5)	-4(5)
C10	40(7)	35(7)	33(6)	2(6)	-4(5)	0(5)
C11	43(8)	47(9)	33(7)	4(6)	-1(6)	1(6)
C12	44(8)	39(8)	32(7)	13(6)	-2(6)	4(6)
C13	40(8)	50(8)	40(7)	9(6)	-5(6)	1(6)
C14	57(9)	51(9)	31(7)	-3(6)	-2(6)	-17(7)
C15	48(8)	33(8)	36(7)	5(6)	-1(6)	-2(6)
C16	43(8)	54(9)	41(8)	8(7)	-7(6)	-4(7)
C17	52(8)	57(9)	42(9)	2(7)	0(6)	-12(6)

C18	51(7)	44(7)	46(7)	-4(6)	-3(6)	-17(5)
C19	75(11)	54(9)	67(9)	-1(7)	1(8)	-27(8)
C20	99(13)	52(8)	92(11)	5(7)	28(10)	-23(7)
C21	42(7)	49(6)	45(9)	18(6)	-7(6)	-14(5)
C22	22(7)	48(7)	58(9)	18(6)	-12(6)	-17(5)
C23	30(7)	46(6)	39(8)	20(6)	-11(6)	-12(5)
C24	39(7)	49(6)	35(8)	5(6)	-1(6)	-15(5)
C25	46(7)	47(6)	25(7)	1(5)	-3(5)	-15(5)
C26	44(7)	45(6)	24(7)	5(5)	-6(6)	-14(5)
C27	47(8)	26(7)	41(7)	-6(5)	9(6)	-4(5)
C28	41(8)	33(8)	49(8)	-13(6)	8(6)	-2(6)
C29	55(10)	33(8)	60(8)	-6(6)	3(7)	-10(7)
C30	39(8)	33(7)	63(8)	-1(6)	13(6)	6(6)
C31	52(9)	45(9)	52(8)	1(6)	14(6)	4(7)
C32	51(9)	54(9)	40(7)	3(6)	10(6)	-2(7)
C33	41(8)	52(9)	77(11)	0(8)	5(7)	-11(6)
C34	39(7)	47(9)	48(8)	-7(7)	2(6)	-9(6)
C35	33(8)	56(10)	56(11)	1(9)	-9(7)	-11(7)
C36	48(11)	47(9)	48(8)	3(7)	-20(8)	-11(8)
C37	63(7)	51(7)	52(10)	1(7)	-12(6)	-20(5)
C38	71(9)	49(7)	36(10)	0(7)	5(7)	-20(6)

C39	77(8)	42(7)	38(10)	-5(7)	6(7)	-16(6)
C40	77(8)	56(8)	24(8)	-9(7)	12(7)	-18(6)
C41	68(8)	51(7)	35(9)	-8(7)	-4(7)	-25(6)
C42	71(8)	50(8)	28(9)	-4(7)	-9(7)	-22(6)
C43	86(10)	77(11)	34(10)	-3(9)	23(8)	-4(8)
C44	91(16)	74(12)	54(9)	-11(8)	-5(9)	-2(10)
C45	49(10)	103(14)	73(13)	6(11)	13(9)	-28(9)
C46	97(8)	59(8)	9(7)	-6(6)	0(6)	-15(6)
C47	96(11)	63(9)	39(10)	6(8)	9(8)	-18(7)
C48	109(10)	61(10)	33(10)	0(8)	3(8)	-11(7)
C49	103(10)	69(9)	27(10)	-12(7)	-8(8)	-15(7)
C50	99(10)	76(9)	36(10)	-1(8)	-2(9)	-15(7)
C51	100(9)	68(10)	18(9)	-4(8)	0(7)	-20(7)
C52	107(12)	84(12)	54(12)	1(10)	-11(10)	-11(9)
N1	46(7)	38(6)	53(6)	3(5)	-9(5)	-7(5)
N2	69(8)	53(7)	48(6)	-5(5)	-5(5)	-23(6)
O1	74(8)	97(8)	51(7)	21(6)	-20(6)	-29(6)
O2	63(8)	68(6)	83(8)	27(6)	-19(7)	-10(5)
O3	32(5)	50(6)	49(7)	3(5)	-10(5)	-4(4)
O4	44(6)	43(5)	38(6)	-5(4)	-3(5)	2(4)
O5	51(6)	60(6)	37(6)	1(5)	2(5)	-11(5)

O6	119(9)	52(6)	32(6)	3(5)	-6(6)	-20(6)
O7	128(10)	63(8)	51(7)	5(6)	-8(7)	-37(7)
O8	41(6)	62(7)	58(7)	23(6)	4(5)	-9(5)
O9	43(7)	50(6)	51(6)	2(5)	6(5)	-12(5)
O10	56(7)	49(6)	77(8)	17(5)	-6(6)	-15(5)
S1	62(3)	60(3)	52(3)	16(2)	-17(3)	-13(2)
S2	103(4)	47(2)	38(2)	4(2)	-10(3)	-23(2)

Table A.11. Hydrogen coordinates ($x10^4$) and isotropic displacement parameters ($Å^2x10^3$) for *N*-tosyl *p*-phenolic *C*-alkylation dimer.

	x	y	z	U(eq)
H1A	-1029	3995	5666	56
H1B	-667	4387	4768	56
H2A	-2098	4591	5532	46
H2B	-1859	4573	4457	46
H4	-2898	5652	4718	43
H9	-219	6063	6044	43
H11	-442	7532	3783	49
H12	548	8378	3809	46
H14	544	8273	6646	56
H15	-465	7462	6577	47
H16A	1283	9396	4068	55
H16B	1855	8703	4163	55
H17A	2014	10075	5131	61
H17B	2493	9853	4224	61
H18	2568	8857	5784	56
H19A	3426	10790	5600	78
H19B	4085	10442	6221	78
H20A	4648	10276	4990	97

H20B	3913	10437	4382	97
H22	5129	9288	3935	51
H28	2439	7394	3611	49
H29	1540	6500	4037	59
H31	2131	6752	6757	60
H32	3046	7640	6329	58
H33A	912	4999	5458	68
H33B	1297	5434	4608	68
H34A	31	5341	4302	54
H34B	222	6202	4484	54
H35A	-3870	6205	4265	72
H35B	-4361	6923	4540	72
H35C	-3995	6415	5341	72
H36A	-1656	8272	3659	71
H36B	-2376	8731	4014	71
H36C	-2475	7896	3631	71
H38	-1242	6431	7340	62
H39	-2441	6966	7367	63
H41	-3406	4934	7494	61
H42	-2219	4355	7365	60
H43A	-4149	6115	7043	98

H43B	-3785	6884	7395	98
H43C	-4026	6258	8136	98
H44A	3892	7189	2710	109
H44B	3778	6348	3064	109
H44C	4610	6668	2897	109
H45A	5770	8707	2713	112
H45B	6297	7998	2912	112
H45C	6119	8581	3732	112
H47	2462	11299	6404	79
H48	1349	11986	6145	81
H50	143	10350	7387	84
H51	1220	9650	7567	74
H52A	-33	12020	6111	122
H52B	-146	12032	7220	122
H52C	-513	11376	6610	122

Table A.12. Torsion angles [°] for *N*-tosyl *p*-phenolic *C*-alkylation dimer

N1-C1-C2-C3	29.3(19)	C4-C3-C8-C9	173.1(13)
C1-C2-C3-C4	-176.5(13)	C2-C3-C8-C9	-4(2)
C1-C2-C3-C8	1(2)	C7-C8-C9-N1	156.7(13)
C8-C3-C4-C5	0(2)	C3-C8-C9-N1	-22.0(18)
C2-C3-C4-C5	177.8(14)	C7-C8-C9-C34	-76.4(17)
C3-C4-C5-O3	-175.8(13)	C3-C8-C9-C34	104.9(15)
C3-C4-C5-C6	5(2)	C6-C7-C10-C11	-75.6(17)
O3-C5-C6-C7	176.2(12)	C8-C7-C10-C11	101.3(16)
C4-C5-C6-C7	-4(2)	C6-C7-C10-C15	101.0(16)
O3-C5-C6-O4	-0.1(19)	C8-C7-C10-C15	-82.1(18)
C4-C5-C6-O4	179.4(12)	C15-C10-C11-C12	0(2)
C5-C6-C7-C8	-1(2)	C7-C10-C11-C12	177.4(13)
O4-C6-C7-C8	175.1(12)	C10-C11-C12-C13	2(2)
C5-C6-C7-C10	175.9(12)	C11-C12-C13-C14	-3(2)
O4-C6-C7-C10	-8.0(19)	C11-C12-C13-O5	-178.9(13)
C6-C7-C8-C3	6(2)	O5-C13-C14-C15	178.0(13)
C10-C7-C8-C3	-170.7(12)	C12-C13-C14-C15	2(2)
C6-C7-C8-C9	-172.7(12)	C13-C14-C15-C10	0(2)
C10-C7-C8-C9	11(2)	C11-C10-C15-C14	-2(2)

C4-C3-C8-C7	-6(2)	C7-C10-C15-C14	-178.4(14)
C2-C3-C8-C7	176.8(13)	O5-C16-C17-C18	62.8(16)
C16-C17-C18-N2	-150.9(13)	C24-C25-C26-C18	-178.9(13)
C16-C17-C18-C26	89.2(16)	C27-C25-C26-C18	-4(2)
N2-C19-C20-C21	-13(3)	N2-C18-C26-C21	-41.8(18)
C19-C20-C21-C26	25(3)	C17-C18-C26-C21	82.1(17)
C19-C20-C21-C22	-149.7(17)	N2-C18-C26-C25	141.7(13)
C26-C21-C22-C23	2(2)	C17-C18-C26-C25	-94.5(16)
C20-C21-C22-C23	176.4(15)	C24-C25-C27-C32	106.5(16)
C21-C22-C23-C24	-1(2)	C26-C25-C27-C32	-68.3(19)
C21-C22-C23-O8	-179.3(13)	C24-C25-C27-C28	-67.2(18)
C22-C23-C24-O9	-171.6(13)	C26-C25-C27-C28	118.0(15)
O8-C23-C24-O9	6(2)	C32-C27-C28-C29	0(2)
C22-C23-C24-C25	3(2)	C25-C27-C28-C29	173.7(14)
O8-C23-C24-C25	-179.4(13)	C27-C28-C29-C30	1(2)
C23-C24-C25-C26	-4(2)	C28-C29-C30-O10	-176.5(13)
O9-C24-C25-C26	170.1(13)	C28-C29-C30-C31	-1(2)
C23-C24-C25-C27	-179.1(13)	C29-C30-C31-C32	1(2)
O9-C24-C25-C27	-5(2)	O10-C30-C31-C32	176.7(13)
C22-C21-C26-C25	-4(2)	C28-C27-C32-C31	-1(2)

C20-C21-C26-C25	-178.2(15)	C25-C27-C32-C31	-174.2(13)
C22-C21-C26-C18	179.9(13)	C30-C31-C32-C27	0(2)
C20-C21-C26-C18	5(2)	O10-C33-C34-C9	-64.1(17)
C24-C25-C26-C21	5(2)	N1-C9-C34-C33	-62.3(15)
C27-C25-C26-C21	179.4(14)	C8-C9-C34-C33	168.9(12)
C42-C37-C38-C39	-3(2)	C34-C9-N1-C1	-76.9(14)
S1-C37-C38-C39	170.8(12)	C8-C9-N1-S1	-87.5(13)
C37-C38-C39-C40	4(2)	C34-C9-N1-S1	143.3(10)
C38-C39-C40-C41	-2(2)	C20-C19-N2-C18	-29(2)
C38-C39-C40-C43	178.6(14)	C20-C19-N2-S2	170.6(14)
C39-C40-C41-C42	-1(2)	C26-C18-N2-C19	54.6(18)
C43-C40-C41-C42	179.1(14)	C17-C18-N2-C19	-70.8(18)
C38-C37-C42-C41	1(2)	C26-C18-N2-S2	-144.2(10)
S1-C37-C42-C41	-172.9(12)	C17-C18-N2-S2	90.3(14)
C40-C41-C42-C37	1(2)	C6-C5-O3-C35	-171.2(13)
C51-C46-C47-C48	-2(2)	C4-C5-O3-C35	9(2)
S2-C46-C47-C48	177.6(13)	C7-C6-O4-C36	108.0(14)
C46-C47-C48-C49	4(3)	C5-C6-O4-C36	-75.7(15)
C47-C48-C49-C50	-5(2)	C14-C13-O5-C16	174.5(13)
C47-C48-C49-C52	178.3(15)	C12-C13-O5-C16	-9(2)

C48-C49-C50-C51	3(3)	C17-C16-O5-C13	-178.6(12)
C52-C49-C50-C51	179.8(16)	C22-C23-O8-C45	1(2)
C49-C50-C51-C46	0(3)	C24-C23-O8-C45	-177.4(14)
C47-C46-C51-C50	0(2)	C23-C24-O9-C44	-69.8(18)
S2-C46-C51-C50	-179.5(13)	C25-C24-O9-C44	115.9(16)
C2-C1-N1-C9	-56.4(17)	C29-C30-O10-C33	14(2)
C2-C1-N1-S1	84.0(14)	C31-C30-O10-C33	-162.0(12)
C8-C9-N1-C1	52.3(16)	C34-C33-O10-C30	-94.4(16)
C1-N1-S1-O1	173.1(10)	C19-N2-S2-O6	-156.2(13)
C9-N1-S1-O1	-48.9(12)	C18-N2-S2-O6	43.4(13)
C1-N1-S1-O2	42.1(12)	C19-N2-S2-O7	-28.7(16)
C9-N1-S1-O2	-179.9(10)	C18-N2-S2-O7	170.8(11)
C1-N1-S1-C37	-71.5(11)	C19-N2-S2-C46	86.6(14)
C9-N1-S1-C37	66.6(11)	C18-N2-S2-C46	-73.8(13)
C42-C37-S1-O1	-149.4(12)	C47-C46-S2-O6	-172.3(13)
C38-C37-S1-O1	36.9(15)	C51-C46-S2-O6	6.8(14)
C42-C37-S1-O2	-19.1(15)	C47-C46-S2-O7	58.2(15)
C38-C37-S1-O2	167.2(13)	C51-C46-S2-O7	-122.7(12)
C42-C37-S1-N1	95.3(14)	C47-C46-S2-N2	-55.6(14)
C38-C37-S1-N1	-78.4(14)	C51-C46-S2-N2	123.5(12)

Figure A.3. View of **2.59** showing the atom labeling scheme. Displacement ellipsoids are scaled to the 50% probability level

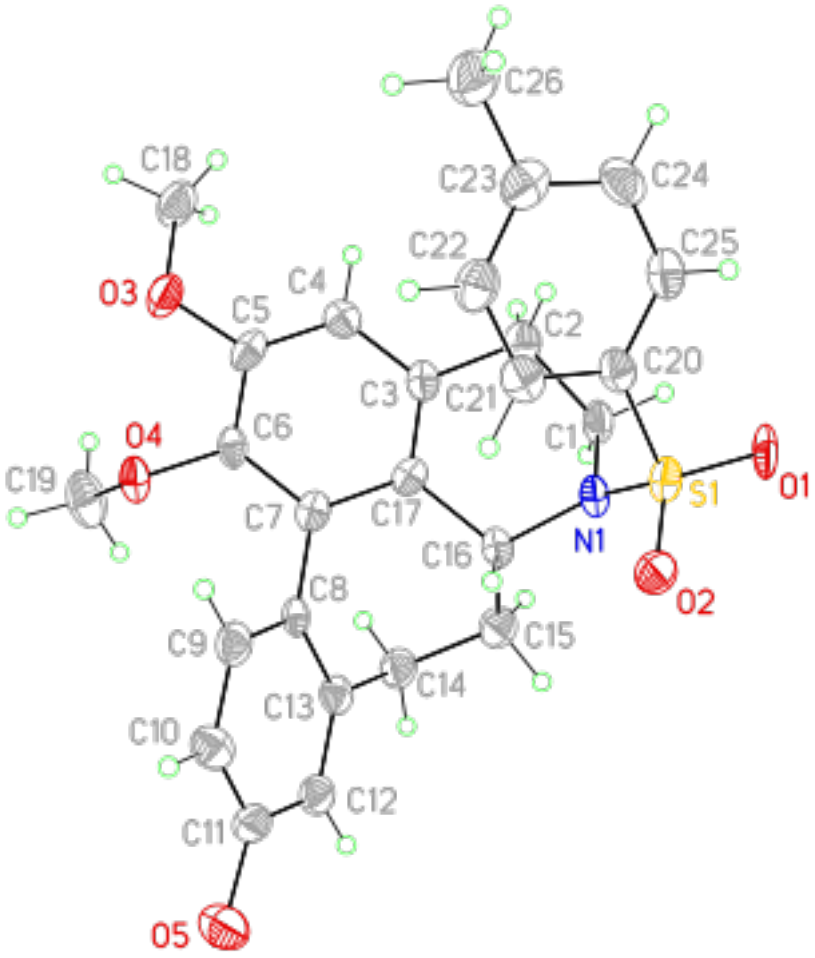

X-ray Experimental for $C_{26}H_{26}NO_5S$ - CH_3OH: Crystals grew as colorless needles by slow evaporation from methanol. The data crystal was cut from a longer crystal and had approximate dimensions; 0.29 x 0.13 x 0.09 mm. The data were collected at -140 °C on a Nonius Kappa CCD diffractometer using a Bruker AXS Apex II detector and a graphite monochromator with MoKα radiation (λ = 0.71073Å). Reduced temperatures were maintained by use of an Oxford Cryosystems 600 low-temperature

device. A total of 366 frames of data were collected using ω and ϕ-scans with a scan range of 1.0° and a counting time of 199 seconds per frame. Details of crystal data, data collection and structure refinement are listed in Table 1. Data reduction were performed using SAINT V8.27B.[322] The structure was solved by direct methods using SIR97[315] and refined by full-matrix least-squares on F^2 with anisotropic displacement parameters for the non-H atoms using SHELXL-2013.[316] Structure analysis was aided by use of the programs PLATON98[317] and WinGX.[318] The hydrogen atoms were calculated in idealized positions.

The function, $\Sigma w(|F_o|^2 - |F_c|^2)^2$, was minimized, where $w = 1/[(\sigma(F_o))^2 + (0.0516*P)^2]$ and $P = (|F_o|^2 + 2|F_c|^2)/3$. $R_w(F^2)$ refined to 0.146, with R(F) equal to 0.0618 and a goodness of fit, S, = 1.01. Definitions used for calculating R(F),$R_w(F^2)$ and the goodness of fit, S, are given below.[319] The data were checked for secondary extinction but no correction was necessary. Neutral atom scattering factors and values used to calculate the linear absorption coefficient are from the International Tables for X-ray Crystallography (1992).[320] All figures were generated using SHELXTL/PC.[321] Tables of positional and thermal parameters, bond lengths and angles, torsion angles and figures are found elsewhere.

Table A.13. Crystal data and structure refinement for **2.59**

Empirical formula	C27 H30 N O6 S	
Formula weight	496.58	
Temperature	133(2) K	
Wavelength	0.71073 Å	
Crystal system	monoclinic	
Space group	P 21/c	
Unit cell dimensions	a = 12.620(2) Å	α= 90°.
	b = 22.056(3) Å	β= 109.127(8)°.
	c = 9.224(2) Å	γ = 90°.
Volume	2425.7(7) $Å^3$	
Z	4	
Density (calculated)	1.360 Mg/m^3	
Absorption coefficient	0.177 mm^{-1}	
F(000)	1052	
Crystal size	0.290 x 0.130 x 0.090 mm	
Theta range for data collection	1.708 to 24.997°.	
Index ranges	-14<=h<=13, -26<=k<=24, -10<=l<=10	
Reflections collected	17000	
Independent reflections	4255 [R(int) = 0.1285]	

Completeness to theta = 25.242°	96.7 %
Absorption correction	Semi-empirical from equivalents
Max. and min. transmission	1.00 and 0.817
Refinement method	Full-matrix least-squares on F^2
Data / restraints / parameters	4255 / 0 / 321
Goodness-of-fit on F^2	1.005
Final R indices [I>2sigma(I)]	R1 = 0.0618, wR2 = 0.1065
R indices (all data)	R1 = 0.1769, wR2 = 0.1456
Extinction coefficient	n/a
Largest diff. peak and hole	0.477 and -0.311 e.$Å^{-3}$

Table A.14. Atomic coordinates ($x10^4$) and equivalent isotropic displacement parameters ($Å^2x10^3$) for **2.59**

U(eq) is defined as one third of the trace of the orthogonalized U^{ij} tensor.

	x	y	z	U(eq)
C1	1447(4)	7146(2)	3164(4)	28(1)
C2	1590(4)	6723(2)	1937(5)	27(1)
C3	2746(4)	6438(2)	2410(5)	21(1)
C4	3075(4)	6143(2)	1287(5)	24(1)
C5	4112(4)	5880(2)	1647(5)	26(1)
C6	4848(4)	5900(2)	3163(5)	21(1)
C7	4530(4)	6182(2)	4301(5)	20(1)
C8	5311(4)	6204(2)	5896(5)	21(1)
C9	5843(4)	5681(2)	6662(5)	28(1)
C10	6610(4)	5705(2)	8119(5)	30(1)
C11	6893(4)	6250(2)	8849(5)	28(1)
C12	6341(4)	6773(2)	8159(5)	29(1)
C13	5570(4)	6754(2)	6687(5)	23(1)
C14	5004(4)	7325(2)	5905(5)	31(1)
C15	3760(4)	7352(2)	5750(5)	31(1)
C16	3130(4)	6756(2)	5182(5)	22(1)
C17	3467(4)	6458(2)	3908(5)	20(1)

C18	3853(4)	5598(2)	-943(5)	42(1)
C19	6664(4)	5978(2)	3013(5)	44(1)
C20	814(4)	5802(2)	4348(5)	26(1)
C21	1633(4)	5355(2)	4603(5)	31(1)
C22	1413(4)	4846(2)	3675(5)	33(1)
C23	409(5)	4773(2)	2505(5)	34(1)
C24	-405(4)	5223(2)	2296(5)	36(1)
C25	-199(4)	5730(2)	3208(5)	33(1)
C26	182(4)	4223(2)	1481(5)	46(1)
C27	8263(5)	7707(2)	11766(6)	66(2)
N1	1922(3)	6891(1)	4723(4)	24(1)
O1	84(3)	6809(1)	5071(3)	38(1)
O2	1755(3)	6348(1)	6951(3)	32(1)
O3	4518(3)	5581(1)	636(3)	32(1)
O4	5891(3)	5628(1)	3515(3)	28(1)
O5	7718(3)	6266(1)	10261(4)	44(1)
O6	8729(3)	7368(2)	10848(4)	56(1)
S1	1122(1)	6480(1)	5400(1)	30(1)

Table A.15. Bond lengths [Å] and angles [°] for **2.59**

C1-N1	1.475(5)	C10-C11	1.368(6)
C1-C2	1.522(5)	C10-H10	0.95
C1-H1A	0.99	C11-O5	1.376(5)
C1-H1B	0.99	C11-C12	1.390(6)
C2-C3	1.516(6)	C12-C13	1.388(6)
C2-H2A	0.99	C12-H12	0.95
C2-H2B	0.99	C13-C14	1.509(6)
C3-C17	1.384(5)	C14-C15	1.530(6)
C3-C4	1.396(5)	C14-H14A	0.99
C4-C5	1.369(6)	C14-H14B	0.99
C4-H4	0.95	C15-C16	1.537(5)
C5-O3	1.372(5)	C15-H15A	0.99
C5-C6	1.403(6)	C15-H15B	0.99
C6-O4	1.385(5)	C16-N1	1.473(5)
C6-C7	1.388(5)	C16-C17	1.524(5)
C7-C17	1.409(6)	C16-H16	1.00
C7-C8	1.479(6)	C18-O3	1.423(5)
C8-C13	1.400(5)	C18-H18A	0.98
C8-C9	1.403(5)	C18-H18B	0.98

C9-C10	1.375(6)	C18-H18C	0.98
C9-H9	0.95	C19-O4	1.433(5)
C19-H19A	0.98	C24-H24	0.95
C19-H19B	0.98	C25-H25	0.95
C19-H19C	0.98	C26-H26A	0.98
C20-C25	1.374(6)	C26-H26B	0.98
C20-C21	1.392(6)	C26-H26C	0.98
C20-S1	1.755(4)	C27-O6	1.396(5)
C21-C22	1.383(6)	C27-H27A	0.98
C21-H21	0.95	C27-H27B	0.98
C22-C23	1.378(6)	C27-H27C	0.98
C22-H22	0.95	N1-S1	1.626(3)
C23-C24	1.396(6)	O1-S1	1.441(3)
C23-C26	1.506(6)	O2-S1	1.421(3)
C24-C25	1.371(6)	O6-H6	0.84
N1-C1-C2	112.5(3)	C3-C2-H2B	109.2
N1-C1-H1A	109.1	C1-C2-H2B	109.2
C2-C1-H1A	109.1	H2A-C2-H2B	107.9
N1-C1-H1B	109.1	C17-C3-C4	119.9(4)
C2-C1-H1B	109.1	C17-C3-C2	122.0(4)

H1A-C1-H1B	107.8	C4-C3-C2	118.2(4)
C3-C2-C1	112.2(3)	C5-C4-C3	120.7(4)
C3-C2-H2A	109.2	C5-C4-H4	119.7
C1-C2-H2A	109.2	C3-C4-H4	119.7
C4-C5-O3	125.4(4)	C11-C12-H12	119.7
C4-C5-C6	119.8(4)	C12-C13-C8	120.4(4)
O3-C5-C6	114.8(4)	C12-C13-C14	120.9(4)
O4-C6-C7	120.3(4)	C8-C13-C14	118.8(4)
O4-C6-C5	119.2(4)	C13-C14-C15	112.8(3)
C7-C6-C5	120.5(4)	C13-C14-H14A	109.0
C6-C7-C17	119.1(4)	C15-C14-H14A	109.0
C6-C7-C8	120.2(4)	C13-C14-H14B	109.0
C17-C7-C8	120.7(4)	C15-C14-H14B	109.0
C13-C8-C9	117.3(4)	H14A-C14-H14B	107.8
C13-C8-C7	120.8(4)	C14-C15-C16	113.5(3)
C9-C8-C7	121.9(4)	C14-C15-H15A	108.9
C10-C9-C8	121.9(4)	C16-C15-H15A	108.9
C10-C9-H9	119.1	C14-C15-H15B	108.9
C8-C9-H9	119.1	C16-C15-H15B	108.9
C11-C10-C9	120.1(4)	H15A-C15-H15B	107.7

C11-C10-H10	119.9	N1-C16-C17	112.9(3)
C9-C10-H10	119.9	N1-C16-C15	107.2(3)
C10-C11-O5	118.9(4)	C17-C16-C15	112.8(3)
C10-C11-C12	119.6(4)	N1-C16-H16	107.9
O5-C11-C12	121.5(4)	C17-C16-H16	107.9
C13-C12-C11	120.6(4)	C15-C16-H16	107.9
C13-C12-H12	119.7	C3-C17-C7	120.1(4)
C3-C17-C16	121.7(4)	C22-C23-C24	118.1(4)
C7-C17-C16	118.1(4)	C22-C23-C26	121.5(5)
O3-C18-H18A	109.5	C24-C23-C26	120.4(5)
O3-C18-H18B	109.5	C25-C24-C23	120.9(5)
H18A-C18-H18B	109.5	C25-C24-H24	119.6
O3-C18-H18C	109.5	C23-C24-H24	119.6
H18A-C18-H18C	109.5	C24-C25-C20	120.4(4)
H18B-C18-H18C	109.5	C24-C25-H25	119.8
O4-C19-H19A	109.5	C20-C25-H25	119.8
O4-C19-H19B	109.5	C23-C26-H26A	109.5
H19A-C19-H19B	109.5	C23-C26-H26B	109.5
O4-C19-H19C	109.5	H26A-C26-H26B	109.5
H19A-C19-H19C	109.5	C23-C26-H26C	109.5

H19B-C19-H19C	109.5	H26A-C26-H26C	109.5
C25-C20-C21	120.0(4)	H26B-C26-H26C	109.5
C25-C20-S1	120.3(3)	O6-C27-H27A	109.5
C21-C20-S1	119.5(4)	O6-C27-H27B	109.5
C22-C21-C20	118.9(4)	H27A-C27-H27B	109.5
C22-C21-H21	120.5	O6-C27-H27C	109.5
C20-C21-H21	120.5	H27A-C27-H27C	109.5
C23-C22-C21	121.7(4)	H27B-C27-H27C	109.5
C23-C22-H22	119.1	C16-N1-C1	114.2(3)
C21-C22-H22	119.1	C16-N1-S1	119.4(3)
C1-N1-S1	118.8(3)	O2-S1-N1	106.64(18)
C5-O3-C18	117.1(3)	O1-S1-N1	105.92(18)
C6-O4-C19	112.7(3)	O2-S1-C20	109.37(19)
C27-O6-H6	109.5	O1-S1-C20	106.9(2)
O2-S1-O1	119.18(18)	N1-S1-C20	108.39(18)

Table A.16. Anisotropic displacement parameters ($Å^2x10^3$) for **2.59**

The anisotropic displacement factor exponent takes the form: $-2\pi^2[h^2 a^{*2}U^{11} + ... + 2 h k a^* b^* U^{12}]$

	U^{11}	U^{22}	U^{33}	U^{23}	U^{13}	U^{12}
C1	24(3)	32(3)	32(3)	3(2)	13(2)	10(2)
C2	28(3)	26(2)	28(3)	5(2)	10(2)	5(2)
C3	22(3)	10(2)	33(3)	3(2)	13(2)	-1(2)
C4	24(3)	19(2)	29(3)	2(2)	8(2)	-2(2)
C5	34(3)	20(3)	29(3)	-3(2)	20(3)	-2(2)
C6	20(3)	14(2)	32(3)	3(2)	12(2)	3(2)
C7	27(3)	9(2)	28(3)	3(2)	14(2)	-1(2)
C8	16(3)	25(3)	26(3)	1(2)	13(2)	1(2)
C9	25(3)	31(3)	33(3)	-2(2)	16(3)	-1(2)
C10	26(3)	32(3)	31(3)	4(2)	9(3)	-2(2)
C11	27(3)	35(3)	23(3)	-2(2)	10(2)	-1(2)
C12	22(3)	33(3)	35(3)	-9(2)	12(2)	-4(2)
C13	20(3)	22(3)	31(3)	-2(2)	12(2)	-4(2)
C14	27(3)	26(3)	40(3)	-9(2)	13(2)	-3(2)
C15	32(3)	25(3)	37(3)	-5(2)	11(2)	3(2)
C16	18(3)	21(2)	29(3)	2(2)	10(2)	2(2)
C17	27(3)	12(2)	24(3)	2(2)	13(2)	-2(2)

C18	47(4)	54(3)	25(3)	-2(2)	13(3)	18(3)
C19	29(4)	54(3)	56(4)	11(3)	24(3)	3(3)
C20	22(3)	30(3)	29(3)	3(2)	11(3)	2(2)
C21	29(3)	34(3)	31(3)	5(2)	10(2)	1(2)
C22	40(4)	23(3)	41(3)	3(2)	17(3)	8(2)
C23	43(4)	32(3)	36(3)	-1(2)	26(3)	-11(3)
C24	24(3)	44(3)	42(3)	0(3)	12(3)	-9(3)
C25	28(3)	35(3)	40(3)	3(2)	17(3)	3(2)
C26	44(4)	48(3)	52(3)	-9(3)	24(3)	-7(3)
C27	62(5)	72(4)	74(4)	-9(3)	38(4)	14(3)
N1	19(2)	27(2)	30(2)	3(2)	12(2)	6(2)
O1	25(2)	43(2)	52(2)	-3(2)	23(2)	14(2)
O2	32(2)	42(2)	24(2)	2(1)	12(2)	1(2)
O3	39(2)	35(2)	26(2)	0(1)	14(2)	12(2)
O4	23(2)	30(2)	35(2)	4(1)	14(2)	9(2)
O5	34(2)	56(2)	36(2)	1(2)	4(2)	2(2)
O6	52(3)	59(2)	62(2)	-19(2)	24(2)	-22(2)
S1	26(1)	35(1)	33(1)	-2(1)	17(1)	3(1)

Table A.17. Hydrogen coordinates ($x10^4$) and isotropic displacement parameters ($Å^2x10^3$) for **2.59**

	x	y	z	U(eq)
H1A	1819	7537	3116	34
H1B	638	7227	2948	34
H2A	1018	6398	1732	33
H2B	1463	6953	974	33
H4	2574	6125	263	29
H9	5668	5300	6161	34
H10	6943	5342	8618	36
H12	6493	7147	8699	35
H14A	5078	7349	4871	37
H14B	5391	7681	6500	37
H15A	3398	7681	5025	38
H15B	3692	7456	6761	38
H16	3316	6469	6069	27
H18A	3131	5400	-1081	63
H18B	4244	5384	-1550	63
H18C	3726	6020	-1284	63
H19A	6343	6053	1908	66
H19B	7370	5755	3229	66

H19C	6806	6366	3561	66
H21	2331	5398	5402	38
H22	1969	4539	3848	40
H24	-1110	5178	1513	44
H25	-762	6033	3049	39
H26A	875	4098	1304	68
H26B	-389	4322	497	68
H26C	-89	3892	1975	68
H27A	8864	7876	12637	98
H27B	7784	7445	12147	98
H27C	7812	8038	11159	98
H6	8425	7025	10684	84

Table A.18. Torsion angles [°] for **2.59**

N1-C1-C2-C3	-42.8(5)	C8-C9-C10-C11	-1.5(6)
C1-C2-C3-C17	13.7(5)	C9-C10-C11-O5	-175.6(4)
C1-C2-C3-C4	-166.9(3)	C9-C10-C11-C12	4.8(6)
C17-C3-C4-C5	-0.9(6)	C10-C11-C12-C13	-5.1(6)
C2-C3-C4-C5	179.7(4)	O5-C11-C12-C13	175.3(4)
C3-C4-C5-O3	-180.0(3)	C11-C12-C13-C8	2.0(6)
C3-C4-C5-C6	0.7(6)	C11-C12-C13-C14	-177.4(4)
C4-C5-C6-O4	179.5(4)	C9-C8-C13-C12	1.3(6)
O3-C5-C6-O4	0.1(5)	C7-C8-C13-C12	-177.2(4)
C4-C5-C6-C7	0.4(6)	C9-C8-C13-C14	-179.3(4)
O3-C5-C6-C7	-179.0(3)	C7-C8-C13-C14	2.3(6)
O4-C6-C7-C17	179.7(3)	C12-C13-C14-C15	-109.2(5)
C5-C6-C7-C17	-1.2(6)	C8-C13-C14-C15	71.4(5)
O4-C6-C7-C8	1.1(6)	C13-C14-C15-C16	-45.3(5)
C5-C6-C7-C8	-179.8(4)	C14-C15-C16-N1	-166.1(3)
C6-C7-C8-C13	127.3(4)	C14-C15-C16-C17	-41.1(5)
C17-C7-C8-C13	-51.2(6)	C4-C3-C17-C7	0.0(6)
C6-C7-C8-C9	-51.1(6)	C2-C3-C17-C7	179.4(4)
C17-C7-C8-C9	130.4(4)	C4-C3-C17-C16	-178.0(3)

C13-C8-C9-C10	-1.6(6)	C2-C3-C17-C16	1.4(6)
C7-C8-C9-C10	176.9(4)	C6-C7-C17-C3	1.1(6)
C8-C7-C17-C3	179.6(3)	C15-C16-N1-S1	-128.5(3)
C6-C7-C17-C16	179.1(3)	C2-C1-N1-C16	59.3(4)
C8-C7-C17-C16	-2.3(5)	C2-C1-N1-S1	-90.0(4)
N1-C16-C17-C3	12.4(5)	C4-C5-O3-C18	6.7(6)
C15-C16-C17-C3	-109.4(4)	C6-C5-O3-C18	-174.0(4)
N1-C16-C17-C7	-165.7(3)	C7-C6-O4-C19	-104.8(4)
C15-C16-C17-C7	72.5(5)	C5-C6-O4-C19	76.0(5)
C25-C20-C21-C22	1.1(6)	C16-N1-S1-O2	37.9(3)
S1-C20-C21-C22	-174.4(3)	C1-N1-S1-O2	-174.4(3)
C20-C21-C22-C23	0.2(6)	C16-N1-S1-O1	165.8(3)
C21-C22-C23-C24	-1.5(6)	C1-N1-S1-O1	-46.5(3)
C21-C22-C23-C26	179.0(4)	C16-N1-S1-C20	-79.8(3)
C22-C23-C24-C25	1.5(6)	C1-N1-S1-C20	67.9(3)
C26-C23-C24-C25	-179.0(4)	C25-C20-S1-O2	143.5(3)
C23-C24-C25-C20	-0.1(6)	C21-C20-S1-O2	-41.0(4)
C21-C20-C25-C24	-1.2(6)	C25-C20-S1-O1	13.2(4)
S1-C20-C25-C24	174.3(3)	C21-C20-S1-O1	-171.3(3)
C17-C16-N1-C1	-42.5(4)	C25-C20-S1-N1	-100.6(4)

C15-C16-N1-C1	82.4(4)	C21-C20-S1-N1	74.9(4)

Table A.19. Hydrogen bonds for **2.59** [Å and °].

D-H...A	d(D-H)	d(H...A)	d(D...A)	<(DHA)
O6-H6...O5	0.84	1.88	2.715(4)	178.3

References

(1) Tojo, E. The Homoaporphine Alkaloids. *J. Nat. Prod.* **1989**, *52*, 909–921.

(2) Tojo, E.; Abu Zarga, M. H.; Sabri, S. S.; Freyer, A. J.; Shamma, M. The Homoaporphine Alkaloids of Androcymbium Palaestinum. *J. Nat. Prod.* **1989**, *52*, 1055–1059.

(3) Badger, G. M.; Bradbury, R. B. The Alkaloids of Kreysigia Multiflora Reichb. Part I. Isolation. *Chem. Commun.* **1960**, 445–447.

(4) Battersby, A. R.; Bradbury, R. B.; Herbert, R. B.; Munro, M. H. G.; Ramage, R. 1 -Phenethylisoquinoline Alkaloids. Part IV. Isolation, Structural Elucidation, and Synthesis of c-Homoaporphines. *J.C.S. Perkin I* **1974**, 1394–1399.

(5) Battersby, A. R.; Bradbury, R. B.; Herbert, R. B.; Munro, M. H. G.; Ramage, R. Structure and Synthesis of Homoaporphines: A New Group of 1 - Phenethylisoquinoline Alkaloids. *Chem. Commun.* **1967**, 450–451.

(6) Battersby, A. R.; Bohler, P.; Munro, M. H. G.; Ramage, R. Biosynthesis. Part XX. Biosynthesis of c-Homoaporphines in Kreysigia Multiflora. *J.C.S. Perkin I* **1974**, 1399–1402.

(7) Battersby, a. R.; McDonald, E.; Munro, M. H. G.; Ramage, R. Homoaporphine Systems and Related Dienones: Isolation, Structure, and Synthesis. *Chem. Commun.* **1967**, 934–935.

(8) R Battersby, A.; Bohler, P.; G Munro, M. H.; Ramage, R. Biosynthesis of Homoaporphines. *Chem. Commun.* **1969**, 1066–1067.

(9) Kupchan, S. M.; Dhingra, O. P.; Kim, C.-K. Efficient Intramolecular Monophenol Oxidative Coupling. *J. Org. Chem.* **1978**, *43*, 4076–4081.

(10) Kupchan, S. M.; Dhingra, O. P.; Kim, C.-K. Efficient Intramolecular Monophenol Oxidative Coupling. *J. Org. Chem.* **1976**, *41*, 4049–4050.

(11) Kupchan, S. M.; Dhingra, O. P.; Kim, C.-K.; Kameswaran, V. Intramolecular Nonphenol Oxidative Coupling of Phenethylisoquinolines. *J. Org. Chem.* **1978**, *43*, 2521–2529.

(12) Taylor, E. C.; Andrade, J. G.; Rall, Gerhardus, J. H.; Mckillop, A. Thallium in Organic Synthesis. 59. Alkaloid Synthesis via Intramolecular Nonphenolic Oxidative Coupling. Preparation of Ocoteine, Acetoxyocoxylonine, 3-Methoxy-N-Acetylnornantenine, Neolisine, Kreysigine, O-Methylkresigine, and Multifloramine. *J. Am. Chem. Soc.* **1980**, *102*, 6513–6519.

(13) Hoshino, O.; Toshioka, T.; Umezawa, B. Studies on Tetrahydroisoquinolines. VI. Synthesis of (±)-Thaliporphine and (±)-Glaucine via a P-Quinol Acetate. *Chem. Pharm. Bull* **1974**, *22*, 1302.

(14) Hara, H.; Shinoki, H.; Hoshino, O.; Umezawa, B. A Synthesis of 3-Hydroxyaporphine and Homoaporphine. *Heterocycles* **1983**, *20*, 2155–2158.

(15) Hara, H.; Shinoki, H.; Komatsu, T.; Hoshino, O.; Umezawa, B. Studies on Tetrahydroisoquinolines. XXVII. A Synthesis of 3-Hydroxyaporphines and 3-Hydroxyhomoaporphines. *Chem. Pharm. Bull* **1986**, *34*, 1924–1928.

(16) Hoshino, O.; Hara, H.; Serizawa, N.; Umezawa, B. Studies on Tetrahydroisoquinolines. IX. The Synthesis of (±)-Domesticine and a Related (±)-Homoaporphine via P-Quinol Acetates. *Chem. Pharm. Bull* **1975**, *23*, 2048–2053.

(17) Hara, H.; Hoshino, O.; Ishige, T.; Umezawa, B. Studieson Tetrahydroisoquinolines. XIX. Synthesis of (±)-Isothebaine, (±)-1-Hydroxy-2,9-Dimethoxy-, (±)-1-Hydroxy-2,10-Dimethoxy-, and (±)-2,10-Dimethoxy-Aporphines, (±)-2,6-Dimethoxyhomomorphinandienone, and (±)-1-Hydroxy-2,10-Dimethoxyhomoaporphine. *Chem. Pharm. Bull* **1981**, *29*, 1083–1087.

(18) Hoshino, O.; Toshioka, T.; Ohyama, K.; Umezawa, B. Studies on Tetrahydroisoquinolins. VII. Synthesis of Homoaporphine via a P-Quinol Acetate; Total Synthesis of (±)-Kreysigine. *Chem. Pharm. Bull* **1974**, *22*, 1307.

(19) Hoshino, O.; Toshioka, T.; Umezawa, B. Synthesis of (±)-Kreysigine via a P-Quinol Acetate. *J.C.S. Chem. Comm.* **1972**, 740–741.

(20) Hara, H.; Hoshino, O.; Umezawa, B. Studies of Tetrahydroisoquinoline. Part 13. Total Syntheses of (±)-O-Methylandrocymbine, (±)-Androcymbine, (±)-Kreysigine, (±)-Multifloramine, and Their Related Phenethylisoquinoline Alkaloids. *J. C. S. Perkin I* **1979**, 2657–2663.

(21) Castro, J. L.; Castedo, L.; Riguera, R. Addition of Dichlorocarbene to Aporphinoids: A New Route to Homoaporphines. *Tetrahedron Lett.* **1985**, *26*, 1561–1564.

(22) Castro, J. L.; Castedo, L.; Riguera, R. Ring C Homologation of Aporphines. A New Synthesis of Homoaporphines. *J. Org. Chem.* **1987**, *52*, 3579–3584.

(23) Kametani, B. T.; Satoh, F.; Fukumoto, K. The Synthesis of Homoproaporphine-Type Compounds by Phenolic Oxidative Coupling. *J. Chem. SOC.* **1968**, 271–275.

(24) Kametani, T.; Satoh, F.; Yagi, H.; Fukumoto, K. Syntheses of Homoproaporphines by Phenolic Oxidative Coupling. II. Separation of Two Isomeric Dienones of Homoproaporphines. *J. Org. Chem.* **1968**, *33*, 690–694.

(25) Kametani, T.; Satoh, F. Novel Rearrangement of Homoproaporphine and the Configuration of Two Isomeric Homoproaporphines. *Chem. Commun.* **1967**, 1103–1105.

(26) Kametani, T.; Yagi, H.; Fukumoto, K.; Satoh, F. The Acid Catalyzed Rearrangement of Homoaporphine under Two Different Conditions. *Chem. Pharm. Bull* **1968**, *16*, 2297–2298.

(27) Kametani, T.; Satoh, F.; Yagi, H.; Fukumoto, K. Rearrangement and Novel Enol-Ether Addition in Homoproaporphines. *J. Chem. Soc. Perkin 1* **1968**, *8*, 1003–1005.

(28) Kametani, T.; Satoh, F.; Yagi, H.; Fukumoto, K. Configuration and Rearrangements of Homoproaporphines. *J. Chem. SOC.* **1970**, 382–385.

(29) Kametani, T.; Fukumoto, K. Total Syntheses of (-)-O-Methylandrocymbine, (-)-Kreysigine, and Alkaloid CC-10 Methyl Ether. *J.C.S. Perkin I* **1972**, 2160–2162.

(30) Kametani, T.; Koizumi, M.; Fukumoto, K. Total Synthesis of O-Methylandrocymbine by a Photo-Pschorr Reaction and Synthesis of Thalifoline. *J. Chem. Soc. C Org.* **1971**, 1792–1796.

(31) Kametani, T.; Koizumi, M.; Fukumoto, K. Total Synthesis of O-Methylandrocymbine by Photolysis of Diazotised Isoquinoline. *J. Chem. Soc. D Chem. Commun.* **1970**, 1157.

(32) Kametani, B. T.; Koizumi, M. Studies on the Syntheses of Heterocyclic Compounds. Part CDXLVI. Total Photolytic Synthesis of (±)Androcymbine and (±)-Multifloramine. *J . Chem. Soc. (C)* **1971**, *19*, 3976–3979.

(33) Kametani, T.; Satoh, Y.; Shibuya, S.; Koizumi, M.; Fukumoto, K. Studies on the Syntheses of Heterocyclic Compounds. CDLI. Alternative Photolytic Total Syntheses of O-Methylandrocymbine and Kreysigine. *J. Org. Chem.* **1971**, *36*, 3733–3736.

(34) Kametani, T.; Koizumi, M.; Shishido, K.; Fukumoto, K. Studies on the Syntheses of Heterocyclic Compounds. Part CD. Total Syntheses of N0(10)-Dimethylhernovine and Kreysigine by Photolysis of Diazotised Lsoquinolines. *J. Chem. Soc.* **1971**, 1923–1927.

(35) Barolo, S. M.; Teng, X.; Cuny, G. D.; Rossi, R. A. Syntheses of Aporphine and Homoaporphine Alkaloids by Intramolecular Ortho-Arylation of Phenols with Aryl Halides via SRN1 Reactions in Liquid Ammonia. *J. Org. Chem.* **2006**, *71*, 8493–8499.

(36) Chaudhary, S.; Harding, W. W. Synthesis of C-Homoaporphines via Microwave-Assisted Direct Arylation. *Tetrahedron* **2011**, *67*, 569–575.

(37) Winstein, S.; Baird, R. The Formation of Dienones Through Ar1-Participation. *J. Am. Chem. Soc.* **1957**, *79*, 756–757.

(38) Murphy, W. S.; Wattanasin, S. Anionic Cyclization of Phenols. *Chem. Soc. Rev.* **1983**, *12*, 213–250.

(39) Masamune, S. Synthesis of 4a,6-Ethano-5.6 7,8-Tetrahydro2(4a)-Naphthalenone. *J. Am. Chem. Soc.* **1961**, *83*, 1009–1010.

(40) Masamune, S. Total Syntheses of Diterpenes and Diterpene Alkaloids. II.1 A Tetracyclic Common Intermediate. *J. Am. Chem. Soc.* **1964**, *86*, 288–289.

(41) Masamune, S. Total Syntheses of Diterpenes and Diterpene Alkaloids. III. Kaurene. *J. Am. Chem. Soc.* **1964**, *86*, 289–390.

(42) Masamune, S. Total Syntheses of Diterpenes and Diterpene Alkaloids. IV. Garryine. *J. Am. Chem. Soc.* **1964**, *86*, 290–291.

(43) Masamune, S. Total Syntheses of Diterpenes and Diterpene Alkaloids. V. Atisine. *J. Am. Chem. Soc.* **1964**, *86*, 291–292.

(44) Magnus, P.; Sane, N.; Fauber, B. P.; Lynch, V. Concise Syntheses of (-)-Galanthamine and (±)-Codeine via Intramolecular Alkylation of a Phenol Derivative. *J. Am. Chem. Soc.* **2009**, *131*, 16045–16047.

(45) Fauber, B. P. Studies Directed Toward The Syntheses of the Biologically Active Alkaloids (-)-Galanthamine and (-)-Lemonomycin. Ph.D. Dissertation, The University of Texas at Austin, 2006.

(46) Sane, N. The Total Synthesis of (±)-Morphine and (-)-Galanthamine. Ph.D. Dissertation, The University of Texas at Austin, 2009.

(47) Shieh, W.-C.; Carlson, J. A. Asymmetric Transformation of Either Enantiomer of Narwedine via Total Spontaneous Resolution Process, a Concise Solution to the Synthesis of (-)-Galanthamine. *J. Org. Chem.* **1994**, *59*, 5463–5465.

(48) Kuenburg, B.; Czollner, L.; Frohlich, J.; Jordis, U. Development of a Pilot Scale Process for the Anti-Alzheimer Drug (–)-Galanthamine Using Large-Scale Phenolic Oxidative Coupling and Crystallisation-Induced Chiral Conversion. *Org. Process Res. Dev.* **1999**, *3*, 425–431.

(49) Czollner, L.; Frantsits, W.; Küenburg, B.; Hedenig, U.; Fröhlich, J.; Jordis, U. New Kilogram-Synthesis of the Anti-Alzheimer Drug (–)-Galanthamine. *Tetrahedron Lett.* **1998**, *39*, 2087–2088.

(50) Kita, Y.; Arisawa, M.; Gyoten, M.; Nakajima, M.; Hamada, R.; Tohma, H.; Takada, T. Oxidative Intramolecular Phenolic Coupling Reaction Induced by a Hypervalent Iodine(III) Reagent: Leading to Galanthamine-Type Amaryllidaceae Alkaloids. *J. Org. Chem.* **1998**, *63*, 6625–6633.

(51) Ghavimi, B.; Magnus, P. Total Synthesis of 8,14-Dihydromorphinandienone Alkaloids. *Org. Lett.* **2014**, *16*, 1708–1711.

(52) Magnus, P.; Seipp, C. Concise Synthesis of the Hasubanan Alkaloid (±)-Cepharatine A Using a Suzuki Coupling Reaction to Effect O,p-Phenolic Coupling. *Org. Lett.* **2013**, *15*, 4870–4871.

(53) Magnus, P.; Marks, K. D.; Meis, A. New Strategy for the Synthesis of Proaporphine and Homoproaporphine-Type Alkaloids from a Common Intermediate. *Tetrahedron* **2015**, *71*, 3872–3877.

(54) Baldwin, J. E.; Kruse, L. I. Rules for Ring Closure. Stereoelectronic Control in the Endocyclic Alkylation of Ketone Enolates. *J. Chem. Soc. Chem. Commun.* **1977**, 233–235.

(55) Gilmore, K.; Alabugin, I. V. Cyclizations of Alkynes: Revisiting Baldwin's Rules for Ring Closure. *Chem. Rev.* **2011**, *111*, 6513–6556.

(56) Marks, K. The Total Synthesis of (±)-Stepharine. M.S. Thesis, The Univeristy of Texas at Austin, 2013.

(57) Ramirez, F.; Burger, A. The Reduction of Phenolic Beta-Nitrostyrenes by Lithium Aluminum Hydride. *J. Am. Chem. Soc.* **1950**, *72*, 2781–2782.

(58) Kabalka, G.; Laila, G.; Varma, R. Selected Reduction of Conjugated Nitroalkenes. *Tetrahedron* **1990**, *46*, 7443–7475.

(59) Pecic, S.; McAnuff, M. A.; Harding, W. W. Nantenine as an Acetylcholinesterase Inhibitor: SAR, Enzyme Kinetics and Molecular Modeling Investigations. *J. Enzyme Inhib. Med. Chem.* **2011**, *26*, 46–55.

(60) Kohno, M.; Sasao, S.; Murahashi, S. I. Synthesis of Phenethylamines by Hydrogenation of Beta-Nitrosyrenes. *Bull. Chem. Soc. Jpn* **1990**, *63*, 1252–1254.

(61) Ueki, R.; Yamaguchi, K.; Nonaka, H.; Sando, S. 1H NMR Probe for in Situ Monitoring of Dopamine Metabolism and Its Application to Inhibitor Screening. *J. Am. Chem. Soc.* **2012**, *134*, 12398–12401.

(62) Pradhan, P. K.; Dey, S.; Jaisankar, P.; Giri, V. S. Fe-HCl: An Efficient Reagent for Deprotection of Oximes as Well as Selective Oxidative Hydrolysis of Nitroalkenes and Nitroalkanes to Ketones. *Synth. Commun.* **2005**, *35*, 913–922.

(63) Vinogradova, V. I.; Yunusov, M. S.; Kuchin, A. V.; Tolstikov, G. A.; Sagandykov, R.; Khaimuratov, K. A.; Alimov, A. Syntheses Based on Beta-Phenylethylamines. *Khimiya Prir. Soedin.* **1990**, *1*, 54–59.

(64) Mans, D. M.; Pearson, W. H. Total Synthesis of (+)-Cocaine via Desymmetrization of a *Meso* -Dialdehyde. *Org. Lett.* **2004**, *6*, 3305–3308.

(65) Maryanoff, B. E.; Zhang, H.-C.; Cohen, J. H.; Turchi, I. J.; Maryanoff, C. a. Cyclizations of N-Acyliminium Ions. *Chem. Rev.* **2004**, *104*, 1431–1628.

(66) Chrzanowska, M.; Rozwadowska, M. D. Asymmetric Synthesis of Isoquinoline Alkaloids. *Chem. Rev.* **2004**, *104*, 3341–3370.

(67) Royer, J.; Bonin, M.; Micouin, L. Chiral Heterocycles by Iminium Ion Cyclization. *Chem. Rev.* **2004**, *104*, 2311–2352.

(68) Yokoyama, A.; Ohwada, T.; Shudo, K. Prototype Pictet-Spengler Reactions Catalyzed by Superacids. Involvement of Dicationic Superelectrophiles. *J. Org. Chem.* **1999**, *64*, 611–617.

(69) Numa, M. M. D.; Lee, L. V; Hsu, C.-C.; Bower, K. E.; Wong, C.-H. Identification of Novel Anthrax Lethal Factor Inhibitors Generated by Combinatorial Pictet-Spengler Reaction Followed by Screening in Situ. *Chembiochem* **2005**, *6*, 1002–1006.

(70) Ponnala, S.; Harding, W. W. A New Route to Azafluoranthene Natural Products via Direct Arylation. *Eur. J. Org. Chem.* **2013**, *3013*, 1107–1115.

(71) Hodges, T. R. The Study of a Codeine Bromohydrin Rearrangement and Investigation of a Phenolic Aklylation Strategy. M.S. Thesis, The University of Texas at Austin, 2013.

(72) Meth-Cohn, O.; Stanforth, S. P. 3.5 – The Vilsmeier–Haack Reaction. In *Comprehensive Organic Synthesis*; 1991; pp. 777–794.

(73) Stirling, C. J. M. Leaving Groups and Nucleofugality in Elimination and Other Organic Reactions. *Acc. Chem. Res.* **1979**.

(74) Jaramillo, P.; Domingo, L. R.; Pérez, P. Towards an Intrinsic Nucleofugality Scale: The Leaving Group (LG) Ability in CH3LG Model System. *Chem. Phys. Lett.* **2006**, *420*, 95–99.

(75) Ghavimi-Alagha, B. Synthesis and Receptor Affinity of 7ß-Substituted Analogs of Coeine; Total Synthesis of 8,14-Dihydromorphinandienone Alkaloids. Ph.D. Dissertation, The Univeristy of Texas at Austin, 2014.

(76) Kupchan, S. M.; Dhingra, O. P.; Kim, C.-K. Efficient Intramolecular Monophenol Oxidative Coupling. *J. Org. Chem.* **1978**, *43*, 4076–4081.

(77) Kupchan, S. M.; Dhingra, O. P.; Kim, C.; Kameswaran, V. Efficient Intramolecular Monophenol Oxidative Coupling. *J. Org. Chem.* **1976**, *41*, 4049–4050.

(78) Kametani, T.; Satoh, F.; Yagi, H.; Fukumoto, K. Novel Rearrangement of Homoproaporphine and the Configuration of Two Isomeric Homoproaporphines. *Chem. Commun.* **1967**, 1103–1105.

(79) Kametani, T.; Satoh, F.; Yagi, H.; Fukumoto, K. Rearrangement and Novel Enol-Ether Addition in Homoproaporphines. *J. Chem. Soc. C Org.* **1968**, 1003–1005.

(80) Brun, R.; Blum, J.; Chappuis, F.; Burri, C. Human African Trypanosomiasis. *Lancet* **2010**, *375*, 148–159.

(81) Usuki, T.; Sato, M.; Hara, S.; Yoshimoto, Y.; Kondo, R.; Zimmermann, S.; Kaiser, M.; Brun, R.; Hamburger, M.; Adams, M. Antitrypanosomal Structure–activity-Relationship Study of Synthetic Cynaropicrin Derivatives. *Bioorg. Med. Chem. Lett.* **2014**, *24*, 794–798.

(82) Koh, C. Y.; Kim, J. E.; Wetzel, A. B.; de van der Schueren, W. J.; Shibata, S.; Ranade, R. M.; Liu, J.; Zhang, Z.; Gillespie, J. R.; Buckner, F. S.; Christophe, L. M.; Fan, E.; Hol, W. G. J. Structures of Trypanosoma Brucei Methionyl-tRNA Synthetase with Urea-Based Inhibitors Provide Guidance for Drug Design against Sleeping Sickness. *PLoS Negl. Trop. Dis.* **2014**, *8*, e2775.

(83) Kristensson, K.; Nygård, M.; Bertini, G.; Bentivoglio, M. African Trypanosome Infections of the Nervous System: Parasite Entry and Effects on Sleep and Synaptic Functions. *Prog. Neurobiol.* **2010**, *91*, 152–171.

(84) Kennedy, P. G. Clinical Features, Diagnosis, and Treatment of Human African Trypanosomiasis (Sleeping Sickness). *Lancet. Neurol.* **2013**, *12*, 186–194.

(85) Barrett, M. P.; Brun, R.; Don, R.; Jacobs, R. T.; Wang, M. Z. Development of Novel Drugs for Human African Trypanosomiasis. *Future Microbiol.* **2011**, *6*, 677–791.

(86) Nagle, A. S.; Khare, S.; Kumar, A. B.; Supek, F.; Buchynskyy, A.; Mathison, C. J. N.; Chennamaneni, N. K.; Pendem, N.; Buckner, F. S.; Gelb, M. H.; Molteni, V. Recent Developments in Drug Discovery for Leishmaniasis and Human African Trypanosomiasis. *Chem. Rev.* **2014**, *114*, 11305–11347.

(87) Bacchi, C. J.; Berens, R. L.; Nathan, H. C.; Klein, R. S.; Elegbe, I. A.; Rao, K. V. B.; McCann, P. P.; Marr, J. J. Synergism between 9-Deazainosine and DL-a-Difluoromethylornithine in Treatment of Experimental African Trypanosomiasis. *Antimicrob. Agents Chemother.* **1987**, *31*, 1406–1413.

(88) Fairlamb, A. H.; Henderson, G. B.; Cerami, A. Trypanothione Is the Primary Target for Arsenical Drugs against African Trypanosomes (Chemotherapy). *Proc. Natl. Acad. Sci. USA* **1989**, *86*, 2607–2611.

(89) Baker, N.; de Koning, H. P.; Mäser, P.; Horn, D. Drug Resistance in African Trypanosomiasis: The Melarsoprol and Pentamidine Story. *Trends Parasitol.* **2013**, *29*, 110–118.

(90) Baker, N.; Alsford, S.; Horn, D. Genome-Wide RNAi Screens in African Trypanosomes Identify the Nifurtimox Activator NTR and the Eflornithine Transporter AAT6. *Mol. Biochem. Parasitol.* **2011**, *176*, 55–57.

(91) Simarro, P. P.; Diarra, A.; Ruiz Postigo, J. A.; Franco, J. R.; Jannin, J. G. The Human African Trypanosomiasis Control and Surveillance Programme of the World Health Organization 2000–2009: The Way Forward. *PLoS Negl. Trop. Dis.* **2011**, *5*, e1007.

(92) Jennings, F. W.; Urquhart, G. M. The Use of the 2 Substituted 5-Nitroimidazole, Fexinidazole (Hoe 239) in the Treatment of chronicT. Brucei Infections in Mice. *Zeitschrift fur Parasitenkd. Parasitol. Res.* **1983**, *69*, 577–581.

(93) Torreele, E.; Bourdin Trunz, B.; Tweats, D.; Kaiser, M.; Brun, R.; Mazué, G.; Bray, M. A.; Pécoul, B. Fexinidazole – A New Oral Nitroimidazole Drug Candidate Entering Clinical Development for the Treatment of Sleeping Sickness. *PLoS Negl. Trop. Dis.* **2010**, *4*, e923.

(94) Pohlig, G.; Bernhard, S. C.; Blum, J.; Burri, C.; Mpanya, A.; Lubaki, J.-P. F.; Mpoto, A. M.; Munungu, B. F.; N'tombe, P. M.; Deo, G. K. M.; Mutantu, P. N.; Kuikumbi, F. M.; Deo, G. K. M.; Mununga, A. K.; Dala, A.; Macharia, S.; Bilenge, C. M. M.; Mesu, V. K.; Franco, J. R.; Dituvanga, N. D.; Tidwell, R. R.; Olson, C. A. Efficacy and Safety of Pafuramidine versus Pentamidine Maleate for Treatment of First Stage Sleeping Sickness in a Randomized, Comparator-Controlled, International Phase 3 Clinical Trial. *PLoS Negl. Trop. Dis.* **2016**, *10*, e0004363.

(95) Pham, J. S.; Dawson, K. L.; Jackson, K. E.; Lim, E. E.; Pasaje, C. F. a; Turner, K. E. C.; Ralph, S. a. Aminoacyl-tRNA Synthetases as Drug Targets in Eukaryotic Parasites. *Int. J. Parasitol. Drugs drug Resist.* **2014**, *4*, 1–13.

(96) Hurdle, J. G.; Neill, A. J. O.; Chopra, I. Prospects for Aminoacyl-tRNA Synthetase Inhibitors as New Antimicrobial Agents. *Antimicrob. Agents Chemother.* **2005**, *49*, 4821–4833.

(97) Nakama, T.; Nureki, O.; Yokoyama, S. Structural Basis for the Recognition of Isoleucyl-Adenylate and an Antibiotic, Mupirocin, by Isoleucyl-tRNA Synthetase. *J. Biol. Chem.* **2001**, *276*, 47387–47393.

(98) Critchley, I. a; Ochsner, U. a. Recent Advances in the Preclinical Evaluation of the Topical Antibacterial Agent REP8839. *Curr. Opin. Chem. Biol.* **2008**, *12*, 409–417.

(99) Ibba, M.; Stoll, D. Aminoacyl-tRNA Synthesis. *Annu. Rev. Biochem.* **2000**, *69*, 617–650.

(100) Laursen, B. S.; Sørensen, H. P.; Mortensen, K. K.; Sperling-Petersen, H. U. Initiation of Protein Synthesis in Bacteria. *Microbiol. Mol. Biol. Rev.* **2005**, *69*, 101–123.

(101) Farhanullah; Kim, S. Y.; Yoon, E. J.; Choi, E. C.; Kim, S.; Kang, T.; Samrin, F.; Puri, S.; Lee, J. Design and Synthesis of Quinolinones as Methionyl-tRNA Synthetase Inhibitors. *Bioorganic Med. Chem.* **2006**, *14*, 7154–7159.

(102) Shibata, S.; Gillespie, J. R.; Kelley, A. M.; Napuli, A. J.; Zhang, Z.; Kovzun, K. V; Pefley, R. M.; Lam, J.; Zucker, F. H.; Van Voorhis, W. C.; Merritt, E. A.; Hol, W. G. M.; Verlinde, C. L. M. J.; Fan, E.; Buckner F. S. Selective Inhibitors of Methionyl-tRNA Synthetase Have Potent Activity against Trypanosoma Brucei Infection in Mice. *Antimicrob. Agents Chemother.* **2011**, *55*, 1982–1989.

(103) Koh, C. Y.; Kim, J. E.; Shibata, S.; Ranade, R. M.; Yu, M.; Liu, J.; Gillespie, J. R.; Buckner, F. S.; Verlinde, C. L. M. J.; Fan, E.; Hol, W. M. G. Distinct States of Methionyl-tRNA Synthetase Indicate Inhibitor Binding by Conformational Selection. *Structure* **2012**, *20*, 1681–1691.

(104) Shibata, S.; Gillespie, J. R.; Ranade, R. M.; Koh, C. Y.; Kim, J. E.; Laydbak, J. U.; Zucker, F. H.; Hol, W. G. J.; Verlinde, C. L. M. J.; Buckner, F. S.; Fan, E. Urea-Based Inhibitors of Trypanosoma Brucei Methionyl-tRNA Synthetase: Selectivity and in Vivo Characterization. *J. Med. Chem.* **2012**, *55*, 6342–6351.

(105) Vincent, I. M.; Creek, D.; Watson, D. G.; Kamleh, M. a.; Woods, D. J.; Wong, P. E.; Burchmore, R. J. S.; Barrett, M. P. A Molecular Mechanism for Eflornithine Resistance in African Trypanosomes. *PLoS Pathog.* **2010**, *6*, 1–9.

(106) Bridges, D. J.; Gould, M. K.; Nerima, B.; Mäser, P.; Burchmore, R. J. S.; de Koning, H. P. Loss of the High-Affinity Pentamidine Transporter Is Responsible for High Levels of Cross-Resistance between Arsenical and Diamidine Drugs in African Trypanosomes. *Mol. Pharmacol.* **2007**, *71*, 1098–1108.

(107) Ranade, R. M.; Gillespie, J. R.; Shibata, S.; Verlinde, C. L. M. J.; Fan, E.; Hol, W. G. J.; Buckner, F. S. Induced Resistance to Methionyl-tRNA Synthetase Inhibitors in Trypanosoma Brucei Is Due to Overexpression of the Target. *Antimicrob. Agents Chemother.* **2013**, *57*, 3021–3028.

(108) Galloway, W. R. J. D.; Isidro-Llobet, A.; Spring, D. R. Diversity-Oriented Synthesis as a Tool for the Discovery of Novel Biologically Active Small Molecules. *Nat. Commun.* **2010**, *1*, 1–13.

(109) Tan, D. S. Diversity-Oriented Synthesis: Exploring the Intersections between Chemistry and Biology. *Nat. Chem. Biol.* **2005**, 74–84.

(110) Burke, M. D.; Schreiber, S. L. A Planning Strategy for Diversity-Oriented Synthesis. *Angew. Chemie Int. Ed.* **2004**, *43*, 46–58.

(111) Schreiber, S. L. Target-Oriented and Diversity-Oriented Organic Synthesis in Drug Discovery. *Science.* **2000**, *287*, 1964–1969.

(112) Nielsen, T. E.; Schreiber, S. L. Towards the Optimal Screening Collection: A Synthesis Strategy. *Angew. Chemie Int. Ed.* **2008**, *47*, 48–56.

(113) Welsch, M. E.; Snyder, S. A.; Stockwell, B. R. Privileged Scaffolds for Library Design and Drug Discovery. *Curr. Opin. Chem. Biol.* **2010**, *14*, 347–361.

(114) Dyker, G. Amino Acid Derivatives by Multicomponent Reactions. *Angew. Chemie Int. Ed.* **1997**, *36*, 1700–1702.

(115) Magedov, I. V; Kornienko, A. Multicomponent Reactions in Alkaloid-Based Drug Discovery. *Chem. Heterocycl. Compd.* **2012**, *48*, 33–38.

(116) Shestopalov, A.; Shestopalov, A.; Rodinovskaya, L. Multicomponent Reactions of Carbonyl Compounds and Derivatives of Cyanoacetic Acid: Synthesis of Carbo- and Heterocycles. *Synthesis (Stuttg).* **2008**, 1–25.

(117) Jiang, B.; Rajale, T.; Wever, W.; Tu, S.-J.; Li, G. Multicomponent Reactions for the Synthesis of Heterocycles. *Chem. - An Asian J.* **2010**, *5*, 2318–2335.

(118) Ruijter, E.; Scheffelaar, R.; Orru, R. V. A. Multicomponent Reaction Design in the Quest for Molecular Complexity and Diversity Angewandte. *Angew. Chemie Int. Ed.* **2011**, *50*, 6234–6246.

(119) D'Souza, D. M.; Muller, J. J. T. Multi-Component Syntheses of Heterocycles by Transition-Metal Catalysis. *Chem. Soc. Rev.* **2007**, *36*, 1095–1108.

(120) Posner, G. H. Multicomponent One-Pot Annulations Forming 3 to 6 Bonds. *Chem. Rev.* **1986**, *86*, 831–844.

(121) Ramón, D. J.; Yus, M. Asymmetric Multicomponent Reactions (AMCRs): The New Frontier. *Angew. Chemie Int. Ed.* **2005**, *44*, 1602–1634.

(122) Touré, B. B.; Hall, D. G. Natural Product Synthesis Using Multicomponent Reaction Strategies. *Chem. Rev.* **2009**, *109*, 4439–4486.

(123) Candeias, N. R.; Montalbano, F.; Cal, P. M. S. D.; Gois, P. M. P. Boronic Acids and Esters in the Petasis-Borono Mannich Multicomponent Reaction. *Chem. Rev.* **2010**, *110*, 6169–6193.

(124) Dömling, A.; Wang, W.; Wang, K. Chemistry and Biology Of Multicomponent Reactions. *Chem. Rev.* **2012**, *112*, 3083–3135.

(125) Shiri, M. Indoles in Multicomponent Processes (MCPs). *Chem. Rev.* **2012**, *112*, 3508–3549.

(126) Estevez, V.; Villacampa, M.; Menedez, C. J. Recent Advances in the Synthesis of Pyrroles by Multicomponent Reactions. *Chem. Soc. Rev.* **2014**, *43*, 4633–4657.

(127) Allais, C.; Grassot, J.-M.; Rodriguez, J.; Constantieux, T. Metal-Free Multicomponent Syntheses of Pyridines. *Chem. Rev.* **2014**, *114*, 10829–10868.

(128) Rotstein, B. H.; Zaretsky, S.; Rai, V.; Yudin, A. K. Small Heterocycles in Multicomponent Reactions. *Chem. Rev.* **2014**, *114*, 8323–8359.

(129) Levi, L.; Müller, T. J. J. Multicomponent Syntheses of Functional Chromophores. *Chem. Soc. Rev.* **2016**, *45*, 2825–2846.

(130) Martin, S. F.; Rueger, H.; Williamson, S. A.; Grzejszczak, S. General Strategies for the Synthesis of Indole Alkaloids. Total Synthesis of (±)-Reserpine and (±)-.alpha.-Yohimbine. *J. Am. Chem. Soc.* **1987**, *109*, 6124–6134.

(131) Martin, S. F.; Benage, B.; Hunter, J. E. A Concise Strategy for the Syntheses of Indole Alkaloids of the Heteroyohimboid and Corynantheioid Families. Total Syntheses of (±)-Tetrahydroalstonine, (±)-Cathenamine and (±)-Geissoschizine. *J. Am. Chem. Soc.* **1988**, *110*, 5925–5927.

(132) Martin, S. F.; Benage, B.; Williamson, S. A.; Brown, S. P. Applications of the Intramolecular Diels-Alder Reactions of Heterodienes to the Syntheses of Indole Alkaloids. *Tetrahedron* **1986**, *42*, 2903–2910.

(133) Trost, B. M.; Balkovec, J. M.; Mao, M. K. T. A Biomimetic Approach to Plumericin. *J. Am. Chem. Soc.* **1983**, *105*, 6755–6757.

(134) Trost, B. M.; Balkovec, J. M.; Mao, M. K. T. A Total Synthesis of Plumericin, Allamcin and Allamandin. Part 2. A Biomimetic Strategy. *J. Am. Chem. Soc.* **1986**, *108*, 4974–4983.

(135) Granger, B. A.; Wang, Z.; Kaneda, K.; Fang, Z.; Martin, S. F. Multicomponent Assembly Processes for the Synthesis of Diverse *Yohimbine* and *Corynanthe* Alkaloid Analogues. *ACS Comb. Sci.* **2013**, *15*, 379–386.

(136) James D. Sunderhaus; Chris Dockendorff, A.; Martin, S. F. Applications of Multicomponent Reactions for the Synthesis of Diverse Heterocyclic Scaffolds. *Org. Lett.* **2007**, *9*, 4223–4226.

(137) Simila, S. T. M.; Martin, S. F. Applications of the Ugi Reaction with Ketones. *Tetrahedron Lett.* **2008**, *49*, 4501–4504.

(138) Sunderhaus, J. D.; Dockendorff, C.; Martin, S. F. Synthesis of Diverse Heterocyclic Scaffolds via Tandem Additions to Imine Derivatives and Ring-Forming Reactions. *Tetrahedron* **2009**, *65*, 6454–6469.

(139) Cheng, B.; Sunderhaus, J. D.; Martin, S. F. Concise Total Synthesis of (±)-Pseudotabersonine via Double Ring-Closing Metathesis Strategy. *Org. Lett.* **2010**, *12*, 3622–3625.

(140) Granger, B. A.; Kaneda, K.; Martin, S. F. Multicomponent Assembly Strategies for the Synthesis of Diverse Tetrahydroisoquinoline Scaffolds. *Org. Lett.* **2011**, *13*, 4542–4545.

(141) Hardy, S.; Martin, S. F. Multicomponent Assembly and Diversification of Novel Heterocyclic Scaffolds Derived from 2-Arylpiperidines. *Org. Lett.* **2011**, *13*, 3102–3105.

(142) Sahn, J. J.; Martin, S. F. Facile Syntheses of Substituted, Conformationally-Constrained Benzoxazocines and Benzazocines via Sequential Multicomponent Assembly and Cyclization. *Tetrahedron Lett.* **2011**, *52*, 6855–6858.

(143) Sahn, J. J.; Su, J. Y.; Martin, S. F. Facile and Unified Approach to Skeletally Diverse, Privileged Scaffolds. *Org. Lett.* **2011**, *13*, 2590–2593.

(144) Granger, B. A.; Kaneda, K.; Martin, S. F. Libraries of 2,3,4,6,7,11 β-Hexahydro-1 *H*-pyrido[2,1-*a*]Isoquinolin-2-Amine Derivatives via a Multicomponent Assembly Process/1,3-Dipolar Cycloaddition Strategy. *ACS Comb. Sci.* **2012**, *14*, 75–79.

(145) Sahn, J. J.; Martin, S. F. Expedient Synthesis of Norbenzomorphan Library via Multicomponent Assembly Process Coupled with Ring-Closing Reactions. *ACS Comb. Sci.* **2012**, *14*, 496–502.

(146) Martin, S. F. Evolution of the Vinylogous Mannich Reaction as a Key Construction for Alkaloid Synthesis. *Acc. Chem. Res.* **2002**, *35*, 895–904.

(147) Alexander, D.; Martin, S. F. Synthesis of Oxygen- and Nitrogen-Containing Heterocycles by Ring-Closing Metathesis. *Chem. Rev.* **2004**, *104*, 2199–2238.

(148) Sunderhaus, J. D.; Martin, S. F. Applications of Multicomponent Reactions to the Synthesis of Diverse Heterocyclic Scaffolds. *Chem. - A Eur. J.* **2009**, *15*, 1300–1308.

(149) Wang, Z.; Kaneda, K.; Fang, Z.; Martin, S. F. Diversity Oriented Synthesis: Concise Entry to Novel Derivatives of Yohimbine and Corynanthe Alkaloids. *Tetrahedron Lett.* **2012**, *53*, 477–479.

(150) Granger, B. A.; Wang, Z.; Kaneda, K.; Fang, Z.; Martin, S. F. Multicomponent Assembly Processes for the Synthesis of Diverse Yohimbine and Corynanthe Alkaloid Analogues. *ACS Comb. Sci.* **2013**, *15*, 379–386.

(151) Wang, Z.; Kaneda, K.; Fang, Z.; Martin, S. F. Diversity Oriented Synthesis: Concise Entry to Novel Derivatives of Yohimbine and Corynanthe Alkaloids. *Tetrahedron Lett.* **2012**, *53*, 477–479.

(152) Yu, H.; Li, J.; Wu, D.; Qiu, Z.; Zhang, Y. Chemistry and Biological Applications of Photo-Labile Organic Molecules. *Chem. Soc. Rev.* **2010**, *39*, 464–473.

(153) Bochet, C. G. Photolabile Protecting Groups and Linkers. *J. Chem. Soc. Perkin Trans. 1* **2001**, 125–142.

(154) Deiters, A. Light Activation as a Method of Regulating and Studying Gene Expression. *Curr. Opin. Chem. Biol.* **2009**, *13*, 678–686.

(155) Shao, Q.; Xing, B. Photoactive Molecules for Applications in Molecular Imaging and Cell Biology. *Chem. Soc. Rev.* **2010**, *39*, 2835.

(156) Mayer, G.; Heckel, A. Biologically Active Molecules with a "Light Switch." *Angew. Chemie Int. Ed.* **2006**, *45*, 4900–4921.

(157) Young, D. D.; Deiters, A. Photochemical Control of Biological Processes. *Org. Biomol. Chem.* **2007**, *5*, 999–1005.

(158) Casey, J. P.; Blidner, R. A.; Monroe, W. T. Caged siRNAs for Spatiotemporal Control of Gene Silencing. *Mol. Pharm.* **2009**, *6*, 669–685.

(159) Deiters, A. Principles and Applications of the Photochemical Control of Cellular Processes. *ChemBioChem* **2009**, *11*, 47–53.

(160) Brieke, C.; Rohrbach, F.; Gottschalk, A.; Mayer, G.; Heckel, A. Light-Controlled Tools. *Angew. Chemie - Int. Ed.* **2012**, *51*, 8446–8476.

(161) Pelliccioli, A. P.; Wirz, J. Photoremovable Protecting Groups: Reaction Mechanisms and Applications. *Photochem. Photobiol. Sci.* **2002**, *1*, 441–458.

(162) Klán, P.; Šolomek, T.; Bochet, C. G.; Blanc, A.; Givens, R.; Rubina, M.; Popik, V.; Kostikov, A.; Wirz, J. Photoremovable Protecting Groups in Chemistry and Biology: Reaction Mechanisms and Efficacy. *Chem. Rev.* **2013**, *113*, 119–191.

(163) Barltrop, J. A.; Schofield, P. Photosensitive Protecting Groups. *Tetrahedron Lett.* **1962**, *3*, 697–699.

(164) Barton, D. H. R.; Chow, Y. L.; Cox, A.; Kirby, G. W. 654. Photochemical Transformatiom. Part XIX. Some Photosensitive Protecting Groups. *J. Chem. Soc.* **1965**, 3571–3578.

(165) Barton, D. H. R.; Chow, Y. L.; Cox, A.; Kirby, G. W. Photosensitive Protection of Functional Groups. *Tetrahedron Lett.* **1962**, *3*, 1055–1057.

(166) Patchornik, A.; Amit, B.; Woodward, R. B. Photosensitive Protecting Groups. *J. Am. Chem. Soc.* **1970**, *92*, 6333–6335.

(167) Bochet, C. G. Photolabile Protecting Groups and Linkers. *J. Chem. Soc. Perkin Trans. 1* **2002**, 125–142.

(168) Papageorgiou, G.; Corrie, J. E. T. Synthesis and Properties of Carbamoyl Derivatives of Photolabile Benzoins. *Tetrahedron* **1997**, *53*, 3917–3932.

(169) Barltrop, J. A.; Plant, P. J.; Schofield, P. Photosensitive Protective Groups. *Chem. Commun.* **1966**, 822–823.

(170) Wang, P. Photolabile Protecting Groups: Structure and Reactivity. *Asian J. Org. Chem.* **2013**, *2*, 452–464.

(171) Zuman, P.; Shah, B. Addition, Reduction, and Oxidation Reactions of Nitrosobenzene. *Chem. Rev* **1994**, *94*, 1621–1641.

(172) Barth, A.; Corrie, J. E. T.; Gradwell, M. J.; Maeda, Y.; Ma, W.; Meier, T.; Trentham, D. R. Time-Resolved Infrared Spectroscopy of Intermediates and Products from Photolysis of 1-(2-Nitrophenyl)ethyl Phosphates: Reaction of the 2-Nitrosoacetophenone Byproduct with Thiols. *J. Am. Chem. Soc.* **1997**, *119*, 4149–4159.

(173) Zou, K.; Cheley, S.; Givens, R. S.; Bayley, H. Catalytic Subunit of Protein Kinase A Caged at the Activating Phosphothreonine. *J. Am. Chem. Soc.* **2002**, *124*, 8220–8229.

(174) Zou, K.; Miller, W. T.; Givens, R. S.; Bayley, H. Caged Thiophosphotyrosine Peptides. *Angew. Chemie Int. Ed.* **2001**, *40*, 3049–3051.

(175) Cameron, J. F.; Frechet, J. M. J. Photogeneration of Organic Bases from O-Nitrobenzyl-Derived Carbamates. *J. Am. Chem. Soc.* **1991**, *113*, 4303–4313.

(176) Neenan, T. X.; Houlihan, F. M.; Reichmanis, E.; Kometani, J. M.; Bachman, B. J.; Thompson, L. F. Photo- and Thermochemistry of Select 2,6-Dinitrobenzyl Esters in Polymer Matrixes: Studies Pertaining to Chemical Amplification and Imaging. *Macromolecules* **1990**, *23*, 145–150.

(177) Hasan, A.; Stengele, K.-P.; Giegrich, H.; Cornwell, P.; Isham, K. R.; Sachleben, R. A.; Pfleiderer, W.; Foote, R. S. Photolabile Protecting Groups for Nucleosides: Synthesis and Photodeprotection Rates. *Tetrahedron* **1997**, *53*, 4247–4264.

(178) Baldwin, J. E.; McConnaughie, A. W.; Moloney, M. G.; Pratt, A. J.; Bo Shin, S. New Photolabile Phosphate Protecting Group. *Tetrahedron* **1990**, *46*, 6879–6884.

(179) Bley, F.; Schaper, K.; Görner, H. Photoprocesses of Molecules with 2-Nitrobenzyl Protecting Groups and Caged Organic Acids. *Photochem. Photobiol.* **2008**, *84*, 162–171.

(180) Bochet, C. G. Wavelength-Selective Cleavage of Photolabile Protecting Groups. *Tetrahedron Letters*. 2000, pp. 6341–6346.

(181) Lusic, H.; Uprety, R.; Deiters, A. Improved Synthesis of the Two-Photon Caging Group 3-Nitro-2- Ethyldibenzofuran and Its Application to a Caged Thymidine Phosphoramidite. *Org. Lett.* **2010**, *12*, 916–919.

(182) Mahmoodi, M. M.; Abate-Pella, D.; Pundsack, T. J.; Palsuledesai, C. C.; Goff, P. C.; Blank, D. A.; Distefano, M. D. Nitrodibenzofuran: A One- and Two-Photon Sensitive Protecting Group That Is Superior to Brominated Hydroxycoumarin for Thiol Caging in Peptides. *J. Am. Chem. Soc.* **2016**, *138*, 5848–5859.

(183) Momotake, A.; Lindegger, N.; Niggli, E.; Barsotti, R. J.; Ellis-Davies, G. C. R. The Nitrodibenzofuran Chromophore: A New Caging Group for Ultra-Efficient Photolysis in Living Cells. *Nat. Methods* **2006**, *3*, 35–40.

(184) Schäfer, F.; Joshi, K. B.; Fichte, M. A. H.; Mack, T.; Wachtveitl, J.; Heckel, A. Wavelength-Selective Uncaging of dA and dC Residues. *Org. Lett.* **2011**, *13*, 1450–1453.

(185) Pirrung, M. C.; Wang, L.; Montague-Smith, M. P. 3‘-Nitrophenylpropyloxycarbonyl (NPPOC) Protecting Groups for High-Fidelity Automated 5‘ → 3‘ Photochemical DNA Synthesis. *Org. Lett.* **2001**, *3*, 1105–1108.

(186) Berroy, P.; Viriot, M. L.; Carré, M. C. Photolabile Group for 5′-OH Protection of Nucleosides: Synthesis and Photodeprotection Rate. *Sensors Actuators B Chem.* **2001**, *74*, 186–189.

(187) Donato, L.; Mourot, A.; Davenport, C. M.; Herbivo, C.; Warther, D.; Léonard, J.; Bolze, F.; Nicoud, J. F.; Kramer, R. H.; Goeldner, M.; Specht, A. Water-Soluble, Donor-Acceptor Biphenyl Derivatives in the 2-(O-Nitrophenyl)propyl Series: Highly Efficient Two-Photon Uncaging of the Neurotransmitter γ-Aminobutyric Acid at λ=800 Nm. *Angew. Chemie - Int. Ed.* **2012**, *51*, 1840–1843.

(188) Onica, V.; Miguel, S.; Bochet, C. G.; Anzazu, A.; Campo, D. Wavelength-Selective Caged Surfaces: How Many Functional Levels Are Possible? *J. Am. Chem. Soc* **2011**, *133*, 5380–5388.

(189) Pirrung, M. C.; Dore, T. M.; Zhu, Y.; Rana, V. S. Sensitized Two-Photon Photochemical Deprotection. *Chem. Commun.* **2010**, *46*, 5313.

(190) Wö, D.; Laimgruber, S.; Galetskaya, M.; Smirnova, J.; Pfleiderer, W.; Rn Heinz, B.; Gilch, P.; Steiner, U. E. On the Mechanism of Intramolecular Sensitization of Photocleavage of the 2-(2-Nitrophenyl)propoxycarbonyl (NPPOC) Protecting Group. *J. Am. Chem. Soc.* **2007**, *129*, 12148–12158.

(191) Bhushan, K. R.; Delisi, C.; Laursen, R. A. Synthesis of Photolabile 2-(2-Nitrophenyl)propyloxycarbonyl Protected Amino Acids. *Tetrahedron Lett.* **2003**, *44*, 8585–8588.

(192) Sheehan, J. C.; Wilson, R. M. Photolysis of Desyl Compounds. A New Photolytic Cyclization. *J. Am. Chem. Soc.* **1964**, *86*, 5277–5281.

(193) Sheehan, J. C.; Wilson, R. M.; Oxford, A. W. The Photolysis of Methoxy-Substituted Benzoin Esters. A Photosensitive Protecting Group for Carboxylic Acids. *J. Am. Chem. Soc.* **1971**, *93*, 7222–7228.

(194) Pirrung, M. C.; Huang, C. Y. Photochemical Deprotection of 3',5'-dimethoxybenzoin (DMB) Carbamates Derived from Secondary Amines. *Tetrahedron Lett.* **1995**, *36*, 5883–5884.

(195) Corrie, J. E. T.; Trentham, D. R. Synthetic, Mechanistic and Photochemical Studies of Phosphate Esters of Substituted Benzoins. *J. Chem. Soc. Perkin Trans. 1* **1992**, 2409.

(196) Shi, Y.; Corrie, J. E. T.; Wan, P. Mechanism of 3‘,5‘-Dimethoxybenzoin Ester Photochemistry: Heterolytic Cleavage Intramolecularly Assisted by the Dimethoxybenzene Ring Is the Primary Photochemical Step. *J. Org. Chem.* **1997**, *62*, 8278–8279.

(197) Pirrung, M. C.; Ye, T.; Zhou, Z.; Simon, J. D. Mechanistic Studies on the Photochemical Deprotection of 3′,5′-Dimethoxybenzoin Esters. *Photochem. Photobiol.* **2006**, *82*, 1258–1264.

(198) Boudebous, H.; Kosmrlj, B.; Sket, B.; Wirz, J. Primary Photoreactions of the 3‘,5‘-Dimethoxybenzoin Cage and Determination of the Release Rate in Polar Media. *J. Phys. Chem. A* **2007**, *111*, 2811–2813.

(199) Wing Sum Chan; Chensheng Ma; Wai Ming Kwok; Peng Zuo, A.; Phillips, D. L. Resonance Raman Spectroscopic and Density Functional Theory Study of Benzoin Diethyl Phosphate. *J. Phys. Chem. A* **2004**, *108*, 4047–4058.

(200) Givens, R. S.; Rubina, M.; Wirz, J. Applications of P-Hydroxyphenacyl (pHP) and Coumarin-4-Ylmethyl Photoremovable Protecting Groups. *Photochem. Photobiol. Sci.* **2012**, *11*, 472–488.

(201) Givens, R. S.; Lee, J.-I. The P-Hydroxyphenacyl Photoremovable Protecting Group. *J. Photoscience* **2003**, *10*, 1–12.

(202) Pelliccioli, A. P.; Wirz, J.; Wirz, J. J. Photoremovable Protecting Groups : Reaction Mechanisms and Applications. *Photochem. Photobiol. Sci.* **2002**, *1*, 441–458.

(203) Park, C.; Givens, R. S. New Photoactivated Protecting Groups. 6. P-Hydroxyphenacyl : A Phototrigger for Chemical and Biochemical Probes. *J. Am. Chem. Soc.* **1997**, *119*, 2453–2463.

(204) Givens, R. S.; Park, C.-H. P-Hydroxyphenacyl ATP: A New Phototrigger. *Tetrahedron Lett.* **1996**, *37*, 6259–6262.

(205) Zhang, K.; Corrie, J. E. T.; Munasinghe, R. N.; Wan, P. Mechanism of Photosolvolytic Rearrangement of P-Hydroxyphenacyl Esters: Evidence for Excited-State Intramolecular Proton Transfer as the Primary Photochemical Step. *J. Am. Chem. Soc.* **1999**, *121*, 5625–5632.

(206) Conrad, P. G.; Givens, R. S.; Hellrung, B.; Rajesh, C. S.; Ramseier, M.; Wirz, J. P -Hydroxyphenacyl Phototriggers : The Reactive Excited State of Phosphate Photorelease. *J. Am. Chem. Soc.* **2000**, *122*, 9346–9347.

(207) Sebej, P.; Lim, B. H.; Park, B. S.; Givens, R. S.; Klan, P. The Power of Solvent in Altering the Course of Photorearrangements. *Org. Lett.* **2011**, *13*, 644–647.

(208) Conrad, P. G.; Givens, R. S.; Weber, F. W.; Kandler, K. New Phototriggers:1 Extending the P-Hydroxyphenacyl $\pi -\pi^*$ Absorption Range. *Org. Lett.* **2000**, *2*, 1545–1547.

(209) Lukeman, M.; Veale, D.; Wan, P.; Ranjit, M. V. N.; Corrie, J. E. T. Photogeneration of 1,5-Naphthoquinone Methides via Excited-State (Formal) Intramolecular Proton Transfer (ESIPT) and Photodehydration of 1- Naphthol Derivatives in Aqueous Solution 1. *Can. J. Chem.* **2004**, *82*, 240–253.

(210) Small, R. D.; Scaiano, J. C. Role of Biradical Intermediates in the Photochemistry of O-Methylacetophenone. *J. Am. Chem. Soc.* **1977**, *99*, 7713–7714.

(211) Das, P. K.; Encinas, M. V.; Small, R. D.; Scaiano, J. C. Photoenolization of O-Alkyl-Substituted Carbonyl Compounds. Use of Electron Transfer Processes to Characterize Transient Intermediates. *J. Am. Chem. Soc.* **1979**, *101*, 6965–6970.

(212) Haag, R.; Wirz, J.; Wagner, P. J. The Photoenolization of 2-Methylacetophenone and Related Compounds. *Helv. Chim. Acta* **1977**, *60*, 2595–2607.

(213) Bong, S. P.; Hye, M. L. New Photosensitive Polymer Containing O-Methylphenacyl Photocage. *Bull. Korean Chem. Soc.* **2008**, *29*, 2054–2056.

(214) Du, L.-H.; Zhang, S.-J.; Wang, Y.-G. *Phenacyl Esters as a New Photocleavable Linker in Liquid-Phase Chemistry*; 2005; Vol. 46.

(215) Pospíšil, T.; Veetil, A. T.; Antony, L. A. P.; Klán, P. Photochemical Synthesis of Substituted Indan-1-Ones Related to Donepezil. *Photochem. Photobiol. Sci.* **2008**, *7*, 625–632.

(216) Andreani, A.; Cavalli, A.; Granaiola, M.; Guardigli, M.; Leoni, A.; Locatelli, A.; Morigi, R.; Rambaldi, M.; Recanatini, M.; Roda, A. Synthesis and Screening for Antiacetylcholinesterase Activity of (1-Benzyl-4-Oxopiperidin-3-Ylidene)methylindoles and -Pyrroles Related to Donepezil. *J. Med. Chem.* **2001**, *44*, 4011–4014.

(217) Wessig, P.; Glombitza, C.; Muller, G.; Teubner, J. Photochemical Preparation of Highly Functionalized 1-Indanones. *J. Org. Chem.* **2004**, *69*, 7582–7591.

(218) Wessig, P.; Teubner, J. Total Synthesis of Pterosines B and C via a Photochemical Key Step. *Synlett* **2006**, *2006*, 1543–1546.

(219) Tseng, S.; Ullman, E. F. Elimination Reactions Induced by Photoenolization of O-Alkylbenzophenones. *J. Am. Chem. Soc.* **1975**, *98*, 541–544.

(220) Atemnkeng, W. N.; Louisiana Ii, L. D.; Yong, P. K.; Vottero, B.; Banerjee, A. -[2-(2-Hydroxyalkyl)phenyl]ethanone: A New Photoremovable Protecting Group for Carboxylic Acids. *Org. Lett.* **2003**, *5*, 4469–4471.

(221) Sobczak, M.; Wagner, P. J. Light-Induced Decarboxylation of (O-Acylphenyl)acetic Acids. *Org. Lett.* **2002**, *4*, 379–382.

(222) Muthukrishnan, S.; Pace, T. C. S.; Li, Q.; Seok, B.; De Jong, G.; Bohne, C.; Gudmundsdottir, A. D. Comparison of Photoenolization and Alcohol Release from Alkyl-Substituted Benzoyl Benzoic Esters. *Can. J. Chem.* **2011**, *89*, 331–338.

(223) Konosonoks, A.; Wright, P. J.; Tsao, M.-L.; Pika, J.; Novak, K.; Mandel, S. M.; Krause Bauer, J. A.; Bohne, C.; Gudmundsdóttir, A. D. Photoenolization of 2-(2-Methyl Benzoyl) Benzoic Acid, Methyl Ester: Effect of E Photoenol Lifetime on the Photochemistry. *J. Org. Chem.* **2005**, *70*, 2763–2770.

(224) Muthukrishnan, S.; Sankaranarayanan, J.; Pace, T. C. S.; Konosonoks, A.; DeMichiei, M. E.; Meese, M. J.; Bohne, C.; Gudmundsdottir, A. D. Effect of Alkyl Substituents on Photorelease from Butyrophenone Derivatives. *J. Org. Chem.* **2010**, *75*, 1393–1401.

(225) Sankaranarayanan, J.; Muthukrishnan, S.; Gudmundsdottir, A. D. Photoremovable Protecting Groups Based on Photoenolization. **2009**.

(226) Sandel, V. R.; Zimmerman, H. E. Mechanistic Organic Photochemistry. II. Solvolytic Photochemical Reactions. *J. Am. Chem. Soc.* **1962**, *85*, 915–922.

(227) Zimmerman, H. E.; Alabugin, I. V. Excited State Energy Distribution and Redistribution and Chemical Reactivity; Mechanistic and Exploratory Organic Photochemistry. *J. Am. Chem. Soc.* **2000**, *122*, 952–953.

(228) Zimmerman, H. E.; Schuster, D. I. The Photochemical Rearrangement of 4,4-Diphenylcyclohexadieneone. Paper I on a General Theory of Photochemical Reactions. *J. Am. Chem. Soc.* **1961**, *83*, 208–210.

(229) Zimmerman, H. E. Meta - Ortho Effect in Organic Photochemistry : Mechanistic and Exploratory Organic. *J. Phys. Chem. A* **1998**, *102*, 5616–5621.

(230) Somasekhara, S.; Zimmerman, H. E. Mechanistic Organic Photochemistry. III. Excited State Solvolyses. *J. Am. Chem. Soc.* **1962**, *85*, 922–927.

(231) Zimmerman, H. E.; Schuster, D. I. Photochemistry of 4,4-Diphenylcyclohexadieneone. *J. Am. Chem. Soc.* **1962**, *84*, 4527–4540.

(232) Misetic, A.; Boyd, M. K. The Pixyl (Px) Group: A Novel Photocleavable Protecting Group for Primary Alcohols. *Tetrahedron Lett.* **1998**, *39*, 1653–1656.

(233) Coleman, M. P.; Boyd, M. K. The S-Pixyl Group: An Efficient Photocleavable Protecting Group for the 5′-Hydroxy Function of Deoxyribonucleosides. *Tetrahedron Lett*. **1999**, *40*, 7911–7915.

(234) Ren, M.-G.; Bi, N.-M.; Mao, M.; Song, Q.-H. 2-(1′-Hydroxyethyl)-Anthraquinone as a Photolabile Protecting Group for Carboxylic Acids. *J. Photochem. Photobiol. A Chem*. **2009**, *204*, 13–18.

(235) Furuta, T.; Torigai, H.; Sugimoto, M.; Iwamura, M. Photochemical Properties of New Photolabile cAMP Derivatives in a Physiological Saline Solution. *J. Org. Chem*. **1995**, *60*, 3953–3956.

(236) Zhou, L.; Yang, H.; Wang, P. Development of Trityl-Based Photolabile Hydroxyl Protecting Groups. *J. Org. Chem*. **2011**, *76*, 5873–5881.

(237) Wang, P.; Zhou, L.; Zhang, X.; Liang, X. Facilitated Photochemical Cleavage of Benzylic C–O Bond. Application to Photolabile Hydroxyl-Protecting Group Design. *Chem. Commun*. **2010**, *46*, 1514–1516.

(238) Yang, H.; Zhang, X.; Zhou, L.; Wang, P. Development of a Photolabile Carbonyl-Protecting Group Toolbox. *J. Org. Chem*. **2011**, *76*, 2040–2048.

(239) Wang, P.; Huayou, H.; Wang, Y. Novel Photolabile Protecting Group for Carbonyl Compounds. *Org. Lett*. **2007**, *9*, 1533–1535.

(240) Hagen, V.; Bendig, J.; Frings, S.; Eckardt, T.; Helm, S.; Reuter, D.; Kaupp, U. B. Highly Efficient and Ultrafast Phototriggers for cAMP and cGMP by Using Long-Wavelength UV/Vis-Action. *Angew. Chem. Int. Ed. Engl*. **2001**, *40*, 1045–1048.

(241) Cameron, J. F.; Frechet, J. M. J. Base Catalysis in Imagine Materials. 1. Design and Synthesis of Novel Light-Sensitive Urethanes as Photoprecursors of Amines. *J. Org. Chem*. **1990**, *55*, 5919–5922.

(242) Givens, R. S.; Matuszewski, B. Photochemistry of Phosphate Esters: An Efficient Method for the Generation of Electrophiles. *J. Am. Chem. Soc*. **1984**, *106*, 6860–6861.

(243) Suzuki, A. A.; Watanabe, T.; Kawamoto, M.; Nishiyama, K.; Yamashita, H.; Ishii, M.; Iwamura, M.; Furuta, T. Coumarin-4-Ylmethoxycarbonyls as Phototriggers for Alcohols and Phenols. *Org. Lett*. **2003**, *5*, 4867–4870.

(244) Cürten, B.; Kullmann, P. H. M.; Bier, M. E.; Kandler, K.; Schmidt, B. F. Synthesis, Photophysical, Photochemical and Biological Properties of Caged GABA, 4-[[(2H-1-Benzopyran-2-One-7-Amino-4-Methoxy) Carbonyl] Amino] Butanoic Acid. *Photochem. Photobiol.* **2007**, *81*, 641–648.

(245) Kotzur, N.; Briand, B.; Beyermann, M.; Hagen, V. Wavelength-Selective Photoactivatable Protecting Groups for Thiols. *J. Am. Chem. Soc.* **2009**, *131*, 16927–16931.

(246) Fonseca, A. S. C.; Gonçalves, M. S. T.; Costa, S. P. G. Photocleavage Studies of Fluorescent Amino Acid Conjugates Bearing Different Types of Linkages. *Tetrahedron* **2007**, *63*, 1353–1359.

(247) Hagen, V.; Kilic, F.; Schaal, J.; Dekowski, B.; Schmidt, R.; Kotzur, N. [8-[Bis(carboxymethyl)aminomethyl]-6-Bromo-7-Hydroxycoumarin-4-Yl]methyl Moieties as Photoremovable Protecting Groups for Compounds with COOH, NH_2, OH, and C=O Functions. *J. Org. Chem.* **2010**, *75*, 2790–2797.

(248) Shembekar, V. R.; Chen, Y.; Carpenter, B. K.; Hess, G. P. Coumarin-Caged Glycine That Can Be Photolyzed within 3ms by Visible Light. *Biochemistry* **2007**, *46*, 5479–5484.

(249) Shembekar, V. R.; Chen, Y.; Carpenter, B. K.; Hess, G. P. A Protecting Group for Carboxylic Acids That Can Be Photolyzed by Visible Light. *Biochemistry* **2005**, *44*, 7107–7114.

(250) Olson, J. P.; Kwon, H. B.; Takasaki, K. T.; Chiu, C. Q.; Higley, M. J.; Sabatini, B. L.; Ellis-Davies, G. C. R. Optically Selective Two-Photon Uncaging of Glutamate at 900 Nm. *J. Am. Chem. Soc.* **2013**, *135*, 5954–5957.

(251) Olson, J. P.; Banghart, M. R.; Sabatini, B. L.; Ellis-Davies, G. C. R. Spectral Evolution of a Photochemical Protecting Group for Orthogonal Two-Color Uncaging with Visible Light. *J. Am. Chem. Soc.* **2013**, *135*, 15948–15954.

(252) Fournier, L.; Gauron, C.; Xu, L.; Aujard, I.; Le Saux, T.; Gagey-Eilstein, N.; Maurin, S.; Dubruille, S.; Baudin, J. B.; Bensimon, D.; Volovitch, M.; Vriz, S.; Jullien, L. A Blue-Absorbing Photolabile Protecting Group for in Vivo Chromatically Orthogonal Photoactivation. *ACS Chem. Biol.* **2013**, *8*, 1528–1536.

(253) Schmidt, R.; Geissler, D.; Hagen, V.; Jürgen, B. Mechanism of Photocleavage of (Coumarin-4-Yl)methyl Esters. *J. Phys. Chem. A* **2007**, *111*, 5768–5774.

(254) Pocker, Y.; Davison, B. L.; Deits, T. L. Decarboxylation of Monosubstituted Derivatives of Carbonic Acid. Comparative Studies of Water- and Acid-Catalyzed Decarboxylation of Sodium Alkyl Carbonates in Water and Water-d2. *J. Am. Chem. Soc.* **1978**, *100*, 3564–3567.

(255) Rossi, F. M.; Margulis, M.; Tang, C.-M.; Kao, J. P. Y. N-Nmoc-L-Glutamate, a New Caged Glutamate with High Chemical Stability and Low Pre-Photolysis Activity. *J. Biol. Chem.* **1997**, *272*, 32933–32939.

(256) Rossi, F. M.; Kao, J. P. Y. Nmoc-DBHQ, a New Caged Molecule for Modulating Sarcoplasmic/Endoplasmic Reticulum Ca 2+ ATPase Activity with Light Flashes. *J. Biol. Chem.* **1997**, *272*, 3266–3271.

(257) Schade, B.; Hagen, V.; Schmidt, R.; Herbrich, R.; Krause, E.; Eckardt, T.; Bendig, J. Deactivation Behavior and Excited-State Properties of (Coumarin-4-Yl)methyl Derivatives. 1. Photocleavage of (7-Methoxycoumarin-4-Yl)methyl-Caged Acids with Fluorescence Enhancement. *J. Org. Chem.* **1999**, *64*, 9109–9117.

(258) Noguchi, M.; Skwarczynski, M.; Prakash, H.; Hirota, S.; Kimura, T.; Hayashi, Y.; Kiso, Y. Development of Novel Water-Soluble Photocleavable Protective Group and Its Application for Design of Photoresponsive Paclitaxel Prodrugs. *Bioorganic Med. Chem.* **2008**, *16*, 5389–5397.

(259) Engels, J.; Schlaeger, E.-J. Synthesis, Structure, and Reactivity of Adenosine Cyclic 3',5'-Phosphate Benzyl Triesters. *J. Med. Chem.* **1977**, *20*, 907–911.

(260) Kaplan, J. H.; Forbush, B.; Hoffman, J. F. Rapid Photolytic Release of Adenosine 5'-Triphosphate from a Protected Analogue: Utilization by the Na:K Pump of Human Red Blood Cell Ghosts. *Biochemistry* **1978**, *17*.

(261) Young, D. D.; Deiters, A. Photochemical Activation of Protein Expression in Bacterial Cells. *Angew. Chemie - Int. Ed.* **2007**, *46*, 4290–4292.

(262) Weber, W.; Fussenegger, M. Artificial Mammalian Gene Regulation Networks—Novel Approaches for Gene Therapy and Bioengineering. *J. Biotechnol.* **2002**, *98*, 161–187.

(263) Buskirk, A. R.; Liu, D. R. Review Creating Small-Molecule-Dependent Switches to Modulate Biological Functions Pressor-DNA Complex and Permitting Transcription and Translation of lacZYA. *Chem. Biol.* **2005**, *12*, 151–161.

(264) Lee, H.-M.; Larson, D. R.; Lawrence, D. S. Illuminating the Chemistry of Life: Design, Synthesis, and Applications of "Caged" and Related Photoresponsive Compounds. *ACS Chem. Biol.* **2009**, *4*, 409–427.

(265) Gardner, L.; Zou, Y.; Mara, A.; Cropp, T. A.; Deiters, A. Photochemical Control of Bacterial Signal Processing Using a Light-Activated Erythromycin. *Mol. Biosyst.* **2011**, *7*, 2554.

(266) Weber, W.; Fux, C.; Daoud-El Baba, M.; Keller, B.; Weber, C. C.; Kramer, B. P.; Heinzen, C.; Aubel, D.; Bailey, J. E.; Fussenegger, M. Macrolide-Based Transgene Control in Mammalian Cells and Mice. *Nat. Biotechnol.* **2002**, *20*, 901–907.

(267) Cambridge, S. B.; Geissler, D.; Calegari, F.; Anastassiadis, K.; Hasan, M. T.; Stewart, A. F.; Huttner, W. B.; Hagen, V.; Bonhoeffer, T. Doxycycline-Dependent Photoactivated Gene Expression in Eukaryotic Systems. *Nat. Methods* **2009**, *6*, 527–531.

(268) Gossen, M.; Freundlieb, S.; Bender, G.; Müller, G.; Hillen, W.; Bujard, H. Transcriptional Activation by Tetracyclines in Mammalian Cells. *Science*. **1995**, *268*, 1766–1769.

(269) Yao, F.; Svensjo, T.; Winkler, T.; Lu, M.; Eriksson, C.; Eriksson, E. Tetracycline Repressor, tetR, rather than the tetR-MammaUan Cell Transcription Factor Fusion Derivatives, Regulates Inducible Gene Expression in Mammalian Cells. *Hum. Gene Ther.* **1998**, *9*, 1939–1950.

(270) Calegari, F.; Huttner, W. B. An Inhibition of Cyclin-Dependent Kinases That Lengthens, but Does Not Arrest, Neuroepithelial Cell Cycle Induces Premature Neurogenesis. *J. Cell Sci.* **2003**, *116*, 4947–4955.

(271) Osumi, N.; Inoue, T. Gene Transfer into Cultured Mammalian Embryos by Electroporation. *Methods* **2001**, *24*, 35–42.

(272) Bennett, B. D.; Wilson, Chalres, J. Spontaneous Activity of Neostriatal Cholinergic Interneurons In Vitro. *J. Neurosci.* **1999**, *19*, 5586–5596.

(273) Pisani, A.; Bonsi, P.; Centonze, D.; Martorana, A.; Fusco, F.; Sancesario, G.; De Persis, C.; Bernardi, G.; Calabresi, P. Activation of b1-Adrenoceptors Excites Striatal Cholinergic Interneurons through a cAMP-Dependent, Protein Kinase-Independent Pathway. *J. Neurosci.* **2003**, *23*, 5272–5282.

(274) Pisani, A.; Bernardi, G.; Ding, J.; Surmeier, D. J. Re-Emergence of Striatal Cholinergic Interneurons in Movement Disorders. *Trends Neurosci*. **2007**, *30*, 545–553.

(275) Pirrung, M. C.; Wang, L.; Montague-Smith, M. P. 3‘-Nitrophenylpropyloxycarbonyl (NPPOC) Protecting Groups for High-Fidelity Automated 5‘ → 3‘ Photochemical DNA Synthesis. *Org*. *Lett*. **2001**, *3*, 1105–1108.

(276) Broca, P. Remarques Sur Le Siege de La Faculte Du Langage Articule Suivies D’une Observation D’aphemie (Perte de La Parole). *Bull*. *Soc*. *Anat*. **1861**, *6*, 330–357.

(277) Rorden, C.; Karnath, H. O. Using Human Brain Lesions to Infer Function: A Relic from a Past Era in the fMRI Age? *Nat*. *Rev*. *Neurosci*. **2004**, *5*, 813–819.

(278) Musso, M.; Moro, A.; Glauche, B.; Rijntjes, M.; Reichenbach, J.; Buchel, C.; Weiller, C. Broca’s Area and He Language Instinct. *Nat*. *Neurosci*. **2003**, *6*, 774–781.

(279) Scoville, W. B.; Milner, B. Loss of Recent Memory after Bilateral Hippocampal Lesions. *J*. *Neurol*. *Neurosurg*. *Psychiatry* **1957**, *20*, 11–21.

(280) Adolphs, R.; Tranel, D.; Damasio, H.; Damasio, A. R. Fear and the Human Amygdala. *J*. *Neurosci*. **1995**, *15*, 5879–5891.

(281) Calder, A. J.; Keane, J.; Manes, F.; Antoun, N.; Young, A. W. Impaired Recognition and Experience of Disgust Following Brain Injury. *Nat*. *Neurosci*. **2000**, *3*, 1077–1078.

(282) Goodale, M. A.; Milner, D. A. Separate Visual Pathways for Perception and Action. *Trends Neurosci*. **1992**, *15*, 20–25.

(283) Raineteau, O.; Schwab, M. E. Plasticity of Motor Systems After Incomplete Spinal Cord injury. *Nat*. *Rev*. *Neurosci*. **2001**, *2*, 263–273.

(284) Amunts, K.; Weiss, P. H.; Mohlberg, H.; Pieperhoff, P.; Eickhoff, S.; Gurd, J. M.; Marshall, J. C.; Shah, N. J.; Fink, G. R.; Zilles, K. Analysis of Neural Mechanisms Underlying Verbal Fluency in Cytoarchitectonically Defined Stereotaxic space—The Roles of Brodmann Areas 44 and 45. *Neuroimage* **2004**, *22*, 42–56.

(285) Farah, M. J. Neuropsychological Inference with an Interactive Brain: A Critique of the "locality" Assumption. *Behav. Brain Sci.* **1994**, *17*, 43.

(286) Ogawa, S.; Tank, D. W.; Menon, R.; Ellermann, J. M.; Kim, S. G.; Merkle, H.; Ugurbil, K. Intrinsic Signal Changes Accompanying Sensory Stimulation: Functional Brain Mapping with Magnetic Resonance Imaging. *Proc. Natl. Acad. Sci. U. S. A.* **1992**, *89*, 5951–5955.

(287) Harel, N.; Ugurbil, K.; Uludag, K.; E., Y. Frontiers of Brain Mapping Using MRI. *J. Magn. Reson. Imaging* **2006**, *23*, 945–957.

(288) Kwong, K. K.; Belliveau, J. W.; Chesler, D. A.; Goldberg, I. E.; Weisskoff, R. M.; Poncelet, B. P.; Kennedy, D. N.; Hoppel, B. E.; Cohen, M. S.; Turner, R. Dynamic Magnetic Resonance Imaging of Human Brain Activity during Primary Sensory Stimulation. *Proc. Natl. Acad. Sci. U. S. A.* **1992**, *89*, 5675–5679.

(289) Gabriel, M.; Brennan, N. P.; Peck, K. K.; Holodny, A. I. Blood Oxygen Level Dependent Functional Magnetic Resonance Imaging for Presurgical Planning. *Neuroimaging Clin. N. Am.* **2014**, *24*, 557–571.

(290) Schilling, K.; Lukt, D.; Morgan, J. I.; Currant, T. Regulation of a *Fos-lacZ* Fusion Gene: A Paradigm for Quantitative Analysis of Stimulus-Transcription Coupling (Oncogene/signal Transduction/gene Regulation). *Proc. Natl. Acad. Sci. U. S. A.* **1991**, *88*, 5665–5669.

(291) Kawashima, T.; Okuno, H.; Nonaka, M.; Adachi-Morishima, A.; Kyo, N.; Okamura, M.; Takemoto-Kimura, S.; Worley, P. F.; Bito, H. Synaptic Activity-Responsive Element in the Arc/Arg3.1 Promoter Essential for Synapse-to-Nucleus Signaling in Activated Neurons. *Proc. Natl. Acad. Sci. U. S. A.* **2009**, *106*, 316–321.

(292) Eguchi, M.; Yamaguchi, S. In Vivo and in Vitro Visualization of Gene Expression Dynamics over Extensive Areas of the Brain. *Neuroimage* **2009**, *44*, 1274–1283.

(293) Barth, A. L.; Gerkin, R. C.; Dean, K. L. Alteration of Neuronal Firing Properties after In Vivo Experience in a FosGFP Transgenic Mouse. *J. Neurosci.* **2004**, *24*, 6466–6475.

(294) Grinevich, V.; Kolleker, A.; Eliava, M.; Takada, N.; Takuma, H.; Fukazawa, Y.; Shigemoto, R.; Kuhl, D.; Waters, J.; Seeburg, P. H.; Osten, P. Fluorescent Arc/Arg3.1 Indicator Mice: A Versatile Tool to Study Brain Activity Changes in Vitro and in Vivo. *J. Neurosci. Methods* **2009**, *184*, 25–36.

(295) Okuno, H.; Akashi, K.; Ishii, Y.; Yagishita-Kyo, N.; Suzuki, K.; Nonaka, M.; Kawashima, T.; Fujii, H.; Takemoto-Kimura, S.; Abe, M.; Natsume, R.; Chowdhury, S.; Sakimura, K.; Worley, P. F.; Bito, H. Inverse Synaptic Tagging of Inactive Synapses via Dynamic Interaction of Arc/Arg3.1 with CaMKIIβ. *Cell* **2012**, *149*, 886–898.

(296) Kawashima, T.; Kitamura, K.; Suzuki, K.; Nonaka, M.; Kamijo, S.; Takemoto-Kimura, S.; Kano, M.; Okuno, H.; Ohki, K.; Bito, H. Functional Labeling of Neurons and Their Projections Using the Synthetic Activity–dependent Promoter E-SARE. *Nat. Methods* **2013**, *10*, 889–895.

(297) Barco, A.; Patterson, S.; Alarcon, J. M.; Gromova, P.; Mata-Roig, M.; Morozov, A.; Kandel, E. R. Gene Expression Profiling of Facilitated L-LTP in VP16-CREB Mice Reveals That BDNF Is Critical for the Maintenance of LTP and Its Synaptic Capture. *Neuron* **2005**, *48*, 123–137.

(298) Mayr, B.; Montminy, M. Transcriptional Regulation by the Phosphorylation-Dependent Factor CREB. *Nat. Rev. Mol. Cell Biol.* **2001**, *2*, 599–609.

(299) Kramer, B. P.; Fischer, M.; Fussenegger, M. Semi-Synthetic Mammalian Gene Regulatory Networks. *Metab. Eng.* **2005**, *7*, 241–250.

(300) Noguchi, N.; Takada, K.; Katayama, J.; Emura, A. Regulation of Transcription of the *mph*(A) Gene for Macrolide 2'-Phosphotransferase I in *Escherichia Col*i: Characterization of the Regulatory Gene *mphR*(A). *J. Bacteriol.* **2000**, *182*, 5052–5058.

(301) Pandey, D.; Katti, S. B.; Haq, W.; Tripathi, C. K. M. Synthesis and Antimicrobial Activity of Erythromycin-A Oxime Analogs. *Bioorganic Med. Chem.* **2004**, *12*, 3807–3813.

(302) Nam, G.; Kang, T. W.; Shin, J. H.; Choi, K. Il. Design, Synthesis, and Anti-Helicobacter Pylori Activity of Erythromycin A (E)-9-Oxime Ether Derivatives. *Bioorg. Med. Chem. Lett.* **2006**, *16*, 569–572.

(303) García-Melchor, M.; Braga, A. A. C.; Lledós, A.; Ujaque, G.; Maseras, F. Computational Perspective on Pd-Catalyzed C-C Cross-Coupling Reaction Mechanisms. *Acc. Chem. Res.* **2013**, *46*, 2626–2634.

(304) Campeau, L.; Parisien, M.; Jean, A.; Fagnou, K. Intramolecular Direct Arylation with Aryl Chlorides, Bromides and Iodides: Developments Leading to New Intermolecular Processes. *J. Am. Chem. Soc.* **2006**, *128*, 581–590.

(305) Shembekar, V. R.; Chen, Y.; Carpenter, B. K.; Hess, G. P. A Protecting Group for Carboxylic Acids That Can Be Photolyzed by Visible. *Biochemistry* **2005**, *44*, 7107–7114.

(306) Bordwell, F. G.; Ji, G.-Z. Equilibrium Acidities and Homolytic Bond Dissociation Energies of the H-0 Bonds in Oximes and Amidoximes. *J. Org. Chem* **1992**, *57*, 3019–3025.

(307) Olmstead, W. N.; Margolin, Z.; Bordwell, F. G. Acidities of Water and Simple Alcohols in Dimethyl Sulfoxide Solution. *J. Org. Chem.* **1980**, *45*, 3295–3299.

(308) Seamon, K. B.; Padgett, W.; Daly, J. W. Forskolin: Unique Diterpene Activator of Adenylate Cyclase in Membranes and in Intact Cells. *Biochemistry* **1981**, *78*, 3363–3367.

(309) Hinrichs, W.; Kisker, C.; Düvel, M.; Müller, a; Tovar, K.; Hillen, W.; Saenger, W. Structure of the Tet Repressor-Tetracycline Complex and Regulation of Antibiotic Resistance. *Science* **1994**, *264*, 418–420.

(310) Pangborn, A. B.; Giardello, M. A.; Grubbs, R. H.; Rosen, R. K.; Timmers, F. J. Safe and Convenient Procedure for Solvent Purification. *Organometallics* **1996**, *15*, 1518–1520.

(311) McDonagh, A. F.; Smith, H. E. Ring-Chain Tautomerism of Derivatives of O-Hydroxybenzylamine with Aldehydes and Ketones. The Nuclear Magnetic Resonance of Immonium Ion. *J. Org. Chem.* **1968**, *33*, 8–12.

(312) Burke, W. J.; Hammer, C. R.; Weatherbee, C. Bis-M-Oxazines from Hydroquinone. *J. Org. Chem.* **1961**, *26*, 4403–4407.

(313) Ihara, M.; Noguchi, K.; Fukumoto, K. Conversion of Indoles into Quinolines Through the N-1-C-2 Fission by Singlet Oxygen as a Model Experiment of Biomimetic Synthesis of Quinine Alkaloids. *Tetrahedron* **1985**, *41*, 2109–2114.

(314) *CrystalClear 1.40*; Rigaku Americas Corporation: The Woodlands, TX, 2008.

(315) Altomare, A.; Burla, M. C.; Camalli, M.; Cascarano, G. L.; Giacovazzo, C.; Guagliardi, A.; Moliterni, A. G. G.; Polidori, G.; Spagna, R. SIR97. A Program for Crystal Structure Solution. *J. Appl. Cryst.* **1999**, *32*, 115–119.

(316) Sheldrick, G. M. SHELXL97. Program for the Refinement of Crystal Structures. *Acta. Cryst.* **2008**, *A64*, 112–122.

(317) Spek, A. L. *PLATON, A Multipurpose Crystallographic Tool*; Utrecht University: The Netherlands, 1998.

(318) Farrugia, L. J. WinGX 1.64. An Integrated System of Windows Programs for the Solutions, Refinement and Analysis of Single Crystal X-Ray Diffraction Data. *Appl. Cryst.* **1999**, *32*, 837–838.

(319) $R_w(F^2) = \{\Sigma w(|F_o|^2 - |F_c|^2)^2/\Sigma w(|F_o|)^4\}^{1/2}$ where w is the weight given each reflection.
$R(F) = \Sigma(|F_o| - |F_c|)/\Sigma|F_o|\}$ for reflections with $F_o > 4(\sigma(F_o))$.
$S = [\Sigma w(|F_o|^2 - |F_c|^2)^2/(n - p)]^{1/2}$, where n is the number of reflections and p is the number of refined parameters.

(320) International Tables for X-ray Crystallography (1992). Vol. C, Tables 4.2.6.8 and 6.1.1.4, A. J. C. Wilson, editor, Boston: Kluwer Academic Press.

(321) Sheldrick, G. M. *SHELXTL/PC (Version 5.03)*; Siemens Analytical X-ray Instruaments, INC.: Madison, Wisconsin, USA, 1994.

(322) *SAINT V8.27B Bruker AXS Inc.*; Madison, Wi, 2012.